DOCTORAL DISSERTATION

Mono- and diradicals derived from dihydrobenzo[*e*][1,2,4]triazin-4-yl

MSc Dominika Katarzyna Pomikło

Supervised by Prof. Piotr Kaszyński

Centre of Molecular and Macromolecular Studies
Polish Academy of Sciences
Division of Organic Chemistry

Łódź, August 2023

ROZPRAWA DOKTORSKA

Mono- oraz dirodniki oparte na dihydrobenzo[*e*][1,2,4]triazyn-4-ylu

mgr inż. Dominika Katarzyna Pomikło

Promotor: prof. zw. dr hab. inż. Piotr Kaszyński

Centrum Badań Molekularnych i Makromolekularnych
Polskiej Akademii Nauk
Dział Chemii Organicznej

Łódź, Sierpień 2023

mgr inż. Dominika Katarzyna Pomikło

Centrum Badań Molekularnych i Makromolekularnych

Polskiej Akademii Nauk

Dział Chemii Organicznej

ul. Henryka Sienkiewicza 112, 90-363 Łódź

email: dominika.pomiklo@cbmm.lodz.pl

Mono- oraz dirodniki oparte na dihydrobenzo[*e*][1,2,4]triazyn-4-ylu

Promotor: prof. zw. dr hab. inż. Piotr Kaszyński

Łódź, Sierpień 2023

Acknowledgments/ Podziękowania

Presented Dissertation was realized in years 2018-2023 with financial support from the following research programs:

Table of Contents

1. Abstract in English

Recent years witness a rapid growth of interest in open-shell organic species for fundamental and applied studies. Such systems exhibit semiconductive properties, which are applicable in areas such as optoelectronic or sensors, and constitute attractive building blocks for magnetic materials employed *e.g.* as spin filters. In this context, stable heterocyclic diradicals based on the benzo[*e*][1,2,4]triazin-4-yl are of particular interest. Various connections of two paramagnetic units can lead to either a closed-shell Kekulè resonance structure with the prefference for a singlet ground state (referred to as diradicaloids) or non-Kekulè molecules, which can exhibit a triplet ground state.

During the last five years, there has been a significant development in the design, characterization and synthesis of diradicals and diradicaloids incorporating the Blatter radical. However many of these derivatives exhibit limited stability and their synthetic access is still cumbersome. Stable diradicals based on the benzo[*e*][1,2,4]triazin-4-yl are also attractive building blocks for the preparation of paramagnetic liquid crystals and near-infrared dichroic dyes. Therefore, further development of methods allowing for convinient and effective preparation of stable Blatter diradicals as well as understanding of the properties of such species opens up access to a wide range of applications in functional materials and constitutes a significant part of this Doctoral Dissertation.

The presented Dissertation is part of a broad project aimed at developing access to a new class of near-IR dichroic dyes. Stable diradicals incorporating the benzo[*e*][1,2,4]triazin-4-yl are envisioned to be suitable precursors to radical cations with substituent-tunable absorption in the NIR region, and which are compatible with LC matrix and exhibit high dichroic ratio. This approach is a response for a rapidly growing interest in diradicals as NIR dyes, and overcomes problems *e.g.* low chemical stability and incompatibility with the liquid crystal host which characterizes already investigated systems.

The development of synthetic access to new classes of mono- and diradicals based on the benzo[*e*][1,2,4]triazin-4-yl and comprehensive analysis of their structure-property relationships (Figure 1.1.) constitute key steps enabling achieving the ultimate goal and is the main focus of this Doctoral Dissertation. Establishing convinient synthetic methods for a series of C(3)-functionalized benzo[*e*][1,2,4]triazines, gave rise to simple preparation of variety of stable monoradicals incorporating benzo[*e*][1,2,4]triazin-4-yl. Developed synthetic pathways and

acquired skills for characterization of such spiecies by spectroscopic and electrochemical methods allowed for understanding structure–property relationships in this class of compounds. These findings constitute a tool for a rational design and preparation of stable diradicals connected either directly (type **A**) or through a π-spacer (type **B**) with properties suitable for application in functional materials (Figure 1.1.). One-electron oxidation of appropriately functionalized diradicals will provide radical cations with substituent-tunable absorption in the NIR region and which are compatible with LC matrix and exhibit high dichroic ratio.
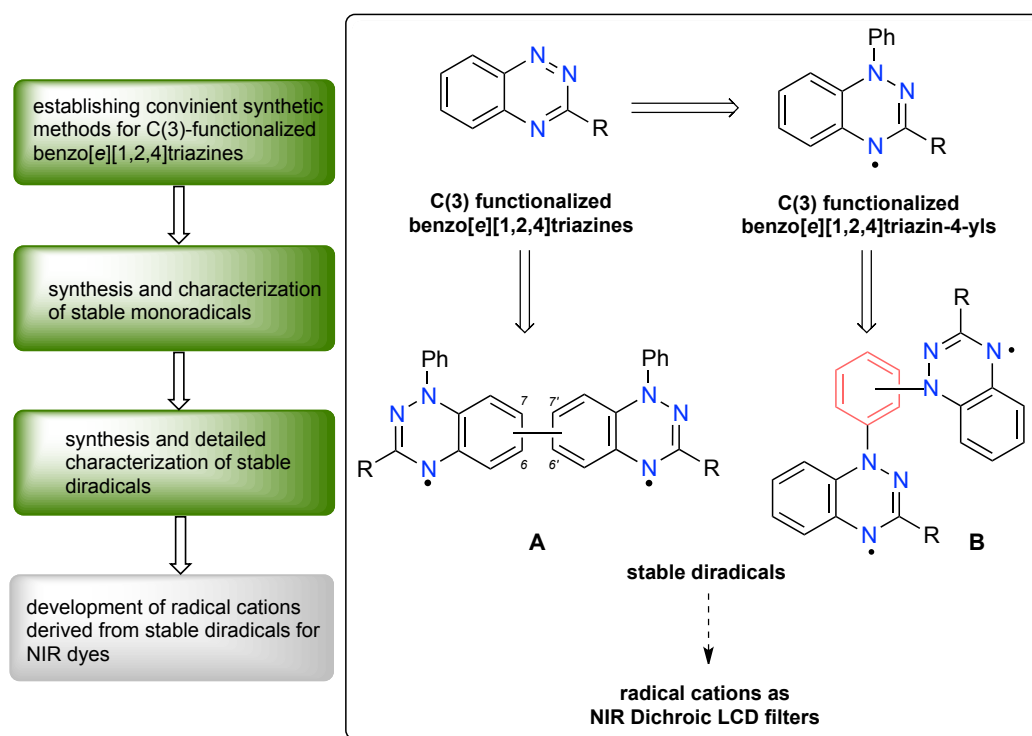
Figure 1.1. A graphical representation of the goals and scope of this Dissertation.

The Introduction discusses the properties of heterocyclic stable organic radicals, with a particular emphasis on mono- and diradicals based on the benzo[*e*][1,2,4]triazin-4-yl, as well as the main techniques for studies of magnetic properties. In Section 4.2.2. the general design of high-spin molecules is discussed, which has been used in the rational development of diradicals based on the benzo[*e*][1,2,4]triazin-4-yl unit and exhibiting either the triplet ground state or a thermally populated triplet state. Section 4.2.5. describes the current state-of-the-art in the field of stable diradicals based on the benzo[*e*][1,2,4]triazin-4-yl reported to date. This part provides an important point of reference for my accomplishments in this area.

The Result and Disscusion part of this Dissertation is initially focused on the development of methods for synthesis of C(3)-functionalized benzo[*e*][1,2,4]triazines and benzo[*e*][1,2,4]triazin-4-yls, and understanding of their properties. Section 6.1 provides a brief description of a facile access to a series of structurally diverse C(3)-substituted derivatives of the benzo[*e*][1,2,4]triazine, which are readily available directly from the 3-chloro or 3-iodobenzo[*e*][1,2,4]triazines. In Section 6.2 the synthesis and characterization of a series of C(3)-functionalized derivatives of the Blatter radical obtained by a new synthetic method are described. This method utilizes the cyclization of *N*-substituted guanidines and amidines leading to the formation of the C(3)-amino and C(3)-alkyl benzo[*e*][1,2,4]triazines respectively and followed by addition of phenyllithium to permit the facile access to a series of benzo[*e*][1,2,4]triazin-4-yls. The presented methodology allows to avoid multistep procedures with poorly soluble intermediates. Section 6.3. contains a description of preparation of a series of C(3)-substituted benzo[*e*][1,2,4]triazin-4-yl radicals by addition of PhLi to benzo[*e*][1,2,4]triazines obtained *via* methodology presented in Section 6.1. As a result, convenient access to a series of C(3)-functionalized derivatives of the Blatter radical was developed and the synthetic limitations of these methods were determined. Detailed characterization of the resulting benzo[*e*][1,2,4]triazin-4-yls by spectroscopic (UV-vis, EPR) and electrochemical (Cyclic Voltammetry) methods was performed. A brief description of these accomplishments is located in Sections 6.1. and 6.2. and 6.3, and details are provided in enclosed publications (Chapter 9).

The last two Sections concern with the synthesis, physicochemical and magnetic studies of a series of stable diradicals based on the benzo[*e*][1,2,4]triazin-4-yl. The first contains a detailed description of the synthesis and investigation of a series of regioisomers of di-Blatter diradicals with controlled electronic and magnetic properties connected through the spin rich positions C(6) and C(7) of the benzo[*e*][1,2,4]triazin-4-yl core. The last section of this Dissertation presents two di-Blatter diradicals connected through a spin-coupler at the N(1) position. Access to these derivatives was possible through an effective, one-step addition of dilithio derivatives to the 3-trifluoromethylbenzo[*e*][1,2,4]triazine. These diradicals are the first examples of a potentially broad class of symmetric high-spin molecules with a controlled singlet-triplet gap.

2. Abstract in Polish (Streszczenie w języku polskim)

W ostatnich latach nastąpił gwałtowny wzrost zainteresowania organicznymi układami otwarto-powłokowymi zarówno w badaniach podstawowych jak i stosowanych. Systemy te wykazują właściwości półprzewodzące, które są istotne w obszarach takich jak, optoelektronika czy sensory oraz stanowią atrakcyjne bloki budulcowe w materiałach magnetycznych wykorzystywanych jako filtry spinowe. W tym kontekście szczególnie interesujące są stabilne dirodniki heterocykliczne oparte na rdzeniu benzo[*e*][1,2,4]triazyn-4-ylu. Różne sposoby połączenia dwóch centrów paramagnetycznych mogą prowadzić do molekuł posiadających zamknięto-powłokową strukturę Kekulềgo i charakteryzujących się singletowym stanem podstawowym (określane terminem diradikaloidy) lub nieposiadających takiej struktury rezonansowej i mogących wykazywać trypletowy stan podstawowy.

W ciągu ostatnich pięciu lat nastąpił znaczny rozwój w projektowaniu, charakteryzacji oraz syntezie dirodników oraz diradikaloidów posiadających w swojej strukturze rodnik Blattera, jednak wiele z takich pochodnych wykazuje ograniczoną stabilność, a ich dostęp syntetyczny w dalszym ciągu jest skomplikowany. Stabilne dirodniki oparte na benzo[*e*][1,2,4]triazyn-4-ylu stanowią również atrakcyjne bloki budulcowe do otrzymywania paramagnetycznych ciekłych kryształów oraz barwników dichroicznych w bliskiej podczerwieni. Opracowanie dogodnego dostępu syntetycznego oraz poznanie właściwości takich dirodników otworzy szereg możliwości aplikacyjnych opartych na nich materiałów funkcjonalnych. W związku z tym dalszy rozwój metod pozwalających na łatwe i efektywne otrzymywanie stabilnych dirodników Blattera jest bardzo istotny i jest przedmiotem znacznej część tej Rozprawy Doktorskiej.

Niniejszej Rozprawa Doktorska, stanowi część rozległego projektu mającego na celu opracowanie dostępu do nowej klasy barwników dichroicznych bliskiej podczerwieni. Stabilne dirodniki oparte na benzo[*e*][1,2,4]triazyn-4-ylu będą wykorzystane jako dogodne prekursory kationorodników kompatybilnych z matrycą ciekłokrystaliczną, wykazujących wysoki stosunek dichroiczny oraz charakteryzujących się modyfikowalną w zależności od podstawnika absorpcją w bliskiej podczerwieni. Przestawione podejście jest odpowiedzią na wzrost zainteresowania dirodnikami oraz kationorodnikami jako elementami fotonicznymi, a także rozwiązuje problemy takie jak niska stabilność czy brak kompatybilności z matrycą ciekłokrystaliczną, którymi charakteryzują się dotychczas badane systemy.

Opracowanie dostępu syntetycznego do nowych klas mono- oraz dirodników opartych na benzo[*e*][1,2,4]triazyn-4-ylu wraz z kompleksową analizą zależności ich struktura–właściwości stanowią kluczowe etapy umożliwiające osiągnięcie ostatecznego celu i są głównym tematem tej Rozprawy Doktorskiej. Dogodne metody otrzymywania C(3)-sfunkcjonalizowanych benzo[*e*][1,2,4]triazyn pozwoliły na łatwy dostęp do różnorodnych stabilnych monorodników zawierających strukturę benzo[*e*][1,2,4]triazyn-4-ylu. Wypracowane umiejętności syntetyczne oraz charakteryzacji takich związków pozwoliły na poznanie relacji ich struktura-właściwości. Proces ten stanowi narzędzie do racjonalnego projektowania oraz syntezy stabilnych dirodników połączonych bezpośrednio (typ **A**) lub za pomocą łącznika π (typ **B**) posiadających właściwości odpowiednie dla ich zastosowania w materiałach funkcjonalnych (Rycina 2.1.). Utlenianie jednoelektronowe odpowiednio sfunkcjonalizowanych dirodników pozwoli na dostęp do kationorodników kompatybilnych z matrycą ciekłokrystaliczną, wykazujących wysoki współczynnik dichroiczny oraz regulowaną za pomocą efektu podstawnika absorpcję w obszarze bliskiej podczerwieni.
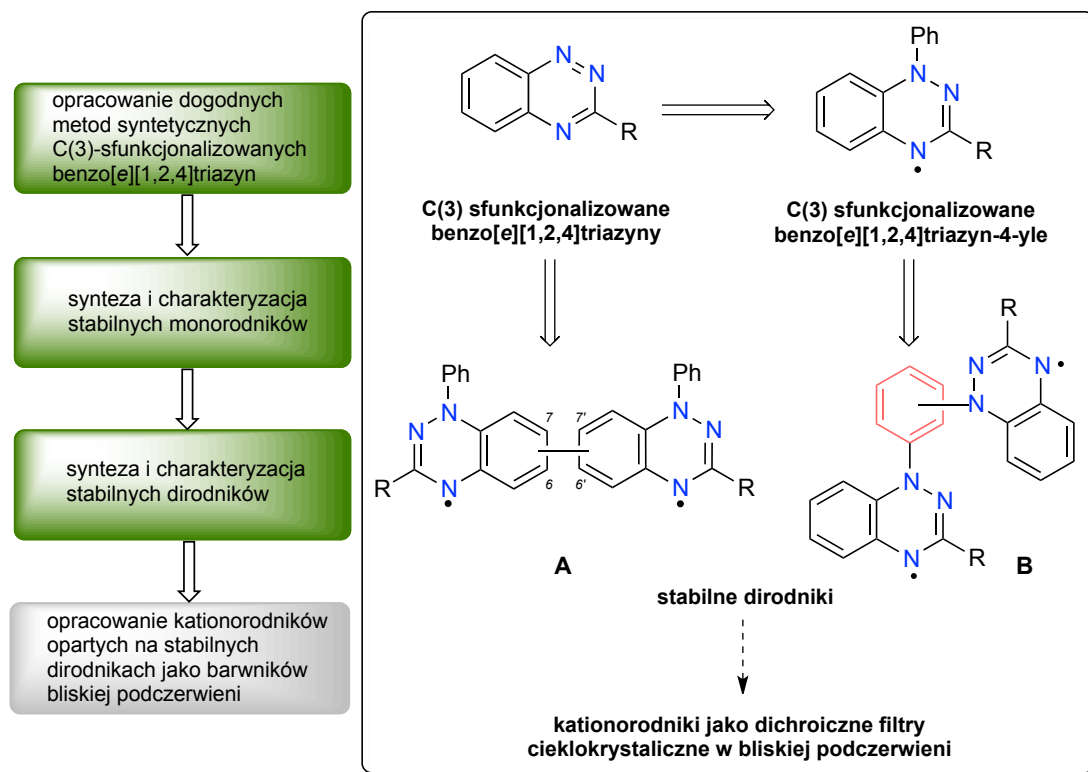
Rycina 2.1. Graficzna prezentacja celów oraz zakresu Rozprawy Doktorskiej.

We wprowadzeniu omówiono właściwości heterocyklicznych stabilnych rodników organicznych ze szczególnym uwzględnieniem mono- oraz dirodników opartych na 1,4-dihydrobenzo[*e*][1,2,4]triazyn-4-ylu, a także główne techniki badań właściwości magnetycznych wraz z analizą wyników pomiarów. W podrozdziale 4.2.2. omówiono zasady projektowania molekuł wysoko-spinowych, stosowane również do racjonalnego tworzenia dirodników opartych na strukturze benzo[*e*][1,2,4]triazin-4-ylu i posiadających stan trypletowy jako stan podstawowy lub możliwość termicznej populacji stanu trypletowego. Podrozdział 4.2.5. zawiera opis dotychczasowych osiągnięć w obszarze stablinych dirodników opartych na benzo[*e*][1,2,4]triazyn-4-ylu. Stanowi on istotny punkt odniesienia do moich dokonań w tej tematyce badawczej.

Część poświęcona omówieniu wyników badań własnych zawiera opis opracowanych metod syntezy C(3)-sfunkcjonalizowanych benzo[*e*][1,2,4]-triazyn oraz benzo[*e*][1,2,4]-triazyn-4-yli i właściwości uzyskanych pochodnych. Podrozdział 6.1. opisuje metodę dostępu do serii benzo[*e*][1,2,4]triazyn podstawionych w pozycji C(3), na drodze bezpośrednich reakcji z 3-chloro lub 3-iodobenzo[*e*][1,2,4]triazyną. W podrozdziale 6.2. przedstawiono syntezę oraz charakteryzację serii C(3)-sfunkcjonalizowanych pochodnych rodnika Blattera otrzymanych za pomocą nowej metody syntetycznej. Polega ona na cyklizacji *N*-aryloguanidyn oraz *N*-aryloamidyn prowadzącej do otrzymywania odpowiednich benzo[*e*][1,2,4]triazyn i następczej addycji fenylolitu. Taka metodologia pozwala na uniknięcie wieloetapowych procedur wykorzystujących słabo rozpuszczalne półprodukty. Sekcja 6.3. zawiera opis otrzymywania szeregu C(3)-podstawionych rodników benzo[*e*][1,2,4]triazyn-4-ylowych poprzez addycję fenylolitu do benzo[*e*][1,2,4]triazyn otrzymanych metodami przedstawionymi w podrozdziale 6.1. W rezultacie opracowano dogodny dostęp do szeregu C(3)-sfunkcjonalizowanych pochodnych rodnika Blattera oraz określono syntetyczne ograniczenia tych metod. Przeprowadzono szczegółową charakterystykę otrzymanych benzo[*e*][1,2,4]triazyn-4-yli metodami spektroskopowymi i elektrochemicznymi. Wyniki te pozwoliły na zrozumienie zależności struktura-właściwość i stanowią narzędzie do dalszych badań. Rezultaty te zostały krótko opisane kolejno w podrozdziałach 6.1. 6.2. oraz 6.3, a także szczegółowo w załączonych materiałach publikacyjnych (Rozdział 9).

W dwóch końcowych podrozdziałach opisano syntezę oraz badania fizykochemiczne i magnetyczne serii stabilnych dirodników opartych na benzo[*e*][1,2,4]triazyn-4-ylu. W pierwszej

części (podrozdział 6.4.1.) opisano syntezę oraz badania nad serią regioisomerów dirodników di-Blattera z kontrolowanymi właściwościami elektronowymi oraz magnetycznymi połaczonych przez kombinację obdarzonych wysoką gęstością spinową atomów węgla w pozycjach C(6) oraz C(7) benzo[*e*][1,2,4]triazyn-4-ylu. Ostatni podrozdział stanowi opis opracowania dostępu syntetycznego oraz badań dwóch dirodnikiów di-Blattera połączonych w pozycjach N(1) za pomocą spin-łącznika. Dostęp do tych dwóch pochodnych był możliwy na drodze efektywnej, jednoetapowej reakcji addycji dilito- pochodnych do 3-trifluorometylobenzo[*e*][1,2,4]triazyny. Dirodniki te, stanowią pierwsze przykłady potencjalnie szerokiej klasy symetrycznych wyskospinowych molekuł z kontrolowaną wartością przerwy energetycznej singlet-tryplet. Opracowanie dostępu syntetycznego do takich pochodnych oraz poznanie ich właściwości fizykochemicznych i magnetycznych otwiera szerokie możliwości do łatwego wykorzystania w ciekłokrystalicznych materiałach samo-organizujących oraz filtrach dichroicznych.

3. List of publications constituting this Doctoral Dissertation

D−1 Bodzioch, A.; Pomikło, D.; Celeda, M.; Pietrzak, A.; Kaszyński, P. 3-Substituted benzo[*e*][1,2,4]triazines: synthesis and electronic effects of the C(3) substituent. *J. Org. Chem.* **2019**, *84*, 6377–6394.

Impact factor (IF) = 4.34

D−2 Pomikło, D.; Bodzioch, A.; Pietrzak, A.; Kaszyński, P. C(3) Functional derivatives of the Blatter radical. *Org. Lett.* **2019**, *21*, 6995–6999.

Impact factor (IF) = 6.09

D−3 Pomikło, D.; Bodzioch, A.; Kaszyński, P. 3-Substituted Blatter radicals: cyclization of *N*-arylguanidines and *N*-arylamidines to benzo[*e*][1,2,4]triazines and PhLi addition. *J. Org. Chem.* **2023**, *88*, 2999–3011.

Impact factor (IF) = 4.34

D−4 Pomikło, D.; Pietrzak, A.; Kishi, R.; Kaszyński, P. Bi-Blatter diradicals: convenient access to regioisomers with tunable electronic and magnetic properties. *Mater. Chem. Front.* **2023**, doi.org/10.1039/D3QM00666B

Impact factor (IF) = 7.0

D−5 Pomikło, D.; Kaszyński, P. Blatter diradicals with a spin coupler at the N(1) position. *Chem. Eur. J.* **2023**, doi.org/10.1002/chem.202301069

Impact factor (IF) = 5.02

4. Introduction

4.1. Stable heterocyclic radicals

4.1.1. Basic concepts and classification of stable radicals

Organic radicals are molecules containing an odd number of electrons *i.e.* possessing an unpaired electron on a singly occupied molecular orbital, SOMO.[1] This property, in most cases, makes such species highly chemically reactive and readily transforming through spontaneous dimerization, disproportionation or hydrogen abstraction reactions.[2] As a consequence of the presence of an unpaired electron, these molecules exhibit paramagnetic properties and the most frequently used technique for their studies is Electron Paramagnetic Resonance spectroscopy (EPR). The use of this technique for mono- as well as diradicals and interpretation of the results are described in details in Sections 4.2.3. and 4.2.4. of this Dissertation.

Since the discovery of the first stable organic radical, triphenylmethyl radical (Figure 4.1.1.), by Gomberg[3-4] in 1900 and isolation of tri(biphenyl)methyl radical by Schlenk[5] in 1910, these species received great attention and numerous organic radicals of different chemical stability have been synthesized. The propeller-like structure of the triphenylmethyl radical (Figure 4.1.1.a), is characterized by the twist angle of *ca.* 30° between phenyl rings and the plane containing the central carbon atom. This moderately low angle allows delocalization of some spin density from the central carbon atom to the three phenyl rings resulting in increased stability. In diluted deoxygenated solutions Gomberg's radical exists in an equilibrium with the dimer formed *via* a sigma-bond between the central carbon of one radical and the *para*-carbon of a phenyl ring in another radical. Selected examples of stable organic radicals,[3-12] which can be stored under ambient conditions are presented in Figure 4.1.1.
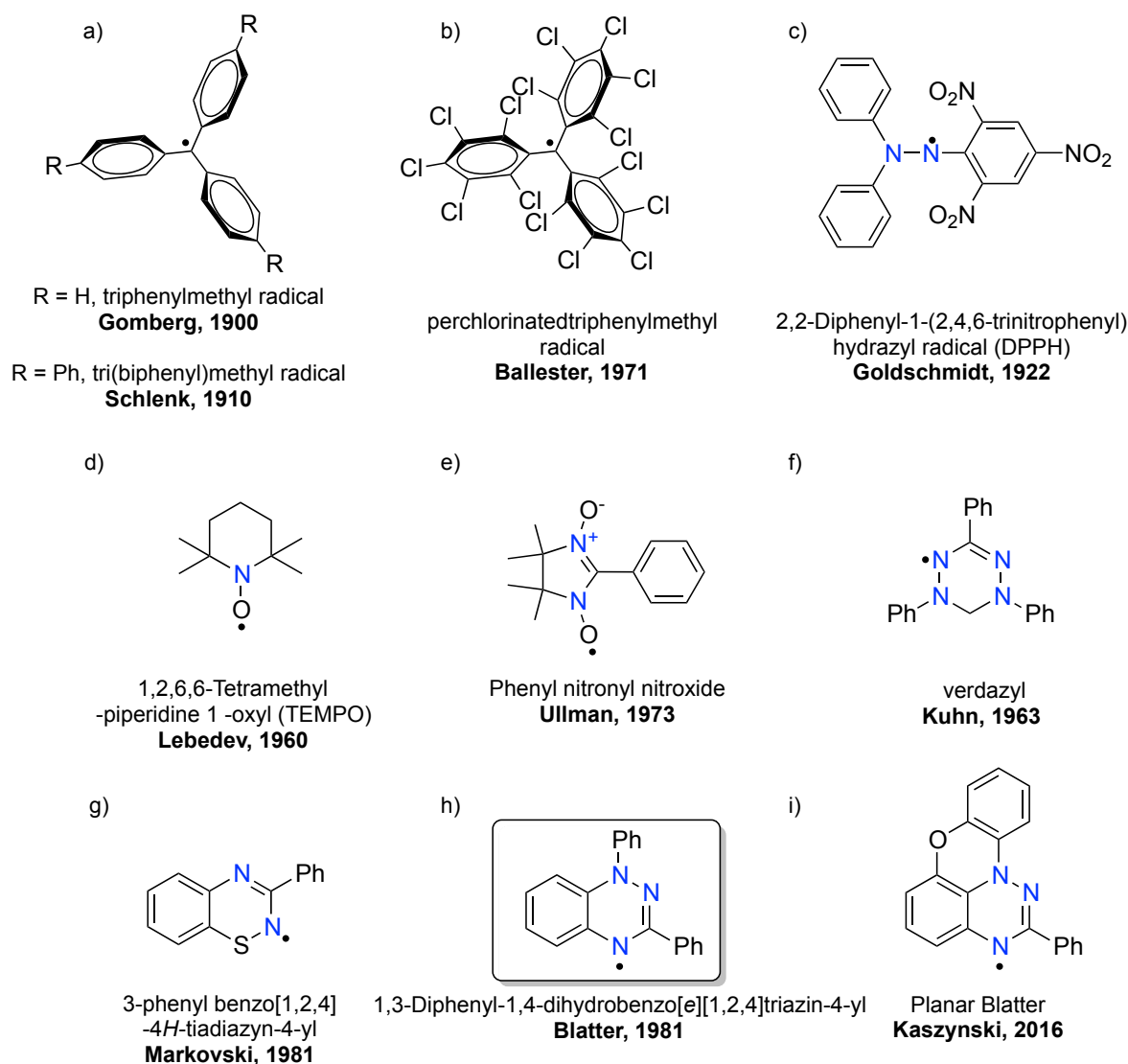
Figure 4.1.1. Structures of selected stable organic radicals.

The stability of radicals presented in Figure 4.1.1. is determined by steric and electronic factors, which can be controlled to some extent. The first method of stabilization relies on substitution with sterically bulky substituents, such as the *tert*-butyl group, or by perchlorination of aromatic rings to protect the spin center from reactions. A good example of this approach is a stable and inert towards oxygen perchlorinated analogue of the Gomberg radical, in which the *ortho*-chlorine atoms of the phenyl rings provide a large steric hindrance (Figure 4.1.1.b).[6] The phenyl rings in the perchlorinated triphenylmethyl radical (PTM) are twisted away from the plane containing the central carbon atom by *ca.* 50° leading to higher localization of spin density on the central carbon atom.
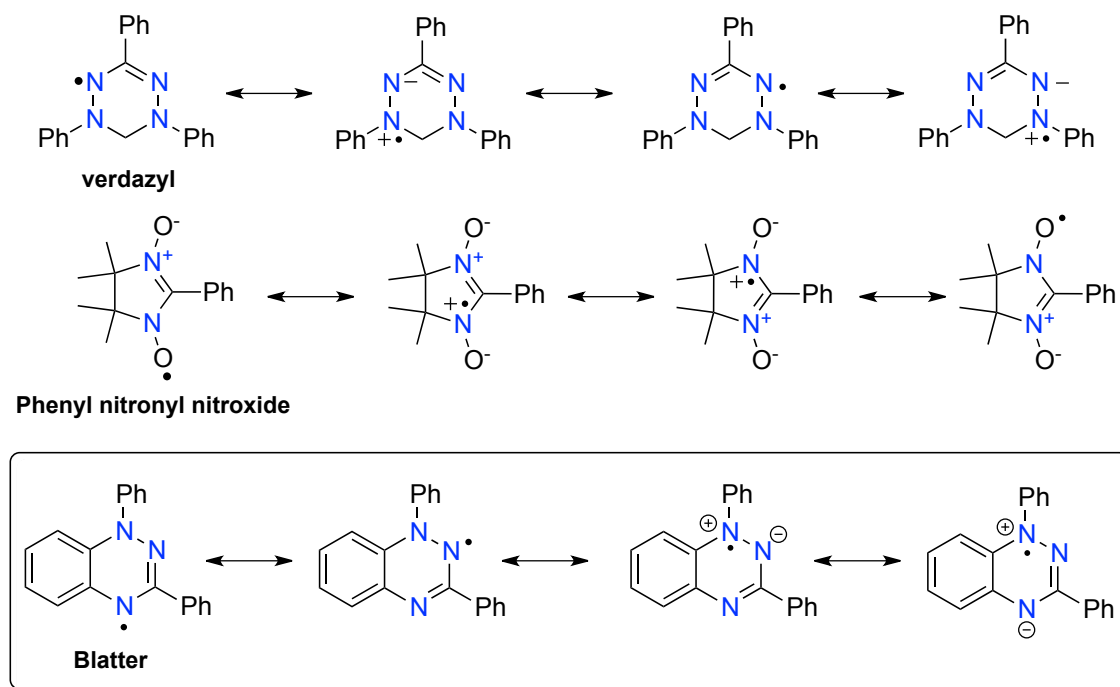
Figure 4.1.2. Selected resonance structures of verdazyl, phenyl nitronyl nitroxide and Blatter radical.

The second factor affecting stability of organic radicals is π-delocalization of the unpaired electron. Such a resonance-improved stability is observed in many radicals *e.g.* verdazyl radical, nitronyl nitroxide and Blatter radical (Figure 4.1.2.). The latter is the main focus in this Dissertation. The verdazyl and phenyl nitronyl nitroxide radicals are stabilized by delocalization of unpaired electrons over the nitrogen and oxygen atoms. The stability of the Blatter radical originates mainly from the extensive delocalization of the spin in two rings. Selected resonance structures of verdazyl, phenyl nitronyl nitroxide and Blatter radicals are presented in Figure 4.1.2. In general, the more resonance structures, the higher delocalization of the unpaired electron and better stabilization of the spin center. The presence of functional groups containing a heteroatom can also increase stability of radicals. In some cases, these factors are synergistic and highly stable and super-stable radicals are formed, which are used as building blocks for advanced magnetic materials. Particularly important are highly stable heterocyclic radicals whose stability can be controlled by modifications of their structure using standard methods of organic synthesis.[13] While many of nitronyl nitroxide and hydrazyl radicals possess an excellent stability, the sulfur–contining benzo[1,2,4]-4*H*-thiadiazin-4-yl (Figure 4.1.1.g) exhibits low stability towards oxygen[14] limiting its application in magnetic and liquid crystalline materials.

4.1.2. 1,4-Dihydrobenzo[*e*][1,2,4]triazin-4-yl – general properties

Among a family of stable radicals, a group of hydrazyl–based species is exceptional. The additional valence on the N atom permits incorporation of the hydrazyl fragment into cyclic structures, such as the six-membered ring of 1,4-dihydrobenzo[*e*][1,2,4]triazin-4-yl. Discovered by Blatter[11] in 1968, 1,3-diphenyl-1,4-dihydrobenzo[*e*][1,2,4]triazin-4-yl **4.1** (Figure 4.1.2.1.) is a prototypical derivative of a family of 1,4-dihydrobenzo[*e*][1,2,4]triazin-4-yl radicals, known as Blatter radical. The fundamental two-ring heterocyclic fragment is an 11-π electron system, isoelectronic with naphthalene radical anion. Thus, it belongs to a group of π* radicals, whose exceptional stability is owed to the antibonding nature of the SOMO, extensive spin delocalization, and aromatic character of the heterocycle. These factors results in thermal stability of certain Blatter radical derivatives up to 290 °C.[15]

Benzo[*e*][1,2,4]triazin-4-yls possess reversible redox properties with a small electrochemical window (*ca.* 1.2 V)[16] and distinct physicochemical properties with a broad absorption in the visible range, high lying SOMO, and significant spin delocalization. These electronic fetures are highly desired for charge and spin transport materials, which make Blatter radicals important building blocks for advanced functional materials. This molecular element has already been studied in the context of advanced magnetic materials,[17-19] particularly as building block for liquid crystals,[17,20-22] organic spintronics,[23] polymer chemistry[24] and photovoltaics.[25]
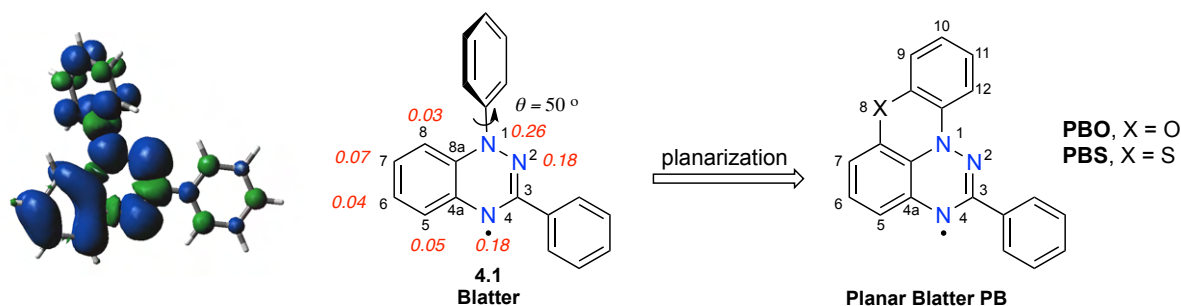
Figure 4.1.2.1. From the left: DFT-derived spin density distribution in the Blatter radical **4.1**, structure of the Blatter radical **4.1** with indicated numbering system and spin densities based on EPR spectroscopy[26] and its planar analogues with indicated numbering system.

All reported derivatives of the 1,4-dihydrobenzo[*e*][1,2,4]triazin-4-yl **4.1** exhibit a common feature, which is the presence of an aryl or *het*-aryl group at the N(1) position.[27] However, high torsion angle (about 50°) between the N(1)–aryl and the heterocycle plane limits the spin delocalization. Results of Electron Paramagnetic Resonance Spectroscopy (EPR) and Density

Functional Theory (DFT) calculations show that less than 10 % of spin density is delocalized to the Ar substituent, while about 70 % is concentrated on three nitrogen atoms of the [1,2,4]triazin-4-yl ring.[26] To expand the spin delocalization the plannar analogues of the Blatter radical were designed by annulation of the N(1)–Ph group with the C(8) position using einther an oxygen (**PBO**, X=O) or a sulfur atom (**PBS**, X = S) and are presented in Figure 4.1.2.1. Moreover, the planarization resulted in enrichment of the aryl substituent at the N(1) position with an additional 9.1% of spin density.[12] Importantly, positive spin is delocalized over both rings of the benzo[*e*][1,2,4]triazin-4-yl system, while the nodal C(3) position has a negative spin density due to spin polarization mechanism (shown in green in Figure 4.1.2.1.) . This distribution is an important aspect in the design of Blatter–based high-spin diradicals, described in Chapter 4.2.4. of this Dissertation.

As described above, 1,4-dihydrobenzo[*e*][1,2,4]triazin-4-yl **4.1** is characterised by high torsion angle between N(1)–Ar and the benzo[*e*][1,2,4]triaziny-yl core, which affects the molecular packing of radicals in the solid state. The torsion angle can be varied using N(1) substituents, which significantly affects magnetic properties of the solids.[12,28] A moderately high spin density resonating at the C(6) and C(7) position of the benzo[*e*][1,2,4]triazin-4-yl makes these sites releatively reactive. According to the literature, lack of protection of the C(7) position results in its oxidative instability and oxidation of the Blatter radical **4.1** to a quinoidal derivative. To prevent it, Koutentis and co-workers introduced the trifluoromethyl group to this position resulting in a "super stable" radical.[15] On the other hand fusing the C(6) and C(7) positions with aromatic rings allows for futher spin delocalization.[29-33] As mentioned before, the node at the C(3) position excludes the possibility of delocalization of the positive spin density to this site of the radical. However, introduction of various substituent at the C(3) position can impact physical properties of the radical by affecting the FMO's.[34-40] Functionalization of the C(3) position of the benzo[*e*][1,2,4]triazinyl was investigated during my research and the results of this work are described in details in Chapter 6.1., Chapter 6.2. and Chapter 6.3. of this Dissertation.

One of the most important aspects of these radicals is their magnetic properties, which depend on the molecular and crystal structures. This research area was initiated[41] by Neugebauer in the late 80s and was continued by Koutentis, Rawson[15,35] and others[12,42] at the beginning of the previous decade. These studies have yielded the fundamental knowledge on magneto–structural correlations and intermolecular spin interactions in the solid state.

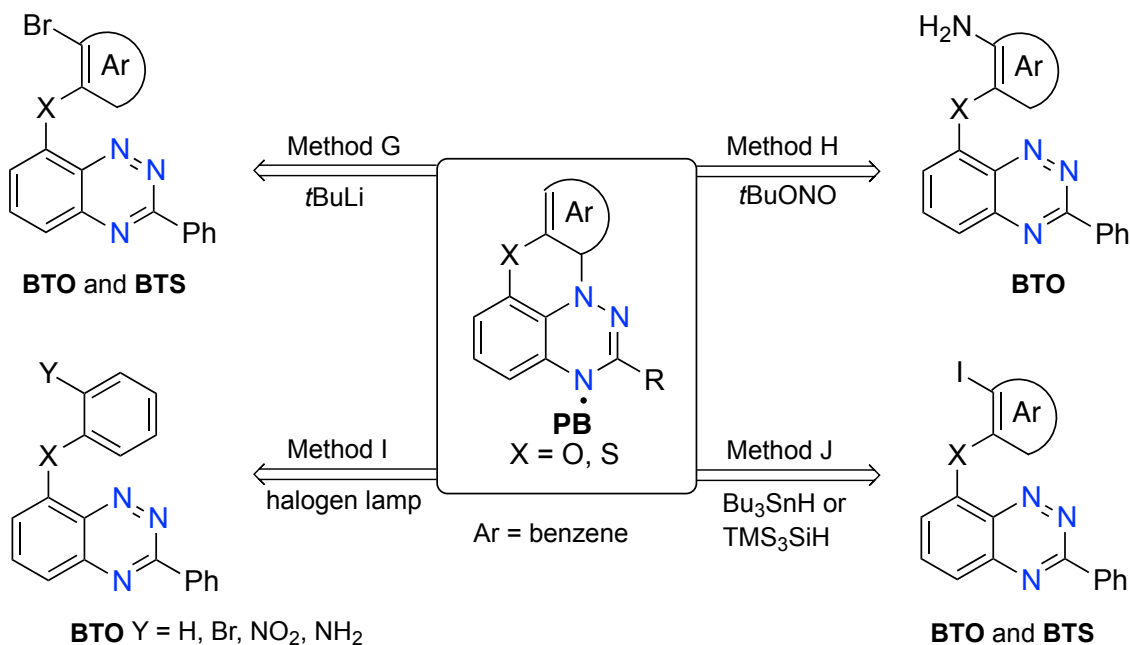## 4.1.3. Synthesis of 1,4-dihydrobenzo[*e*][1,2,4]triazin-4-yl radicals

During the past decade there was a rapidly increasing interest in the benzo[*e*][1,2,4]triazin-4-yl skeleton resulting in a continuously expanding and improving set of synthetic tools for construction of the heterocycle and for functional group transformations in the presence of the unpaired electron.[12,43-44] Thus, Koutentis has developed two synthetic approaches to benzo[*e*][1,2,4]triazin-4-yls.[16,45] The first approach is the optimization of the original method and involves oxidation of amidrazones followed by a 6-π electrocyclization process (Method A, Figure 4.1.3.1.).[16,45-48] He has also developed an alternative process, in which reductive cyclocondensation of nitro hydrazides leads to benzo[*e*][1,2,4]triazin-4-yls (Method B, Figure 4.1.3.1.).[16,43,49] Both of these approaches have a number of limitations including the stability of starting materials, low yields and poor availability of arylhydrazines, which are key substrates in these methods. Another synthetic method employs the aza-Wittig reaction of *N*-aryliminophosphoranes with 1-(*het*)aroyl-2-aryldiazenes at high temperatures (Method C, Figure 4.1.3.1.).[50] The formation of 3-amino-1,4-dihydrobenzo[*e*][1,2,4]triazin-4-yl was also observed in spontaneous hydrolysis of a stable triazolin carbene in wet acetonitrile solutions (Method D, Figure 4.1.3.1.).[51] Efficient methods have also been developed for postcyclization ring substitutions,[43,46-47,49,52] functional group transformations,[43] and ring annulation,[29,32-33] which significantly expanded the structural variety of the parent 1,4-dihydrobenzo[*e*][1,2,4]triazin-4-yl.

In 2016 Kaszyński presented a simple method for preparation of 1,4-dihydrobenzo[*e*][1,2,4]triazin-4-yl radicals by azaphilic addition of an organometallic reagent to easily available benzo[*e*][1,2,4]triazines followed by oxidation of the resulting anions to the desired radicals (Method E, Figure 4.1.3.1.).[44] This method is potentially general, permits introduction of a substituent at the N(1) position in the post-cyclization step, and avoids the use of arylhydrazines. It is often used tool in our laboratory and has provided access to a number of derivatives of the Blatter radical, including its planar analogues. To expand functionality of the Blatter radicals we have developed an alternative access to benzo[*e*][1,2,4]triazines as the key precursors in Method E, which involves cyclization of *N*-arylguanidines and *N*-arylamidines (Method F). Subsequent reduction of benzo[*e*][1,2,4]triazine *N*-oxides to benzo[*e*][1,2,4]triazines followed by ArLi addition lead to C(3)-functionalized benzo[*e*][1,2,4]triazin-4-yls (Method E, Figure 4.1.3.1.).[40] C(3)-functionalization of the Blatter radical is one of the most explored topics in my doctoral work and is described in a separate chapter of this Dissertation (Chapter 6).
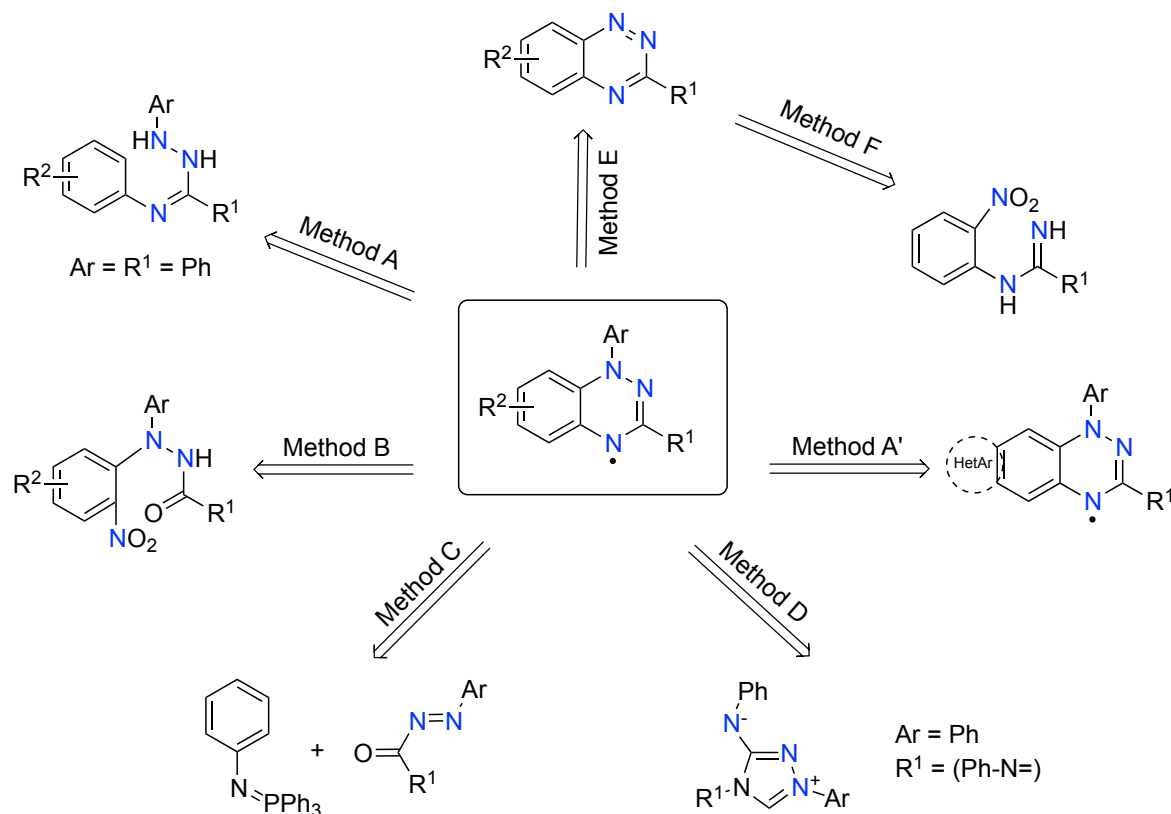
Figure 4.1.3.1. Synthetic methodologies for Blatter radical derivatives (Methods A-F).

Recent advances in the chemistry of the benzo[*e*][1,2,4]triazinyl led to the discovery of planar Blatter radicals.[12] The two parent planar radicals, containing phenoxazine and phenothiazine rings, were obtained *via* the intramolecular azaphilic addition of ArLi, which was generated *in situ* from the appropriate C(8)-substituted benzo[*e*][1,2,4]triazine (Method G, Figure 4.1.3.2.).[12] A much improved access to functional derivatives of plannar Blatter radicals **PB** was demonstrated with the aza-Pschorr cyclization reaction (Method H, Figure 4.1.3.2.).[53-56] Futher progress in the synthesis of ring-fused derivatives containing the phenoxazine ring involved photocyclization of appropriate C(8)-substituted benzo[*e*][1,2,4]triazines (Method I, Figure 4.1.3.2.).[57] Unfortunately, neither of the latter two methods was suitable for the preparation of sulfur containing radicals.[58] Recently, Kaszyński presented an efficient Bu$_3$SnH– and TMS$_3$SiH– assisted radical chain intramolecular cyclization of aryl iodides on the [1,2,4]triazine N(1)-atom and the formation of planar Blatter radicals (Method J, Figure 4.1.3.2.). The latter method was applied to the synthesis of four previously reported radicals and to the preparation of the first functionalized sulfur-containing planar Blatter radical.[58]

Figure 4.1.3.2. Synthetic methodologies for planar Blatter radical derivatives **PB** (Methods G-J).

The exceptional stability of 1,4-dihydrobenzo[*e*][1,2,4]triazin-4-yl radicals enabled a series of classical functional group transformations to be carried out in the presence of the unpaired spin.[43] Particularly important transformations include palladium catalyzed carbon-carbon coupling reactions, such as Suzuki-Miyaura,[59] Negishi[60] and Sonogashira[61] reactions. These transformations usually lead to complex mixtures and decomposition products in the case of other stable radicals, such as verdazyls.[62]

A series of other transformations, such as reduction of the nitro group to aniline derivatives, hydrolysis of esters and Heck coupling, can be performed without loss of the radical (Figure 4.1.3.3.).[43] Moreover, debenzylation of the –OCH$_2$Ph group in the presence of a palladium catalyst, and subsequent acylation or alkylation of the resulting phenols was performed successfully (Figure 4.1.3.3.).[43] Azaphilic addition of arylllithium to properly functionalized benzo[*e*][1,2,4]triazines (Method F, Figure 4.1.3.1.) constitutes the most convenient method of synthesis of benzo[*e*][1,2,4]triazin-4-yl radicals and diradicals and allows the access to all such derivatives invesitigated during my research.

X, Y = OBn, OBz, NO₂, I, CO₂Me
Z = H, 7-CF₃, 6-CF₃, 7-I,

X, Y = OH, OR, OCOR, NH₂, NHR,
NHCOR, Ar, C≡CAr, CH=CHR, CO₂H
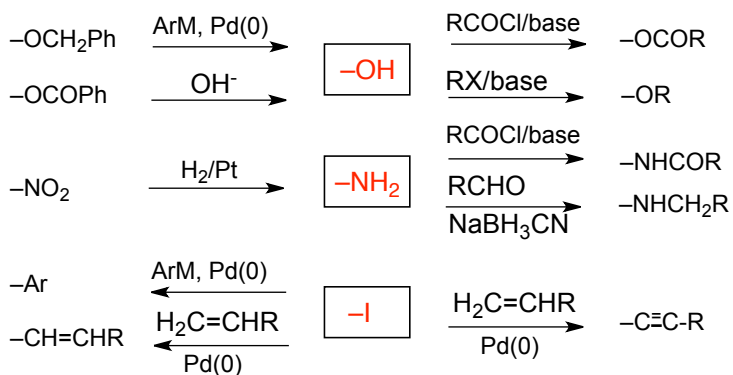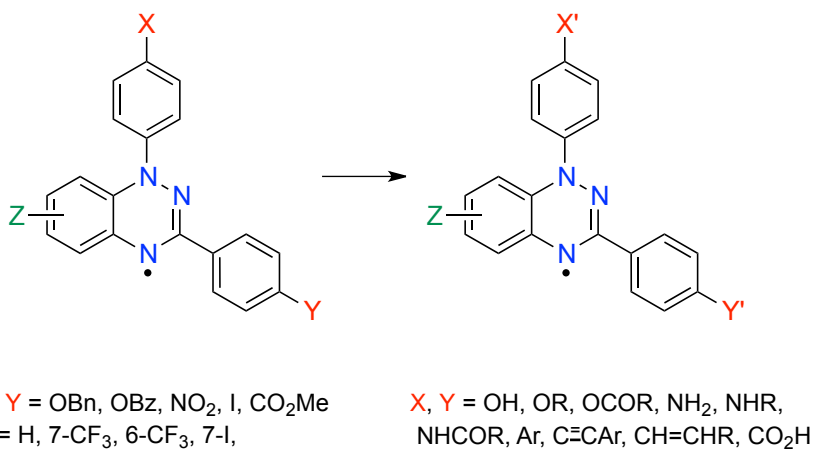
Figure 4.1.3.3. Transformations of functional groups (X→X' and Y→Y') in 1,4-dihydrobenzo[*e*][1,2,4]triazin-4-yl radicals.[43]

4.2. Stable heterocyclic diradicals

4.2.1. Basic concepts of stable diradicals

Diradicals and biradicals are the molecules possessing two unpaired electrons in two energetically degenerate or nearly-degenerate orbitals. The term biradical refers to molecules in which two electrons act independently or nearly independently and the electron exchange interaction (J) is negligible because of the large separation (r) between these two electrons.[63] Furthermore, when two molecular orbitals occupied by two electrons are nearly degenerate in energy and the molecule still possess the diradical character, these open-shell molecules are called diradicaloids. When the magnitude of the spin-spin interaction is large enough two produce two spin states, the molecular species with the two unpaired electrons is referred to as a diradical. If two unpaired electrons (spins) are antiparallel to each other, the spin quantum number $S = 0$ (antiferromagnetic coupling) and spin multiplicity $2S+1 = 1$. In case of parallel orientation of two unpaired electrons, the spin quantum number $S = 1$ (ferromagnetic coupling) and spin multiplicity $2S+1 = 3$. Thus, diradicals have two states: a singlet state ($S = 0$) and a triplet state ($S = 1$). The strength of the exchange coupling is proportional to the energy difference between the singlet and triplet states ($\Delta E_{ST} = E_S - E_T$). In the case of ferromagnetic coupling (spins parallel, triplet ground state) a positive value of the singlet-triplet energy gap ΔE_{ST} is obtained (triplet state is lower in energy than the singlet state) as shown in Figure 4.2.1.1. Negative J value indicates antiferromagnetic interaction and a singlet ground state is preferred.

E $S = 0$, singlet

$\Delta E_{ST} = 2J$
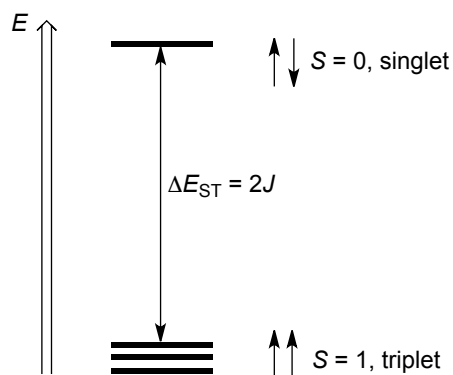
$S = 1$, triplet

Figure 4.2.1.1. Energy diagram for high-spin diradicals

The exchange interaction between energy levels of singlet and triplet state, is typically represented by the Heisenberg Hamiltonian for two electron spins:

$$\hat{H} = -2J\hat{S}_1 \cdot \hat{S}_2$$

where *J* is the exchange interaction constant and indicates the coupling type/strength (ferromagnetic or antiferromagnetic), and S_1 and S_2 are spin quantum operators.

A prototypical diradicaloid system, which is the highly reactive *p*-quinodimethane (**II**, Figure 4.2.1.2.),[64] can be described by the principal open-shell (OS) *p*-xylylenediyl and closed-shell (CS) quinoidal resonance forms.[65] The dominant contribution of the latter form to the actual electronic structure[66] of **II** in large part results from a competition between the stability of the aromatic Clar's sextet,[67] experimentally estimated at 35 ± 1 kcal mol^{-1},[68] and stability of the π bond (58 ± 3 kcal mol^{-1} in ethylene).[69] Extension of **II** by one benzene ring leads to a favorable balance of two Clar's sextets *vs* one C–C π bond in biphenoquinodimethane (**III**, Figure 4.2.1.2.) and, consequently, recovery of aromaticity and stabilization of the diradical form with a significant open-shell singlet (OSS) character (diradical index[70-71] $y = 0.32$; where $y = 0$ for pure CS and $y = 1$ for pure OSS)[72] and a much smaller separation between the S and T states (DFT energy gap, $\Delta E_{\text{S-T}} = -5.1$ kcal mol^{-1}).[73] For this reason **III** constitutes an attractive fundamental structural element for open-shell systems, such as type **IV** (Figure 4.2.1.2.), in which the diradicaloid character and the S–T gap can be tuned by judicious choice of substituents at the terminal positions and the degree of spin delocalization.
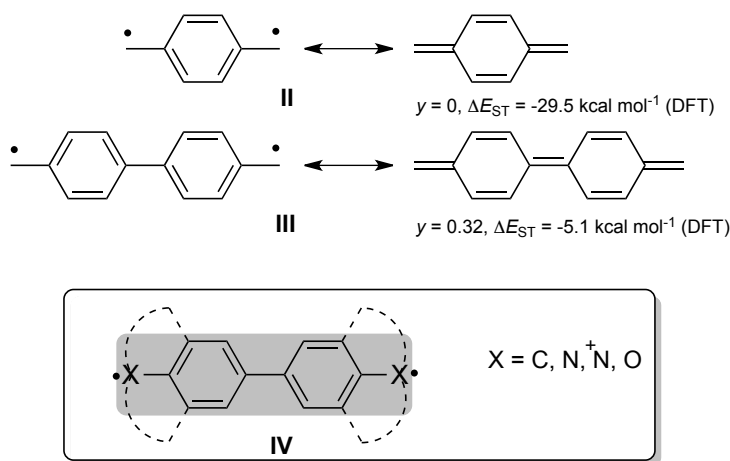
Figure 4.2.1.2. The structure of the prototypical one- and two-benzene ring diradicals: *p*-quinodimethane (**II**) and 4,4'-biphenoquinodimethane (**III**) and diradicals of the general structure **IV** based on the biphenoquinodimethane fragment (**III**). Data from ref.[73]

4.2.2. The molecular design of high spin organic molecules

The molecular design of high-spin molecules is still challenging. The interactions between two unpaired electrons take place through bond and through space and may lead to the stabilization of either a singlet or triplet ground state. There are several ways to control the diradical ground state and the crucial aspect of this control is topology (connectivity) of the electronic system (manifold), which may lead to Kekulé or non-Kekulé structure. The preference for ferromagnetic or antiferromagnetic exchange interaction in these two types of structures will be discussed below.
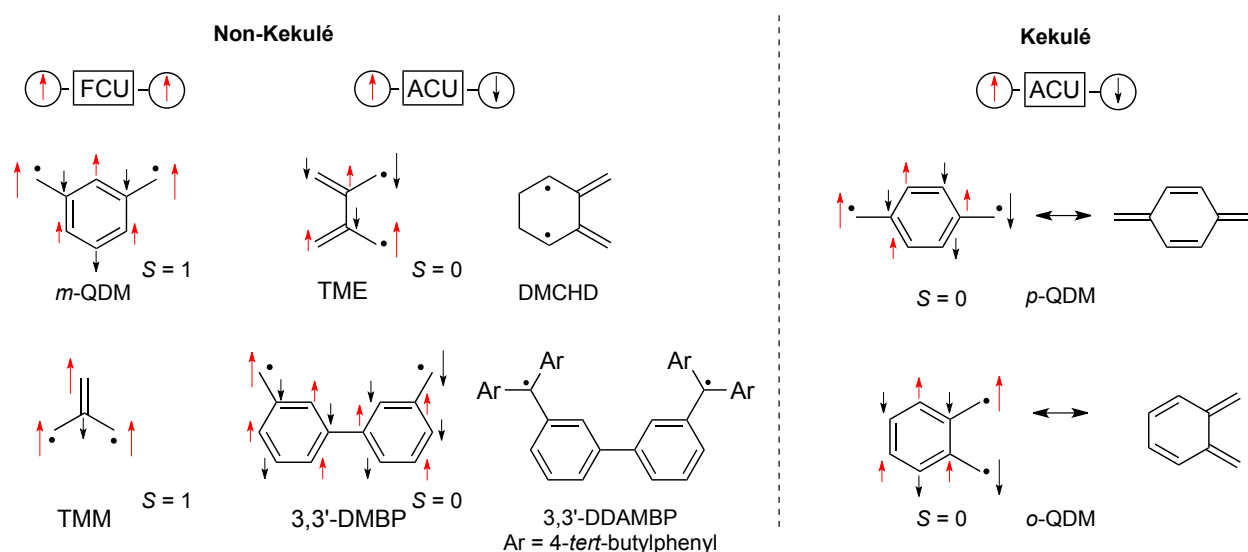
Figure 4.2.2.1. High ($S = 1$) or low ($S = 0$) spin ground states predicted using Ovchinnikov's parity model.

Non-Kekulé delocalized molecules are fully conjugated hydrocarbons containing at least two atoms that are not π-bonded. The classical examples of such systems are *meta*-quinodimethane (*m*-QDM), trimethylenemethane (TMM) and tetramethylenethane (TME) (Figure 4.2.2.1.). In diradicals, fragments formally possessing one unpaired electron can be defined as spin centers (SCs). The through-bond exchange interactions between the spin centers are prevailing in π-conjugated planar diradicals. In such systems ferromagnetic or antiferromagnetic exchange coupling between SCs can be qualitatively predicted using simple Ovchinnikov's parity model.[74] This concept assumes that each adjacent spin in the π-system is assigned to possess the opposite sign of its neighbor (the first spin is assigned as up (or down) label, and the neighbors in the system are assigned with opposite label). The preference of the

spin at the ground state is obtained by $S = (n_\uparrow - n_\downarrow)/2$, where $n_\uparrow$ is a number of spin up ($\uparrow$) centers and $n_\downarrow$ is a number of spin down ($\downarrow$) centers. Coupling units (*m*-QDM and TMM) that lead to ferromagnetic interactions between SCs (spins parallel) are termed ferromagnetic coupling units (FCU's, Figure 4.2.2.1.) and those that lead to antiferromagnetic coupling (*p*-QDM and *o*-QDM) are termed antiferromagnetic coupling units (ACU's, Figure 4.2.2.1.).[75] As illustrated in Figure 4.2.2.1., application of the above described method indicates triplet $S = 1$ ground state for *meta*-quinodimethane (*m*-QDM, $S = (5-3)/2 = 1$), for which the experimental singlet-triplet energy gap is determined $\Delta E_{ST} = 9.6 \pm 0.2$ kcal mol^{-1}.[76] The simplest among non-Kekulé molecules trimethylenemethane, possess a triplet ground state ($S = (3-1)/2 = 1$) with the experimentally determined singlet-triplet energy gap ΔE_{ST} of 16.1 6 $\pm$ 0.1 kcal mol^{-1}.[77] This structural element constitutes an important and robust ferromagnetic spin coupler (FCU) utilized in the design of stable high-spin diradicals.[63, 78] As predicted by the parity model, tetramethylenethane (TME) should possesses a singlet ground state. This prediction was supported by the experimental results for its analogue, 2,3-dimethylenecyclohexane-1,4-diyl (DMCHD), which demonstrated a small ΔE_{ST} of -0.002 kcal mol^{-1}.[79] Similarly, 3,3'-dimethylenebiphenylene diradical (3,3'-DMBP) containing two methyl radicals connected *via* biphenyl-3,3'-diyl unit, shows singlet ground state with a small ΔE_{ST} = -0.1 kcal mol^{-1} determined experimentally for its analogue 3,3'di[(diaryl)methylene]-biphenylene (Figure 4.2.2.1.).[75, 80]

In contrast to non-Kekulé *meta*-quinodimethane, which exhibit a robust triplet ground state, Kekulé molecules, such as *para*-quinodimethane (*p*-QDM) and *ortho*-quinodimethane (*o*-QDM) (Figure 4.2.2.1.), exhibit a singlet ground state in accordance to $S = (4-4)/2 = 0$ and can serve as antiferromagnetic coupling units (ACU's). Although this simple parity model is useful for a qualitative assessment of the ground state multiplicity, they do not address the strength of exchange interactions (ΔE_{ST}), especially in non-Kekulé molecules. For a better understanding, the energetics of the singly occupied orbitals (SOMO) in the diradicals need to be considered. According to Borden and Davidson, SOMOs can be classified as either non-disjoint (spatially coinciding at some atoms) or disjoint (not spatially coinciding at any atoms) as illustrated for *m*-QDM, TMM and TME in Figure 4.2.2.2.[81] The exchange interaction is weak for disjoint SOMOs, while it is strong for non-disjoint SOMOs. This is caused by the fact that when two unpaired electrons align parallel, a node is introduced in the spatial part of the wave function, and as a result the Coulombic repulsion is reduced effectively in the spatially coinciding area.[82]

The non-Kekulé molecules listed above possess two unpaired electrons, which are located in energetically degenerate singly occupied non-bonding molecular orbitals (NBMOs). When these NBMOs are non-disjoint (their atomic spin densities have at least an atom in common), the triplet state experiences less electron repulsion than the singlet state, leading to a triplet ground state. Thus, the first two diradicals (*m*-QDM and TMM) are categorized as non-disjoint-type diradicals, which have a triplet ground state.[63] The design of novel triplet ground state diradicals relies on connection of two paramagnetic centers *via* robust ferromagnetic spin couplering units (*e.g. m*-QDM or TMM). In contrast to *m*-QDM and TMM diradicals, tetramethylenethane (TME), which is also a non-Kekulé system, possess a singlet triplet degenerate ground state. In TME, the NBMOs are disjoint (their atomic spin densities have no atoms in common). Therefore the exchange interaction is negligible and there is no preference for either triplet or singlet ground state.[83]
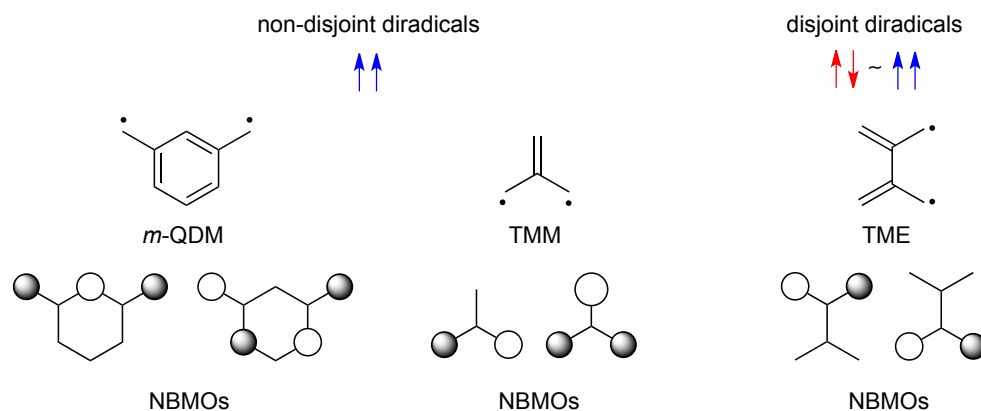
Figure 4.2.2.2. Non-Kekulé diradicals with non-disjoint (*m*-QDM and TMM) and disjoint (TME) non-bonding MOs.

In conclusion, there are two general strategies for the design of diradicals possessing a triplet ground state. The first method involves joining two radical fragments directly with sites of the opposite sign spin densities. In the second strategy two radicals need to be connected with sites of the same spin density through a robust ferromagnetic coupling unit (FCU), such as *meta*-quinodimethane (*m*-QDM) or trimethylenemethane (TMM). In addition, the greater the spin density at the connecting points, the stronger triplet state stabilization. Connection of sites with the same sign of spin densities in the first method, opposite in the second method or incorporation of antiferromagnetic coupling unit (ACU), for connection of two radicals, lead to a singlet ground state of the diradical.

4.2.3. Organic radicals as magnetic materials

In recent years, paramagnetic compounds, including stable radicals and diradicals, have attracted much attention as organic magnetic materials.[84-85] Characterization methods of such compounds enable the understanding of molecular structure–property relationships and rational design of diradicals with desired magnetic properties for the needs of modern advanced materials in areas such as molecular electronics and spintronics (charge and spin transport).[23] Among the techniques employed for magnetic studies two main methods can be distinguished: Electron Paramagnetic Resonance (EPR) spectroscopy and Superconductive Quantum Interference Device (SQUID) magnetometery. With the former, paramagnetic susceptibility can be precisely analyzed, while SQUID magnetometry is used to measure the total magnetic susceptibility. In my research, Electron Paramagnetic Resonance spectroscopy was used primarily for magnetic characterization. For this reason, the main assumptions and principles of measurements utilizing this technique are discussed below.

A fundamental quantum mechanical property of the unpaired electron is known as spin. The intrinsic magnetic moment of a particle is directly related to the property of spin and is defined in equation 4.2.3.1. In quantum mechanics, each electron has an intrinsic angular momentum (spin), which is expressed as a spin quantum number $S = ½$. Since an electron is a spinning charge, it creates a small magnetic field at which the magnetic moment $\boldsymbol{\mu}$ is proportional to the spin angular momentum $\mathbf{S}$:

$$\boldsymbol{\mu} = g\mu_B \, \mathbf{S} \qquad\qquad \text{(eq. 4.2.3.1.)}$$

where, electron g-factor (2.00232), μ_B (-9.274×10^{-24} J T^{-1}) is the Bohr magneton. A single electron has two magnetic components, $m_S = 1/2$ and $-1/2$. Thus, the spin multiplicity is determined as 2 by the $2S + 1$ relationship; therefore monoradicals possess a doublet state. When an external magnetic field is applied to a single electron in one direction, its spin aligns either parallel (α, $m_S = 1/2$) or antiparallel (β, $m_S = -1/2$) to the field. The resulting two magnetic states ($m_S = 1/2$ and $-1/2$) undergo splitting and have different energy levels given by $E = m_S g e \mu_B B$. This interaction between a single electron and external magnetic flied is called Zeeman effect (Figure 4.2.3.1.). The difference in energy between the two states is dependent on the strength of the applied magnetic field: $\Delta E = E_\alpha - E_\beta = \Delta m_S g \mu_B B = g\mu_B B$.

The transition between the states can be induced, when the energy of the photon $h\nu$ (ν is the frequency) matches that of the ΔE, $h\nu = \Delta E$. Such transitions can be observed in EPR spectroscopy.
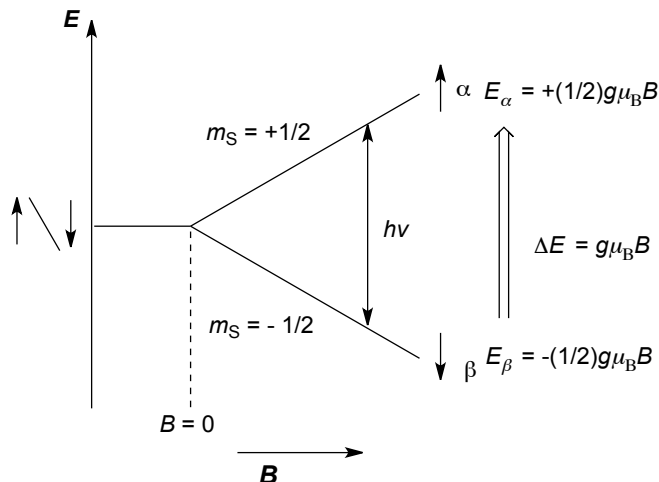
Figure 4.2.3.1. Zeeman effect of an unpaired electron.

4.2.4. Magnetic properties of diradicals – characterization methods

Magnetic susceptibility (χ) is the basic constant, which indicates the degree of magnetization (M) of a materials in response to an external magnetic field (H) determined by the formula:

$$\chi = \frac{M}{H}$$ (eq. 4.2.4.1.)

where M – magnetization of the material; magnetic dipole moment per unit volume (A m^{-1}), H is the magnetic field strength (A m^{-1}) .

Depending on the type of interactions between spins we can distinguish systems with non-interacting (isolated) magnetic moments (typical for paramagnetism) and magnetically ordered systems, such as ferromagnetic and antiferromagnetic presented in Figure 4.2.4.1.
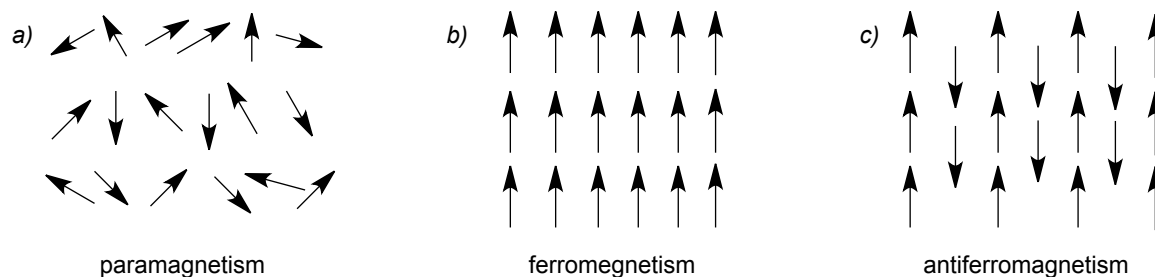
Figure 4.2.4.1. Three fundamental arrangements of spins in: a) paramegnetic, b) ferromagnetic, c) antiferromagnetic materials.

Since each substance possesses diamagnetic properties, the total magnetic susceptibility, χ_{Tot}, is the sum of the temperature-dependent paramagnetic susceptibility, χ_p, and the temperature-independent diamagnetic susceptibility, χ_{dia} (equation 4.2.4.2.).

$$\chi_{Tot} = \chi_p + \chi_{dia} \qquad \text{(eq. 4.2.4.2.)}$$

Electron Paramagnetic Resonance (EPR) spectroscopy is a particularly convenient technique for studying magnetic properties of radicals and to determine the extent of spin delocalization, ground state of diradicals, and to measure the singlet-triplet energy gaps. As mentioned above, this technique does not take the diamagnetic component into account and responses to the paramagnetic component only. Therefore, the dependence of the paramagnetic susceptibility on temperature is reproduced more accurately with EPR than using SQUID measurements of total magnetization. The second advantage of the EPR technique is a small experimental error, even at high temperatures (up to 440 K), and high sensitivity of the measurement. A typical experiment involves recording spectra either in a frozen glass / fluid solution or solid solutions in a polymer (*e.g.* polystyrene) at concentrations $\sim 10^{-4}$–10^{-3} M at a broad temperature range (typically between 100 K and 350 K). Another significant benefit of this technique is the possibility to investigate exchange and spin-spin dipolar interactions, which are not as thoroughly investigated with SQUID. The Variable-Temperature Electron Paramagnetic Resonance (VT–EPR) measurements in solid solutions of diradicals is dictated by minimization of intermolecular spin-spin exchange interactions. Most commonly used matrixes for VT-EPR, such as glasses [PhMe:CHCl$_3$), polystyrene, benzophenone, benzothiophene or polyvinyl chloride.

4.2.4.1. Background for experimental determination of singlet-triplet gap ΔE_{ST}

The magnitude of the singlet−triplet energy gap ($\Delta E_{ST} = E_S - E_T$) in diradicals provides direct information on the extent of the interaction between the two unpaired electron states. Accurate determination of ΔE_{ST} is essential for understanding the diradical character and its magnetic properties. The most important assumptions of the EPR theory and a discussion of practical aspects and analysis of the variable-temperature measurements are presented below.[63, 86]

As spin quantum number of a singlet states equals to zero and the Zeeman effect (Figure 4.2.3.1.) does not apply to such species, the triplet states are the only EPR-active species in diradicals. Thus, EPR spectroscopy is an effective method for distinguishing between these two spin states, the singlet and the triplet. Since the doublet species are also EPR–active, the issue of distinction between the doublet and triplet species need to be addressed. For doublet species randomly oriented in a rigid matrix, only one resonance absorption can be observed, because of a single transition between two states, $m_S = \frac{1}{2}$ and $m_S = -\frac{1}{2}$ in the presence of the external magnetic field, as shown in Figure 4.2.3.1. (Section 4.2.3.). In contrast, three resonanance absorptions are typically observed for triplet spiecies in a rigid solid state (Figure 4.2.4.1.1.). Two of the resonance signals correspond to the allowed $\Delta m_S \pm 1$ transitions, whereas the third resonance signal corresponds to the formally forbidden transition of $\Delta m_S = 2$, that is from $m_S = -1$ to $m_S = +1$. The three magnetic axes of x, y and z, cause the appearance of two allowed transitions as six lines in the triplet EPR spectrum. The observation of the formally forbidden transition signal, which appears at about half–field with respect to the $\Delta m_S = 1$, is a strong evidence of the triplet diradicals, however, it can be quite difficult to detect it.

Figure 4.2.4.1.1. Energy splitting diagram for triplet diradicals in the solid state.

An internal magnetic field, produced by a dipolar coupling of the two spins in triplet diradicals, splits the energy level into three levels at zero magnetic field. This energy splitting is called zero–field splitting (zfs), as shown in Figure 4.2.4.1.1., and is derived from the dipol–dipol interaction. The relative energies of the three energy levels are described by two zero–field splitting paramaters D and E. In real triplet EPR spectra, the two allowed transitions are expected to appear as six lines because of three magnetic axes x, y and z. Parameter D is related to the average distance r between the two unpaired electrons, and thus the average distance r can be calculated by the point-dipole approximation:

$$D = 1.39 \times 10^4 \left(\frac{g}{r^3}\right) \qquad\qquad \text{(eq. 4.2.4.1.1.)}$$

where D – half–way between the maxiumum and minimum of peak height of EPR signal from $\Delta m_S = 1$ transition (G), g –the g-factor of the triplet diradical value, r – the average distance between two unpaired electrons (Å).

The zero-field splitting parameter E is related to the symmetry of the two electrons in triplet diradicals (it is a measure of the deviation of the electron distribution from the axial symmetry). In a structure with 3-fold or higher symmetry, the two triplet sublevels of E_x and E_y are degenerate. Therefore the EPR spectra of the allowed transitions appear as 4 lines. Typically, in the description of EPR simulation data, both of these parameters are given in the form of $|D/hc|$ and $|E/hc|$, where: D and E - energy values (J), h - Planck's constant ($h = 6.62 \times 10^{-34}$ J s) and c – speed of light ($\sim 3.0 \times 10^{10}$ cm s^{-1}).

The relative intensity between the signal of the allowed transition $|\Delta m_s = 1|$ and that of the forbidden transition $|\Delta m_s = 2|$ is related to the average spin−spin distance r according to the equation:

$$\frac{|\Delta m_S = 2|}{|\Delta m_S = 1|} = F/r^6 \left(\frac{9.1}{v}\right)^2 \qquad\qquad \text{(eq. 4.2.4.1.2.)}$$

where v – the resonance frequency (X-band ~9.5 GHz for EPR) and $F = 19.5$ for organic radicals.

The average distance between the two unpaired electrons can be calculated based on experimentally determined D values and intensity ratio. The distance r of less than ~ 10 Å can be determined by a combination of the two methods. Since the intensity of the half–field transition is

proportional to r^{-6} according equation 4.2.4.1.2., the intensity of $\Delta m_s = 2$ trasition becomes extremely weak or vanishes for spin-spin distances greater than ~ 10 Å. In other words, the forbidden half–field transition signal is absent in EPR spectra when D parameter has a small value ($D < 25$ G).

Thermal equilibrium of triplet and singlet states results in dependence of the intensity (I) of the triplet EPR signal on the temperature (T). Therefore a typical plot of χT *vs T* for a system with the triplet or singlet ground–state should be non-linear: the intensity of EPR signal should turn downward for triplet ground state diradicals as the temperature increases and an opposite temperature effect on the EPR signal intensity is observed for singlet ground state diradicals. The intensity of the allowed $|\Delta m_s = 1|$ transitions signals is sensitive to a saturation effect particularly at lower temperatures. Due to this fact, it is more proper to apply the intensity of the forbidden half-field transition signal for the $\chi T(T)$ plots, however not always possible, as discussed above.

Double integration of the intensity of the EPR signal allows to determine the number of spins in the tested sample and is proportional to the paramagnetic susceptibility (χ_p) of the material. The signal intensity is related to the paramagnetic susceptibility χ_p according to the Bloch equation: [87]

$$\chi_p = \frac{2\mu_B g I'_m \Delta H_{pp}^2}{\sqrt{3h\nu H_1}} \qquad\qquad \text{(eq. 4.2.4.1.3.)}$$

where μ_B – the Bohr magneton, g –is the g-factor value, I'_m – maxiumum peak height (I'_m and - I'_m), ΔH_{pp} – peak–to–peak line width, h – Planck's constant, ν – the frequency of the absorbed electromagnetic wave, H_1 – the amplitude of the oscillating magnetic field.

Analysis of Variable Temperature EPR (VT-EPR) results, involves double integration of the EPR signal (either at half-field or at full field) and normalization of spectra measured in a temperature range (e.g. 120–340 K) is used. The resulting double integration $DI_{(rel)}$ as a function of temperature, $DI_{rel}T(T)$ is analyzed, using a modified Bleaney-Bowers model for two interacting spins:[88]

$$\chi \bullet T = \frac{Ng^2\mu_B^2}{k}\left(\frac{2}{3+e^{-\frac{2J}{kT}}}\right)(1-\rho) + \frac{Ng^2\mu_B^2}{2k}\rho \qquad\qquad \text{(eq. 4.2.4.1.4.)}$$

where ρ – fraction of monoradical impurity, N – Avogadro constant (6.022×10^{23}), k – Boltzman contstant (1.38×10^{-23} m^2 kg s^{-2} K^{-1}), T –temperature (K), J – exchange integral.

For numerical fitting to Bleaney-Bowers equation, a three-parameter equation is used:

$$DI_{rel} \times T = m1 \left(\frac{2}{3 + e^{-\frac{m2}{m0}}} \right) (1 - m3) + 0.5 \times m1 \times m3 \qquad \text{(eq. 4.2.4.1.5.)}$$

where, $m0 = T$, $m1 = \frac{Ng^2\mu_B^2}{k}$, $m2 = -\frac{2J}{k}$, $m3 = \rho$.

When the ground state is singlet, the exchange interaction J will assume a negative value $(J < 0)$, while for the triplet state J is positive $(J > 0)$.

$$\Delta E_{ST} = E_S - E_T = 2J \qquad \text{(eq. 4.2.4.1.6.)}$$

4.2.5. Stable heterocyclic diradicals derived from benzo[*e*][1,2,4]triazin-4-yl

Among stable diradicals there are benzo[*e*][1,2,4]triazin-4-yl–based stable diradicals, which due to the general characteristic of the Blatter radical (discussed in Chapter 4.1.2.), constitute a class of particularly attractive magnetic systems.

A combination of the readily accessible high-spin states, electrochemical properties, low excitation energies and intermolecular spin-spin interactions of diradicals are attractive for a range of advanced applications, such as near-IR dyes,[89-90] non-linear optics,[91] sensors,[92] and singlet fission systems.[93-94] In addition, high-spin diradicals are of particular importance for organic spintronics[23] (*e.g.* aciting as spin filters)[95-97] and as building elements for molecular magnetic materials.[85, 98] For these reasons there is an increasing effort in developing of robust diradicals with controlled ground state multiplicity (singlet or triplet) and tunable singlet-triplet energy gap (ΔE_{ST}).

Molecules with Kekulé structures (diradicaloids), constitute a significant group among stable diradicals. Since the first report on Thiele's hydrocarbon[99] (Figure 4.2.5.10.), there have been significant efforts devoted to stabilize these open-shell species. In this context, several strategies, including delocalization, steric hindrance, and introduction of heteroatoms, have been developed.[63, 100] Moreover, several reports on their use in organic field-effect transistors (OFETs) and organic photodetectors (OPDs) have appeared.[101-103] Expansion of structural variety of stable diradicaloids will result in futher development of their applications in modern technologies. In this context, stable diradicaloids based on the benzo[*e*][1,2,4]triazin-4-yl are of particular interest and several have been reported.[92, 104-107] Therefore, development of methods for the formation of multispin systems incorporating two or more Blatter radicals is particularly important to take full advantage of the exceptional thermal and air stability of the benzo[*e*][1,2,4]triazin-4-yl spin source. In recent years, this area has been intensively explored, as the theory and design of such systems has matured. My contribution to this field is significant, and results of this work are discussed in Section 6.4.

Analysis of the prototypical Blatter radical (**4.1**, Fig. 4.2.5.1.) indicates that among positions capable of substitution only one position, C(3), has a negative spin density, and the highest spin density is located at the N(1) position, which is significantly greater than that on the carbon positions.[26] Another important aspect that needs to be considered in the designing of the diradicals is the amplitude of the SOMO at the connection site and coplanarity of the interacting

π systems. In general: the greater the overlap the stronger the interactions. This characteristic of Blatter radical determines the topology of diradicals derived from the benzo[*e*][1,2,4]triazin-4-yl with the desired ground state preference and the size of the singlet-triplet gap, ΔE_{ST}.
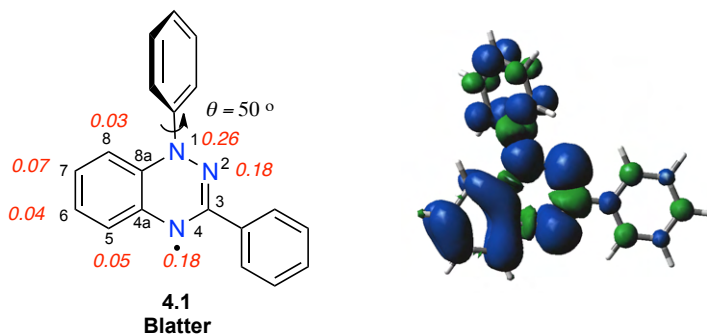

Figure 4.2.5.1. Structure of the Blatter radical with indicated numbering system and spin densities based on EPR spectroscopy,[26] and DFT-derived spin density map in the Blatter radical.

The following section of this Chapter includes a collection of designed diradicals based on two benzo[*e*][1,2,4]triazin-4-yl moieties connected either directly or through a π-spacer. This part demonstrates possible directions and rationalize formation of a high-spin diradicals incorporating this key structural element. The latter part of this Chapter includes the current state-of-the-art in the field of stable diradicals based on the benzo[*e*][1,2,4]triazin-4-yl.

Benzo[*e*][1,2,4]triazin–4–yls connected directly

When two benzo[*e*][1,2,4]triazin-4-yls are connected directly, a triplet ground state is obtained when sites with the opposite sign of spin densities are connected. Thus, it is necessary to involve the C(3) position of one benzo[*e*][1,2,4]triazin-4-yl to obtain high-spin ground state diradicals. Considering that the highest (0.07), among the carbon atoms, spin density is at the C(7) position, the strongest preference for the triplet ground state is expected for the C(3)–C(7) connected bi-Blatter diradical **4.2**. A lower spin density at the C(6) position should lead to a lower preference for a triplet ground state in the C(3)–C(6) connected diradical **4.3**. Another important aspect in the design of such molecules is the torsion angle between two benzo[*e*][1,2,4]triazin–4–yls, which can limit π overlap and exchange interactions between the spin centers.
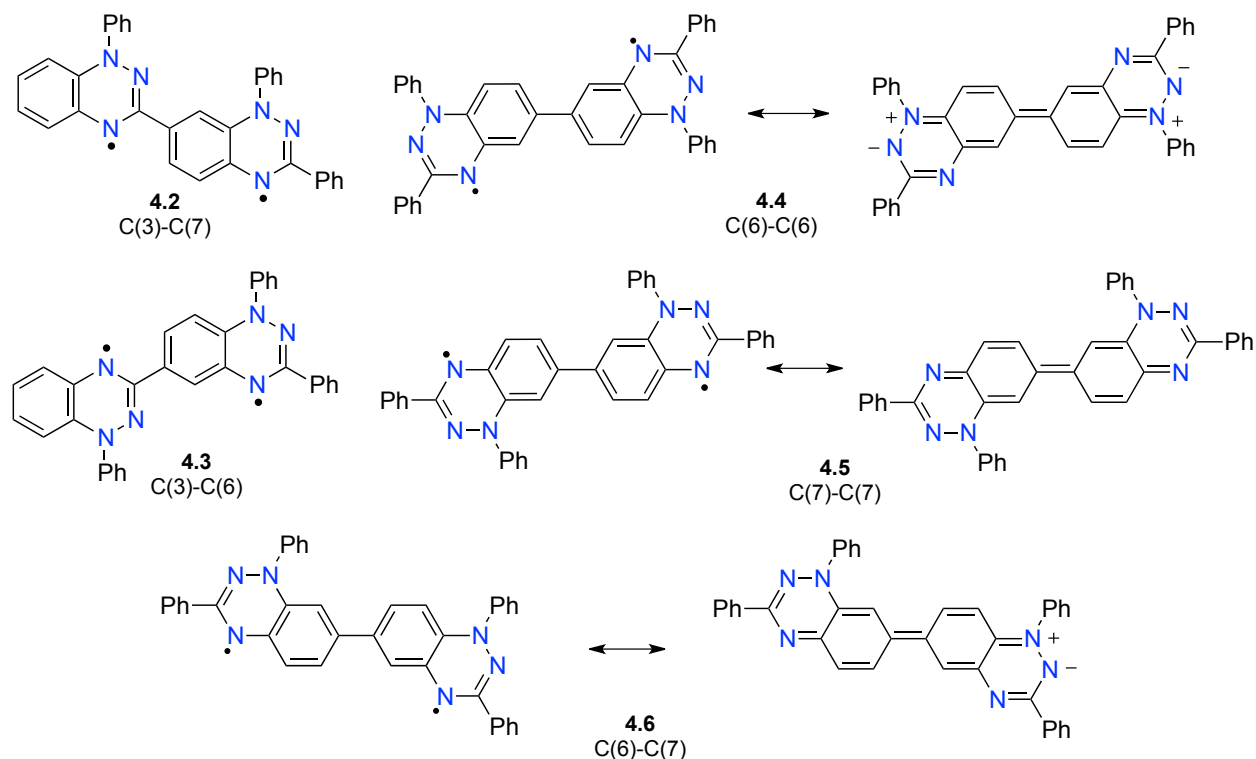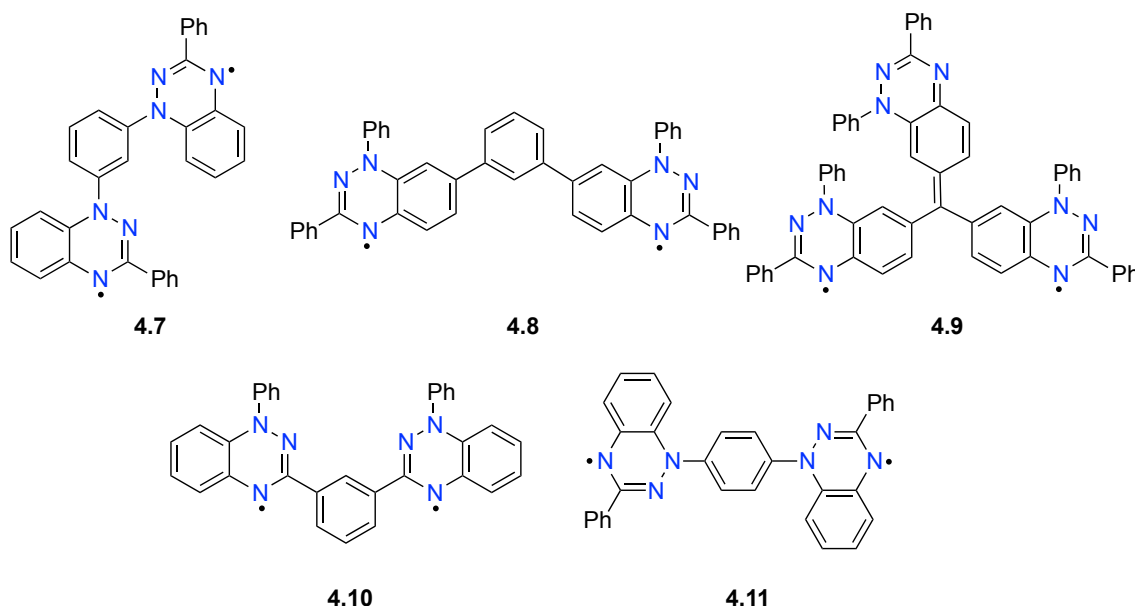
Figure 4.2.5.2. Structures of diradicals with directly connected benzo[*e*][1,2,4]triazin-4-yls units.

On the other hand, direct connection of two sites of the benzo[*e*][1,2,4]triazin-4-yls with the same sign of spin density will lead to a singlet ground state. Utilizing the most accessible positions C(6) and C(7) there are three possible regioisomers **4.4-4.6** presented in Figure 4.2.5.2. The C(7)-C(7) connected diradical **4.5** was already reported in the literature[106] and results of this work are described later in this Chapter. It possesses a Kekulè resonance form as shown below and exhibits a moderate preference for a singlet ground state (ΔE_{ST} = -1.27 kcal mol^{-1}). In this kind of molecules the singlet–triplet energy gap ΔE_{ST} is dictated by a balance between aromaticity of the 6–membered rings and a closed-shell structure (electrons paired). Synthesis and characterization of such three diradicals is part of my work and is described in Section 6.4.1.

Benzo[*e*][1,2,4]triazin–4–yls connected through a π spacer

Connecting two radicals through a ferromagnetic spin coupling unit (FC) at the sites with the same sign of spin density lead to high–spin ground state diradicals. Thus benzo[*e*][1,2,4]triazin–4–yl diradicals **4.7 – 4.11** presented in Figure 4.2.5.3. are expected to possess a triplet ground state. On the other hand, connection of the sites with the same sign of spin density *via* antiferromagnetic spin coupling unit (AFC) leads to a singlet ground state in the case of diradical **4.11**.

Figure 4.2.5.3. Structures of benzo[*e*][1,2,4]triazin-4-yls units connected through a spacer.

There are three general classes of diradicals based on the benzo[*e*][1,2,4]triazin-4-yl moiety (classes **A – C**) and most of them were reported during the last five years. In class **A** two [1,2,4]triazinyl rings are fused with a central ring system and all exhibit a singlet ground state (**4.12–4.14**), Figure 4.2.5.4.).[105, 108-109] In the second class of diradicals (class **B**) two benzo[*e*][1,2,4]triazin-4-yl units (**4.15–4.17** and **4.19**) or benzo[*e*][1,2,4]triazin-4-yl and another radical (**4.18a**, **4.18b**) are connected with a spin coupling unit (SC). Among five diradicals in this group only one, **4.16** contains a TMM-derived ferromagnetic unit.[106-107, 109-110] The third class of diradicals (class **C**) constitute those, in which two benzo[*e*][1,2,4]triazin-4-yl radicals (**4.5**, **4.20** and **4.21**)[92, 104, 106, 111] or benzo[*e*][1,2,4]triazinyl and another radical (**4.22-4.24**) are connected at a carbon atom and the resulting diradicals exhibit either a singlet or a triplet ground state depending on the connectivity.[112-113]

[1,2,4]Triazin-4-yl – based diradicals

4.12, A = benzene
4.13, A = naphthalene
4.14, A = carbazole

4.15, R = Blatter, Ar = Ph, SC = Alk–N⟨
4.16, R = Blatter, Ar = Ph, SC = Ph$_2$C=C⟨
4.17, R = Blatter, Ar = Ph, SC = −CPh=CPh
4.18a, B = 7-t-Bu, Ar = 1-(4-nitrononitroxylphenyl)
4.18b, B = 7-t-Bu, Ar = 1-(4-iminonitroxylphenyl)
4.19, R = Blatter, Ar = Ph, SC = 1,4-C$_6$H$_4$

4.5, R = 7,7-biBlatter
4.20, R = fluorenyl-fused biBlatter
4.21, R = 3,7-biBlatter
4.22, R = 7-(nitronylnitroxide)
4.23, R = 7-(phenoxyl)
4.24, R = 6-(phenoxyl)
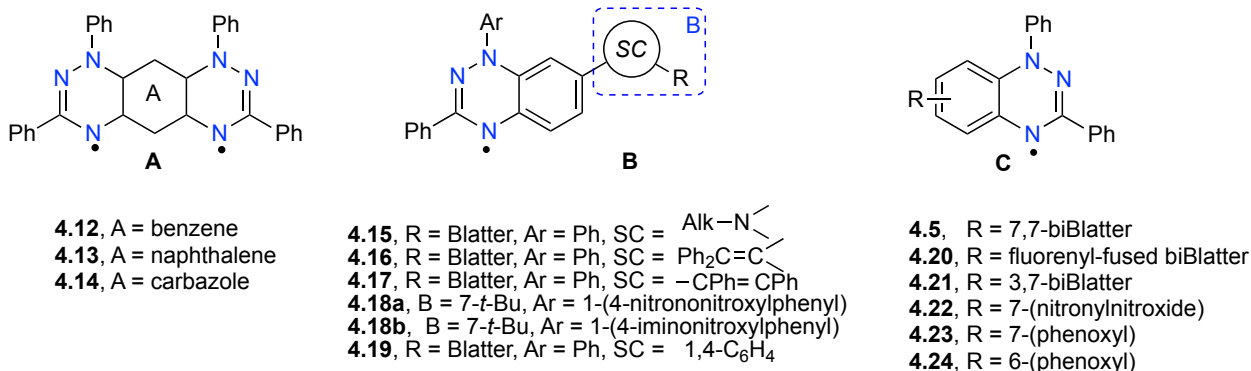
Figure 4.2.5.4. Three classes of diradicals derived from the [1,2,4]triazin-4-yl.

In 1998 Wudl *et al*. prepared the first compound involving two Blatter radical moieties, by linking two of benzo[*e*][1,2,4]triazinyl units in a single molecule resulting in the zwitterionic biscyanine of tetraphenylhexaazaanthracene **4.12**. 1,8-Diazabicyclo[5.4.0]undec-7-ene (DBU)-mediated air oxidative cyclization of the isolable, but reportedly unstable bisamidrazone **4.25** gave tetraphenylhexaazaanthracene **4.12** in a low yield of 17%.[108] Bisamidrazone **4.25** was derived from *N′,N″*-(*m*-phenylene)dibenzimidoyl dichloride **4.26** in reaction with phenylhydrazine following a general procedure described by Potts *et al.* for the preparation of mono amidrazones (Scheme 4.2.5.1).[114]
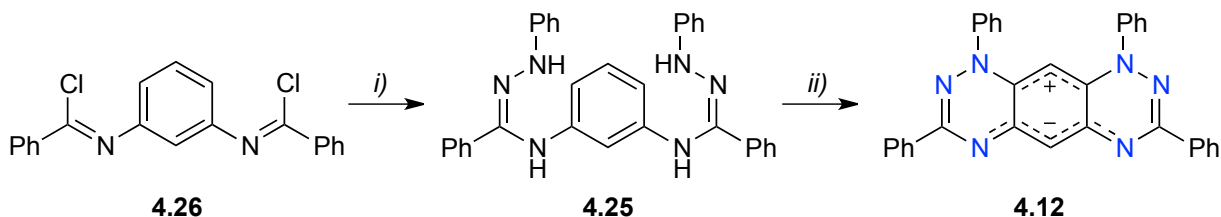
Scheme 4.2.5.1. Synthetic route to **4.12**. Reaction conditions: (*i*) phenylhydrazine, *n*-hexane, 0°C to rt, overnight, 63% yield. (*ii*) DBU, MeOH, air, rt, 14 days, 17% yield.

This molecule was designed with the goal of generating a stable triplet ground state molecule **4.12T**, however cyanine stabilization over the aromatic Clar's sextet was the driving force for parting their π electrons and loss of aromaticity.[92, 108, 115] The benzo-fused analogue of Blatter's radical was found to exists as an exceptionally stable zwitterion defined by its large singlet-triplet energy gap ΔE_{ST} of −20.1 kcal mol^{-1}.[116] It undergoes a photoexcitation to a triplet excited state in **4.12T** (Figure 4.2.5.5.).[117-118]
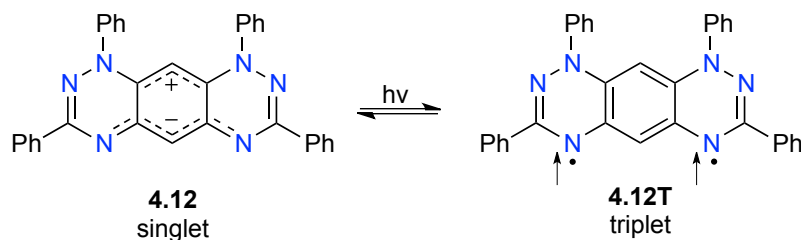
Figure 4.2.5.5. Structures of **4.12** and **4.12T**.

Toward the goal of preparing a stable, neutral open–shell system, a series of *p*-phenyl-substituted 3,5,7,9-hexaazaacridine **4.27** (X = N) and 3,5,7,9-hexaazaanthracene **4.12** (X = C) derivatives was synthesized and the effects of substitution on molecular electronic properties were probed both experimentally and computationally by Schreiner *et al.* in 2008.[118] Systematic computations of the substituent effect were used to help to explain the electronic properties of the prepared compounds and to predict ways to minimize the ΔE_{ST} value.

The synthesis of 3,5,7,9-hexaazaacridines **4.27a-i** (X = N) was conducted according to the classical protocol involving oxidation of amidrazones **4.29a-i** followed by a 6-π electrocyclization process (Method A, Figure 4.1.3.1). The latter were obtained *via* condensation of phenyl- and tolylhydrazine with **4.30a-f**. The reaction of 2,6-diaminopyridine with aromatic acid chlorides afforded the bis(amides) **4.31a-f** which were transformed into the bis(imidoyl) dichlorides **4.30a-f** (Scheme 4.2.5.2.). The desired products **4.27a-i** were obtained with overall yields ranging from 6 to 27 % (Table 4.2.5.1.).[118]
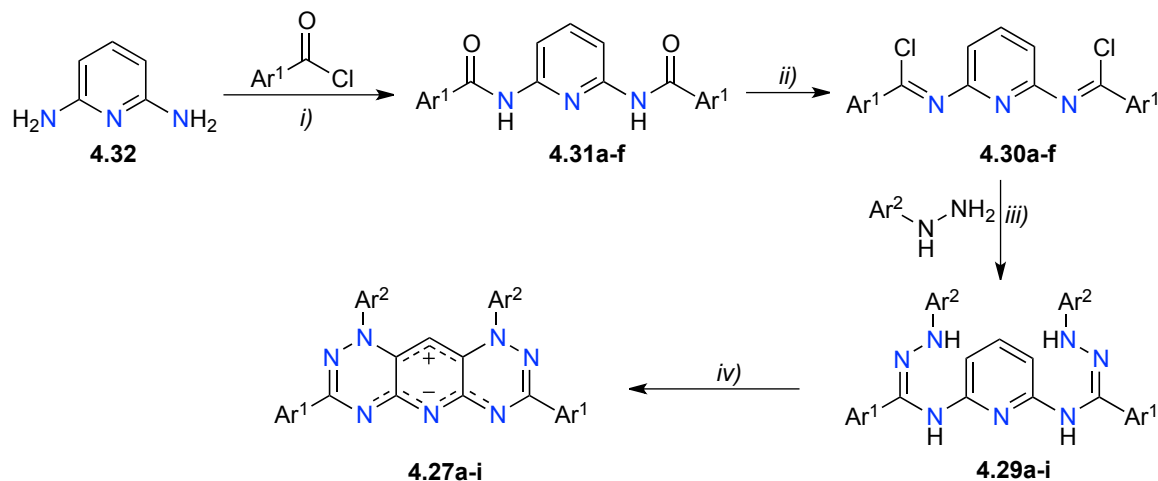
Scheme 4.2.5.2. Synthetic route to 3,5,7,9-hexaazaacridines **4.27a-4.27i**. Reaction conditions: (*i*) Et₃N, DCM, 0 °C to rt, 14 h. (*ii*) PCl₅, toluene, rt, 1.5 h, then 110 °C, 2 h. (*iii*) *n*-hexane, 0 °C to rt, 14 h. (*iv*) DBU, MeOH (EtOH for **4.27h** and **4.27i)**, air, rt, 4–14 days.

Table 4.2.5.1. Synthesis and characterization of aciridines **4.27a-4.27i** and anthracenes **4.12** and **4.12a**.
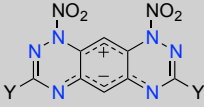
Acridine/ Anthracene	Ar^1	Ar^2	yield %	$\Delta E_{ST}{}^a$ kcal mol^{-1}
4.27a	Ph	Ph	23	−20.8
4.27b	Ph	p-MeC$_6$H$_4$	14	−21.0
4.27c	p-MeC$_6$H$_4$	Ph	6	−20.7
4.27d	p-ClC$_6$H$_4$	Ph	23	−21.0
4.27e	p-ClC$_6$H$_4$	p-MeC$_6$H$_4$	11	−21.1
4.27f	p-NO$_2$C$_6$H$_4$	Ph	14	−21.5
4.27g	p-NO$_2$C$_6$H$_4$	p-MeC$_6$H$_4$	11	−21.6
4.27h	naphth-2-yl	Ph	21	−21.2
4.27i	pyrid-4-yl	Ph	27	−21.0
4.12	Ph	Ph	7	−18.9
4.12a	p-MeC$_6$H$_4$	Ph	10	−16.2

^{a} Obtained at the B3LYP/6-31G(d,p)level of theory.

For the comparison purpose, the novel zwitterionic TPH-anthracene **4.12a** was prepared from 1,3-diaminobenzene in 10 % yield following the procedure previously used for the synthesis of acridines **4.27a-i**. Anthracene **4.12a** represents the carba-analogue of acridine derivative **4.27c**. Anthracene **4.12** (the analogue of **4.27a**) was prepared following the procedure reported by Wudl and coworkers.[108] In contrast to this report, despite much synthetic efforts, pure **4.12** was isolated, in only 7% yield.[118]

The ΔE_{ST} values for the studied hexaazaanthracenes **4.12** and **4.12a** are generally smaller than those of the related hexaazaacridines **4.27a-4.27i** (Table 4.2.5.1.). As the TPH-acridines generally display dipole moments larger than those of TPH-anthracenes, these results might imply that the greater charge separation or the higher polarity, the larger the singlet-triplet energy splitting.

Table 4.2.5.2. Structure of 3,5,7,9-hexaazaanthracene **4.33** and DFT derived[a] singlet–triplet gaps ΔE_{ST} of **4.33a–4.33i**.

Anthracene **4.33**	Y	ΔE_{ST}[a] kcal mol^{-1}
a	OMe	−10
b	NMe$_2$	−8.5
c	NH$_2$	−9
d	H	−9
e	CF$_3$	−10.5
f	C(O)Me	−10
g	CN	−10.4
h	NO$_2$	−10.5
i	BH$_2$	−8.4

[a] Obtained at the B3LYP/6-31G(d,p)level of theory.

A systematic computational analysis revealed that the electronic properties, the number, and the position of the substituents have a large effect on the ΔE_{ST} values (Table 4.2.5.2.). Nitrogen-bonded substituents show larger effects than those bonded to carbon, owing to the general molecular orbital structure of these systems that favors the involvement of π-delocalization via the nitrogen atoms. The ΔE_{ST} values in N-bonded pull-pull electronic systems are smaller than those in pull-push and push-push systems. While the experimentally prepared structures have large singlet-triplet energy gaps (from -21.6 to -16.2 kcal mol^{-1}), systems with smaller singlet-triplet energy separations (from -10.5 to -8.4 kcal mol^{-1}) can be realized through systematic variation of the substituent numbers, types, and patterns. As presented above, a whole set of analogues of **4.12** have been proposed, however no example of such derivative possessing a triplet ground state have been demonstrated experimentally thus far.

Potential for obtaining of an organic molecular magnet based on tetraphenylhexaazaanthracene **4.12** was explored by computational methods by Ali *et al.* in 2022, through adaptation of two different strategies (Figure 4.2.5.6.).[119] In the first strategy, as the length of the coupler between the two radical moieties was increased the zwitterionic ground state was destabilized in favor of a diradical state (Figure 4.2.5.6a.). For a large *n*, the compounds

exhibited a triplet ground state. For example, molecule **4.44** (n = 2) exhibits a closed shell ground-state similarly to **4.12** (open-shell singlet OSS state lying 0.27 kcal mol^{-1} above the closed-shell singlet CSS). However, for molecules **4.45** (n = 3) and **4.46** (n = 4), larger values of $\Delta E_{OSS\text{-}CSS}$ were observed, indicating instability of the CSS structure and preference for OSS as the ground state. Moreover, further expansion of the coupler resulted in a substantial increase of the $\Delta E_{T\text{–}CSS}$ for molecules **4.47** (n = 5) and **4.48** (n = 6) exhibiting the preference for the triplet ground state. In another approach, the *push-pull* effect of substituents in molecules with **4.12** skeleton was explored to obtain diradicaloids and, in some cases, even a triplet ground state. It is believed that the resonating structure of **4.49f** (Figure 4.2.5.6.c) suppress the partition of 16π electrons into 10π-negative and 6π-positive parts and, thus, displays a transition from zwitterionic **4.12** to a diradicaloid.[119]
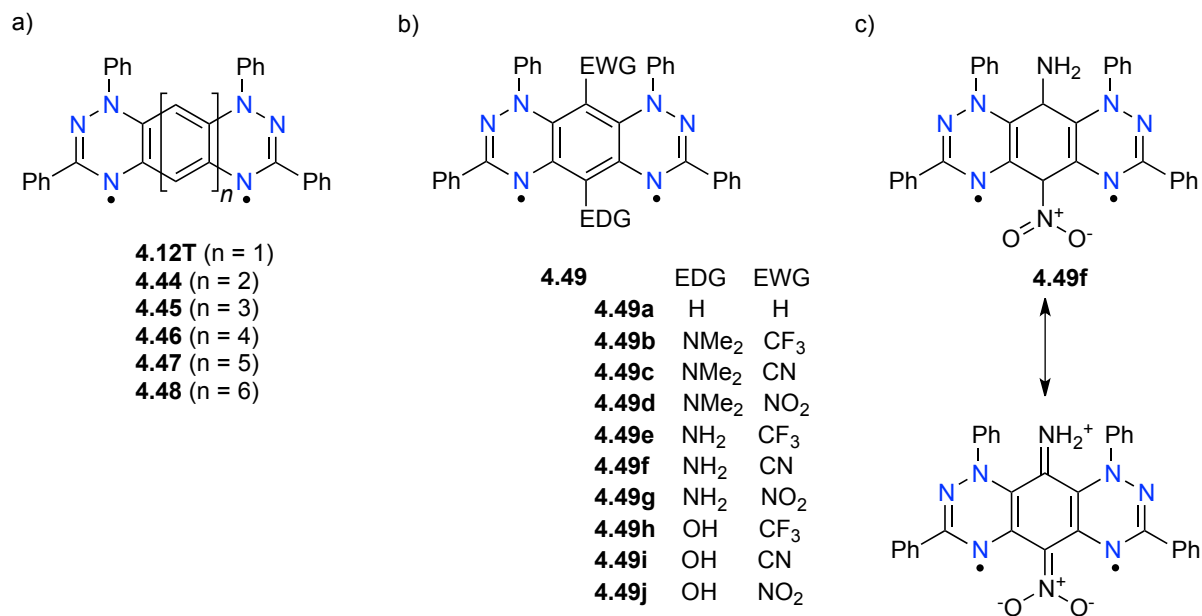
Figure 4.2.5.6. Modeled diradicals designed with: (a) extended coupler, (b) simultaneous substitution of electron donating groups (EDGs) and electron withdrawing groups (EWGs) on the parent **4.12T** and (c) the resonance structure **4.49f**.

The following years resulted in another fused benzo[*e*][1,2,4]triazin-4-yl based diradicals prepared and characterized by Zheng *et al.* in 2019. Taking into account good charge-transport properties, chemical stability and suitable bandgaps of carbazole based materials for organic light emitting diodes (OLEDs), diradical **4.14** was designed.[109] Another fused diradicaloid **4.13** was reported in 2020 by the same group (Figure 4.2.5.7.)[105]
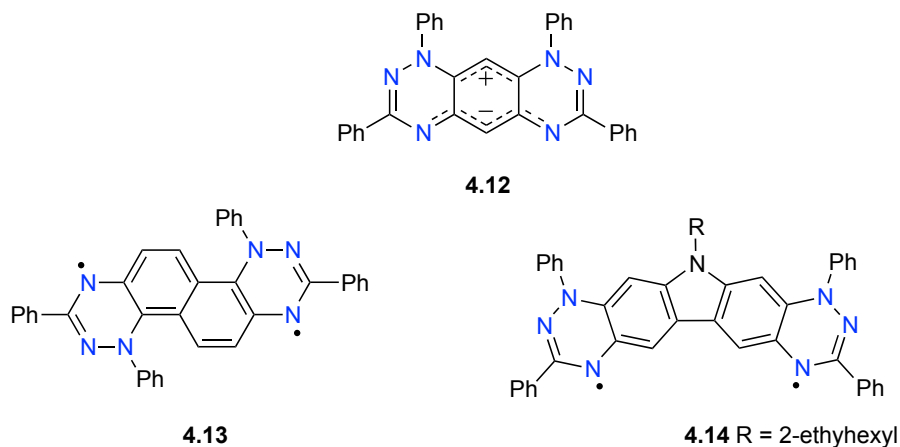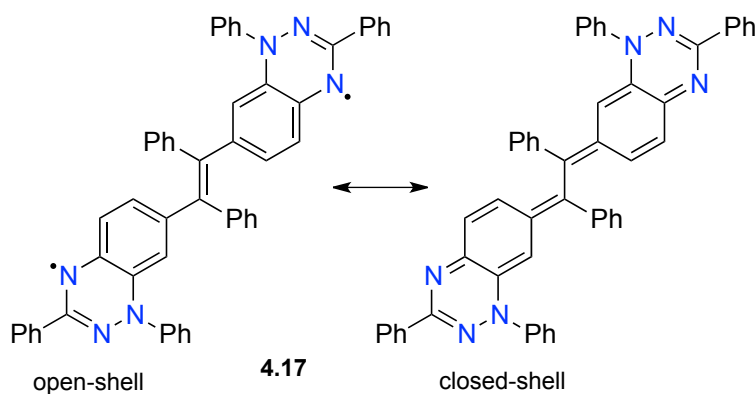
Figure 4.2.5.7. Diradicals incorporating the benzo[*e*][1,2,4]triazinyl constituting class **A**.

As mentioned before, the second class of diradicals (**B**) constitutes those of incorporating two benzo[*e*][1,2,4]triazinyl units (**4.15**–**4.17** and **4.19**) or benzo[*e*][1,2,4]triazin-4-yl and another radical (**4.18a**, **4.18b**) are connected with a spin coupling unit (SC). (Figure 4.2.5.8.). The unfused **4.15,** which is an analogue of **4.14**, is the earliest example of such a system. This work demonstrates the bridging effect on the diradical character, singlet-triplet gap and stability of the diradicals. According to expectations based on the topological rules, the unfused **4.15** turned out to be a singlet ground state diradical with a diradical character index y_0 = 0.89 and a moderate singlet-triplet gap of -1.16 kcal mol^{-1}.[109] In contrast, it was found that planarization of **4.15** decreased its chemical and photostability. Meanwhile, planar **4.14** possess a significantly lower diradical character (y_0 = 0.68) and an increased singlet-triplet gap (ΔE_{ST} = -2.38 kcal mol^{-1}).[109]
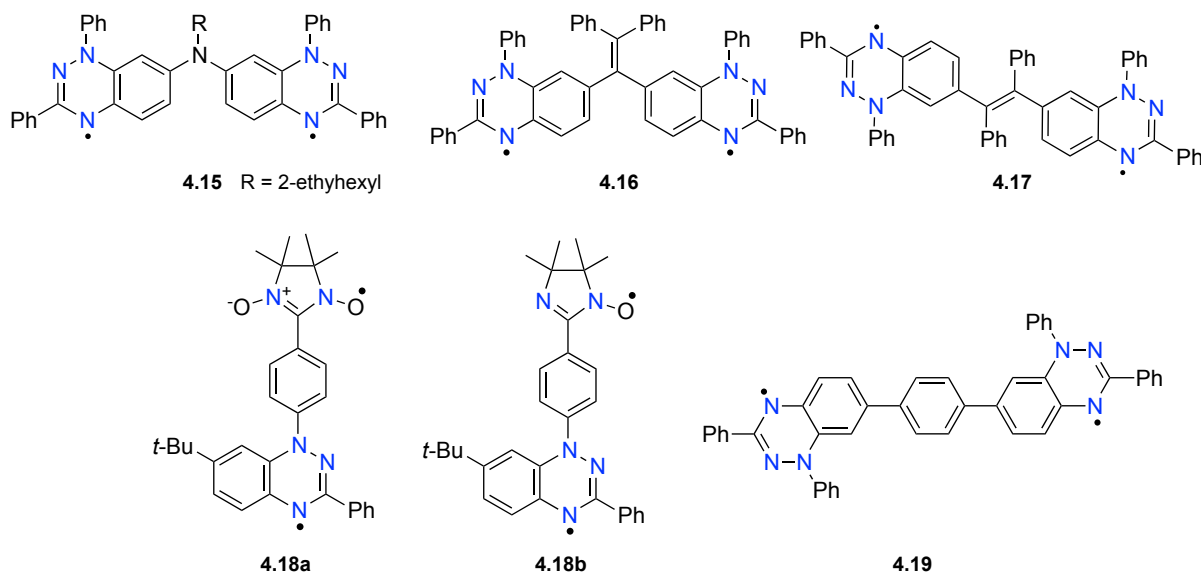
Figure 4.2.5.8. Diradicals incorporating the benzo[*e*][1,2,4]triazinyl constituting class **B**

In an attempt to access stable high-spin molecules, Zheng *et al.* reported non-Kekulé TMM type diradical **4.16** and Kekulé **4.17** by appending the spin centers of two Blatter radicals on the tetraphenylethylene framework (Figure 4.2.5.9.). These diradicals exhibit a remarkable stability under ambient conditions. As expected based on the topology rules, connection *via* the TMM-derived ferromagnetic coupling unit, should result in a triplet ground state of **4.16**. Contrary to expectations, a weak preference for the singlet ground state was found, apparently due to conformational reasons.[107] Both diradicals possess small singlet–triplet energy gaps with -0.21 kcal mol^{-1} for **4.16** and -0.18 kcal mol^{-1} for **4.17**, leading to a readily thermally accessible triplet excited state. Furthermore, the two diradicals were proved to be stable in solution for six months under ambient conditions, even upon irradiation with a high power lamp (400 W) for one day without obvious degradation. Remarkably, diradical **4.16** exhibits an excellent thermal stability up to 270 °C in the solid state.[107]

Figure 4.2.5.9. Structure of Kekulé **4.17** diradical with a closed-shell resonance form (right).

Among the diradicals incorporating a spin coupling unit, there is also reported in 2019, stable diradicaloid, **4.19**. Similarly to the previously described diradicals (**4.15-4.17**), two benzo[*e*][1,2,4]triazin-4-yl moieties were connected at the C(7) position, possessing the highest among the carbon atoms spin density ($\rho_7 = 0.07$).[26] In this work a comparison of analogues of Tschitschibabin's **4.5** and Müller hydrocarbon **4.19** (Figure 4.2.5.10.) were reported constituting a valuable demonstration of stable nitrogen-centered analogues of its reactive carbon predecessors. It was found that the latter systems usually have small singlet-triplet gaps with a thermally accessible triplet excited state. As predicted by the topology, both diradicaloids **4.5** and **4.19** possess singlet ground states, and excellent thermal and chemical stabilities in comparison to the hydrocarbon analogues. The two diradicaloids exhibit smaller singlet-triplet energy gaps

(ΔE_{ST} from -1.05 to -1.27 kcal mol^{-1}) than the carbon centered diradicaloids with the same bridges, thus can easily be populated to triplet excited states. Such small ΔE_{ST} values are due to the weak through–bond intramolecular electron exchange interactions (J) caused by terminal triazinyl rings dominating spin density distribution.

4.51 (n = 1) **Thiele Hydrocarbon**
4.52 (n = 2) **Tschitschibabin's Hydrocarbon**
4.53 (n = 3) **Müller's Hydrocarbon**

4.5 (n = 0)
4.19 (n = 1)

open-shell diradical   closed-shell quinoid
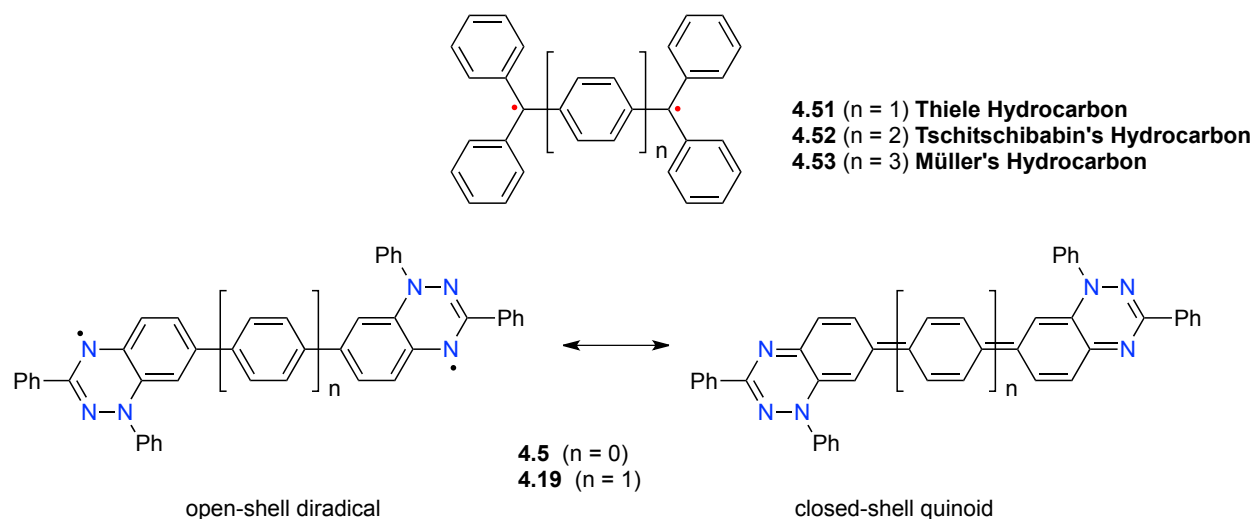
Figure 4.2.5.10. Structures of carbon-centered diradicaloids **4.51–4.52** and their nitrogen-centered analogues **4.5** and **4.19**.

The third class of diradicals (**C**) constitute those, in which two benzo[*e*][1,2,4]triazin-4-yl radicals (**4.5**, **4.20** and **4.21**)[106, 111] or benzo[*e*][1,2,4]triazinyl and another radical (**4.22-4.24**) are connected at a carbon atom. Beside the singlet ground state diradicaloid **4.5**, a series of high-spin diradicals reported by Rajca *et. al* belongs to this group. The connection of two benzo[*e*][1,2,4]triazin-4-yl rings (**4.21**), benzo[*e*][1,2,4]triazin-4-yl and nitronyl nitroxide radical (**4.22**) *via* the C(7) position, resulted in the access to remarkably stable triplet ground state Blatter–based diradicals (Figure 4.2.5.11.).[110-112]
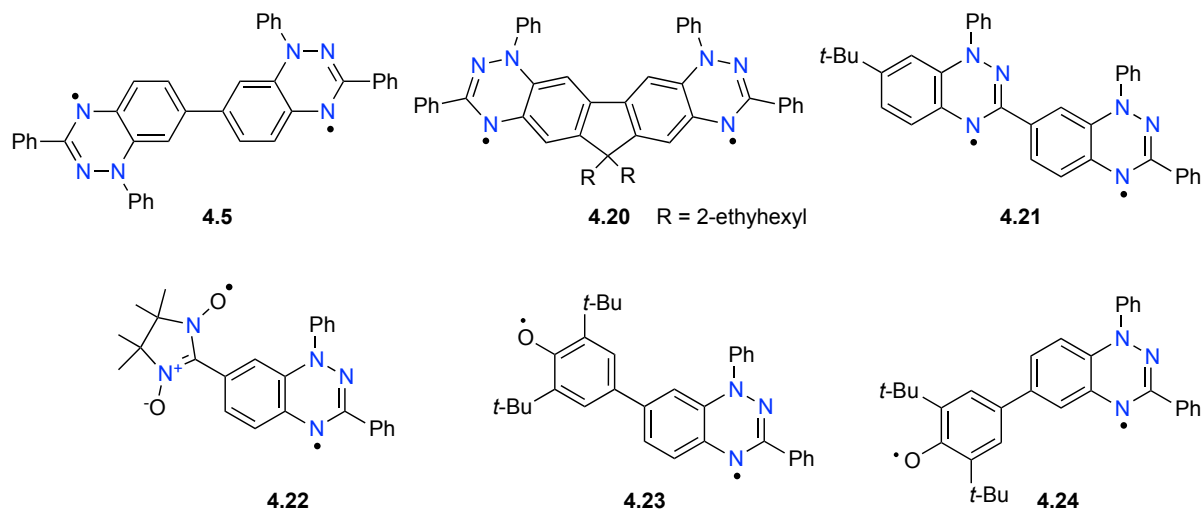
Figure 4.2.5.11. Diradicals incorporating the benzo[*e*][1,2,4]triazinyl constituting class **C**.

The 6,6-bis(2-ethylhexyl)-1,1',3,3'-tetraphenyl-4,6-dihydro-1*H*-fluoreno[2,3,8,9][1,2,4]-ditriazin-4-yl[92] (**4.20**) is an excellent, near-infrared photodetector, which exhibits doublet character in the solution but the electron spin resonance (ESR) spectra of polycrystalline sample resulted in the discovery of an unprecedented formation of stable dimers showing an intermolecular quintet state at room temperature. The synthetic route to **4.20** followed the classical procedure for the formation of benzo[*e*][1,2,4]triazin-4-yls, shown in Scheme 4.2.5.3.[45, 92]
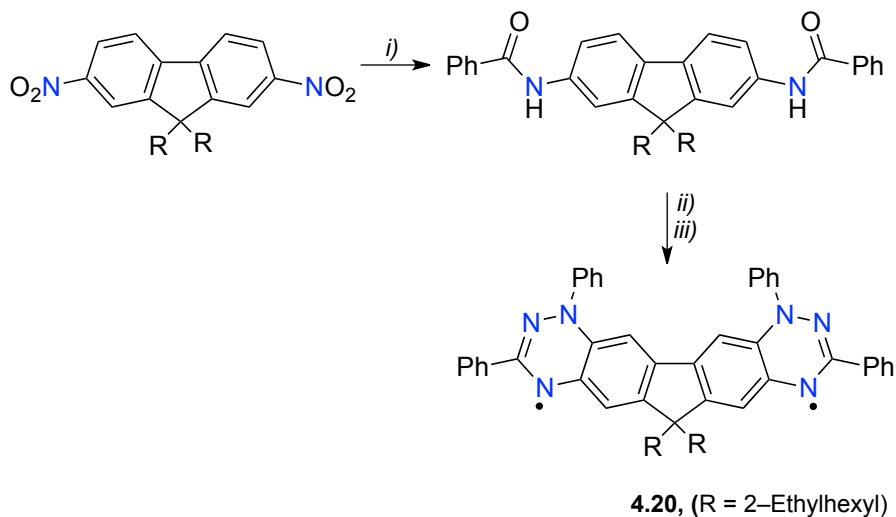
Scheme 4.2.5.3. Synthetic route to diradicaloid **4.20**. Reaction conditions: (*i*) 1. $NH_2NH_2 \cdot H_2O$, Pd/C, EtOH, reflux; 2. Benzoyl chloride, Et$_3$N, THF, rt, 1h, 85 % yield. (*ii*) 1. PCl$_5$, toluene, reflux, 6h; 2. Et$_3$N, phenylhydrazine, THF, 0 °C to rt, 24h (*iii*) DBU, Pd/C, DCM, air, rt, 24h, 11% yield.[92]

The interest in the development of organic materials suitable for application as dopants through a charge transfer process has mostly been focused on closed-shell molecules, which constituted the majority of organic semiconductors till 2015. Further research on **4.20** and its bromo-analogue **4.50** by Wudl was intended to yield materials with a temperature tunable electrical conductivity. The intermolecular electron transfer between the open-shell diradical and closed-shell quinoidal form (Figure 4.2.5.12.a.) leads to a radical anion–radical cation–radical pair (Figure 4.2.5.12.b.) and opens an avenue to a new type of self-doped semiconductor.[104]
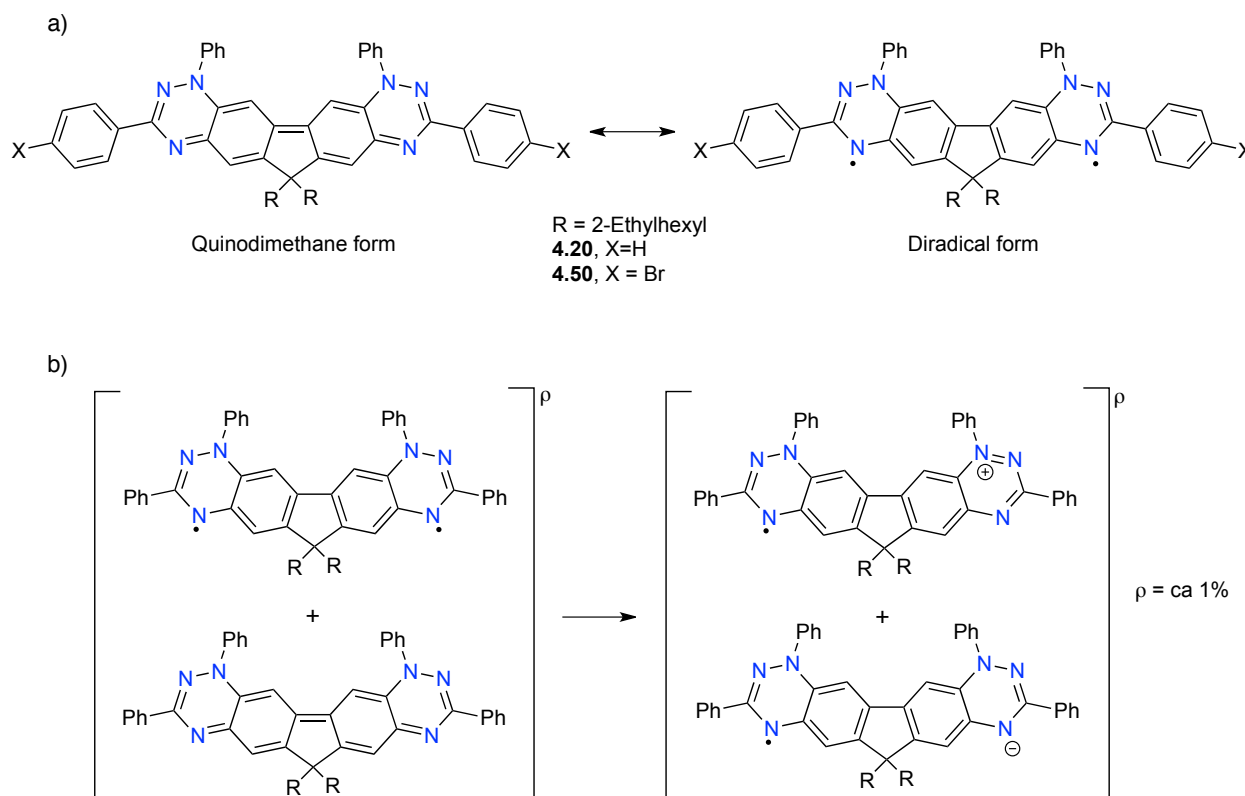
Figure 4.2.5.12. a) Structures of closed-shell (quinodimethane form) and open-shell (diradical form) of **4.20** and **4.50** diradicaloids. b) Example of the formation of a radical anion–radical cation pair.

Successfully, self-doping in solution-processable organic diradicaloids that are electrically and magnetically stable at adfmbient conditions were observed. The observed self-doping lead to a drastic improvement of the electrical conductivity in a controllable fashion, which, in association with the spin properties, opens up an avenue for advanced optoelectronic device applications with low fabrication cost.[104]

The analysis of the parity models, spin density distribution and general strategies for the design of high-spin ground state diradicals led to the design of di-Blatter diradical **4.21**. Taking advantage of the negative spin density at the C(3) position and possessing the highest among the carbon atoms positive value of spin density C(7) position, a triplet ground state of diradical was postulated. To take full advantage of its excellent thermal and air stability, diradical based entirely on the Blatter radical building blocks were designed, however the authors faced a tremendous challenge during synthesis of this analogue. Fortunately, after various unsuccessful convergent synthetic approaches, a breakthrough was achieved using a divergent route presented below (Scheme 4.2.5.4.).[111]
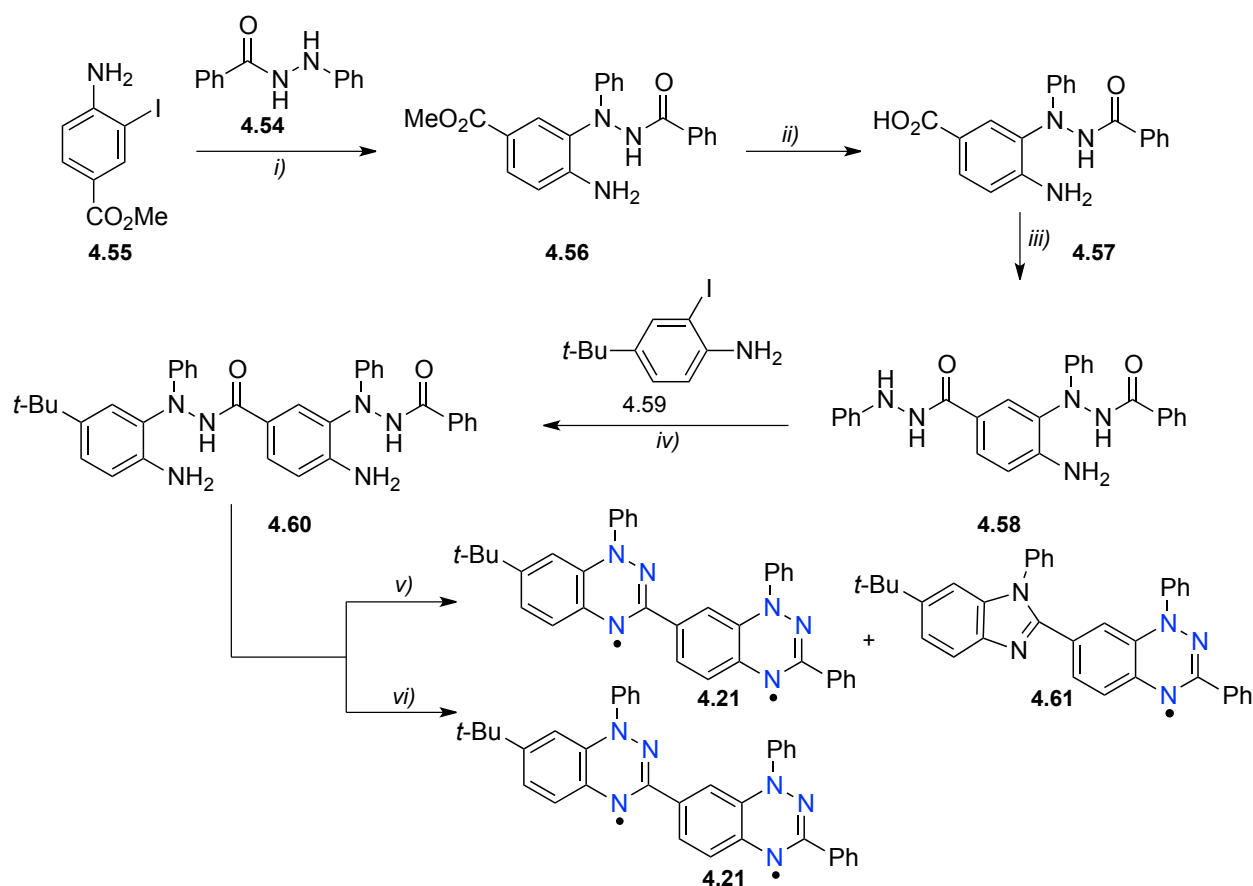
Scheme 4.2.5.4. Synthetic route to diradical **4.21**. Reaction conditions: (*i*) K$_2$CO$_3$, CuI, DMSO, 60 °C, 6 h, 84–85 % yield. (*ii*) LiOH, MeOH/H$_2$O, rt, 12 h, 64-78 % yield. (*iii*) 1. 1,1'-Carbonyldiimidazole (CDI); 2. Phenylhydrazine, DCM, rt, 12 h, 84-94 % yield. (*iv*) K$_2$CO$_3$, CuI, DMSO, 60 °C, 6 h, 65–81 % yield. (*v*) 1. *p*-TsOH, toluene, reflux, 24 h; 2. NaOH, MeOH, air, rt, 12 h, **4.21** 40-43 % yield, **4.61** 21-52 % yield. (*vi*) 1. *p*-TsOH, toluene, reflux, 2 h; 2. NaOH, MeOH, air, rt, 12 h, 50-54 % yield.[111]

The synthesis of **4.21** starts with the copper-catalyzed C−N coupling reaction of **4.54** with methyl 4-amino-3-iodo-benzoate **4.55**, to produce hydrazide **4.56**. The ester group in **4.56** was hydrolyzed, and the resulting carboxylic acid **4.57** was activated with 1,1′-carbonyldiimidazole (CDI), and reacted with phenylhydrazine. The resultant intermediate **4.58** was subjected to a C−N coupling reaction with 4-*tert*-butyl-2-iodoaniline **4.59** to provide compound **4.60**. Acid-catalyzed double cyclization of **4.60** was followed by air oxidation under basic conditions to produce diradical **4.21** in about 50% isolated yield. Notably, when the cyclization step was carried out for 24 h, instead of 2 h, an approximately equimolar mixture of diradical **4.21** and byproduct monoradical **4.61** was isolated (Scheme 4.2.5.4.).[111]

The diradical **4.21** exhibits a triplet ground state and robust thermal stability, with an onset of decomposition above 264 °C, which is the highest temperature among high-spin diradicals or triradicals studied by TGA. Remarkably, single crystals of **4.21** exhibit electrical conductivity at room temperature. [111]

With the ultimate goal of developing an all-organic ferromagnet, polyradicals possessing a stable high-spin ground state are the most sought-after, but also the least commnon examples in the literature. The thermally and magnetically robust triplet ground state diradical **4.22** with a large ΔE_{ST} of ≥1.7 kcal mol^{-1}, corresponding to a nearly exclusive (98 %) triplet occupancy at room temperature, constitutes one of the most unusual examples of diradicals incorporating the benzo[*e*][1,2,4]triazinyl reported to date. The difficulty in designing of high spin polyradicals is compounded by the often desire to establish long-range interactions in polycrystalline solids and films. Here, **4.22** is unusual in so far, that it forms antiferromagnetic one-dimensional chains in the polycrystalline phase, with a coupling constant of $J/k = -14$ K being "by far the strongest among all studied 1D, $S = 1$ chains of organic radicals".[112, 120] Compounds **4.21, 4.22, and 4.18a** are the only known examples of diradicals, which have been thermally sublimed in ultra-high vacuum to obtain thin films on silicon substrates, with near full retention of the diradical character for at least 18 h. These features make them promising candidates for device fabrication, however more effort in this area are still needed. [110-112]

Recently, the synthesis and characterization of two conjugated asymmetric diradical isomers, consisting of phenoxyl (acceptor) and Blatter (donor) radical moieties connected *via* the C(7) (**4.23**) or C(6) (**4.24**) position were repored by Zheng *et. al* (Figure 4.2.5.13.)[113] These molecules were designed to explore the electronic properties resulting from two concepts:

electron delocalization effect and electron-pair splitting effect. The number of molecules that simultaneously execute both of these effects over the same π-core is limited, and the main difficulty in the design of such molecules is the ability of balance these competitive effects.
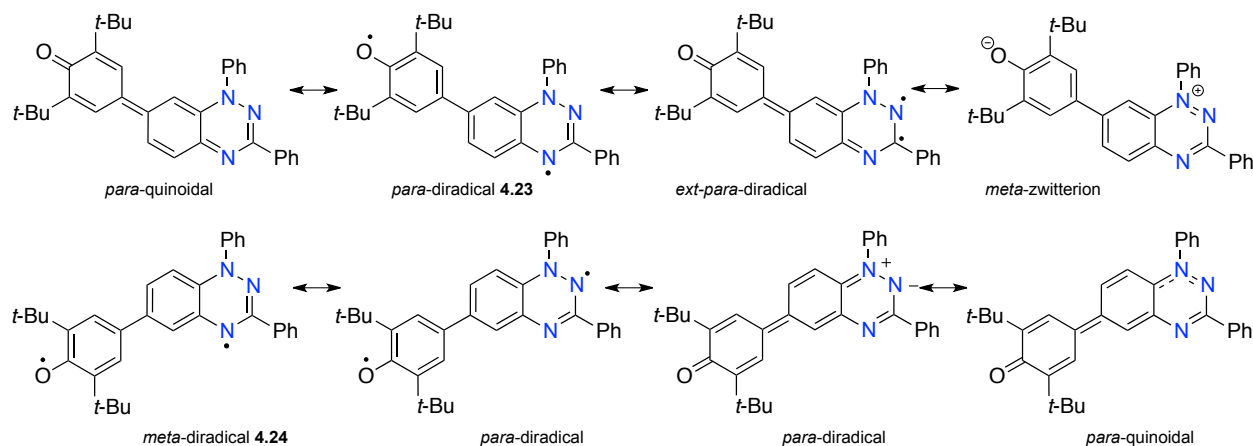
Figure 4.2.5.13. Resonance structures of asymmetric diradicals **4.23** and **4.24**.[113]

The subtle balance that shapes up the electronic structure of open-shell molecules is controlled by diradical-zwitterion relation, which is challenging in the case of asymmetric systems, such as the phenoxyl–Blatter diradicals. The stabilization of charge-separated states (zwitterion-like structures) is required for the purpose of obtaining of conducting and photoconducting materials. The charge-transfer processes in the excited states is also of relevance for the application of stable diradicals in photovoltaics, which makes these diradicals promisssing candidates for technological needs.[113]

The next challenge in the area of stable polyradicals incorporating the benzo[*e*][1,2,4]triazinyl moiety, namely access to a stable triradical was first reported by Koutentis *et. al* in 2020 (Figure 4.2.5.14.).[121] A C(3)–symmetric, star–shaped triradical **4.62** was prepared *via* reductive condensation of tricarbohydrazide in an overall yield of 58 %. The claimed quartet ground state was confirmed by theoretical calculations initially with the doublet-quartet energy gap $\Delta E_{DQ} = 0.109$ kcal mol^{-1}. Further experimental studies using continuous wave (CW) and pulse EPR spectroscopy were performed to confirm the postulated[122] quartet ground state of **4.62**.[123]

4.62   **4.63**
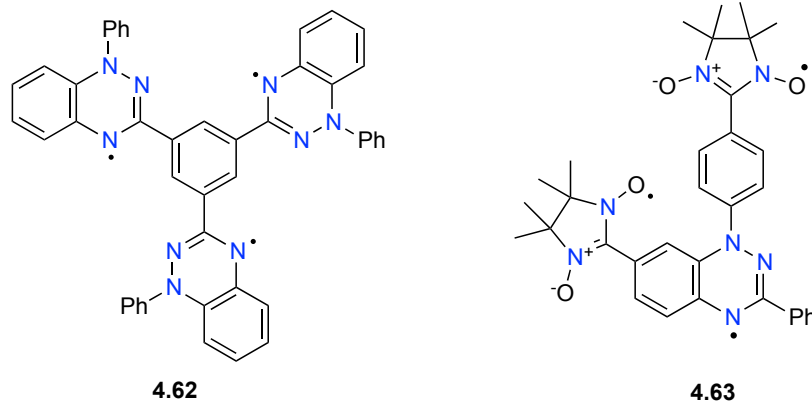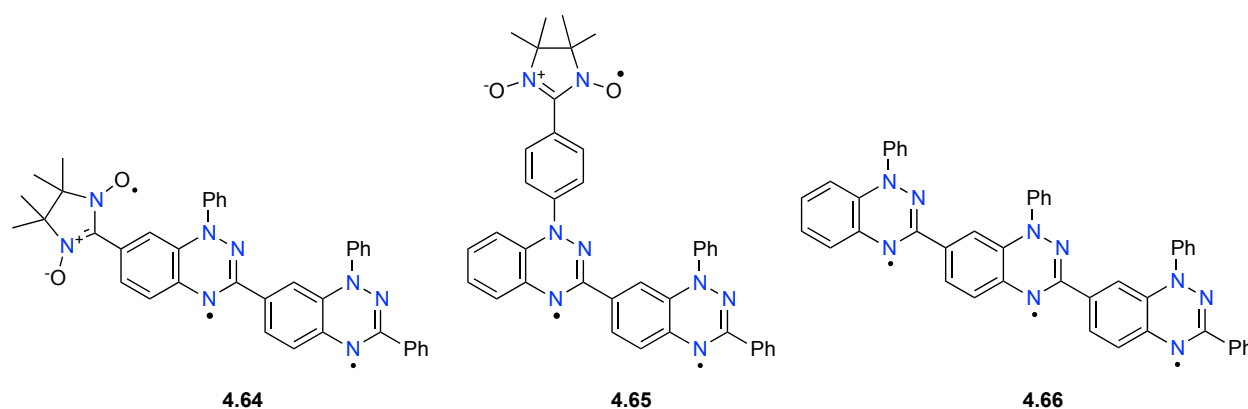
Figure 4.2.5.14. Triradicals incorporating benzo[*e*][1,2,4]triazinyl moiety reported to date.

In 2021 Rajca with co-workers reported the synthesis and study of the second Blatter-based triradical **4.63**.[122] The molecular design comprises of two nitronyl-nitroxide radicals connected to benzo[*e*][1,2,4]triazinyl *via* the most spin rich positions N(1) and C(7) of its core. The triradical **4.63** was synthesized by a Pd(0)-catalyzed radical-radical cross-coupling reaction. Previously, the development of the cross-coupling reactions in the synthesis of organic radicals has faced tremendous obstacles, largely due to the inherent reactivity of organic radicals, which affect both the activation of the starting materials and the search for a suitable catalyst.[46] Rajca *et. al* reported the synthesis and study of high-spin (S = 3/2) triradical **4.63**, in which they exploit the Pd(0)-catalyzed radical−radical cross-coupling reactions between di-iodo-substituted Blatter radical and nitronyl nitroxides. Triradical **4.63** has two doublet−quartet energy gaps, $\Delta E_{DQ} \approx$ 0.2−0.3 kcal mol^{-1} and $\Delta E_{DQ2} \approx$ 1.2−1.8 kcal mol^{-1}, *i.e.*, same order of magnitude as the thermal energy at room temperature, thus possessing a quartet ground state that is 70% populated at room temperature. Triradical **4.63** is thermally robust, with an onset of decomposition at ~160 °C under an inert atmosphere and was thermally evaporated under ultrahigh vacuum to form thin films. These studies provide the first example of the preparation and characterization of a thin film of high-spin (S = 3/2) organic triradical.[122]

Growing interest in robust organic triradicals with quartet ground-state provide promising applications in molecular magnets or spintronics. In this context, triradicals **4.62** and **4.63** were investigated computationally by the standard broken symmetry (BS)-DFT methods, which can result in somewhat overestimated energies in comparison to the eperimentally observed values.[124]
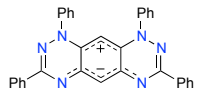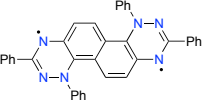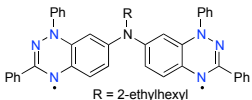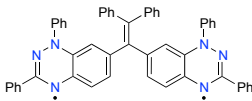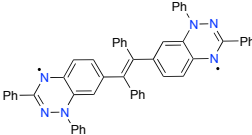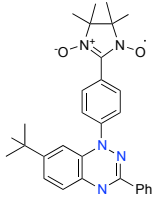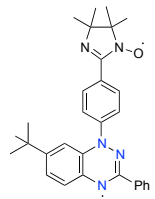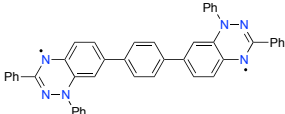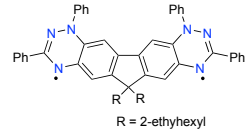
In order to avoid this problem Ali *et. al* employed different computational methods using **4.63** as the prototypical system to obtain more accurate doublet-quartet energy gaps ΔE_{DQ} for this triradical.[124] The spin constraint broken symmetry (CBS)-DFT method has been used to reduce the overestimation of energy gaps from (BS)-DFT. To address the issues of spin-contamination and multi-reference nature of low-spin states affecting the DFT methods, they have computed the energy gaps using appropriately state-averaged CASSCF and NEVPT2 methods. Furthermore, they have proposed and modeled other three triradicals based on the benzo[*e*][1,2,4]triazin-4-yl, which can be of interest for experimental exploration (Figure 4.2.5.15.).
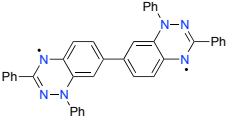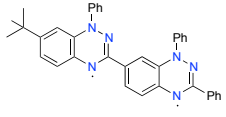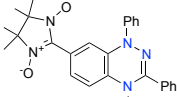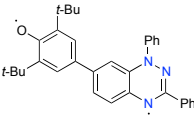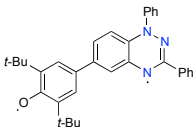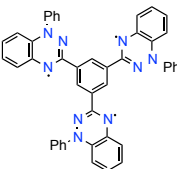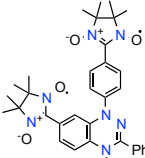

Figure 4.2.5.15. Modeled triradicals incorporating benzo[*e*][1,2,4]triazin-4-yl.[124]

In conclusion, scientific interest in stable diradicals incorporating the benzo[*e*][1,2,4]triazin-4-yl increased significantly during last 5 years. Since the first report on di-Blatter diradical **4.20**, seventeen new di- and triradicals based on this key structural element appeared in the literature resulting in about twenty publications in high–quality journals. The latter is a consequence of accessible high-spin states, electrochemical properties and spin-spin interactions of such compounds desired for technological needs. The most important paramateres, including the absorption maxima, oxidation and reduction potentials, singlet–triplet gaps ΔE_{ST}, diradical character index *y* and zero–field splitting parameters *D* and *E* for discussed diradicals, are listed in Tables 4.2.5.3. and 4.2.5.4. All the reported diradicals exhibit long absorption in the visible range tailing to the NIR region up to 990 nm. Electronic interactions in most of the synthesized derivatives were tested with electrochemical methods. EPR spectroscopy of solid solutions of diradicals confirmed their predicted ground states except for TMM-coupled derivative **4.16** due to conformational reasons. Also the analysis of C(3)-C(7) connected diradical **4.21** revealed the ground state dependence on the rigid medium. Three high–spin ground state diradicals incorporating the benzo[*e*][1,2,4]triazin-4-yl and another radical **4.18a** and **4.22** or two benzo[*e*][1,2,4]triazin-4-yl units were reported to date, and all of them were sublimed in under ultra-high vacuum (UHV) on surface, which make them candidates for device fabrication. Synthetic access to most of the derivatives is complicated and resulting derivatives were prepared in low yields. For that reason further investigation and development of convenient access using general intermediates to diradicals with controllable singlet–triplet energy gap by judicious choice of connection position or using couplers (SC) is still needed. The reported diradicals offer new platforms for molecular and supramolecular engineering in the context of magnetostructural studies, molecular electronics, photovoltaics and spintronics. It is also the first step towards electroactive multi-spin and functionalized systems including polymeric high-spin materials.

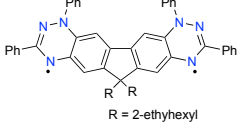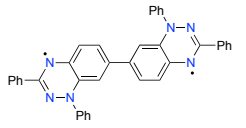**Table 4.2.5.3.** Selected experimental parameters of reported diradicals.
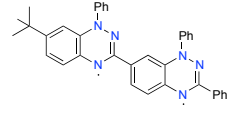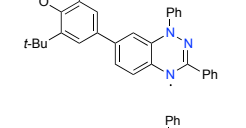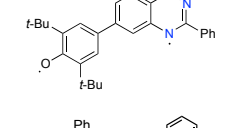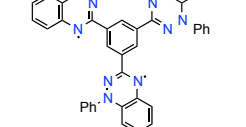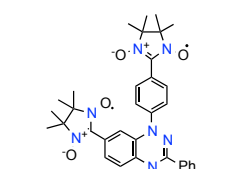
diradical	structure	λ_{max} exp /nm	$E_{1/2}^{2-/-}$ ^{b}/V	$E_{1/2}^{-/0}$ ^{b}/V	$E_{1/2}^{0/+}$ ^{b}/V	$E_{1/2}^{+/2+}$ ^{b}/V
4.12[108, 115]		589 ^{a}	–	–	–	–
4.13[105]		773 ^{a}	–0.93		0.24	0.69
4.14[109]		934 ^{a}	–	–0.95	0.07	0.47
4.15[109]		695 ^{a}	–	–0.96	0.05	0.51
4.16[107]		528 ^{a}	–	–	–	–
4.17[107]		659 ^{a}	–	–	–	–
4.18a[110]		–	–	–	–	–
4.18b[110]		–	–	–	–	–
4.19[106]		524 ^{a}	–0.89		0.32	
4.20[104-105]		736 ^{a}	≈ –0.9		–	–

	Structure	λ				
4.5[106]		728 ^{a}		–		–0.15	0.09
4.21[111]		720 ^{a}	–1.6	–1.33	–0.28	–0.04
4.22 [122] 112		547 ^{a}		–1.31		–0.1	0.56
4.23[113]		820 ^{a}	–1.33	–1.15	–0.18	0.13
4.24[113]		990 ^{a}	–1.54	–1.22	–0.50	–0.11
4.62[121]		595 ^{a}	–	–1.28	–0.08	–
4.63[122]		545 ^{a}	–	–1.19	–0.05	0.51

^{a} The lowest energy absorption band recorded in CH_2Cl_2. ^{b} Potentials *vs.* Fc/Fc$^+$ couple recorded in CH_2Cl_2 with $[n\text{-}Bu_4N]^+[PF_6]^-$ (100 mM), at *ca.* 20 ^{o}C.

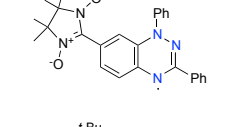**Table 4.2.5.4.** Selected experimental parameters of reported diradicals.

diradical	structure	ΔE_{ST} exp kcal mol^{-1}	ΔE_{ST} DFT kcal mol^{-1}	y	D cm^{-1}	E cm^{-1}	r Å
4.12[108, 115]		−20.1	−0.77	–	–	–	–
4.13[105]		−1.54 [a]	−3.75			0.0044	8.4
4.14[109]		−2.38 [b]		0.68	0.0027	0.00083	9.87
4.15[109]		−1.16 [b]		0.89	0.0057	0.00067	7.69
4.16[107]		−0.21 [e]	−0.1	0.84	0.0042	0.0013	8.5
4.17[107]		−0.18 [e]	−0.3	0.78	0.0048	0.00099	8.2
4.18a[110]		0.50 ±0.02 [d]	1.4	–	0.00232	0.00014	–
4.18b[110]		–			0.00558	0.00013	–
4.19[106]		−1.05 [a]		0.85	0.0021	–	–

Compound	Structure						
4.20 [104-105]		-1.40 [a]	-2.57	0.38	0.29	0.0012	12.9
4.5 [106]		-1.27 [a]	-0.95	0.63	0.0025	–	10.1
4.21 [111]		0.5 [c]			0.013	0.00113	–
4.22 [122] [112]		1.74 ±0.07 [c]	3.5	–	0.0081	0.00117	–
4.23 [113]		-1.71 [e]	-4.04	0.43	–	–	–
4.24 [113]		-1.01 [e]	-1.81	0.50	0.0029	0.00056	9.64
4.62 [121]		–	–	–	–	–	–
4.63 [122]		–	–	–	–	–	–

[a] Determination of ΔE_{ST} for diradical in benzophenone solid solution [b] Determination of ΔE_{ST} for diradical in benzothiophene. [c] Determination of ΔE_{ST} for diradical in polystyrene. [d] Determination of ΔE_{ST} for diradical in dibuthyl phthalate or toluene/CH$_3$Cl glass. [e] Determination of ΔE_{ST} for diradical in powder form usig SQUID. [f] Determination of ΔE_{ST} for diradical in a frozen glass (toluene:CHCl$_3$ v/v = 4:1).

5. Goal and scope of this Dissertation

The presented Dissertation is part of a broad project aimed at the development of a new class of near-IR dichroic dyes. The main goal of this work was access to stable diradicals incorporating benzo[*e*][1,2,4]triazin-4-yl, as precursors to radical cations with substituent-tunable absorption in the NIR region. Such compounds are expected to be compatible with LC matrix and exhibit high dichroic ratio important to telecommunication industry. To accomplish this goal, development of convinient synthetic methods to a series of new classes of mono- and diradicals based on benzo[*e*][1,2,4]triazin-4-yl and detailed analysis of their structure-property relationships was necessary. The first goal was to establish convient synthetic access to a series of C(3) substituted benzo[*e*][1,2,4]triazines, which are presursors to stable C(3)-functionalized monoradicals. Developed synthetic pathways and acquired skills for characterization of such spiecies were necessary for a rational design and preparation of stable diradicals connected either directly (type **A**) or through a π-spacer (type **B**) with properties suitable for application in functional materials (Figure 5.1.). One-electron oxidation of appropriately functionalized diradicals will provide radical cations with substituent-tunable absorption in the NIR region, and which are compatible with LC matrix and exhibit high dichroic ratio.
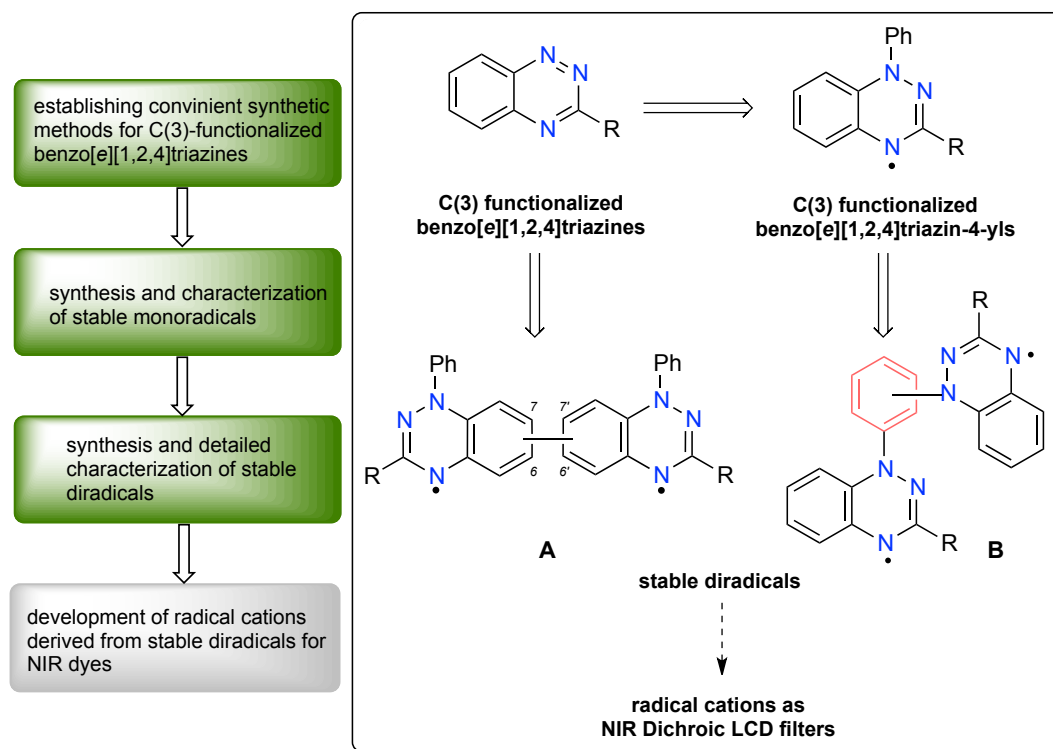
Figure 5.1. A graphical representation of the goals and scope of this Dissertation area.

In the first stage of the presented work, the scope and the influence of C(3) substituents on stability and spectroscopic (UV-vis) and electrochemical (Cyclic Voltammetry) properties of a series of functionalized benzo[*e*][1,2,4]triazines and benzo[*e*][1,2,4]triazin-4-yl monoradicals had to be developed. Previously reported functionalization of C(3) position of benzo[*e*][1,2,4]triazine included a few members of 3-phenyl, 3-aryl, 3-amino and 3-alkyl derivatives and was insufficient to accomplish goals established in this project. Access to a new class of near-IR dichroic dyes based on the radical cations incorporating benzo[*e*][1,2,4]triazin-4-yl requires C(3)-N(Alkil)$_2$ substituent, which will deliver significant red-shift of the absorption spectrum and compatibility with the nematic matrix.

The established scope of substituents at the C(3) position and the electronic and chemical properties of both the C(3) functionalized benzo[*e*][1,2,4]triazines and benzo[*e*][1,2,4]triazin-4-yls *via* two methods[34, 40,125] gave a tool for further investigation of such systems. This opened up new opportunities in structural manipulation with the C(3) substituent of benzo[*e*][1,2,4]triazin-4-yls providing a tool for the designing of mono- and diradicals that show greater functional flexibility and structural variety for modern materials applications.

In the next stage of research the access to a new class of air and temperature stable high-spin molecules of types **A** and **B** (Figure 5.1.) with magnetically coupled two delocalized spins was needed to be developed. The centerpiece of the molecular design of diradicals consisted of two benzo[*e*][1,2,4]triazin-4-yl fragments, which supposed to be connected either directly (**A**) or through a π-spacer (**B**) (Figure 5.1.).

Our hypothesis states that singlet–triplet gap in diradicals derived from the benzo[e][1,2,4]triazin-4-yls can be controlled by judicious choice of the molecular structure and connectivity between the radicals.

Initially a series of regioisomers of di-Blatter diradicals with controlled electronic and magnetic properties connected through the spin rich positions C(6) and C(7) of the benzo[*e*][1,2,4]triazin-4-yl core was invesigated. For this purpose the development of easily accesible, common presursors was necessary, which will allow for convient functionalization of such derivatives. Available synthetic methods for synthesis of directly connected diradicals incorporating benzo[*e*][1,2,4]triazin-4-yl, were complicated and inefficient.

The access to di-Blatter diradicals connected through a spin-coupler at the N(1) position was envisioned through, a one-step addition of dilithio derivatives to the 3-substituted

benzo[*e*][1,2,4]triazine. These diradicals were proposed as the first examples of a potentially broad class of symmetric high-spin molecules with a controlled singlet-triplet gap. Judicious choice of the connection position on the benzo[*e*][1,2,4]triazin-4-yl will permit the control of the ground state multiplicity and the singlet–triplet energy gap.

The obtained diradicals with the most linear shapes, sufficient solubility and accessible starting materials will serve as precursors for radical cations with predicted substantially red shifted electronic absorption. Group R will be used to control absorption wavelength and compatibility with nematic matrix.

6. Results and Discussion

6.1. 3-Substituted benzo[*e*][1,2,4]triazines: Synthesis and electronic effects of the C(3) substituent

Results of this work were analyzed, described and published. My contribution to this publication consisted of: development of synthetic methods, synthesis and characterization of precursors and final products, characterization of final products by UV-vis spectroscopy, preparation of Experimental Part and Supporting Information for the manuscript, participation in the revision of the manuscript. A summary of the main assumptions of the project is presented below. For details, please refer to the attached publication: Bodzioch, A.; Pomikło, D.; Celeda, M.; Pietrzak, A.; Kaszyński, P. 3-Substituted benzo[*e*][1,2,4]triazines: synthesis and electronic effects of the C(3) substituent. *J. Org. Chem.* **2019**, *84*, 6377–6394 (Chapter 9).

In spite of broad applications of benzo[*e*][1,2,4]triazine derivatives, there were surprisingly few investigations of their molecular and electronic structures. For instance, there has been no systematic investigation of the effect of the C(3) substituent on the electronic properties of the benzo[*e*][1,2,4]triazine ring. My interest in this class of derivatives stems from the understanding of these electronic effects and accessing C(3)-substituted benzo[*e*][1,2,4]triazin-4-yl radicals. Thus, the goal of this project was to develop a facile access to a series of structurally diverse C(3)-substituted derivatives **6.1** of the parent benzo[*e*][1,2,4]triazine (**6.1a**) and their complete characterization by spectroscopic (UV-vis, NMR) and electrochemical methods.
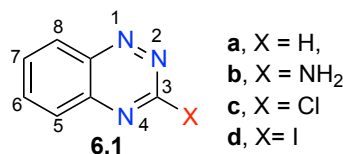
Figure 6.1.1. The parent benzo[*e*][1,2,4]triazine (**6.1a**) and other derivatives with the numbering system.
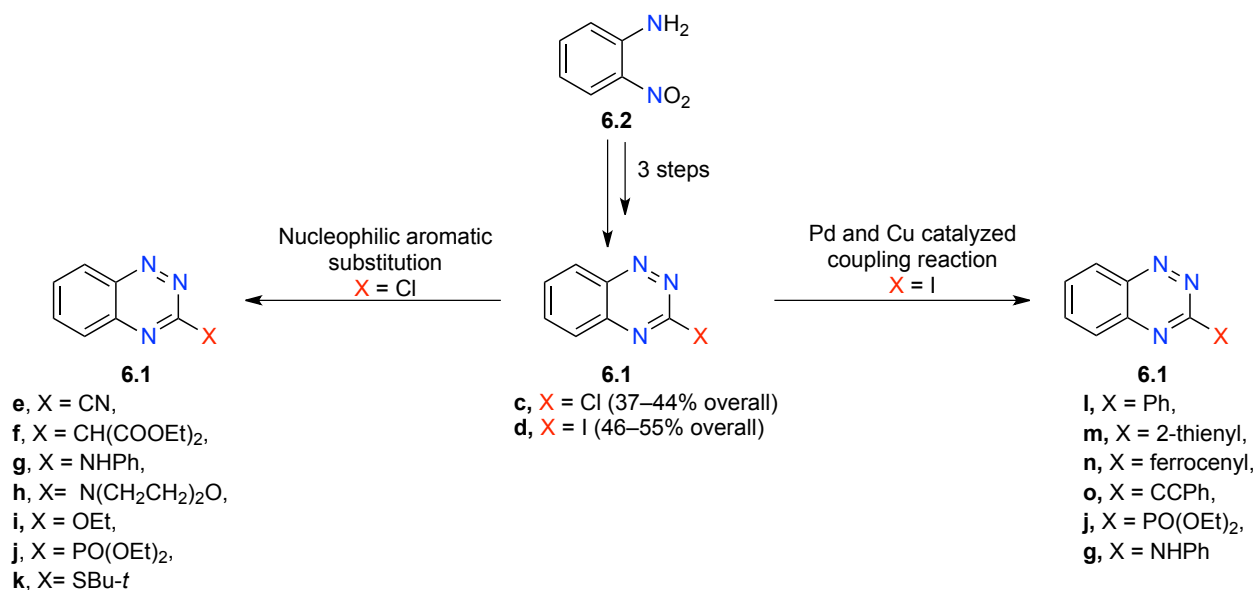
Figure 6.1.2. The general access to C(3)–functionalized benzo[*e*][1,2,4]triazines with a scope of substituents.

Access to a variety of C(3)-substituted derivatives **6.1** was envisioned from a common precursor, 3-aminobenzo[*e*][1,2,4]triazine (**6.1b**). As a result of my work, benzo[*e*][1,2,4]triazines with a wide range of substituents at the C(3) position are readily available directly from 3-halo derivatives **6.1c** and **6.1d**, which are obtained in three simple steps from 2-nitroaniline (**6.2**). The chloride **6.1c** is a convenient substrate for direct and efficient introduction of substituents such as OR, NHAr, NR_2, SR, and soft C-nucleophiles (CN and malonate) *via* S_N2Ar nucleophilic substitution reactions, while the iodo derivative **6.1d** provided access to C(3) (*het*)aryl (Suzuki), acetylene (Sonogashira), and phosphonate through Pd- or Cu- catalyzed substitution reactions. These methods failed to obtain 3-CF_3 (**6.1p**), 3-carboxyl (**6.1r**), and 3-pentyl (**6.1s**) derivatives from **6.1d** using the Ruppert, Pd-catalyzed carbonylation, and Negishi reactions, respectively. The use of iodo N-oxide **6.5** instead of **6.1d** allowed to obtain 3-pentyl derivative **6.1s** in good yields, but failed again to provide access to **6.1p** and **6.1r**. In search for convient synthetic access to C(3)-amino and C(3)-alkyl benzo[*e*][1,2,4]triazines **6.1**, an alternative synthetic method was developed (Section 6.2). Simplified availability of a variety of derivatives **6.1** offers a broader and simpler access to C(3)-functionalized 1,4-dihydrobenzo[*e*][1,2,4]triazin-4-yl radicals by addition of ArLi reagents.

6.2. 3-Substituted Blatter radicals: Cyclization of *N*-arylguanidines and *N*-arylamidines to benzo[*e*][1,2,4]triazines and PhLi addition

Results of this work were analyzed, described and published. My contribution to this publication consisted of: development of synthetic methods, synthesis and characterization of precursors and final products, performing Cyclic Voltammetry, UV-vis spectroscopy and Electron Paramagnetic Resonance Spectroscopy measurements, describing results, preparation of Experimental Part and Supporting Information of the manuscript, participation in preparation and revision of manuscript. A summary of the main assumptions of the project is presented below. For details, please refer to the attached publication: Pomikło, D.; Bodzioch, A.; Kaszyński, P. 3-Substituted Blatter radicals: cyclization of *N*-arylguanidines and *N*-arylamidines to benzo[*e*][1,2,4]triazines and PhLi addition. *J. Org. Chem.* **2023**, *88*, 2999–3011 (Chapter 9).

Analysis of the previously obtained data[125] (Section 6.1) indicated that the 3-amino substituent in benzo[*e*][1,2,4]triazin-4-yl derivatives is particularly effective in modification of electronic properties of the radicals: it effects a significant cathodic shift of the oxidation potential and a bathochromic shift in the electronic absorption, relative to the prototypical Blatter radical **4.1**.[34] Similar, although less pronounced effects were observed for the 3-pentyl derivative **6.1s**.[34] For these reasons, C(3)-amino and C(3)-alkyl derivatives are of interest for fine tuning of electronic properties of the benzo[*e*][1,2,4]triazinyl system, and also in the context of our program in self-organizing paramagnetic materials with controlled photophysical and redox behavior.

The existing methods[34, 51] for the preparation of 3-amino and 3-alkyl derivatives relayed mainly on benzo[*e*][1,2,4]triazines **6.1**.[125] Thus, the requisite amines **6.1g** (X = NHPh) and **6.1h** (X = morpholinyl) were obtained from 3-chlorobenzo[*e*][1,2,4]triazine **6.1c**, while the 3-pentyl derivative **6.1s** was prepared in two steps from 3-iodobenzo[*e*][1,2,4]triazine-1-oxide (**6.5**) as presented in Section 6.1.[125] Although the two halo derivatives, **6.1c** and **6.5**, are general intermediates to a variety of such C(3) substituted radicals,[34] their synthesis is a multi-step process and involves poorly soluble intermediates, which is problematic for the preparation of polyradicals and more complex molecular systems. Therefore, in search for an alternative, more direct and convenient method for the preparation of **6.1**, we focused on *N*-substituted guanidines and amidines **6.6** as the starting materials. In comparison to the existing methods for the

preparation of 3-amino and 3-alkyl derivatives of benzo[*e*][1,2,4]triazine **6.1**, the presented methodology allows one to avoid multistep procedures with poorly soluble intermediates. It ofers an alternative access to benzo[*e*][1,2,4]triazines **6.1**, which serve as convenient precursors to radicals **6.3** with greater control of their electrochemical and spectroscopic properties. This opens up new opportunities in structural manipulation with the C(3) substituent of benzo[*e*][1,2,4]triazin-4-yls providing a tool for the designing of radicals that show greater functional exibility and structural variety for modern materials applications.
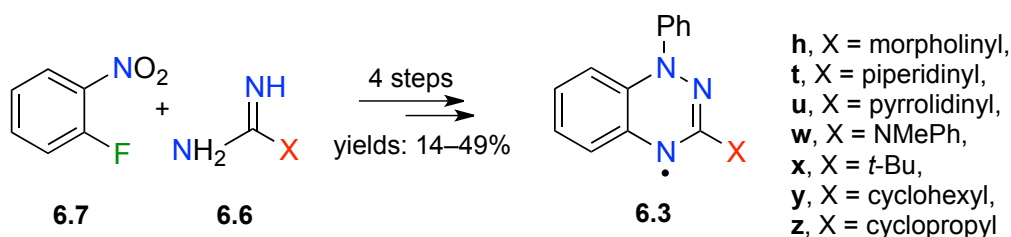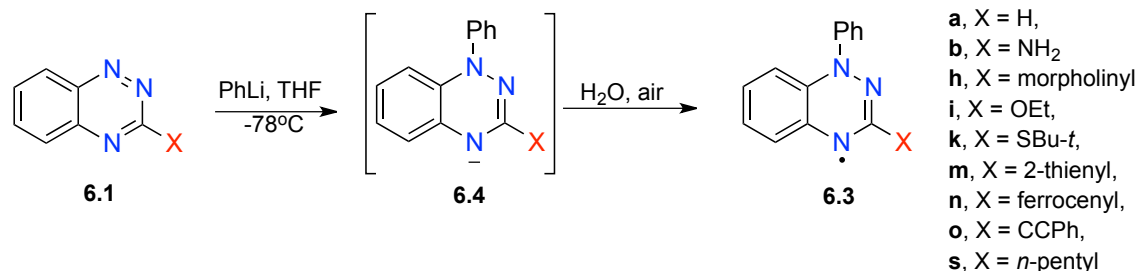

Figure 6.2.1. The access to C(3)-functionalized benzo[*e*][1,2,4]triazin-4-yls **6.3** using guanidines and amidines.

As a result, a series of 3-amino- and 3-alkyl substituted 1-phenyl-1,4-dihydrobenzo[*e*][1,2,4]triazin-4-yls **6.3** was prepared in four steps involving *N*-arylation, cyclization of *N*-arylguanidines and *N*-arylamidines, reduction of the resulting *N*-oxides to benzo[*e*][1,2,4]triazines **6.1** and subsequent addition of PhLi followed by aerial oxidation. The resulting seven C(3)–substituted benzo[*e*][1,2,4]triazin-4-yls **6.3h, 6.3t-6.3z** (Figure 6.2.1.) were analyzed by spectroscopic and electrochemical methods augmented with DFT methods. Electrochemical data were compared to DFT results and correlated with Hammett parameters.

6.3. C(3) Functional derivatives of the Blatter radical

Results of this work were analyzed, described and published. My contribution to this publication consisted of: synthesis and characterization of precursors and final products, performing Cyclic Voltammetry, UV-vis spectroscopy and Electron Paramagnetic Resonance Spectroscopy measurements, describing results, preparation of Experimental Part and Supporting Information of the manuscript, participation in preparation and revision of manuscript. A summary of the main assumptions of the project is presented below. For details analysis, please refer to the attached publication: Pomikło, D.; Bodzioch, A.; Pietrzak, A.; Kaszyński, P. C(3) Functional derivatives of the Blatter radical. *Org. Lett.* **2019**, *21*, 6995–6999 (Chapter 9).

The goal of this project was to prepare a series of C(3)-substituted benzo[*e*][1,2,4]triazin-4-yl radicals **6.3** by addition of PhLi to the readily available benzo[*e*][1,2,4]triazines **6.1** and their complete characterization by spectroscopic (UV-vis, EPR) and electrochemical methods. Since the C(3) position of the benzo[*e*][1,2,4]triazinyl system is the only functionalizable position with a sizable negative spin density, the substituent is expected to have a significant impact on electronic properties of the radical.

a, X = H,
b, X = NH$_2$
h, X = morpholinyl
i, X = OEt,
k, X = SBu-*t*,
m, X = 2-thienyl,
n, X = ferrocenyl,
o, X = CCPh,
s, X = *n*-pentyl

Figure 6.3.1. The access to C(3)-functionalized benzo[*e*][1,2,4]triazin-4-yls **6.3**.

The access to benzo[*e*][1,2,4]triazin-4-yls with a significantly expanded range and diversity of substituents at the C(3) position was successfully demonstrated. The newly available derivatives include the electroactive C(3)-ferrocenyl derivative **6.3n**, C(3)-acetylene derivative **6.3o**, and derivative **6.3b** containing a particularly important and versatile NH$_2$ functionality. The limitation of the azaphilic addition method and its incompatibility with some C(3) substituents, such as COO$^-$, NHPh, CN, and PO(OR)$_2$, were also established. The expanded series of derivatives **6.3** permitted analysis of C(3) substituent effects on electronic properties of the benzo[*e*][1,2,4]triazin-4-yl system, which, in turn, provides a tool for designing of radicals with greater functional flexibility and structural variety for modern materials applications.

6.4. Topologically coupled stable diradicals with tunable S-T gaps for molecular materials

6.4.1. Bi-Blatter diradicals: Convenient access to regioisomers with tunable electronic and magnetic properties

Results of this work were analyzed, described and currently are under publication process. My contribution to this publication consisted of: development of synthetic methods, synthesis and characterization of precursors and final products, performing Cyclic and Differential Pulse Voltammetry, UV-vis spectroscopy and Variable-Temperature Electron Paramagnetic Resonance Spectroscopy measurements, simulation of EPR spectra using Easy Spin, describing results, preparation of Experimental Part and Electronic Supporting Information of the manuscript, partial preparation and revision of manuscript. Pomikło, D.; Pietrzak, A.; Kishi, R.; Kaszyński, P. Bi-Blatter diradicals: Convenient access to regioisomers with tunable electronic and magnetic properties. *Mater. Chem. Front.* **2023**, (Accepted Manuscript). doi.org/10.1039/D3QM00666B

As presented before (Chapter 4.2.5.), the oxidatively and thermally stable 7,7'-bi-Blatter diradical **4.5** has one of the lowest among a series of ring-fused [1,2,4]triazin-4-yls S–T energy gaps ($\Delta E_{\text{S-T}}$ = -1.27 kcal mol^{-1}) and a moderate diradical index y = 0.63 (Table 4.2.5.4.).[106] The high propensity of the benzo[*e*][1,2,4]triazinyl for spin delocalization was used to stabilize an open-shell structure in phenoxy diradicals **4.23** and **4.24**.[113] These and other[107, 109] results demonstrate a significant potential of the benzo[*e*][1,2,4]triazinyl as a structural element of a broad class of chemically stable diradicals with controllable electronic and magnetic properties.

Analysis of spin distribution in the benzo[*e*][1,2,4]triazinyl unit of the prototypical Batter radical[11] (**4.1**, Fig. 4.2.4.1) indicates that only one position, C(3), has the negative spin density, which can be used to form bi-Blatter radicals with the triplet ground state.[26] All other bi-benzo[*e*][1,2,4]triazinyls not involving connection through the C(3) position are expected to posses the singlet ground state. This has been demonstrated for diradical **4.5**, but unfortunately, its synthesis was complicated and low yield, while the diradical itself has low solubility.[106] Therefore, it is highly desirable to establish simple access to diradicals such, as **4.5** and its isomers, and to investigate the degree of tunability of the diradicaloid character and the S–T energy gap by judicious choice of connectivity and substituents.
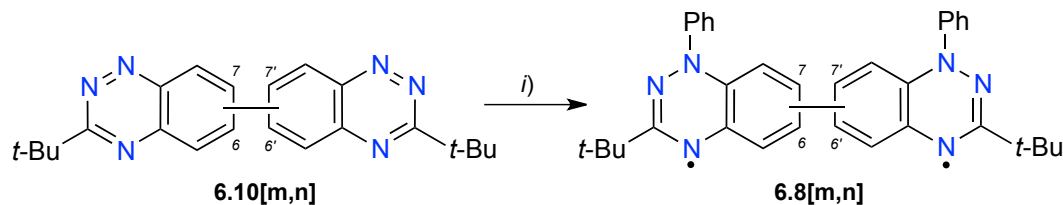
Synthesis

Herein a simple and concise synthetic access to three regioisomers of bi-Blatter diradicals **6.8[m,n]** is demonstrated (Figure 6.4.1.1.) and systematic studies of their electronic and magnetic properties as a function of the connectivity. The three regioisomers are investigated with spectroscopic (UV-vis-NIR and variable temperature EPR), electrochemical and structural analysis (single crystal XRD) methods. The experimental data are compared to those obtained for the analogous monoradical **6.9** and augmented with DFT computational results. The thermal and solution photochemical stability of the diradicals is briefly investigated.
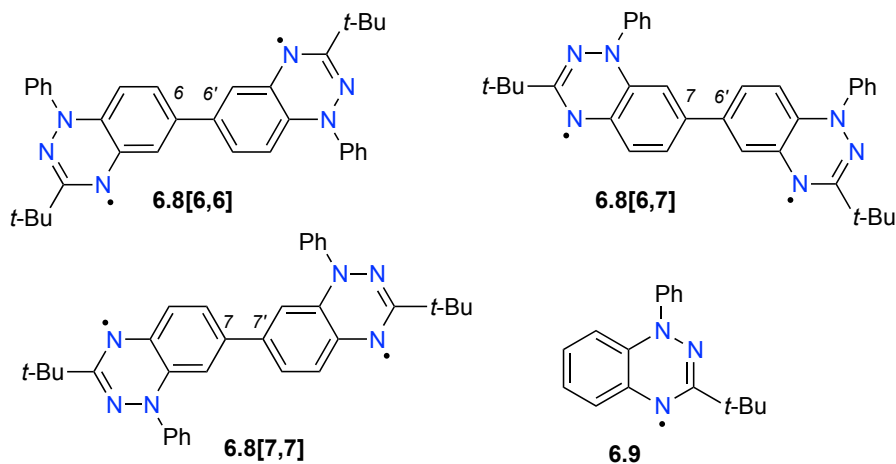
Figure 6.4.1.1. Molecular structures of bi-benzo[*e*][1,2,4]triazin4-yl diradicals **6.8[m,n]** and monoradical **6.9**. Numerals **m** and **n** denote the connecting positions, C(6) or C(7).

The strategy used in the synthesis of diradicals **6.8[m,n]** relies on azaphilic addition of ArLi to benzo[*e*][1,2,4]triazines.[44] Thus, addition of excess PhLi to bi-benzo[*e*][1,2,4]triazines **6.10[m,n]** followed by aerial oxidation of the intermediate dianions gave the title diradicals in 53–77% yield (Scheme 6.4.1.1.).[44] To maximize the yields, reaction times at each step were extended relative to those in the original procedure. For solubility reasons diradicals **6.8[m,n]** contain the *t*-Butyl groups substituted at the C(3) position of the benzo[*e*][1,2,4]triazine ring instead of the typical Ph group.

Scheme 6.4.1.1. Synthesis of diradicals **6.8[m,n].** *Reagents and conditions*: (*i*) 1. PhLi, -78 °C, 40 min, then rt, 1 h, 2. H₂O, air, overnight; yield: **6.8[6,6]** 65–75%, **6.8[6,7]** 66–77%, **6.8[7,7]** 53–56%. Numerals **m** and **n** denote the connecting positions, C(6) or C(7).

The requisite symmetric bi-benzo[*e*][1,2,4]triazines **6.10[6,6]** and **6.10[7,7]** were obtained starting from fluoroiodonitrobenzenes **6.11a** and **6.11b**, respectively, as shown in Scheme 6.4.1.2. Thus, Ullmann coupling[126] of **6.11** in DMSO[127] gave the corresponding biphenyls **6.12[m,n]** in moderate yields up to 49%. The same reaction conducted in dried DMF or DMA gave significant amounts of byproducts containing the NMe₂ group. A subsequent reaction of **6.12[m,n]** with pivalohydrazide in DMSO provided bishydrazides **6.13[m,n]** in about 75% yield. Reductive cyclization of **6.13[m,n]** with Sn powder in AcOH furnished the bi-benzo[*e*][1,2,4]triazines **6.10[6,6]** and **6.10[7,7]** in about 60% yield.

The same strategy did not work for the unsymmetric derivative **6.10[6,7]**. The Ullmann reaction of the two iodoarenes **6.11a** and **6.11b** in dry xylene, DMF, DMA or DMSO gave complex mixtures, including deiodinated products and substituted with Me₂NH, with very little, if at all, of the desired product. Therefore the synthetic strategy was changed.
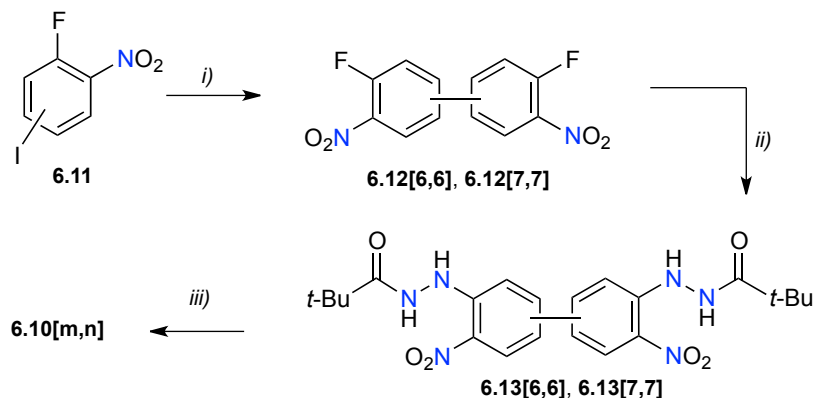
Scheme 6.4.1.2. Synthesis of symmetric bi-benzo[*e*][1,2,4]triazines **6.10[6,6]** and **6.10[7,7]**. *Reagents and conditions*: (*i*) Cu, DMSO, 165 °C, overnight, yield: **6.12[6,6]** 49%, **6.12[7,7]** 35%; (*ii*) DMSO, 110 °C, 72 h, yield **6.13[6,6]** 62-80%, **6.13[7,7]** 65-75%; (*iii*) 1. Sn, AcOH, rt, overnight, then 115–120 °C, 8 h, 2. NaIO₄, MeOH/CH₂Cl₂ (1:1), rt, overnight; yields: **6.10[6,6]** 56-59%, **6.10[7,7]** 60-66%.

The new approach to bi-benzo[*e*][1,2,4]triazine **6.10[6,7]** was based on conversion of the phenolic OH functionality to a leaving group (instead of fluorine) and Suzuki coupling instead of Ullmann coupling for the preparation of the requisite biphenyl (Scheme 6.4.1.3.). Thus, a reaction of boronic ester[128] **6.14** with 5-bromo-2-nitrophenol (**6.15**) in the presence of a Pd catalyst gave an inseparable mixture of the desired 3',4-dinitro-3,4'-dihydroxybiphenyl (**6.16[6,7]**) with the unreacted borolane **6.14** in a 1:2 ratio (¹H NMR). Additional portions of the phenol and/or the catalyst did not improve the conversion ratio. Also resubmitting the isolated mixture of **6.14** and **6.16[6,7]** to the reaction conditions with fresh portions of the phenol resulted in even lower amounts of the desire product. Ultimately, the mixture containing **6.14** and **6.16[6,7]** was submitted to oxidative hydrolysis,[129] and the analytically pure biphenyl **6.16[6,7]** was isolated in low yields up to 20%.

Suspecting the interference of the OH group with the Suzuki coupling process, the synthesis of the diphenol **6.16[6,7]** was modified by masking the OH functionality as the OMe group. Thus, Suzuki coupling of borolane **6.17**[130]with 4-bromo-2-methoxy-1-nitrobenzene (**6.18**) resulted in the dimethoxybiphenyl **6.19[6,7]**, which upon treatment with BBr₃ gave the desired diphenol **6.16[6,7]** in nearly quantitative yield, or 64% overall yield for two steps (Scheme 6.4.1.3.).
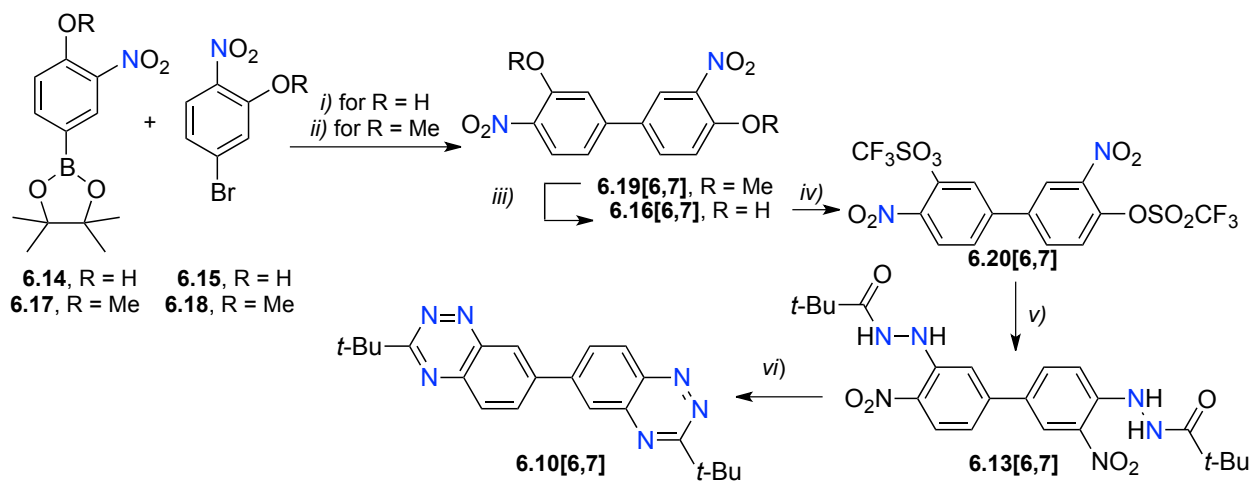
Scheme 6.4.1.3. Synthesis of bi-benzo[*e*][1,2,4]triazine **6.10[6,7]**. *Reagents and conditions*: (*i*) 1. Pd(dppf)Cl₂, KOAc, 1,4-dioxane, 110 °C, overnight, 2. NaIO₄, THF/H₂O (4:1), rt, 30 min, then HCl (drop), rt, 1h, <20% yield; (i*i*) Pd(dppf)Cl₂, KOAc, 1,4-dioxane, 110 °C, overnight, 66% yield; (*iii*) BBr₃, CH₂Cl₂, -70 °C then -30 °C, 96% yield; (*iv*) Tf₂O, Py, CH₂Cl₂, 0 °C, then rt, 20 h, 90% yield; (*v*) Pivalohydrazide, DMSO, 110 °C, 72 h, 71% yield; (*vi*) 1. Sn, AcOH, rt, overnight, then 115-120 °C, 8 h, 2. NaIO₄, MeOH/CH₂Cl₂ (1:1), rt, overnight, 55% yield.

The resulting biphenyl **6.16[6,7]** was converted to triflate **6.20 [6,7]** in 90% yield by treatment with fresh triflic anhydride in CH_2Cl_2 (Scheme 6.4.1.3.). The subsequent di-substitution reaction of **6.20[6,7]** with pivalohydrazide gave **6.13[6,7]** in 71% yield, which was converted to bi-benzo[*e*][1,2,4]triazine **6.10[6,7]** in 55% yield.

The requisite iodide **6.11a** was obtained using the literature[131] iodination of 2-fluoronitrobenzene (Scheme 6.4.1.4.). The reaction time was extended to 2 hr and the iodide was obtained in a nearly quantitative yield. Iodide **6.11b** was obtained from nitroaniline **6.21** using general conditions for the Sandmayer reaction.[132] Aniline **6.21** was prepared following a literature procedure,[133] while borolane **6.14** according to general reaction conditions[134] (Scheme 6.4.1.4.). Methylation of borolane **6.14** with MeI gave the reported[130] methoxy derivative **6.17**.
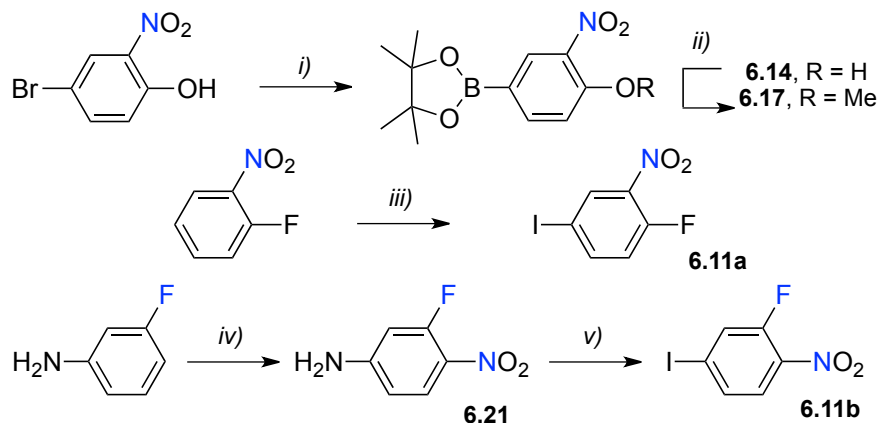

Scheme 6.4.1.4. Synthesis of key precursors. *Reagents and conditions*: *i*) bis(pinacolato)diboron, Pd(dppf)Cl$_2$, KOAc, 1,4-dioxane, 110 °C, overnight, 69% yield; *ii*) MeI, K$_2$CO$_3$, acetone, 99% yield; *iii*) *N*-iodosuccinimide, TfOH, rt, 2 h, 99% yield, ref.[131]; *iv*) 1. C$_6$H$_5$CHO, 80 °C, 1 h; 2. H$_2$SO$_4$, HNO$_3$, 0 °C, 1 h, 35% yield, ref.[133]; *v*) 1. NaNO$_2$, H$_2$O, H$_2$SO$_4$, 0 °C, 1 h, 2. KI, H$_2$O, 0 °C, 1 h, 82% yield.

X-ray crystallography

Black-green crystals of **6.8[m,n]** were grown by a liquid-liquid diffusion method using the CH_2Cl_2/hexane solvent system. Solid-state structures for all three compounds were determined by low temperature single-crystal X–ray diffraction methods. Crystals of **6.8[6,7]** were fragile and faintly diffracting. Despite the weaker data, the crystal structure determination was successful. Results are shown in Figures 6.4.1.2.–6.4.1.5., while full information is provided in the Experimental Section (Chapter 6.6.).

The diradicals **6.8[6,6]**, **6.8[6,7]** and **6.8[7,7]** form monoclinic crystals with the $P2_1/n$, $I2/a$ and $P2_1/c$ space group, respectively. Diradical **6.8[6,6]** is centrosymmetric with the inversion center located on the C(6)–C(6') bond, which, consequently leads to crystals with a half of the molecule in the asymmetric unit. In contrast, diradicals **6.8[6,7]** and **6.8[7,7]** contain two symmetry independent molecules in the asymmetric unit. Unique molecules of **6.8[7,7]** adopt similar conformations charactecrized by their superposition RMSD value of 0.14, while the difference in geometry of the two unique molecules of **6.8[6,7]** is defined by the RMSD value of 0.71. The individual benzo[*e*][1,2,4]triazinyl rings in all three diradicals are approximately planar with typical interatomic dimensions[28] (Figure 6.4.1.2.). The *t*-Bu group at the C(3) position adopts orientation roughly eclipsing the C(3)–N(2) bond. The only exception is one of the two unique molecules of **6.8[6,7]**, in which the *t*-Bu group is in a nearly ideal staggered orientation relative to the [1,2,4]triazine ring. The orientation of the N(1)–Ph ring relative to the [1,2,4]triazine is characterized by a typically high torsion angle between the Ph and [1,2,4]triazine planes, which ranges between 32° and 51° with an average of $44(6)^o$ for all three diradicals. The value for the analogous torsion angle found in **4.5**,[106] a close analogue of **6.8[7,7]**, is higher, 58.4^o. In each diradical both N(1)–Ph rings are oriented pseudo parallel to each other. These structural features are well reproduced in full geometry optimization at the UB3LYP/6-311(d,p) level of theory. DFT results demonstrate a nearly eclipsed conformation of the *t*-Bu group (the N(2)–C(3)–C–C angle of $\sim2^o$) and an average Ph/[1,2,4]triazine interplanar angle of $49.5(7)^o$ for all three diradicals.
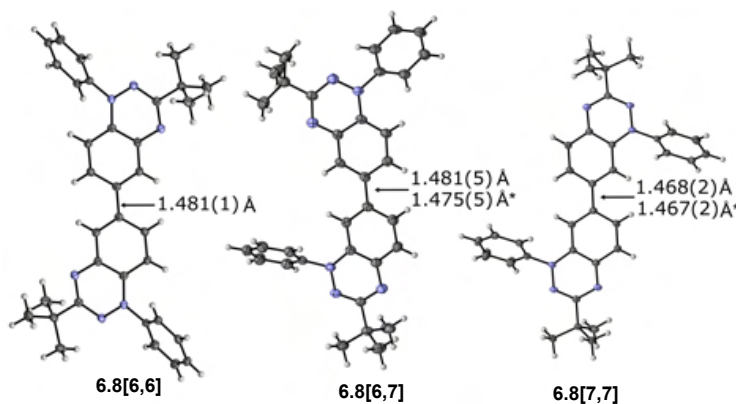

Figure 6.4.1.2. Molecular structures of **6.8[6,6]**, **6.8[6,7]** and **6.8[7,7]**. Atomic displacement ellipsoids are drawn at 50% probability level. For diradicals **6.8[6,7]** and **6.8[7,7]** only one molecule from the asymmetric unit is shown. Asterisk refers to the value for the second symmetry-independent molecule.

The C–C bond between two benzo[*e*][1,2,4]triazine units appears to decrease from 1.481(1) Å in **6.8[6,6]** to 1.467(2) in **6.8[7,7]** in response to the increasing tendency for spin pairing (Figure 6.4.1.2.). The last value compares favorably to 1.463(4) determined for the C(7)– C(7') distance in **4.5**,[106] and is longer than the Ph–Ph bond in Tschitschibabin's hydrocarbon **4.52** (1.448(4) Å),[135] but significantly shorter than that in biphenyl (1.493(3) Å).[136] This trend is well reproduced by the DFT method, which predicts a systematic decrease from 1.481 Å in **6.8[6,6]**, through 1.4775 Å in **6.8[6,7]** to 1.474 Å in **6.8[7,7]** with a simultaneous increase of Wiberg's bond order index from 1.050 to 1.076. The coplanarity between the benzo[*e*][1,2,4]triazine units, measured as an angle between the benzene rings planes, varies in the experimental structures from 0° (ideally coplanar) in **6.8[6,6]** to 7.2° and 24.8° in two unique molecules of **6.8[6,7]**. For **6.8[7,7]** this value is about 10° for both symmetry-independent molecules, while in **4.5** the two heterocycles are co-planar.[106] DFT modeling revealed higher interplanar angles, which decrease from 35.5° in **6.8[6,6]**, through 31.9° in **6.8[6,7]** to 31.2° in **6.8[7,7]**. This trend parallels that found for the C–C distance between the two heterocycles. A comparison of the experimental and DFT–calculated interplanar angles for Ph/[1,2,4]triazine and benzene/benzene rings indicate significant planarization of the structures in the solid-state, presumably due to crystal packing forces.

Molecular packing in the crystals of **6.8[6,6]** is the most interesting. Molecules are assembled in sheets with voids (meshes) extended parallel to the (110) plane (Figure 6.4.1.3a.), which are rotated by 39.9° relative to each other (Figure 6.4.1.3b.). In each sheet molecules interact through π⋅⋅⋅π contacts between phenyl groups of the adjacent molecules for which C⋅⋅⋅C nonbonding contacts are 0.066 Å shorter than the sum of Van der Waals (VdW) radii. Additionally, stacking interactions are supported by C–H⋅⋅⋅π interactions of the phenyl group and π–electron system of the benzo[*e*][1,2,4]triazine heterocycle. The resulting C(Ph)– H⋅⋅⋅C(8a)/C(8a') distances are 0.066 Å inside the VdW radii. Adjacent sheets are pinned through the C–H⋅⋅⋅π interactions between benzo[*e*][1,2,4]triazine C–H fragments and π-electron system of the phenyl group with the C(7)–H⋅⋅⋅C(Ph) contact of 0.038 Å inside the VdW radii. Additionally, the contact between sheets is augmented by the *t*-Bu groups filling the voids in the adjacent sheets.
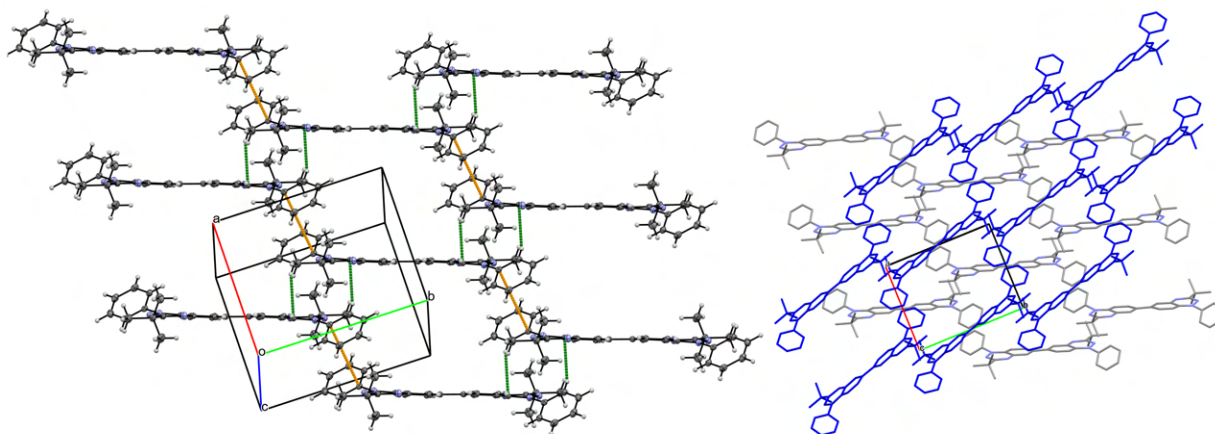
Figure 6.4.1.3. Left: single sheet formed by molecules of **6.8[6,6]** with marked intermolecular interactions: $\pi\cdots\pi$ interactions between phenyl groups of adjacent molecules (orange dotted lines) and C–H$\cdots\pi$ interactions (C(Ph)–H$\cdots$C(8a)/C(8a'), green dotted lines). Right: the relative orientation of the adjacent sheets in **6.8[6,6]**. Hydrogen atoms are omitted for clarity.
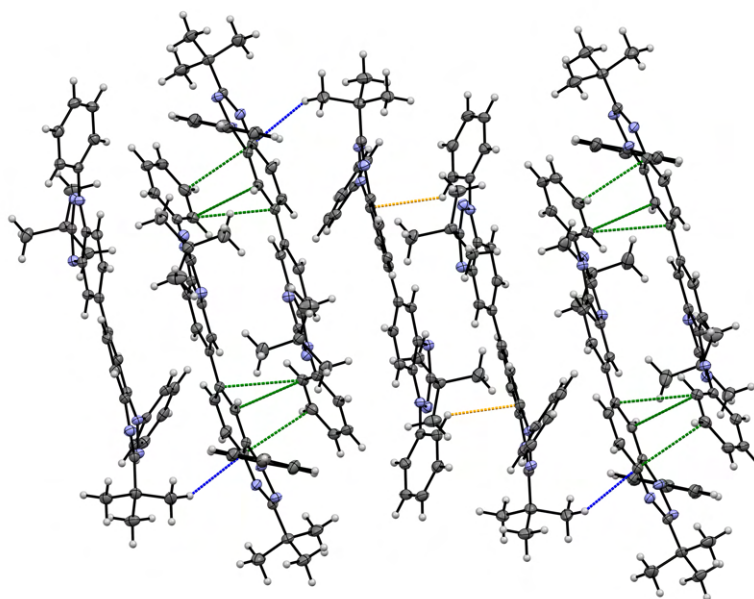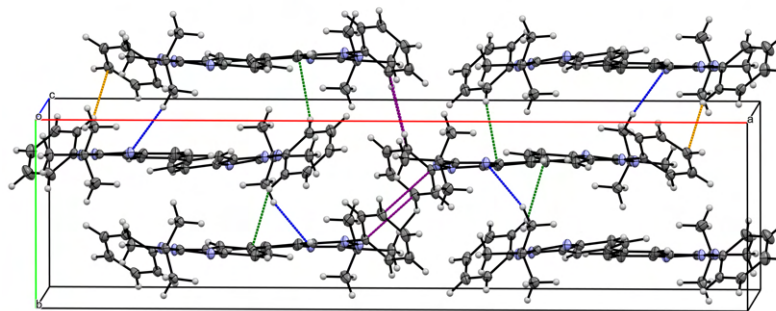

Figure 6.4.1.4. Partial packing diagram of **6.8[6,7]** with marked intermolecular interactions: $\pi\cdots\pi$ interactions between phenyl and benzo[*e*][1,2,4]triazine fragments characterized by C(Ph)$\cdots$C(4a), C(Ph)$\cdots$C(7) and C(Ph)$\cdots$C(8) contacts (green dotted lines); C–H$\cdots\pi$ interactions between the phenyl ring and the benzo[*e*][1,2,4]triazine core (C(Ph)-H$\cdots$C(8a)/(8a'), orange dotted lines); C–H$\cdots\pi$ interactions of *t*-Bu group and π-electron system of the core (blue dotted lines).

The crystal system of **6.8[6,7]** is maintained by many short contacts. Symmetry-independent molecules A and B form A···A and B···B discrete dimers. The A···A dimers are stabilized through π···π interactions between phenyl and benzo[*e*][1,2,4]triazine moieties characterized by C(Ph)···C(4a), C(Ph)···C(7) and C(Ph)···C(8) contacts of 0.202 Å, 0.140 Å and 0.170 Å shorter than the sum of the VdW radii, respectively. The shortest contacts in the B···B dimer involve the C–H···π interactions between the phenyl ring and the benzo[*e*][1,2,4]triazine core. The relevant C(Ph)–H···C(8a)/(8a') contact is 0.100 Å inside the VdW separation. Dimers A···A and B···B are connected through C–H···π interactions of the *t*-Bu group and the benzo[*e*][1,2,4]triazine moiety, which are 0.222 Å shorter than the sum of the VdW radii. These dimers are assembled one above another forming stacks extended in the [100] direction (Figure 6.4.1.4.).

Molecules of **6.8[7,7]** assembly in stacks extending along the *b* axis (Figure 6.4.1.5.). The stacks are formed through the C–H···N interactions between *t*-Bu groups and N(4) or N(4') atoms with contacts 0.088 Å and 0.100 Å shorter than the sum of the VdW radii, respectively. The association is augmented by C–H···π interactions between the phenyl rings (0.027 Å inside the VdW radii) and between a hydrogen of the N(1)–phenyl ring and π–electron system of the core (the C(Ph)–H···C(7)/C(7') and C(Ph)···C(8)/C(8') are 0.103 Å and 0.004 Å inside the the VdW radii, respectively). The neighboring stacks are connected through π···π interactions between phenyl groups of adjacent symmetry-equivalent molecules with the C···C contact of 0.061 Å shorter than the sum of the VdW radii.

Figure 6.4.1.5. Partial packing diagram of **6.8[7,7]** with marked intermolecular interactions: C–H···N interactions between the *t*-Bu group and N(4)/N(4') atoms (blue dotted lines); C–H···π interactions formed between phenyl rings (orange dotted lines), C–H···π interactions between a hydrogen of phenyl ring and π-electron system of the core (C(Ph)–H···C(7)/C(7)' and C(Ph)···C(8)/C(8'), green dotted lines); π···π interaction between phenyl groups (purple dotted line).

Electronic spectroscopy and electrochemistry

The impact of the regioconnectivity of the benzo[*e*][1,2,4]triazinyl units on electronic properties of diradicals **6.8[m,n]** was probed with spectroscopic and electrochemical methods.
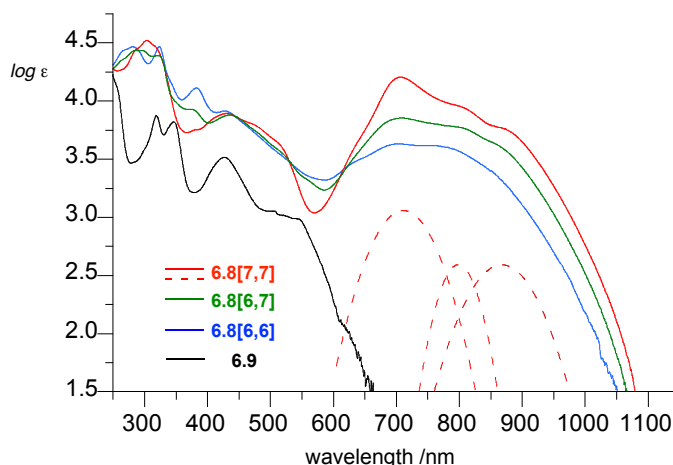
Figure 6.4.1.6. UV−vis–NIR absorption spectra of diradicals **6.8[m,n]** and monoradical **6.9** recorded in CH_2Cl_2. The doted lines represent a deconvoluted low energy portion of **6.8[7,7]** spectrum with arbitrary intensity.

UV-vis-NIR spectroscopy of diradicals **6.8[m,n]** revealed two broad, intense and poorly resolved multicomponent absorption bands in the visible range: up to 600 nm with maxima at about 430 nm and the second, above 600 nm tailing to nearly 1100 nm with maxima at about 710 nm (Figure 6.4.1.6., Table 6.4.1.1.). This is consistent with the reported $\lambda_{max} = 728$ nm for the C(3)–phenyl analogue **4.5**.[106] The intensity of the low energy band increases from **6.8[6,6]** to **6.8[7,7]**, which indicates increasing electronic communication and parallels trends in the bond distance and the degree of planarization between the heterocyclic units. A comparison of these spectra to that of the reference monoradical **6.9** demonstrates that the high energy band is related to excitations within individual benzo[*e*][1,2,4]triazinyl units, while the low energy absorption is unique to the diradicals. Deconvolution of the latter band revealed three components for **6.8[7,7]** (Figure 6.4.1.6.) and **6.8[6,7]**, and two components for **6.8[6,6]** (see Chapter 6.6.). Analysis shows that for diradicals **6.8[6,6]**, **6.8[6,7]**, and **6.8[7,7]** the lowest energy deconvoluted absorption bands are at 769, 884 and 868 nm respectively, while the most intense absorption peak in this spectral range is at 722, 726 and 711 nm, respectively.

Table 6.4.1.1. Selected experimental and calculated electronic parameters for diradicals **6.8[m,n]**.

| diradical	λ_{max} [a] /nm	λ_{max} [b] /nm	$E_g(opt)$ [c] /eV	$E_{\beta\text{-HOMO}}$ [d] /eV	$E_{\beta\text{-LUMO}}$ [d] /eV
6.8[6,6]	703	769	1.30	-6.24	-1.77
6.8[6,7]	709	884	1.29	-6.21	-1.80
6.8[7,7]	706	868	1.27	-6.22	-1.82

[a] Maximum of the lowest energy absorption band (recorded in CH_2Cl_2). [b] Maximum of the lowest energy deconvoluted absorption band. [c] Optical band gap calculated from the onset of absorption, l_{onset}. [d] Obtained at the TD-DFT UCAM-B3LYP/6-311++G(d,p) // UB3LYP/6-311G(d,p)level of theory for OSS in CH_2Cl_2 dielectric medium.

TD-DFT analysis performed at the UCAM-B3LYP/6-311++G(d,p) // UB3LYP/6-311G(d,p) level of theory suggests that the observed lowest energy absorption bands in OSS diradicals **6.8[m,n]** (calculated at 498 nm f = 0.112 for **6.8[6,6]**, at 507 nm f = 0.164 for **6.8[6,7]**, 521 nm f = 0.262 for **6.8[7,7]**,) involve mainly the HOMO→LUMO (40–60%) and HOMO→LUMO+1 (19–28%) transitions (Figure 6.4.1.7.) with approximately equal contribution from both electron manifolds in the symmetric diradicals. In contrast, this excitation in the unsymmetric diradical **6.8[6,7]** has a larger contribution from the β electron manifold than from the α, which coincides with slightly higher β-HOMO (localized on the C(7) connected ring) and β-LUMO (localized on the C(6) connected ring) by 36 and 14 meV, respectively, relative to the α-FMOs. This double HOMO to double LUMO excitation is characteristic for diradicals. In general, in the series **6.8[6,6]**, **6.8[6,7]**, and **6.8[7,7]** the energy of this excitation decreases, the intensity increases and the percentage of the HOMO→LUMO transition increases at the expense of the HOMO→LUMO+1 transition.
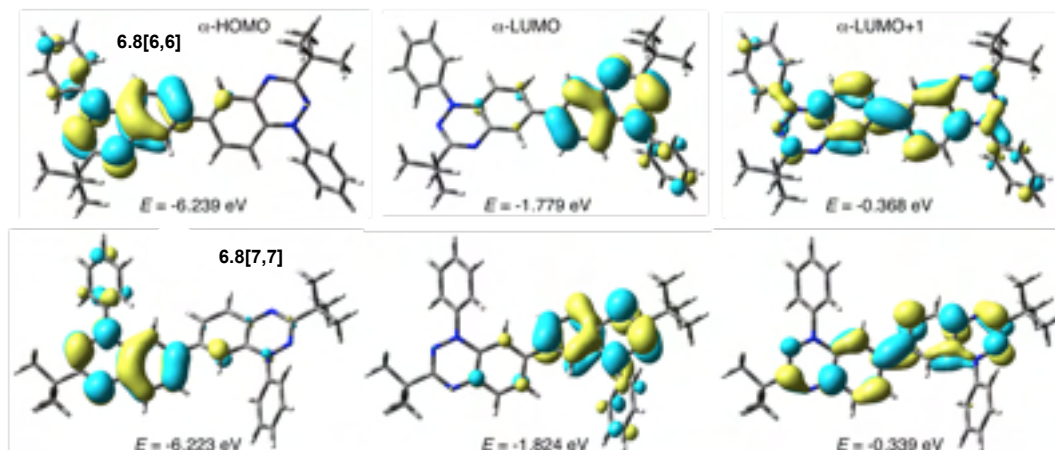
Figure 6.4.1.7. TD-DFT-derived contours and energies of the α-HOMO (left), α-LUMO (middle) and α-LUMO+1 (right) for OSS **6.8[6,6]** (top) and **6.8[7,7]** (bottom). MO isovalue = 0.03, density = 0.0004.

Electrochemical analysis confirmed strong electronic interaction between the two benzo[*e*][1,2,4]triazinyl units in **6.8[m,n]**. Thus, cyclic voltammetry (CV) and differential pulse voltammetry (DPV) analyses revealed that all three diradicals **6.8[m,n]** exhibit two quasi-reversible one-electron oxidation processes with similar half-wave potentials $E_{1/2}^{0/+}$ at about -0.30 V and $E_{1/2}^{+/+2}$ at -0.05 V *vs* Fc/Fc$^+$ with separation of about 0.25 V (Figure 6.4.1.8. and Table 6.4.1.2.). This indicates similar electronic communication between two benzo[*e*][1,2,4]triazine units in all three isomers. Reduction of the diradicals also exhibits two quasi-reversible although less separated processes, at about -1.4 and -1.5 V *vs* Fc/Fc$^+$. A comparison of these potentials to those reported[40] for the monoradical **6.9** demonstrates that $E_{1/2}^{0/+}$ of the diradicals is shifted cathodically by about 0.04, while the $E_{1/2}^{-/0}$ appears to be shifted anodically, resulting in an overall smaller-than-typical[16] ΔE_{cell}, consistent with a low optical band gap of about 1.3 eV (Table 6.4.1.2.). This suggests that connecting of two monoradicals **6.9** and formation of diradicals **6.8[m,n]** shifts the FMO's to higher energies. Inspection of the MOs indicates that the HOMO for **6.8[6,6]**, **6.8[6,7]** and **6.8[7,7]** is indeed higher by 25, 52 and 40 meV than the SOMO for **6.9**, which correlates with the more cathodic $E_{1/2}^{0/+}$ potentials.
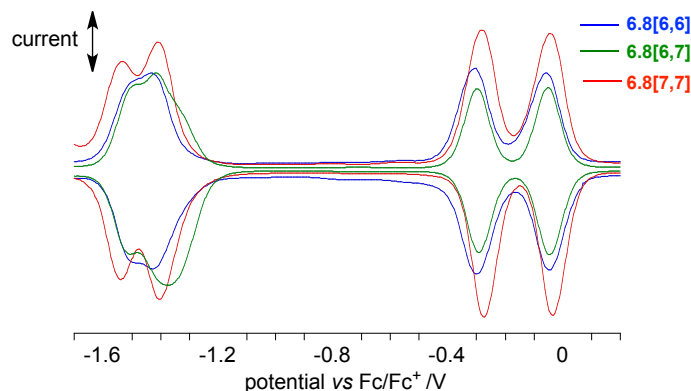
Figure 6.4.1.8. Differential pulse voltammograms (DVP) of diradicals **6.8[m,n]** in 0.1 M [Bu$_4$N]$^+$PF$_6^-$ in CH$_2$Cl$_2$. Scan rate 5 mV s^{-1}. For details see the Experimental Section (Chapter 6.6.).

Table 6.4.1.2. Electrochemical data for diradicals **6.8[m,n]** and monoradical **6.9**.

diradical	$E_{1/2}^{2-/-}$ [a] /V	$E_{1/2}^{-/0}$ [a] /V	$E_{1/2}^{0/+}$ [a] /V	$E_{1/2}^{+/2+}$ [a] /V	$\Delta E_{cell(1)}$ [b] /V
6.8[6,6] [c]	-1.49	-1.43	-0.30	-0.06	1.13
6.8[6,7] [c]	-1.53	-1.40	-0.28	-0.04	1.12
6.8[7,7] [c]	-1.52	-1.37	-0.30	-0.05	1.07
6.9 [d]	–	-1.49 [e]	-0.26	–	–

[a] Potentials *vs.* Fc/Fc$^+$ couple (0.46 V *vs.* SCE).[137] Recorded in CH$_2$Cl$_2$ with [*n*-Bu$_4$N]$^+$[PF$_6$]$^-$ (100 mM), at *ca.* 20 °C, 5 mV s^{-1}, glassy carbon working electrode. [b] $\Delta E_{cell(1)} = E_{1/2}^{+/0} - E_{1/2}^{-/0}$. [c] Potentials from DPV. [d] Potentials from CV; ref[40] [e] Irreversible reduction. Cathodic peak potential.

Redox properties of **6.8[7,7]** are significantly different from those measured for the C(3)–Ph analogue **4.5** under comparable conditions.[106] Thus, the oxidation half-wave potentials $E_{1/2}^{0/+}$ and $E_{1/2}^{+/+2}$ are about 0.6 V more anodic for **4.5** than for **6.8[7,7]**, which seems too high considering that the replacement of the C(3)–Ph in the prototypical Blatter radical with the C(3)–*t*-Bu in **6.9** lowers $E_{1/2}^{0/+}$ by 0.06 V,[40] and connecting two radicals **6.9** lowers further the first oxidation potential by 0.04 V. Thus, it is likely, that the half-wave potentials for **4.5** are reported *vs* SCE, not *vs* Fc/Fc$^+$ (0.46 V *vs* SCE), as claimed in the report.[106] The reduction reported[106] for **4.5** at $E_{1/2}^{-/0}$ = -0.17 V is too anodic relative to the analogous value for **6.8[7,7]** ($E_{1/2}^{-/0}$ = -1.37 V *vs* Fc/Fc$^+$). The $E_{1/2}^{-/0}$ value expected for **4.5** should be at about -1.25 V.

The S–T energy gap

EPR spectroscopy of solid solutions of diradicals **6.8[m,n]** in polystyrene demonstrated signals characteristic for a triplet state with some doublet impurities (Figure 6.4.1.9.). The signal intensity was increasing with increasing temperature, which is consistent with an open-shell singlet ground state. Since none of the diradicals showed the forbidden $|\Delta m_s| = 2$ transition, the analysis focused on the relative intensity of the $|\Delta m_s| = 1$ EPR signal, $DI_{(rel)}$, obtained by double integration and normalization of spectra measured in a temperature range 120–340 K. The signal intensity as a function of temperature, $DI_{rel}T(T)$, was analyzed on the basis of Heisenberg Hamiltonian for two electron system, $\hat{H} = -2J\hat{S}_1 \cdot \hat{S}_2$, using a modified Bleaney-Bowers[88] equation (eq 6.4.1.1.).

$$\chi T = \frac{Ng^2\mu_B^2}{k}\left(\frac{2}{3+e^{-\frac{2J}{kT}}}\right)(1-\rho) + \frac{Ng^2\mu_B^2}{2k}\rho \qquad \text{(eq 6.4.1.1.)}$$

Numerical fit of the $DI_{rel}T(T)$ data to a three parameter function (eq 6.4.1.1.) gave the energy difference $\Delta E_{\text{S-T}} = 2J$ between the singlet and triplet states -0.81(1), -1.13(2), -1.33(8) kcal mol^{-1} for diradicals **6.8[6,6]**, **6.8[6,7]**, and **6.8[7,7]**, respectively (Table 6.4.1.3.). The last value is in a good agreement with that reported for the C(3)–Ph analogue **4.5** (ΔE_{ST} = -1.27 kcal mol^{-1}) measured in a benzophenone solution.[106]

Table 6.4.1.3. Results of VT EPR analysis and DFT calculations of diradicals **6.8[m,n]**.

6.8[m,n]		ΔE_{ST} /kcal mol^{-1}		ΔE_{OS-CS} /kcal mol^{-1}	y_0 [c]	$\|D/hc\|$ /cm^{-1} ×10^{-3}	$\|E/hc\|$ /cm^{-1} ×10^{-4}
	exp	DFT[a]	DFT[b]	DFT[b]			
6.8[6,6]	-0.81(1)	-0.18	-0.30	-6.02	0.99	7.97	5.55
6.8[6,7]	-1.13(2)	-0.74	-1.19	-8.64	0.94	5.44	5.58
6.8[7,7]	-1.33(8)	-1.12	-1.89	-6.95	0.81	4.44	11.4

[a] Adiabatic $\Delta E_{ST} = E_S - E_T$ obtained with the spin-flip non-collinear time-dependent DFT (SF-NC-TDDFT) using PBE5050/6-311G(d,p) // UB3LYP/6-311G(d,p) level with the ZPE correction. [b] Adiabatic ΔE_{ST} with ZPE correction obtained with the Yamaguchi formalism[138] at the UB3LYP/6-311G(d,p) level. [c] Adiabatic energy difference between the OSS and CS states. [d] PUHF/6-311G(d) // BS-UB3LYP/6-311G(d,p) method. For details see the ESI. For details see the Experimental Section (Chapter 6.6.).
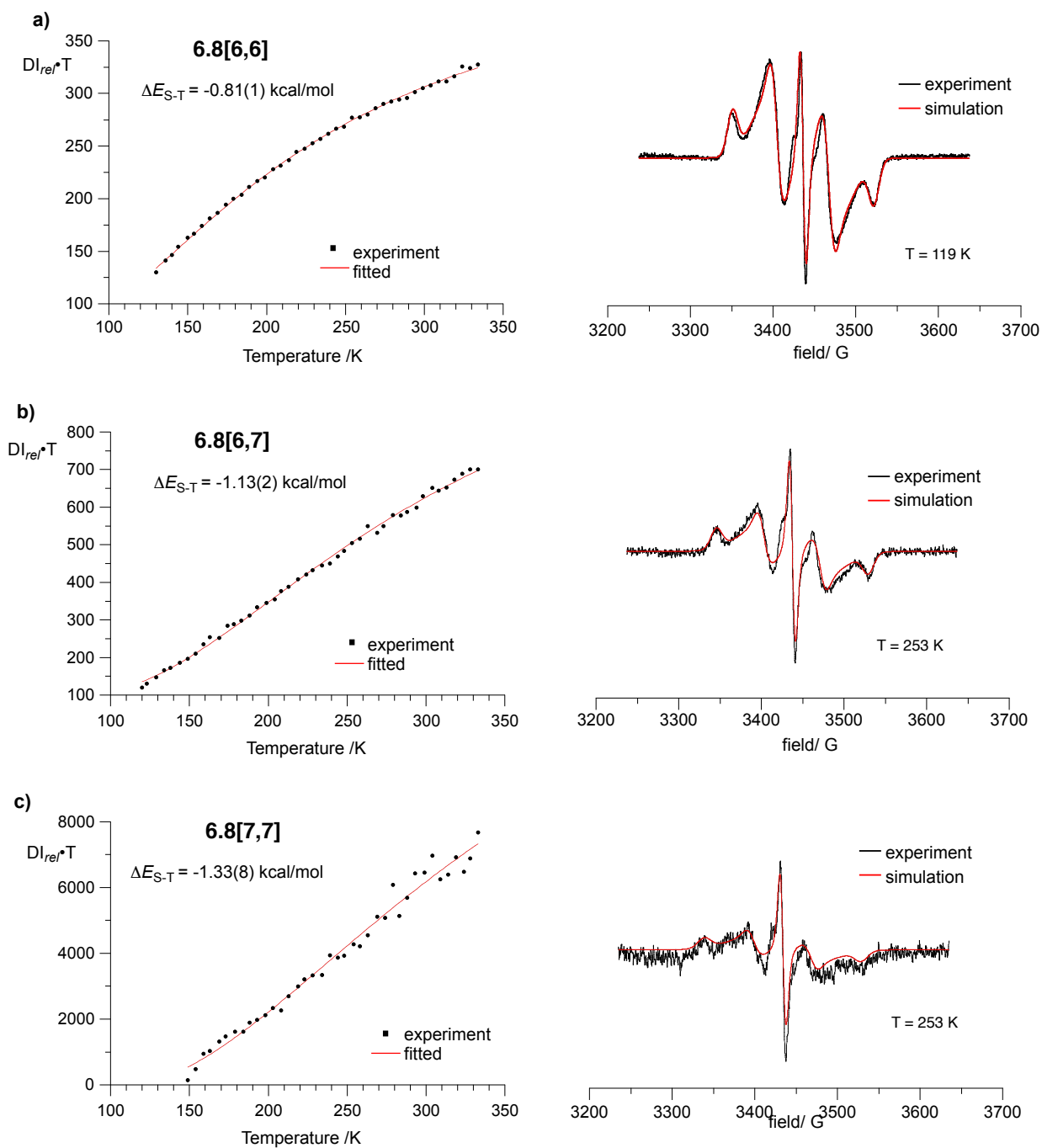
Figure 6.4.1.9. Left: Experimental (black dots) $DI_{rel}T(T)$ curves for **6.8[6,6]** (a), **6.8[6,7]** (b) and **6.8[7,7]** (c) obtained from VT EPR spectra in polystyrene solid solutions. The red lines represent fitting experimental data to the Bleaney-Bowers model (eq 6.4.1.1.). Right: experimental (black) and simulated (red) EPR spectra of **6.8[m,n]** in polystyrene solid solutions.

Analysis of the triplet spectra of diradicals **6.8[m,n]** provided the zero-field splitting (*zfs*) parameters $|D/hc|$ and $|E/hc|$ (Table 6.4.1.3.). The former increases in the series from 7.97×10^{-3} cm^{-1} to 8.80×10^{-3} cm^{-1}, which indicates increasing spin separation from 8.7 Å in **6.8[6,6]** to 9.9 Å in **6.8[7,7]**, according to the point-dipole approximation model. The DFT spin maps for two diradicals are shown in Figure 6.4.1.10.

6.8[6,6]   **6.8[6,7]**
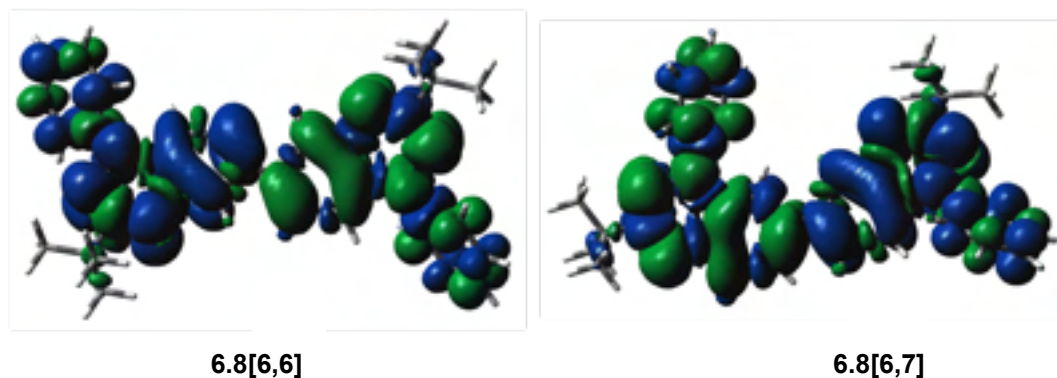
Figure 6.4.1.10. TD-DFT-derived spin density map for OSS **6.8[6,6]** and **6.8[6,7]** (isovalue =0.0004).

DFT calculations confirmed the open-shell singlet (OSS) character of diradicals **6.8[m,n]** showing that the closed-shell singlet (CS) is 6–8.6 kcal mol^{-1} higher that the OSS state. The S–T energy gaps, ΔE_{S-T}, for series **6.8[m,n]** calculated using two approaches, give the same trends consistent with the experimental results (Table 6.4.1.3.). The spin-flip non-collinear time-dependent DFT method[139] underestimated the ΔE_{S-T} for all diradicals **6.8[m,n]**, while the Yamaguchi formalism[138] gave closer energies for **6.8[6,6]** and **6.8[6,7]** and overestimated for the **6.8[7,7]** isomer (Table 6.4.1.3.). Similar results were reported for the C(3)–Ph analogues of **6.8[m,n]** using DFT and CASSCF methods, which concluded a slightly better performance of the traditional BS-DFT approach.[140]

The order of ΔE_{S-T}, energies parallels the trend in the diradicaloid character of **6.8[m,n]**. Thus, increasing ΔE_{S-T} in the series is paralleled by decreasing diradicaloid index y_0 from 0.99 for nearly pure OSS in **6.8[6,6]** to 0.81 in **6.8[7,7]**, and the decreasing C–C distance, which indicates an increasing magnetic coupling between the benzo[*e*][1,2,4]triazinyl units in the series. These results and trends are consistent with those recently observed for another series of diradicaloids.[141]

Fine tuning of the S–T energy gap

The progressively stronger magnetic and electronic coupling in the series **6.8[6,6]**, **6.8[6,7]** and **6.8[7,7]** is related to the higher spin density at the C(7) position than in the C(6) (0.07 *vs* 0.04, Figure 4.2.4.1.), and the less favorable resonance form for the CS singlet state involving a zwitterionic structure for the C(6) connected heterocycle (Figure 6.4.1.11.). The appearance of the zwitterionic resonance form in **6.8[6,6]** and **6.8[6,7]** opens up a possibility of fine tuning of the $\Delta E_{\text{S-T}}$ and y_0 parameters in these diradicals by judicious choice of the N(1) and C(3) substituents affecting stability of charge polarization in the [1,2,4]triazine ring. DFT calculations for a series of **6.8[6,7]** derivatives demonstrate that this indeed is the case. Thus, changing the N(1)–Ph substitunet in **6.8[6,7]** to an electron withdrawing N(1)–(2-Pyridyl) destabilizes the OSS state and narrows the $\Delta E_{\text{S-T}}$ gap by 0.11 kcal mol^{-1}, while an electron donating group, Ar = PhNMe$_2$-4, opens it up by 0.06 kcal mol^{-1} (Figure 6.4.1.11.). A smaller effect is observed when the C(3)–*t*-Bu group is replaced with R = CF$_3$ or R = NMe$_2$: the former slightly destabilizes and the latter stabilizes the OSS state by about 0.03 kcal mol^{-1}. Finally, using a combination of N(1) and C(3) substituents a synergistic effect can be obtained in the case of R = CF$_3$, Ar = PhNMe$_2$-4 (change by 0.08 kcal mol^{-1}), while no such a synergistic effect is observed for a combination of R = NMe$_2$ and Ar = 2-Pyridyl. Stronger substituent effects are expected for derivatives of **6.8[6,6]**, in which both [1,2,4]triazinyl rings experience significant charge polarization in the CS state. These derivatives are easily synthetically available using general intermediates **6.12[m,n]** or **6.20[m,n]** and methods developed for substituting amino, alkyl, aryl and CF$_3$ groups in the C(3) position[40] and aryl and hetaryl with different electronic properties[44] at the N(1) positions of the benzo[*e*][1,2,4]triazinyl ring.
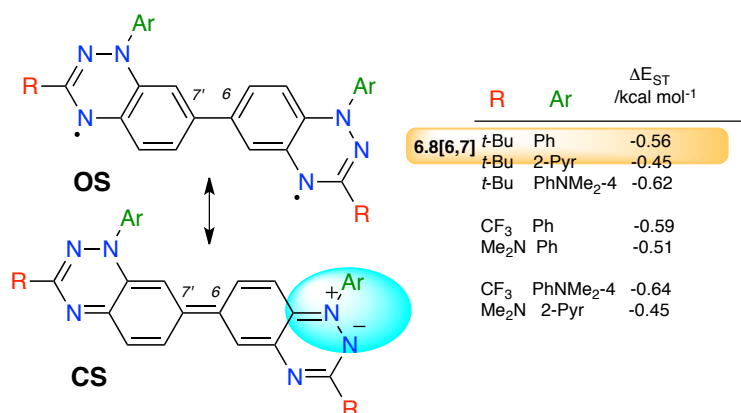
Figure 6.4.1.11. Open-shell (OS) and closed-shell (CS) resonance forms for **6.8[6,7]** and DFT-calculated $\Delta E_{\text{S-T}}$ with the Yamaguchi formalism[138] at the UB3LYP/6-311G(d,p) level of theory.

Stability of diradicals 6.8[m,n]

Thermogravimetric analysis (TGA) of three diradicals **6.8[m,n]** revealed minimal mass loss up to nearly 300 °C (Figure 6.4.1.12.). Differential analysis of the TGA curves indicates the onset of a major mass loss at about 270 °C for **6.8[6,6]** and **6.8[6,7]**, and at lower temperature, 255 °C for **6.8[7,7]** with the peak at about 315 °C for all three diradicals (For details see Experimental Section Chapter 6.6.).
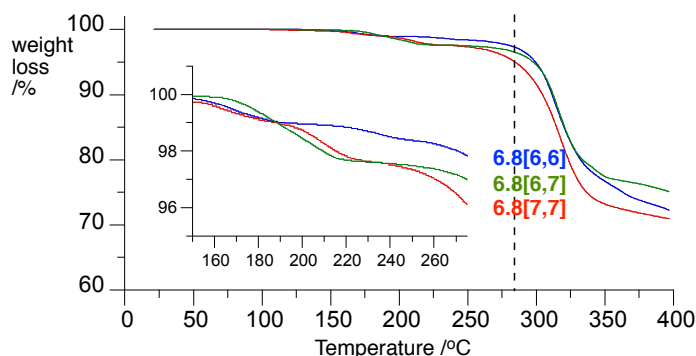
Figure 6.4.1.12. Thermogravimetric analysis of **6.8[m,n]**. Heating rate 10 K min^{-1}.

Photostability of diradicals **6.8[m,n]** was investigated using a broad-band unfiltered halogen light. Thus, irradiation of 1.0×10^{-4} M solutions in CH_2Cl_2 in a quartz cuvette opened to air led to a slow decrease of the absorption band at about 700 nm and appearance of new, higher energy bands at about 580 and 630 nm for **6.8[6,6]** and **6.8[6,7]** (Figure 6.4.1.13.). The rate of the photo bleaching monitored at 705 nm decreases in the order **6.8[7,7]** ($-0.019(1)$ h^{-1}) > **6.8[6,7]** ($-0.0079(2)$ h^{-1}) > **6.8[6,6]** ($-0.0072(3)$ h^{-1}). This trend parallels that of the magnitude of extinction coefficients in the diradicals. When normalized for the initial optical density at 705 nm, all three diradicals exhibit similar bleaching rate. The half-life for the process appears to be shortest for the **6.8[6,6]** isomer ($t_{1/2} = 25$ h) and longest for the **6.8[6,7]** isomer ($t_{1/2} = 36$ h). For **6.8[7,7]** $t_{1/2} = 33$ h.
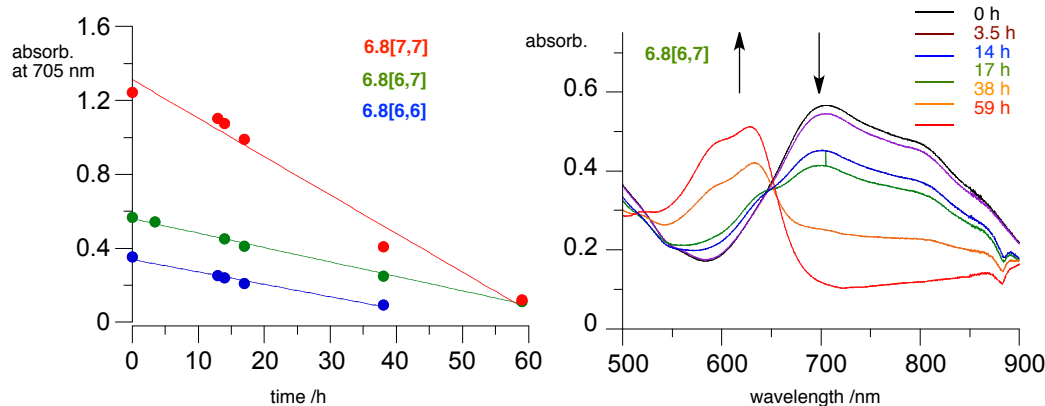
Figure 6.4.1.13. Photostability of **6.8[m,n]** in CH_2Cl_2 (1.0×10^{-4} M) irradiated with unfiltered 400 W halogen lamp light in a 10 mm quartz cuvette. Left: rate of bleaching at 705 nm. Right: spectral changes in **6.8[6,7]**.

Conclusions

A concise and efficient strategy for the preparation of open-shell singlet bi-benzo[*e*][1,2,4]triazin-4-yl diradicals with high chemical stability and variable ΔE_{S-T} has been demonstrated. The presented three prototypical diradicals **6.8[m,n]** containing the *t*-Bu group at the 3 and 3' positions demonstrate that the regioconnectivity has a significant impact on their diradical character and is related to the total spin concentration at the connecting sites C(6) and C(7) of the benzo[*e*][1,2,4]triazin-4-yl units. Thus, as the total spin density increases from 0.08 in the C(6)–C(6') connected diradical **6.8[6,6]** to 0.14 in the C(7)–C(7') isomer **6.8[7,7]**, the S–T separation increases from -0.81 to -1.33 kcal mol^{-1} and diradicaloid index y_0 decreases from 0.99 to 0.81. These trends in electronic and magnetic communication between the two radical sites are consistent with those for structural parameters (XRD) and the progressive hyperchromic shift in the series **6.8[m,n]** observed in the UV-vis-NIR spectra.

Results for diradicals **6.8[m,n]** demonstrate that in contrast to the 3,3'-diphenyl derivative **4.5**, they exhibit all four well-defined quasi-reversible one-electron redox processes, which is desired for electronic applications. They also exhibit one of the smallest S–T separations and the highest *y* indices among benzo[*e*][1,2,4]triazin-4-yls, with high chemical stability. These favorable electronic properties combined with potentially easily modifiable electronic structures of bi-Blatter diradicals constitute an attractive direction for the development of materials with tunable properties for emerging applications.

The presented synthetic strategy opens up convenient access to a range of diradicals with properties tailored by judicious choice of substituents at the N(1) and C(3) positions, including C(3)–C(3')-heterodisubstituted derivatives with a push-pull effect, using general intermediates **6.12[m,n]** and **6.19[m,n]**. This provides additional means for fine-tuning of the $\Delta E_{\text{S-T}}$ and in such bi-Blatter diradicals of the general structure **6.8[m,n]**. The described methodology and intermediate **6.12[6,6]** have already been used for the preparation of diradicals of the general structure **O** with cathodically shifted oxidation potentials, bathochomically shifted absorption bands and higher stability of the OSS state that those for **6.8[6,7]**.
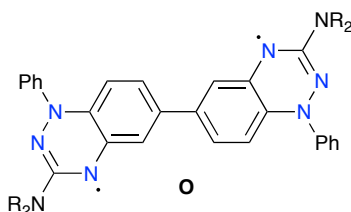
6.4.2. Blatter diradicals with a spin coupler at the N(1) position

Results of this work were analyzed, described and currently are under publication process. My contribution to this publication consisted of: development of synthetic methods, synthesis and characterization of precursors and final products, performing Cyclic and Differential Pulse Voltammetry, UV-vis spectroscopy and Variable-Temperature Electron Paramagnetic Resonance Spectroscopy measurements, simulation of EPR spectra using Easy Spin, describing results, preparation of Experimental Part and Electronic Supporting Information of the manuscript, partial preparation and revision of manuscript. Pomikło, D.; Kaszyński, P. "Blatter diradicals with a spin coupler at the N(1) position" *Chem. Eur. J.* **2023**, (Accepted Manuscript). doi.org/10.1002/chem.202301069

Herein an investigation of a new paradigm in air stable diradicals with controllable S–T energy gap, $\Delta E_{S\text{-}T}$, by using spin coupling units, SC, connecting to the most spin rich N(1) position of each radical is presented. This Chapter reports a convergent and efficient synthesis and also extensive characterization of two prototypical diradicals **6.22p** and **6.22m** (Figure 6.4.2.1.) by spectroscopic and electrochemical methods. Experimental results for the diradicals are compared to those for the analogous monoradical **6.23** and are augmented with density functional theory (DFT) analysis. The latter includes DFT calculations of the $\Delta E_{S\text{-}T}$ for **6.22** and several related diradicals with different SC units.
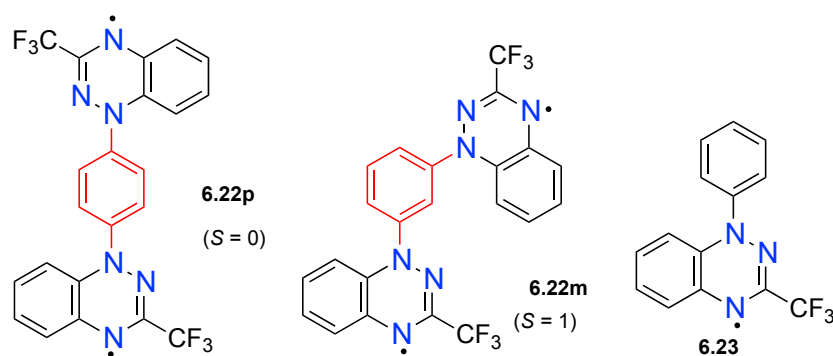
Figure 6.4.2.1. Structure of diradicals **6.22p** and **6.22m**, and monoradical **6.23**.

Synthesis of radicals

Diradicals **6.22p** and **6.22m** were obtained in 56% and 32% yield, respectively, using azaphilic addition[34, 44] of dilithiobenzene, generated from appropriate diiodobenzene and *t*-BuLi, to the readily available[125] benzo[*e*][1,2,4]triazine **3** and subsequent aerial oxidation of the resulting dianions (Scheme 6.4.2.1.). For comparison purposes, monoradical **6.23** was obtained by reacting **6.24** with PhLi.[34, 125] The CF$_3$ group at the C(3) position is intended to enhance solubility of the diradicals.
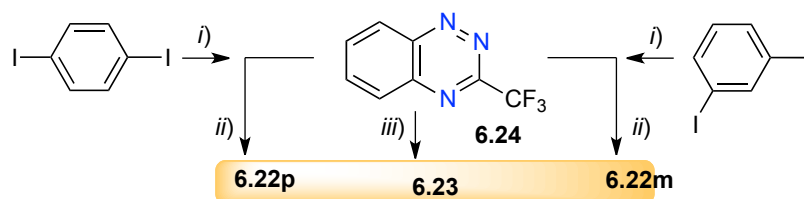

Scheme 6.4.2.1. Preparation of diradicals **6.22** and radical **6.23**. Reagents and conditions: *i*) *t*-BuLi, THF, -78°C, 40 min; *ii*) 1. THF, -78 °C, 50 min, 2. rt, 40 min, 3. rt, air, overnight, yield 56% **6.22p** and 32% **6.22m**. *iii*) 1. PhLi, THF, -78 °C, yield 81%, ref [34].

**Molecular geometry and conformational preference**

All attempts at obtaining single crystals of **6.22p** and **6.22m** suitable for single crystal X-ray structural analysis were unsuccessful. Therefore molecular structures of the two diradicals were obtained at the UB3LYP/6-31G(2d,p) level of theory and results are shown in Figure 6.4.2.2. Such a computational analysis appears more relevant to solid solutions presently investigated (*vide infra*) than the solid-state structures.

Geometry optimization of **6.22p** in the open-shell singlet (OSS) configuration and limited conformational search gave the most thermodynamically stable structure with two benzo[*e*][1,2,4]triazine (BT) systems nearly coplanar and relative *anti* orientation. The connecting 1,4-phenylene linker is twisted out of plane forming a dihedral angle C(8a)–N(1)–C$_{Ph}$–C$_{Ph}$ of 49° for the triplet state, 42° for the open-shell singlet, and 28° for the zwitterion, with both heterocycles. At the same time, the N(1)–C$_{Ph}$ distance is contracting from 1.425 Å, through 1.416 Å to 1.381 Å in the zwitterion. This is consistent with the progressive tendency for a more effective π–π overlap and formation of a closed-shell structure as shown in Figure 6.4.2.3.

6.22p-S   **6.22m-T**
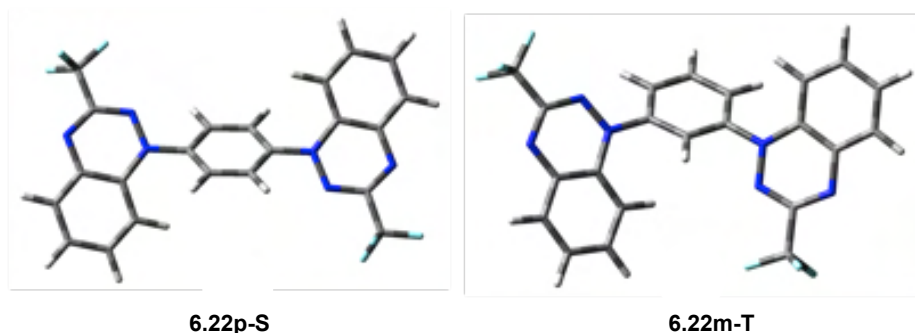
Figure 6.4.2.2. Optimized geometries for **6.22p-OSS** and **6.22m-T** in gas phase at the UB3LYP/6-31G(2d,p) level of theory.

Similar analysis for the *meta* isomer **6.22m**, optimized in the triplet state (T) revealed a non-planar structure with the relative *anti* orientation of the BT heterocycles in the most stable conformer (Figure 6.4.2.2.). The central 1,3-phenylene linker forms dihedral angles C(8a)–N(1)–C_{Ph}–C_{Ph} 47.6° and 43.6° in the triplet state, and 49.0° and 45.0° for the open-shell singlet. The N(1)–C_{Ph} bonds remain essentially the same for both open-shell structures, ~1.425 Å.
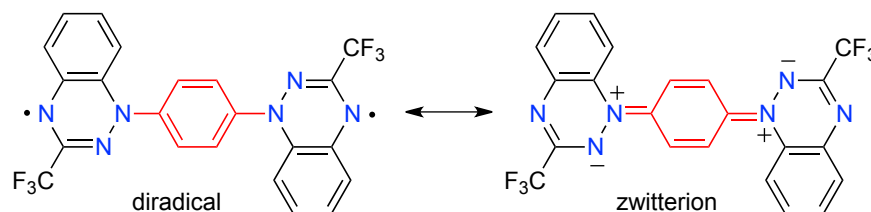
Figure 6.4.2.3. Two resonance forms for **6.22p**.

Spectroscopic and electrochemical characterization

The electronic structure of the two isomeric radicals was probed with optical and electron paramagnetic resonance (EPR) spectroscopy and also electrochemical analysis. Spectroscopic investigation demonstrated that the UV-vis spectrum of *meta* isomer **6.22m** is similar to that of the monoradical **6.23** although more intense (two BT chromophores in **6.22m** instead of one in **6.23**) and red shifted by about 25 nm (Figure 6.4.2.4.). In contrast, the electronic spectrum of the *para* isomer **6.22p** exhibits a significantly stronger absorption in the visible range tailing to the near IR region. These observed hyperchromic and bathochromic shifts are consistent with stronger electron delocalization. Deconvolution of the broad absorption in **6.22p** with a maximum at 593 nm (*log* e = 3.75) revealed two medium intensity bands at λ_{max} = 598 nm and 732 nm.
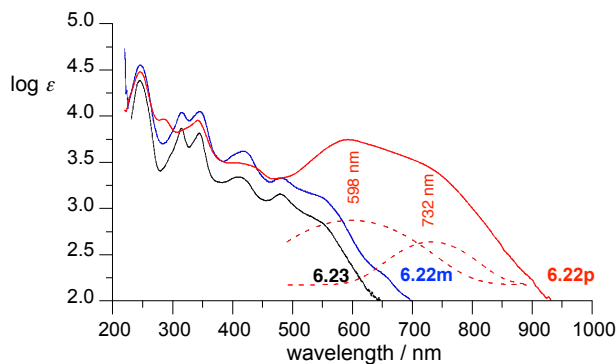
Figure 6.4.2.4. UV-vis absorption spectra for diradicals **6.22p** (red) and **6.22m** (blue) and monoradical **6.23** (black) in CH_2Cl_2. The red dotted lines represent a deconvoluted portion of spectrum of **6.22p** with indicated positions of the maxima.

Time-dependent DFT (TD–DFT) analysis indicates that the two lowest energy excitations in the open-shell singlet **6.22p-OSS** with a significant oscillator strength (calculated at 500 nm f = 0.196 for state 1 and 462 nm f = 0.222 for state 4) involve mainly the HOMO→LUMO+1 (38% in the former and 48% in the latter) and, to a lesser extent, HOMO→LUMO and HOMO-1→LUMO transitions (Figure 6.4.2.5.) with equal participation of both electron manifolds. Such double (HOMO,HOMO to LUMO,LUMO) excitations are characteristic for singlet biradicals and biradicaloids with significant resonance structures involving the p bridge joining the spin centers, such as in **6.22p**. In contrast, this behavior is not observed when the π bridge is connected to the nodal position of a spin system.[142]

The same analysis for the meta isomer **6.22m-T** revealed higher energy excitations with over an order of magnitude lower oscillator strength and involving mainly (~75%) the α electron manifold with the dominant α-HOMO→ α-LUMO and α-HOMO–1→ α-LUMO transitions for state 1 (491 nm f = 0.011) and α -HOMO-1→ α-LUMO+1 and α-HOMO→ α-LUMO+1 transitions for state 2 (490 nm f = 0.010). Transitions in the β electron manifold are prominent (about 70%) in the next two excitations involving the β-HOMO–1→ β-LUMO, β-HOMO→ β-LUMO and β-HOMO→ β-LUMO+1 transitions in states 3 and 4 (443 nm f = 0.036, and 440 nm f = 0.081). Excitation with a significant oscillator strength is found in state 10 with energy of 321 nm. This behavior is similar to that found in monoradical **6.23**, in which the lowest energy excitation at 503 nm (f = 0.003) is solely due to the α-HOMO→ α-LUMO transition (84%) and the next lowest excitation at 431 nm (f = 0.054) is due to the β-HOMO→ β-LUMO transition

(77%). Like in **6.22m-T**, the first excitation with a significant oscillator strength has high energy (316 nm). These results are consistent with the experimental data.
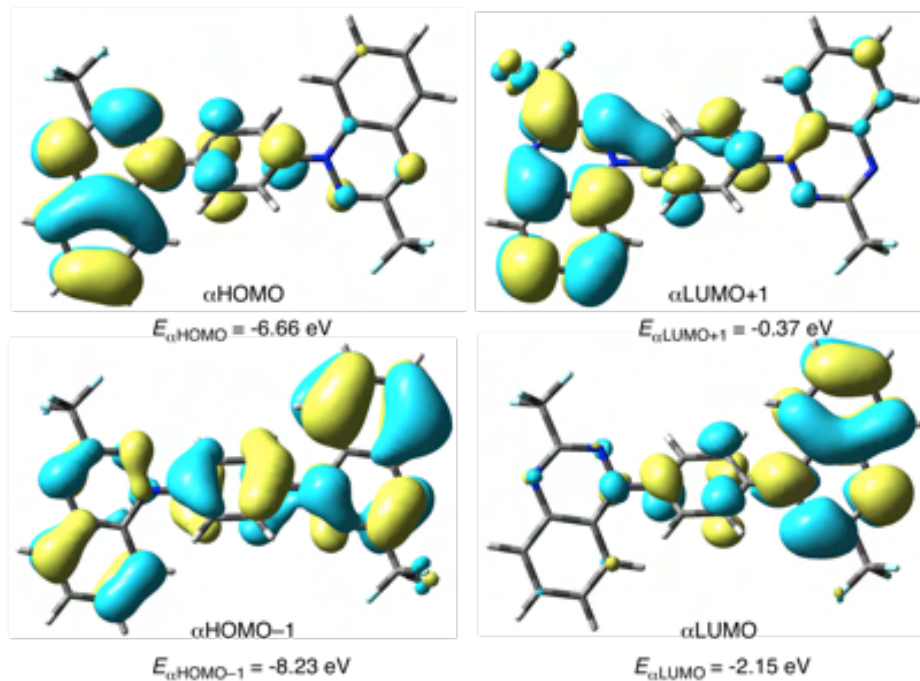
Figure 6.4.2.5. DFT-derived contours and energies of the a-MO relevant to low energy excitations in open-shell singlet **6.22p-OSS**. MO isovalue = 0.02, density = 0.0004.

Analysis of the solvent effect on the electronic spectrum of **6.22p** revealed a modest positive solvatochromic effect indicating slightly more polar excited state that the ground state. For instance, maximum of absorption in Et_2O ($E_T30 = 34.5$ kcal mol^{-1}) at 582.2 nm shifts to 598.8 nm in DMSO ($E_T30 = 45.1$ kcal mol^{-1}).

Evidence for strong electronic communication in both isomers **6.22p** and **6.22m** was provided by electrochemical analysis. Cyclic voltammetry (CV) aided with differential pulse voltammetry (DPV) conducted in CH_2Cl_2 solutions revealed two distinct quasi-reversible reduction processes, $E_{1/2}^{-1/0}$ and $E_{1/2}^{-2/-1}$, separated by 0.29 (**6.22p**) and 0.24 V (**6.22m**, Figure 6.4.2.6, Table 6.4.2.1.). In contrast, anodic scan revealed a single, two-electron quasi-reversible oxidation process for the *meta* isomer, **6.22m**, while diradical **6.22p** exhibited two closely spaced (0.08 V) oxidation processes in the anodic direction and a single 2e processes in the cathodic direction.
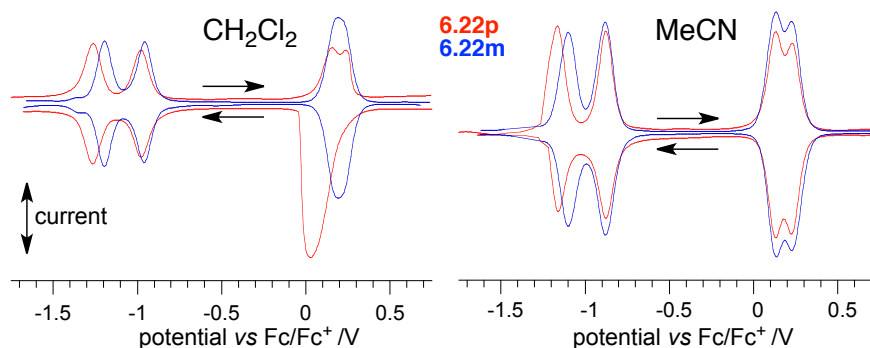
Figure 6.4.2.6. Differential Pulse Voltammetry (DPV) of diradicals **6.22p** (red) and **6.22m** (blue) in 0.1 M $[Bu_4N]^+PF_6^-$ in CH_2Cl_2 (left) and MeCN (right). Scan rate 5 mV s^{-1}.

For a better resolution of the current peaks, electrochemical analysis of **6.22** was conducted in MeCN instead of CH_2Cl_2. Analysis revealed that both radicals exhibit two quasi-reversible one-electron reduction and oxidation processes. The oxidation processes are separated by about 0.1 V, while separation of the reduction peaks remains nearly the same: 0.30 and 0.22 V for **6.22p** and **6.22m**, respectively.

A comparison of the two diradicals demonstrates that both have similar redox potentials except for $E_{1/2}^{-2/-1}$, which is 0.07 V lower for **6.22p**, consistent with a wider separation of the two reduction processes. Relative to the monoradical **6.23**, the $E_{1/2}^{-1/0}$ $E_{1/2}^{0/+1}$ processes for diradicals **6.22** are more anodic by about 0.13 and 0.05 V, respectively (Table 6.4.2.1.).

Table 6.4.2.1. Electrochemical data for diradicals **6.22p**,**6.22m** and monoradical **6.23**.[a]

radical	solvent	$E_{1/2}^{2-/-}$ /V	$E_{1/2}^{-/0}$ /V	$E_{1/2}^{0/+}$ /V	$E_{1/2}^{+/2+}$ /V
6.22p	CH_2Cl_2	-1.27	-0.98	0.16 [b]	0.24 [b]
6.22m	CH_2Cl_2	-1.20	-0.96	0.19 [c]	–
6.23 [d]	CH_2Cl_2	–	-1.12	0.13	–
6.22p	MeCN	-1.17	-0.87	0.13	0.23
6.22m	MeCN	-1.10	-0.88	0.14	0.23
6.23 [d]	MeCN	–	-1.01	0.09	–

[a] Potentials *vs* Fc/Fc$^+$ obtained from DPV. For details, see the SI. [b] Irreversible process. One two-electron peak on cathodic scan. [c] Reversible one two-electron process. [d] Data from CV measurements.

Determination of the singlet-triplet gap

EPR spectroscopy confirmed the expected ground state multiplicity of diradicals **6.22**: singlet for **6.22p** and triplet for **6.22m**. To establish the singlet–triplet energy gaps, diradicals were investigated as solid solutions in polystyrene by variable temperature EPR spectroscopy in a temperature range of 120–340 K (Figure 6.4.2.7). Both diradicals **6.22** exhibited EPR signals characteristic for a triplet state with minimum doublet impurities, but neither showed the forbidden $|\Delta m_s| = 2$ transition. Therefore, analysis focused on the relative intensity of the $|\Delta m_s| = 1$ signal, $DI_{(rel)}$, which was analyzed on the basis of Heisenberg Hamiltonian for two electrons $\hat{H} = -2J\hat{S}_1 \cdot \hat{S}_2$. The intensity of the spectrum markedly increased with increasing temperature for **6.22p**, consistent with the thermally populated triplet state, and had a moderately decreasing character for **6.22m**, indicating thermal population of the singlet state. Numerical fitting of the $DI_{rel}(T)$ datapoints to the Bleaney-Bowers equation[88] (eq 6.4.2.1.) gave the singlet–triplet energy gap ΔE_{S-T} (as $2J$) of -3.02(11) kcal mol^{-1} for **6.22p**. This value is significantly greater than that reported for **4.5** and **4.17** (ΔE_{S-T} = -1.27 and -1.05 kcal mol^{-1}, respectively),[106] in which two Blatter radicals are connected with their C(7) positions either directly (**4.5**) or through the 1,4-phenylene (**4.19**). DFT calculations predicted that the OSS state is only 2.04 kcal mol^{-1} more stable than the triplet.

$$\chi = \frac{Ng^2\mu_B^2}{kT}\left(\frac{2}{3+e^{-\frac{2J}{kT}}}\right)$$
6.4.2.1.

The same analysis of the VT EPR data for the *meta* isomer **6.22m** surprisingly resulted in a slightly negative ΔE_{S-T} = -0.16(1) kcal mol^{-1} instead of a positive value expected on the basis of the parity rules. Similar results were obtained for other diradicals based on the benzo[*e*][1,2,4]triazinyl despite the expected GS triplet.[107, 111] Particularly relevant is the case of diradical **4.21**, for which the character of the $DI_{rel}(T)$ curves was matrix dependent: data obtained in the PS solutions gave the expected ferromagnetic exchange interaction (ΔE_{S-T} = 0.55(7) kcal mol^{-1}), while the same analysis of data obtained from a frozen toluene/CHCl$_3$ matrix gave a significantly antiferromagnetic exchange interaction (ΔE_{S-T} = -0.33(3) kcal mol^{-1} from analysis of the original data).[111] The latter result was attributed to a coexistence of two major conformers with diametrically different GS preferences ($\Delta E_{S-T}(1)$ = 0.44(14) and $\Delta E_{S-T}(2)$ = -0.67(7) kcal mol^{-1}).[111]

This example indicates, that conformational properties and distribution of conformers in solid solutions and/or aggregation and specific interactions can play critical role in the mean value of the exchange interaction for a diradical. This is even more important in case of **6.22m** in which the Ar–N(1) junction, unlike the Ar–C(3) in **4.21**,[111] is characterized by a high torsion angle calculated at about 45°. This not only limits the effectiveness of the orbital overlap and hence exchange interaction, but also is particularly susceptible to conformational variations. A brief gas phase DFT analysis of **6.22m** in several conformational minima demonstrated that S–T energy gaps are in a range 0.31–0.42 kcal mol^{-1}, which suggests that some non-equilibrium conformers might be responsible for the observed mean antiferromagnetic interactions.[140]
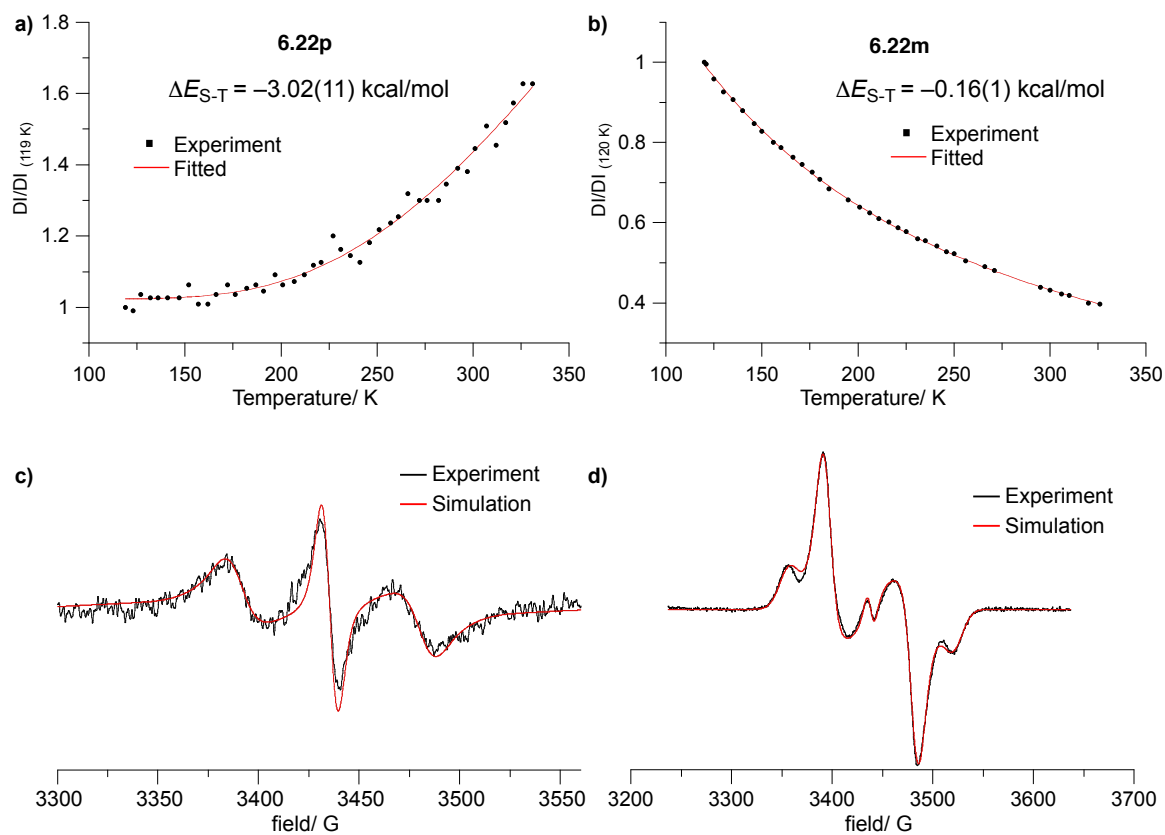
Figure 6.4.2.7. Experimental DI_{rel} *vs* *T* data points (black dots) and Bleaney-Bowers fitting curves (red line) for **6.22p** (a) and **6.22m** (b). Experimental (black) and simulated (red) EPR spectra of **6.22p** (c) and **6.22m** (d) in polystyrene solid solution at 120 K.

Simulation of the experimental triplet pattern obtained at 120 K for **6.22m** (Figure 6.4.2.7d.) gave zero-field splitting (*zfs*) parameters $|D/hc| = 7.60×10^{-3}$ cm^{-1} and $|E/hc|$ $2.07×10^{-4}$, which are smaller than those for **6.22p** ($|D/hc| = 8.93×10^{-3}$ cm^{-1} and $|E/hc|$ $9.41×10^{-5}$ cm^{-1}). These results indicate a slightly larger separation of the spin centers for the *meta* isomer **6.22m-T** (8.8 Å) than in the *para* analogue **6.22p-T** (8.4 Å) and are in qualitative agreement with spin density maps for both diradicals (Figure 6.4.2.8.).

6.22p-BS   **6.22m-T**
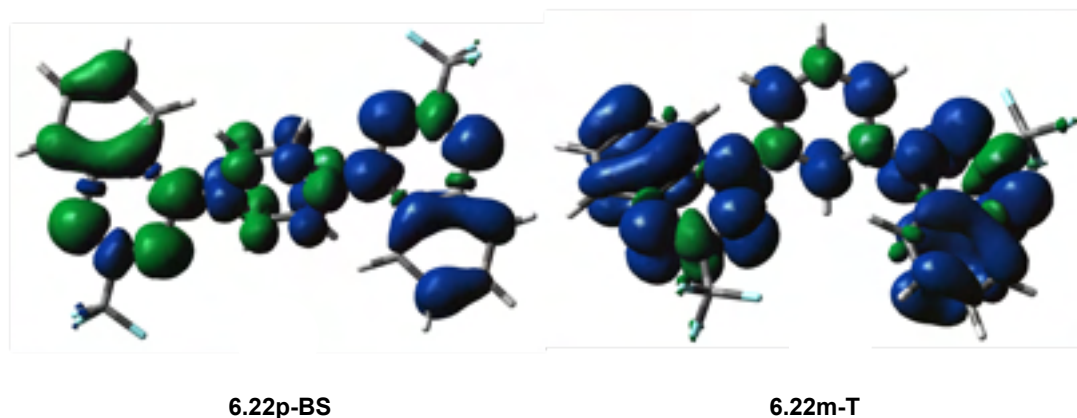
Figure 6.4.4.8. Spin density map for **6.22p-OSS** and **6.22m-T** (*density* =0.0014).

For comparison purposes the exchange interactions in diradicals **6.22p** and **6.22m** were calculated at the UB3LYP/6-31G(2d,p) level of theory giving the $\Delta E_{\text{S-T}}$ values of -2.04 for **6.22p** and 0.42 kcal mol^{-1} for **6.22m**. In addition, spin-restricted calculations revealed that the closed-shell (CS) singlet **6.22p-CS** is 6.69 kcal mol^{-1} above the open-shell form **6.22p-OSS**.

Diradicals **6.22p** and **6.22m** are the first examples of a potentially rich class of symmetric high-spin compounds accessible through organolithium addition to benzo[*e*][1,2,4]triazines (Scheme 6.4.2.1.). The strength of ferromagnetic exchange interactions and the overall spin delocalization in such derivatives can be controlled by varying the connecting unit (SC). The SC structure effect on the strength of exchange interactions 2*J* was briefly investigated with DFT methods and results showed that the $\Delta E_{\text{S-T}}$ can be controlled with substituents on the *m*-phenylene SC (Figure 6.4.2.9.). Thus, electron-withdrawing CF$_3$ group stabilizes the triplet state, while the donating NMe$_2$ narrows the S–T gap. This result is in agreement with conclusions of a more extensive computational analysis of Schlenk diradical derivatives.[143] Similar stabilization of the triplet state is observed in the pyridine derivative **6.22Pyr** and, as it might have been expected, addition of a CF$_3$ group increases further the $\Delta E_{\text{S-T}}$ energy up to 0.63 kcal mol^{-1} in

6.22PyrCF$_3$ (Figure 6.4.2.9.). The same effect is obtained, when pyridine in **6.22Pyr** is replaced with pyrazine in **6.22Pyraz**.

SC	DFT	ΔE_{S-T}
		/ kcal mol^{-1}
6.22m, X = H		0.42
6.22mNMe$_2$, NMe$_2$		0.32
6.22mCF$_3$, CF$_3$		0.48
6.22Pyr, X = CH		0.53
6.22PyrCF$_3$, CCF$_3$		0.63
6.22Pyraz, N		0.64
6.22NH, X = NH		-5.48
6.22O, O		-5.20
6.22S, S		-5.16

Figure 6.4.2.9. DFT-calculated singlet triplet energy gaps, ΔE_{S-T}, for several derivatives **6.22**.

Five membered heterocyclic SC connectors stabilize the singlet state in di-Blatter diradical derivatives in Figure 6.4.2.9., which is consistent with experimental results for other diradicals.[144-146] The main reason for this over twice stronger preference for low spin is the less aromatic character of these connecting units and hence lower thermodynamic penalty for the quinoid structure. All derivatives in Figure 6.4.2.9. are potentially accessible through the method shown in Scheme 6.4.2.1.

Finally DFT calculations for the analogue of **6.22m** in which the C(3)–CF$_3$ group was replaced with the C(3)–CH$_3$ group gave essentially identical ΔE_{S-T} of 0.42 kcal mol^{-1}.

Summary and Conclusions

We have demonstrated a simple and efficient, convergent strategy to access symmetrical diradicals with a potentially controllable singlet–triplet energy gap by judicious choice of the spin coupler (SC). This concept was demonstrated for two diradicals: robust open-shell singlet **6.22p** ($\Delta E_{S-T} = -3.02(11)$ kcal mol^{-1}) and a triplet GS **6.22m**. Analysis of PS solid solution of the latter gave a negative mean exchange interaction energy suggesting a dominance of conformer(s) or aggregates with significant antiferromagnetic exchange interactions. Gas phase DFT calculations of **6.22m** indicate that modest ferromagnetic exchange interactions are expected and the preference for the triplet GS can be increase by up to 50% by using SC units with low LUMO (electron withdrawing groups, pyridine, pyrazine), while the substituent at the C(3) position has little or no effect on the ΔE_{S-T} value.

6.5. Conclusion

This Doctoral Dissertation presents a comprehensive study of synthetic access and analysis of structure–property relationships of series of mono- and diradicals derived from benzo[*e*][1,2,4]triazin-4-yl.

A convinient acess to benzo[*e*][1,2,4]triazines **6.1** and benzo[*e*][1,2,4]triazin-4-yls **6.3** with a wide range of substituents at the C(3) position using two methods was developed. Simplified availability of a variety of benzo[*e*][1,2,4]triazines **6.1** offered a broader and simpler access to C(3)-functionalized benzo[*e*][1,2,4]triazin-4-yl radicals **6.3** by addition of PhLi. A series of 15 structurally diverse radicals was synthesized and stability of the resulting benzo[*e*][1,2,4]triazin-4-yls **6.3** and their properties were investigated with spectroscopic (UV-vis and EPR) and electrochemical methods (Cyclic Voltammetry). The limitation of the azaphilic addition method was established. The expanded series of derivatives permitted analysis of the C(3) substituent effects on electronic properties of the benzo[*e*][1,2,4]triazin-4-yl system, which, in turn, provides a tool for designing of radicals with greater functional flexibility and structural variety for modern materials applications.

The developed synthetic methods were applied to synthesis of benzo[*e*][1,2,4]triazin-4-yl based diradicals. A concise and efficient strategy for the preparation of three open-shell singlet bi-benzo[*e*][1,2,4]triazin-4-yl diradicals connected directly with high chemical stability and variable ΔE_{S-T} has been demonstrated. The presented three prototypical diradicals **6.8[m,n]** demonstrate that the regioconnectivity has a significant impact on their diradical character and is related to the total spin concentration at the connecting sites C(6) and C(7) of the benzo[*e*][1,2,4]triazin-4-yl units. Thus, as the total spin density increases, the S–T separation increases and diradicaloid index y_0 decreases. Diradicals **6.8[m,n]** exhibit all four well-defined quasi-reversible one-electron redox processes, which is desired for electronic applications. They also exhibit one of the smallest S–T separations and the highest y indices among benzo[*e*][1,2,4]triazin-4-yls, with high chemical stability. These favorable electronic properties combined with potentially easily modifiable electronic structures of bi-Blatter diradicals constitute an attractive direction for the development of materials with tunable properties for emerging applications.

These studies enable access to radical cations derived from appropriately functionalized diradicals **6.8[m,n]** with substituent-tunable absorption in the NIR region, high dichroic ratio and

which are compatible with LC matrix. One electron oxidation of such diradicaloids gives rise to highly delocalized radical cations with predicted substantially red shifted electronic absorption. The C(3) substituent is used to control absorption wavelength and compatibility with the nematic matrix. The successfully demonstrated novel approach using cyclization of *N*-arylguanidines (Section 6.2) will be extended to preparation of diradicals possessing electro-donating groups with linear shapes, and will open up wide opportunities in structural manipulation with the C(3) substituent needed for tuning properties of radical cations. Preparation of such derivatives is currently being developed in our laboratory.

In the context of investigation of diradicals with triplet ground state, a simple and efficient, convergent strategy to symmetrical diradicals connected with spin coupler (SC) was demonstrated. Judicious choice of the spin coupling unit lead to potentially controllable singlet–triplet energy gap in such molecules. This concept was demonstrated for two diradicals: robust open-shell singlet **6.22p** and a triplet GS **6.22m**. Analysis of variable temperature EPR measurements of polystyrene solid solution of the **6.22m** gave a negative mean exchange interaction energy suggesting a dominance of conformer(s) or aggregates with significant antiferromagnetic exchange interactions. Gas phase DFT calculations of **6.22m** indicate that modest ferromagnetic exchange interactions are expected and the preference for the triplet GS can be increased by using SC units with low LUMO (electron withdrawing groups, pyridine, pyrazine), while the substituent at the C(3) position has little or no effect on the $\Delta E_{\text{S-T}}$ value.

6.6. Experimental Section for Bi-Blatter diradicals: Convenient access to regioisomers with tunable electronic and magnetic properties
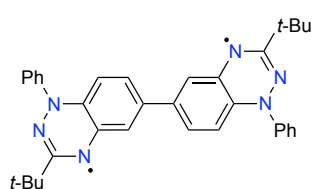
6.6.1. General information

Reagents and solvents were obtained commercially. Reactions were carried out under inert atmosphere (N_2 or A_r gas), and subsequent reaction work-ups were conducted in air. Heat for the reaction requiring elevated temperatures was supplied using oil baths. Volatiles were removed under reduced pressure. Reaction mixtures and column eluents were monitored by TLC using aluminum backed thin layer chromatography (TLC) plates (Merck Kieselgel 60 F_{254}). The plates were observed under UV light at 254 and 365 nm. Melting points were determined on Melt-Temp II Apparatus in capillaries and they are uncorrected. ^{1}H, ^{13}C, ^{19}F and ^{11}B NMR spectra were obtained at 400 MHz, 100 MHz, 377 MHz and 128 MHz respectively, on a Bruker AVANCE NMR spectrometer in CDCl$_3$ and referenced[147] to the solvent (δ = 7.26 ppm for ^{1}H and δ = 77.16 ppm for ^{13}C{^{1}H} in DMSO-d_6 and referenced to the solvent (δ = 2.50 ppm for ^{1}H and δ = 39.52 ppm for ^{13}C{^{1}H} or in acetone-d_6 and referenced to the solvent (δ = 2.05 ppm for ^{1}H and δ = 29.84 ppm for ^{13}C{^{1}H} unless otherwise specified. UV-vis-NIR spectra were recorded on a Jasco V770 spectrophotometer in spectroscopic-grade CH$_2$Cl$_2$ at concentrations in a range 1.9–10×10^{-5} M. IR spectra were recorded using Nexus FT-IR Thermo Nilolet IR spectrometer in KBr pellets. High-resolution mass spectrometry (HRMS) measurements were performed using SYNAPT G2-Si High-Definition Mass Spectrometry equipped with an ESI mass analyzer.

6.6.2. Synthetic details

Preparation of diradicals 6.8[m,n]. A general procedure. A 1.75 M solution of phenyllithium (1.49 mL, 2.6 mmol, 2.6 equiv.) in *n*-dibutyl ether was added dropwise to a stirred solution of bibenzo[*e*][1,2,4]triazine **6.10[m,n]** (1 mmol, 1 equiv.) in dry THF (3 mL, 0.33 M) at -78 °C under Ar atmosphere and the resulting mixture was stirred for 40 min at -78 °C and then for 1 h at rt. The reaction flask was opened and stirring was continued overnight in air at rt. After evaporation of the solvent, the residue was dissolved in CH$_2$Cl$_2$ (10 mL), water (10 mL) was added, the organic phase was separated, washed with water (10 mL) and dried (Na$_2$SO$_4$). The solvent was evaporated and the resulting crude product was purified by column chromatography (SiO$_2$ passivated with 1% Et$_3$N in CH$_2$Cl$_2$, hexane/AcOEt, 4:1) to afford diradicals **6.8[m,n]**.

Analytically pure diradicals were obtained by recrystallization from *n*-heptane/MeCN mixture or Et$_2$O.
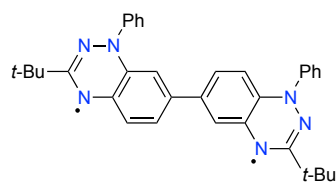
Diradical 6.8[6,6]. Following the general procedure, diradical **6.8[6,6]** (62.6 mg, 0.119 mmol, 75% yield; 65–75% in several runs) was obtained from 3,3'-di-(*tert*-butyl)-6,6'-bibenzo[*e*][1,2,4]triazine (**6.10[6,6]**, 59.1 mg, 0.159 mmol) as dark green crystals: mp 246–248 °C (*n*-heptane/MeCN). IR *v* 3062, 2950, 1587, 1479, 1403, 1299, 1191, 991, 862, 771, 697, 621 cm^{-1}. UV-vis (CH$_2$Cl$_2$) λ_{max} (*log* ε) 281 (4.47), 323 (4.47), 383 (4.11), 427 (3.91), 703 (3.63) nm. ESI(+)–MS, *m/z* 527 (100, [M + H]$^+$). HRMS (ESI+–TOF) *m/z* [M+H]$^+$ calcd for C$_{34}$H$_{35}$N$_6$ 527.2923, found 527.2911. Anal. Calcd for C$_{34}$H$_{34}$N$_6$: C, 77.54; H, 6.51; N, 15.96. Found: C, 77.53; H, 6.52; N, 15.94.
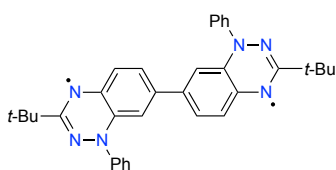
Diradical 6.8[6,7]. Following the general procedure, diradical **6.8[6,7]** (39.8 mg, 0.076 mmol, 77% yield; 66–77% in several runs) was obtained from 3,3'-di-(*tert*-butyl)-6,7'-bibenzo[*e*][1,2,4]triazine (**6.10[6,7]**, 36.4 mg, 0.098 mmol) as dark green crystals: mp 250–252 °C (Et$_2$O). IR *v* 2961, 1589, 1478, 1401, 1195, 1154, 994, 857, 828, 804, 756, 696, 618, 586 cm^{-1}. UV-vis (CH$_2$Cl$_2$) λ_{max} (*log* ε) 291 (4.44), 322 (4.39), 374 (3.93), 436 (3.88), 709 (3.85) nm. ESI(+)–MS, *m/z* 527 (40, [M + H]$^+$), 264 (100). HRMS (ESI+–TOF) *m/z* [M + H]$^+$ calcd for C$_{34}$H$_{35}$N$_6$ 527.2923, found 527.2911. Anal. Calcd for C$_{34}$H$_{34}$N$_6$: C, 77.54; H, 6.51; N, 15.96. Found: C, 77.51; H, 6.48; N, 15.92.

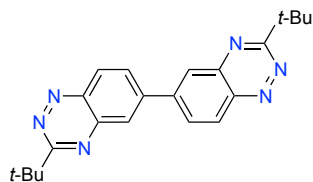***Diradical 6.8[7,7]***. Following the general procedure, diradical **6.8[7,7]** (63.7 mg, 0.121 mmol, 56% yield; 53–56% in several runs) was obtained from 3,3'-di-(*tert*-butyl)-7,7'-bibenzo[*e*][1,2,4]triazine (**6.10[7,7]**, 81.2 mg, 0.217 mmol) as a dark green crystals: mp 228-230 °C (*n*-heptane/MeCN). IR *v* 3087, 2976, 1516, 1419, 1335, 1167, 1054, 962, 846 cm^{-1}. UV-vis (CH$_2$Cl$_2$) λ_{max} (*log* ε) 246 (4.28), 304 (4.52), 431 (3.89), 706 (4.20) nm. ESI(+)–MS, *m/z* 527 (100, [M + H]$^+$), 264 (40). HRMS (ESI+–TOF) *m/z* [M + H]$^+$ calcd for C$_{34}$H$_{35}$N$_6$ 527.2923, found 527.2901. Anal. Calcd for C$_{34}$H$_{34}$N$_6$: C, 77.54; H, 6.51; N, 15.96. Found: C, 77.61; H, 6.61; N, 15.98.

Preparation of bibenzo[*e*][1,2,4]triazines 6.10[m.n]. A general procedure. Bishydrazide **6.13[m,n]** (1 mmol, 1 equiv.) was dissolved in glacial acetic acid (8 mL, 0.13 M), Sn powder (8 mmol, 8 equiv.) was added, and the solution was left stirring vigorously overnight at rt. The reaction mixture was then heated at 115–120 °C for 8 h and cooled. AcOEt (10 mL) followed by H$_2$O (20 mL) were added, and the resulting biphasic mixture was passed through a layer of Cellite. The organic layer was separated, and the aqueous layer was extracted with AcOEt (2×10 mL). The combined organic extracts were washed with sat. NaHCO$_3$ and dried (Na$_2$SO$_4$). The solvent was removed, the solid residue was dissolved in a MeOH/CH$_2$Cl$_2$ mixture (1:1, 10 mL, 0.1 M), and solid NaIO$_4$ (3.0 mmol, 3 equiv.) was added. The mixture was stirred overnight at rt. Inorganic salts were filtered, solvents evaporated, and the resulting yellow solid residue was passed through a short SiO$_2$ column (pet. eter/AcOEt, 9:1) giving bibenzo[*e*][1,2,4]triazine **6.10[m.n]** as a yellow solid. Recrystallization from *n*-heptane/AcOEt mixture gave the analytically pure product.
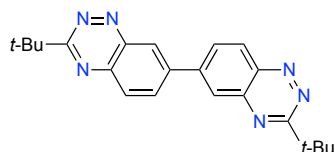
***3,3'-Di-tert-butyl-6,6'-bibenzo[e][1,2,4]triazine (6.10[6,6])**.* Following the general procedure, bibenzo[*e*][1,2,4]triazine **6.10[6,6]** (48.8 mg, 0.131 mmol, 59% yield; 56–59% in several runs) was obtained from bishydrazide **6.13[6,6]** (105.1 mg, 0.222 mmol) as an analytically pure microcrystalline yellow solid: mp 182–184 °C (*n*-heptane/AcOEt). ^{1}H NMR (CDCl$_3$, 400 MHz) δ 8.67 (d, *J* = 8.8 Hz, 2H), 8.44 (d, *J* = 1.9 Hz, 2H), 8.23 (dd, *J$_1$* = 8.8 Hz, *J$_2$* = 2.0 Hz, 2H), 1.67 (s, 18H). ^{13}C{^{1}H} NMR (CDCl$_3$, 100 MHz) δ 173.2, 145.3, 145.2, 140.9, 130.6, 129.4, 128.1, 39.4, 29.8. ESI(+)–MS, *m/z* 373 (100, [M + H]$^+$). HRMS (ESI+–TOF) *m/z* [M + H]$^+$ calcd for C$_{22}$H$_{25}$N$_6$: 373.2141, found: 373.2138. Anal. Calcd for C$_{22}$H$_{24}$N$_6$: C, 70.94; H, 6.49; N, 22.56. Found: C, 70.95; H, 6.49; N, 22.53.

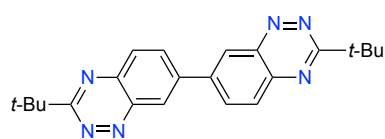***3,3'-Di-tert-butyl-6,7'-bibenzo[e][1,2,4]triazine (6.10[6,7])**.* Following the general procedure, bibenzo[*e*][1,2,4]triazine **6.10[6,7]** (82.7 mg, 0.222 mmol, 55% yield; 50–60% for several runs) was obtained from bishydrazide **6.13[6,7]** (190.7 mg, 0.404 mmol) as an analytically pure microcrystalline yellow solid: mp 186–188 °C (*n*-heptane/AcOEt). ^{1}H NMR δ (CDCl$_3$, 400 MHz) 8.89 (d, *J* = 2.1 Hz, 1H), 8.67 (d, *J* = 8.8 Hz, 1H), 8.43 (d, *J* = 1.9 Hz, 1H), 8.37 (dd, *J$_1$* = 8.8 Hz, *J$_2$* = 2.0 Hz, 1H), 8.25 (dd, *J$_1$* = 8.8 Hz, *J$_2$* = 1.9 Hz, 1H), 8.20 (d, *J* = 8.8 Hz, 1H), 1.66 (s, 18H).

^{13}C{^{1}H} NMR (CDCl$_3$, 100 MHz) δ 173.1, 172.9, 145.9, 145.3, 145.2, 140.9, 140.7, 140.3, 134.4, 130.6, 130.3, 129.4, 128.2, 127.5, 39.41, 39.37, 29.8 (2C). ESI(+)–MS, *m/z* 373 (100, [M + H]$^+$). HRMS (ESI+–TOF) *m/z* [M + H]$^+$ calcd for C$_{22}$H$_{25}$N$_6$: 373.2141, found: 373.2146. Anal. Calcd for C$_{22}$H$_{24}$N$_6$: C, 70.94; H, 6.49; N, 22.56. Found: C, 70.96; H, 6.42; N, 22.52.

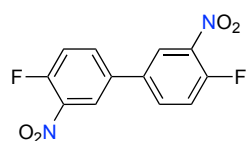***3,3'-Di-tert-butyl-7,7'-bibenzo[e][1,2,4]triazine (6.10[7,7])***. Following the general procedure, bibenzo[*e*][1,2,4]triazine **6.10[7,7]** (139.5 mg, 0.374 mmol, 66% yield; 60–66% in several runs) was obtained from bishydrazide **6.13[7,7]** (266.8 mg, 0.565 mmol) as analytically pure flake-like yellow crystals: mp 274–276 °C (*n*-heptane/AcOEt). ^{1}H NMR (CDCl$_3$, 400 MHz) δ 8.88 (d, *J* = 2.0 Hz, 2H), 8.40 (dd, *J$_1$* = 8.9 Hz, *J$_2$* = 2.0 Hz, 2H), 8.22 (d, *J* = 8.8 Hz, 2H), 1.67 (s, 18H). ^{13}C{^{1}H} NMR (CDCl$_3$, 100 MHz) δ 172.9, 146.0, 140.6, 140.3, 134.4, 130.3, 127.7, 39.4, 29.8. ESI(+)–MS, *m/z* 373 (100, [M + H]$^+$). HRMS (ESI+–TOF) *m/z* [M + H]$^+$ calcd for C$_{22}$H$_{25}$N$_6$: 373.2141, found: 373.2137. Anal. Calcd for C$_{22}$H$_{24}$N$_6$: C, 70.94; H, 6.49; N, 22.56. Found: C, 70.92; H, 6.48; N, 22.57.

Preparation of difluorodinitrobiphenyls 6.12[m,n]. A general procedure. To the solution of fluoroiodonitrobenzene **6.11** (1 mmol, 1 equiv.) in dry DMSO (2 mL, 0.5 M) activated copper bronze[148] (6 mmol, 6 equiv.) was added under inert atmosphere. The mixture was heated to 165 °C and stirred overnight. After cooling, AcOEt (10 mL) followed by H$_2$O (20 mL) were added, and the resulting biphasic mixture was passed through a layer of Cellite. The organic layer was separated, and the aqueous layer was extracted with AcOEt (2×10 mL). The combined organic extracts were dried (Na$_2$SO$_4$), the solvent was evaporated, and the crude residue was purified by column chromatography (pet. ether/CH$_2$Cl$_2$ 3:1) to afford compound **6.12[m,n]**. Analytically pure products **6.12[m,n]** were obtained by recrystallization from *n*-heptane/CH$_2$Cl$_2$ mixture.

***4,4'-Difluoro-3,3'-dinitrobiphenyl (6.12[6,6])***. Following the general procedure, biphenyl **6.12[6,6]** (1.041 g, 3.718 mmol, 49% yield; 45–55% in several runs) was obtained from 1-fluoro-4-iodo-2-nitrobenzene[131, 149] (**6.11a**, 2.025 g, 7.584 mmol) and activated copper bronze (2.892 g, 45.504 mmol) as a pale yellow solid: mp 208–210 °C (*n*-heptane/CH$_2$Cl$_2$). ^{1}H NMR (CDCl$_3$, 400 MHz) δ 8.27 (dd, *J$_1$* = 6.8, *J$_2$* = 2.5 Hz, 2H), 7.88-7.81 (m, 2H), 7.45 (dd, *J$_1$* = 10.3, *J$_2$* = 8.6 Hz, 2H). ^{13}C{^{1}H} NMR (CDCl$_3$, 100

MHz) δ 155.7 (d, $^1J_{FC}$ = 267.7 Hz), 137.9, 134.9 (d, $^3J_{FC}$ = 4.2 Hz), 133.9 (d, $^2J_{FC}$ = 8.7 Hz), 124.7 (d, $^3J_{F\text{-}C}$ = 2.5 Hz), 119.8 (d, $^2J_{F\text{-}C}$ = 21.5 Hz). ^{19}F NMR (CDCl$_3$, 377 MHz) δ -116. AP(-)– MS *m/z* 280 (30, [M]$^-$), 250 (100). HRMS (AP- –TOF) *m/z* [M]$^-$ calcd for C$_{12}$H$_6$F$_2$N$_2$O$_4$ 280.0296, found 280.0295. Anal. Calcd for C$_{12}$H$_6$F$_2$N$_2$O$_4$: C, 51.44; H, 2.16; N, 10.00. Found: C, 51.41; H, 2.12; N, 10.27.

***3,3'-Difluoro-4,4'-dinitrobiphenyl (6.12[7,7])*.**[150] Following the general procedure, biphenyl
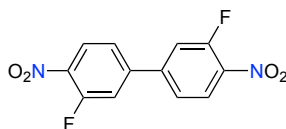

6.12[7,7] (1.064 g, 3.800 mmol, 35% yield; 31-42% yield for several runs) was obtained from 2-fluoro-4-iodo-1-nitrobenzene[151] (**6.11b**, 2.898 g, 10.854 mmol) and activated copper bronze (4.139 g, 65.124 mmol) as a pale yellow solid: mp 204–206 °C (*n*-heptane/CH$_2$Cl$_2$), (lit.[150] mp 197.5–198.5 °C, MeOH). ^{1}H NMR (CDCl$_3$, 400 MHz) δ 8.22 (t, *J* = 7.8 Hz, 2H), 7.58-7.50 (m, 4H). ^{13}C{^{1}H} NMR (CDCl$_3$, 100 MHz) δ 156.0 (d, $^1J_{F\text{-}C}$ = 266.6 Hz), 145.1 (d, $^2J_{F\text{-}C}$ = 8.0 Hz), 137.6 (d, $^3J_{FC}$ = 6.7 Hz), 127.4 (d, $^4J_{F\text{-}C}$ = 2.4 Hz), 123.4 (d, $^3J_{F\text{-}C}$ = 4.1 Hz), 117.5 (d, $^2J_{F\text{-}C}$ = 22.1 Hz). ^{19}F NMR (CDCl$_3$, 377 MHz) δ -114.5. AP(-)–MS *m/z* 280 (100, [M]$^-$), 250 (30). HRMS (AP(-)–TOF) *m/z* [M]$^-$ calcd for C$_{12}$H$_6$F$_2$N$_2$O$_4$ 280.0296, found 280.0307. Anal. Calcd for C$_{12}$H$_6$F$_2$N$_2$O$_4$: C, 51.44; H, 2.16; N, 10.00. Found: C, 51.39; H, 2.18; N, 10.19.

Preparation of *N',N'''-*(dinitrobiphenyldiyl)bis(pivalohydrazides) 6.13[m,n]. A general procedure. A solution of difluoro-dinitrobiphenyl **6.12[m,n]** (1 mmol, 1 equiv.) and pivalohydrazide[152] (2.6 mmol, 2.6 equiv.) in dry DMSO (4 mL, 0.25 M) was stirred at 110 °C for 72 h. After cooling, AcOEt (25 mL) followed by H$_2$O (15 mL) were added to the reaction mixture and the organic layer was separated. The aqueous layer was extracted twice with large portions of AcOEt (2×40 mL). The combined organic layers were dried (Na$_2$SO$_4$), the solvent was evaporated and the solid residue was dissolved in hot CH$_3$CN (25 mL). Cooling down of the solution gave the product as an orange powder. Recrystallization from EtOH gave analytically pure microcrystalline product.
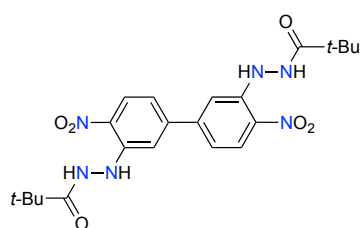
***N',N'''-*(3,3'-dinitrobiphenyl-4,4'-diyl)bis(pivalohydrazide) (6.13[6,6])*.** Following the general
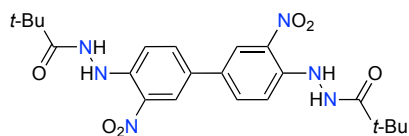
procedure, **6.13[6,6]** (253.1 mg, 0.536 mmol, 75% yield; 62– 80% in several runs) was obtained from 4,4'-difluoro-3,3'- dinitrobiphenyl (**6.12[6,6]**, 200.0 mg, 0.714 mmol) and

pivalohydrazide [152] (215.3 mg, 1.856 mmol) as a microcrystalline orange solid: mp 334–336 °C (EtOH). ^{1}H NMR (DMSO-d_6, 400 MHz) δ 10.01 (s, 2H), 9.24 (s, 2H), 8.33 (d, J = 2.2 Hz, 2H), 7.97 (dd, J_1 = 8.9 Hz, J_2 = 2.3 Hz, 2H), 7.10 (d, J = 8.9 Hz, 2H), 1.23 (s, 18H). ^{13}C{^{1}H} NMR (DMSO-d_6, 100 MHz) δ 177.0, 145.0, 134.2, 132.0, 127.4, 122.5, 115.6, 37.7, 27.1. ESI(+)–MS, m/z 473 (100, [M + H]$^+$), 372 (78). HRMS (ESI+–TOF) m/z [M + H]$^+$ calcd for $C_{22}H_{29}N_6O_6$: 473.2149, found: 473.2147. Anal. Calcd for $C_{22}H_{28}N_6O_6$: C, 55.92; H, 5.97; N, 17.79. Found: C, 55.79; H, 6.02; N, 17.65.
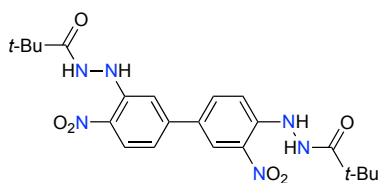
N',N'''-(4,4'-dinitrobiphenyl-3,3'-diyl)bis(pivalohydrazide) (6.13[7,7]). Following the general procedure, **6.13[7,7]** (308.1 mg, 0.652 mmol, 73% yield; 65–75% in several runs) was obtained from 3,3'-difluoro-4,4'-dinitrobiphenyl (**6.12[7,7]**, 250.0 mg, 0.893 mmol) and pivalohydrazide [152] (269.3 mg, 2.322 mmol) as a microcrystalline orange solid: mp 284–286 °C (EtOH). ^{1}H NMR (DMSO-d_6, 400 MHz) δ 9.99 (s, 2H), 9.33 (s, 2H), 8.25 (d, J = 8.8 Hz, 2H), 7.13 (d, J = 2.0 Hz, 2H), 7.00 (dd, J_1 = 8.8 Hz, J_2 = 2.0 Hz, 2H), 1.22 (s, 18H). ^{13}C{^{1}H} NMR (DMSO-d_6, 100 MHz) δ 177.0, 145.9, 145.8, 131.6, 127.3, 116.1, 112.6, 37.8, 27.2. ESI(-)–MS, m/z 471 (100, [M – H]$^-$), 372 (78). HRMS (ESI- –TOF) m/z [M – H]$^-$ calcd for $C_{22}H_{27}N_6O_6$: 471.1992, found: 471.2002. Anal. Calcd for $C_{22}H_{28}N_6O_6$: C, 55.92; H, 5.97; N, 17.79. Found: C, 55.79; H, 5.88; N, 17.65.

N',N'''-(3',4-dinitrobiphenyl-3,4'-diyl)bis(pivalohydrazide) (6.13[6,7]). A solution of bis-triflate **6.20[6,7]** (356.8 mg, 0.660 mmol, 1 equiv.) and pivalohydrazide[152] (199.1 mg, 1.716 mmol, 2.6 equiv.) in dry DMSO (2.6 mL, 0.25 M) was stirred at 110 °C for 48 h. After cooling AcOEt (20 mL) followed by H_2O (10 mL) were added to the reaction mixture and the organic layer was separated. The aqueous layer was extracted twice with large portions of AcOEt (2×30 mL). The combined organic layers were dried (Na_2SO_4), the solvent was evaporated and the solid residue was purified by column chromatography (hexane/AcOEt 2:1 to AcOEt). Recrystallization from an EtOH/AcOEt mixture gave an analytically pure orange microcrystalline solid **6.13[6,7]** (221.5 mg, 0.469 mmol, 71% yield): mp 276–278 °C (EtOH/AcOEt). ^{1}H NMR (DMSO-d_6, 400 MHz) δ 10.05 (s, 1H), 10.03 (s, 1H), 9.42 (s, 1H), 9.27 (s, 1H), 8.35 (d, J = 2.2 Hz, 1H), 8.18 (d, J = 8.7 Hz), 7.94 (dd, J_1 = 9.0 Hz, J_2 = 2.2

Hz, 1H), 7.21 (dd, J_1 = 8.7 Hz, J_2 = 2.0 Hz, 1H), 7.20 (s, 1H), 7.14 (d, J = 9.0 Hz, 1H), 1.26 (s, 9H), 1.23 (s, 9H). ^{13}C{^{1}H} NMR (DMSO-d_6, 100 MHz) δ 176.9, 176.8, 146.1, 146.0, 145.1, 134.4, 131.7, 130.7 127.1, 126.8, 123,8, 115.7, 115.8, 110.7, 37.8, 37.7, 27.1 (2C). ESI(+)–MS, m/z 473 (100, [M + H]$^+$). HRMS (ESI+–TOF) m/z [M + H]$^+$ calcd for $C_{22}H_{29}N_6O_6$: 473.2149, found: 473.2142. Anal. Calcd for $C_{22}H_{28}N_6O_6$: C, 55.92; H, 5.97; N, 17.79. Found: C, 55.86; H, 5.98; N, 17.76.
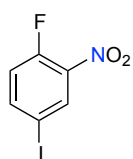
3',4-Dinitro-3,4'-bis(trifluoromethanesulfonyloxy)biphenyl (6.20[6,7]). Following a modified general literature procedure,[153] to a solution of 3',4-dinitrobiphenyl-3,4'-diol (**6.16[6,7]**, 140.5 mg, 0.509 mmol, 1 equiv.) in dry CH_2Cl_2 (4.2 mL, 0.12 mL), pyridine (0.043 mL, 3.054 mmol, 6 equiv.) was added at 0 °C. Subsequently Tf$_2$O (0.41 mL, 2.443 mmol, 4.8 equiv.) in dry CH_2Cl_2 (1 mL, 0.41 M) was added dropwise maintaining 0 °C. The resulting mixture was stirred for 20 h at rt and then quenched by addition of AcOEt (5 mL) and 1N HCl (5 mL). The organic phase was separated and washed with sat. NaHCO$_3$ and brine, and then dried (Na$_2$SO$_4$). The solvent was evaporated, and the solid residue was passed through a short SiO$_2$ pad (hexane/CH_2Cl_2, 9:1) giving bistriflate **6.20[6,7]** (246.5 mg, 0.456 mmol, 90% yield) as a brownish oil. ^{1}H NMR (CDCl$_3$, 400 MHz) δ 8.38 (d, J = 2.4 Hz, 1H), 8.35 (d, J = 8.5 Hz, 1H), 7.96 (dd, J_1 = 8.6 Hz, J_2 = 2.4 Hz, 1H), 7.81 (dd, J_1 = 8.5 Hz, J_2 = 1.9 Hz, 1H), 7.66 (d, J = 6.2 Hz, 1H), 7.65 (s, 1H). ^{13}C{^{1}H} NMR (CDCl$_3$, 100 MHz) δ 144.3, 142.28, 142.23, 141.6, 138.4, 133.8, 133.6, 128.0, 127.8, 125.7, 123.2, 118.7 (q, $^1J_{\text{F-C}}$ = 321.0 Hz) (2C). ^{19}F NMR (CDCl$_3$, 377 MHz) δ -72.09, -72.12. ESI(-)–MS, m/z 538 (40, [M – H]$^-$), 584 (100). HRMS (ESI- –TOF) m/z [M – H]$^-$ calcd for $C_{14}H_5F_6N_2O_{10}S_2$: 538.9290, found: 538.9284.
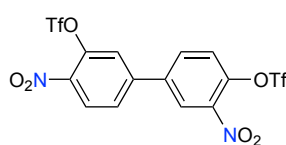
1-Fluoro-4-iodo-2-nitrobenzene (6.11a).[131, 149] Following a modified literature procedure,[131] to a solution of 1-fluoro-2-nitrobenzene (3.000 g, 21.26 mmol, 1 equiv.) in triflic acid (9.4 mL, 106.48 mmol, 5 equiv.) *N*-iodosuccinimide (5.760 g, 25.66 mmol, 1.2 equiv.) was added portionwise at 0 °C and the mixture was stirred at rt for 2 h. The mixture was quenched by the addition of water (250 mL) and extracted with diethyl ether (3×150 mL). The combined organic layers were washed with water, aqueous $Na_2S_2O_3$, brine and dried (Na_2SO_4). The solvent was evaporated and the crude residue was purified by passing through a short silica plug (pet. ether/AcOEt, 9:1) to afford pure product **6.11a** as a pale yellow

oil (5.415 g, 20.28 mmol, 99% yield; 95–99% in several runs): ^{1}H NMR (CDCl$_3$, 400 MHz) δ 8.35 (dd, J_1 = 6.9 Hz, J_2 = 2.3 Hz, 1H), 7.93 (ddd, J_1 = 8.8 Hz, J_2 = 4.2 Hz, J_3 = 2.2 Hz, 1H), 7.07 (dd, J_1 = 10.5 Hz, J_2 = 8.7 Hz, 1H). ^{13}C{^{1}H} NMR (CDCl$_3$, 100 MHz) δ 155.6 (d, $^1J_{F\text{-}C}$ = 266.5 Hz), 144.5 (d, $^2J_{F\text{-}C}$ = 8.2 Hz), 138.1, 134.7 (d, $^3J_{F\text{-}C}$ = 2.9 Hz), 120.5 (d, $^2J_{F\text{-}C}$ = 21.5 Hz), 86.2 (d, $^3J_{F\text{-}C}$ = 4.7 Hz). ^{19}F NMR (CDCl$_3$, 377 MHz) δ -118.4. ASAP(+)–MS, m/z 267 (100, [M + H]$^+$). HRMS (ASAP+–TOF) m/z [M + H]$^+$ calcd for C$_6$H$_3$FINO$_2$: 266.9192, found: 266.9202.

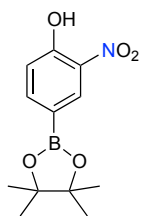***2-Fluoro-4-iodo-1-nitrobenzene (6.11b).***[150-151] Following a general procedure,[132] NaNO$_2$ (1.313 g, 19.03 mmol, 1.1 equiv.) in water (4.3 mL, 4.6 M) was added to a solution of 3-fluoro-4-nitroaniline (**6.21**, 2.870 g, 18.64 mmol, 1 equiv.) in 32% aq. H$_2$SO$_4$ (10 mL) at 0 °C. The resulting mixture was stirred at 0 °C for 1 h. A solution of KI (4.846 g, 29.19 mmol, 1.5 equiv.) in water (6 mL, 4.6 mL) was added at 0 °C, and the resulting mixture was stirred at 0 °C for 1h. The aqueous solution was extracted with AcOEt (2×50 mL) and the combined organic layers were washed with aqueous Na$_2$S$_2$O$_3$ and dried (Na$_2$SO$_4$). The solvent was evaporated and the crude residue was purified by column chromatography (pet. ether/AcOEt, 9:1) to afford the pure product **6.11b** as a pale yellow solid. Analytically pure product (4.025 g, 15.08 mmol, 82% yield; 75–85% in several runs) was obtained by recrystallization from EtOH to give pale yellow crystals: mp 116–118 °C (EtOH, lit.[150] mp 118–118.5 °C). ^{1}H NMR (CDCl$_3$, 400 MHz) δ 7.78 (t, J = 8.1 Hz, 1H), 7.74–7.64 (m, 2H). ^{13}C{^{1}H} NMR (CDCl$_3$, 100 MHz) δ 154.9 (d, $^1J_{F\text{-}C}$ = 270.7 Hz), 137.2, 134.2 (d, $^3J_{F\text{-}C}$ = 4.4 Hz), 128.0 (d, $^2J_{F\text{-}C}$ = 22.9 Hz, 127.1 (d, $^3J_{F\text{-}C}$ = 2.7 Hz), 101.5 (d, $^2J_{F\text{-}C}$ = 7.5 Hz). ^{19}F NMR (CDCl$_3$, 377 MHz) δ -114.6. ASAP(+)–MS, m/z 268 (100, [M + H]$^+$). HRMS (ASAP+ –TOF) m/z [M + H]$^+$ calcd for C$_6$H$_4$FINO$_2$: 267.9271, found: 267.9288. Anal. Calcd for C$_6$H$_3$FINO$_2$: C, 26.99; H, 1.13; N, 5.25. Found: C, 26.87; H, 1.19; N, 5.49.
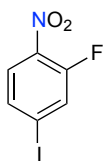
2-Nitro-4-(4,4,5,5-tetramethyl[1,3,2]dioxaborolan-2-yl)phenol (6.14).[128] Following an analogous literature procedure,[134] the solution of 4-bromo-2-nitrophenol (1.500 g, 6.88 mmol, 1 equiv.), bis(pinacolato)diboron (2.098 g, 8.26 mmol, 1.2 equiv.) and KOAc (2.026 g, 20.64 mmol, 3 equiv.) in dioxane (10 mL, 0.7 M) was degassed (oil pomp) and purged with N$_2$ (three times). PdCl$_2$(dppf) (251.7 mg, 0.344 mmol, 0.05 equiv.) was added and the mixture was stirred at 110 °C overnight. After cooling, AcOEt (25 mL) was added and the resulting mixture was passed through a layer of Cellite. Water (25 mL)

was added and the organic layer was separated, and the aqueous layer was extracted with AcOEt (2×25 mL). The combined organic extracts were dried (Na_2SO_4), the solvent was evaporated, and the residue was purified by column chromatography (hexane/CH_2Cl_2 3:1 to CH_2Cl_2) to afford pure product **6.14** as a pale yellow solid. Analytically pure product **6.14** (1.259 g, 4.75 mmol, 69% yield; 65–72% in several runs) was obtained as pale yellow flake-like crystals by recrystallization from hexane/CH_2Cl_2 mixture: mp 104–105 °C. ^{1}H NMR (CDCl$_3$, 400 MHz) δ 10.78 (s, 1H), 8.55 (s, 1H), 7.96 (dd, J_1 = 8.3 Hz, J_2 = 1.5 Hz, 1H), 7.13 (d, J = 8.4 Hz, 1H), 1.34 (s, 12H). ^{13}C{^{1}H} NMR (CDCl$_3$, 100 MHz) δ 157.3, 143.5, 133.6, 132.3, 119.5, 84.5, 25.0. ^{11}B{^{1}H} NMR (CDCl$_3$, 128 MHz, ref to BF$_3$•EtO) δ 29.9 (s). ESI(-)–MS, m/z 264 (70, [M – H][-]), 182 (100); HRMS (ESI- –TOF) m/z [M – H][-] calcd for $C_{12}H_{15}BNO_5$: 264.1043, found: 264.1050. Anal. Calcd for $C_{12}H_{16}BNO_5$: C, 54.37; H, 6.08; N, 5.28. Found: C, 54.38; H, 6.09; N, 5.32.

***3',4-Dinitrobiphenyl]-3,4'-diol (6.16[6,7]).* Method A.** The solution of 5-bromo-2-nitrophenol (**6.15**, 782.6 mg, 3.590 mmol, 1 equiv.), 2-nitro-4-(4,4,5,5-tetramethyl-1,3,2-dioxaborolan-2-yl)phenol (**6.14**, 1.046 g, 3.946 mmol, 1.1 equiv.) and KOAc (1.057 g, 10.770 mmol, 3 equiv.) in dioxane (6 mL, 0.6 M) was degassed (oil pomp) and purged with N_2 (three times). PdCl$_2$(dppf) (131.7 mg, 0.180 mmol, 0.05 equiv.) was added, and the mixture was stirred at 110 °C overnight. After cooling, AcOEt (15 mL) was added and the resulting mixture was passed through a layer of Cellite. Water (15 mL) was added, the organic layer was separated, and the aqueous layer was extracted with AcOEt (2×15 mL). The combined organic extracts were dried (Na_2SO_4), the solvent was evaporated, and the residue was purified by column chromatography (pet. ether/CH_2Cl_2 3:1) to afford inseparable mixture of the desired product **6.16[6,7]** and starting borolane **6.14** in a 2:1 ratio (^{1}H NMR). This mixture was submitted to oxidative hydrolysis reaction according to a general literature procedure:[129] the mixture of **6.16[6,7]** and **6.14** (499.4 mg) and NaIO$_4$ (1.970 mg, 7.440 mmol) was stirred in 4:1 THF/H_2O mixture (4 mL) for 30 min and a drop of HCl was added to the suspension. The reaction mixture was stirred for 1 h at rt and the solvent was evaporated. AcOEt (10 mL) followed by H_2O (5 mL) were added. The organic layer was separated, and the aqueous layer was extracted with AcOEt (2×6 mL). The combined organic extracts were dried (Na_2SO_4), the solvent was evaporated, and the crude residue was purified by column chromatography (pet. ether/CH_2Cl_2 3:1) to afford pure product **6.16[6,7]** as a yellow solid. Analytically pure product

was obtained as yellow flake-like crystals by recrystallization from an *n*-heptane/CH_2Cl_2 mixture (148.7 mg, 0.538 mmol, 15% yield; 8–20% in several runs).

3',4-Dinitrobiphenyl-3,4'-diol (6.16[6,7]). Method B. Following a similar procedure,[154] a 1.0 M solution of boron tribromide (0.08 mL, 0.077 mmol, 1.2 equiv.) in CH_2Cl_2) was added dropwise to the solution of 3,4'-dimethoxy-3',4-dinitrobiphenyl (**6.19[6,7]**, 19.5 mg, 0.064 mmol, 1 equiv.) in dry CH_2Cl_2 (2 mL) at -70 °C under Ar atmosphere. The resulting mixture was stirred for 1 h at -70 °C and then for 30 min at -30 °C. Water (3 mL) was added and the resulting mixture was stirred for 15 min at rt. The organic layer was separated, and the aqueous layer was extracted with CH_2Cl_2 (5 mL). The combined organic extracts were dried (Na_2SO_4), the solvent was evaporated, and the residue was passed through a short diatomaceous earth pad, and the solvent was evaporated giving pure product **6.16[6,7]** (17.0 mg, 0.062 mmol, 96% yield) as a yellow solid. Analytically pure product was obtained as yellow flake-like crystals by recrystallization from an *n*-heptane/CH_2Cl_2 mixture: mp 190–192 °C (*n*-heptane/CH_2Cl_2). ^{1}H NMR ($CDCl_3$, 400 MHz) δ 10.71 (s, 1H), 10.70 (s, 1H), 8.39 (d, $J = 2.3$ Hz, 1H), 8.20 (d, $J = 8.8$ Hz, 1H), 7.87 (dd, $J_1 = 8.8$ Hz, $J_2 = 2.3$ Hz, 1H), 7.35 (d, $J = 2.0$ Hz, 1H), 7.31 (d, $J = 8.8$ Hz, 1H), 7.20 (dd, $J_1 = 8.8$ Hz, $J_2 = 2.0$ Hz, 1H). ^{13}C{^{1}H} NMR ($CDCl_3$, 100 MHz) δ 155.8, 155.6, 147.4, 136.1, 134.0, 133.1, 130.8, 126.2, 123.8, 121.3, 118.7, 117.6. ESI(-)-MS, *m/z* 275 (100, [M − H]$^-$). HRMS (ESI- –TOF) *m/z* [M − H]$^-$ calcd for $C_{12}H_7N_2O_6$: 275.0304, found: 275.0299. Anal. Calcd for $C_{12}H_8N_2O_6$: C, 52.18; H, 2.92; N, 10.14. Found: C, 51.95; H, 2.97; N, 9.98.
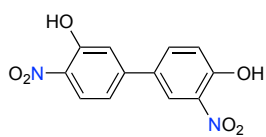
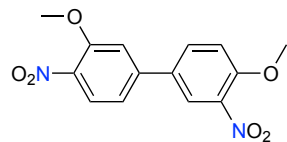***3,4'-Dimethoxy-3',4-dinitrobiphenyl (6.19[6,7]).*** Following an analogous procedure,[155] the solution of 4-bromo-2-methoxy-1-nitrobenzene (**6.18**, 67.5 mg, 0.291 mmol, 1 equiv.), 2-(4-methoxy-3-nitrophenyl)-4,4,5,5-tetramethyl-1,3,2-dioxaborolane (**6.17**, 89.0 mg, 0.32 mmol, 1.1 equiv.) and KOAc (85.7 mg, 0.873 mmol, 3 equiv.) in dioxane (4 mL) was degassed (oil pomp) and purged with N_2 (three times). $PdCl_2$(dppf) (11.0 mg, 0.015 mmol, 0.05 equiv.) was added and the mixture was stirred at 110 °C overnight. After cooling, AcOEt (10 mL) was added and the resulting mixture was passed through a layer of Cellite. Water (10 mL) was added and the organic layer was separated, and the aqueous layer was extracted with AcOEt (2×10 mL). The combined organic extracts were dried (Na_2SO_4), the solvent was evaporated, and the residue was purified by column chromatography

(hexane/CH_2Cl_2 9:1 to CH_2Cl_2). Recrystallization (*n*-heptane/CH_2Cl_2 mixture) gave analytically pure product **6.19[6,7]** (58.7 mg, 0.193 mmol, 66% yield) as pale yellow crystals: mp 164–165 °C. ^{1}H NMR (CDCl$_3$, 400 MHz) δ 8.09 (d, *J* = 2.4 Hz, 1H), 7.96 (d, *J* = 9.0 Hz, 1H), 7.78 (dd, *J$_1$* = 8.7 Hz, *J$_2$* = 2.4 Hz, 1H), 7.22 (d, *J* = 8.9 Hz, 1H), 7.20–7.17 (m, 2H), 4.05 (s, 3H), 4.03 (s, 3H). ^{13}C{^{1}H} NMR (CDCl$_3$, 100 MHz) δ 153.8, 153.5, 144.9, 140.0, 138.9, 132.9, 131.7, 126.9, 124.5, 118.7, 114.4, 111.8, 56.94, 56.86. TPF AP(-)–MS, *m/z* 304 (5, [M]$^-$), 289 (100, [M-Me]). HRMS (AP(-)–TOF) *m/z* [M]$^-$ calcd for $C_{14}H_{12}N_2O_6$: 304.0695, found: 304.0697. Anal. Calcd for $C_{14}H_{12}N_2O_6$: C, 55.27; H, 3.98; N, 9.21. Found: C, 55.25; H, 4.02; N, 9.38.

3-Fluoro-4-nitroaniline (6.21).[156] Following a reported procedure,[133] 3-fluoroaniline (5.000 g, 44.96 mmol, 1 equiv.) and benzaldehyde (5.000 g, 47.12 mmol, 4.81 mL, 1.1 equiv.) were heated at 80 °C for 1h. The reaction mixture was cooled in an ice bath, conc. H_2SO_4 (20 mL) was slowly added, and the mixture was stirred at rt until complete dissolution of the resulting solid. The reaction mixture was then cooled to 0 °C with an ice bath and a mixture of conc. HNO_3 (3 mL) and conc. H_2SO_4 (10 mL) was added dropwise, maintaining the temperature at 0 °C. The resulting mixture was stirred at 0°C for 1h and then poured into a saturated solution of K_2CO_3 in water. The aqueous solution was extracted with AcOEt (2×50 mL) and the combined organic layers were collected and dried (Na_2SO_4). The solvent was evaporated and the residue was purified by column chromatography (pet. ether/AcOEt, 3:1) to afford the title product as a yellow solid. The analytically pure product **6.21** (2.459 g, 15.75 mmol, 35% yield; 32–37% for several runs) was obtained by recrystallization from EtOH as yellow needles: mp 162–164 °C (EtOH lit. [157] 146-148 °C). ^{1}H NMR (acetone-d_6, 400 MHz) δ 7.92 (t, *J* = 9.0 Hz, 1H), 6.56 (dd, *J$_1$* = 9.1, *J$_2$* = 2.3 Hz, 1H), 6.53 (dd, *J$_1$* = 14.0, *J$_2$* = 2.3 Hz, 1H), 6.31 (bs, 2H). ^{13}C{^{1}H} NMR (acetone-d_6, 100 MHz) δ 159.2 (d, $^1J_{F-C}$ = 259.4 Hz), 157.4 (d, $^2J_{F-C}$ = 12.7 Hz), 129.3 (2C), 110.1, 101.1 (d, $^2J_{F-C}$ = 24.4 Hz). ^{19}F NMR (acetone-d_6, 377 MHz) δ -110.9. ESI(-)–MS, *m/z* 155 (100, [M – H]$^-$). HRMS (ESI- –TOF) *m/z* [M – H]$^-$ calcd for $C_6H_4FN_2O_2$: 155.0257, found: 155.0264. Anal. Calcd for $C_6H_5FN_2O_2$: C, 46.16; H, 3.23; N, 17.94. Found: C, 46.22; H, 3.21; N, 18.23.
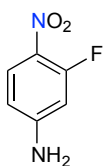
6.6.3. NMR spectra
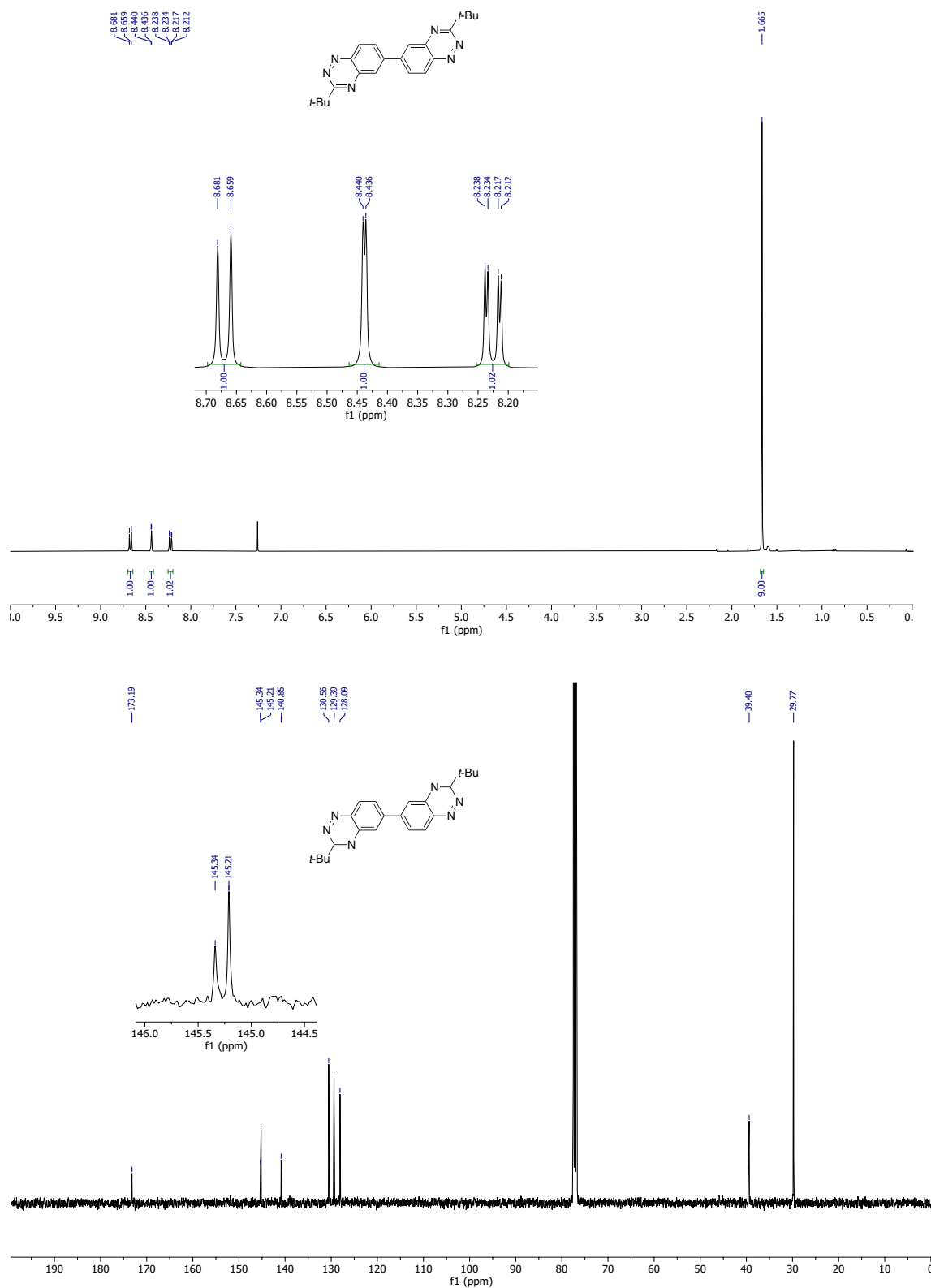
Figure 6.6.3.1. ^{1}H NMR (400 MHz) and ^{13}C{^{1}H} NMR (100 MHz) spectra of **6.10[6,6]** (CDCl$_3$).
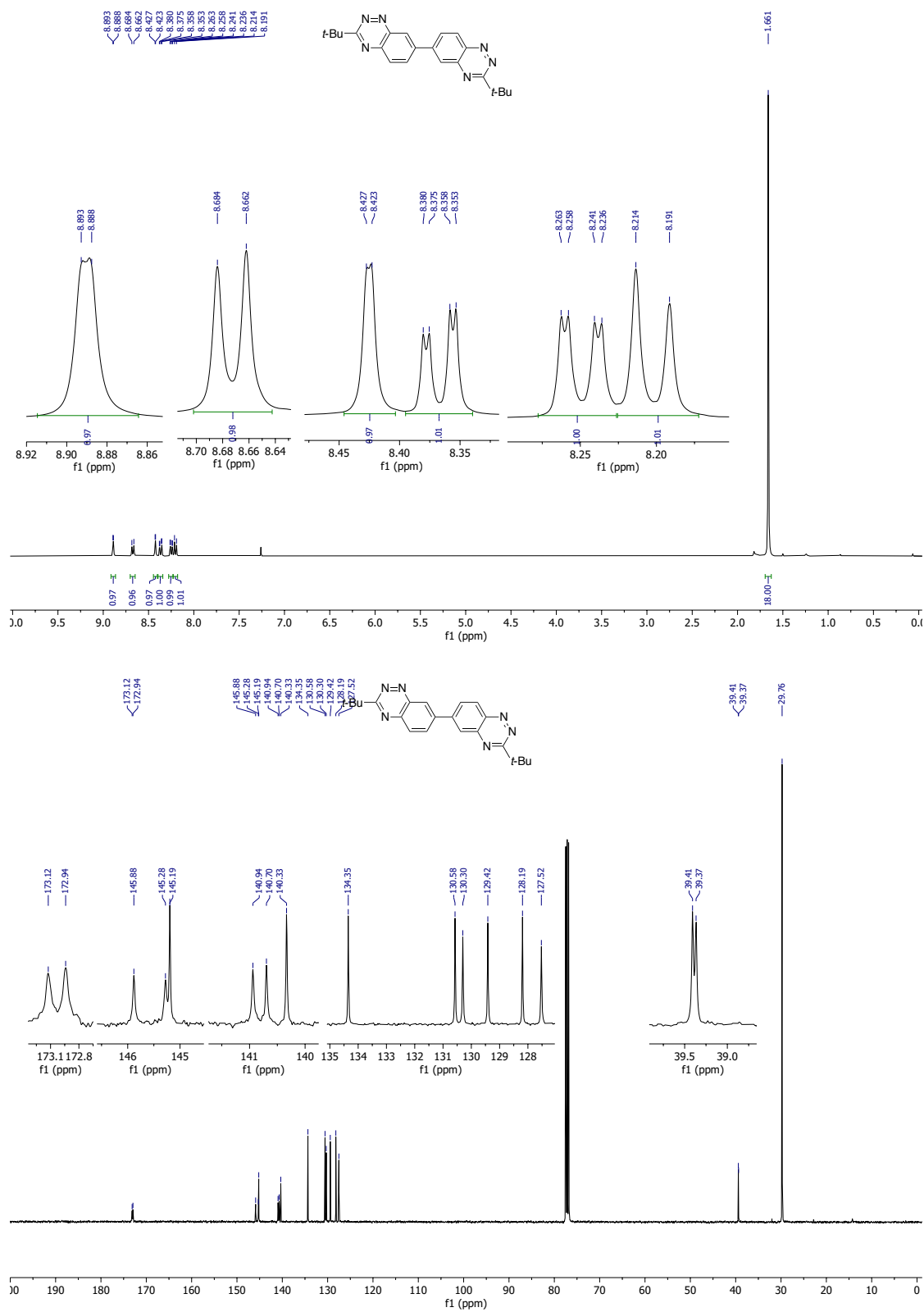
Figure 6.6.3.2. ^{1}H NMR (400 MHz) and ^{13}C{^{1}H} NMR (100 MHz) spectra of **6.10[6,7]** (CDCl${}_3$).
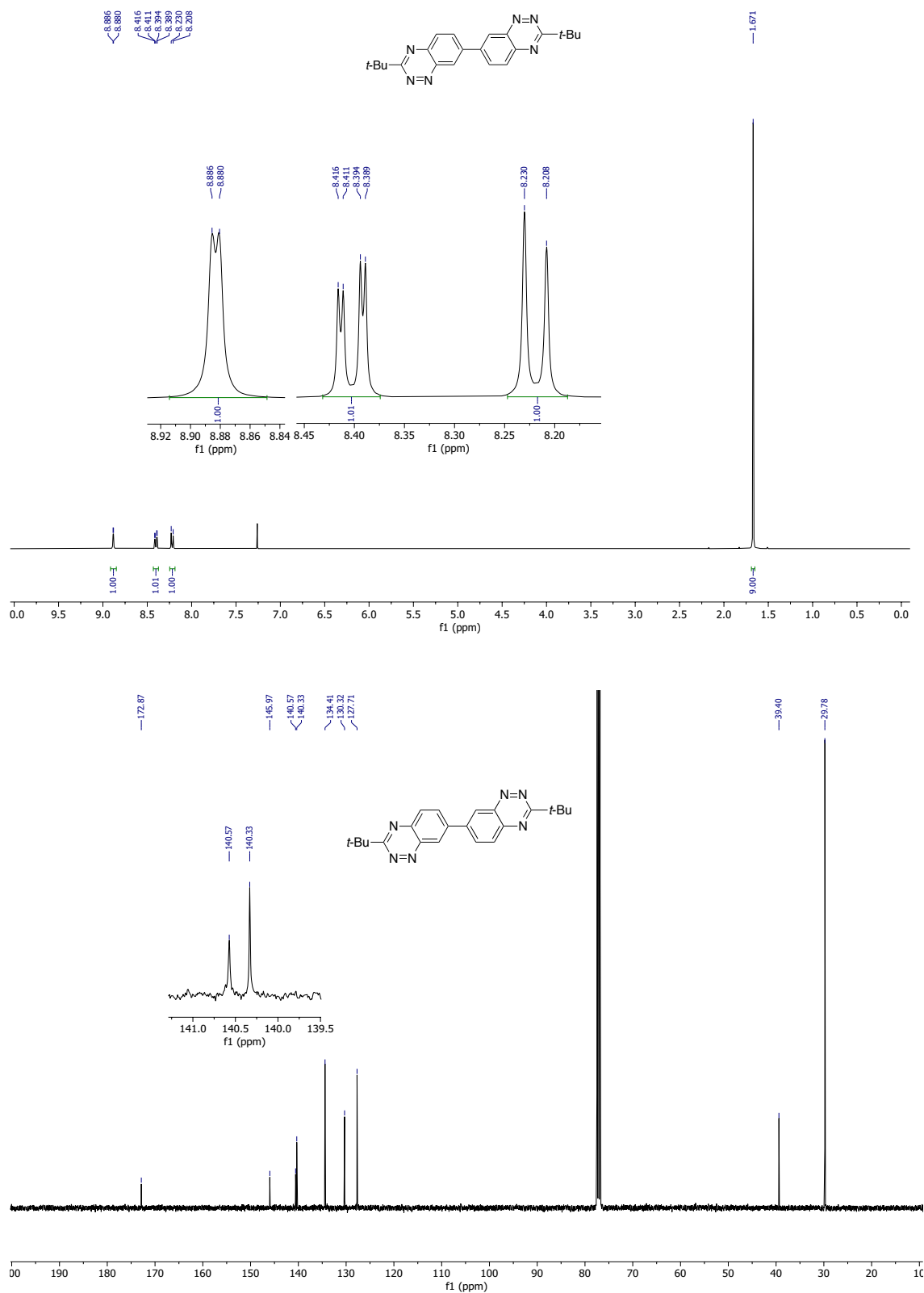
Figure 6.6.3.3. ¹H NMR (400 MHz) and ¹³C{¹H} NMR (100 MHz) spectra of **6.10[7,7]** (CDCl₃).
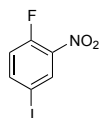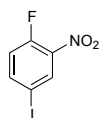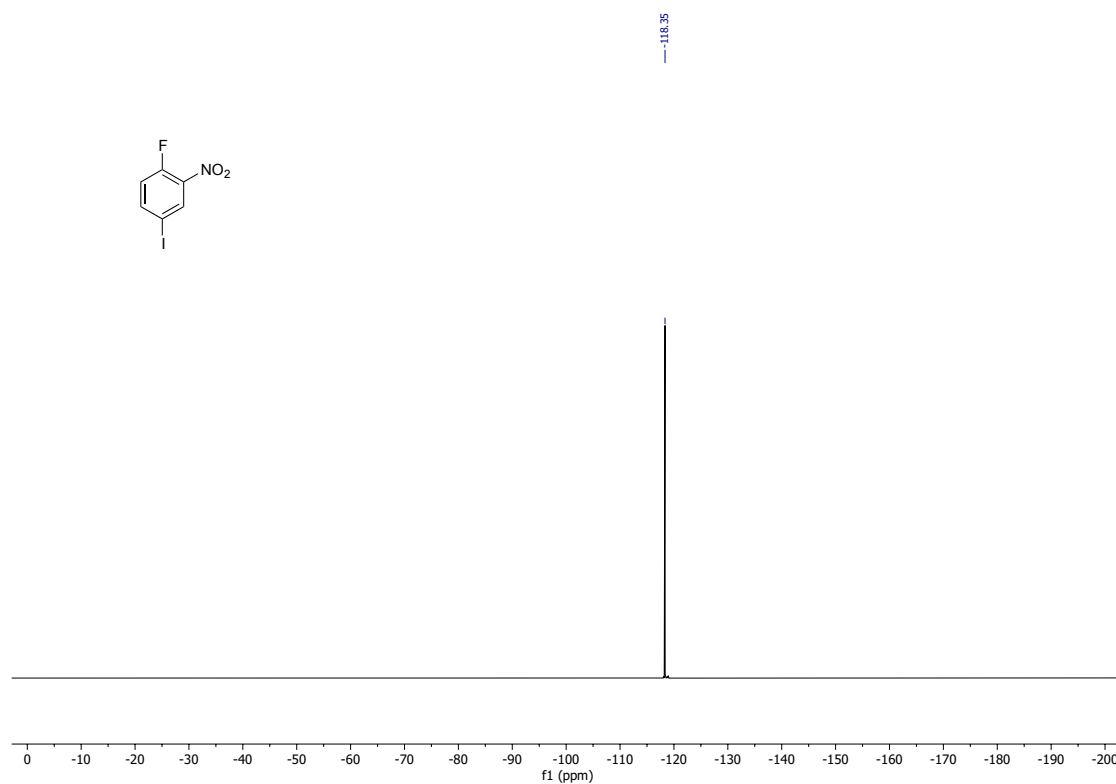
Figure 6.6.3.4. ^{1}H NMR (400 MHz), ^{13}C{^{1}H} NMR (100 MHz) and ^{19}F NMR (377 MHz) spectra of **6.11a** (CDCl$_3$).

---114.64
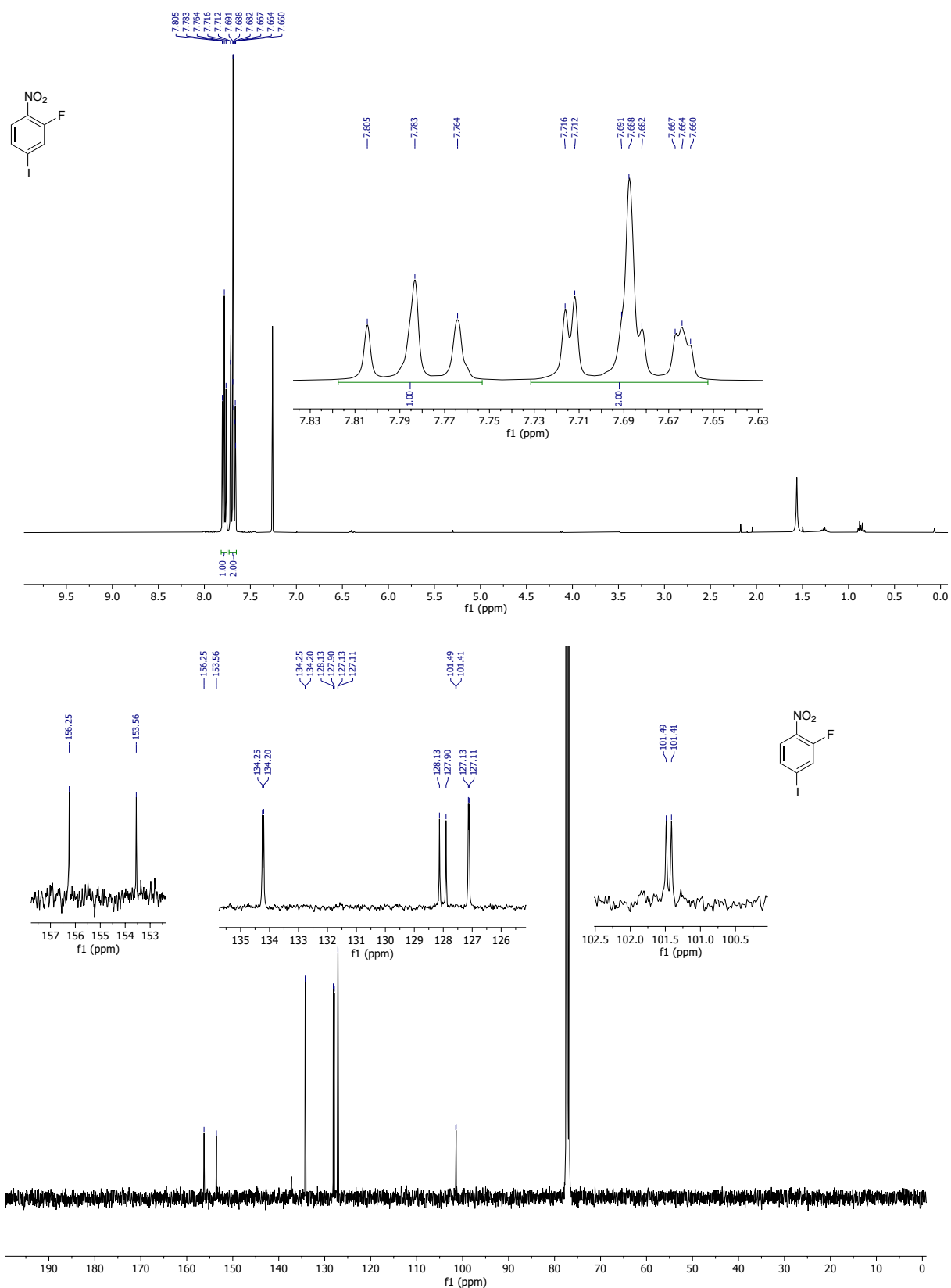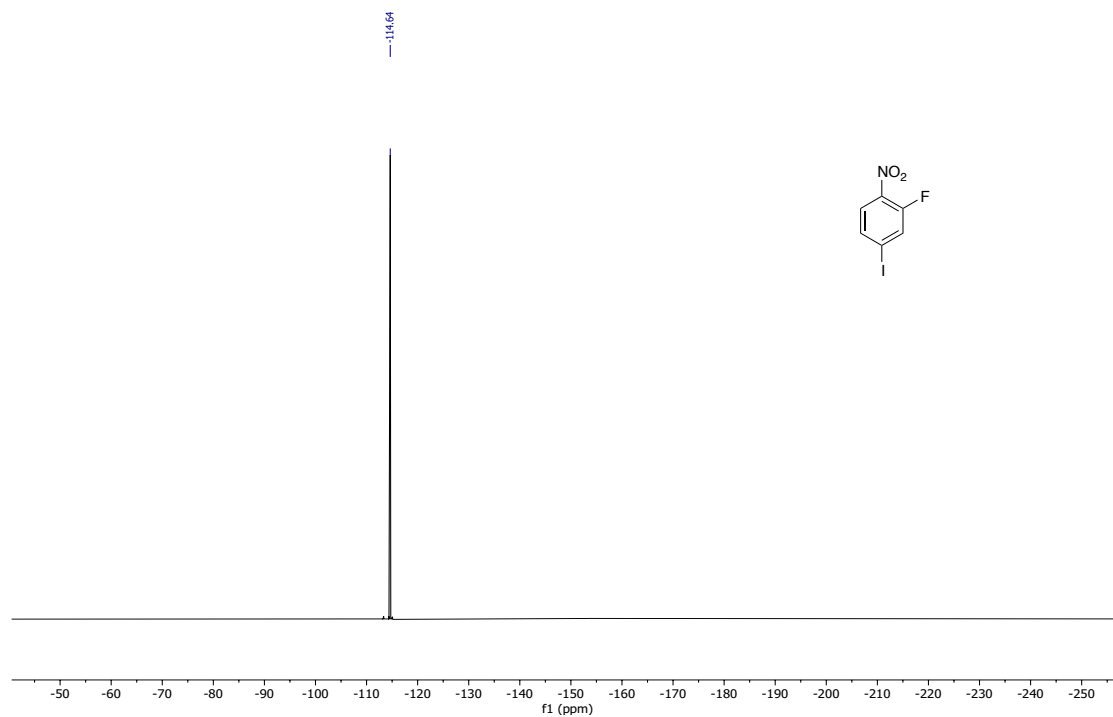
Figure 6.6.3.5. ^{1}H NMR (400 MHz), ^{13}C{^{1}H} NMR (100 MHz) and ^{19}F NMR (377 MHz) spectra of **6.11b** (CDCl$_3$).
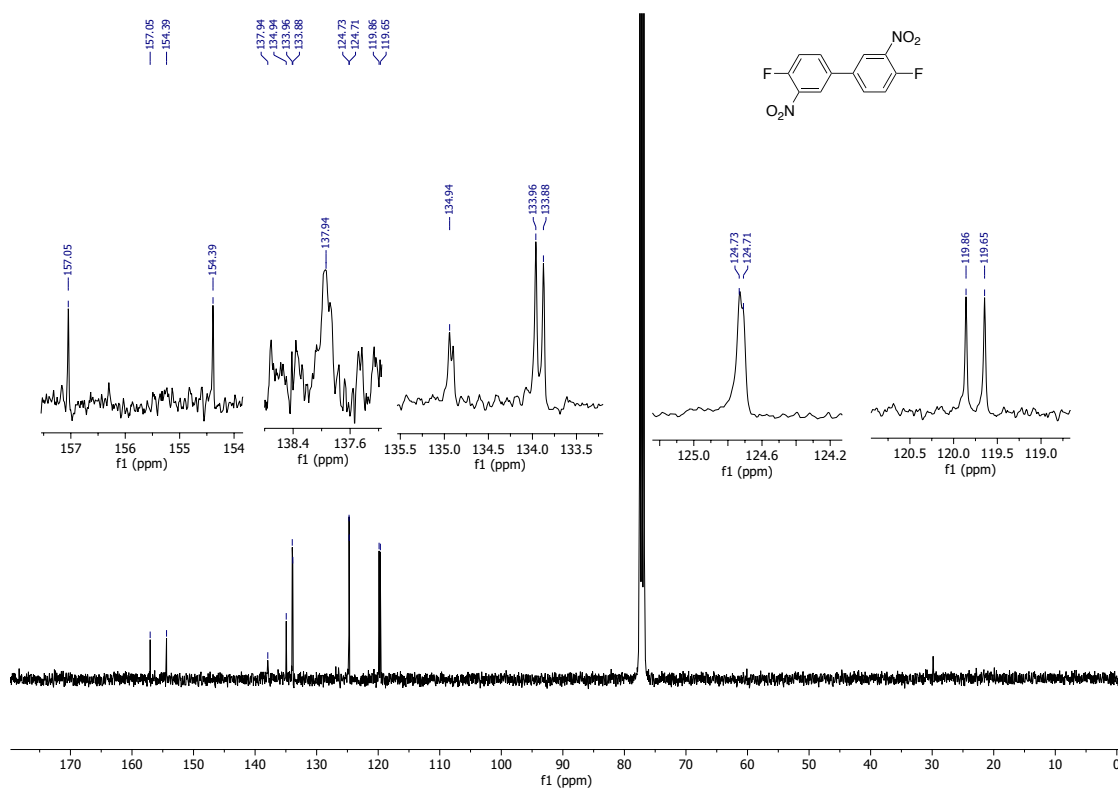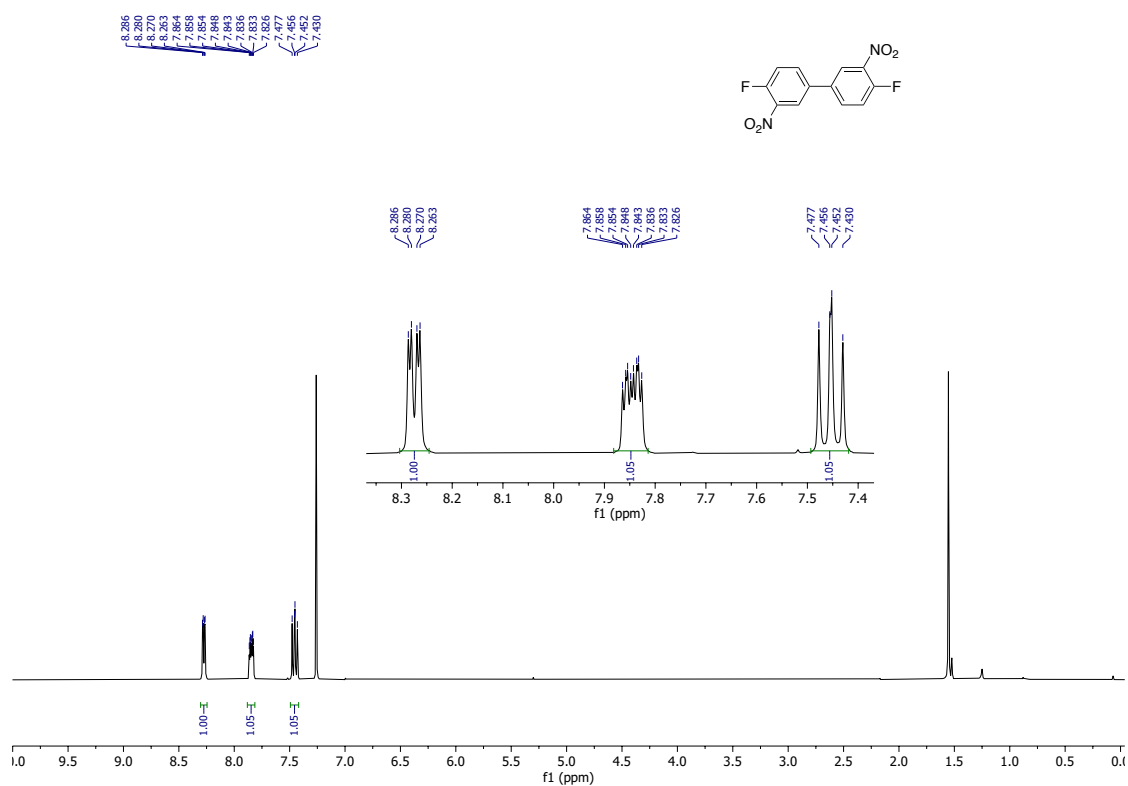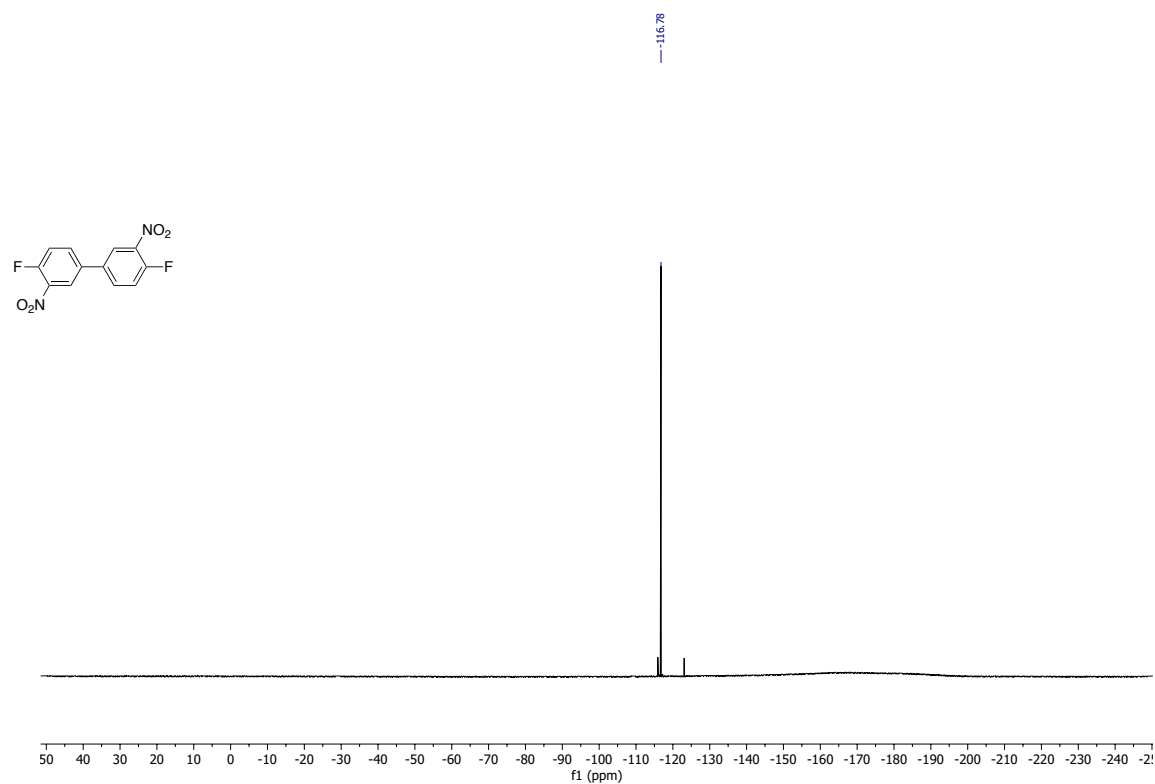
Figure 6.6.3.6. ^{1}H NMR (400 MHz), ^{13}C{^{1}H} NMR (100 MHz) and [19]F (377 MHz) spectra of **6.12[6,6]** (CDCl$_3$).
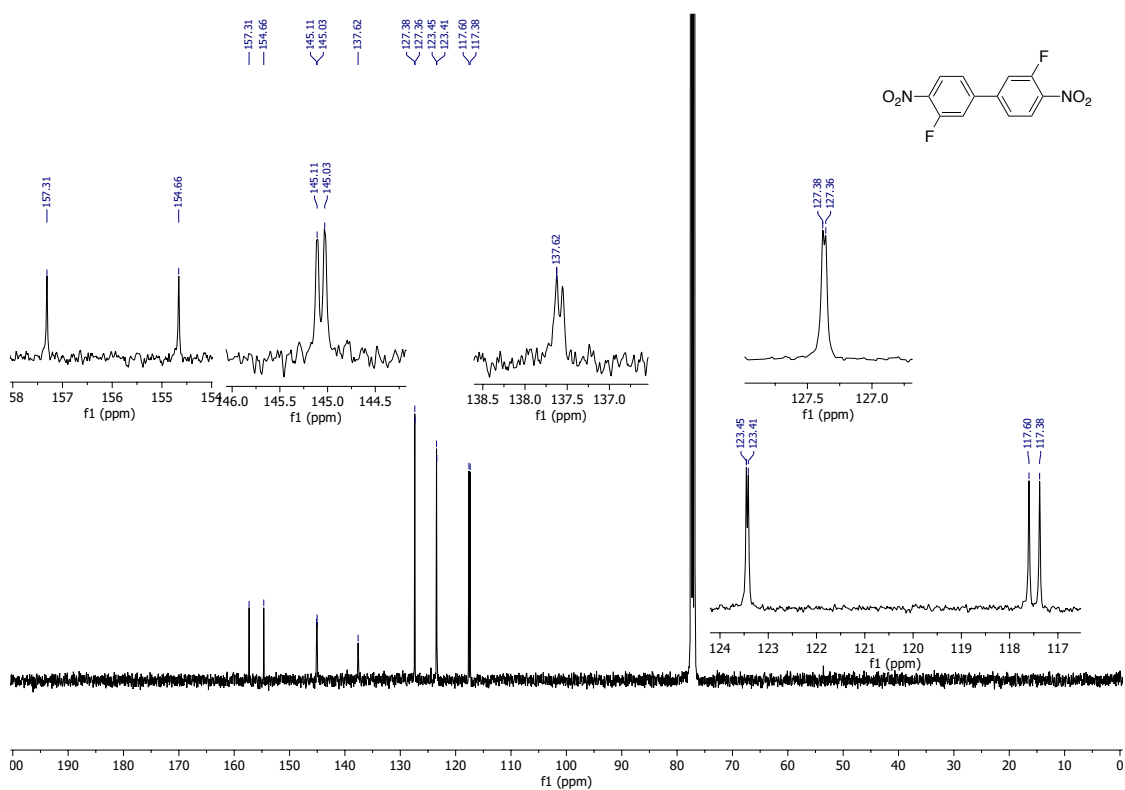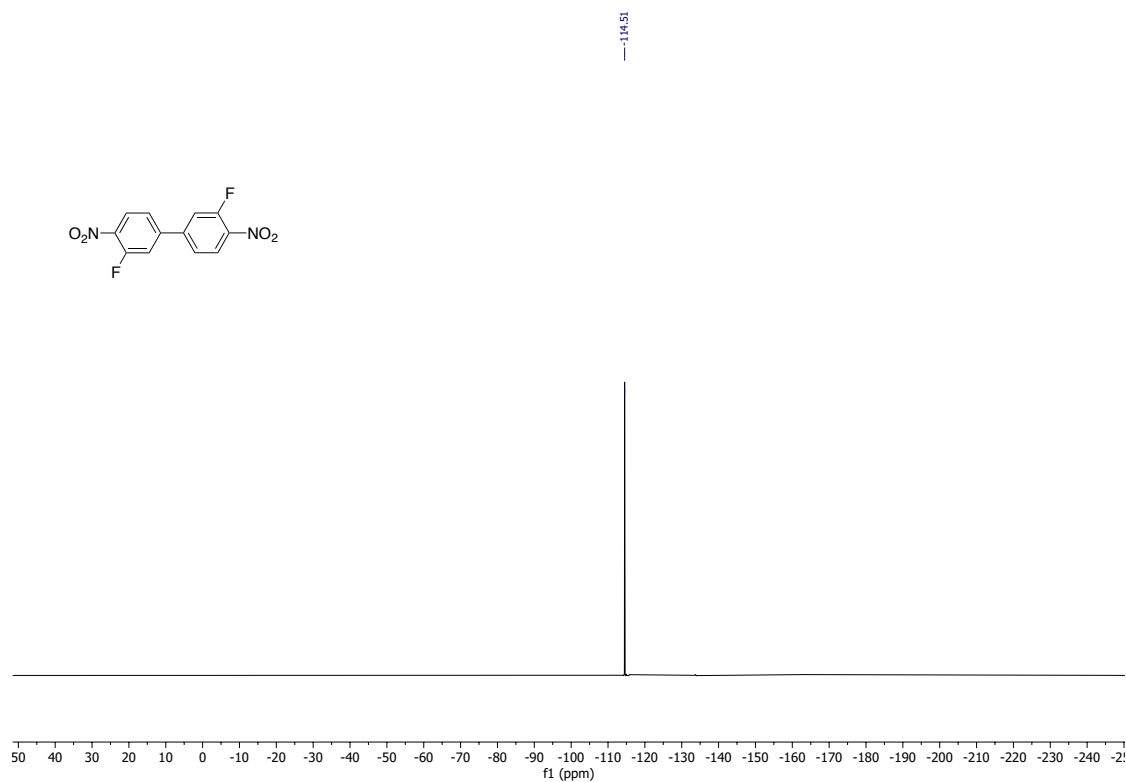
Figure 6.6.3.7. ^{1}H NMR (400 MHz), ^{13}C{^{1}H} NMR (100 MHz) and ^{19}F NMR (377 MHz) spectra of **6.12[7,7]** (CDCl$_3$).
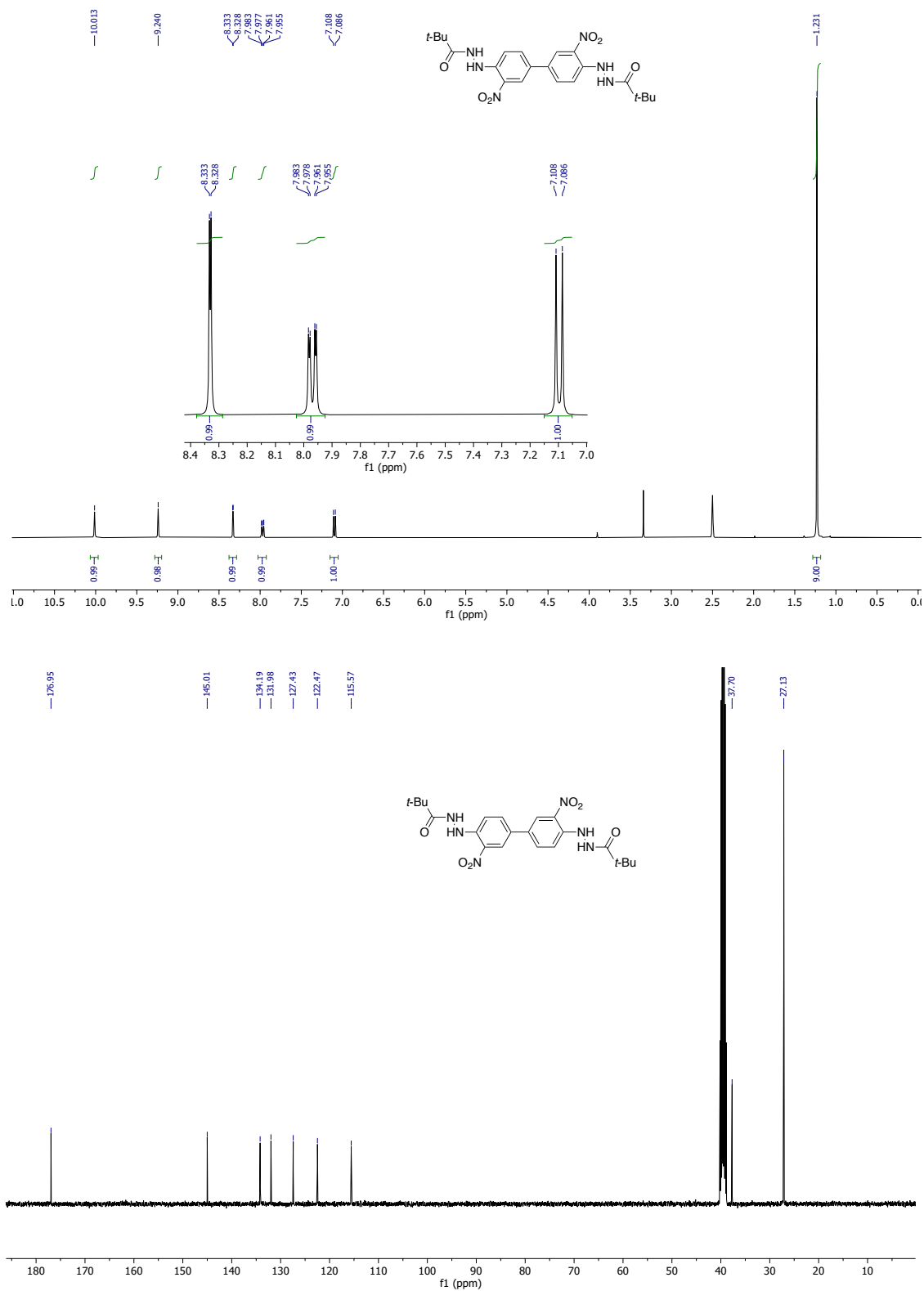
Figure 6.6.3.8. ^{1}H NMR (400 MHz) and ^{13}C{^{1}H} NMR (100 MHz) spectra of **6.13[6,6]** (DMSO-d_6).
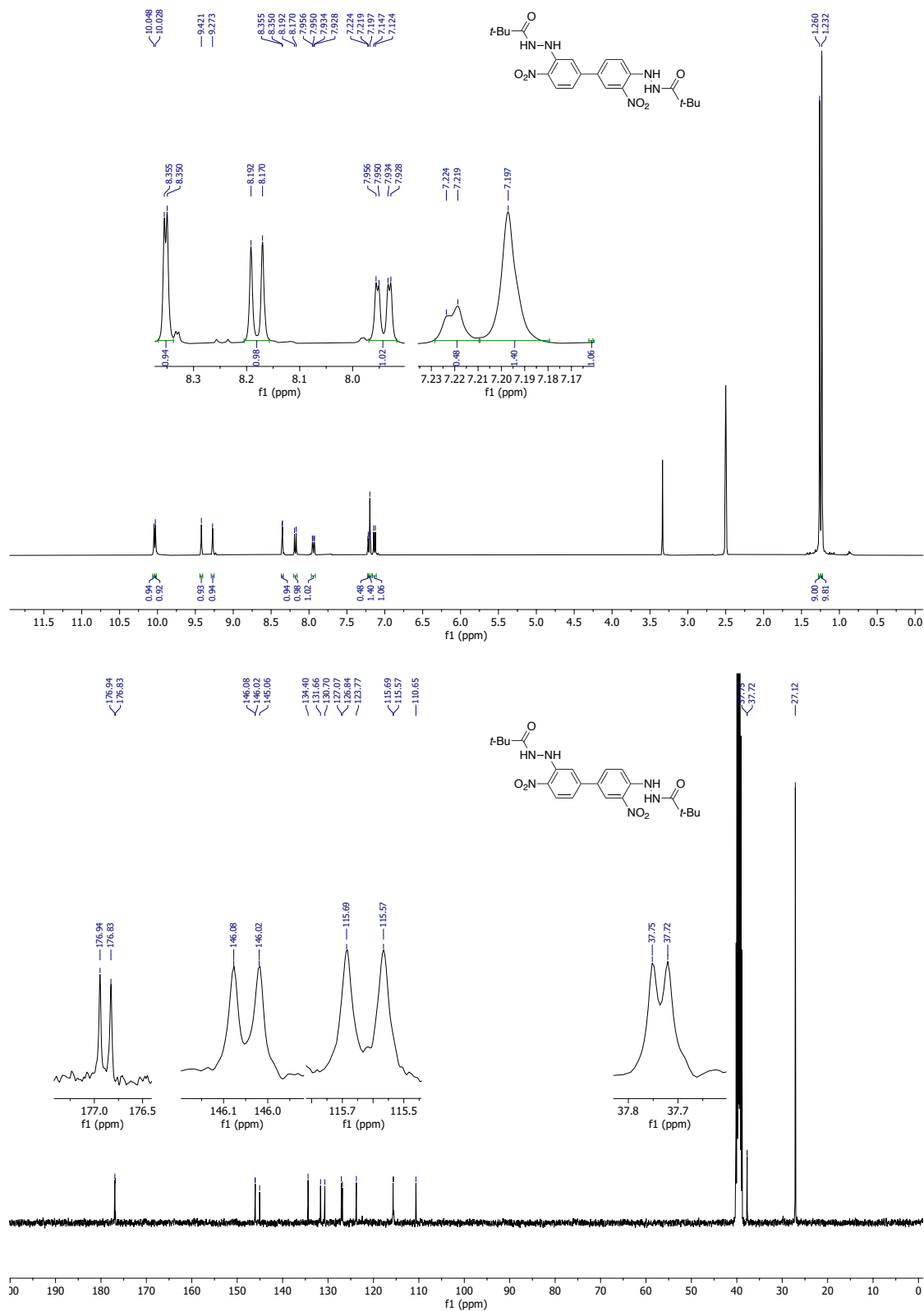
Figure 6.6.3.9. ¹H NMR (400 MHz) and ¹³C{¹H} NMR (100 MHz) spectra of **6.13[6,7]** (DMSO-*d₆*).
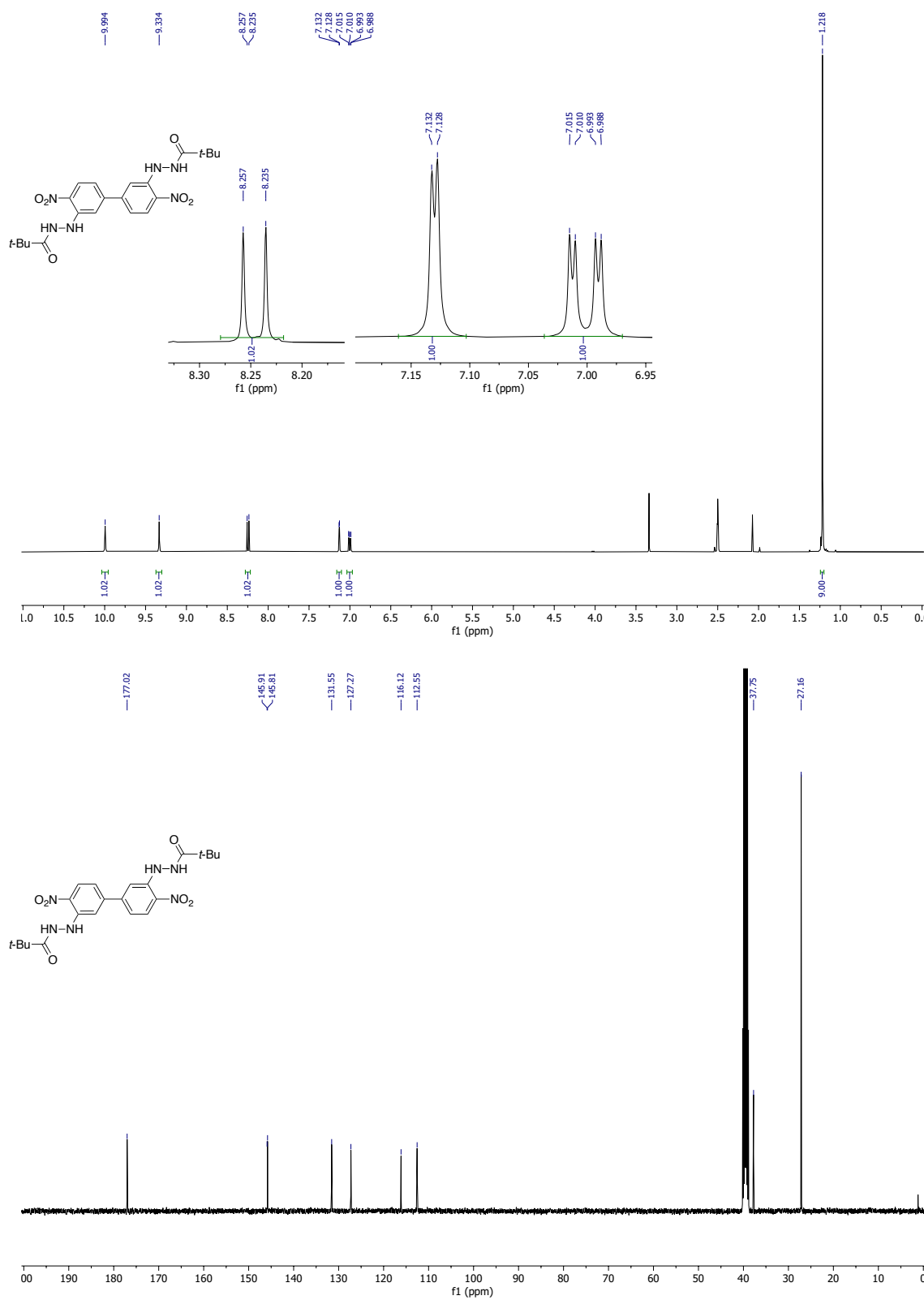
Figure 6.6.3.10. ^{1}H NMR (400 MHz) and ^{13}C{^{1}H} NMR (100 MHz) spectra of **6.13[7,7]** (DMSO-d_6).
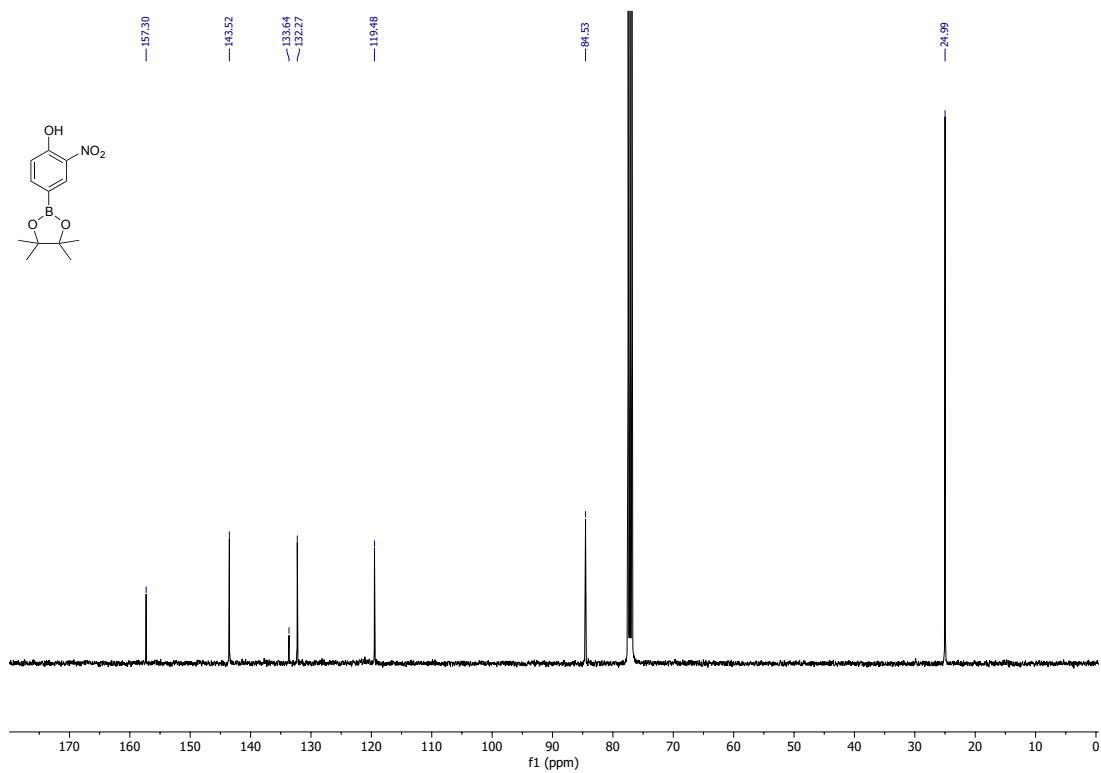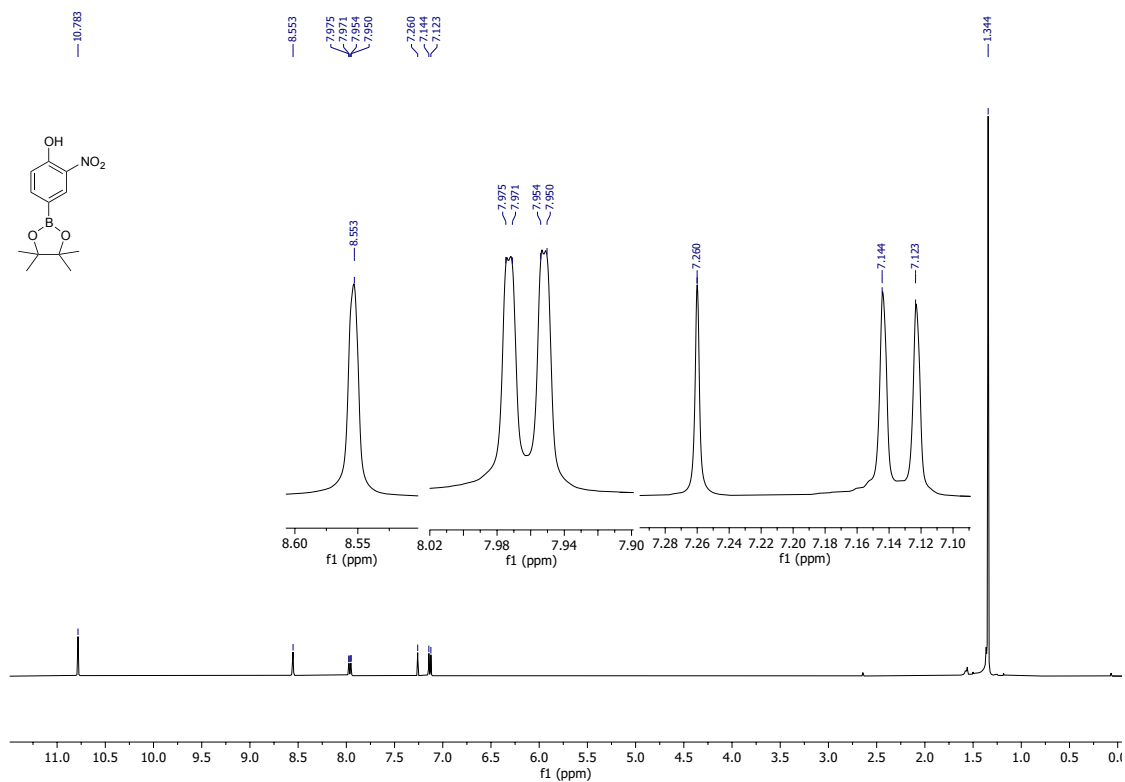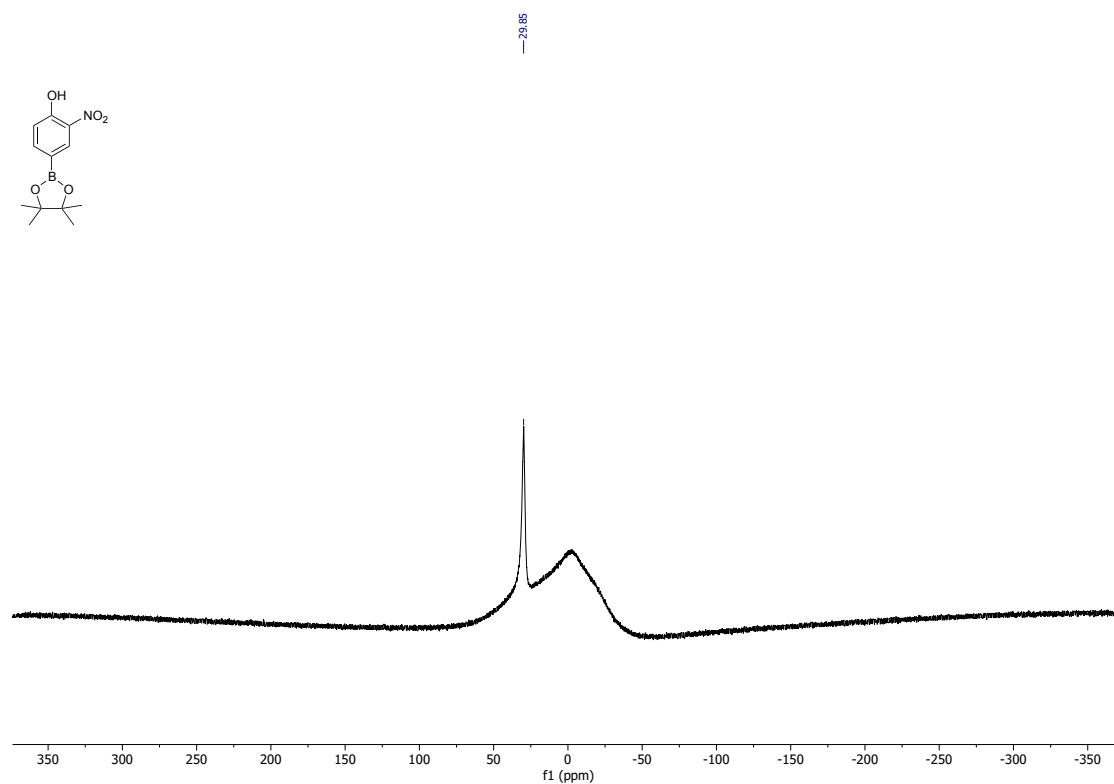
Figure 6.6.3.11. ¹H NMR (400 MHz), ¹³C{¹H} NMR (100 MHz) and ¹¹B{¹H} NMR (128 MHz) spectra of **6.14** (CDCl₃).
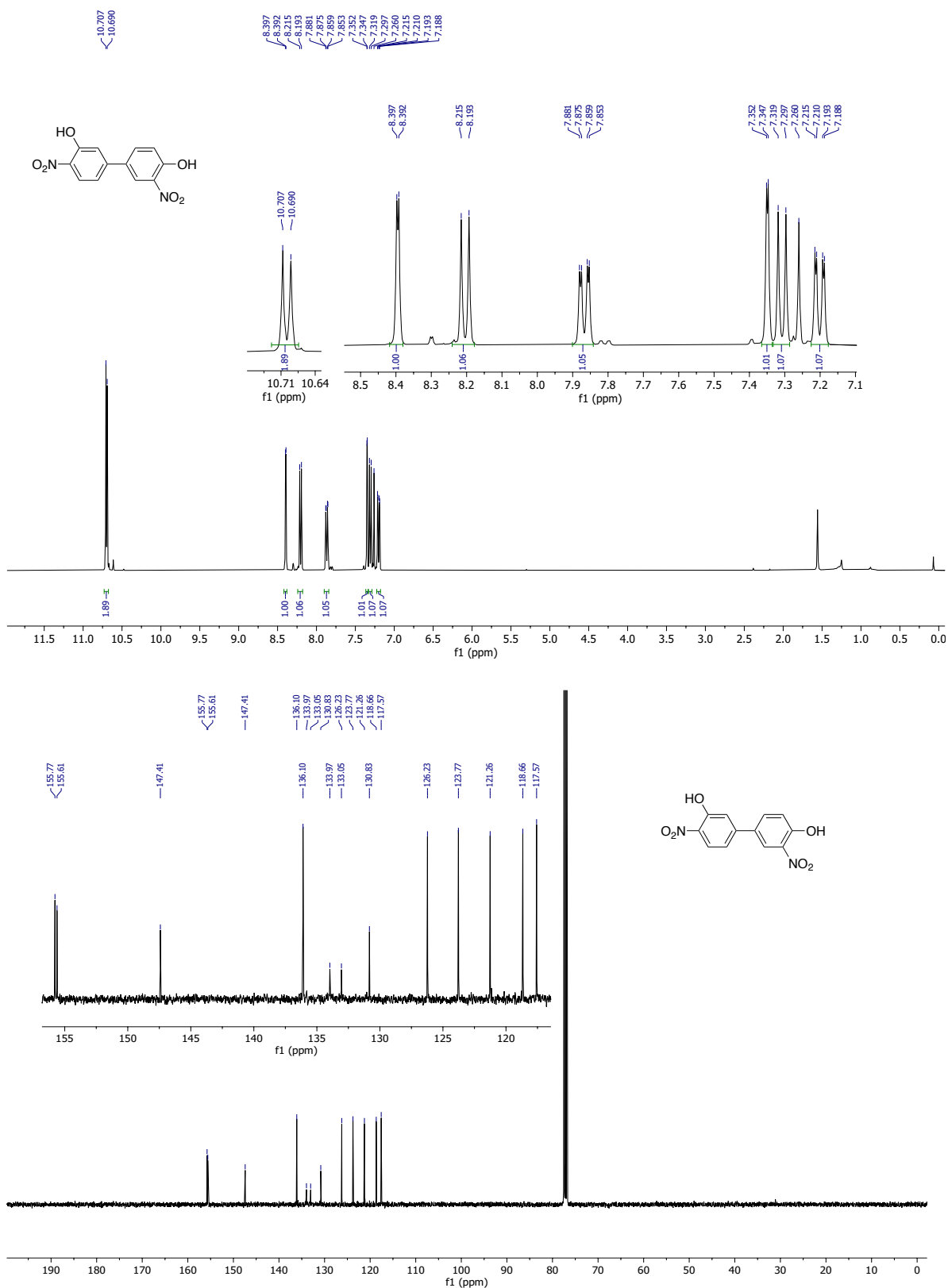
Figure 6.6.3.12. ¹H NMR (400 MHz) and ¹³C{¹H} NMR (100 MHz) spectra of **6.16[6,7]** (CDCl₃).

Figure 6.6.3.13. ^{1}H NMR (400 MHz) and ^{13}C{^{1}H} NMR (100 MHz) spectra of **6.19[6,7]** (CDCl$_3$).
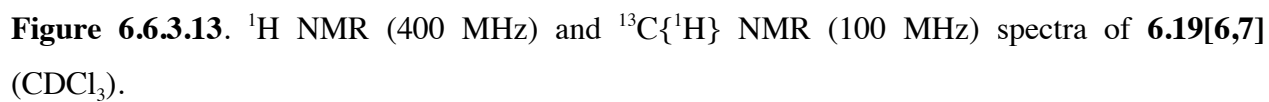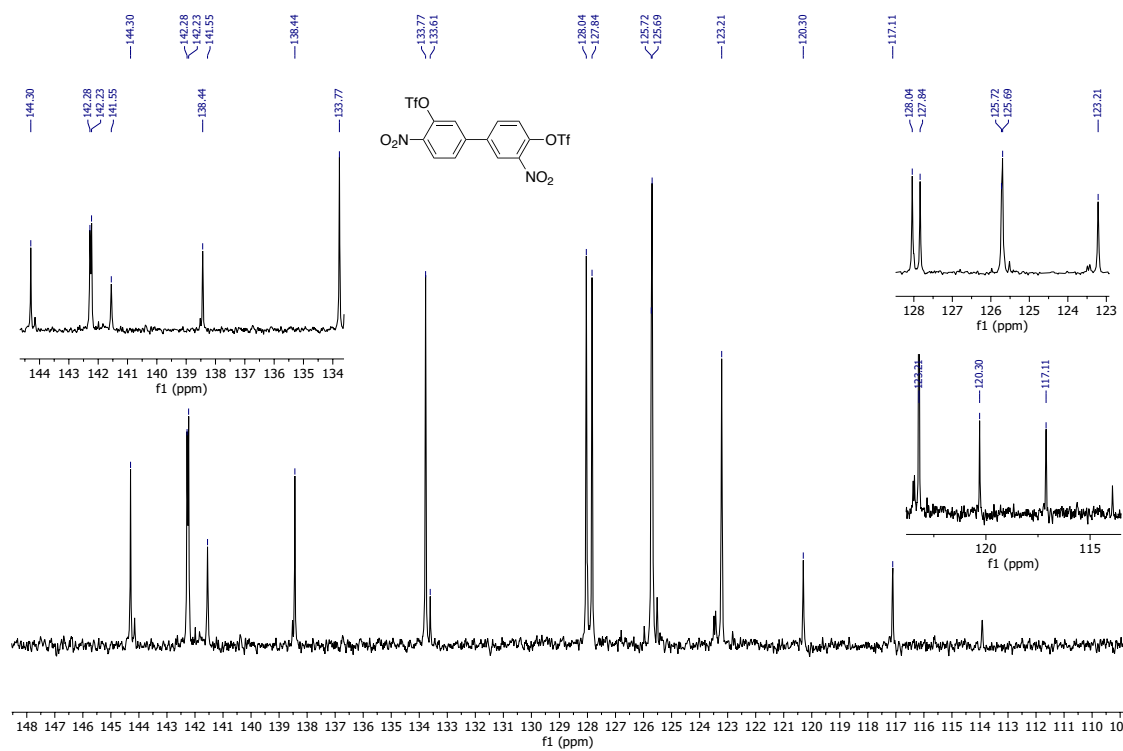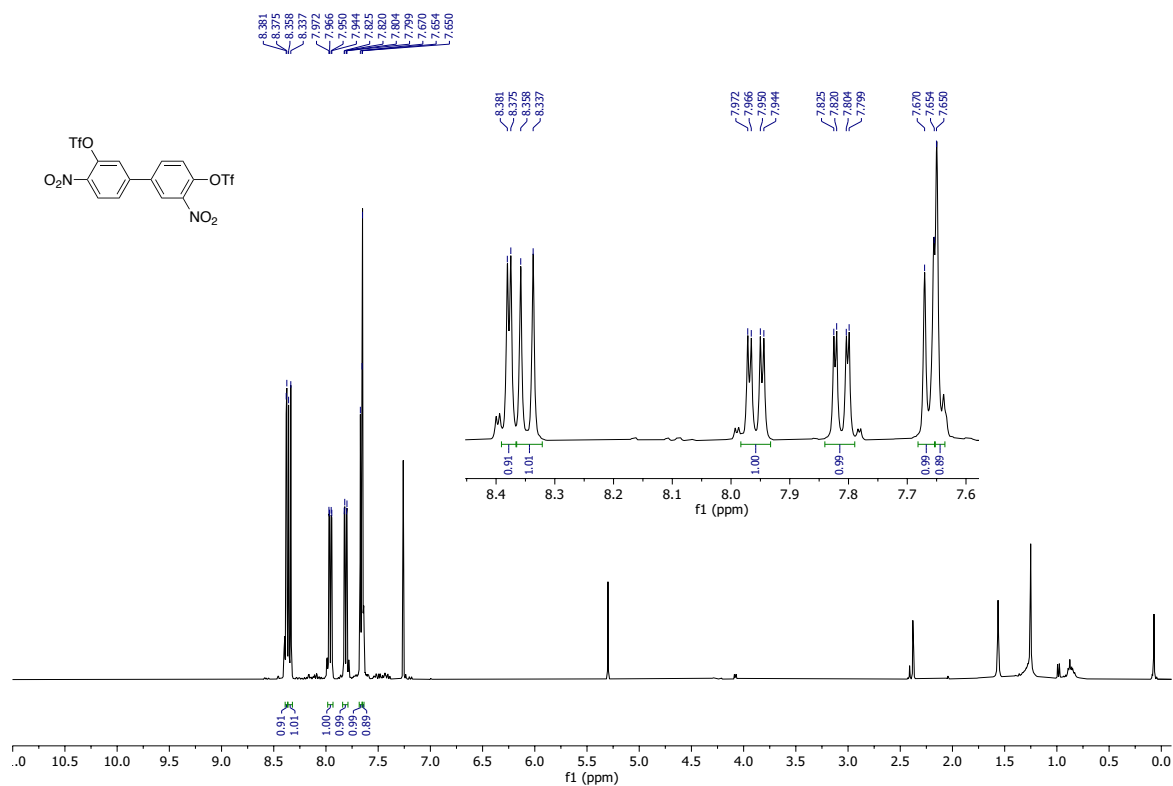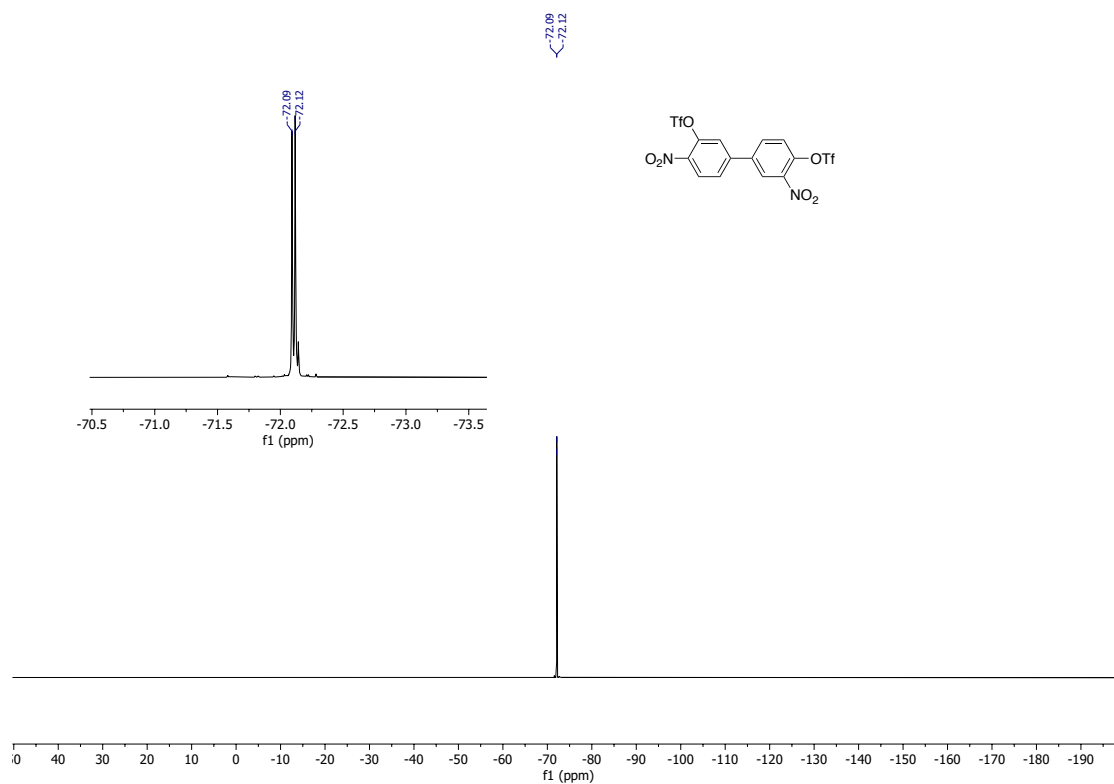
Figure 6.6.3.14. ^{1}H NMR (400 MHz), ^{13}C{^{1}H} NMR (100 MHz) and ^{19}F NMR (377 MHz) spectra of **6.20[6,7]** (CDCl$_3$).
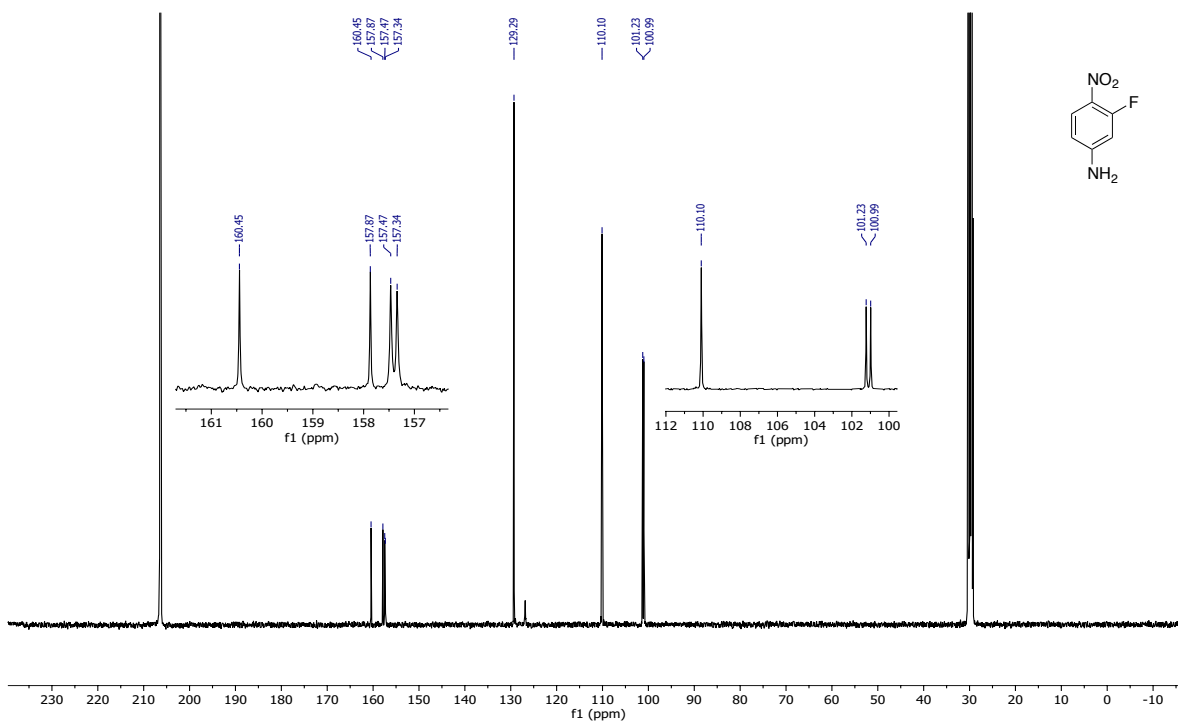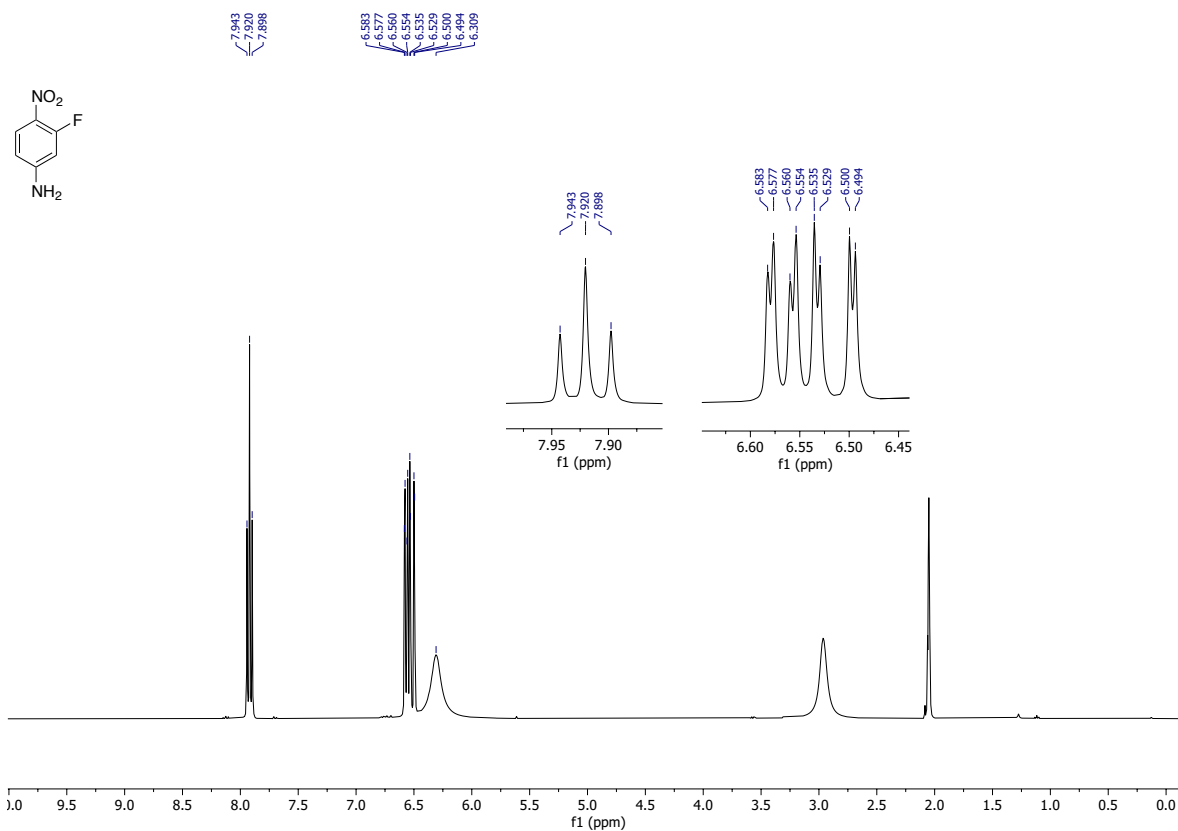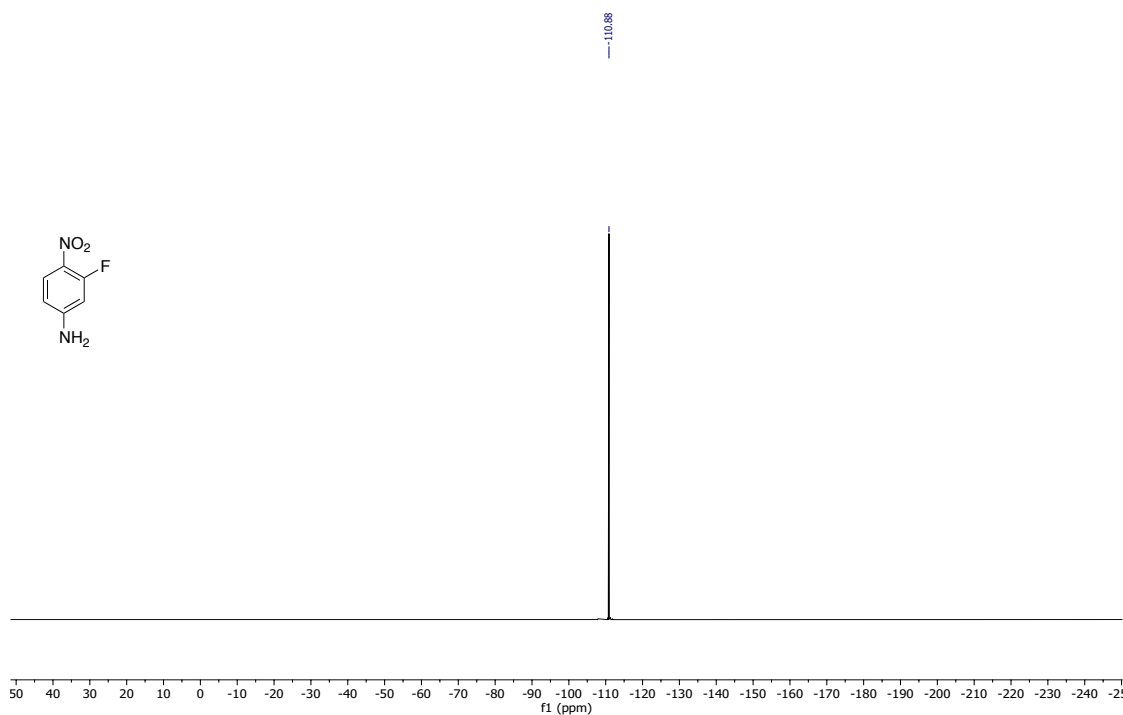
Figure 6.6.3.15. ^{1}H NMR (400 MHz), ^{13}C{^{1}H} NMR (100 MHz) and ^{19}F NMR (377 MHz) spectra of **6.21** (acetone-d_6).

6.6.4. IR spectra

FT-IR spectra were recorded in KBr pellets and results are shown in Figures 6.6.3.16–6.6.3.18.
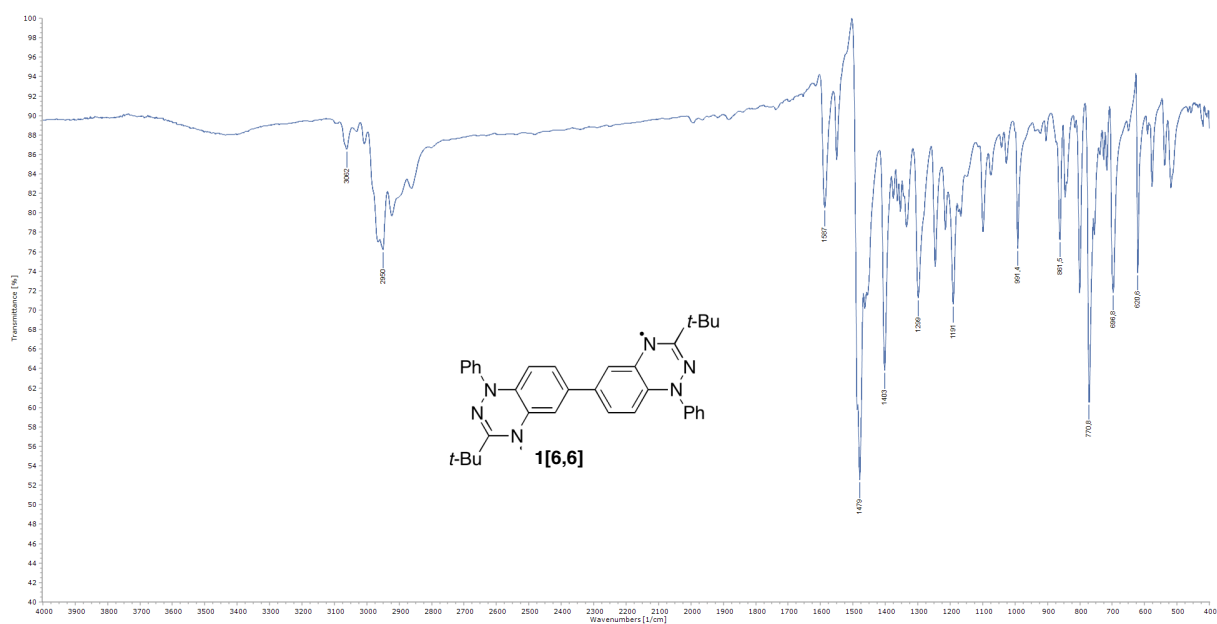
Figure 6.6.3.16. IR spectrum for diradical **6.8[6,6]** recorded in KBr.
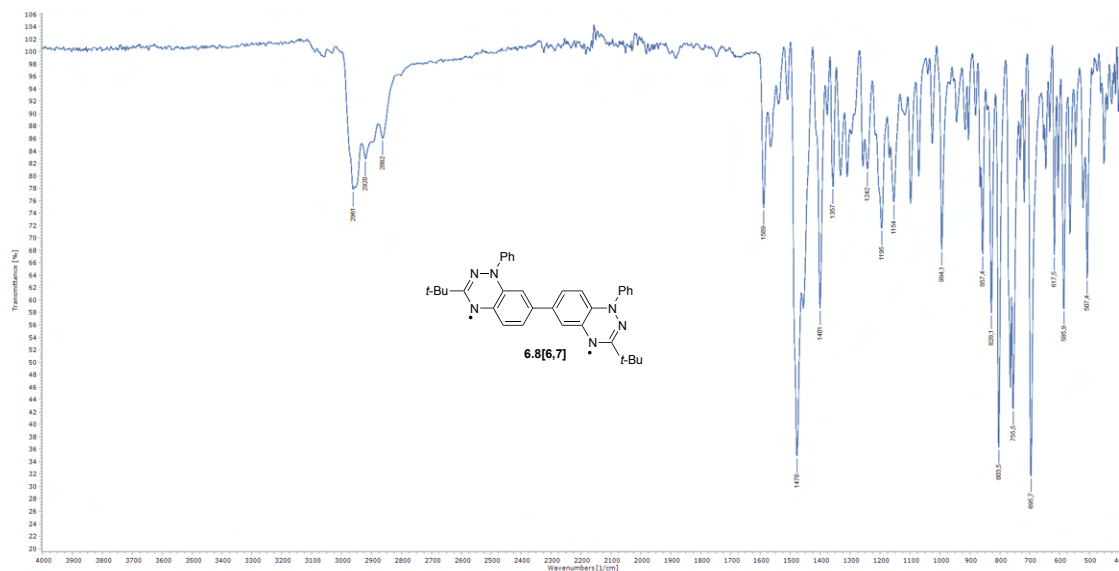
Figure 6.6.3.17. IR spectrum for diradical **6.8[6,7]** recorded in KBr.
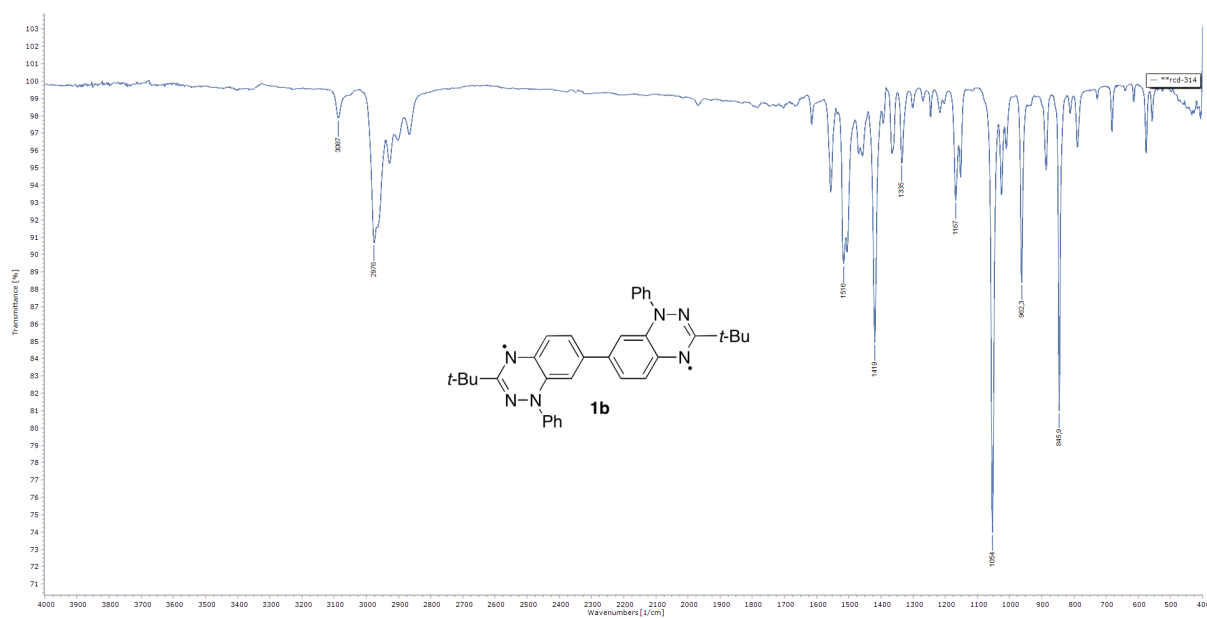
Figure 6.6.3.18. IR spectrum for diradical **6.8[7,7]** recorded in KBr.

6.7.4. XRD data collection and refinement

Data Collection

Crystals of diradicals **6.8[6,6]**, **6.8[6,7]** and **6.8[7,7]** were grown by liquid-liquid diffusion method using CH_2Cl_2/hexane solvent system.

Single-crystal X-ray diffraction measurements for **6.8[6,6]**, **6.8[6,7]** and **6.8[7,7]** were performed with XtaLAB Synergy, Pilatus 300 K diffractometer. All measurements were conducted at

100.0(1) K using Cu$K\alpha$ radiation ($\lambda = 1.54184$ Å). The data were integrated using CrysAlisPro program. Intensities for absorption were corrected using SCALE3 ABSPACK scaling algorithm implemented in CrysALisPro program.[158]

Structure solution and refinement

All structures were solved with the ShelXT structure solution program[159] using Intrinsic Phasing and refined by the full-matrix least-squares minimization on F^2 with the ShelXL refinement package.[159] All non-hydrogen atoms were refined anisotropically. All hydrogen atoms were generated geometrically and refined isotropically using the riding model.

The crystal data and structure refinement descriptors are presented in Table 6.6.3.1, while molecular structures are shown in Figures 6.6.3.19–6.6.3.21.

Table 6.6.3.1. Crystal data and refinement details for diradicals **6.8[m,n]**.

Compound	6.8[6,6]	6.8[6,7]	6.8[7,7]
CCDC	2250028	2255380	2250029
Empirical formula	$C_{34}H_{34}N_6$	$C_{34}H_{34}N_6$	$C_{34}H_{34}N_6$
Formula weight	526.28	526.28	526.28
Crystal system	monoclinic	monoclinic	monoclinic
Space group	$P2_1/n$	$I2/a$	$P2_1/c$
a/Å	9.1253(10)	30.2422(10)	31.6231(5)
b/Å	11.2591(2)	10.3658(3)	8.2908(10)
c/Å	13.6478(2)	39.1965(13)	21.4175(4)
α/°	90	90	90
β/°	90.020(1)	114.998(4)	96.233(2)
γ/°	90	90	90
Volume/Å^3	1402.21(4)	11136.4(7)	5582.1(2)
Z	2	16	8
Goodness-of-fit	1.037	1.061	1.057
Final R indexes [I>=2δ (I)]	$R_1 = 0.0340$ wR_2 =0.0854	$R_1 = 0.0657$ wR_2 =0.1456	$R_1 = 0.0461$ wR_2 =0.1250
Final R indexes [all data]	$R_1 = 0.0362$ wR_2 =0.0869	$R_1 = 0.1043$ wR_2 =0.1647	$R_1 = 0.0585$ wR_2 =0.1334

Selected geometrical parameters of **6.8[6,6]**, **6.8[7,7]** and **6.8[6,7]** are listed in Tables 6.6.3.2–6.6.3.4. For comparison purposes Table 6.6.3.4 contains literature data for diradical **4.5.**[106]
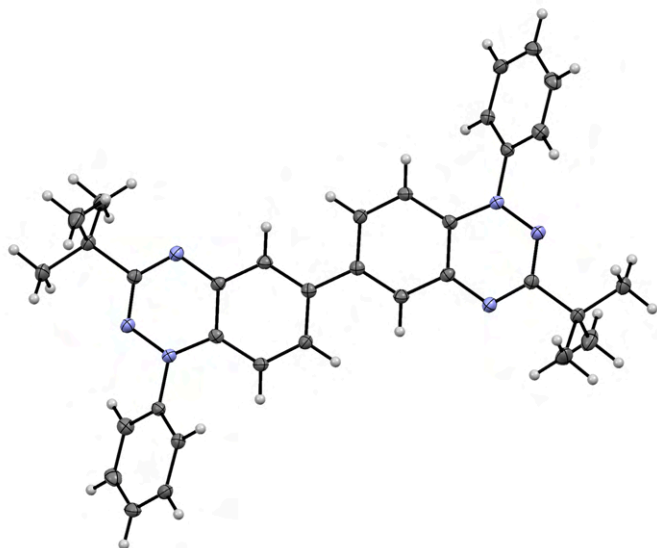
Figure 6.6.3.19. Atomic displacement ellipsoid diagram for diradical **6.8[6,6]**. Ellipsoids are drawn at 50% probability level.
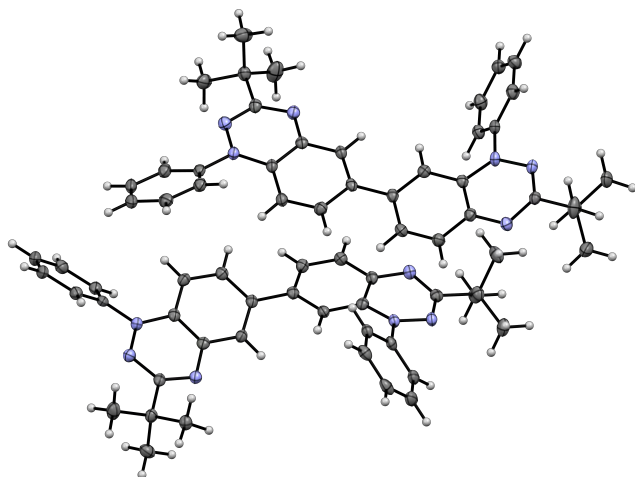
Figure 6.6.3.20. Atomic displacement ellipsoid diagram for two unique molecules of diradical **6.8[6,7]**. Ellipsoids are drawn at 50% probability level.
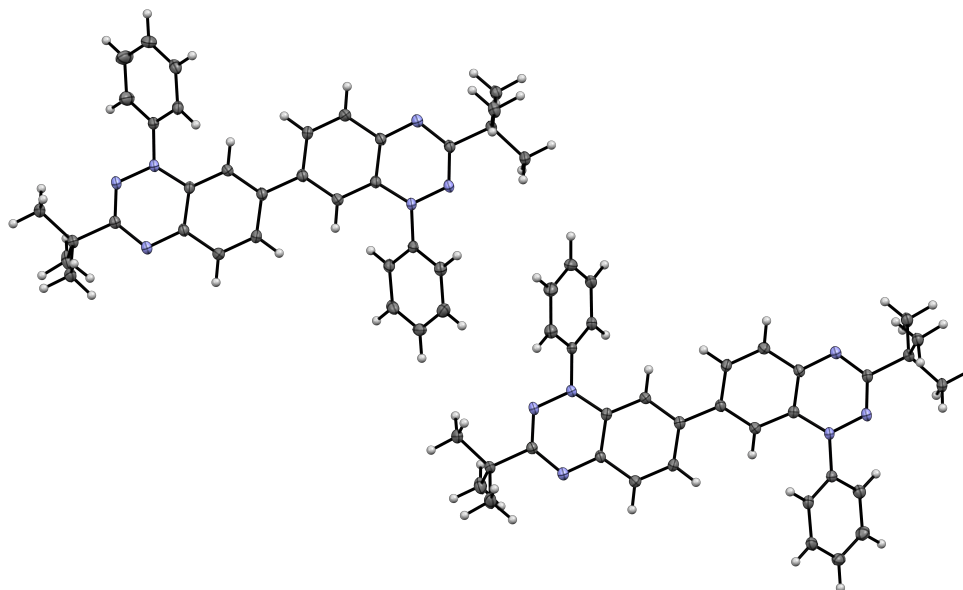
Figure 6.6.3.21. Atomic displacement ellipsoid diagram for two unique molecules of diradical **6.8[7,7]**. Ellipsoids are drawn at 50% probability level.

Table 6.6.3.2. Selected interatomic distances and angles for diradical **6.8[6,6]**.

	6.8[6,6]
N(1)-C(9)	1.431(1)
N(1)-N(2)	1.377(1)
N(2)-C(3)	1.332(1)
C(3)-N(4)	1.337(1)
C(3)-*t*Bu	1.528(1)
N(4)-C(4a)	1.372(1)
C(4a)-C(5)	1.400(1)
C(5)-C(6)	1.392(1)
C(6)-C(7)	1.412(1)
C(7)-C(8)	1.378(1)
C(8)-C(8a)	1.403(1)
C(8a)-N(1)	1.381(1)
C(8a)-C(4a)	1.417(1)
C(6)-C(6')	1.481(1)
C(9)-C(10)	1.391(1)
C(10)-C(11)	1.390(2)
C(11)-C(12)	1.388(2)
N(1)-N(2)-C(3)	115.60(8)
N(2)-C(3)-N(4)	127.97(9)
N(2)-N(1)-C(9)-C(10)	40.5(1)
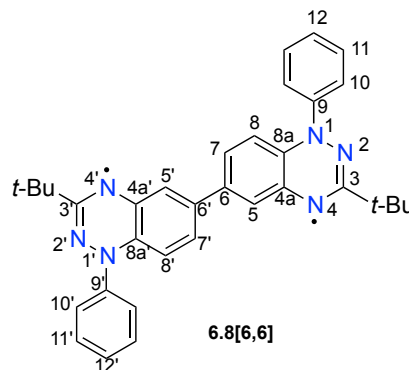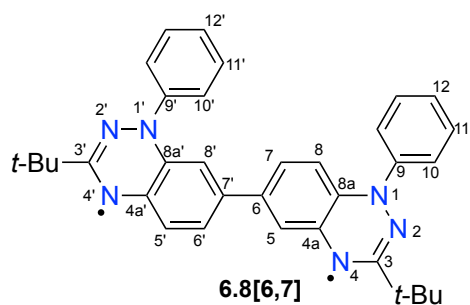
6.8[6,7]

Table 6.6.3.3. Selected interatomic distances and angles for diradical **6.8[6,7]**.

	molecule 1	molecule 2		molecule 1	molecule 2
N(1)-C(9)	1.426(4)	1.439(4)	N(1')-C(9')	1.424(4)	1.429(4)
N(1)-N(2)	1.380(3)	1.381(4)	N(1')-N(2')	1.387(4)	1.388(4)
N(2)-C(3)	1.332(4)	1.333(4)	N(2')-C(3')	1.323(4)	1.310(4)
C(3)-N(4)	1.335(4)	1.340(4)	C(3')-N(4')	1.343(4)	1.350(4)
C(3)-*t*Bu	1.534(4)	1.522(4)	C(3')-*t*Bu	1.526(4)	1.529(5)
N(4)-C(4a)	1.371(4)	1.367(4)	N(4')-C(4a')	1.366(4)	1.360(4)
C(4a)-C(5)	1.399(4)	1.405(5)	C(4a')-C(5')	1.409(5)	1.419(5)
C(5)-C(6)	1.393(4)	1.388(4)	C(5')-C(6')	1.373(5)	1.364(5)
C(6)-C(7)	1.406(4)	1.411(5)	C(6')-C(7')	1.407(4)	1.405(4)
C(7)-C(8)	1.374(4)	1.376(5)	C(7')-C(8')	1.399(4)	1.407(5)
C(8)-C(8a)	1.400(4)	1.394(4)	C(8')-C(8a')	1.392(5)	1.397(5)
C(8a)-N(1)	1.388(4)	1.387(4)	C(8a')-N(1')	1.389(4)	1.392(4)
C(8a)-C(4a)	1.406(4)	1.423(5)	C(8a')-C(4a')	1.417(4)	1.406(4)
C(6)-C(7')	1.481(5)	1.475(5)	C(6)-C(7)	1.481(2)	1.475(5)
C(9)-C(10)	1.376(4)	1.392(5)	C(9')-C(10')	1.388(4)	1.387(5)
C(10)-C(11)	1.385(4)	1.385(5)	C(10')-C(11')	1.378(4)	1.376(4)
C(11)-C(12)	1.390(5)	1.380(5)	C(11')-C(12')	1.395(4)	1.386(5)
N(1)-N(2)-C(3)	115.3(2)	116.5(3)	N(1')-N(2')-C(3')	116.2(2)	116.0(2)
N(2)-C(3)-N(4)	128.2(3)	127.3(3)	N(2')-C(3')-N(4')	127.4(3)	128.0(3)
N(2)-N(1)-C(9)-C(10)	41.2 (4)	30.0(4)	N(2')-N(1')-C(9')-C(10')	-37.0(4)	- 49.4(4)
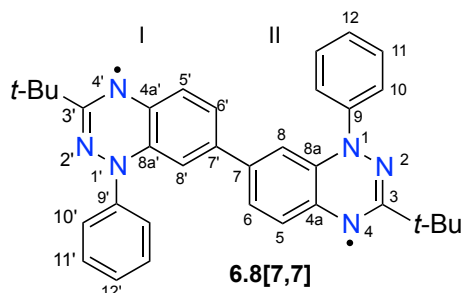
6.8[7,7]

Table 6.6.3.4. Selected interatomic distances and angles for diradical **6.8[7,7]** and **4.5**.

	6.8[7,7] (two molecules)					**4.5** [a]
	molecule 1	molecule 2		molecule 1	molecule 2	
N(1)-C(9)	1.427(2)	1.429(2)	N(1')-C(9')	1.427(2)	1.422(2)	1.431(3)
N(1)-N(2)	1.377(1)	1.375(2)	N(1')-N(2')	1.376(1)	1.375(1)	1.375(2)
N(2)-C(3)	1.313(2)	1.316(2)	N(2')-C(3')	1.317(2)	1.313(2)	1.317(3)
C(3)-N(4)	1.359(2)	1.354(2)	C(3')-N(4')	1.357(2)	1.360(2)	1.356(3)
C(3)-*t*Bu	1.525(2)	1.528(2)	C(3')-*t*Bu	1.528(2)	1.525(2)	1.483(3)
N(4)-C(4a)	1.346(2)	1.353(2)	N(4')-C(4a')	1.354(2)	1.349(2)	1.353(3)
C(4a)-C(5)	1.420(2)	1.416(2)	C(4a')-C(5')	1.419(2)	1.419(2)	1.411(3)
C(5)-C(6)	1.367(2)	1.372(2)	C(5')-C(6')	1.370(2)	1.369(2)	1.366(3)
C(6)-C(7)	1.424(2)	1.421(2)	C(6')-C(7')	1.421(2)	1.421(2)	1.412(3)
C(7)-C(8)	1.404(2)	1.404(2)	C(7')-C(8')	1.403(2)	1.406(2)	1.406(3)
C(8)-C(8a)	1.389(2)	1.384(2)	C(8')-C(8a')	1.388(2)	1.388(2)	1.384(3)
C(8a)-N(1)	1.396(2)	1.399(2)	C(8a')-N(1')	1.394(2)	1.396(2)	1.392(3)
C(8a)-C(4a)	1.428(2)	1.426(2)	C(8a')-C(4a')	1.424(2)	1.424(2)	1.416(3)
C(6)-C(7')	1.467(2)	1.468(2)	C(6)-C(7')	1.467(2)	1.468(2)	1.463(4)
C(9)-C(10)	1.392(2)	1.389(2)	C(9')-C(10')	1.389(2)	1.390(2)	1.380(3)
C(10)-C(11)	1.387(2)	1.388(3)	C(10')-C(11')	1.392(2)	1.388(2)	1.390(3)
C(11)-C(12)	1.390(2)	1.380(2)	C(11')-C(12')	1.383(2)	1.383(2)	1.390(4)
N(1)-N(2)-C(3)	116.8(1)	116.5(1)	N(1')-N(2')-C(3')	116.4(1)	116.9(1)	116.19 (19)
N(2)-C(3)-N(4)	127.1(1)	127.3(1)	N(2')-C(3')-N(4')	127.4(1)	127.0(1)	127.30(19)
N(2)-N(1)-C(9)-C	-37.9 (2)	- 46.9(2)	N(2')-N(1')-C(9')-C	46.0(2)	42.7(2)	55.6 (3)

[a] Ref [106]

6.7.5. Electronic absorption spectroscopy

Electronic absorption spectra of diradicals **6.8[m,n]** were recorded on a Jasco V770 spectrophotometer in spectroscopic grade CH_2Cl_2 at concentrations in a range of 1.9 to 10.0×10^{-5} mol·L^{-1} and the measurements were recorded immediately after. The measured UV-vis spectra

were fitted to the Beer–Lambert law ($A = \varepsilon c l$), the molar absorption coefficient (ε) was derived from the linear plots. Results are shown in Figures 6.6.3.22–6.6.3.24.
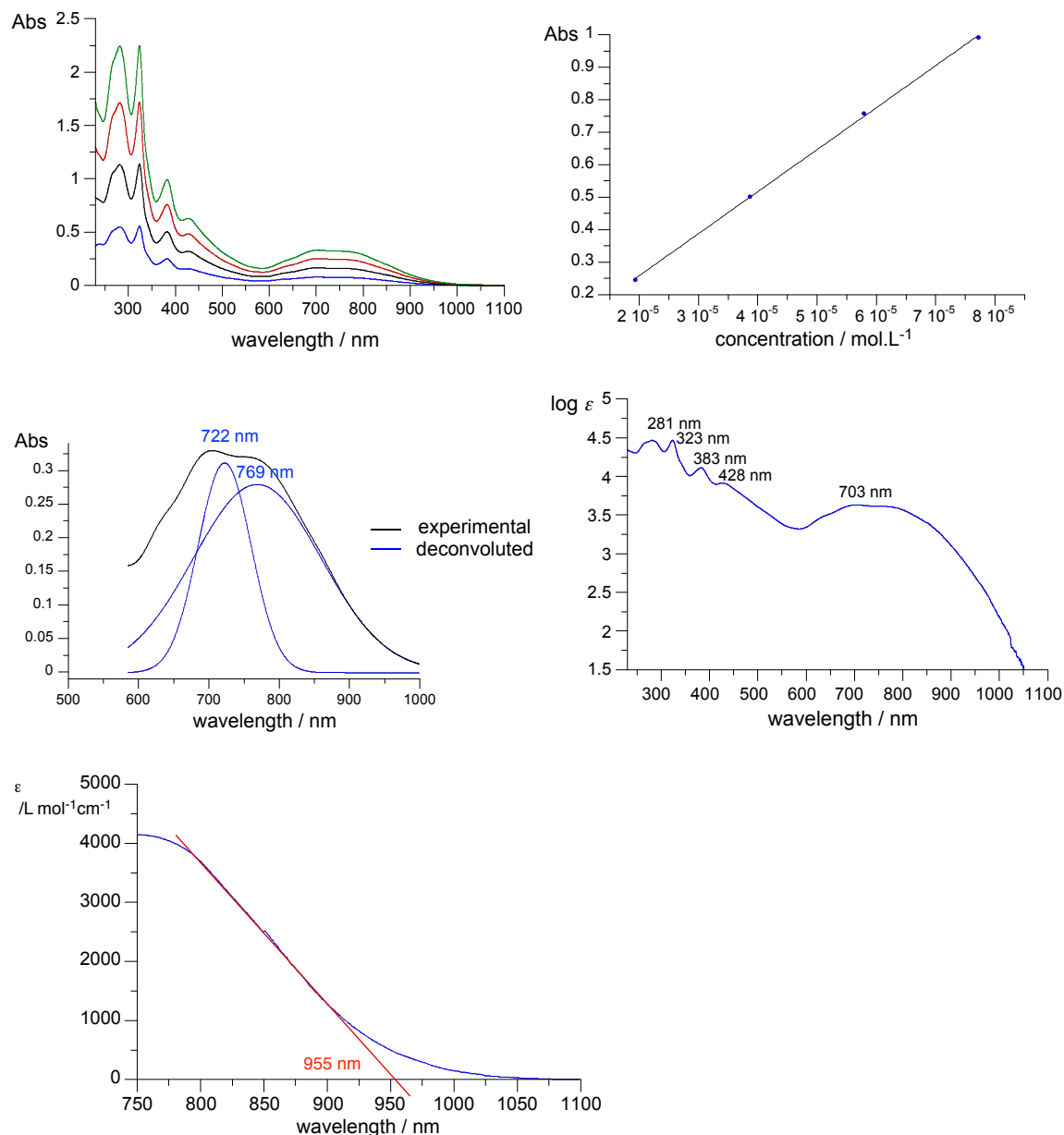
Figure 6.6.3.22. Clockwise: electronic absorption spectra of diradical **6.8[6,6]** in CH_2Cl_2 for four different concentrations, determination of molar extinction coefficient ε at $\lambda = 382.6$ nm (best fit function: $\varepsilon = 12934(65) \times conc$, $r^2 = 0.9996$), molar extinction log (ε) plot, deconvolution of the lowest energy portion of the spectrum and the onset of absorption.
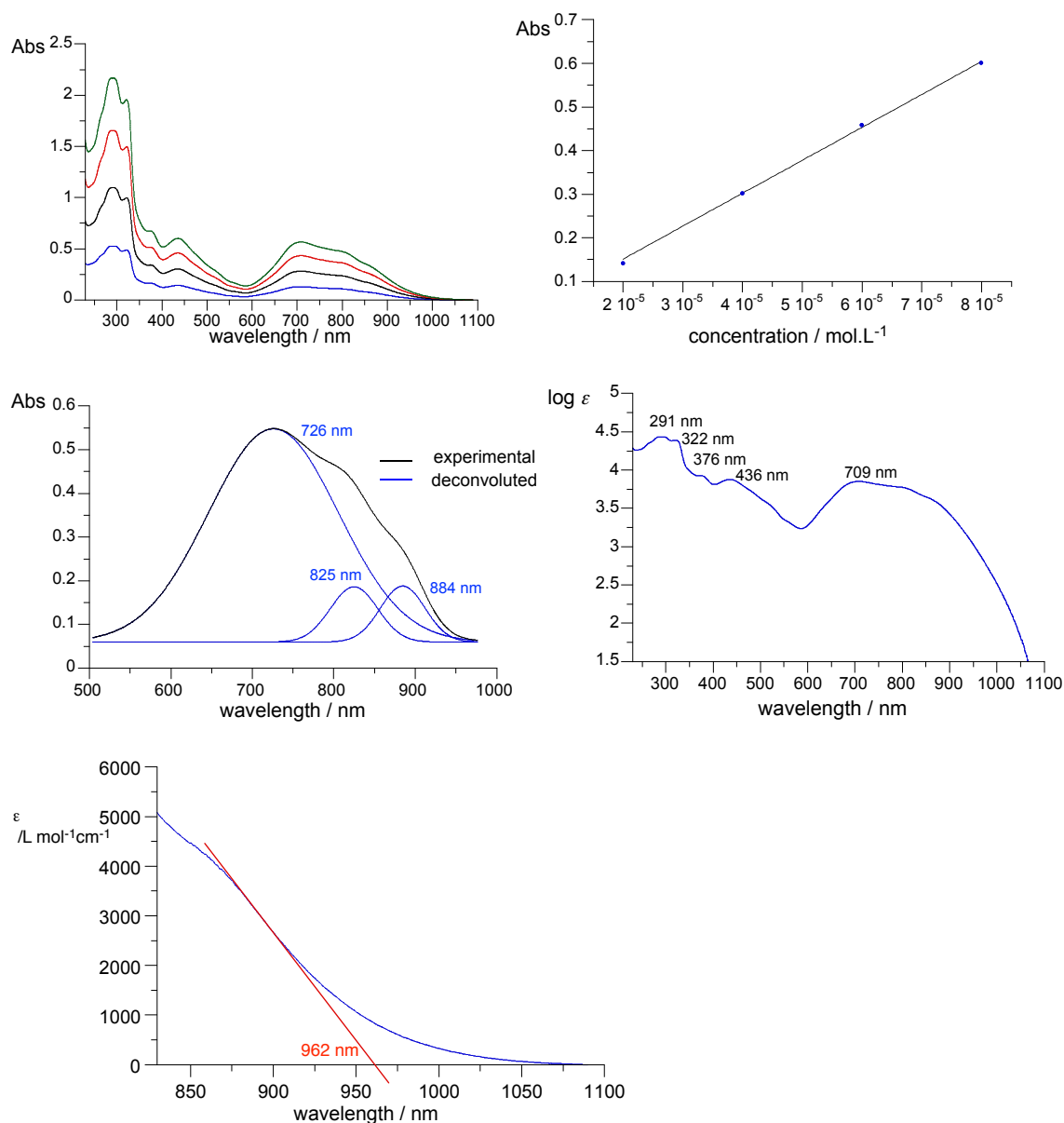
Figure 6.6.3.23. Clockwise: electronic absorption spectra of diradical **6.8[6,7]** in CH_2Cl_2 for four different concentrations, determination of molar extinction coefficient ε at $\lambda = 435.6$ nm (best fit function: $\varepsilon = 7554.5(62) \times conc$, $r^2 = 0.9988$), molar extinction log (ε) plot, deconvolution of the lowest energy portion of the spectrum and the onset of absorption.
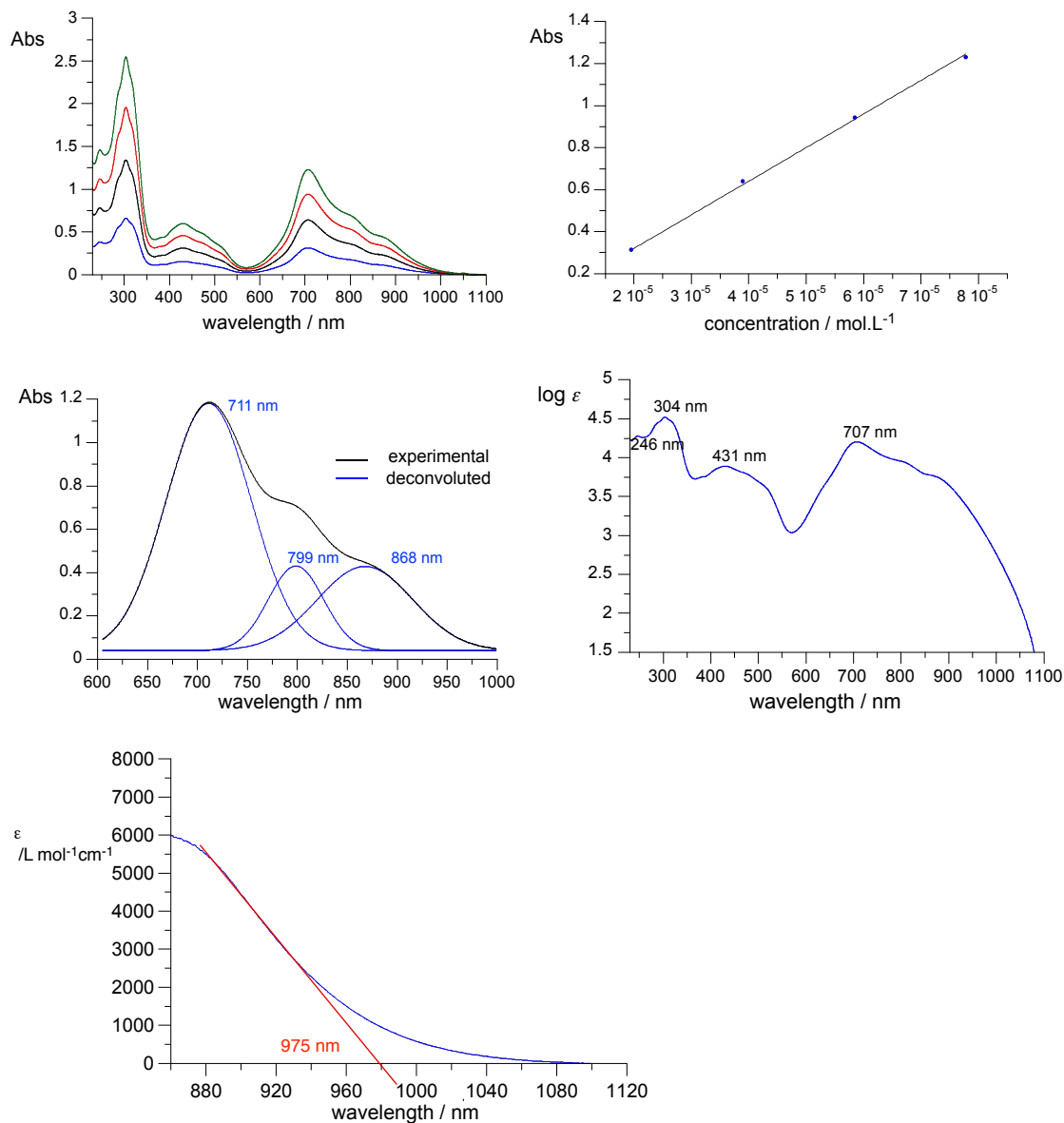
Figure 6.6.3.24. Clockwise: electronic absorption spectra of diradical **6.8[7,7]** in CH_2Cl_2 for four different concentrations, determination of molar extinction coefficient ε at $\lambda = 706.2$ nm (best fit function: $\varepsilon = 16000(129) \times$ conc, $r^2 = 0.9988$), molar extinction log (ε) plot, deconvolution of the lowest energy portion of the spectrum and the onset of absorption.

6.7.6. Electrochemical results

Electrochemical characterization of diradicals **6.8[m,n]** was conducted using a Metrohm Autolab PGSTAT 128N potentiostat/galvanostat instrument. Diradical **6.8[m,n]** was dissolved in dry, spectroscopic grade CH_2Cl_2 (concentration 1.5 mM) in the presence of $[n\text{-}Bu_4N]^+[PF_6]^-$ as an electrolyte (concentration 100 mM) and the resulting solution was degassed by purging with Ar gas for 20 minutes. A three-electrode electrochemical cell was used with glassy carbon disk as the working electrode (ϕ 2 mm, alumina polished), Pt wire as the counter electrode and Ag/AgCl wire as the pseudoreference electrode. All samples were measured without internal reference once and afterwards with $FcMe_{10}$ as the internal reference couple with a scan rate of 50 mV s^{-1} (CV) or 5 mV s^{-1} (DPV) at *ca.* 20 °C. The oxidation potential for the $FcMe_{10}/FcMe_{10}^+$ couple was established at -0.556 V in CH_2Cl_2 *vs* Fc/Fc$^+$, by comparison with the oxidation potential for the Fc/Fc$^+$ couple (0.0 V).

Cyclic voltammetry (CV) measurements were started from 0.0 V in the oxidative direction, while differential pulse voltammetry (DPV) measurements were conducted starting from -1.6 V in the oxidative direction (black line) and starting from 0.9 V in the reductive direction (red line). Cyclic voltammetry (CV) and Differential pulse voltammetry (DPV) plots are shown in Figures 6.6.3.25–6.6.3.27 and numerical results are shown in Table 6.6.3.5.
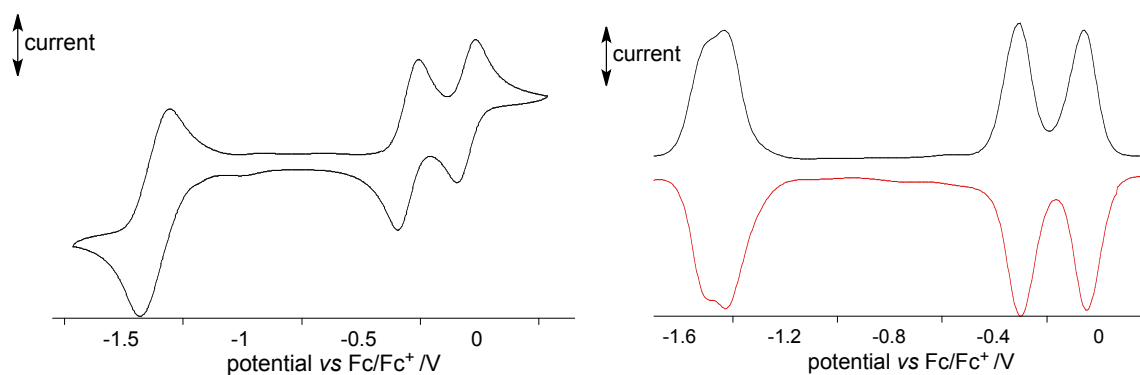
Figure 6.6.3.25. Cyclic voltammogram (CV, left) and differential pulse voltammogram (DPV, right) for **6.8[6,6]** in CH_2Cl_2 referenced to the Fc/Fc$^+$ couple.
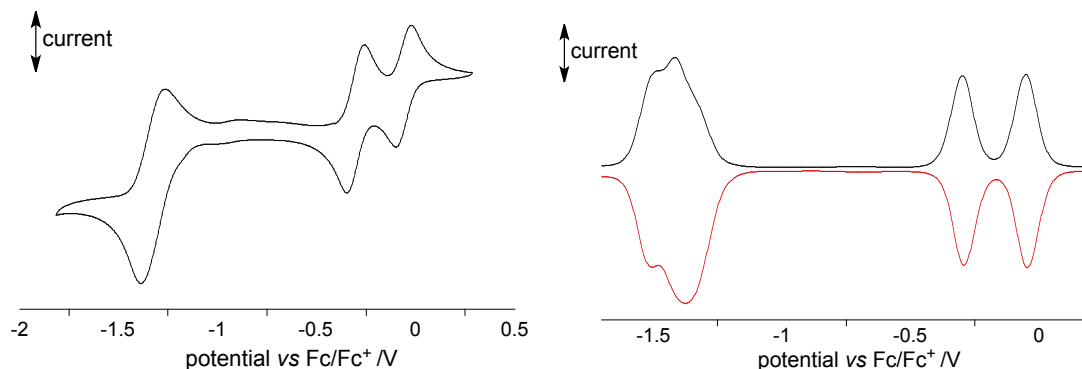
Figure 6.6.3.26. Cyclic voltammogram (CV, left) and differential pulse voltammogram (DPV, right) for **6.8[6,7]** in CH_2Cl_2 referenced to the Fc/Fc$^+$ couple.
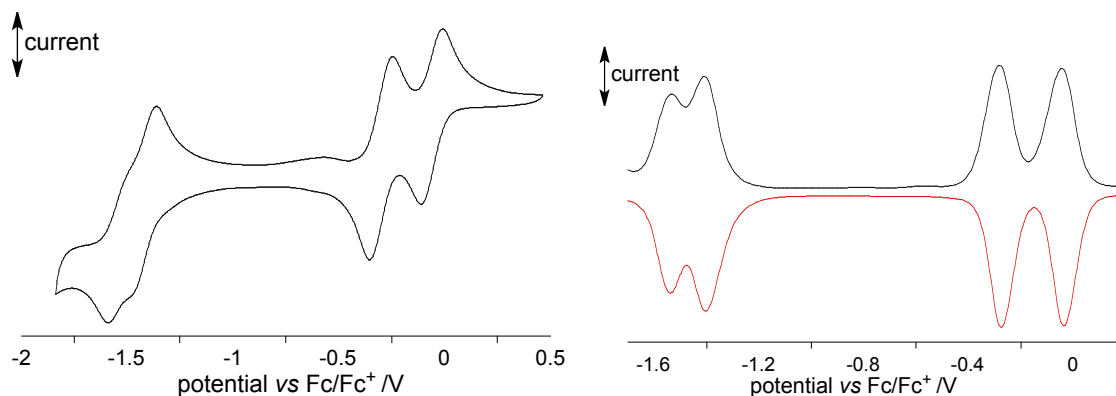
Figure 6.6.3.27. Cyclic voltammogram (CV, left) and differential pulse voltammogram (DPV, right) for **6.8[7,7]** in CH_2Cl_2 referenced to the Fc/Fc$^+$ couple.

Table 6.6.3.5. Electrochemical properties of diradicals **6.8[m,n]**.[a]

diradical	$E_{1/2}^{2-/-}$ (V)	$E_{1/2}^{-/0}$ (V)	$E_{1/2}^{+/0}$ (V)	$E_{1/2}^{2+/+}$ (V)	$\Delta E_{cell}(1)^b$ (V)	$\Delta E_{cell}(2)^b$ (V)
6.8[6,6] [c]	-1.49	-1.43	-0.30	-0.06	1.13	1.43
6.8[6,7] [c]	-1.52	-1.37	-0.30	-0.05	1.07	1.47
6.8[7,7] [c]	-1.53	-1.40	-0.28	-0.04	1.12	1.49

[a]Measured in CH_2Cl_2 [n-Bu$_4$N]$^+$[PF$_6$]$^-$ (100 mM), *ca.* 20 °C, 50 mVs^{-1} (CV); 5 mVs^{-1} (DPV), glassy carbon electrode. Potentials referenced to Fc/Fc$^+$). [b]$\Delta E_{cell}(1) = E_{1/2}^{+/0} - E_{1/2}^{-/0}$; $\Delta E_{cell}(2) = E_{1/2}^{2+/+} - E_{1/2}^{2-/-}$. [c] Data from DPV measurements.

6.7.7. VT EPR spectroscopy
a) sample preparation

A solution of polystyrene (500.2 mg, $d = 1.04$ g cm^{-3}) in dry and distilled CH_2Cl_2 (4 mL) was degassed in vacuum and diradical **6.8[m,n]** (1.317 mg, 2.5×10^{-3} mmol) was added and mixed till a homogenous mixture was formed. The resulting mixture was degassed in vacuum till complete evaporation of the solvent and formation of a fragile polystyrene film. The film was then dried for 1 h, divided into smaller pieces, placed in EPR tube and tightly packed using a glass rod. The EPR tube containing the sample was blown with argon gas, tightly closed, and variable temperature measurement was performed.

b) measurement

Variable temperature EPR spectra for diradicals **6.8[m,n]** were recorded on an X-band EMX-Nano EPR spectrometer equipped with a frequency counter and nitrogen flow temperature control (120 K to 340 K) in degassed solid polystyrene solutions (5.2 mM) at 120 K exhibit patterns with randomly oriented triplets contaminated with signal from the doublet impurity (the middle singlet). No half-field transition $|\Delta m_s| = 2$ was observed in either of the diradicals. Variable-temperature EPR spectra for diradicals **6.8[m,n]** are shown in the Figures 6.6.3.28–6.6.3.30.

c) spectra analysis and simulation

EPR spectra were double integrated and the resulting DI intensities were normalized for the intensity at the lowest temperature. The resulting DI$_{rel}$ are shown in Tables 6.6.3.6–6.6.3.8.

Table 6.6.3.6. Double integral and normalized data for **6.8[6,6]**.

Temp /K	DI	DI/DI_{130}	$DI_{rel} \cdot T$	Temp /K	DI	DI/DI_{130}	$DI_{rel} \cdot T$
130	9040	1	130	234	9930	1.0985	257.04
136	9400	1.0398	141.42	239	9890	1.094	261.47
140	9460	1.0465	146.5	244	9870	1.0918	266.4
144	9680	1.0708	154.19	249	9740	1.0774	268.28
150	9820	1.0863	162.94	254	9860	1.0907	277.04
154	9780	1.0819	166.61	259	9680	1.0708	277.34
159	9910	1.0962	174.3	264	9590	1.0608	280.06
164	9990	1.1051	181.23	269	9610	1.0631	285.96
169	9970	1.1029	186.39	274	9570	1.0586	290.06
174	10100	1.1173	194.4	279	9470	1.0476	292.27
179	10100	1.1173	199.99	284	9360	1.0354	294.05
184	10000	1.1062	203.54	289	9250	1.0232	295.71
189	10100	1.1173	211.16	294	9260	1.0243	301.15
194	10100	1.1173	216.75	299	9220	1.0199	304.95
199	10000	1.1062	220.13	304	9150	1.0122	307.7
204	10100	1.1173	227.92	309	9110	1.0077	311.39
209	10000	1.1062	231.19	314	8970	0.99226	311.57
214	10000	1.1062	236.73	319	8970	0.99226	316.53
219	10100	1.1173	244.68	324	9090	1.0055	325.79
224	9990	1.1051	247.54	329	8910	0.98562	324.27
229	9980	1.104	252.81	334	8860	0.98009	327.35

Table 6.6.3.7. Double integral and normalized data for **6.8[6,7]**.

Temp /K	DI	DI/DI_{120}	$DI_{rel} \cdot T$	Temp /K	DI	DI/DI_{120}	$DI_{rel} \cdot T$
120	2670	1	120	228	5060	1.8951	432.09
123	2850	1.0674	131.29	234	5070	1.8989	444.34
129	3040	1.1386	146.88	239	5030	1.8839	450.25
134	3310	1.2397	166.12	244	5130	1.9213	468.81
138	3330	1.2472	172.11	248	5210	1.9513	483.93
144	3460	1.2959	186.61	253	5320	1.9925	504.1
149	3530	1.3221	196.99	258	5340	2	516
154	3650	1.367	210.52	263	5580	2.0899	549.64
159	3950	1.4794	235.22	269	5280	1.9775	531.96
163	4170	1.5618	254.57	273	5370	2.0112	549.07
169	3980	1.4906	251.92	279	5540	2.0749	578.9
174	4370	1.6367	284.79	284	5430	2.0337	577.57
178	4330	1.6217	288.67	288	5440	2.0375	586.79
183	4350	1.6292	298.15	294	5440	2.0375	599.01
188	4430	1.6592	311.93	298	5640	2.1124	629.48
193	4620	1.7303	333.96	304	5720	2.1423	651.27
199	4630	1.7341	345.08	308	5580	2.0899	643.69
204	4640	1.7378	354.52	313	5560	2.0824	651.79
208	4840	1.8127	377.05	318	5650	2.1161	672.92
213	4870	1.824	388.51	323	5690	2.1311	688.34
219	4980	1.8652	408.47	328	5700	2.1348	700.22
224	5020	1.8801	421.15	333	5620	2.1049	700.92

Table 6.6.3.8. Double integral and normalized data for **6.8[7,7]**.

Temp /K	DI	DI/DI$_{149}$	DI$_{rel}$•T	Temp /K	DI	DI/DI$_{149}$	DI$_{rel}$•T
149	82	1	149	244	1300	15.854	3868.3
154	257	3.1341	482.66	248	1300	15.854	3931.7
159	491	5.9878	952.06	254	1380	16.829	4274.6
163	523	6.378	1039.6	258	1340	16.341	4216.1
169	641	7.8171	1321.1	263	1420	17.317	4554.4
173	701	8.5488	1478.9	269	1560	19.024	5117.6
179	741	9.0366	1617.5	274	1520	18.537	5079
184	721	8.7927	1617.9	279	1790	21.829	6090.4
188	826	10.073	1893.8	283	1490	18.171	5142.3
193	842	10.268	1981.8	288	1620	19.756	5689.8
198	879	10.72	2122.5	293	1800	21.951	6431.7
203	945	11.524	2339.5	299	1770	21.585	6454
208	892	10.878	2262.6	304	1880	22.927	6969.8
213	1040	12.683	2701.5	309	1660	20.244	6255.4
219	1120	13.659	2991.2	314	1670	20.366	6394.9
223	1180	14.39	3209	319	1780	21.707	6924.6
228	1200	14.634	3336.6	324	1640	20	6480
234	1170	14.268	3338.8	328	1720	20.976	6880
239	1350	16.463	3934.8	333	1890	23.049	7675.2

The singlet-triplet energy gap ΔE_{S-T} (2J) was estimated by fitting DI$_{rel}$•T to a modified Bleaney-Bowers equation[88] (eq 6.6.3.1).

$$\chi \bullet T = \frac{N g^2 \mu_B^2}{k} \left(\frac{2}{3 + e^{-\frac{2J}{kT}}} \right) (1 - \rho) + \frac{N g^2 \mu_B^2}{2k} \rho \qquad \text{eq 6.6.3.1}$$

For numeral fitting to the eq 6.6.3.1, a three-parameter equation 6.6.3.2 was used.

$$DI_{rel} \times T = m1 \left(\frac{2}{3 + e^{-\frac{m2}{m0}}} \right) (1 - m3) + 0.5 \times m1 \times m3 \qquad \text{eq 6.6.3.2}$$

Results are shown in Figures 6.6.3.28–6.6.3.30 and in Table 6.6.3.9.
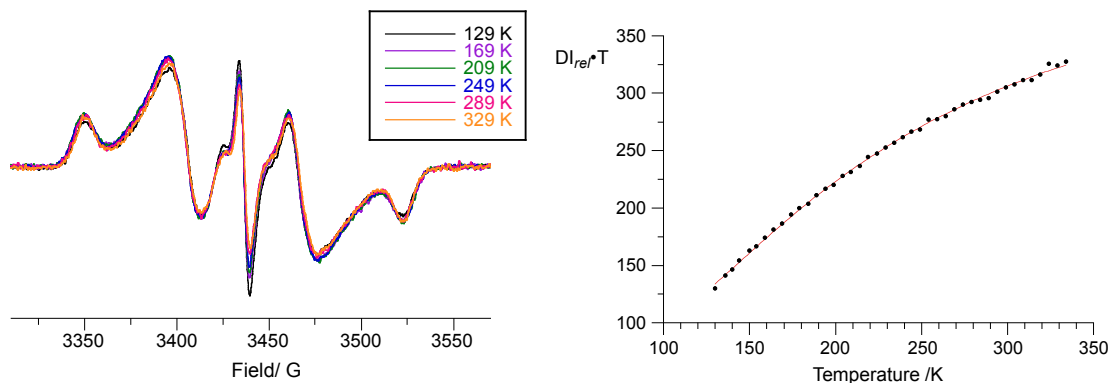
Figure 6.6.3.28. Determination of ΔE_{ST} for 5.2 mM diradical **6.8[6,6]** in polystyrene. Left: variable temperature spectra in the temperature range 129–329 K. Right: plot of $DI_{rel} \cdot T$ *vs T*, in the temperature range 130–334 K. Red line represents the best fitting function (eq. 6.6.3.2) with the following parameters: $m1 = 950(6)$, $m2 = 2J/k = -406(7)$ K, $m3 = 0.150$, $r^2 = 0.999$.
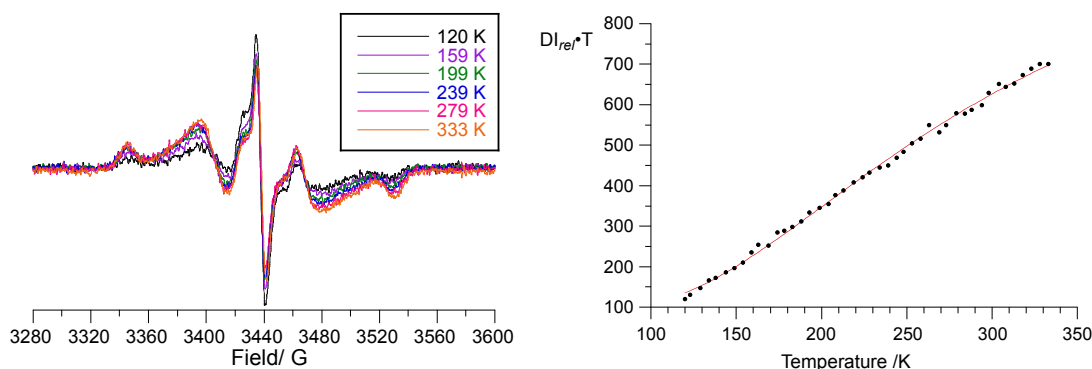
Figure 6.6.3.29. Determination of ΔE_{ST} for 5.2 mM diradical **6.8[6,7]** in polystyrene. Left: variable temperature spectra in the temperature range 120–333 K. Right: a plot of $DI_{rel} \cdot T$ *vs T* in the temperature range 120–333 K. The red line represents the best fitting function (eq. 6.6.3.2) with the following parameters: $m1 = 2764(50)$, $m2 = 2J/k = -569(10)$ K, $m3 = 0.066$, $r^2 = 0.997$.
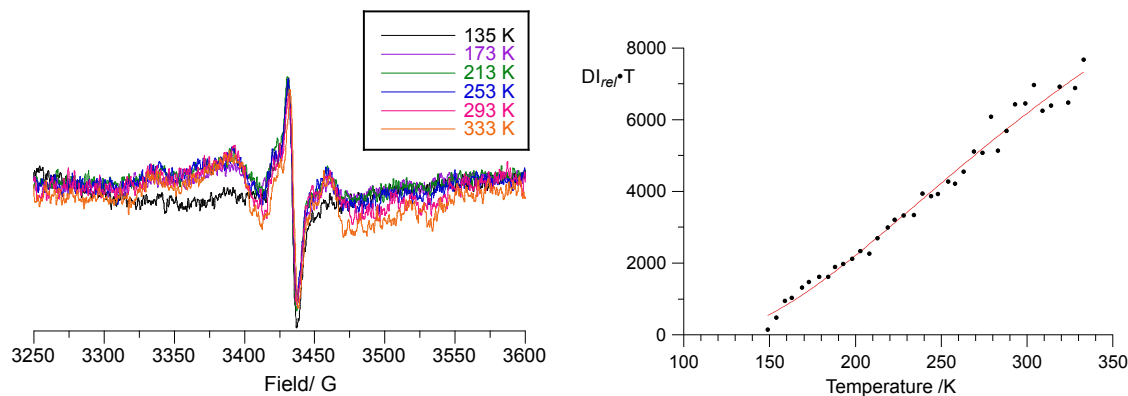
Figure 6.6.3.30. Determination of ΔE_{ST} for 5.2 mM diradical **6.8[7,7]** in polystyrene. Left: variable temperature spectra in the temperature range 135–333 K. Right: a plot of $DI_{rel}\cdot T$ *vs T* in the temperature range 149–333 K. The red line represents the best fitting function (eq. 6.6.3.2) with the following parameters: $m1 = 39640(2965)$, $m2 = 2J/k = -673(38)$ K, $m3 = -0.016(15)$, $r^2 = 0.983$.

Table 6.6.3.9. The singlet-triplet energy gap $\Delta E_{S\text{-}T}$ (2J) for diradicals **6.8[m,n]** determined by fitting to the Bleaney-Bowers equation eq 6.6.3.1.

	Matrix	$\Delta E_{S\text{-}T}$ /kcal/mol
6.8[6,6]	PS	-0.81(1)
6.8[6,7]	PS	-1.13(2)
6.8[7,7]	PS	-1.33(8)

Simulation of triplet EPR spectra for diradicals **6.8[m,n]** was conducted using the *pepper* module in *EasySpin* (Matlab),[160] and results are shown in Figures 6.6.3.31–6.6.3.33. Assuming an isotropic *g* value, the resulting absolute values of zero field splitting parameters (*zfp*), |*D/hc*| and |*E/hc*|, are shown in Table 6.6.3.10. Assuming a point dipole approximation, the mean distance between the spin centers was estimated using equation 6.6.3.3.

$$r = ((D/2g)\times7.19\times10^{-5})^{-1/3} \qquad\qquad \text{eq 6.6.3.3}$$

where *D* (in gauss) is the fitting parameter in the simulated EPR spectrum.
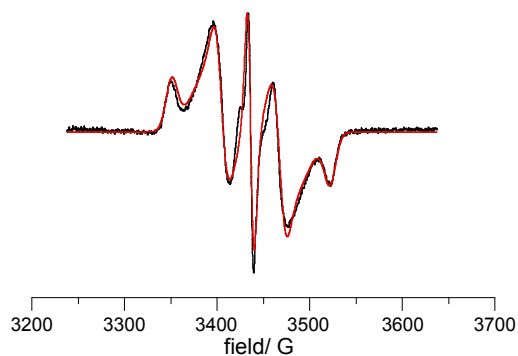
Figure 6.6.3.31. A complete set of fitting parameters for EPR spectrum of 5.2 mM diradical **6.8[6,6]** in polystyrene (119 K, ν = 9.644 GHz). Simulation $|\Delta m_S|$ = 1 region (*pepper*, *EasySpin*, rmsd = 0.0821065): Component A, weight = 1.0000, S = 1, D = 238.77 MHz, E = 16.63 MHz, g_{iso} = 2.00492; H-strain (MHz): H_x = 37.0232, H_y = 120.226, H_z = 40.7546; D-strain (MHz): D = 80.00, E = 30.00; component B, S =1/2, weight = 0.146923, g_{iso}= 2.00497, H-strain (MHz): H_x = 50.00, H_y = 50.00, H_z = 87.00.
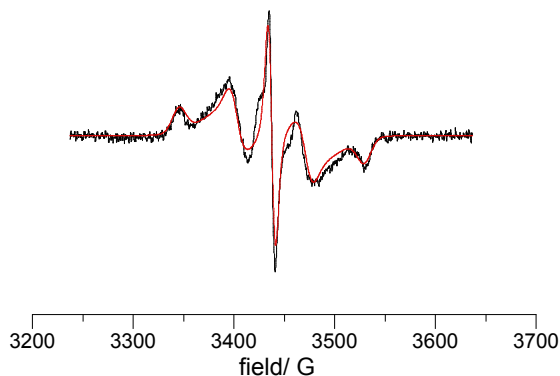
Figure 6.6.3.32. A complete set of fitting parameters for EPR spectrum of 5.2 mM diradical **6.8[6,7]** in polystyrene (253 K, ν = 9.644 GHz). Simulation $|\Delta m_S|$ = 1 region (*pepper*, *EasySpin*, rmsd = 0.0464004): Component A, weight = 1.0000, S = 1, D = 255.30 MHz, E = 16.72 MHz, g_{iso} = 2.00455, H-strain (MHz): H_x = 38.376, H_y = 169.137, H_z = 43.438; D-strain (MHz): D = 80.00, E = 30.00; component B, S =1/2, weight = 0.2324777, g_{iso} = 2.00443; H-strain (MHz): H_x = 50.00, H_y = 50.00, H_z = 87.00.
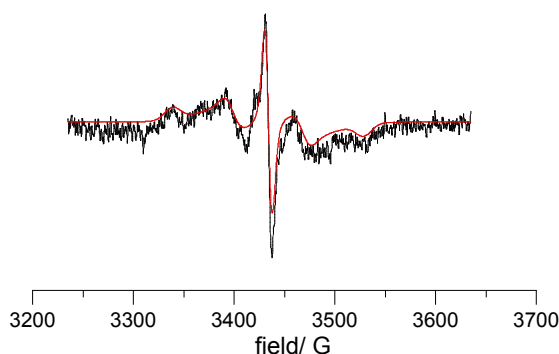
Figure 6.6.3.33. A complete set of fitting parameters for the EPR spectrum of 5.2 mM diradical **6.8[7,7]** in polystyrene (253 K, ν = 9.644 GHz). Simulation $|\Delta m_S|$ = 1 region (pepper, EasySpin, rmsd = 0.0443615): Component A, weight = 1.0000, S = 1, D = 263.629 MHz, E = 17.876 MHz, g_{iso} = 2.00666; H-strain (MHz): H_x = 42.446, H_y = 191.877, H_z = 50.029; D-strain (MHz): D = 80.00, E = 30.00; component B, S =1/2, weight = 0.294611, g_{iso} = 2.0065; H-strain (MHz): H_x = 50.00, H_y = 50.00, H_z = 87.00.

Table 6.6.3.10. Zero field splitting parameters simulated for di-Blatter diradicals **6.8[m,n]**.

compound	Matrix, temp/ K	$|D/hc|$ /cm^{-1}	$|E/hc|$ /cm^{-1}	g	r /Å ^{a}
6.8[6,6]	PS, 119	7.97×10^{-3}	5.55×10^{-4}	2.00492	8.68
6.8[6,7]	PS, 253	8.52×10^{-3}	5.58×10^{-4}	2.00455	8.97
6.8[7,7]	PS, 253	8.80×10^{-3}	5.97×10^{-3}	2.00666	9.86

^{a} Calculated using equation 6.6.3.3.

6.7.8. Stability testing
a) thermal stability

Thermal stability of diradicals **6.8[m,n]** was investigated with a thermogravimetric method (TGA) using a TA Instruments TGA 5500 at a heating rate of 10 K min^{-1} under nitrogen atmosphere. Results are shown in Figures 6.6.3.34–6.6.3.36.
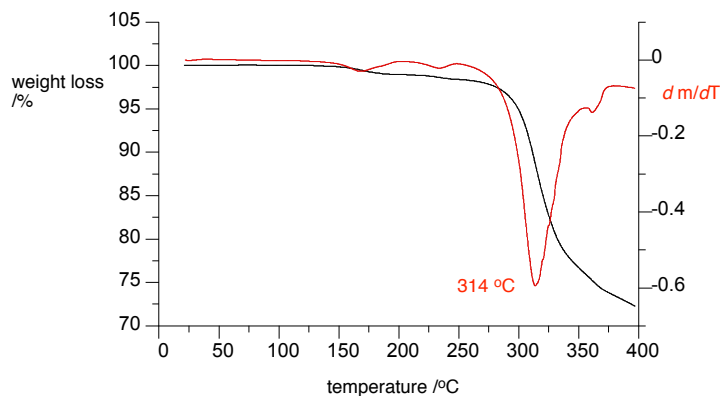
Figure 6.6.3.34. Termogravimetric analysis of diradical **6.8[6,6]**. Heating rate of 10 K min^{-1}.
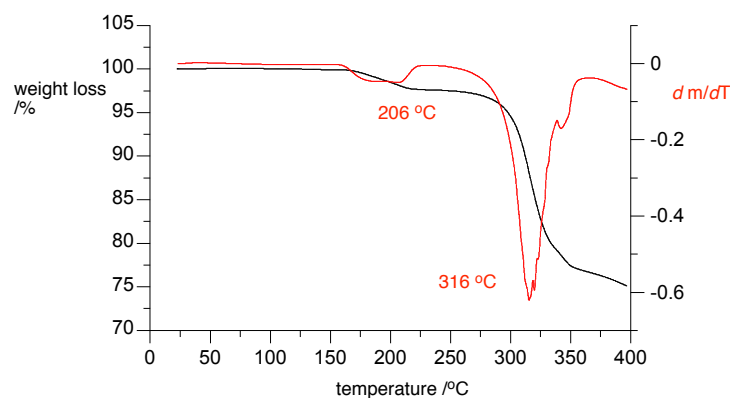
Figure 6.6.3.35. Termogravimetric analysis of diradical **6.8[6,7]**. Heating rate of 10 K min^{-1}.
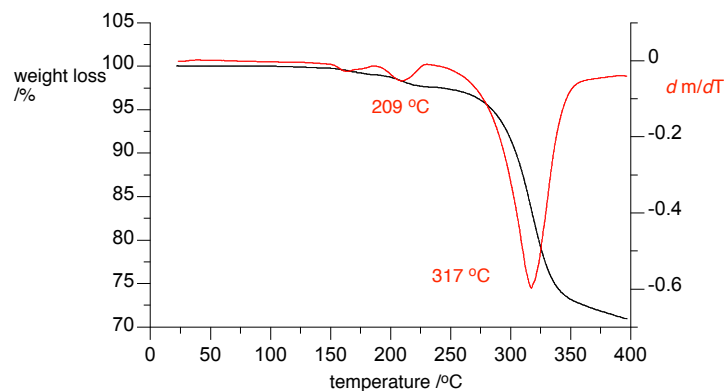
Figure 6.6.3.36. Termogravimetric analysis of diradical **6.8[7,7]**. Heating rate of 10 K min^{-1}.

b) photo stability

Photostability of diradicals **6.8[m,n]** was investigated in CH_2Cl_2 solutions in a quartz cuvette and the absorbance at 705 nm was measured periodically. If needed, fresh solvent was added to maintain the original volume of the solution before each measurement.

Solutions of diradicals in spectroscopic grade CH_2Cl_2 and concentration of 1.0×10^{-4} $mol \cdot L^{-1}$ in a quartz cuvette with the optical path of 1.0 cm were irradiated with unfiltered light produced by a 400 W halogen lamp placed in a distance of 30 cm. Cuvettes were cooled during irradiation with a fan. Electronic absorption spectra of diradicals were recorded on a Jasco V770 spectrophotometer. Results are shown in Figure 6.6.3.37.
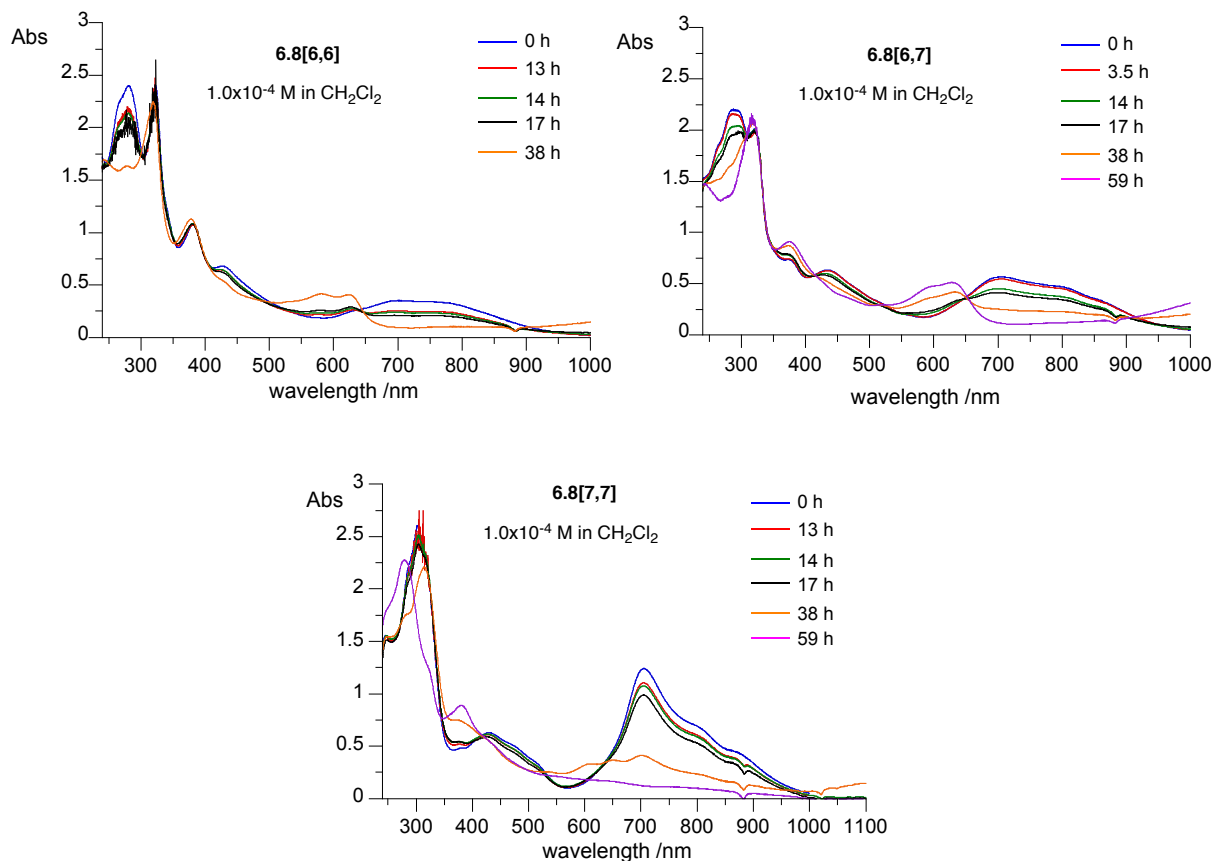
Figure 6.6.3.37. Electronic absorption spectra of 1.0x10-4 M solution of diradicals **6.8[m,n]** in CH_2Cl_2 irradiated with unfiltered white light (400 W halogen lamp)

Photodecomposition products of **6.8[7,7]** diradical were separated using semipreparative TLC and hexane / ethyl acetate / methanol (6:6:1) as the eluent. The resulting 6 fractions and the baseline material were analyzed by TOF MS ES(+) analysis and results are shown in Figure 6.6.3.38.

fraction 1

230710_pr_1D 18 (0.251) Cm (15:20-42:54)

TOF MS ES+
2.57e6

526.2843
540.2639
541.2676
317.1216
318.1254
257.1367
199.0946
255.1207
169.0840
127.0371
451.2132
583.3494

fraction 2

230710_pr_2B 14 (0.217) Cm (9:15)

TOF MS ES+
1.63e6

540.2632
541.2682
271.1387
270.6352
271.6405
272.1424
527.2885
542.2728
515.2648
432.2381
561.2240
317.1515
227.1257
137.5048
108.0091

fraction 3

230710_pr_3_A 14 (0.217) Cm (11:18-3:6)

TOF MS ES+
1.24e6

561.2530
525.2755
562.2562
575.2346
524.2668
595.2169
458.2200
424.2382
263.1389
202.1341
270.1315
319.7046
394.3474
178.1587
203.1371
111.1184

fraction 4

fraction 5

fraction 6
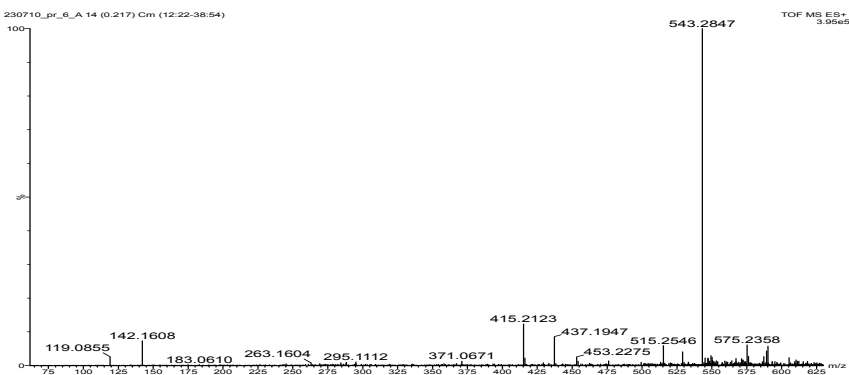
baseline
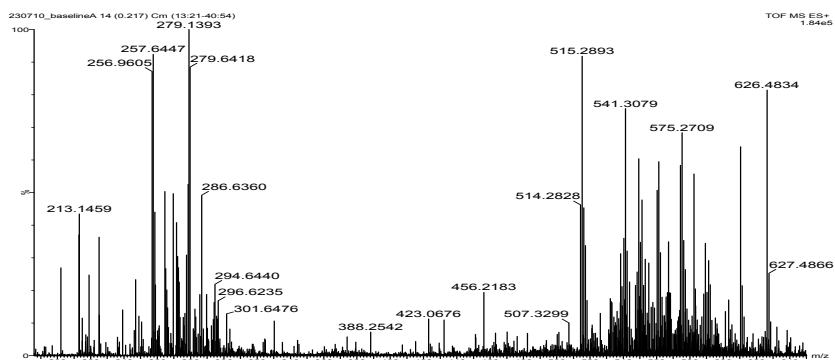
Figure 6.6.3.38. Mass spectra of six fractions in the order of increasing polarity from the top and the baseline material (bottom).

High-resolution mass spectrometry (HRMS) analysis was conducted for selected *m/z* peaks and results are listed in Table 6.6.3.11.

Table 6.6.3.11. High-resolution mass spectra (HRMS) results for selected *m/z* signals in the photodegradation products of diradical **6.8[7,7]**.[a]

Measured mass	Calculated mass	Error /mDa	/ppm	Conf /%	formula
577.2477	577.2483	-0.6	-1.0	100	$C_{34}H_{34}N_6ClO$
576.2386	576.2404	-1.8	-3.1	n/a	$C_{34}H_{33}N_6ClO$
561.2530	561.2533	-0.3	-0.5		$C_{34}H_{34}N_6Cl$
543.2857	543.2872	-1.5	-2.8	94	$C_{34}H_{34}N_9O$
540.2639	540.2638	1.5	32.8	51	$C_{34}H_{32}N_9O$
527.2923[b]	527.2901				$C_{34}H_{35}N_6$ $[M+H]^+$

[a] Obtained using the TOF MS ES(+) method. [b] HRMS for diradical **1[7,7]**.

6.7. Experimental Section for Blatter diradicals with a spin coupler at the N(1) position

6.7.1. General information

Reagents and solvents were obtained commercially. Reactions were carried out under inert atmosphere (N_2 gas) and subsequent reaction work-ups were conducted in air. Volatiles were removed under reduced pressure. Reaction mixtures and column eluents were monitored by TLC using aluminum-backed thin layer chromatography (TLC) plates (Merck Kieselgel 60 F_{254}). The plates were observed under UV light at 254 and 365 nm. Melting points were determined on a Melt-Temp II apparatus in capillaries, and they are uncorrected. IR spectra were recorded using Nexus FT-IR Thermo Nilolet IR spectrometer in KBr pellets. High-resolution mass spectrometry (HRMS) measurements were performed using SYNAPT G2-Si High-Definition Mass Spectrometry equipped with an ESI mass analyzer. Electronic absorption spectra were recorded on a Jasco V770 Uv-vis-NIR spectrophotometer in spectroscopic grade CH_2Cl_2. The electrochemical characterization was conducted using a Metrohm Autolab PGSTAT 128N potentiostat/galvanostat instrument. EPR spectra were recorded on an X-band EMX-Nano EPR spectrometer equipped with a frequency counter and nitrogen flow temperature control.

6.7.2. Synthesis

Preparation of diradicals 6.22. A general procedure. Following a general procedure,[34, 44] 1.7 M solution of *tert*-butyllithium (2.47 mL, 4.2 mmol, 4.2 equiv.) in pentane was added dropwise to a stirred solution of appropriate diiodobenzene (1 mmol, 1 equiv.) in dry THF (3 mL, 0.33 M) at -78 °C under inert atmosphere and stirred for 40 min at -78 °C. A solution of 3-(trifluoromethyl)benzo[*e*][1,2,4]triazine[125] (**6.24**, 2 mmol, 2 equiv.) in dry THF (3 mL, 0.66 M) was cooled to -78 °C and added dropwise to the resulting mixture. The reaction mixture was stirred for 50 min at -78 °C and then at rt for 40 min. The reaction flask was opened and stirring was continued overnight in air at rt. Solvents were evaporated, water and CH_2Cl_2 were added and the organic phase was separated, washed with water and dried (Na_2SO_4). After evaporation of the solvent, the resulting crude product was purified by column chromatography (SiO_2 passivated with 1% Et_3N in CH_2Cl_2, pet. ether/Et_2O/CH_2Cl_2, 2/2/1). The resulting solid was washed with hot *n*-pentane (5 x 5 mL) to afford analytically pure diradicals **6.22**.

Diradical 6.22p. (271.3 mg, 0.572 mmol, 56% yield) was obtained from 1,4-diiodobenzene (336.9 mg, 1.021 mmol) and 3-(trifluoromethyl)benzo[e][1,2,4]triazine[125] (**6.24**, 406.4 mg, 2.042 mmol) as a blue-black solid: mp 216-218 °C (*n*-pentane). IR *v* 3056, 2928, 2856, 1567, 1492, 1261, 1196, 1142, 1081, 990, 850, 758, 591 cm^{-1}. UV-vis (CH$_2$Cl$_2$) λ_{max} (log ε) 246.5 (4.49), 285 (3.97), 342 (3.96), 405 (3.50), 593 (3.75) nm. ESI(+)–MS, *m/z* 475 (100, [M + H]$^+$). HRMS (ESI+–TOF) *m/z* [M + H]$^+$ calcd for C$_{22}$H$_{13}$N$_6$F$_6$ 475.1106, found 475.1099(7). Anal. Calcd for C$_{22}$H$_{12}$N$_6$F$_6$•H$_2$O: C, 53.67; H, 2.87; N, 17.07. Found: C, 53.99; H, 2.75; N, 16.81.

Diradical 6.22m. (163.1 mg, 0.344 mmol, 32% yield) was obtained from 1,3-diiodobenzene (351.1 mg, 1.064 mmol) and 3-(trifluoromethyl)benzo[*e*][1,2,4]triazine[125] (**6.24**, 423.5 mg, 2.128 mmol) as a dark maroon solid: mp 231-233 °C (*n*-pentane). IR *v* 3074, 3045, 2972, 1585, 1485, 1460, 1262, 1198, 1171, 1139, 1098, 993, 928, 798, 757, 703, 625 cm^{-1}. UV-vis (CH$_2$Cl$_2$) λ_{max} (log ε) 246.5 (4.61), 315.5 (4.08), 345.5 (4.09), 418 (3.66), 481 (3.37) nm. ESI(+)–MS, *m/z* 475 (100, [M + H]$^+$). HRMS (ESI+–TOF) *m/z* [M + H]$^+$ calcd for C$_{22}$H$_{13}$N$_6$F$_6$ 475.1106, found 475.1099(6). Anal. Calcd for C$_{22}$H$_{12}$N$_6$F$_6$: C, 55.70; H, 2.55; N, 17.72. Found: C, 55.62; H, 2.55; N, 17.63.

6.7.3. IR spectra

FT-IR spectra were recorded in KBr pellets.
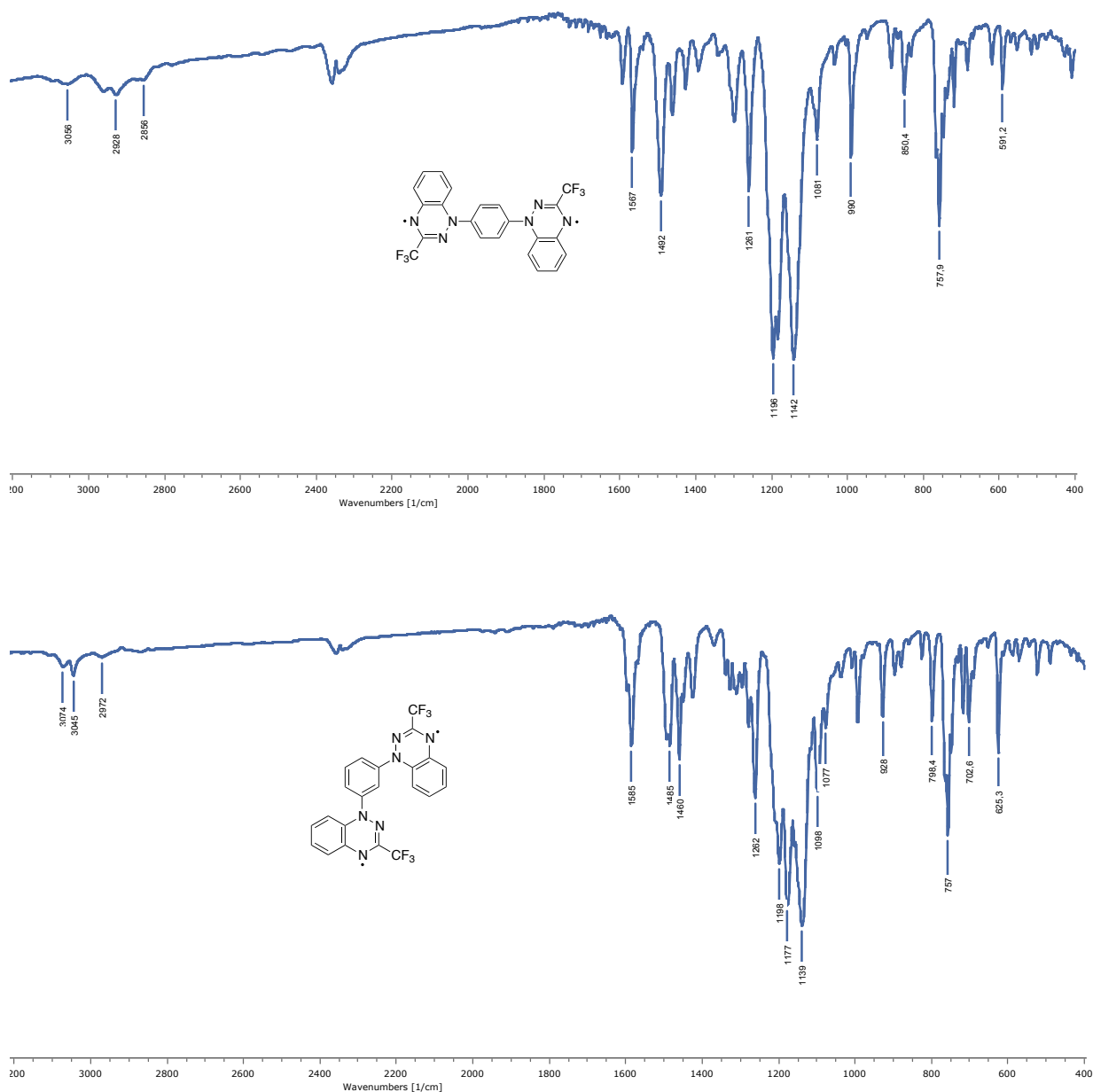
Figure 6.7.3.1. IR spectra for diradicals **6.22p** (top) and **6.22m** (bottom) recorded in KBr.

6.7.4. Electronic absorption spectroscopy
a) *spectra for 6.22p and 6.22m in CH₂Cl₂*

Electronic absorption spectra for radicals **6.22p** and **6.22m** were recorded on Jasco V-770 spectrophotometer in spectroscopic grade CH_2Cl_2 at concentrations in a range 1.0–10×10^{-5} mol·L^{-1} .The measured UV-vis spectra were fitted to the Beer–Lambert law ($A = \varepsilon c l$), the molar absorption coefficient (ε) was derived from the linear plot. Results are shown in Figures 6.7.3.2 and 6.7.3.3.
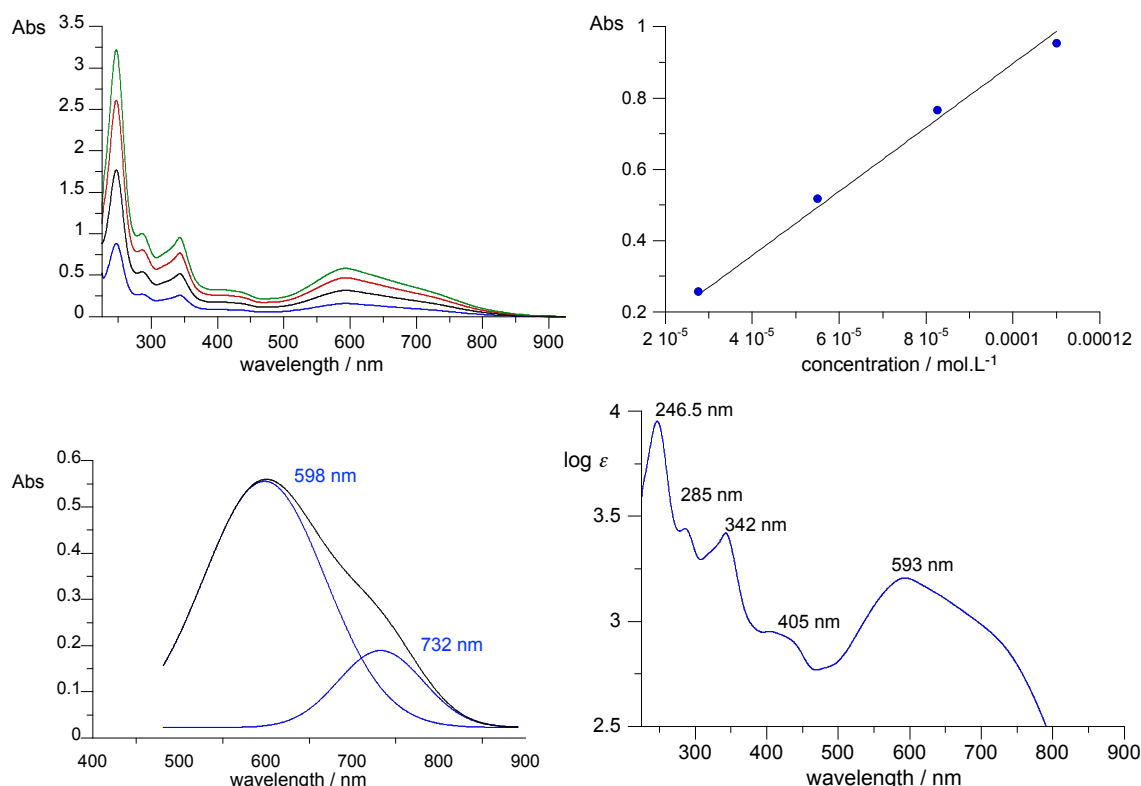
Figure 6.7.3.2. Clockwise: electronic absorption spectra of 1,4-diradical **6.22p** in CH_2Cl_2 for four concentrations (top left), determination of molar extinction coefficient ε at $\lambda = 342.2$ nm (top right, best fit function: $\varepsilon = 9052(61)\times$conc, $r^2 = 0.9997$), molar extinction log (ε) plot (bottom right) and deconvolution of a low energy portion of the spectrum.
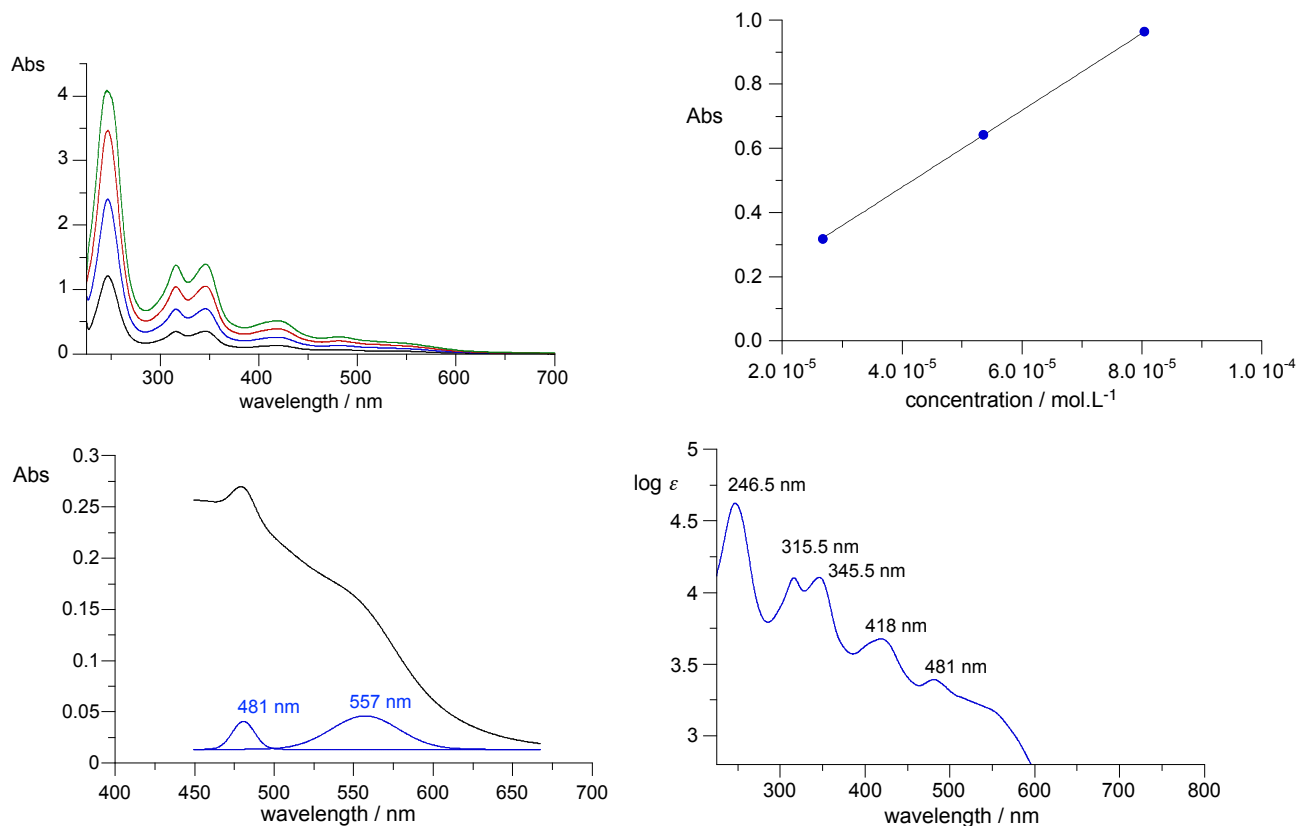
Figure 6.7.3.3. Clockwise: electronic absorption spectra of 1,3-diradical **6.22m** in CH_2Cl_2 for three concentrations (top left), determination of molar extinction coefficient ε at λ = 315.5 nm (top right, best fit function: ε = 11976(23)×conc, r^2 = 0.9999), molar extinction log (ε) plot (bottom right) and deconvolution of a low energy portion of the spectrum.

b) solvatochromism studies of **6.22p**

10×10^{-5} M solutions of **6.22p** in several solvents were measured at ambient temperature in a cuvette with 10 mm optical path. Lower solubility was observed for some polar solvents and the results were unreliable. Resulting maxima of absorption are shown in Figure 6.7.3.4.
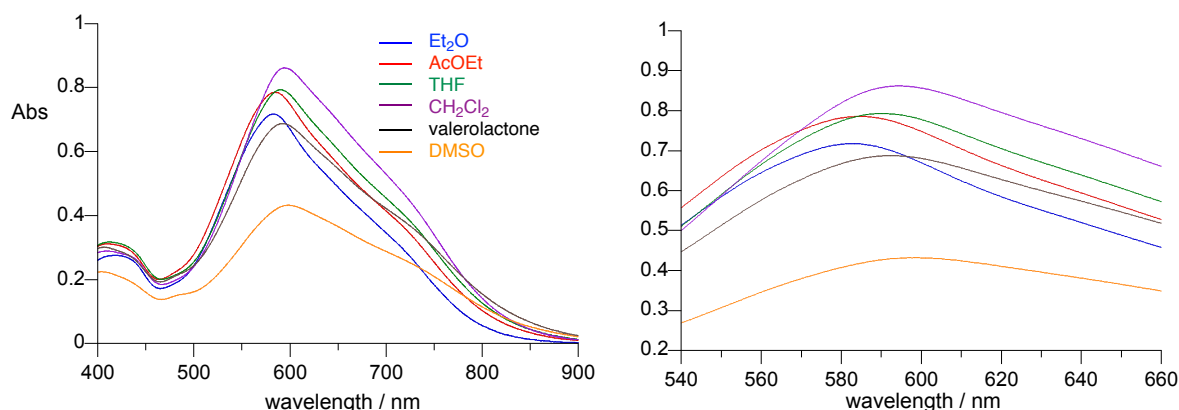
Figure 6.7.3.4. Low energy portion of the electronic spectra of **6.22p** in several solvents. Concentration 10×10^{-5} M.

Table 6.7.3.1. Dependence of the low energy absorption maximum of **6.22p** on solvent polarity.[a]

solvent	$E_T(30)$	λ_{max} /nm
Et$_2$O	34.5	582.2
THF	37.4	590.0
AcOEt	38.1	584.4
CH$_2$Cl$_2$	40.7	593.4
valerolactone	44.3	592.8
DMSO	45.1	598.8

[a] Measured at concentration 10×10^{-5} M.

6.7.5. Electrochemical results

Electrochemical characterization of diradicals **6.22** and radical **6.23** was conducted using a Metrohm Autolab PGSTAT 128N potentiostat/galvanostat instrument. The analyzed radical was dissolved in dry, spectroscopic grade CH$_2$Cl$_2$ (concentration 1.5 mM) or CH$_3$CN (concentration 1.5 mM) in the presence of [n-Bu$_4$N]$^+$[PF$_6$]$^-$ as an electrolyte (concentration 100 mM) and the resulting solution was degassed by purging with Ar gas for 20 minutes. A three-electrode electrochemical cell was used with a glassy carbon disk as the working electrode (ϕ 2 mm, alumina polished), Pt wire as the counter electrode and Ag/AgCl wire as the pseudoreference electrode. All samples were measured without internal reference once and afterwards with FcMe$_{10}$ as the internal reference with a scan rate of 50 mV s^{-1} (CV) or 5 mV s^{-1} (DPV) at *ca.* 20 °C. The oxidation potential for the FcMe$_{10}$/FcMe$_{10}$$^+$ couple was established at -0.556 V in CH$_2$Cl$_2$ and -0.507 V in MeCN *vs* Fc/Fc$^+$,

respectively, by comparison with the oxidation potential for the Fc/Fc^+ couple (0.0 V, Figure 6.7.3.5).

Figure 6.7.3.5. Cyclic voltammogram (CV) for decamethylferrocene ($FeMe_{10}$) and ferrocene (Fc) in CH_2Cl_2 (left) and MeCN (right) referenced to the Fc/Fc^+ couple.

Cyclic voltammetry (CV) measurements were started from 0.0 V in the oxidative direction, while differential pulse voltammetry (DPV) measurements were conducted starting from -1.4 V in the oxidative direction (black line) and starting from 1.2 V in the reductive direction (red line). Cyclic voltammetry (CV) and differential pulse voltammetry (DPV) plots are shown in Figures 6.7.3.6–6.7.3.11 and numerical results are shown in Tables 6.7.3.2 and 6.7.3.3.

Figure 6.7.3.6. Cyclic voltammogram (CV, left) and differential pulse voltammogram (DPV, right) for **6.22p** in CH_2Cl_2 referenced to the Fc/Fc^+ couple.

Figure 6.7.3.7. Cyclic voltammogram (CV, left) and differential pulse voltammogram (DPV, right) for **6.22m** in CH$_2$Cl$_2$ referenced to the Fc/Fc$^+$ couple.

Figure 6.7.3.8. Cyclic voltammogram (CV) for radical **6.23** in CH$_2$Cl$_2$ referenced to the Fc/Fc$^+$ couple.

Table 6.7.3.2. Electrochemical properties of **6.22** and **6.23** in CH$_2$Cl$_2$.[a]

compound	$E_{1/2}^{2-/-}$ (V)	$E_{1/2}^{-/0}$ (V)	$E_{1/2}^{+/0}$ (V)	$E_{1/2}^{2+/+}$ (V)	$\Delta E_{cell}(1)^{b}$ (V)	$\Delta E_{cell}(2)^{b}$ (V)
6.22p [c]	-1.27	-0.98	0.16 [d]	0.24 [d]	1.08	1.42
6.22m [c]	-1.20	-0.96	0.19		1.15	1.39
6.23 [e]	–	-1.12	0.13	–	1.25	–

[a] Measured in CH$_2$Cl$_2$ [n-Bu$_4$N]$^+$[PF$_6$]$^-$ (100 mM), *ca.* 20 °C, 50 mVs^{-1} (CV); 5 mVs^{-1} (DPV), glassy carbon electrode. Potentials referenced to Fc/Fc$^+$. [b] $\Delta E_{cell}(1) = E_{1/2}^{+/0} - E_{1/2}^{-/0}$; $\Delta E_{cell}(2) = E_{1/2}^{2+/+} - E_{1/2}^{2-/-}$. [c] Data from DPV measurements. [d] Irreversible process. [e] Data from CV measurement.

Figure 6.7.3.9. Cyclic voltammogram (CV, left) and differential pulse voltammogram (DPV, right) for **6.22p** in MeCN referenced to the Fc/Fc$^+$ couple.

Figure 6.7.3.10. Cyclic voltammogram (CV, left) and differential pulse voltammogram (DPV, right) for **6.22m** in MeCN referenced to the Fc/Fc$^+$ couple.

Figure 6.7.3.11. Cyclic voltammogram (CV) for radical **6.23** in MeCN referenced to the Fc/Fc$^+$ couple.

Table 6.7.3.3. Electrochemical properties of **6.22** and **6.23** in MeCN.[a]

compound	$E_{1/2}^{2-/-}$ (V)	$E_{1/2}^{-/0}$ (V)	$E_{1/2}^{+/0}$ (V)	$E_{1/2}^{2+/+}$ (V)	$\Delta E_{\text{cell}}(1)^{b}$ (V)	$\Delta E_{\text{cell}}(2)^{b}$ (V)
6.22p [c]	-1.17	-0.88	0.13	0.23	1.01	1.39
6.22m [c]	-1.10	-0.88	0.14	0.23	1.02	1.33
6.23 [d]	–	-1.01	0.09	–	1.10	–

[a] Measured in MeCN [n-Bu$_4$N]$^+$[PF$_6$]$^-$ (100 mM), *ca.* 20 °C, 50 mVs^{-1} (CV); 5 mVs^{-1} (DPV), glassy carbon electrode. Potentials referenced to Fc/Fc$^+$. [b] $\Delta E_{\text{cell}}(1) = E_{1/2}^{+/0} - E_{1/2}^{-/0}$; $\Delta E_{\text{cell}}(2) = E_{1/2}^{2+/+} - E_{1/2}^{2-/-}$. [c] Data from DPV measurements. [d] Data from CV measurement.

6.7.6. VT EPR spectroscopy and data analysis
b) *sample preparation*

A solution of polystyrene (500.2 mg, $d = 1.04$ g cm^{-3}) in dry and distilled CH$_2$Cl$_2$ (4 mL) was degassed in vacuum and diradical **6.22** was added and mixed till a homogenous mixture was formed. The resulting mixture was degassed in vacuum till complete evaporation of the solvent and formation of a fragile polystyrene film. The film was then dried for 1 h, divided into smaller pieces, placed in EPR tube and tightly packed using a glass rod. The EPR tube containing the sample was blown with argon gas, tightly closed, and variable temperature measurement was performed.

b) *measurement*

Variable temperature EPR spectra for diradicals **6.22** were recorded on an X-band EMX-Nano EPR spectrometer equipped with a frequency counter and nitrogen flow temperature control (120 K to 340 K) in degassed solid polystyrene solutions (5.2 mM) at 120 K exhibit patterns with randomly oriented triplets contaminated with signal from the doublet impurity (the middle singlet). No half-field transition $|\Delta m_{\text{s}}| = 2$ was observed in either of the diradicals. Variable-temperature EPR spectra for diradicals **6.22p** and **6.22m** are shown in the Figures 6.7.3.12 and 6.7.3.13.

c) *spectra analysis and simulation*

Variable EPR spectra were double integrated and the resulting DI intensities were normalized for the intensity at the lowest temperature. The resulting DI$_{\text{rel}}$ are shown in Tables 6.7.3.4 and 6.7.3.5.

Table 6.7.3.4. Double integral and normalized data for **6.22p**.

Temp /K	DI	DI/DI$_{120}$	Temp /K	DI	DI/DI$_{120}$
119.00	1100.0	1.0000	227.00	1320.0	1.2000
123.00	1090.0	0.99091	231.00	1280.0	1.1636
127.00	1140.0	1.0364	236.00	1260.0	1.1455
132.00	1130.0	1.0273	241.00	1240.0	1.1273
136.00	1130.0	1.0273	246.00	1300.0	1.1818
141.00	1130.0	1.0273	251.00	1340.0	1.2182
147.00	1130.0	1.0273	257.00	1360.0	1.2364
152.00	1170.0	1.0636	261.00	1380.0	1.2545
157.00	1110.0	1.0091	266.00	1450.0	1.3182
162.00	1110.0	1.0091	272.00	1430.0	1.3000
166.00	1140.0	1.0364	276.00	1430.0	1.3000
172.00	1170.0	1.0636	282.00	1430.0	1.3000
176.00	1140.0	1.0364	286.00	1480.0	1.3455
182.00	1160.0	1.0545	292.00	1530.0	1.3909
187.00	1170.0	1.0636	297.00	1520.0	1.3818
191.00	1150.0	1.0455	301.00	1590.0	1.4455
197.00	1200.0	1.0909	307.00	1660.0	1.5091
201.00	1170.0	1.0636	312.00	1600.0	1.4545
207.00	1180.0	1.0727	317.00	1670.0	1.5182
212.00	1200.0	1.0909	321.00	1730.0	1.5727
217.00	1230.0	1.1182	326.00	1790.0	1.6273
221.00	1240.0	1.1273	331.00	1790.0	1.6273

Table 6.7.3.5. Double integral and normalized data for **6.22m**.

Temp /K	DI	DI/DI$_{120}$	Temp /K	DI	DI/DI$_{120}$
120.00	21600	1.0000	225.00	12500	0.57870
121.00	21500	0.99537	231.00	12100	0.56019
125.00	20700	0.95833	235.00	12000	0.55556
130.00	20000	0.92593	241.00	11700	0.54167
135.00	19600	0.90741	246.00	11400	0.52778
140.00	19000	0.87963	250.00	11300	0.52315
146.00	18300	0.84722	256.00	10900	0.50463
150.00	17900	0.82870	266.00	10600	0.49074
156.00	17300	0.80093	271.00	10400	0.48148
160.00	17000	0.78704	295.00	9500.0	0.43981
166.00	16500	0.76389	300.00	9330.0	0.43194
171.00	16100	0.74537	306.00	9130.0	0.42269
176.00	15700	0.72685	310.00	9050.0	0.41898
180.00	15300	0.70833	320.00	8650.0	0.40046
185.00	14800	0.68519	326.00	8570.0	0.39676
195.00	14200	0.65741			
201.00	13800	0.63889			
206.00	13500	0.62500			
211.00	13200	0.61111			
216.00	13000	0.60185			
221.00	12700	0.58796			

The singlet-triplet energy gap $\Delta E_{S\text{-}T} = 2J$ for each diradical was estimated by fitting experimental VT EPR data points (DI$_{rel}$ *vs* T) to the Bleaney-Bowers equation[88] (eq 6.7.3.1) and the results are shown in Figures 6.7.3.12 and 6.7.3.13.

$$\chi = \frac{Ng^2\mu_B^2}{kT}\left(\frac{2}{3+e^{-\frac{2J}{kT}}}\right) \qquad \text{eq 6.7.3.1}$$

For numeral fitting to the eq S1, a three-parameter equation 6.7.3.2 was used:

$$DI_{rel} = \frac{m1}{T}\left(\frac{2}{3+e^{-\frac{m2}{T}}}\right) + m3$$

Figure 6.7.3.12. Determination of ΔE_{ST} for 5.2 mM diradical **6.22p** in polystyrene. Left: variable temperature spectra in a temperature range 122 – 321 K. Right: plot of DI$_{rel}$ *vs T*. Fitting (red line) the data points to three-parameter eq. 6.7.3.1, gave $2J/k_B = -1524(58)$ K, $r^2 = 0.983$.

Figure 6.7.3.13. Determination of ΔE_{S-T} for 5.2 mM diradical **6.22m** in polystyrene. Left: variable temperature spectra in a temperature range from 125 – 320 K. Right: plot of DI$_{rel}$ *vs T*, Fitting (red line) the data points to three-parameter eq. 6.7.3.1, gave $2J/k_B = -83(3)$ K, $r^2 = 0.999$.

Simulation of triplet EPR spectra for both radicals recorded at the lowest temperature (119 for **6.22p** and 120 K for **6.22m**) was conducted using *pepper* module in *EasySpin* (Matlab),[160] and results are shown in Figures 6.7.3.14 and 6.7.3.15. Assuming an isotropic *g* value, the resulting absolute values zero field splitting parameters (*zfp*), |*D/hc*| and |*E/hc*|, are shown in Table 6.7.3.6. Assuming a point-dipole approximation, the mean distance between the spin centers was estimated using eq 6.7.3.2.

$$r = ((D/g)\times 7.19\times 10^{-5})^{-1/3}$$ eq. 6.7.3.2
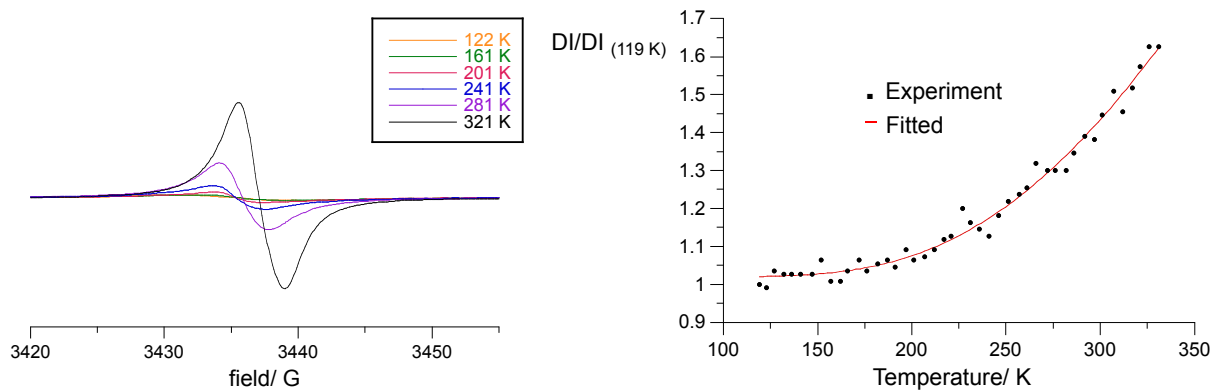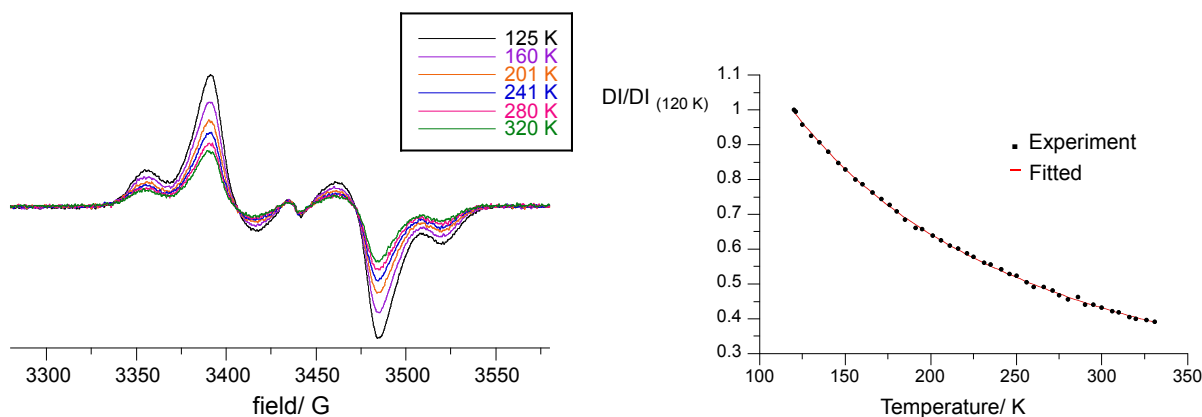
where D (in gauss) is the fitting parameter in the simulated EPR spectrum.
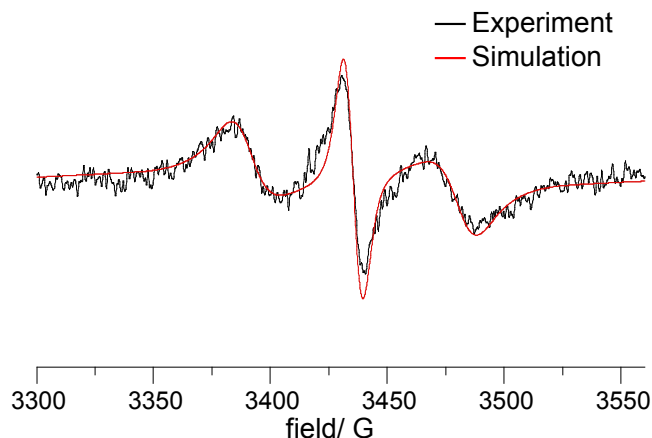
Figure 6.7.3.14. Complete set of fitting parameters for the spectrum in Figure 9 (main text): EPR (119 K, ν = 9.644 GHz) spectrum for 5.2 mM diradical **6.22p** in polystyrene. Simulation $|\Delta m_S|$ = 1 region (*pepper*, *EasySpin*, rmsd = 0.0821065): Component A, weight = 1.0000, S = 1, D = 267.62 MHz, E = 2.81 MHz, g_{iso} = 2.0053, H-strain (MHz): H_x = 39.907, H_y = 117.32, H_z = 174.703; D-strain (MHz): D = 80.00, E = 30.00; component B, S =1/2, weight = 0.336664, g_{iso} = 2.00569, H-strain (MHz)): H_x = 50.00, H_y = 50.00, H_z = 87.00.
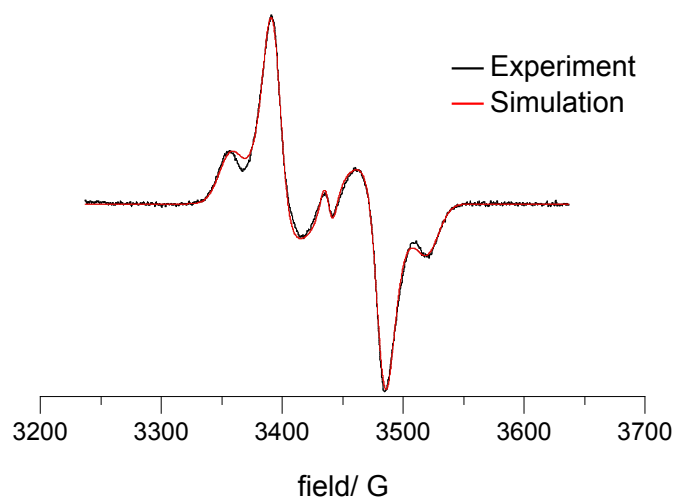
Figure 6.7.3.15. Complete set of fitting parameters for the spectrum in Figure 9 (main text): EPR (120 K, ν = 9.644 GHz) spectrum for 5.2 mM diradical **6.22m** in polystyrene. Simulation $|\Delta m_S|$ = 1 region (*pepper, EasySpin*, rmsd = 0.0169852): Component A, weight = 1.0000, S = 1, D = 227.64 MHz, E = -6.19 MHz, g_{iso} = 2.00388; H-strain (MHz): H_x = 40.567, H_y = 118.54, H_z = 63.19; D-strain (MHz): D = 80.00, E = 30.00; component B, S =1/2, weight = 0.020969, g_{iso} = 2.00401; H-strain (MHz)): H_x = 50.00, H_y = 50.00, H_z = 87.00.

Table 6.7.3.6. Zero field splitting parameters simulated for Blatter diradicals **6.22**.

compound	matrix, temp/ K	$\|D/hc\|$ /cm^{-1}	$\|E/hc\|$ /cm^{-1}	g	r /Å [a]
6.22p-T	PS, 119	8.93×10^{-3}	9.41×10^{-5}	2.0053	8.4
6.22m-T	PS, 120	7.60×10^{-3}	2.07×10^{-4}	2.00388	8.8

[a] Calculated using equation eq 6.7.3.2.

7. References

1.   Hicks, R. G., *Stable Radicals: Fundamentals and applied aspects of odd–electron compounds*. Wiley&Sons: 2010.

2.   Hicks, R. G., What's new in stable radical chemistry? *Org. Biomol. Chem.* **2007,** *5*, 1321-1338.

3.   Gomberg, M., Triphenylmethyl, ein Fall von dreiwerthigem Kohlenstoff. *Ber. Dtsch. Chem. Ges.* **1900,** *33*, 3150-3163.

4.   Gomberg, M., An instance of trivalent carbon: triphenylmethyl. *J. Am. Chem. Soc.* **1900,** *22*, 757-771.

5.   Schlenk, W.; Weickel, T.; Herzenstein, A., Ueber triphenylmethyl and analoga des triphenylmethyls in der biphenylreihe. [Zweite mittheilung uber "Triarylmethylene".]. *Justus Liebigs Ann. Che,.* **1910,** *372*, 1-20.

6.   Ballester, M.; Riera-Figueras, J.; Castaner, J.; Badfa, C.; Monso, J. M., Inert carbon free radicals. I. Perchlorodiphenylmethyl and perchlorotriphenylmethyl radical series. *J. Am. Chem. Soc.* **1971,** *93*, 2215-2225.

7.   Goldschmidt, S.; Renn, K., Zweiwertiger sticlstoff: uber das *a,a*-diphenyl-*b*-trinitrophenyl hydrazyl. *Ber. Dtsch. Chem. Ges. B* **1922,** *B55*, 628-643.

8.   Lebedev, O. L.; Kazarnovskii, S. N., Catalytic oxidation of aliphatic amines with hydrogen peroxide. *Zh. Obshch. Khim* **1960,** *30*, 1631-1635.

9.   Call, L.; Ullman, E. F., Stable free radicals XI. Photochemistry of a nitronyl nitroxide. *Tetrahedron Lett.* **1973,** *14*, 961-964.

10.   Kuhn, R.; Trischmann, H., Surprisingly stable nitrogenous free radicals. *Angew. Chem. Int. Ed. Engl.* **1963,** *2*, 155.

11.   Blatter, H. M.; Lukaszewski, H., A new stable free radical. *Tetrahedron Lett.* **1968,** *9*, 2701–2705.

12.   Kaszyński, P.; Constantinides, C. P.; Young, V. G., The plannar Blatter radical: Structural chemistry of 1,4-dihydrobenzo[*e*][1,2,4]triazin-4-yls. *Angew. Chem. Int. Ed.* **2016,** *55*, 11149-11152.

13.   Constantinides, C. P.; Koutentis, P. A., Chapter Seven – Stable N– and N/S–rich heterocyclic radicals: synthesis and applications. *Adv. Heterocycl. Chem.* **2016,** *119*, 173-207.

14.   Zienkiewicz, J.; Kaszyński, P.; Young, V. G., Experimental and theoretical studies of fused–ring persistent [1,2,4]thiadiazinyl radicals. *J. Org. Chem.* **2004,** *69*, 7525–7536.

15.   Constantinides, C. P.; Koutentis, P. A.; Krassos, H.; Rawson, J. M.; Tasiopoulos, A. J., Characterization and magnetic properties of a "super stable" radical 1,3-diphenyl-7-trifluoromethyl-1,4-dihydro-1,2,4-benzotriazin-4-yl. *J. Org. Chem.* **2011,** *76*, 2798-2806.

16.   Berezin, A. A.; Zissimou, G. A.; Constantinides, C. P.; Beldjoudi, Y.; Rowson, J. M.; Koutentis, P. A., Route to benzo- and pyrido-fused 1,2,4-triazinyl radicals via *N'*-(het)-aryl-*N'*-[2-nitro(het)aryl]-hydrazides. *J. Org. Chem.* **2014,** *79*, 314–327.

17.   Jasiński, M.; Szczytko, J.; Pociecha, D.; Monobe, H.; Kaszyński, P., Substituent-dependent magnetic behaviour of discotic benzo[*e*][1,2,4]triazinyls. *J. Am. Chem. Soc.* **2016,** *138*, 9421–9424.

18.   Morgan, I. S.; Peuronen, A.; Hanninen, M. M.; Reed, R. W.; Clerac, R.; Tuononen, H. M., 1-Phenyl-3-)pyrid-2-yl_benzo[*e*][1,2,4]triazinyl: the first "Blatter radical" for coordination chemistry. *Inorg. Chem.* **2014,** *53*, 33-35.

19. Morgan, I. S.; Mansikkamaki, A.; Zissimou, G. A.; Koutentis, P. A.; Rouzieres, M.; Clerac, R.; Tuononen, H. M., Coordination complexes of a neutral 1,2,4-benzotriazinyl radical ligand: synthesis, molecular and electronic structures, and magnetic properties. *Chem. Eur. J.* **2015,** *21*, 15843–15853.

20. Kapuściński, S.; Gardias, A.; Pociecha, D.; Jasiński, M.; Szczytko, J.; Kaszyński, P., Magnetic behavior of bent-core mesogens derived from the 1,4-dihydrobenzo[*e*][1,2,4]triazin-4-yl. *J. Mater. Chem. C* **2018,** *6*, 3079–3088.

21. Kapuściński, S.; Szczytko, J.; Pociecha, D.; Jasiński, M.; Kaszyński, P., Discs, dumbbels and superdiscs: Molecular and supermolecular architecture dependent magnetic behavior of mesogenic Blatter radical derivatives. *Mater. Chem. Front.* **2021,** *5*, 6512–6521.

22. Jasiński, M.; Kapuściński, S.; Kaszyński, P., Stability of a columnar liquid cristalline phase in isomeric derivatives of the 1,4-dihydrobenzo[*e*][1,2,4]triazin-4-yl: Conformational effect in the core *J. Mol. Liq.* **2019,** *277*, 1054–1059.

23. Sanvito, S., Molecular spintronics. *Chem. Soc. Rev.* **2011,** *40*, 3336–3355.

24. Demetriou, M.; Berezin, A. A.; Koutentis, P. A.; Krasia-Christoforou, T., Benzotriazinyl–mediated controlled radical polymerization of styrene. *Polym. Int.* **2014,** *63*, 674–679.

25. Ciofini, I.; Adamo, C.; Teki, Y.; Tuyeras, F.; Laine, P. P., *Chem. Eur. J.* **2008,** *14*, 11385.

26. Neugebauer, F. A.; Umminger, I., Über 1,4-dihydro-1,2,4-benzotriazinyl-radikale. *Chem. Ber.* **1980,** *113*, 1205–1225.

27. Ji, Y.; Long, L.; Zheng, Y., Recent advances of stable Blatter radicals: synthesis, properties and applications. *Mater. Chem. Front.* **2020,** *4*, 3433–3443.

28. Gardias, A.; Kaszyński, P.; Obijalska, E.; Trzybiński, D.; Domagała, S.; Woźniak, K.; Szczytko, J., Magnetostructural investigation of orthogonal 1-aryl-3-phenyl-1,4-dihydrobenzo[*e*][1,2,4]triazin-4-yl derivatives. *Chem. Eur. J.* **2018,** *24*, 1317-1329.

29. Constantinides, C. P.; Berezin, A. A.; Manoli, M.; Leitus, G. M.; Zissimou, G. A.; Bendikov, M.; Rawson, J. M.; Koutentis, P. A., Structural, magnetic, and computational correlations of some imidazolo-fused 1,2,4-benzotriazinyl radicals. *Chem. Eur. J.* **2014,** *20*, 5388-5396.

30. Zheng, Y.; Miao, M.; Kemei, M. C.; Seshadri, R.; Wudl, F., The pyreno-triazinyl radical-magnetic and sensor properties. *Isr. J. Chem.* **2014,** *54*, 774-778.

31. Constantinides, C. P.; Berezin, A. A.; Manoli, M.; Leitus, G. M.; Bendikov, M.; Rawson, J. M.; Koutentis, P. A., Effective exchange coupling in alternating-chains of a II-extended 1,2,4-benzotriazin-4-yl. *New. J. Chem.* **2014,** *38*, 949-954.

32. Berezin, A. A.; Constantinides, C. P.; Mirallai, S. I.; Manoli, M.; Cao, L. L.; Rawson, J. M.; Koutentis, P. A., Synthesis and properties of imidazolo-fused benzotriazinyl radicals. *Org. Biomol. Chem.* **2013,** *11*, 6780-6795.

33. Berezin, A. A.; Constantinides, C. P.; Drouza, C.; Manoli, M.; Koutentis, P. A., From Blatter radical to 7-substituted 1,3-diphenyl-1,4-dihydrothiazolo[5'4':4,5]-benzo[1,2 - 2][1,2,4]triazin-4-yls: toward multifunctional materials. *Org. Lett.* **2012,** *14*, 5586-5589.

34. Pomikło, D.; Bodzioch, A.; Pietrzak, A.; Kaszyński, P., C(3) Functional derivatives of the Blatter radical. *Org. Lett.* **2019,** *21*, 6995–6999.

35. Constantinides, C. P.; Berezin, A. A.; Zissimou, G. A.; Manoli, M.; Leitus, G. M.; Bendikov, M.; Probert, M. R.; Rawson, J. M.; Koutentis, P. A., A magnetostructural investigation of an abrupt spin transition for 1-phenyl-3-trifluoromethyl-1,4-dihydrobenzo[*e*][1,2,4]triazin-4-yl. *J. Am. Chem. Soc.* **2014,** *136*, 11906-11909.

36.	Yan, B.; Cramen, J.; McDonald, R.; Frank, N. L., Ferromagnetic spin-delocalized electron donors for multifunctional materials: II-conjugated benzotriazinyl radicals. *Chem. Commun.* **2011,** *47*, 3201-3203.

37.	Takahashi, Y.; Miura, Y.; Yoshioka, N., Synthesis and properties of the 3-tert-butyl-7-trifluoromethyl-1,4-dihydro-1-phenyl-1,2,4-benzotriazin-4-yl radical. *New. J. Chem.* **2015,** *39*, 4783-4789.

38.	Mukai, K.; Inoue, K.; Achiwa, N.; Jarnali, J. B.; Krieger, C.; Neugebauer, F. A., 1,4-dihydro-1,2,4-benzotriazin-4-yl radicals. *Chem. Phys. Lett.* **1994,** *224*, 569-575.

39.	Constantinides, C. P.; Berezin, A. A.; Zissimou, G. A.; Manoli, M.; Leitus, G. M.; Koutentis, P. A., The suppression of columnar II-stacking in 3-adamantyl-1-phenyl-1,4-dihydrobenzo[*e*][1,2,4]triazin-4-yl. *Molecules* **2016,** *21*, 636-642.

40.	Pomikło, D.; Bodzioch, A.; Kaszyński, P., 3-Substituted Blatter radicals: cyclization of *N*-arylguanidines and *N*-arylamidines to benzo[*e*][1,2,4]triazines and PhLi addition. *J. Org. Chem.* **2023,** *88*, 2999-3011.

41.	Neugebauer, F. A.; Rimmler, G., *Magn. Reson. Chem.* **1988,** *26*, 595.

42.	Takahashi, Y.; Tsuchiya, N.; Miura, Y.; Yoshioka, N., Megneto-structural correlation of cyano-substituted 3-*tert*-butyl-1-phenyl-1,2,4-benzotriazin-4-yl: spin transition behaviour observed in a 6-cyano derivative. *New. J. Chem.* **2018,** *42*, 9949–9955.

43.	Bodzioch, A.; Zheng, M.; Kaszyński, P.; Utecht, G., Functional group transformations in derivatives of 1,4-dihydrobenzo[1,2,4]triazinyl radical. *J. Org. Chem.* **2014,** *79*, 7294-7310.

44.	Constantinides, C. P.; Obijalska, E.; Kaszyński, P., Access to 1,4-dihydrobenzo[*e*][1,2,4]triazin-4-yl derivatives. *Org. Lett.* **2016,** *18*, 916–919.

45.	Koutentis, P. A.; Lo Re, D., Catalytic oxidation of *N*-phenyl amidrazones to 1,3-diphenyl-1,4-dihydro-1,2,4-benzotriazin-4-yls: An improved synthesis of Blatter's radical. *Synthesis* **2010,** *12*, 2075–2079.

46.	Constantinides, C. P.; Koutentis, P. A.; Loizou, G., Synthesis of 7-aryl/heteraryl-1,3-diphenyl-1,2,4-benzotriazinyls *via* palladium catalyzed Stille and Suzuki-Miyaura reactios. *Org. Biomol. Chem.* **2011,** *9*, 3122–3125.

47.	Constantinides, C. P.; Koutentis, P. A.; Rawson, J. M., Antiferromagnetic interactions in 1D Heisenberg linear chains of 7-(4-fluorophenyl) and 7-phenyl-substituted 1,3-diphenyl-1,4-dihydro-1,2,4-benzotriazin-4-yl radicals. *Chem. Eur. J.* **2012,** *18*, 15433-15438.

48.	Miura, Y.; Yoshioka, N., II-Stacked structure of thiadiazolo-fused benzotriazinyl radical: crystal structure and magnetic properties. *Chem. Phys. Lett.* **2015,** *626*, 11-14.

49.	Takahashi, Y.; Miura, Y.; Yoshioka, N., Introduction of three aryl groups to benzotriazinyl radical by Suzuki-Miyaura cross-coupling reaction. *Chem. Lett.* **2014,** *43*, 1236-1238.

50.	Savva, A. C.; Mirallai, S. I.; Zissimou, G. A.; Berezin, A. A.; Demetriades, M.; Kourtllaris, A.; Constantinides, C. P.; Nicolaides, C.; Tripiniotis, T.; Koutentis, P. A., Preparation of Blatter radicals via aza-Wittig chemistry: The reaction of *N*-aryliminophosphoranes with 1-(Het)aroyl-2-aryldiazenes. *J. Org. Chem.* **2017,** *82*, 7564–7575.

51.	Grant, J. A.; Lu, Z.; Tucker, D. E.; Hockin, B. M.; Yufit, D. S.; Fox, M. A.; Kataky, R.; Chechik, V.; o'Donoghue, A. C., New Baltter-type radicals from a bench-stable carben. *Nature Commun.* **2017,** *8*, 15088.

52.	Constantinides, C. P.; Carter, E.; Murphy, D. M.; Manoli, M.; Leitus, G. M.; Bendikov, M.; Rawson, J. M.; Koutentis, P. A., Spin-triplet excitons in 1,3-diphenyl-7-(fur-2-yl)-1,4-dihydro-1,2,4-benzotriazin-4-yl. *Chem. Commun.* **2013,** *49*, 8662-8664.

53.   Bartos, P.; Anand, B.; Pietrzak, A.; Kaszyński, P., Functional planar Blatter radical through Pschorr-type cyclization. *Org. Lett.* **2020,** *22*, 180-184.

54.   Hande, A. A.; Darrigan, C.; Bartos, P.; Baylere, P.; Pietrzak, A.; Kaszyński, P.; Chrostowska, A., UV-photoelectron spectroscopy of stable radicals: the electronic structure of planar Blatter radicals as materials for organic electronics. *Phys. Chem. Chem. Phys.* **2020,** *22*, 23637-23644.

55.   Bartos, P.; Hande, A. A.; Pietrzak, A.; Chrostowska, A.; Kaszyński, P., Substituent effects on the electronic structure of the flat Blatter radical: Correlation analysis of experimental and computational data. *New. J. Chem.* **2021,** *45*, 22876-22887.

56.   Shivakumar, K. I.; Pociecha, D.; Szczytko, J.; Kapuściński, S.; Monobe, H.; Kaszyński, P., Photoconductive bent-core liquid crystalline radicals with a paramagnetic polar switchable phase. *J. Mater. Chem. C* **2020,** *8*, 1083-1088.

57.   Bartos, P.; Young, V. G.; Kaszyński, P., Ring-fused 1,4-dihydro[1,2,4]triazin-4-yls through photocyclization. *Org. Lett.* **2020,** *22*, 3835-3840.

58.   Bartos, P.; Celeda, M.; Pietrzak, A.; Kaszyński, P., Planar Blatter radicals through Bu3SnH- and TMS3SiH- assisted cyclization of aryl iodides: azaphilic radical addition *Org. Chem. Front.* **2022,** *9*, 929-938.

59.   Miyaura, N.; Yamada, K.; Suzuki, A., A new stereospecific cross-coupling by the palladium-catalyzed reaction of 1-alkenylboranes with 1-alkenyl or 1-alkynyl halides. *Tetrahedron Lett.* **1979,** *20*, 3437–3440.

60.   King, A. O.; Okukado, N.; Negishi, E., Highly general stereo-, regio-, and chemo-selective synthesis of terminal and internal conjugated enyenes by the Pd-catalysed reaction of alkynylzinc reagents with alkenyl halides. *J. Chem. Soc., Chem. Commun.* **1977,** *19*, 683–684.

61.   Sonogashira, K., Development of Pd–Cu catalyzed cross-coupling of terminal acetylenes with sp2-carbon halides. *J. Organomet. Chem.* **2002,** *653*, 46–49.

62.   Jasiński, M.; Gerding, J. S.; Jankowiak, A.; Gębicki, K.; Romański, J.; Jastrzębska, K.; Sivaramamoorthy, A.; Mason, K.; Evans, D. H.; Celeda, M.; Kaszyński, P., Functional Group Transformations in Derivatives of 6-Oxoverdazyl. *J. Org. Chem.* **2013,** *78*, 7445-7454.

63.   Abe, M., Diradicals. *Chem. Rev.* **2013,** *113*, 7011-7088.

64.   Casado, J., *Para*-Quinodimethanes: A unified review of the quinoida-versus-aromatic competition and its implications. *Top. Curr. Chem.* **2017,** *375*, 209–248.

65.   Nakano, M., Electronic structure of open-shell singlet molecules: Diradical character viewpoint. *Top. Curr. Chem.* **2017,** *375*, 1–67.

66.   Bobrowski, M.; Skurski, P.; Freza, S., The electronic structure of p-xylylene and its reactivity with vinyl molecules. *Chem. Phys.* **2011,** *382*, 20–26.

67.   Solà, M., Forty years of Clar's aromatic π-sextet rule. *Front. Chem.* **2013,** *1*, 22.

68.   Beckhaus, H.-D.; Faust, R.; Matzger, A. J.; Mohler, D. L.; Rogers, D. W.; Rüchardt, C.; Sawhney, A. K.; Verevkin, S. P.; Vollhardt, K. P. C.; Wolff, S., The heat of hydrogenation of (a) cyclohexatriene. *J. Am. Chem. Soc.* **2000,** *122*, 7819–7820.

69.   Qi, F.; Sorkhabi, O.; Suits, A. G., Evidence of triplet ethylene produced from photodissociation of ethylene sulfide *J. Chem. Phys.* **2000,** *112*, 10707–10710.

70.   Yamaguchi, K.; Kawakami, T.; Takano, Y.; Kitagawa, Y.; Yamashita, Y.; Fujita, H., Analytical and *ab initio* studies of effective exchange interactions, polyradical character, unpaired electron density, and information entropy in radical clusters $(R)_N$: Allyl radical cluster (N = 2–10) and hydrogen radical cluster (N = 50). *J. Quantum Chem.* **2002,** *90*, 370–385.

71.   Döhnert, D.; Koutecký, J., Occupation numbers of natural orbitals as a criterion for biradical character. Different kinds of biradicals. *J. Am. Chem. Soc.* **1980,** *102*, 1789–1796.

72.   PK, The value of the *y* index depends of the computational method. For details see ref. 36.

73.   Kuriakose, F.; Commodore, M.; Hu, C.; Fabiano, C. J.; Sen, D.; Li, R. R.; Bisht, S.; Üngör, Ö.; Lin, X.; Strouse, G. F.; DePrince III, A. E.; Lazenby, R. A.; Mentink-Vigier, F.; Shatruk, M.; Alabugin, I. V., Design and synthesis of kKekulè and non-Kekulè diradicaloids via the radical periannulation strategy: The power of seven Clar's sextets. *J. Am. Chem. Soc.* **2022,** *144*, 23448–23464.

74.   Ovchinnikov, A. A., Multiplicity of the ground state of large alternant organic molecules with conjugated bonds. *Theoret. Chim. Acta* **1978,** *47*, 297-304.

75.   Gallagher, N. M.; Olankitwanit, A.; Rajca, A., High-spin organic molecules. *J. Org. Chem.* **2015,** *80*, 1291-1298.

76.   Wenthold, P. G.; Kim, J. B.; Lineberger, W. C., Photoelectron spectroscopy of *m*-xylylene anion. *J. Am. Chem. Soc.* **1997,** *119*, 1354-1359.

77.   Wenthold, P. G.; Hu, J.; Squires, R. R.; Lineberger, W. C., Photoelectron spectroscopy of the trimethylene- methane negative ion. The singlet-triplet splitting of trimethylenemethane. *J. Am. Chem. Soc.* **1996,** *118*, 475-476.

78.   Yang, N. C.; Castro, A. J., Synthesis of a stable biradical. *J. Am. Chem. Soc.* **1960,** *82*, 6208-6208.

79.   Matsuda, K.; Iwamura, H., Demonstration of the degeneracy of the singlet and triplet states in 2,3-dimethylenecyclohexane-1,4-diyl by measurement of its magnetic properties. *J. Chem. Soc., Perkin Trans. 2* **1998**, 1023-1026.

80.   Rajca, A.; Rajca, S., Intramolecular antiferromagnetic vs ferromagnetic spin coupling through the biphenyl unit. *J. Am. Chem. Soc.* **1996,** *118*, 8121-8126.

81.   Borden, W. T.; Davidson, E. R., Effects of electron repulsion in conjugated hydrocarbon diradicals. *J. Am. Chem. Soc.* **1977,** *99*, 4587-4594.

82.   Rajca, A., Organic diradicals and polyradicals: from spin coupling to magnetism? *Chem. Rev.* **1994,** *94*, 871-893.

83.   Matsuda, K.; Iwamura, H., Singlet and triplet states are degenerate in 2,3-dimethylenecyclohexane-1,4-diyl. *J. Am. Chem. Soc.* **1997,** *119*, 7412–7413.

84.   Veciana, J.; Iwamura, H., Organic Magnets. *MRS Bulletin* **2000,** *25*, 41–51.

85.   Ratera, I.; Veciana, J., Playing with organic radicals as building blocks for functional molecular materials. *Chem. Soc. Rev.* **2012,** *41*, 303-349.

86.   Weil, J. A.; Bolton, J. R.; Wertz, J. E., *Electron Paramagnetic Resonance*. Wiley Interscience: 1994.

87.   Bloch, F., Nuclear Induction. *Phys. Rev.* **1946,** *70*, 460–474.

88.   Bleaney, B.; Bowers, K. D., Anomalous paramagnetism of copper acetate. *Proc. R. Soc. London, Ser. A.* **1952,** *214*, 451-465.

89.   Ni, Y.; Wu, J., Diradical approach toward organic near infrared dyes. *Tetrahedron Lett.* **2016,** *57*, 5426-5434.

90.   Kamada, K.; Fuku-en, S.; Minamide, S.; Ohta, K.; Kishi, R.; Nakano, M.; Matsuzaki, H.; Okamoto, H.; Higashikawa, H.; Inoue, K.; Kojima, S.; Tamamoto, Y., Impact of diradical character on two-photon absorption: bis(acridine) dimers synthesized from allenic precursor. *J. Am. Chem. Soc.* **2013,** *135*, 232-241.

91.   Fakuda, K.; Nagami, T.; Fujiyoshi, J.; Nakano, M., Interplay between open-shell character, aromaticity, and secod hyperpolarizabilities in indenofluorenes. *J. Phys. Chem. A* **2015,** *119*, 10620-10627.

92.   Zheng, Y.; Miao, M.-s.; Dantelle, G.; Eisenmenger, N. D.; Wu, G.; Yavuz, I.; Chabinyc, M. L.; Houk, K. N.; Wudl, F., A solid-state effect responsible for an organic quintet state at room temperature and ambient pressure. *Adv. Mater.* **2015,** *27*, 1718-1723.

93.   Ito, S.; Minami, T.; Nakano, M., Diradical character based design for singlet fission of condensed-ring systems with 4nII electrons. *J. Phys. Chem. C* **2012,** *116*, 19729-19736.

94.   Ito, S.; Nagami, T.; Nakano, M., Diradical- character-based design for singlet fission of bisanthene derivatives: aromatic-ring attachment and II-plane twisting. *J. Phys. Chem. Lett.* **2016,** *7*, 3925-3930.

95.   Gaudenzi, R.; Burzuri, E.; Reta, D.; Moreira, I. d. P. R.; Bromley, S. T.; Rovira, C.; Veciana, J.; van der Zant, H. S. J., Exchange coupling inversion in a high-spin organic triradical molecule. *Nano. Lett.* **2016,** *16*, 2066-2071.

96.   Tsuji, Y.; Hoffmann, R.; Strange, M.; Solomon, G. C., Close relation between quantum interference in molecular conductance and diradical existence. *Proc. Natl. Acad. Sci. U. S. A.* **2016,** *113*, E413-E419.

97.   Shil, S.; Bhattacharya, D.; Misra, A.; Klein, D., A high-spin organic diradical as a spin filter. *J. Phys. Chem. Chem. Phys.* **2015,** *17*, 23378-23383.

98.   Iwamura, H., What role has organic chemistry played in the development of molecule-based magnets. *Polyhedron* **2013,** *66*, 3-14.

99.   Thiele, J.; Balhorn, H., Ueber einen chinoiden Kohlenwasserstoff. *Ber. Dtsch. Chem. Ges.* **1904,** *37*, 1463-1470.

100.   Sun, Z.; Ye, Q.; Chi, C.; Wu, J., Low band gap polycyclic hydrocarbons: from closed-shell near infrared dyes and semiconductors to open-shell radicals. *Chem. Soc. Rev.* **2012,** *41*, 7857-7889.

101.   Kubo, T.; Shimizu, A.; Sakamoto, M.; Uruichi, M.; Yakushi, K.; Nakano, M.; Shiomi, D.; Sato, K.; Takui, T.; Morita, Y.; Nakasuji, K., Synthesis, intermolecular interaction, and semiconductive behavior of a delocalized singlet biradical hydrocarbon. *Angew. Chem. Int. Ed.* **2005,** *44*, 6564-6568.

102.   Rudebusch, G. E.; Zafra, J. L.; Jorner, K.; Fakuda, K.; Marshall, J. L.; Arrechea-Marcos, I.; Espejo, G. L.; Ponce Ortiz, C. J.; Gomez-Garcia, C. J.; Zakharov, L. N.; Nakano, M.; Ottosson, H.; Casado, J.; Haley, M. M., Diindeno-fusion of anthracene as a design strategy for sutable organic biradicals. *Nat. Chem.* **2016,** *8*, 753-759.

103.   Koike, H.; Chikamatsu, M.; Azumi, R.; Tsutsumi, J.; Ogawa, K.; Yamane, W.; Nishiuchi, T.; Kubo, T.; Hasegawa, T.; Kanai, K., Stable delocalized singlet biradical hydrocarbon for organic field-effect transistors. *Adv. Funct. Mater.* **2016,** *26*, 277-283.

104.   Zhang, Y.; Zheng, Y.; Zhou, H.; Miao, M.-S.; Wudl, F.; Nguyen, T.-Q., Temperature tunable self-doping in stable diradicaloid thin-film devices. *Adv. Mater.* **2015,** *27*, 7412-7419.

105.   Hu, X.; Chen, H.; Xue, G.; Zheng, Y., Correlation between the strength of conjugation and spin-spin interactions in stable diradicaloids. *J. Mater. Chem. C* **2020,** *8*, 10749-10754.

106.   Hu, X.; Chen, H.; Zhao, L.; Miao, M.; Han, J.; Wang, J.; Guo, J.; Hu, Y.; Zheng, Y., Nitrogen analogues of Chchibabin's and Muller's hydrocarbon with small singlet-triplet energy gaps. *Chem. Commun.* **2019,** *55*, 7812-7815.

107.   Hu, X.; Zhao, L.; Chen, H.; Ding, Y.; Zheng, Y.-Z.; Miao, M.-s.; Zheng, Y., Air stable high-spin blatter diradicals: non-Kekule *versus* Kekule structures. *J. Mater. Chem. C* **2019,** *7*, 6559-6563.

108.   Hutchison, K.; Srdanov, G.; Hicks, R.; Yu, H.; Wudl, F.; Strassner, T.; Nendel, M.; Houk, K. N., Tetraphenylhexaazaanthracene: a case for dominance of cyanine ion stabilization overhelming 16II antiaromaticity. *J. Am. Chem. Soc.* **1998,** *120*, 2989-2990.

109.   Hu, X.; Chen, H.; Zhao, L.; Miao, M.-s.; Zheng, X.; Zheng, Y., Nitrogen-coupled blatter diradicals: the fused *versus* unfused bridges. *J. Mater. Chem. C* **2019,** *7*, 10460-10464.

110.   Gallagher, N. M.; Bauer, J. J.; Pink, M.; Rajca, S.; Rajca, A., High-spin organic diradical with robust stability. *J. Am. Chem. Soc.* **2016,** *138*, 9377-9380.

111.   Zhang, S.; Pink, M.; Junghoefer, T.; Zhao, W.; Hsu, S.-N.; Rajca, S.; Calzolari, A.; Boudouris, B. W.; Casu, M. B.; Rajca, A., High-spin (S = 1) Blatter diradical with robust stability and electrical conductivity. *J. Am. Chem. Soc.* **2022,** *144*, 6059-6070.

112.   Gallagher, N.; Zhang, H.; Junghoefer, T.; Giangrisostomi, E.; Ovsyannikov, R.; Pink, M.; Rajca, S.; Casu, M. B.; Rajca, A., Thermally and magnetically robust triplet ground state diradical. *J. Am. Chem. Soc.* **2019,** *141*, 4764-4774.

113.   Miao, F.; Ji, Y.; Han, B.; Moles Quintero, S.; Chen, H.; Xue, G.; Cai, L.; Casado, J.; Zheng, Y., Asymmetric and zwitterionic Blatter diradicals. *Chem. Sci.* **2023,** *14*, 2698-2705.

114.   Potts, K. T.; Roy, S. K.; Jones, D. P., 1,2,4-Triazoles. XVII. Meso-ionic compounds. 2. Derivatives of the s-triazole series. *J. Org. Chem.* **1967,** *32*, 2245-2252.

115.   Constantinides, C. P.; Zissimou, G. A.; Berezin, A. A.; Ioannou, T. A.; Manoli, M.; Tsokkou, D.; Theodorou, E.; Hayes, S. C.; Koutentis, P. A., Tetraphenylhexaazaanthracenes: 16Π weakly antiaromatic species with singlet ground states. *Org. Lett.* **2015,** *17*, 4026-4029.

116.   Wudl, F.; Koutentis, P. A.; Weitz, A.; Ma, B.; Strassner, T.; Houk, K. N.; Khan, S. I., Polyazaacenes: new tricks for old dogs. *Pure & Appl. Chem.* **1999,** *71*, 295-302.

117.   Hutchison, K.; Hasharoni, K.; Wudl, F.; Berg, A.; Shuali, Z.; Levanon, H., A time-resolved EPR study of a new zwitterion undergoing photoinduced intramolecular electron transfer. *J. Am. Chem. Soc.* **1998,** *120*, 6362-6365.

118.   Langer, P.; Amiri, S.; Bodtke, A.; Saleh, N. N. R.; Weisz, K.; Gorls, H.; Schreiner, P. R., 3,5,7,9-Substituted hexaazaacridines: toward structures with nearly degenerate singlet-triplet energy separations. *J. Org. Chem.* **2008,** *73*, 5048-5063.

119.   Khurana, R.; Bajaj, A.; Ali, M. E., Tuning the magnetic properties of a diamagnetic di-Blatter's zwitterion to antiferro- and ferromagnetically coupled diradicals. *Phys. Chem. Chem. Phys.* **2022,** *24*, 2543-2553.

120.   Rogers, F. J. M.; Norcott, P. L.; Coote, M. L., Recent advances in the chemistry of benzo[*e*][1,2,4]triazinyl radicals. *Org. Biomol. Chem.* **2020,** *18*, 8255-8277.

121.   Zissimou, G. A.; Berezin, A. A.; Manoli, M.; Nicolaides, C.; Tripiniotis, T.; Koutentis, P. A., 3,3',3''-(Benzene-1,3,5-triyl)tris(1-phenyl-1H-benzo[e][1,2,4]triazin-4-yl): a C3 symmetrical Blatter-type triradical. *Tetrahedron* **2020,** *76*, 131077.

122.   Shu, C.; Pink, M.; Junghoefer, T.; Nadler, E.; Rajca, S.; Casu, M. B.; Rajca, A., Synthesis of thin films of thermally robust quartet (S = 3/2) ground state triradical. *J. Am. Chem. Soc.* **2021,** *143*, 5508-5518.

123.   Boudalis, A. K.; Constantinides, C. P.; Chrysochos, N.; Carmieli, R.; Leitus, G.; Kourtellaris, A.; Lawson, D. B.; Koutentis, P. A., Deciphering the ground state of a C3-symmetrical Blatter-type triradical by CW and pulse EPR spectroscopy. *J. Magn. Reson.* **2023,** *349*, 107406-.

124.   Khurana, R.; Bajaj, A.; Shamasundar, K. R.; Ali, M. E., High-spin Blatter's triradicals. **2023**.

125.   Bodzioch, A.; Pomikło, D.; Celeda, M.; Pietrzak, A.; Kaszyński, P., 3-substituted benzo[*e*][1,2,4]triazines: Synthesis and electronic effects of the C(3) substituent. *J. Org. Chem.* **2019,** *84*, 6377–6394.

126.   Nelson, T. D.; Crouch, R. D., Cu, Ni, and Pd mediated homocoupling reactions in biaryl syntheses: the Ullmann reaction. *Org. React.* **2004,** *63*, 265-555.

127. Kalk, W.; Bien, H.-S.; Schündehütte, K.-H., Ullmann-Reaktionenanortho-(Acy1amino)halogenaromaten. *Liebigs Ann. Chem.* **1977**, 329-337.

128. Mihai, M. T.; Williams, B. D.; Phipps, R. J., *Para*-Selective C-H borylation of common arene building blocks enabled by ion-pairing with bulky countercation. *J. Am. Chem. Soc.* **2019,** *141*, 15477-15482.

129. Tzschucke, C. C.; Murphy, J. M.; GHartwig, J. F., Arenes to anilines and aryl ethers by sequential iridium-catalyzed borylation and copper-catalyzed coupling. *Org. Lett.* **2007,** *9*, 761-764.

130. Osei, M. K.; Mirzaei, S.; Bogetti, X.; Castro, E.; Rahman, M. A.; Saxena, S.; Sánchez, R. H., Synthesis of Square Planar Cu4 Clusters. *Angew. Chem. Int. Ed.* **2022,** *61*, e202209529.

131. Linnanen, T.; Wohlfahrt, G.; Nanduri, S.; Ujjinamatada, R.; Rajagopalan, S.; Mukherjee, S. Protein kinase inhibitors. 2013.

132. Smith, N. D.; Payne, J.; Bonnefous, C.; Duron, S.; Zhuang, H.; Chen, X.; Govek, S.; Lindstrom, A. K. Isoquinolines useful as inducible nitric oxide synthase inhibitors. 2008.

133. Surleraux, N. D. L.; P., W. P. T. B.; Voets, M. C. J.; Vendeville, S. M. H.; De Kock, H. A.; Vergouwen, B. J. B. Broadspectrum substituted benzimidazole sulfonamide HIV protease inhibitors. 2003.

134. Qiu, J.; Zhao, B.; Shen, Y.; Lin, H., Synthesis, biological evaluation and modeling studies of terphenyl topoisomerase IIα inhibitors as anticancer agents. *Eur. J. Med. Chem.* **2015,** *94*, 427-435.

135. Montgomery, L. K.; Huffman, J. C.; Jurczak, E. A.; Grendze, M. P., The molecular structures of Thiele's and Chichibabin's hydrocarbons. *J. Am. Chem. Soc.* **1986,** *108*, 6004-6011.

136. Charbonneau, G.-P.; Delugeard, Y., Bi-phenyl: three-dimensional data and new refinement at 293 K. **1977,** *33B*, 1586–1588.

137. Connelly, N. G.; Geiger, W. E., Chemical redox agents for organometallic chemistry. *Chem. Rev.* **1996,** *96*, 877-910.

138. Yamaguchi, K.; Takahara, Y.; Fueno, T.; Nasu, K., Ab initio MO calculations of effective exchange integrals between transition-metal ions via oxygen dianions: Nature of the copper-oxygen bonds and superconductivity. *Jpn. J. Appl. Phys* **1987,** *26*, L1362.

139. Bernard, Y. A.; Shao, Y.; Krylov, A. I., General formulation of spin-flip time-dependent density functional theory using non-collinear kernels: theory, implementation, and benchmarks. *J. Chem. Phys.* **2012,** *136*, 204103.

140. Khurana, R.; Bajaj, A.; Ali, M. E., How plusible is getting ferromagnetic interactions by coupling Blatter's radical *via* its fused benzene ring? *J. Phys. Chem. A* **2020,** *124*, 6707–6713.

141. Su, Y.; Wang, X.; Zheng, X.; Zhang, Z.; Song, Y.; Sui, Y.; Li, Y.; Wang, X., Tuning Ground States of Bis(triarylamine) Dications: From a Closed-Shell Singlet to a Diradicaloid with an Excited Triplet State. *Angew. Chem. Int. Ed.* **2014,** *53*, 2857–2861.

142. Gilroy, J. B.; McKinnon, S. D. J.; Kennepohl, P.; Zsombor, M. S.; Ferguson, M. J.; Thompson, L. K.; Hicks, R. G., Probing electronic communication in stable benzene–bridged verdazyl diradicals. *J. Org. Chem.* **2007,** *72*, 8062–8069.

143. Latif, I. A.; Hansda, S.; Datta, S. N., High magnetic exchange coupling constants: a density functional theory based study of substituted Schlenk diradicals. *J. Phys. Chem. A* **2012,** *116*, 8599–8607.

144. Roques, N.; Gerbier, P.; Schatzschneider, U.; Sutter, J.-P.; Guionneau, P.; Vidal-Gancedo, J.; Veciana, J.; Rentschler, E.; Guerin, C., Experimental and Theoretical Studies of Magnetic Exchange in Silole- Bridged Diradicals. *Chem. Eur. J.* **2006,** *12*, 5547–5562.

145.   Takahashi, T.; Matsuoka, K.-i.; Takimiya, K.; Otsubo, T.; Aso, Y., Extensive Quinoidal Oligothiophenes with Dicyanomethylene Groups at Terminal Positions as Highly Amphoteric Redox Molecules. *J. Am. Chem. Soc.* **2005,** *127*, 8928–8929.

146.   Kolanji, K.; Ravat, P.; Bogomyakov, A. S.; Ovcharenko, V. I.; Schollmeyer, D.; Baumgarten, M., Mixed Phenyl and Thiophene Oligomers for Bridging Nitronyl Nitroxides. *J. Org. Chem.* **2017,** *82*, 7764–7773.

147.   Fulmer, G. R.; Miller, A. J. M.; Sherden, N. H.; Gottlieb, H. E.; Nudelman, A.; Stoltz, B. M.; Bercaw, J. E.; Goldberg, K. I., NMR Chemical Shifts of Trace Impurities: Common Laboratory Solvents, Organics, and Gases in Deuterated Solvents Relevant to the Organometallic Chemist. *Organometallics* **2010,** *29*, 2176-2179.

148.   Vogel, A. I., Textbook of practical organic chemistry **1974**, 192-193.

149.   Fu, Z.; Jiang, Y.; Wang, S.; Song, Y.; Guo, S.; Cai, H., Pd-Catalyzed decarboxylative *ortho*-halogenation of aryl carboxylic acids with sodium halide NaX using carboxyl as a traceless directing group. *Org. Lett.* **2019,** *21*, 3003-3007.

150.   Fletcher, L. T.; Namkung, M. J.; Wetzel, W. H.; Pan, H.-L., Defivatives of fluorene. X. Fluorofluorenes. III. *J. Org. Chem.* **1960,** *25*, 1342–1348.

151.   Ye, F.; Wang, C.; Zhang, Y.; Wang, J., Synthesis of aryldiazoacetates through palladium(0)-catalyzed deacylative cross-coupling of aryl iodides with aryldiazoacetates. *Angew. Chem. Int. Ed.* **2014,** *53*, 11625-11628.

152.   Li, B.; Bemish, R. J.; Bill, D. R.; Brenek, S.; Buzon, R. A.; Chiu, C. K.-F.; Newell, L.; Coleman, C.; Wipf, P. A., Preparation of puvaloyl hydrazide in water [Propanoic acid, 2,2-dimethyl-, hydrazide]. *Org. Synth.* **2005,** *81*, 254-261.

153.   Ren, J.; Klaasen, H.; Witteler, M. C.; Viergutz, L.; Neugebauer, J.; Gao, H.-Y.; Studer, A.; Fuchs, H., Aryl triflates in on-surface chemistry. *Chem. Eur. J.* **2020,** *26*, 16727-16732.

154.   Ruah, H. S. S.; Miller, M. T.; Bear, B.; McCartney, J.; Grootenhuis, P. D. J. Modulators of ATP-binding cassette transporters. 2008.

155.   Qiu, J.; Zhao, B.; Zhong, W.; Shen, Y.; Lin, H., Synthesis, biological evaluation and modeling studies of terphenyl topoisomerase IIα inhibitors as anticancer agents. *Eur. J. Med. Chem.* **2015,** *94*, 427–435.

156.   Mąkosza, M.; Bialecki, M., Nitroarylamines via vicarious nucleophilic substitution of hydrogen: amination, alkylamination, and arylamination of nitroarenes with sulfonamides *J. Org. Chem.* **1998,** *63*, 4878-4888.

157.   Harvey, I. W.; McFarlane, M. D.; Moody, D. J.; Smith, D. M., *o*-Nitroaniline derivatives. Part 9. Benzimidazole *N*-oxides unsubstituted at N-1 and C-2. *J. Chem. Soc., Perkin Trans. 1* **1988**, 681-690.

158.   RigakuOD, C. P., Rigaku Oxformd Diffraction Ltd, 2018, Yarnton, Oxfordshire, England.

159.   Sheldrick, G. M., SHELXT- Integrated space-group and crystal-structure determination. *Acta Cryst., Sect.* **2015,** *A71*, 3-8.

160.   Stoll, S.; Schweiger, A., EasySpin, a comprehensive software package for spectral simulation and analysis in EPR. *J. Magn. Reson.* **2006,** *178*, 42–55.

8.Other scientific activities

8.1. Participation in scientific and research projects

Project co-contractor:

1. TEAM (2017-2021) „Supramolecular materials designed for fundamental studies and energy conversion technologies" Foundation for Polish Science. Number: TEAM/2016-3/24 (phD student position; supervisor: Prof. Piotr Kaszyński).

2. OPUS (2020–2023) „Topologically coupled stable diradicals with tunable S-T gaps for molecular materials" National Science Centre Poland. Number: 2019/33/B/ST4/02807 (project contractor position; supervisor: Prof. Piotr Kaszyński).

3. MAESTRO (2021–) „Advanced functional materials from organic paramagnetic building blocks" National Science Centre Poland. Number: 2020/38/A/ST4/00597 (project contractor position; supervisor: Prof. Piotr Kaszyński).

8.2. List of conference presentations

8.2.1. Oral presentations

1. "3-Substituted 1,4-dihydrobenzo[*e*][1,2,4]triazin-4-yls: synthesis and electronic effects of the C(3) substituent" 40th European Meeting on Physical Organic Chemistry; Poland, Spała 03-07.06.2019

8.2.2. Poster presentations

1. "Rodnik benzo[*e*][1,2,4]triazynylowy - modyfikacja pozycji C(3)" VI Łódzkie Sympozjum Doktorantów Chemii; Poland, Łódź 11-12.05.2019

2. "Synteza C(3)-funkcjonalizowanych benzo[*e*][1,2,4]triazyn" 61 Zjazd Polskiego Towarzystwa Chemicznego; Poland, Kraków 17-21.09.2018

3. "Synthesis of C(3)-functionalized benzo[*e*][1,2,4]triazines" XXI International Symposium Advances In The Chemistry of Heteroorganic Compounds; Poland, Łódź 23.11.2018

4. "Modyfikacja pozycji C(3) rodnika1,4-dihydrobenzo[*e*][1,2,4]triazyn-4-ylowego" VII Łódzkie Sympozjum Doktorantów Chemii; Poland, Łódź 09-10.05.2019

5. "Modyfikacja pozycji C(3) rodnika 1,4-dihydrobenzo[*e*][1,2,4]triazyn-4-ylowego" 62 Zjazd Polskiego Towarzystwa Chemicznego; Poland, Warszawa 02-06.09.2019

6. "Topologically coupled stable diradicals" XXII International Symposium Advances In The Chemistry of Heteroorganic Compounds; Poland, Łódź 22.11.2019

7. "Topologically coupled stable diradicals with tunable S-T gaps for molecular materials" VIII Łódzkie Sympozjum Doktorantów Chemii; Poland, Łódź 24.09.2021

8. "Exceptionally stable diradicals with tunable S-T gaps for molecular materials", poster presentation; ISNA19: The 19th International Symposium on Novel Aromatic Compounds, 3-8.07.2022, Warsaw, Poland

9. "Stable radical cations derived from topologically coupled diradicals for NIR dyes", poster presentation; 22nd Tetrahedron Symposium, 28.06-01.07.2022, Lisbon, Portugal

10. "Topologically coupled Blatter diradicals with tunable S-T gaps and exceptional stability for molecular materials", poster presentation; XXIII International Symposium „Advances in the Chemistry of Heteroorganic Compounds", 28.10.2022, Łódź, Poland

8.2.3. Awards

2018 - Scholarship of CBMM PAS Director for the best PhD students.

9. Publications constituting this Doctoral Dissertation

3-Substituted Benzo[*e*][1,2,4]triazines: Synthesis and Electronic Effects of the C(3) Substituent

Agnieszka Bodzioch,[†] Dominika Pomikło,[†] Małgorzata Celeda,[‡] Anna Pietrzak,[§,‖] and Piotr Kaszyński*[,†,‡,§]

[†]Centre of Molecular and Macromolecular Studies, Polish Academy of Sciences, 90-363 Łódź, Poland

[‡]Faculty of Chemistry, University of Łódź, 91-403 Łódź, Poland

[§]Department of Chemistry, Middle Tennessee State University, Murfreesboro, Tennessee 37132, United States

[‖]Faculty of Chemistry, Łódź University of Technology, 90-924 Łódź, Poland

Ⓢ *Supporting Information*

ABSTRACT: A series of 19 structurally diverse C(3)-substituted derivatives of benzo[*e*][1,2,4]triazine were synthesized from 3-chloro- (**1c**) and 3-iodobenzo[*e*][1,2,4]triazine (**1d**) obtained in three steps from 2-nitroaniline in 37−55% yields. Nucleophilic aromatic substitution and metal-catalyzed (Pd, Cu) reactions led to functional derivatives that include alkyl (C_5H_{11}), (het)aryl (Ph, 2-thienyl, ferrocenyl), ArC≡C, amine (NHPh and morpholine), $PO(OEt)_2$, sulfanyl (SBu-*t*), alkoxide (OEt, OMe), and CN. The synthesis of C(3)−CF_3 derivative **1g** via the Ruppert reaction with **1d** and its 1-oxide analogue **2d** led to the substitution followed by formal addition of HCF_3 to the C≡N bond. Pd-catalyzed carbonylation reactions of **1d** and **2d** did not give the corresponding C(3)-carboxylic acids. Therefore, acid **1f** was obtained through hydrolysis of the CN. The substituent effect on the electronic structure of the benzo[*e*][1,2,4]triazine ring was investigated by spectroscopic methods (UV−vis and NMR) augmented with density functional theory calculations. Results show significant effect of the C(3) substituent on the $\pi-\pi^*(1)$ transition energy and good correlation of the ^{1}H NMR chemical shift with the substituent constant σ_p. Molecular and crystal structures of six derivatives were established with the single-crystal X-ray diffraction method, and the substituent impact on the molecular geometry was investigated.
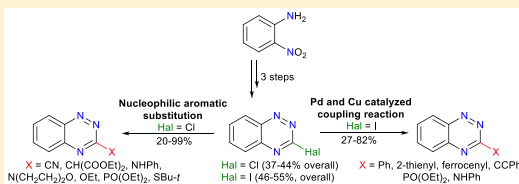
INTRODUCTION

In the past two decades, an increased interest has been observed in chemistry and applications of derivatives of the benzo[*e*]-[1,2,4]triazine[1] (**1a**, Figure 1) in pharmacology and material
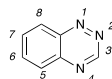
Figure 1. Parent benzo[*e*][1,2,4]triazine (**1a**) with the numbering scheme.

science. For instance, 3-aminobenzo[*e*][1,2,4]triazines posses antimalarial activity[2] and can act as *Src* kinase inhibitors with antitumor activity[3,4] and inhibitors of *Abl* and *Abl*-T315I enzymes.[5] Other derivatives have been described as PARP[6] and sodium-glucose co-transporter 2 inhibitors,[7] microbicides,[8] and antiviral agents.[9] One of the most biologically important classes of benzo[*e*][1,2,4]triazine derivatives are 3-aminobenzo[*e*]-[1,2,4]triazine-1,4-dioxides, which act as bioreductive antitumor agents and are selectively toxic to oxygen-deprived (hypoxic) cells.[10−12] On the other hand, benzo[*e*][1,2,4]-triazine has been used as a structural element of organic

materials, such as organic and electrochemical light emitters,[13] and its derivatives are convenient precursors to exceptionally stable benzo[*e*][1,2,4]triazinyl radicals.[14]

In spite of such a broad application of benzo[*e*][1,2,4]triazine derivatives, there are surprisingly few investigations of their molecular and electronic structures. Thus, only five experimental solid-state structures have been reported to date,[15−19] and UV−vis spectroscopy has been limited to the parent[20,21] and a few members of 3-phenyl,[22] 3-aryl,[23] 3-amino,[24] and 3-alkyl[21] derivatives. There has been no systematic investigation of the effect of 3-substituent on the electronic properties of the benzo[*e*][1,2,4]triazine ring. Our interest in this class of heterocycles stems from understanding of the electronic effects of the C(3) substituent and accessing C(3)-substituted benzo[*e*][1,2,4]triazinyl radicals.

Analysis of the literature indicates that there are several classes of benzo[*e*][1,2,4]triazine derivatives, each accessible through a separate pathway (Figure 2). One of the most convenient methods in the synthesis of the benzo[*e*][1,2,4]-triazine skeleton is condensation of 2-nitroanilines with
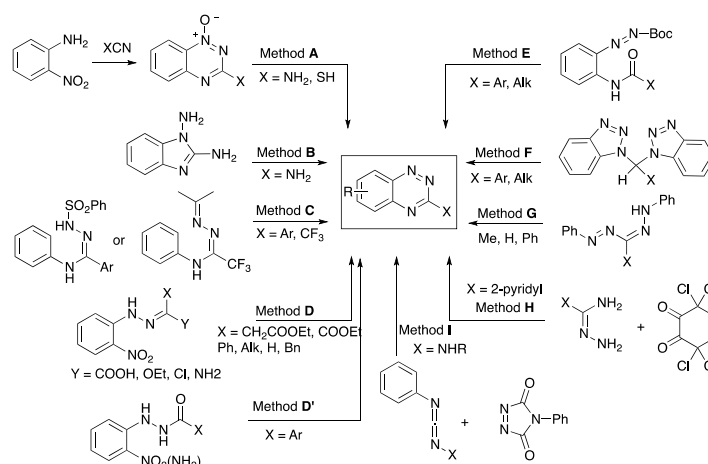
Figure 2. General methods for construction of the benzo[*e*][1,2,4]triazine skeleton.

cyanamide[25] followed by reductive deoxygenation of the resulting 3-aminobenzo[*e*][1,2,4]triazine-1-oxides, achieving 67−80% yield (method A, Figure 2).[2,5,10,26,27] Alternatively, using KSCN and benzoyl chloride in the condensation with 2-nitroanilines, 3-mercapto derivatives are obtained.[28] Oxidation of 1,2-diaminobenzimidazoles with $Pb(OAc)_4$ or $PhI(OAc)_2$ gives the corresponding 3-aminobenzo[*e*][1,2,4]triazines in good yields (method B, Figure 2).[29,30] On the other hand, oxidation of 2-NHPh and 2-NHMe derivatives of 1-amino-benzimidazole with $Pb(OAc)_4$ affords the corresponding benzo[*e*][1,2,4]triazines in low yields (up to 25%).[24] Another method involves the formation of benzo[*e*][1,2,4]triazine ring via oxidative cyclization of the corresponding *N*-arylbenzami-drazones (method C, Figure 2).[23,31,32] Although the reaction allows for the formation of a wide range of 3-aryl[23] and 3-trifluoromethyl-substituted[32] benzo[*e*][1,2,4]triazines in moderate yields, the method suffers from demanding synthesis of amidrazones and use of HgO.[23]

Another method for the preparation of the benzo[*e*][1,2,4]-triazine ring relies on reductive cyclization of 2-nitrophenylhy-drazones,[21,22] 2-nitrophenylhydrazono esters,[33] and 2-nitro-phenylhydrazides[34] (method D, Figure 2). This route allows for the formation of benzo[*e*][1,2,4]triazine derivatives with H, Me, Et, CH_2Ph, Ph, and CH_2COOEt groups at C(3) position in low to moderate yields. Also, the preparation of C(3)−COOR derivatives follows a similar pathway starting with appropriate hydrazonoyl chlorides (Y = Cl), which are transformed to the corresponding amidrazones (Y = NH_2).[35]

A direct synthesis of 3-arylbenzo[*e*][1,2,4]triazines was achieved through a Cu_2O-catalyzed reaction of 2-iodoanilines and aryl hydrazides[16] (method D', Figure 2), resulting in 22−75% yield. Cyclization of azo compounds, obtained by Cu-catalyzed coupling of 2-hydrazino acetanilides and *N*-Boc-protected hydrazine, provides 3-alkyl and 3-aryl (e.g., Ph and 2-thienyl)-substituted benzo[*e*][1,2,4]triazines in excellent yields (method E, Figure 2).[36] A recent report of an unprecedented rearrangement of bis(benzotriazol-1-yl)methylarenes in the presence of allylsamarium bromide demonstrates the formation of the corresponding 3-arylbenzo[*e*][1,2,4]triazines in moderate yields (method F, Figure 2).[37,38]

Another route to 3-aryl derivatives is based on an intramolecular cyclization of formazones in sulfuric acid[20,39,40] or in BF_3/AcOH[9,41] (method G, Figure 2). Benzo[*e*][1,2,4]-triazines with 2-pirydyl substituent at C(3) position were obtained using method H by condensation of 2-picolinoami-drazone with tetrachloro-1,2-cyclohexanedione.[42]

The last method for the preparation of the benzo[*e*][1,2,4]-triazine skeleton involves the [4 + 2] cycloaddition of unsymmetrical carbodiimides to 4-phenyl[1,2,4]triazoline-3,5-dione. This two-step reaction allows for the formation of a series of 3-arylamino- and 3-alkylaminobenzo[*e*][1,2,4]-tria-zines in 59−95% yield (method I, Figure 2).[43]

The above-mentioned synthetic methods[44] are often specific for a particular class of substituents at the C(3) position and in many cases require multistep preparation of precursors for cyclization to the benzo[*e*][1,2,4]triazine skeleton. For instance, methods A, B, and I lead to 3-amino derivatives. Essentially all other methods are used mainly to obtain 3-aryl and 3-heteroaryl derivatives. Only several 3-alkyl derivatives have been obtained using methods D−G. The preparation of the parent benzo[*e*][1,2,4]triazine (**1a**) was demonstrated using methods D and G, while the CF_3 group was introduced at the C(3) position using method C.

Most useful derivatives for further functionalization in the context of pharmacological studies are those containing the NH_2, COOH, and CH_2COOH groups at the C(3) position. They can be transformed into carbonyl derivatives, such as amides and hydrazides, while the C(3)-amino derivatives (e.g., **1b**) can undergo condensation or diazotization reactions, e.g., to form C(3)−Cl derivative **1c**. The chloride **1c** appears to be a synthetically useful intermediate since, in principle, chlorine can be replaced with a number of nucleophiles in the S_NAr process, but only a handful of such transformations have been demonstrated to date: the synthesis of C(3)−$NHNH_2$,[26,45] C(3)−NH_2,[46] and C(3)−OEt derivatives.[45] It should be mentioned that 3-chlorophenanthro[9,10-*e*][1,2,4]triazine, a ring-condensed analogue of the benzo[*e*][1,2,4]triazine, was demonstrated to react with trialkyl phosphites to give phosphonate esters in good yields.[47] In another approach, nucleophilic substitution of the C(3)−SMe group[48] with secondary amines,[48] hydrazine,[28] and MeO[49] was described.

Scheme 1. Synthesis of 3-Halobenzo[e][1,2,4]triazines 1c and 1d[a]

[a]Reagents and conditions: (i) (1) NH₂CN, HCl, 100 °C; (2) NaOH, H₂O, 100 °C, 0.5 h, 82−85% yield; (ii) HN=C(NH₂)₂·HCl, t-BuOK, tetrahydrofuran (THF), 70 °C, 6 h, 96% yield, ref 58; (iii) H₂, Pd/C, EtOH/EtOAc, room temperature (rt), overnight, >98%; alternatively Na₂S₂O₄, EtOH/H₂O, 33−63% yield; (iv) CuCl₂·2H₂O, t-BuONO, MeCN, 60 °C, 0.5 h, 48−52% yield; (v) CuI, I₂, t-BuONO, THF, reflux, 2 h, 59−65% yield for 1d and 41−51% for 2d; (vi) NaNO₂, H₂SO₄/H₂O, 0 °C, 3 h then rt, overnight, 95% yield; (vii) POCl₃, reflux, 2 h, 57% yield; (viii) Zn, NH₄Cl, H₂O, rt, 48 h, <39% yield.

Surprisingly, neither chloride 1c nor any other C(3) halides have been investigated in Pd-catalyzed C−C cross-coupling reactions, even though such a process could, in principle, provide an easy access to a variety of (het)aryl, alkyl, and other substituents at the C(3) position of the benzo[e][1,2,4]triazine ring. The analogous C(3)-bromide is only mentioned in the literature,[25] while the C(3)-iodide 1d is unknown. On the other hand, 3-chloro-[26] (2c), 3-bromo-,[26,50] and 3-iodo-benzo[e]-[1,2,4]triazine-1-oxides[51] (2d) have been successfully used in Pd-catalyzed C−C coupling reactions with a dozen substituted aromatic and heteroaromatic boronic acids (Suzuki conditions)[50,52] and several organotin reagents (Et₄Sn, Me₄Sn, Bu₃SnCH=CH₂, and Bu₃SnCH₂CH=CH₂; Stille conditions).[51−53]

In the context of our investigation of functional benzo[e]-[1,2,4]triazin-4-yl radicals,[54−57] we are interested in an easy access to a variety of C(3)-substituted derivatives of 1a available from a common precursor. For this purpose, we selected the 3-aminobenzo[e][1,2,4]triazine (1b), which can be converted to 3-chloro- (1c) and 3-iodobenzo[e][1,2,4]triazines (1d) to serve as reagents for the formation of C−N (amines), C−O (ether), C−S (sulfides), C−C (COOH, CN, alkyl, aryl, hetaryl, ethynyl, CF₃, acetic acid), and C−P (phosphonates) bonds either by nucleophilic aromatic substitution or through metal-catalyzed (Pd and Cu) coupling reactions. Selected benzo[e]-[1,2,4]triazine derivatives were characterized by X-ray diffraction (XRD) and spectroscopic methods, and the effect of the substituent at the C(3) position on NMR and electronic absorption spectra was investigated. The experimental data are supported with density functional theory (DFT) computational results.
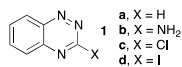
RESULTS AND DISCUSSION

Synthesis of Precursors and Reference Compounds. The requisite 3-halobenzo[e][1,2,4]triazines 1c and 1d were obtained in three steps from 2-nitroaniline in 37−44 and 46−55% overall yields, respectively, as shown in Scheme 1. Thus, a reaction of 2-nitroaniline and cyanamide in concentrated HCl gave 3-aminobenzo[e][1,2,4]triazine-1-oxide (2b) in 82−85% yield.[10,26] The reaction is exothermic and requires careful control in a large scale. An alternative preparation of 2b involves a two-step process starting with a nucleophilic substitution of 2-

fluoronitrobenzene, as shown in Scheme 1.[58] Subsequent catalytic hydrogenation (Pd/C) of the N-oxide 2b in EtOH/AcOEt gave 3-aminobenzo[e][1,2,4]triazine (1b) in a nearly quantitative yield. This method is more convenient and efficient than the literature protocol[10] for deoxygenation of 2b with Na₂S₂O₄ (33−63% yield). The resulting amine 1b was converted to 3-halobenzo[e][1,2,4]triazines 1c and 1d via a substitutive deamination reaction, according to a general literature method[59] and a method for the preparation of 3-iodo derivative 2d,[51] respectively. Thus, a reaction of 1b with t-BuONO in the presence of CuCl₂ hydrate or CuI/I₂ afforded 1c and 1d in 54 and 62% yields, respectively (Scheme 1).

This strategy for the preparation of 3-chloro derivative 1c constitutes a more efficient alternative to the literature procedure involving 3-hydroxy derivative 2e and N-oxide 2c (Scheme 1).[26] The main limitation of this method appears to be deoxygenation of N-oxide 2c with Zn powder, which in our hands gave the desired 1c in yields no greater than 39%. The 3-iodobenzo[e][1,2,4]triazine-1-oxide (2d) was obtained from amine 2b in 41−51% yield according to the literature procedure (Scheme 1).[51] For comparison purposes, the parent benzo[e]-[1,2,4]triazine (1a) was prepared from amine 1b by reductive deamination, according to a general literature procedure[60] (Scheme 2).

Scheme 2. Synthesis of Benzo[e][1,2,4]triazine (1a)[a]
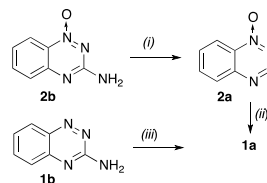
[a]Reagents and conditions: (i) t-BuONO, dimethylformamide (DMF), 60 °C, 2 h; (ii) H₂, Pd/C, EtOH/EtOAc, rt, overnight, 48% overall; (iii) t-BuONO, DMF, 60 °C, 2 h, 23%.

Alternatively, 1a was obtained by reductive deamination of 2b followed by catalytic reduction of the resulting crude benzo[e][1,2,4]triazine-1-oxide (2a). The latter method is more efficient (overall yield 48%) than the literature one using H₂/Pd reduction of chloride 2c.[10] The parent heterocycle 1a

turned out to be sensitive to silica gel, and the crude product was best purified by vacuum sublimation.

Two other reference compounds were prepared according to literature protocols for similar derivatives: benzo[*e*][1,2,4]-triazine-3-carboxylic acid[35,61] (**1f**, Scheme 3) and 3-

Scheme 3. Synthesis of Benzo[*e*][1,2,4]triazine-3-carboxylic Acid (1f)[*a*]

[*a*]Reagents and conditions: (i) (1) NaNO$_2$, HCl, MeOH/H$_2$O, 15 min; (2) MeCOCHClCOOEt, 0 °C to rt, 1.5 h, 73% yield; (ii) NH$_3$, THF, rt, overnight, quant.; (iii) Fe, conc. HCl, AcOH, H$_2$O, rt, overnight, 29% yield; (iv) (1) 0.1 N KOH/EtOH, THF/H$_2$O, rt, 10 min; (2) 10% HCl, quant. yield.
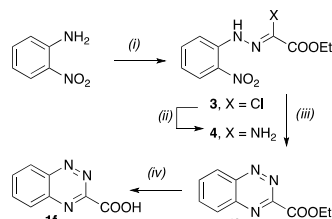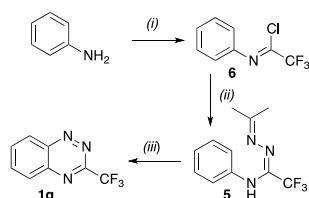
Scheme 4. Synthesis of 3-(Trifluoromethyl)-benzo[*e*][1,2,4]triazine (1g)[*a*]

[*a*]Reagents and conditions: (i) CF$_3$COOH, PPh$_3$, Et$_3$N, CCl$_4$, 0 °C → rt → 100 °C, 5 h, 61% yield, ref 62; (ii) Me$_2$C=NN=CMe$_2$, NH$_2$NH$_2$·H$_2$O, DMF, rt, 5 h, 87% yield; (iii) *t*-BuOCl, CH$_2$Cl$_2$, −70 °C to rt, 4 h, 37% yield, ref 32.

(trifluoromethyl)benzo[*e*][1,2,4]triazine[32] (**1g**, Scheme 4) in yields similar to those reported for their analogues. Thus, 2-nitroaniline was diazotized and reacted with ethyl 2-chloroacetoacetate to yield derivative **3** (Scheme 3). Subsequent treatment of **3** with NH$_3$ gave the amidrazone **4**, which under reductive conditions provided the ethyl ester **1h** in 29%

overall yield. Hydrolysis of the ester under basic conditions gave the desired carboxylic acid **1f**.

Synthesis of the CF$_3$ derivative **1g** involved cyclization of amidrazone **5**, obtained from imidoyl chloride **6**,[62] under oxidative conditions, as shown in Scheme 4.

Nucleophilic Substitution Reactions of 3-Chlorobenzo[*e*][1,2,4]triazine (1c). Chloride **1c** was reacted with a selection of C, N, O, P, and S nucleophiles under typical conditions leading to products **1i−o**, as shown in Table 1. Thus, a reaction of **1c** with [Et$_4$N]$^+$CN$^-$ in MeCN gave benzo[*e*][1,2,4]triazine-3-carbonitrile (**1i**) in a nearly quantitative yield. Reactions of **1c** with NaCN or KCN in the presence of 1,4-diazabicyclo[2.2.2]octane, in aqueous (aq) dimethyl sulfoxide (DMSO)[63] or with CuCN in DMF at 100 °C[64] gave only the unreacted chloride **1c**.

A reaction of **1c** with sodium diethyl malonate in DMF, conditions used for an analogous reaction of 2-chloropyrimidine,[65] gave diethyl 2-(benzo[*e*][1,2,4]triazin-3-yl)malonate (**1j**) in a nearly quantitative yield. Similarly, chloride **1c** reacted with aniline and morpholine in EtOH affording the desired amines **1k** and **1l** in 85 and 89% yields, respectively. Also, a reaction of **1c** with sodium *tert*-butylthiolate in DMF gave sulfide **1o** in 95% yield (Table 1).

In contrast, the formation of the phosphonate ester **1n** was significantly less efficient. Thus, a reaction of **1c** with neat P(OEt)$_3$ gave a mixture of products, of which the desired ester **1n** was isolated in 20% yield. Higher yields of **1n** were obtained using iodide **1d** (vide infra).

Metal-Catalyzed Substitution Reactions of 3-Iodobenzo[*e*][1,2,4]triazine (1d) and 3-Iodobenzo[*e*][1,2,4]-triazine-1-oxide (2d). Several types of standard Pd-catalyzed C−C coupling reactions, such as Suzuki−Miyaura, Sonogashira, Negishi, and carbonylation, were tested with 3-iodobenzo[*e*][1,2,4]triazine (**1d**). Access to those products, which could not be obtained in satisfactory yields, was attempted in a two-step process using 3-iodobenzo[*e*][1,2,4]-triazine-1-oxide (**2d**) and subsequent catalytic deoxygenation (Scheme 5).

Reactions of 3-iodobenzo[*e*][1,2,4]triazine (**1d**) with phenylboronic and 2-thiopheneboronic acids under standard Suzuki−Miyaura conditions gave the corresponding coupling products **1p** and **1r** in good yields (Table 2). A similar reaction of **1d** with ferrocenylboronic was problematic and much less efficient: the desired 3-ferrocenyl derivative **1s** was obtained only in 27% yield after resubmission of the inseparable mixture of the unreacted **1d** and **1s** to the reaction conditions. A reaction of iodide **1d** with phenylacetylene cleanly afforded

Table 1. Nucleophilic Substitution in 3-Chloro-benzo[*e*][1,2,4]triazine (1c)

	X	conditions	isolated yield (%)
1i	CN	[Et$_4$N]$^+$CN$^-$, MeCN, 20 min, rt	98
1j	CH(COOEt)$_2$	NaH, diethyl malonate, DMF, 2 h, 0 °C to rt	99
1k	NHPh	aniline, EtOH, overnight, rt	85
1l	N(CH$_2$CH$_2$)$_2$O	morpholine, EtOH, 2 h, rt	89
1m	OEt	EtONa, EtOH, 0.5 h, rt	95
1n	PO(OEt)$_2$	P(OEt)$_3$, 6 h, 100 °C	20
1o	SBu-*t*	NaH, *t*-BuSH, DMF, 2 h, rt	95

Scheme 5. 3-Iodo Derivatives 1d and 2d as Precursors to C—C Coupling Products
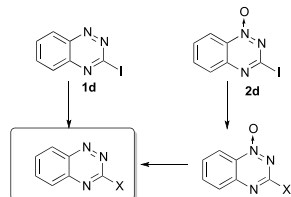
Table 2. Pd-Catalyzed C—C Coupling Reactions of 3-Iodobenzo[e][1,2,4]triazine (1d)

	X	conditions	isolated yield (%)
1p	Ph	PhB(OH)$_2$, Pd(OAc)$_2$, K$_2$CO$_3$, toluene/H$_2$O	82
1r	2-thienyl	thiophene-2-B(OH)$_2$, Pd(OAc)$_2$, K$_2$CO$_3$, toluene/H$_2$O	69
1s	ferrocenyl	ferrocene-B(OH)$_2$, PdCl$_2$(dppf), K$_3$PO$_4$, toluene	27
1t	CCPh	PhCCH, Pd(PPh$_3$)$_4$, CuI, Et$_3$N, THF, 10 min	79

derivative **1t** in 79% yield under standard Sonogashira conditions.

In contrast, carbonylation and Negishi coupling reactions of **1d** were much less successful (Schemes 6 and 7).[66] In

Scheme 6. Attempted Preparation of Carboxylic Acid 1f and Its Esters[a]
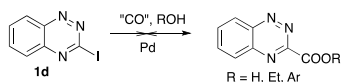
[a]For reaction conditions, see the text and the Supporting Information (SI).

particular, attempts at the preparation of carboxylic acid **1f** or its esters via palladium-catalyzed hydroxycarbonylation, ethoxycarbonylation, or aryloxycarbonylation of 3-iodobenzo[e]-[1,2,4]triazine (**1d**) using several literature protocols and carbon monoxide sources, such as HCOONa in DMF,[67] HCOOH in DMF,[68] HCOOH in toluene,[69] and 2,4,6-trichlorophenyl formate in toluene,[70] gave no reaction or complex mixtures of products, which included **1a**. An attempt at CuI-catalyzed carbonylation of iodide **1d** with CO$_2$ in the presence of Et$_2$Zn and tetramethylethylenediamine in DMSO[71] gave no reaction. Similar results were obtained for ethoxycarbonylation[69] of 3-chlorobenzo[e][1,2,4]triazine (**1c**) and aryloxycarbonylation[70] of 3-iodobenzo[e][1,2,4]triazin-1-oxide (**2d**).

The Negishi cross-coupling reaction of 3-iodo-benzo[e]-[1,2,4]triazine (**1d**) with pentylzinc in THF in the presence of PEPPSI-IPr, Pd(PPh$_3$)$_2$Cl$_2$, Pd(OAc)$_2$/Xantphos, Pd$_2$(dba)$_3$/PPh$_3$, Pd$_2$(dba)$_3$/P(2-OMeC$_6$H$_4$), Pd$_2$(dba)$_3$/Xantphos, or Pd$_2$(dba)$_3$/P(c-Hex)$_2$(Ph-C$_6$H$_4$) in the temperature range of rt to 50 °C surprisingly gave no reaction (Scheme 7) and the

formation of the desired 3-pentylbenzo[e][1,2,4]triazine (**1u**) was not observed.

Scheme 7. Preparation of 3-Pentylbenzo[e][1,2,4]triazine (1u)[a]
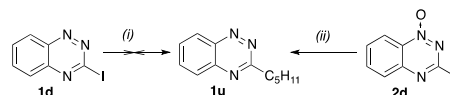
[a]Reagents and conditions: (i) ZnCl$_2$, n-C$_5$H$_{11}$MgBr, PEPPSI-IPr, THF, 0 °C, 15 min → rt, 20 min; (ii) (1) ZnCl$_2$, n-C$_5$H$_{11}$MgBr, PEPPSI-IPr, THF, 0 °C, 15 min → rt, 20 min; (2) H$_2$, 10% Pd/C, EtOH/AcOEt, rt, overnight (55−58% yield).

In contrast to **1d**, the reactivity of N-oxide analogue **2d** in these catalytic systems was much higher even at ambient temperature. Thus, reactions of **2d** with C$_5$H$_{11}$ZnBr in the presence of Pd(PPh$_3$)$_4$, Pd(PPh$_3$)$_2$Cl$_2$, or Pd$_2$(dba)$_3$/PPh$_3$ gave a complex mixture of products with small amounts of the expected 3-pentylbenzo[e][1,2,4]triazine-1-oxide (**2u**, Scheme 8). Changing the catalyst to PEPPSI-IPr greatly improved the

Scheme 8. CuI-Mediated Substitution Reactions of 3-Iodobenzo[e][1,2,4]triazine (1d)[a]
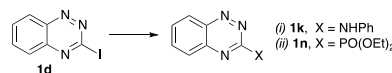
[a]Reagents and conditions: (i) PhNH$_2$, CsF, CuI, DMSO, 60 °C, overnight, 65% yield; (ii) HP(O)(OEt)$_2$, CuI, Et$_3$N, toluene, 60 °C, 2 h, 75% yield.

process conducted at ambient temperature, and the desired product **2u** was isolated in 40% yield. The reaction run with 2 or 4 equiv of C$_5$H$_{11}$ZnBr at 0 °C gave a mixture of the expected product **2u** and its deoxygenated analogue **1u** in a 3:2 ratio, which after catalytic reduction provided **1u** in 55−58% overall yield.

Three copper(I)-mediated C−N, C−P, and C−C coupling reactions of **1d** were investigated. Thus, a ligand-free Ullmann-type C−N coupling reaction[72] of **1d** with aniline in the presence of CuI and CsF in DMSO afforded the desired 3-aminophenyl derivative **1k** in 65% yield (Scheme 8), which is comparable to that obtained in nucleophilic substitution of **1c**. Similarly, a reaction of **1d** with HPO(OEt)$_2$ in the presence CuI and Et$_3$N gave the phosphonate ester **1n** in 75% yield.

The Cu(I)-catalyzed trifluoromethylation[73] of 3-iodobenzo-[e][1,2,4]triazine (**1d**) with the Ruppert reagent (Me$_3$SiCF$_3$) and the preparation of 3-(trifluoromethyl)benzo[e][1,2,4]-triazine (**1g**) proved to be challenging. All attempts at the direct transformation of the iodo derivative **1d** to **1g** were unsuccessful (Scheme 9).

A reaction of **1d** with 2 equiv of Me$_3$SiCF$_3$ in the presence of CsF and CuI gave unreacted **1d** and a new, less polar product in a 1:2 ratio (NMR). A similar result was obtained when chloride **1c** was used in place of the iodide **1d** and no CuI catalysis was used (dimethoxyethane solvent). The new product was different from the expected **1g**. Its detailed analysis revealed the presence of a broad singlet at 4.70 ppm, characteristic for NH, and 2 equiv CF$_3$ groups, which suggested structure **7** (Scheme 9). It could be formed by a formal addition of HCF$_3$ to the C=N bond[73] of the expected product **1g**. The lack of

Scheme 9. Attempted Preparation of 3-(Trifluoromethyl)-benzo[e][1,2,4]triazine (1g)[a]
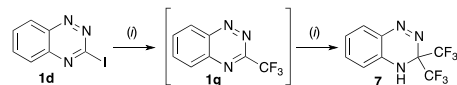
[a]Reagents and conditions: TMSCF$_3$, CsF, CuI, 1,10-phenanthroline, DMF, 60 °C, 1 h. For other reaction conditions, see the text and the SI.

detection of **1g** in the reaction mixture even with 1.3 equiv of Me$_3$SiCF$_3$ is related to the high susceptibility of **1g** to the addition reaction.

A similar result was obtained in a reaction of 3-iodo derivative **1d** with 2 equiv of the Ruppert reagent[73] in the presence of CuI, 1,10-phenanthroline, and CsF in a mixture of DMF and N-methyl-2-pyrrolidone (1:1).[74] In this case, compound **7** was formed in about 65% yield based on ^{1}H NMR, after 3 h at 60 °C. On the other hand, reaction of iodide **1d** with Me$_3$SiCF$_3$ under similar conditions using KF[75] instead of CsF led to recovery of the starting iodide. Attempts at synthesis of **1g** using CF$_3$B(OMe)$_3$K as the trifluoromethylating reagent in DMSO at 60 °C in the presence of CuI and 1,10-phenanthroline[76] gave only 3-methoxybenzo[e][1,2,4]triazine (**1v**), which was isolated in 51% yield. Reactions of 3-iodo N-oxide **2d** with the Ruppert reagent under conditions described by Oishi were more successful.[74] Thus, a reaction of **2d** with 2 equiv of Me$_3$SiCF$_3$ in the presence of CsF and CuI gave full conversion of the iodide in 1 h, resulting in a mixture of products, from which two compounds were isolated. The desired product **2g** was isolated in 7% yield, while the main product of this reaction was less polar derivative **8**, an analogue of **7**, isolated in 24% yield (Scheme 10). Its structure was confirmed by single-crystal XRD analysis (vide infra).

Scheme 10. Trifluoromethylation of 3-Iodo-benzo[e][1,2,4]triazine-1-oxide (2d)[a]
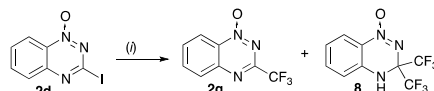
[a]Reagents and conditions: TMSCF$_3$, CsF, CuI, 1,10-phenanthroline, DMF, 60 °C, 1 h; **2g**, 7% yield; **8**, 24% yield.

A test reaction of **2d** with 1 equiv of Me$_3$SiCF$_3$ demonstrated that the reaction is completed in less than 10 min and the ratio of the main components **2d**/**2g**/**8** is 4:1:2. This suggests that the rate of formal addition of HCF$_3$ to the desired product **2g** is comparable to its formation.

Attempted deoxygenation of **2g** under catalytic conditions (H$_2$/Pd/C) gave a complex mixture of products with the desired **1g** being a minor component.

Functional Group Transformations. In light of a failure of carbonylation of **1d**, an alternative access to the carboxylic acid **1f** was investigated through hydrolysis of the nitrile **1i**. Thus, acidic hydrolysis with conc. HCl at ambient temperature gave amide **1w** after 72 h (Scheme 11). Its structure was confirmed by independent synthesis from acid **1f**. Conversion of the amide to the acid **1f** was accomplished in 98% yield using NaNO$_2$ in aqueous HCl/AcOH. When hydrolysis of nitrile **1i** with conc. HCl was conducted at 70 °C, only the parent

Scheme 11. Hydrolysis of Benzo[e][1,2,4]triazine-3-carbonitrile (1i)[a]
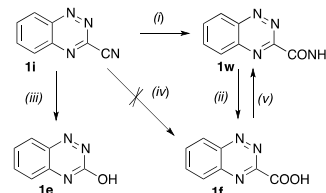
[a]Reagents and conditions: (i) conc. HCl, rt, 72 h, quant.; (ii) NaNO$_2$, 20% HCl, AcOH; rt overnight, 98% yield; (iii) (1) 30% NaOH, 60 °C, 2 h; (2) 20% HCl, rt; (iv) conc. HCl, 70 °C; (v) (1) (COCl)$_2$, CH$_2$Cl$_2$, cat DMF; (2) CH$_2$Cl$_2$/25% NH$_4$OH, quant.

benzo[e][1,2,4]triazine (**1a**) was isolated in 55% yield. A possibility of formation of **1a** by decarboxylation of **1f** was demonstrated by heating of acid **1f** in conc. HCl. Interestingly, treatment of nitrile **1i** with aqueous NaOH gave a mixture of the expected amide **1w** and apparently the substitution product, the 3-hydroxy derivative **1e**, in about 1:7 ratio on the basis of ^{1}H NMR spectroscopy (Scheme 11).

Acylation of amine **1b** with 1 equiv of PhCOCl in the presence of Et$_3$N gave only the dibenzoylated product **1x** and the starting amine **1b** (Scheme 12). No monobenzoylated product was observed. No reaction was observed when NaHCO$_3$ was used as the base.

Scheme 12. Acylation of 3-Aminobenzo[e][1,2,4]triazine (1b)[a]
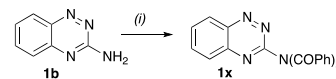
[a]Reagents and conditions: (i) 1.5 equiv BzCl, Et$_3$N, CH$_2$Cl$_2$, rt, overnight, 75% yield.

The malonate ester **1j** was converted to the acetate ester **1y** in 89% yield upon heating with sodium chloride in DMSO (Scheme 13), following a procedure described for a pyrimidine analogue.[65]

Scheme 13. Preparation of Ethyl Benzo[e][1,2,4]triazine-3-acetate (1y)[a]
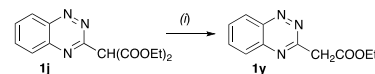
[a]Reagents and conditions: (i) NaCl, H$_2$O, DMSO, 180 °C, 20 min, 89% yield.

Molecular and Crystal Structures. Yellow crystals of 3-morpholinyl (**1l**) and 3-phenyl (**1p**) derivatives suitable for X-ray diffraction studies were obtained by slow evaporation of n-heptane solutions, while crystals of 3-iodo (**1d**) and 3-dibenzoylamino (**1x**) derivatives were grown from MeCN solutions. Crystals of 3-trifluoromethyl derivative **1g** were obtained from a petroleum ether/EtOAc (8:1) solution on cooling, and crystals of 3,3-bis(trifluoromethyl) derivative **8** were grown by slow evaporation of an EtOH/MeCN solution. Single-crystal X-ray diffraction experiments were performed at

Table 3. Selected Interatomic Distances and Angles for Five Benzo[e][1,2,4]triazine Derivatives[a]

	1d[b]	1g[c]	1l[d]	1p[e]	1x[f]
N(1)–N(2)	1.323(4)	1.318(1)	1.305(2)	1.308(1)	1.312(2)
N(2)–C(3)	1.366(4)	1.357(2)	1.385(2)	1.357(1)	1.368(2)
C(3)–N(4)	1.310(5)	1.308(2)	1.331(2)	1.323(1)	1.305(2)
N(4)–C(4a)	1.357(5)	1.361(2)	1.358(2)	1.355(1)	1.366(2)
C(4a)–C(5)	1.407(6)	1.410(2)	1.421(3)	1.416(1)	1.413(2)
C(5)–C(6)	1.366(7)	1.367(2)	1.369(3)	1.367(1)	1.372(2)
C(6)–C(7)	1.426(7)	1.424(2)	1.419(3)	1.420(1)	1.422(2)
C(7)–C(8)	1.364(6)	1.360(2)	1.361(3)	1.363(1)	1.361(2)
C(8)–C(8a)	1.417(6)	1.418(2)	1.419(3)	1.416(1)	1.419(2)
C(8a)–N(1)	1.365(6)	1.357(2)	1.364(3)	1.357(1)	1.365(2)
C(8a)–C(4a)	1.421(6)	1.424(2)	1.409(3)	1.418(1)	1.413(2)
N(1)–N(2)–C(3)	117.3(3)	117.4(1)	118.3(2)	119.05(8)	117.3(1)
N(2)–C(3)–N(4)	128.1(3)	129.0(1)	125.9(2)	125.76(8)	128.6(1)

[a]The numbering system according to the chemical nomenclature. For details, see the SI. [b]The C(3)−I distance is 2.105(3) Å. [c]The C(3)−CF$_3$ distance is 1.519(2) Å. [d]The C(3)−N distance is 1.366(2) Å. [e]The C(3)−Ph distance is 1.481(1) Å; BT−Ph interplanar angle 5.1°. [f]The C(3)−N distance is 1.425(2) Å.
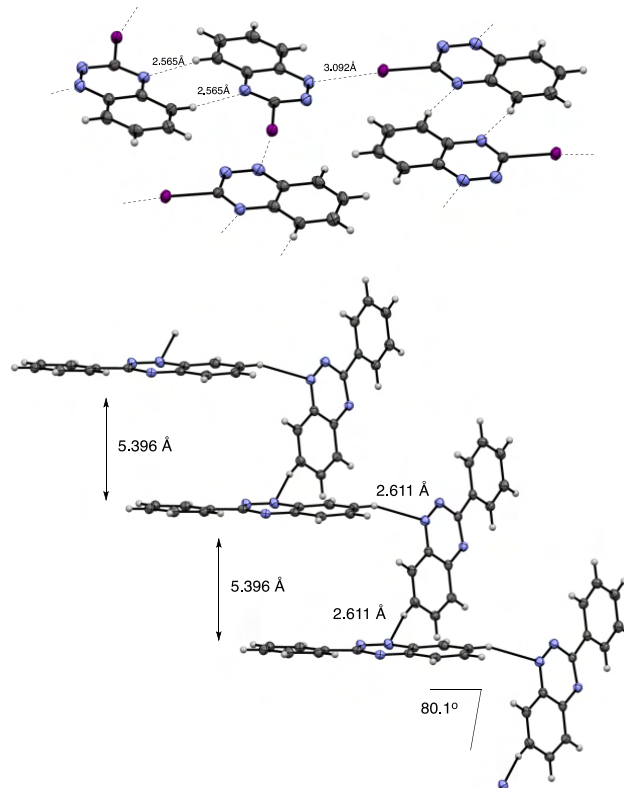
Figure 3. Partial packing diagrams for **1d** (top) showing molecular arrangements in a single sheet and for **1p** (bottom).

100 K. Crystal data, data collection, and structure refinement details are presented in the SI. Selected interatomic distances and angles for investigated derivatives are summarized in Table 3. Respective crystal structures of **1d**, **1l**, **1p**, **1x**, and **8** are shown in Figures 3−5.

All five 3-substituted benzo[e][1,2,4]triazines crystallize with one unique molecule, while derivative **8** with two unique molecules in the asymmetric unit of the crystal lattice. Derivatives **1d**, **1g**, and **8** crystallize in the monoclinic $P2_1/c$ space group, while **1l** and **1p** are in $P2_1/n$ and $C2/c$ settings,
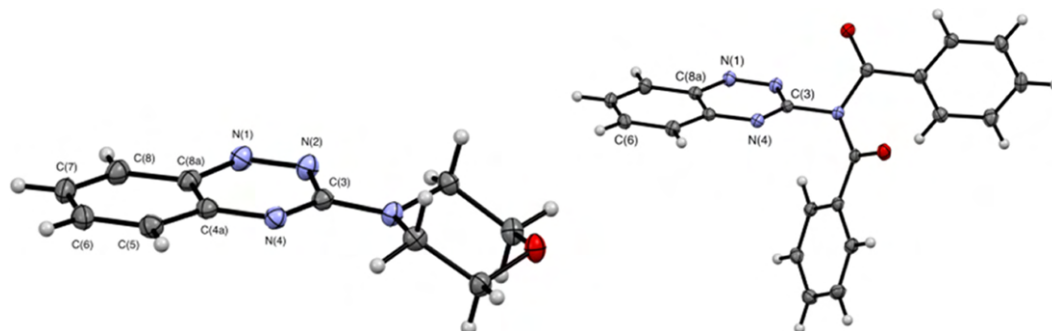
Figure 4. Thermal ellipsoid diagram for **1l** (left) and **1x** (right). For selected geometrical parameters, see Table 3. Ellipsoids are drawn at 50% probability, and the numbering system according to the chemical nomenclature.
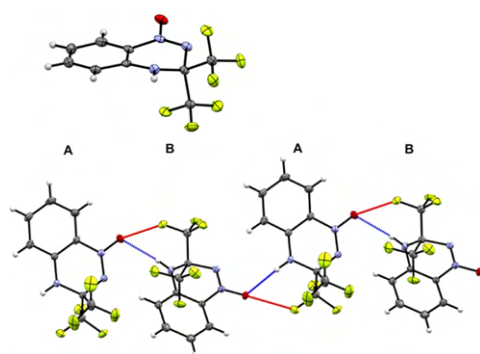
Figure 5. Top: thermal ellipsoid diagram for molecule A of compound **8**. Pertinent geometrical parameters: N(1)−O 1.260(2) Å, N(1)−N(2) 1.283(2) Å, N(2)−C(3) 1.465(2) Å, C(3)−N(4) 1.427(2) Å, C(3)−CF$_3$ 1.547(3) and 1.558(3) Å. Bottom: partial packing diagrams for **8** showing an alternating chain of molecules with close contacts O⋯F 0.112 and 0.186 Å and O⋯H 0.487 and 0.592 Å inside the van der Waals (VDW) separation. Ellipsoids are drawn at 50% probability, and the numbering system according to the chemical nomenclature.

Figure 6. Structures of previously structurally characterized benzo-[*e*][1,2,4]triazine derivatives.

respectively. Compound **1x** crystallizes in the orthorhombic *Pca*2$_1$ space group. Analysis of crystal packing indicates some specific features for each investigated derivative. Most interesting is the 3-iodo derivative **1d**, which forms a dimeric structure with two mutual C(5)−H⋯N(4) nonbonding interactions (0.185 Å inside the VDW separation, Figure 3). The dimers are then interconnected through strong I⋯N(1) interactions (0.438 Å inside the VDW separation), which result in parallel sheets separated by 3.312 Å (Figure 3). In the 3-phenyl derivative **1p**, there are two interacting slipped stacks oriented at 80.1° relative to each other with a distance between the heterocycle planes of 5.396 Å (Figure 3). Molecules of 3,4-dihydrobenzo[*e*][1,2,4]triazine derivative **8** form an infinite chain of type ⋯ABABA⋯ through two types of close contacts: N(4)−H⋯O and F⋯O, which are 0.487/0.592 and 0.112/0.186 Å inside the VDW separation, respectively (Figure 5).

The benzo[*e*][1,2,4]triazine ring is planar in all five derivatives (Figures 3 and 4), and interatomic distances shown in Table 3 are consistent with those found in the five derivatives **9**,[17,18] **10**,[16] **11**,[15] and **12**[19] with known structures (Figure 6).

Analysis of data in Table 3 demonstrates that the dimensions of the [1,2,4]triazine ring respond to electronic effects of the substituent at the C(3) position. Thus, the increase of the electron-withdrawing ability of the substituent results in lengthening of the N(1)−N(2) bond and shortening of the N(2)−C(3), C(3)−N(4), and C(4a)−C(5) distances. These observations are consistent with DFT results (M06-2x/6-31G(2d,p) level) for a set of 11 derivatives.[66] They demonstrate that the C(3) substituent exerts the strongest effect on the N(2)−C(3) distance, which contracts upon increasing the electron-withdrawing character of the substituent. About a half as strong effect is observed on the C(3)−N(4) bond, which also contracts, and on the N(1)−N(2) bond, which expands when the value of the σ_p parameter increases. The calculated changes in all three bonds show reasonable correlation with the σ_p parameter.[66] Effect on other bonds in the benzo[*e*][1,2,4]-triazine skeleton is much weaker or negligible.[66]

Orientation of the C(3) substituents in the five experimentally investigated derivatives of the benzo[*e*][1,2,4]triazine is noteworthy. Thus, the phenyl group in **1p** is nearly coplanar with the heterocycle ring (interplanar angle, 5.6°), which is consistent with the predicted fully planar geometry at the conformational minimum. The morpholine ring in **1l** is oriented parallel to the heterocycle plane (Figure 4) allowing for full interactions of the nitrogen's lone pair with the heterocycle π system. The morpholine nitrogen atom is nearly planar with a distance of 0.156 Å from the plane defined by its three substituents. In the dibenzoyl derivative **1x**, all three π substituents of the imide nitrogen atom, the heterocycle and the two benzoyl groups, are arranged in a propeller-like mode (Figure 4). The nitrogen is slightly pyramidalized, and the distance from the plane defined by its three sp^2-hybridized substituents is 0.184 Å. All of these molecular features are fully consistent with the DFT computational results obtained at the M06-2x/6-31G(2d,p) level of theory.[66]

`Article`

Table 4. Selected Experimental[a] and Calculated[b] Electronic Transition Energies and Oscillator Strength Values

compound	experimental[a]		theoretical[b]		
X	λ_{max} (n → π*)/nm (log ε)	λ_{max} (π → π*)/nm (log ε)	n → π* (A″)/nm (f)	π → π* (A′)/nm (f)	π → π* (A′)/nm (f)
1a, H	443 (2.52)	333 (2.89),[c] 303 (3.57)	415.8 (0.005)	293.7 (0.054)	264.9 (0.110)
1c, Cl	427 (2.44)	339 (3.41), 305 (3.55)	404.2 (0.004)	305.6 (0.049)	271.9 (0.131)
1g, CF$_3$	433 (2.52)	309 (3.50)	409.0 (0.004)	299.8 (0.039)	269.2 (0.080)
1i, CN	431 (2.27)	320 (3.17)	409.1 (0.004)	308.4 (0.039)	278.0 (0.056)
1l, N(C$_2$H$_4$)$_2$O	[d]	416 (3.28), 304 (3.22)[c]	419.8 (0.004)	360.0 (0.103)	270.8 (0.066)
1m, OEt	429 (2.55)	354 (3.47), 295 (3.62)	405.9 (0.004)	309.8 (0.082)	265.9 (0.166)
1p, Ph	454 (2.52)	352 (3.65), 272 (4.44)	429.5 (0.003)	318.1 (0.179)	261.8 (0.864)
1r, thienyl	453 (2.56)[c]	378 (3.73), 301 (4.33)	419.0 (0.004)	335.2 (0.249)	277.0 (0.489)
1t, CCPh	439 (2.66)[c]	355 (3.86), 301 (4.38)	415.6 (0.004)	326.3 (0.499)	281.6 (0.784)

[a]Recorded in CH$_2$Cl$_2$. [b]Obtained with the TD-CAM-B3LYP/6-31++G(2d,p)//M06-2x/6-31G(2d,p) method in CH$_2$Cl$_2$ dielectric medium. [c]After deconvolution; see the SI. [d]Overlap with the π → π* transition.

Analysis of the molecular structure of derivative **8** demonstrated a puckered [1,2,4]triazine ring with the tetrasubstituted C(3) atom displaced from the 3,4-dihydrobenzo[*e*][1,2,4]triazine plane by 0.25 and 0.43 Å in the two unique molecules. The two CF$_3$ groups are orthogonal to the heterocycle plane, as indicated by the angle between the heterocycle and the CF$_3$−C(3)−CF$_3$ planes in both molecules.

Electronic Absorption Spectroscopy. For a better understanding of the C(3) substituent effect on the electronic structure of the benzo[*e*][1,2,4]triazine system, UV−vis absorption spectra were obtained for series **1** in CH$_2$Cl$_2$ solutions with the focus on low-energy absorption bands above 250 nm. Results are shown in Table 4 and Figure 7.
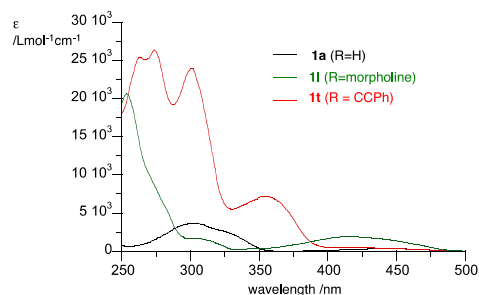
Figure 7. Electronic absorption spectra for **1a** (black), **1l** (green), and **1t** (red) in CH$_2$Cl$_2$.

The spectrum of the parent heterocycle **1a** exhibits two medium-intensity absorptions bands at 303 and 333 nm (after deconvolution; see the SI) corresponding to π → π* transitions and a low-intensity n → π* band at 443 nm (Figure 7). This is consistent with spectra recorded for **1a** in EtOH (304.5, 321sh, and 434 nm).[21] Substitution of the C(3) position affects the energy of all three absorption bands, with the position of the n−π* band being least affected by the nature of the C(3) substituent. It is around 430 nm and oscillates in a range of 427−454 nm. In contrast, the π → π* transition is shifted to higher energies for electron-accepting substituents (CN and CF$_3$), while for substituents with a lone pair (morpholine and EtO), the π → π* absorption bands are at lower energies. A particularly large bathochromic shift is observed for the amino derivative **1l** (Table 4 and Figure 7), for which the first π → π* band is shifted by −0.74 eV to 416 nm. Extended π substituents

at the C(3), such as phenyl (**1p**), thienyl (**1r**), and phenylethynyl (**1t**), also cause bathochromic shift of the first π → π* band with a simultaneous hyperchromic shift. For instance, the first π → π* band in **1p** is shifted by −0.20 eV and in thienyl **1r** by −0.44 eV to lower energies and have over 5 times higher molar extinction than **1a**. This hyperchromic effect is even larger, over 9 times, for acetylene derivative **1t** (Table 4 and Figure 7).

Time-dependent (TD) DFT computational analysis of all members of series **1** in CH$_2$Cl$_2$ dielectric medium reproduced trends in excitation energies and also the relative intensities (Table 4). The calculated transition energies are systematically overestimated for all three bands (0.17 eV for n−π*, 0.5 eV for π−π*1). In the parent benzo[*e*][1,2,4]triazine (**1a**), the lowest-energy absorption band at 443 nm (calculated at 416 nm) is related to n−π* excitation from the highest occupied molecular orbital (HOMO), involving the lone pairs of the nitrogen atoms, to the lowest unoccupied molecular orbital (LUMO), delocalized over the heterocycle (Figure 8). The two lowest-energy π−π* excitations involve mainly the HOMO−1 → LUMO and HOMO−2 → LUMO transitions, respectively, which also include the extended π systems (Figure 9). This simple description cannot be applied to derivative **1s**, due to the
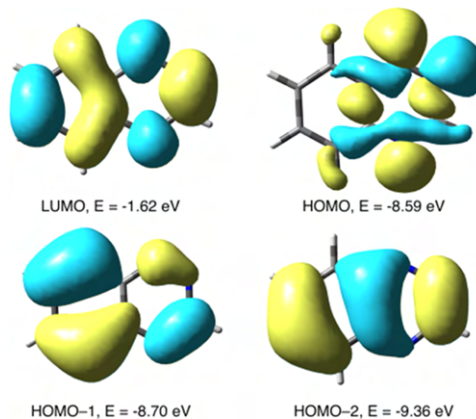
Figure 8. TD-CAM-B3LYP/6-31++G(2d,p)//M06-2x/6-31G(2d,p)-derived contours and energies of molecular orbitals for **1a** in CH$_2$Cl$_2$ dielectric medium relevant to the lowest-energy transitions.
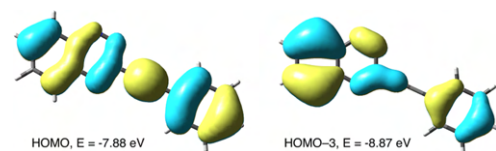
Figure 9. TD-CAM-B3LYP/6-31++G(2d,p)// M06-2x/6-31G(2d,p)-derived contours and energies of selected molecular orbitals for **1t** in CH_2Cl_2 dielectric medium.

extensive involvement of the ferrocene electron manifold in low-energy transitions. Calculations demonstrate that the C(3) substituent affects the energy of the π orbitals involved in these three lowest-energy transitions. Thus, energy of these orbitals decreases with an increasing electron-withdrawing character of the substituent σ_m,[77] with the strongest effect observed for the highest π-symmetry occupied molecular orbital (MO) (π1).[66] While correlation factor r^2 between energy of the MOs and σ_m is modest ($r^2 = 0.66$) and good ($r^2 = 0.915$), essentially no reasonable correlation was found for the calculated three lowest-energy excitation energies and the substituent constant σ.

NMR Spectroscopy. The availability of benzo[*e*][1,2,4]-triazines with a relatively broad range of substituents at the C(3) position allowed for another glimpse into the distribution of electronic effects in the heterocyclic ring through a correlation analysis of ^{1}H NMR shifts in the fused benzene ring. For this purpose, the ^{1}H NMR signals observed in the aromatic region were assigned to positions C(5)−H through C(8)−H of benzo[*e*][1,2,4]triazine on the basis of multiplicity, coupling constants, correlation spectroscopy, and trends in DFT computational results.[66]

A comparison of calculated and experimental chemical shifts (δ) for a series of 17 derivatives **1** in $CDCl_3$ demonstrates high correlation factors for all aromatic hydrogen atoms ($r^2 \geq 0.96$) with the slope being essentially a unity.[66] In contrast, the same correlation of ^{13}C NMR shifts for the C(3) atom shows a significant discrepancy for **1d**, due to heavy atom effect of the iodine atom, **1b** and **1k**. In the latter two cases, the calculated and experimental values differ by over 10 ppm, which suggests that the imino tautomeric forms **1b′** and **1k′** might be dominant (Figure 10). For instance, the calculated C(3) NMR chemical

Figure 10. Tautomeric equilibrium for amines **1b** and **1k**.

shifts for **1k** and **1k′** are 158.3 and 144.0 ppm, respectively, while the observed signal is found at 141.2 ppm. The dominance of tautomer **1k′** in the sample is consistent with significant deshielding of the N−H proton (8.46 ppm) and the presence of an intense band at 1557 cm^{-1} in the IR spectrum (DFT calculated at $\nu_{C=N} = 1641$ cm^{-1}). Therefore, further correlation analysis excluded data also for **1b** and **1k**.

A correlation of experimental ^{1}H NMR chemical shifts for each position of the fused benzene ring in 15 derivatives with available substituent parameters σ_p revealed a linear relationship with the correlation parameter r^2 in a range of 0.88−0.92. Excluding data for the parent **1a** improved the correlation ($r^2 =$

0.89−0.94) shown in Figure 11. Analysis of the best-fit lines shows that the slopes are nearly twice larger for correlations of
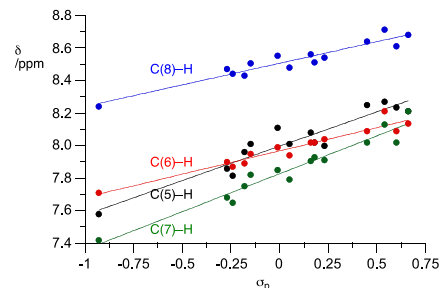
Figure 11. Correlation of ^{1}H NMR chemical shifts (δ) obtained in $CDCl_3$ for 14 derivatives of benzo[*e*][1,2,4]triazines **1** and the substituent parameter σ_p. Best-fit lines: $\delta_{H5} = 8.00 + 0.42 \times \sigma_p$, $r^2 = 0.89$; $\delta_{H6} = 7.97 + 0.29 \times \sigma_p$, $r^2 = 0.93$; $\delta_{H7} = 7.83 + 0.47 \times \sigma_p$, $r^2 = 0.94$; $\delta_{H8} = 8.50 + 0.27 \times \sigma_p$, $r^2 = 0.91$.

C(5)−H and C(7)−H chemical shifts (0.42 and 0.47, respectively) than for those of the other two positions (0.29 and 0.27). The results indicate that all four protons of the benzene ring undergo deshielding upon increase of the electron-withdrawing character of the C(3) substituent, and its impact on the electron density is approximately twice larger for positions C(5)−H and C(7)−H than for those in positions C(6)−H and C(8)−H. This effect is about 80% of that observed for the C(4) position in monosubstituted benzene derivatives (slope 0.55 ± 0.03 for 12 derivatives).[66]

The observed good-quality correlation of the chemical shifts with the parameter σ_p permitted the estimate of the substituent parameter σ_p for the CH_2COOEt group: 0.11 ± 0.01 as an average value obtained from correlation for all four H atoms.

■ SUMMARY AND CONCLUSIONS

We have demonstrated that benzo[*e*][1,2,4]triazines with a wide range of substituents at the C(3) position are readily available directly from the corresponding 3-halo derivatives **1c** and **1d**, which are obtained in three simple steps from 2-nitroaniline. The chloride **1c** is a convenient substrate for direct and efficient introduction of substituents such as OR, NHAr, NR_2, SR, and soft C-nucleophiles (CN and malonate) via S_N2Ar nucleophilic substitution reactions, while the iodo derivative **1d** provided access to C(3) (het)aryl (Suzuki), acetylene (Sonogashira), and phosphonate through Pd- or Cu-catalyzed substitution reactions. These methods failed to obtain 3-CF$_3$ (**1g**), 3-carboxyl (**1f**), and 3-alkyl (**1u**) derivatives from **1d** using the Ruppert, Pd-catalyzed carbonylation, and Negishi reactions, respectively. The use of iodide *N*-oxide **2d** instead of **1d** allowed to obtain 3-pentyl derivative **1u** in good yields, but failed again to provide access to **1g** and **1f**. Analysis of reaction products suggested that the 3-CF$_3$ derivatives **1g** and **2g** are highly electrophilic and their formation under the Ruppert conditions competes with addition of a second equivalent of the "CF$_3$" anion to the C=N bond in the [1,2,4]triazine ring. The carboxylic acid **1f** is susceptible to decarboxylation under acidic conditions, and this tendency may be at the root of failure to carbonylate iodides **1d** and **2d**. The carboxylic acid **1f** was prepared in high yield by a two-step hydrolysis of nitrile **1i**.

Table 5. Comparison of Methods for Preparation of Functional Derivatives 1 in This Work and Previously Used[a]

functionality	this work (from 2-nitroaniline)	previous methods
3-COOH (**1f**)	six steps, 38 avrg% yield	four steps from 2-nitroaniline, 21% yield (method D)[b]
3-alkyl (**1u**)	four steps, 28 avrg% yield	three steps from 2-iodoaniline, 65% yield (method E)[c]
3-(het)aryl (**1p** and **1r**)	four steps, 39 avrg% yield	three steps from 2-iodoaniline, 36% yield (method E)[c]
3-CH₂COOEt (**1y**)	five steps, 36 avrg% yield	three steps from 2-nitrophenylhydrazine and ethyl 3-amino-3-ethoxyacry-late, 43% yield (method D)[d]
3-amino (**1k** and **1l**)	four steps, 35 avrg% yield	multistep processes[e]

^{a}See Figure 2 for methods. ^{b}Refs 35, 61. ^{c}Ref 36. ^{d}Ref 33. ^{e}Refs 24, 48.

Table 5 compares efficiencies of preparation of functional derivatives in this work with those previously reported.

Among the prepared compounds, there are several new functional derivatives of benzo[*e*][1,2,4]triazine. They include malonate **1j**, phosphonate ester **1n**, ferrocene **1s**, acetylene **1t**, and amides **1w** and **1x**. It should be added that two other important functional groups, NHNH₂, which was obtained from chloride **1c**, and N₃ prepared from the C(3)−NHNH₂ derivative, have been useful for the preparation of other heterocyclic systems.[28,45] Also the cyano group in **1i** offers access to other functionalities and heterocyclic systems through standard transformations.[78] Thus, a variety of derivatives of **1a** are available from common easily accessible intermediates.

Spectroscopic analysis augmented with DFT calculations revealed three low-intensity principal absorption bands above 250 nm corresponding to n → π* and π → π* transitions. The C(3) substituent has a significant impact on the position of the lower-energy π → π* transition through considerable interactions with the π-symmetry highest-energy-occupied MO (π1).

NMR and IR analyses demonstrate that the tautomeric imino form is dominant in derivatives containing the NHR group at the C(3) position (compounds **1b** and **1k**). Analogously, the keto form is expected to be the main tautomer in C(3)−OH derivatives (**1e**). Analysis of ^{1}H NMR chemical shifts indicates that the C(3) substituent affects primarily positions C(5) and C(7). The magnitude of this effect in series **1** is comparable to that in monosubstituted benzene at the C(4) position.

Simplified availability of a variety of derivatives **1** offers a broader and simpler access to C(3)-functionalized 1,4-dihydrobenzo[*e*][1,2,4]triazin-4-yl radicals by addition of ArLi reagents. These results will be reported elsewhere.

COMPUTATIONAL DETAILS

Quantum-mechanical calculations were carried out using Gaussian 09 suite of programs.[79] Geometry optimizations were undertaken at the M06-2x/6-31G(2d,p) level of theory using tight convergence limits and appropriate symmetry constraints. Calculations involving iodine and iron used the LANL2DZdp effective core potential basis set (available from http://www.emsl.pnl.gov/forms/-basisform.html) and 6-31G-(2d,p) for the remaining elements implemented with the GEN keyword. The nature of stationary points was confirmed with vibrational frequency calculations.

Zero-point energy corrections were scaled by 0.9806.[80] Electronic excitation energies in CH₂Cl₂ dielectric medium were obtained at the CAM-B3LYP/6-31++G(2d,p)//M06-2x/6-31G(2d,p) level using the time-dependent DFT method[81] supplied in the Gaussian package. The same method was used to obtain isotropic shielding constants requested with the NMR = GIAO keyword and performed in CHCl₃ dielectric medium. Solvation models in both types of calculations were implemented with the polarizable continuum model[82] using

SCRF(solvent = CH₂Cl₂) and SCRF(solvent = chloroform) keywords, respectively.

EXPERIMENTAL SECTION

Reagents and solvents were obtained commercially. Heat in reactions involving elevated temperatures was supplied using oil baths, and reported temperature refers to that of the bath.

NMR spectra were obtained at 500 or 600 MHz (^{1}H) and 125 or 150 MHz (^{13}C) in CDCl₃ or DMSO-d_6. Chemical shifts were referenced to the solvent (^{1}H and ^{13}C: 7.26 and 77.16 ppm for CDCl₃, and 2.50 and 39.52 ppm for DMSO-d_6, respectively).[83] Mass spectra were typically recorded in a positive-ion mode on a G2-Si Waters Synapt HDMS instrument fitted with an atmospheric pressure ionization electrospray source. Melting points are uncorrected. UV−vis spectra were recorded in spectroscopic grade CH₂Cl₂ at concentrations in the range of $(2−20) \times 10^{-5}$ M. Molar extinction coefficients ε were obtained by fitting the maximum absorbance against concentration in agreement with Beer's law. More details are provided in the SI.

Benzo[*e*][1,2,4]triazine (1a).[10] *Method A.* Following the general procedure,[60] *t*-BuONO (0.32 mL, 2.68 mmol) was added to a stirred solution of 3-aminobenzo[*e*][1,2,4]triazine (**1b**, 0.195 g, 1.34 mmol) in DMF (7 mL) and the resulting mixture was stirred at 60 °C (oil bath) for 2 h. The mixture was diluted with water (20 mL) and extracted with AcOEt. The combined organic layers were dried (Na₂SO₄) and the solvent was evaporated. The residue was purified by column chromatography (SiO₂; hexane/AcOEt, 4:1) giving 0.041 g (23% yield; 19−23% in several runs) of benzo[*e*][1,2,4]triazine (**1a**) as a yellow solid.

Method B. *t*-BuONO (0.66 mL, 5.56 mmol) was added to a stirred solution of 3-aminobenzo[*e*][1,2,4]triazine-1-oxide (**2b**, 0.448 g, 2.77 mmol) in DMF (10 mL) and the resulting mixture was stirred at 60 °C (oil bath) for 2 h. The mixture was diluted with water (20 mL) and extracted with EtOAc. The combined organic layers were dried (Na₂SO₄) and the solvent was evaporated. The residue was dissolved in EtOH/EtOAc (1:1, 50 mL) and the mixture was stirred overnight with 10% Pd/C (0.040 g) under H₂ (balloon). The mixture was filtered through Celite, which was washed with EtOH, and the filtrate was evaporated. The residue was passed through a SiO₂ plug (AcOEt) giving 0.186 g (51% yield) of benzo[*e*][1,2,4]triazine (**1a**), which was further purified by vacuum sublimation (60 °C, 2.25 Tr): mp (*n*-heptane) 70−71 °C (lit.[10] mp (petroleum ether/AcOEt) 75−76 °C); ^{1}H NMR (CDCl₃, 500 MHz) δ 7.94 (ddd, J_1 = 1.2 Hz, J_2 = 6.9 Hz, J_3 = 8.3 Hz, 1H), 8.04 (ddd, J_1 = 1.4 Hz, J_2 = 6.9 Hz, J_3 = 8.4 Hz, 1H), 8.11 (d, J = 8.5 Hz, 1H), 8.57 (d, J = 8.6 Hz, 1H), 9.97 (s, 1H); ^{13}C{^{1}H} NMR (CDCl₃, 125 MHz) δ 129.1, 129.9, 131.3, 135.8, 141.2, 148.5, 153.9; UV−vis (CH₂Cl₂), λ_{max}(log ε) 303 (3.57), 333 (2.89), 443 (2.54) nm; mass spectrometry (MS) (atmospheric pressure chemical ionization (CI)-time-of-flight (TOF)) m/z 132 (100, [M]$^+$); high-resolution mass spectrometry (HRMS) (electrospray ionization (ESI)-TOF) m/z: [M + H]$^+$ calcd for C₇H₆N₃ 132.0562, found 132.0565. Anal. Calcd for C₇H₅N₃: C, 64.11; H, 3.84; N, 32.04. Found: C, 63.95; H, 3.92; N, 32.05.

3-Aminobenzo[*e*][1,2,4]triazine (1b).[10] *Method A.* A mixture of 3-aminobenzo[*e*][1,2,4]triazine-1-oxide (**2b**, 1.00 g, 6.17 mmol) and 10% Pd/C (0.130 g, 1.23 mmol) in EtOH/AcOEt (1:1, 100 mL) was stirred overnight at rt in the atmosphere of H₂ (balloon). When the thin-layer chromatography (TLC) showed absence of the starting

The Journal of Organic Chemistry   Article

material, the mixture was filtered through Celite and the solvent was evaporated giving 0.892 g (99% yield; 95−99% in several runs) of amine **1b** as a yellow solid.

Method B. Following a literature procedure,[10] a solution of 3-aminobenzo[*e*][1,2,4]triazine-1-oxide (**2b**, 2.00 g, 12.3 mmol) and sodium dithionite (3.21 g, 18.5 mmol) in 70% aqueous ethanol was heated at reflux (oil bath) for 10 min. The hot suspension was filtered, the filtrate was concentrated, then diluted with water (15 mL), and extracted with chloroform (4 × 50 mL). The combined organic extracts were dried (MgSO$_4$) and the solvent was evaporated giving 1.13 g (63% yield; 33−63% in several runs) of amine **1b** as a yellow solid: mp (CHCl$_3$) 204−206 °C (lit.[10] mp (MeOH/CHCl$_3$) 200−203 °C); ^{1}H NMR (DMSO-d_6, 600 MHz) δ 7.45 (ddd, J_1 = 0.8 Hz, J_2 = 6.8 Hz, J_3 = 8.0 Hz, 1H), 7.53 (d, J = 8.5 Hz, 2H), 7.58 (bs, 2H), 7.78 (ddd, J_1 = 1.1 Hz, J_2 = 6.9 Hz, J_3 = 8.2 Hz, 1H), 8.19 (d, J = 8.3 Hz, 1H); ^{13}C{^{1}H} NMR (DMSO-d_6, 150 MHz) δ 124.7, 125.8, 129.2, 135.6, 141.9, 142.1, 160.5; UV−vis (CH$_2$Cl$_2$), λ_{max}(log ε) 298 (3.55), 384 (3.58) nm; electron ionization (EI)-MS, m/z 146 (56 [M][+]), 118 (100 [M][+] − N$_2$). Anal. Calcd for C$_7$H$_6$N$_4$: C, 57.53; H, 4.14; N, 38.33. Found: C, 57.39; H, 4.23; N, 38.14.

3-Chlorobenzo[*e*][1,2,4]triazine (1c).[26] *Method A.* Following a general procedure,[59] 3-aminobenzo[*e*][1,2,4]-triazine (**1b**, 0.699 g, 4.79 mmol) was added to a mixture of CuCl$_2$·2H$_2$O (0.980 g, 5.75 mmol) and *t*-BuONO (0.68 mL, 5.75 mmol) in MeCN (100 mL). The reaction mixture was stirred at 60 °C (oil bath) for 30 min, then poured into 10% aqueous HCl (10 mL), and extracted with AcOEt (2 × 20 mL). The combined organic extracts were dried (Na$_2$SO$_4$), and the solvent was evaporated. The residue was purified by column chromatography (SiO$_2$; hexane/AcOEt, 3:1) giving 0.401 g (51% yield; 48−52% in several runs) of chloride **1c**.

Method B. Following a literature procedure,[26] Zn powder (1.12 g) and NH$_4$Cl (0.84 g) were added to a suspension of 3-chlorobenzo-[*e*][1,2,4]triazine-1-oxide (**2c**, 2.80 g, 0.015 mol) in H$_2$O (70 mL). The reaction mixture was stirred at rt for 48 h, and then glacial acetic acid (70 mL) was added. The mixture was placed in a beaker and Na$_2$CO$_3$ was added in small portions until the evolution of CO$_2$ was ceased. The resulting mixture was extracted with CH$_2$Cl$_2$ (3 × 50 mL). The combined organic extracts were dried (MgSO$_4$) and the solvent was evaporated giving 1.00 g (39% yield) of chloride **1c** as a yellow solid: mp (hexane) 99−100 °C (lit.[26] mp (pentane) 96−98 °C); ^{1}H NMR (CDCl$_3$, 600 MHz) δ 7.92 (ddd, J_1 = 1.0 Hz, J_2 = 6.8 Hz, J_3 = 8.2 Hz, 1H), 8.00 (d, J = 8.2 Hz, 1H), 8.05 (ddd, J_1 = 0.8 Hz, J_2 = 6.8 Hz, J_3 = 8.3 Hz, 1H), 8.55 (d, J = 8.4 Hz, 1H); ^{13}C{^{1}H} NMR (CDCl$_3$, 150 MHz) δ 128.1, 129.8, 131.4, 137.2, 142.1, 146.4, 159.6; IR ν 1560, 1495, 1039, 769 cm^{-1}; UV−vis (CH$_2$Cl$_2$), λ_{max}(log ε) 305 (3.55), 339 (3.41), 427 (2.44) nm; EI-MS, m/z 167 and 165 (15 [M][+]), 139 and 137 (100 [M][+] − N$_2$). Anal. Calcd for C$_7$H$_4$N$_3$Cl: C, 50.78; H, 2.43; N, 25.38. Found: C, 50.68; H, 2.46; N, 25.46.

3-Iodobenzo[*e*][1,2,4]triazine (1d). Following a literature procedure for the preparation of **2d**,[51] *t*-BuONO (2.1 mL, 17.6 mmol) was added to a stirred solution of 3-aminobenzo[*e*][1,2,4]-triazine (**1b**, 0.859 g, 5.88 mmol), I$_2$ (1.49 g, 5.88 mmol), and CuI (1.12 g, 5.88 mmol) in THF (100 mL). The resulting mixture was stirred at reflux (oil bath) for 2 h. The mixture was cooled, filtered through a short plug of alumina, and washed with THF (100 mL). The filtrate was evaporated. The residue was dissolved in CH$_2$Cl$_2$; washed with Na$_2$SO$_3$ solution, water, and brine; dried (Na$_2$SO$_4$); and the solvent was evaporated. The residue was purified by column chromatography (SiO$_2$; hexane/AcOEt, 20:1) giving 0.931 g (62% yield; 59−65% in several runs) of iodide **1d** as a yellow solid: mp (MeCN) 184−185 °C; ^{1}H NMR (CDCl$_3$, 600 MHz) δ 7.93 (ddd, J_1 = 1.7, 6.3, 8.3 Hz, 1H), 8.00−8.03 (m, 2H), 8.51 (d, J = 8.9 Hz, 1H); ^{13}C{^{1}H} NMR (CDCl$_3$, 150 MHz) δ 128.2, 130.0, 130.1, 131.6, 136.8, 142.6, 146.5; CI-MS (isobutane) m/z 258 (100 [M][+]), 229 (20 [M][+] − N$_2$). Anal. Calcd for C$_7$H$_4$N$_3$I: C, 32.71; H, 1.57; N, 16.35. Found: C, 32.65; H, 1.63; N, 16.22.

Benzo[*e*][1,2,4]triazine-3-carboxylic Acid (1f).[61,84] *Method A.* A solution of ethyl ester **1h** (0.90 g, 4.43 mmol) in THF/H$_2$O (9:1, 50 mL) was treated with 0.1 N KOH in EtOH (1.5 equiv, 66.4 mmol). The reaction mixture was stirred for 10 min at rt and poured into 10%

HCl (20 mL). The resulting mixture was extracted with AcOEt, and the organic layer was washed with H$_2$O and dried (Na$_2$SO$_4$). The solvent was removed giving 0.773 g (99% yield) of carboxylic acid **1f** as an orange solid.

Method B. A mixture of benzo[*e*][1,2,4]triazine-3-carboxamide (**1v**, 0.055 g, 0.31 mmol), 20% HCl (1 mL), CH$_3$COOH (1 mL), and NaNO$_2$ (0.043 mg, 0.62 mmol) was stirred at rt overnight. The resulting mixture was poured into water, and the product was extracted with AcOEt (3 × 10 mL). The combined organic layers were dried (MgSO$_4$), and the solvent was evaporated giving 54.7 mg (98% yield) of acid **1f** as an orange solid: mp (MeCN) 192−194 °C (lit.[84] mp 215−216 °C); ^{1}H NMR (DMSO-d_6, 500 MHz) δ 8.14 (ddd, J_1 = 2.2 Hz, J_2 = 5.9 Hz, J_3 = 8.4 Hz, 1H), 8.22−8.26 (m, 1H), 8.68 (d, J = 8.4 Hz, 1H); ^{13}C{^{1}H} NMR (DMSO-d_6, 125 MHz) δ 129.1, 129.3, 133.5, 137.2, 139.9, 147.2, 152.9, 164.2; IR ν 3443 (OH) and 1731 (CO) cm^{-1}; EI-MS m/z 175 (10 [M][+]), 147 (50 [M][+] − N$_2$). Anal. Calcd for C$_8$H$_5$N$_3$O$_2$: C, 54.86; H, 2.88; N, 23.99. Found: C, 54.82; H, 3.01; N, 23.73.

3-(Trifluoromethyl)benzo[*e*][1,2,4]triazine (1g). Following a general procedure,[32] to a solution of amidrazone **5**[32] (4.35 g, 17.9 mmol) in CH$_2$Cl$_2$ (45 mL) was added dropwise a solution of *t*-BuOCl (4.25 g, 39.2 mmol) in CH$_2$Cl$_2$ (24 mL) at −70 °C. The resulting orange mixture was stirred at rt for 4 h. Then, aq solution of Na$_2$S$_2$O$_4$ (100 mL) was added and the mixture was extracted with CH$_2$Cl$_2$ (2 × 30 mL). Combined organic layers were dried (Na$_2$SO$_4$) and the solvent was evaporated. The residue was purified by flash chromatography (SiO$_2$; petroleum ether/AcOEt, 8:2) giving 1.30 g (37% yield) of the trifluoromethyl derivative **1g** as an orange solid: mp (petroleum ether) 82−84 °C; ^{1}H NMR (CDCl$_3$, 600 MHz) δ 8.10 (t, J = 7.9 Hz, 1H), 8.18 (t, J = 8.0 Hz, 1H), 8.24 (d, J = 8.4 Hz, 1H), 8.68 (d, J = 8.5 Hz, 1H); ^{13}C{^{1}H} NMR (CDCl$_3$, 150 MHz) δ 120.2 (q, J_{HF}[1] = 276 Hz), 129.5, 129.9, 133.5, 137.4, 140.1, 148.5, 152.7 (q, J_{HF}[2] = 37 Hz); UV−vis (CH$_2$Cl$_2$), λ_{max}(log ε) 309 (3.50), 433 (2.52) nm. Anal. Calcd for C$_8$H$_4$N$_3$O$_2$: C, 48.25; H, 2.02; N, 21.10. Found: C, 48.31; H, 2.13; N, 21.21.

Attempted Preparation of 3-(Trifluoromethyl)-benzo[*e*]-[1,2,4]triazine (1g). *3-Methoxy-benzo[*e*][1,2,4]triazine (1v).* Following a general procedure,[76] to a dried flask charged with CuI (0.024 g, 0.128 mmol), 1,10-phenanthroline (0.023 g, 0,128 mmol), and CF$_3$B(OMe)$_3$ (1.69 g, 9.57 mmol) was added anhydrous, deoxygenated DMSO (4 mL). Then, 3-iodobenzo[*e*][1,2,4]triazine (**1d**, 0.164 g, 0.638 mmol) was added directly to the flask and the resulting mixture was stirred at 60 °C (oil bath) for 48 h until TLC showed absence of the starting **1d**. After cooling, the solution was diluted with AcOEt (20 mL) and washed with 1 N HCl (10 mL) and water (10 mL). The washing was reextracted with AcOEt (2 × 10 mL), combined organic layers were dried (Na$_2$SO$_4$), and solvent was evaporated. The residue was separated by column chromatography (SiO$_2$; petroleum ether/AcOEt, 9:1) giving 0.052 g (51% yield) of 3-methoxybenzo[*e*][1,2,4]-triazine (**1v**) as a yellow solid: mp (MeCN) 102−104 °C (lit.[49] mp (hexane) 104−105 °C); ^{1}H NMR (CDCl$_3$, 500 MHz) δ 4.24 (s, 1H), 7.68 (ddd, J_1 = 1.4 Hz, J_2 = 6.7 Hz, J_3 = 8.3 Hz, 1H), 7.86 (d, J = 8.3 Hz, 1H), 7.90 (ddd, J_1 = 1.3 Hz, J_2 = 6.7 Hz, J_3 = 8.1 Hz, 1H), 8.47 (d, J = 8.4 Hz, 1H); ^{13}C{^{1}H} NMR (CDCl$_3$, 125 MHz) δ 55.5, 127.4, 127.9, 129.9, 136.2, 141.9, 144.9, 162.9. Anal. Calcd for C$_8$H$_7$N$_3$O: C, 59.62; H, 4.38; N, 26.07. Found: C, 59.64; H, 4.42; N, 26.14.

Attempted Preparation of 3-(Trifluoromethyl)benzo[*e*]-[1,2,4]triazine (1g). *3,3-Bis(trifluoromethyl)-3,4-dihydrobenzo[e]-[1,2,4]triazine (7).* Following a general literature procedure,[74] to a mixture of CsF (0.083 g, 0.545 mmol), CuI (5.2 mg, 0.027 mmol), 1,10-phenanthroline (4.9 mg, 0.028 mmol), and iodide **1d** (0.071 g, 0.272 mmol) in dry DMF at 60 °C (oil bath) was added TMSCF$_3$ (0.08 mL, 0.545 mmol). The reaction mixture was stirred at 60 °C for 1 h, then quenched with H$_2$O, and extracted with AcOEt (3 × 20 mL). Combined organic layers were dried (Na$_2$SO$_4$) and solvent was evaporated. The residue was separated by column chromatography (SiO$_2$; petroleum ether/AcOEt, 10:1) giving 0.021 g (29% yield) of **7** as a yellow solid: mp (MeOH) 80−82 °C; ^{1}H NMR (CDCl$_3$, 500 MHz) δ 4.70 (s, 1H), 6.67 (dd, J_1 = 0.7 Hz, J_2 = 8.1 Hz, 1H), 6.99 (td,

J_1 = 1.1 Hz, J_2 = 7.8 Hz, 1H), 7.38 (td, J_1 = 1.5 Hz, J_2 = 8.0 Hz, 1H), 7.92 (d, J = 7.9 Hz, 1H); $^{13}C\{^1H\}$ NMR (CDCl$_3$, 125 MHz) δ 75.7 (sept, $J_{HF}{}^2$ = 32 Hz), 114.0, 121.1 (q, $J_{HF}{}^1$ = 289 Hz), 121.2, 127.1, 131.9, 132.7, 136.5; ^{19}F NMR (CDCl$_3$, 188 MHz) δ −77.1; HRMS (ESI-TOF) m/z: [M + H]$^+$ calcd for C$_9$H$_6$N$_3$F$_6$ 270.0466, found 270.0474.

Ethyl Benzo[*e*][1,2,4]triazine-3-carboxylate (1h).[61] Following a general literature procedure,[35] to a stirred mixture of iron (7.80 g, 139.4 mmol), H$_2$O (43 mL), and conc. HCl (36.8 mL) was added dropwise a solution of amidrazone **4** (8.84 g, 36.9 mmol) in a mixture of CH$_3$COOH (178 mL) and conc. HCl (18.5 mL). The resulting mixture was stirred overnight at rt. The reaction mixture was portioned between ethyl acetate (100 mL) and H$_2$O (100 mL). The layers were separated, and the aqueous phase was extracted with ethyl acetate (3 × 50 mL). The combined organic extract was washed with brine and dried (MgSO$_4$). After evaporation of solvent, the residue was purified by flash chromatography (SiO$_2$; petroleum ether/ethyl acetate, 1:1) giving 2.06 g (29% yield) of ester **1h** as a yellow solid: mp 77−79 °C (ref[61] mp (EtOH) 93 °C); ^1H NMR (CDCl$_3$, 600 MHz) δ 1.52 (t, J = 7.1 Hz, 3H), 4.66 (q, J = 7.1 Hz, 2H), 8.02 (t, J = 8.2 Hz, 1H), 8.09 (ddd, J_1 = 1.2 Hz, J_2 = 7.0 Hz, J_3 = 8.2 Hz, 1H), 8.26 (d, J = 8.5 Hz, 1H), 8.64 (d, J = 8.5 Hz, 1H); $^{13}C\{^1H\}$ NMR (CDCl$_3$, 150 MHz) δ 14.4, 63.4, 129.8, 129.9, 133.0, 136.6, 140.5, 148.0, 152.6, 163.1; IR ν 1737 (CO), 1252, 1066, 785 cm^{-1}. Anal. Calcd for C$_{10}$H$_9$N$_3$O$_2$: C, 59.11; H, 4.46; N, 20.68. Found: C, 59.31; H, 4.45; N, 20.82.

Benzo[*e*][1,2,4]triazine-3-carbonitrile (1i). To a solution of 3-chlorobenzo[*e*][1,2,4]triazine (**1c**, 0.050 g, 0.321 mmol) in dry MeCN (2 mL) was added [Et$_4$N]$^+$CN$^-$ (0.052 g, 0.333 mmol). The resulting mixture was stirred at rt for 20 min and solvent was evaporated. The residue was purified by column chromatography (SiO$_2$; hexane/AcOEt, 20:1) giving 0.049 g (98% yield; 95−98% in several runs) of nitrile **1i** as a yellow solid: mp (*n*-heptane) 96−97 °C; ^1H NMR (CDCl$_3$, 500 MHz) δ 8.12−8.15 (m, 1H), 8.20−8.21 (m, 2H), 8.68 (d, J = 8.5 Hz, 1H); $^{13}C\{^1H\}$ NMR (CDCl$_3$, 125 MHz) δ 115.2, 129.2, 130.1, 134.3, 137.8, 140.1, 142.4, 147.3; UV−vis (CH$_2$Cl$_2$), λ_{max}(log ε) 249 (4.26), 320 (3.17), 431 (2.27) nm. Anal. Calcd for C$_8$H$_4$N$_4$: C, 61.54; H, 2.58; N, 35.88. Found: C, 61.52; H, 2.51; N, 35.69.

Diethyl 2-(Benzo[*e*][1,2,4]triazin-3-yl)malonate (1j). Following a similar procedure,[65] to the stirred solution of NaH (0.045 g, 1.2 mmol) in dry DMF (0.5 mL) under nitrogen atmosphere at 0 °C was added dropwise a solution of diethyl malonate (0.17 mL, 1.2 mmol) in dry DMF (1 mL). The resulting mixture was stirred at rt for 2 h, followed by addition of 3-chlorobenzo[*e*][1,2,4]triazine (**1c**, 0.093 g, 0.56 mmol) in DMF (1 mL). The reaction mixture was stirred at 100 °C (oil bath) for 1 h until TLC showed absence of the starting **1c**. The reaction mixture was cooled, quenched with sat. ammonium chloride solution, and then extracted with AcOEt (3 × 5 mL). The combined organic layers were washed with water and brine and dried (Na$_2$SO$_4$). After evaporation of the solvent, the crude product was purified by column chromatography (SiO$_2$; petroleum ether/AcOEt, 6:1) giving 0.160 g (99% yield) of malonate **1j** as a yellow oil: ^1H NMR (CDCl$_3$, 500 MHz) δ 1.30 (t, J = 7.2 Hz, 3H), 4.33 (q, J = 7.2 Hz, 2H), 5.59 (s, 1H), 7.91 (ddd, J_1 = 1.2 Hz, J_2 = 6.8 Hz, J_3 = 8.3 Hz, 1H), 8.01 (ddd, J_1 = 1.3 Hz, J_2 = 6.8 Hz, J_3 = 8.3 Hz, 1H), 8.08 (d, J = 8.5 Hz, 1H), 8.56 (d, J = 8.5 Hz, 1H); $^{13}C\{^1H\}$ NMR (CDCl$_3$, 125 MHz) δ 14.1, 60.5, 62.5, 129.1, 129.7, 131.4, 136.1, 140.9, 146.6, 159.3, 166.3; IR ν 1737 (CO), 1216, 757 cm^{-1}; HRMS (ESI-TOF) m/z: [M + H]$^+$ calcd for C$_{14}$H$_{16}$N$_3$O$_4$ 290.1141, found 290.1152.

3-Phenylaminobenzo[*e*][1,2,4]triazine (1k).[24] *Method A.* To a solution of 3-chlorobenzo[*e*][1,2,4]triazine (**1c**, 0.050 g, 0.303 mmol) in absolute ethanol (1.5 mL), aniline (0.056 mL, 0.606 mmol) was added dropwise. The resulting mixture was stirred overnight at rt, then concentrated in vacuo. The residue was treated with water and extracted with CH$_2$Cl$_2$. The combined organic layers were dried (Na$_2$SO$_4$) and the solvent was evaporated. The crude product was purified by recrystallization from *n*-heptane giving 0.057 g (85% yield) of amine **1k** as an orange solid.

Method B. According to a general method,[72] to a solution of 3-iodobenzo[*e*][1,2,4]triazine (**1d**, 0.200 g, 0.778 mmol), aniline (0.14 mL, 1.56 mmol), and CsF (0.237 g, 1.56 mmol) in DMSO (5 mL),

CuI (0.015 g, 0.078 mmol) was added. The resulting mixture was stirred overnight at 60 °C (oil bath), diluted with AcOEt (20 mL), and washed with water. The organic layer was dried (Na$_2$SO$_4$), solvent was evaporated, and the crude product was purified by column chromatography (SiO$_2$; hexane/AcOEt, 9:1) giving 0.112 g (65% yield) of amine **1k** as an orange solid: mp (*n*-heptane) 198−200 °C (lit.[24] mp (EtOH) 197 °C); ^1H NMR (CDCl$_3$, 500 MHz) δ 7.14 (t, J = 7.4 Hz, 1H), 7.43 (t, J = 7.5 Hz, 2H), 7.54 (ddd, J_1 = 1.5 Hz, J_2 = 6.6 Hz, J_3 = 8.2 Hz, 1H) 7.78 (d, J = 7.7 Hz, 1H) 7.82 (ddd, J_1 = 1.2 Hz, J_2 = 6.7 Hz, J_3 = 8.5 Hz, 1H), 7.92 (d, J = 8.7 Hz, 2H), 8.34 (d, J = 8.4 Hz, 1H), 8.47 (bs, 1H); $^{13}C\{^1H\}$ NMR (CDCl$_3$, 125 MHz) δ 119.2, 123.5, 126.3, 127.2 129.2, 130.0, 136.0, 138.8, 141.3; IR ν 3442, 3256 (NH), 1557 (C=N) cm^{-1}; EI-MS m/z 222 (40 [M]$^+$), 194 (100 [M]$^+$−N$_2$). Anal. Calcd for C$_{13}$H$_{10}$N$_4$: C, 70.26; H, 4.54; N, 25.21. Found: C, 70.03; H, 4.81; N, 25.10.

3-(Morpholin-4-yl)benzo[*e*][1,2,4]triazine (1l).[48] To a solution of 3-chlorobenzo[*e*][1,2,4]triazine (**1c**, 0.100 g, 0.61 mmol) in absolute ethanol (3 mL), morpholine (0.1 mL, 1.2 mmol) was added dropwise. The resulting mixture was stirred for 2 h at rt, then concentrated in vacuo. The residue was treated with water and extracted with CH$_2$Cl$_2$. The combined organic layers were dried (Na$_2$SO$_4$) and the solvent was evaporated. The crude product was purified by recrystallization from *n*-heptane giving 0.117 g (89% yield) of amine **1l** as a yellow solid: mp (*n*-heptane) 123−125 °C (lit.[48] mp 125 °C, cyclohexane); ^1H NMR (CDCl$_3$, 500 MHz) δ 3.86 (t, J = 5.1 Hz, 4H), 4.09 (t, J = 4.4 Hz, 4H), 7.42 (ddd, J_1 = 1.1 Hz, J_2 = 6.8 Hz, J_3 = 8.1 Hz, 1H), 7.58 (d, J = 8.2 Hz, 1H), 7.71 (ddd, J_1 = 1.4 Hz, J_2 = 6.8 Hz, J_3 = 8.4 Hz, 1H), 8.24 (dd, J_1 = 0.8 Hz, J_2 = 8.4 Hz, 1H); $^{13}C\{^1H\}$ NMR (CDCl$_3$, 125 MHz,) δ 44.3 (2C), 67.0 (2C), 125.4, 126.7, 129.9, 135.7, 142.4, 142.8, 158.7; UV−vis (CH$_2$Cl$_2$), λ_{max}(log ε) 254 (4.31), 278 (3.72), 304 (3.22), 416 (3.28) nm; EI-MS m/z 216 (45 [M]$^+$), 188 (50 [M]$^+$ − N$_2$), 131 (100 [M]$^+$ − C$_4$H$_8$NO). Anal. Calcd for C$_{11}$H$_{12}$N$_4$O: C, 61.10; H, 5.59; N, 25.91. Found: C, 61.12; H, 5.67; N, 25.85.

3-Ethoxybenzo[*e*][1,2,4]triazine (1m).[45] A solution of NaOEt [prepared by dissolving Na (8.3 mg) in absolute ethanol (3.6 mL)] was added to a solution of 3-chlorobenzo[*e*][1,2,4]triazine (**1c**, 0.060 g, 0.4 mmol) in absolute ethanol (1.2 mL). The resulting mixture was refluxed (oil bath) for 0.5 h. The precipitate was filtered off and the filtrate was concentrated in vacuo. The residue was neutralized with 3 N HCl and extracted with CH$_2$Cl$_2$. Combined organic layers were dried (Na$_2$SO$_4$), solvent was evaporated, and the resulting crude product was recrystallized (*n*-heptane) giving 0.060 g (95% yield) of ether **1m** as a yellow solid: mp (*n*-heptane) 83−85 °C (lit.[45] mp (benzene) 74−75 °C); ^1H NMR (CDCl$_3$, 500 MHz,) δ 1.55 (t, J = 7.1 Hz, 3H), 4.65 (q, J = 7.1 Hz, 2H), 7.65 (ddd, J_1 = 1.4 Hz, J_2 = 6.8 Hz, J_3 = 8.3 Hz, 1H), 7.82 (dd, J_1 = 1.1 Hz, J_2 = 8.5 Hz, 1H), 7.87 (ddd, J_1 = 1.4 Hz, J_2 = 6.7 Hz, J_3 = 8.5 Hz, 1H), 8.44 (d, J = 8.5 Hz, 1H); $^{13}C\{^1H\}$ NMR (CDCl$_3$, 125 MHz) δ 14.5, 64.4, 127.3, 127.7, 129.9, 136.1, 142.0, 144.8, 162.4; UV−vis (CH$_2$Cl$_2$), λ_{max}(log ε) 295 (3.62), 354 (3.47), 429 (2.55) nm; EI-MS m/z 175 (30 [M]$^+$), 147 (40 [M]$^+$ − N$_2$), 119 (110). Anal. Calcd for C$_9$H$_9$N$_3$O: C, 61.70; H, 5.18; N, 23.99. Found: C, 61.73; H, 5.22; N, 23.95.

Diethyl Benzo[*e*][1,2,4]triazin-3-ylphosphonate (1n). *Method A.* Following a general procedure,[47] a mixture of 3-chlorobenzo[*e*][1,2,4]triazine (**1c**, 0.02 g, 0.121 mmol) and triethyl phosphite (0.07 mL, 0.42 mmol) was heated at 100 °C (oil bath) for 6 h until **1c** was no longer detected by TLC. The reaction mixture was separated by column chromatography (SiO$_2$; petroleum ether/AcOEt, 1:10) giving 6.4 mg (20% yield) of phosphonate **1n** as a yellow oil.

Method B. To a mixture of 3-iodobenzo[*e*][1,2,4]triazine (**1d**, 0.05 g, 0.195 mmol), CuI (3.8 mg, 0.0195 mmol), and Et$_3$N (0.001 mL, 0.0195 mmol) in toluene (1 mL) was added diethyl phosphite (0.031 mL, 0.234 mmol). The resulting mixture was stirred at 60 °C (oil bath) for 20 h. The solvent was evaporated, and the crude product was purified by column chromatography (SiO$_2$; petroleum ether/AcOEt, 1:10) giving 0.041 mg (79% yield) of phosphonate **1n** as a yellow oil: ^1H NMR (CDCl$_3$, 500 MHz) δ 1.44 (t, J = 7.1 Hz, 6H), 4.46−4.50 (m, 4H), 8.01 (ddd, J_1 = 0.9 Hz, J_2 = 7.0 Hz, J_3 = 8.1 Hz, 1H), 8.08 (ddd, J_1 = 1.4 Hz, J_2 = 6.9 Hz, J_3 = 8.3 Hz, 1H), 8.22 (d, J = 8.5 Hz, 1H), 8.59

The Journal of Organic Chemistry　　　　　　　　　　　　　　　　　　　　　Article

(d, J = 8.5 Hz, 1H); $^{13}C\{^1H\}$ NMR (CDCl$_3$, 125 MHz) δ 16.6 (d, J = 6.2 Hz, 2C), 64,5 (d, J = 5.8 Hz, 2C), 129.6, 129.8, 132.9, 136.5, 140.1 (d, J = 17.2 Hz), 147.5, 159.3 (d, J = 262 Hz); ^{31}P NMR (CDCl$_3$, 81 MHz) δ 4.79; HRMS (ESI-TOF) m/z: [M + H]$^+$ calcd for C$_{11}$H$_{15}$N$_3$O$_3$P 268.0851, found 268.0856.

3-(*tert*-Butylthio)benzo[*e*][1,2,4]triazine (1o). Following a general procedure,[85] to a suspension of NaH (0.029 g, 1.2 mmol) in dry DMF (2 mL), 2-methylpropane-2-thiol (0.054 g, 0.6 mmol) was added dropwise. The mixture was stirred for 30 min at rt, then 3-chlorobenzo[*e*][1,2,4]triazine (1c, 0.100 g, 0.6 mmol) was added, and the resulting mixture was stirred for 2 h at rt. The mixture was treated with water, and the residue was extracted with ethyl acetate. The combined organic layers were dried (Na$_2$SO$_4$) and the solvent was evaporated. The crude product was purified by recrystallization from *n*-heptane giving 0.126 mg (95% yield) of sulfide 1o as a yellow solid: mp (*n*-heptane) 67−68 °C; ^{1}H NMR (CDCl$_3$, 500 MHz,) δ 1.73 (s, 9H), 7.70 (ddd, J_1 = 1.9 Hz, J_2 = 6.2 Hz, J_3 = 8.3 Hz, 1H), 7.84−7.90 (m, 2H), 8.39 (d, J = 8.3 Hz, 1H); $^{13}C\{^1H\}$ NMR (CDCl$_3$, 125 MHz) δ 30.1 (3C), 48.5, 127.7, 129.0, 129.9, 135.8, 140.9, 144.8, 170.8; EI-MS m/z 191 (25 [M]$^+$ − N$_2$), 135 (68), 57 (100). Anal. Calcd for C$_{11}$H$_{13}$N$_3$S: C, 60.25; H, 5.98; N, 19.16. Found: C, 60.31; H, 6.02; N, 19.19.

3-Phenylbenzo[*e*][1,2,4]triazine (1p).[34] To a solution of 3-iodobenzo[*e*][1,2,4]triazine (1d, 0.08 g, 0.31 mmol) in degassed toluene (2 mL) were added successively phenylboronic acid (0.091 g, 0.75 mmol), Pd(OAc)$_2$ (0.004 g, 0.016 mmol), K$_2$CO$_3$ (0.066 g, 0.62 mmol), and water (0.01 mL). The reaction mixture was refluxed (oil bath) overnight, and the progress of the reaction was controlled by TLC. When 1d was no longer detected by TLC, the mixture was filtered through Celite and concentrated in vacuo. The crude product was purified by column chromatography (SiO$_2$; hexane/AcOEt, 20:1) giving 0.053 g (82% yield) of 3-phenylbenzo[*e*][1,2,4]-triazine (1p) as a yellow solid: 122−123 °C (lit.[34] mp 120−124 °C); ^{1}H NMR (CDCl$_3$, 500 MHz) δ 7.58−7.61 (m, 3H), 7.85 (ddd, J_1 = 1.3 Hz, J_2 = 6.9 Hz, J_3 = 8.3 Hz, 1H), 7.99 (ddd, J_1 = 1.4 Hz, J_2 = 6.8 Hz, J_3 = 8.3 Hz, 1H), 8.11 (dd, J_1 = 0.5 Hz, J_2 = 8.5 Hz, 1H), 8.55 (dd, J_1 = 0.7 Hz, J_2 = 8.5 Hz, 1H), 8.76−8.78 (m, 2H); $^{13}C\{^1H\}$ NMR (CDCl$_3$, 125 MHz) δ 128.9, 129.1, 129.3, 129.7, 130.4, 131.6, 135.7, 135.8, 141.3, 146.6, 160.0; UV−vis (CH$_2$Cl$_2$), λ_{max}(log ε) 259 (4.47), 272 (4.44), 3.52 (3.65), 454 (2.52). Anal. Calcd for C$_{13}$H$_9$N$_3$: C, 75.35; H, 4.38; N, 20.28. Found: C, 75.14, H, 4.42; N, 20.25.

3-(Thiophen-2-yl)benzo[*e*][1,2,4]triazine (1r).[36] Following the procedure for preparation of 1p, the thiophene derivative 1r was obtained in 69% yield from 0.101 g of 3-iodobenzo[*e*][1,2,4]triazine (1d) as a yellow solid: mp (*n*-heptane) 133−135 °C; ^{1}H NMR (CDCl$_3$, 500 MHz) δ 7.25−7.26 (m, 1H), 7.62 (dd, J_1 = 1.2 Hz, J_2 = 5.0 Hz, 1H), 7.79 (ddd, J_1 = 1.2 Hz, J_2 = 6.8 Hz, J_3 = 8.2 Hz, 1H), 7.94 (ddd, J_1 = 1.4 Hz, J_2 = 6.8 Hz, J_3 = 8.4 Hz, 1H), 8.01 (d, J = 8.5 Hz, 1H), 8.36 (dd, J_1 = 1.1 Hz, J_2 = 3.7 Hz, 1H), 8.48 (dd, J_1 = 0.6 Hz, J_2 = 8.4 Hz, 1H); $^{13}C\{^1H\}$ NMR (CDCl$_3$, 125 MHz) δ 128.8 (2C), 129.2 (2C), 130.8, 131.5, 135.9, 140.9, 141.1, 146.2, 157.5; UV−vis (CH$_2$Cl$_2$), λ_{max}(log ε) 277 (4.26), 301 (4.33), 378 (3.73), 4.53 (2.56); EI-MS m/z 213 (10 [M]$^+$), 185 (100 [M]$^+$ − N$_2$). Anal. Calcd for C$_{11}$H$_7$N$_3$S: C, 61.95; H, 3.31; N, 19.70. Found: C, 61.74; H, 3.47; N, 19.52.

3-(Ferrocenyl)benzo[*e*][1,2,4]triazine (1s). To a solution of 3-iodobenzo[*e*][1,2,4]triazine (1d, 0.110 g, 0.428 mmol) in degassed toluene (3 mL) were added successively ferroceneboronic acid (0.148 g, 0.642 mmol), K$_3$PO$_4$ (0.272 g, 1.28 mmol), and PdCl$_2$(dppf) (0.016 g, 0.0214 mmol). The reaction mixture was refluxed (oil bath) for 8 h, with an additional portion of ferroceneboronic acid (0.148 mmol, 0.642 mmol), and the reaction mixture was refluxed overnight. The mixture was filtered through Celite and concentrated in vacuo. The crude product was purified by column chromatography (SiO$_2$; petroleum ether) giving 0.065 g of inseparable mixture of starting 1d and product 1s. The mixture was dissolved in degassed toluene (2 mL), and ferroceneboronic acid (0.074 g, 0.321 mmol), K$_3$PO$_4$ (0.136 g, 0.64 mmol), and PdCl$_2$(dppf) (0.008 g, 0.0107 mmol) were added successively. The reaction mixture was refluxed (oil bath) overnight, filtered through Celite, and concentrated in vacuo. The residue was

separated by column chromatography (SiO$_2$; petroleum ether) giving 0.036 g (27% yield) of 3-(ferrocenyl)benzo[*e*][1,2,4]triazine (1s) as a dark red solid: mp (CHCl$_3$) 177−179 °C; ^{1}H NMR (CDCl$_3$, 500 MHz) δ 4.10 (s, 5H), 4.64 (t, J = 1.8 Hz, 2H), 5.45 (t, J = 1.8 Hz, 2H), 7.75 (ddd, J_1 = 1.3 Hz, J_2 = 6.8 Hz, J_3 = 8.3 Hz, 1H), 7.89 (ddd, J_1 = 1.3 Hz, J_2 = 6.4 Hz, J_3 = 7.9 Hz, 1H), 7.96 (d, J = 8.0 Hz, 1H), 8.43 (dd, J_1 = 0.7 Hz, J_2 = 8.4 Hz, 1H); $^{13}C\{^1H\}$ NMR (CDCl$_3$, 125 MHz) δ 69.7 (2C$_{Cp}$), 70.1 (5C$_{Cp}$), 71.9 (2C$_{Cp}$), 79.8, 128.5, 129.1, 129.9, 135.4, 141.5, 145.5, 166.0; HRMS (ESI-TOF) m/z: [M + H]$^+$ calcd for C$_{17}$H$_{14}$N$_3$Fe 316.0537, found 316.0543. Anal. Calcd for C$_{17}$H$_{13}$N$_3$Fe: C, 64.79; H, 4.16; N, 13.33. Found: C, 64.72; H, 4.11; N, 13.14.

3-(Phenylethynyl)benzo[*e*][1,2,4]triazine (1t). To a stirred solution of 3-iodobenzo[*e*][1,2,4]triazine (1d, 0.102 g, 0.4 mmol), in dry THF (3 mL) under a nitrogen atmosphere, Pd(PPh$_3$)$_4$ (9.2 mg, 2 mol %) was added. After 5 min, Et$_3$N (0.3 mL) and CuI (3.1 mg, 0.016 mmol) were added and the mixture was stirred for 5 min. Then, phenylacetylene (0.04 mL, 0.4 mmol) was added dropwise and the resulting mixture was stirred for additional 10 min. The solution was filtered through Celite and concentrated in vacuo. The crude product was purified by column chromatography (Al$_2$O$_3$; hexane/AcOEt, 20:1) giving 0.071 g (79% yield) of acetylene 1t as a yellow solid: mp (*n*-heptane) 125−127 °C; ^{1}H NMR (CDCl$_3$, 500 MHz) δ 7.41−7.48 (m, 3H), 7.78 (dt, J_1 = 2.0 Hz, J_2 = 8.2 Hz, 2H), 7.91 (ddd, J_1 = 1.3 Hz, J_2 = 6.8 Hz, J_3 = 8.2 Hz, 1H), 8.02 (ddd, J_1 = 1.3 Hz, J_2 = 6.8 Hz, J_3 = 8.4 Hz, 1H), 8.08 (d, J = 8.1 Hz, 1H), 8.56 (d, J = 8.4 Hz, 1H); $^{13}C\{^1H\}$ NMR (CDCl$_3$, 500 MHz) δ 86.9, 92.3, 121.1, 128.7 (2C), 129.9, 130.3, 131.4, 132.9, 136.3, 140.5, 145.5, 150.4; UV−vis (CH$_2$Cl$_2$), λ_{max}(log ε) 263 (4.40), 274 (4.42), 301 (4.38), 353 (3.86), 439 (2.66) nm. Anal. Calcd for C$_{15}$H$_9$N$_3$: C, 77.91; H, 3.92; N, 18.17. Found: C, 77.94; H, 4.05; N, 17.92.

3-Pentylbenzo[*e*][1,2,4]triazine (1u). A suspension of dry ZnCl$_2$ (0.092 g, 0.68 mmol) in dry THF (2 mL) at 0 °C was treated with a 2 M solution of pentylmagnesium bromide in diethyl ether (0.34 mL, 0.68 mmol). The reaction mixture was stirred at 0 °C for 15 min and then at rt for 20 min. PEPPSI-IPr (11.6 mg, 0.017 mmol) was added, and the reaction mixture was stirred for 10 min, followed by addition of iodide 2d (50.0 mg, 0.17 mmol, obtained according to ref [51]). The reaction mixture was stirred at 0 °C for 20 min, filtered through Celite, and concentrated in vacuo. The residue was purified by column chromatography (SiO$_2$; hexane/AcOEt, 10:1) giving a mixture of 2u and 1u as a brown oil. The oil was dissolved in EtOH/AcOEt (1:1, 10 mL), Pd/C (11 mg, 10 mol %) was added, and the resulting mixture was stirred overnight at rt in the atmosphere of H$_2$ (balloon). The resulting yellow solution was filtered through Celite, and the solvent was evaporated giving 20.2 mg (58% yield) of product 1u as a brown oil, which was short-path-distilled (85 °C/225 Torr): ^{1}H NMR (CDCl$_3$, 500 MHz,) δ 0.91 (t, J = 7.2 Hz, 3H), 1.38−1.46 (m, 4H), 2.01 (quint, J = 7.7 Hz, 2H), 3.39 (t, J = 7.8 Hz, 2H), 7.82 (ddd, J_1 = 1.3 Hz, J_2 = 6.8 Hz, J_3 = 8.3 Hz, 1H), 7.95 (ddd, J_1 = 1.3 Hz, J_2 = 6.7 Hz, J_3 = 8.1 Hz, 1H), 8.00 (d, J = 8.5 Hz, 1H), 8.50 (d, J = 8.5 Hz, 1H); $^{13}C\{^1H\}$ NMR (CDCl$_3$, 125 MHz) δ 14.1, 22.6, 28.8, 31.7, 37.9, 128.6, 129.7, 130.0, 135.5, 141.0, 146.3, 166.8; HRMS (ESI-TOF) m/z: [M + H]$^+$ calcd for C$_{12}$H$_{16}$N$_3$ 202.1344, found 202.1349.

Benzo[*e*][1,2,4]triazine-3-carboxamide (1w). *Method A.* To nitrile 1i (0.050 g, 0.32 mmol) conc. HCl (1 mL) was added, and resulting mixture was stirred at rt for 72 h. The mixture was evaporated giving 55.8 mg (100% yield) of amide 1w as a yellow solid.

Method B. To a suspension of acid 1f (0.150 g, 0.857 mmol) in CH$_2$Cl$_2$ (3 mL) was added DMF (cat.) and oxalyl chloride (0.22 mL, 2.57 mmol). The reaction mixture was stirred at rt for 1 h, and the solvent was evaporated to remove volatiles. The solid residue was dissolved in CH$_2$Cl$_2$ (3 mL) and poured into conc. aq NH$_4$OH (10 mL). The precipitate was filtered giving 0.149 g (99% yield) of amide 1w: mp (MeOH) 248−250 °C; ^{1}H NMR (DMSO-d_6, 500 MHz) δ 8.13−8.16 (m, 1H), 8.20 (bs, 1H), 8.24−8.26 (m, 2H), 8.65 (dd, J_1 = 1.9 Hz, J_2 = 8.4 Hz, 1H), 8.72 (bs, 1H); $^{13}C\{^1H\}$ NMR (DMSO-d_6, 125 MHz) δ 129.2, 133.1, 137.2, 140.0, 147.2, 153.9, 163.6; HRMS (ESI-TOF) m/z: [M + H]$^+$ calcd for C$_8$H$_7$N$_4$O 175.0620, found 175.0619. Anal. Calcd. for C$_8$H$_6$N$_4$O: C, 55.17; H, 3.47; N, 32.17. Found: C, 55.24; H, 3.59; N, 32.14.

Attempted Preparation of Benzo[*e*][1,2,4]triazine-3-carboxamide (1w). *3-Hydroxybenzo[*e*][1,2,4]triazine (1e).* Nitrile **1i** (50 mg, 0.32 mmol) was stirred with NaOH (0.026 g, 0.65 mmol) in water (0.5 mL) at 55 °C (oil bath) for 2 h. Evaporation of the solvent gave a mixture of the expected amide **1w** and 3-hydroxy derivative **1e** in a ratio of 1:7 (based on ^{1}H NMR) as a yellow solid: ^{1}H NMR (DMSO-d_6, 500 MHz) major signals δ 7.01 (t, J = 7.3 Hz, 1H), 7.16 (d, J = 8.3 Hz, 1H), 7.42 (t, J = 7.4 Hz, 1H), 7.88 (d, J = 8.1 Hz, 1H); ^{13}C{^{1}H} NMR (DMDO-d_6, 125 MHz) major signals δ 119.8, 125.4, 128.8, 132.7, 139.2, 145.6, 165.7; IR ν 3059 (br) and 1577 (br) cm^{-1}; HRMS (ESI-TOF) *m/z*: [M + H]$^+$ calcd for C$_7$H$_6$N$_3$O 148.0511, found 148.0515.

3-(*N,N*-Dibenzoylamino)benzo[*e*][1,2,4]triazine (1x). A solution of amine **1b** (0.079 g, 0.541 mmol) and Et$_3$N (0.11 mL, 0.812 mmol) in dry CH$_2$Cl$_2$ (3 mL) was treated with benzoyl chloride (0.10 mL, 0.812 mmol). The reaction mixture was stirred overnight at rt, diluted with CH$_2$Cl$_2$, and washed with H$_2$O. The organic layer was dried (Na$_2$SO$_4$), and the solvent was evaporated. The residue was purified by column chromatography (SiO$_2$; hexane/AcOEt, 4:1) giving 0.090 g (75% yield) of amide **1x** as a yellow solid: mp (MeCN) 202−203 °C; ^{1}H NMR (CDCl$_3$, 500 MHz) δ 7.37 (t, J = 7.5 Hz, 4H), 7.48 (t, J = 8.6 Hz, 2H), 7.82−7.85 (m, 3H), 7.91 (d, J = 0.7 Hz, J_2 = 8.5 Hz, 1H), 7.97 (ddd, J_1 = 1.3 Hz, J_2 = 6.6 Hz, J_3 = 8.4 Hz, 1H), 8.50 (d, J = 8.4 Hz, 1H); ^{13}C{^{1}H} NMR (CDCl$_3$, 125 MHz) δ 128.5, 128.9, 129.6, 129.7, 131.2, 133.2, 134.1, 136.6, 141.6, 145.5, 157.9, 172.5; IR ν 1699 (CO) cm^{-1}. Anal. Calcd for C$_{21}$H$_{14}$N$_4$O$_2$: C, 71.18; H, 3.98; N, 15.81. Found: C, 71.07; H, 3.95; N, 15.83.

Ethyl 2-(Benzo[*e*][1,2,4]triazin-3-yl)acetate (1y).[33] Following an analogous procedure,[65] to the stirred solution of malonate **1j** (0.116 g, 0.4 mmol) in DMSO (0.3 mL) was added a solution of NaCl (0.047 g, 0.8 mmol) in water (0.3 mL). The resulting mixture was heated overnight at 180 °C (oil bath). Then, the reaction was cooled to rt, quenched with water, and extracted with ethyl acetate (3 × 5 mL). The combined organic layers were washed with water and brine and dried (Na$_2$SO$_4$). After evaporation of solvent, the crude product was purified by column chromatography (SiO$_2$; petroleum ether/CH$_2$Cl$_2$, 7:3) giving 0.070 g (89% yield) of acetate **1y** as a dark yellow oil; ^{1}H NMR (CDCl$_3$, 500 MHz) δ 1.30 (t, J = 7.2 Hz, 6H), 4.33 (q, J = 7.2 Hz, 4H), 4.46 (s, 1H), 7.88 (ddd, J_1 = 1.4 Hz, J_2 = 6.8 Hz, J_3 = 8.2 Hz, 1H), 8.05 (dd, J_1 = 0.6 Hz, J_2 = 8.5 Hz, 1H), 8.54 (dd, J_1 = 0.5 Hz, J_2 = 8.4 Hz, 1H); ^{13}C{^{1}H} NMR (CDCl$_3$, 125 MHz) δ 14.3, 43.9, 61.7, 128.8, 129.7, 130.9, 135.9, 141.0, 146.5, 160.1, 169.4; IR ν 1737 (CO) cm^{-1}; HRMS (ESI-TOF) *m/z*: [M + H]$^+$ calcd for C$_{11}$H$_{12}$N$_3$O$_2$ 218.0930, found 218.0933.

3-Aminobenzo[*e*][1,2,4]triazine-1-oxide (2b).[26] Following a literature procedure,[26] a mixture of 2-nitroaniline (20.0 g, 0.14 mol) and cyanamide (20.0 g, 0.47 mol) was melted at 100 °C (oil bath), cooled to rt, and conc. HCl (50 mL) was slowly added to the reaction (Caution: the reaction is strongly exothermic). The mixture was cooled to rt, and H$_2$O (50 mL) and NaOH (40 g) were carefully added. The mixture was stirred at 100 °C (oil bath) for 0.5 h, cooled to rt, and diluted with water (100 mL). The resulting yellow solid was filtered, washed with H$_2$O, and dried under vacuum to give 19.80 g (82% yield; 82−85% in several runs) of oxide **2b**: mp (EtOH) 277−278 °C (lit.[26] mp (EtOH) 284−287 °C); ^{1}H NMR (DMSO-d_6, 600 MHz) δ 7.30−7.33 (m, 3H), 7.52 (d, J = 8.4 Hz, 1H), 7.76 (t, J = 7.5 Hz, 1H), 8.12 (d, J = 8.5 Hz, 1H); ^{13}C{^{1}H} NMR (DMSO-d_6, 150 MHz) δ 119.8, 124.6, 125.8, 129.9, 135.6, 148.7, 160.2. Anal. Calcd for C$_7$H$_6$N$_4$O: C, 51.85; H, 3.73; N, 34.55. Found: C, 51.85; H, 3.79; N, 34.60.

3-Chlorobenzo[*e*][1,2,4]triazine-1-oxide (2c).[26] Following a literature procedure,[26] a solution of 3-hydroxybenzo[*e*][1,2,4]triazine-1-oxide (**2e**, 15.50 g) in POCl$_3$ (120 mL) was stirred at reflux (oil bath) for 2 h. The reaction was concentrated, poured onto ice, diluted with H$_2$O (150 mL), and then extracted with CHCl$_3$ (3 × 100 mL). The combined organic fraction was dried (Na$_2$SO$_4$) and the solvent was evaporated giving 9.80 g (57% yield) of chloride **2c**: mp (hexane/CH$_2$Cl$_2$) 116−117 °C (lit.[10] mp (CH$_2$Cl$_2$) 119−119.5 °C); ^{1}H NMR (CDCl$_3$, 600 MHz) δ 7.76 (ddd, J = 2.0, 5.6, 8.4 Hz, 1H), 7.97−8.01 (m, 2H), 8.39 (d, J = 8.6 Hz, 1H); ^{13}C{^{1}H} NMR (CDCl$_3$, 150 MHz)

δ 120.4, 128.6, 131.1, 133.9, 136.9, 147.4, 157.1. Anal. Calcd for C$_7$H$_4$N$_3$OCl: C, 46.30; H, 2.22; N, 23.14. Found: C, 46.30; H, 2.24; N, 23.38.

3-Hydroxybenzo[*e*][1,2,4]triazine-1-oxide (2e).[26] Following a literature procedure,[26] a solution of NaNO$_2$ (32.9 g) in H$_2$O (45 mL) was added dropwise for 1 h to a stirred solution of 3-aminobenzo-[*e*][1,2,4]triazine-1-oxide (**2b**, 16.9 g, 0.1 mol) in H$_2$O (180 mL) and conc. H$_2$SO$_4$ (66 mL) at 0 °C. The reaction mixture was stirred at this temperature for 2 h and then overnight at rt. The precipitate was filtered, washed with H$_2$O, and dried under vacuum giving 16.10 (95% yield) of 3-hydroxy derivative **2e**: mp (MeOH) 239−240 °C dec. (lit[26] mp (MeOH) 241−244 °C); ^{1}H NMR (DMSO-d_6, 600 MHz) δ 7.32 (t, J = 7.4 Hz, 1H), 7.35 (d, J = 8.2 Hz, 1H), 7.80 (ddd, J = 1.0, 7.2, 8.2 Hz, 1H), 8.09 (d, J = 8.4 Hz, 1H), 12.53 (s, 1H); ^{13}C{^{1}H} NMR (DMSO-d_6, 150 MHz) δ 116.3, 120.9, 123.8, 129.3, 136.4, 136.6, 152.8. Anal. Calcd for C$_7$H$_5$N$_3$O$_2$: C, 51.54; H, 3.09; N, 25.76. Found: C, 51.55; H, 3.12; N, 25.76.

3-(Trifluoromethyl)benzo[*e*][1,2,4]triazine-1-oxide (2g). Following a general literature procedure,[74] to a mixture of 3-iodobenzo-[*e*][1,2,4]triazine-1-oxide (**2d**, 0.199 g, 0.732 mmol, obtained according to ref [51]), CuI (0.014 mg, 0.073 mmol), 1,10-phenanthroline (0.013 g, 0.073 mmol), and CsF (0.222 g, 1.46 mmol) in dry DMF (2 mL) at 60 °C (oil bath) was added the Ruppert reagent (0.22 mL, 1.46 mmol). The reaction mixture was stirred at this temperature for 1 h in the atmosphere of Ar, then cooled to rt, and quenched with H$_2$O. The mixture was extracted with EtOAc (3 × 20 mL). Combined organic layers were dried (Na$_2$SO$_4$), and the solvent was evaporated. The residue was purified by column chromatography (SiO$_2$; petroleum ether/AcOEt, 10:1) giving 0.050 g (24% yield) of **8** as a yellow solid (first fraction) and 0.011 g (7% yield) of 3-(trifluoromethyl)benzo-[*e*][1,2,4]-triazine-1-oxide (**2g**) as a yellow solid (second fraction): mp 63−65 °C (AcOEt); ^{1}H NMR (CDCl$_3$, 500 MHz) δ 7.92 (ddd, J_1 = 1.2 Hz, J_2 = 7.1 Hz, J_3 = 8.5 Hz, 1H), 8.10 (ddd, J_1 = 1.3 Hz, J_2 = 7.1 Hz, J_3 = 8.4 Hz, 1H), 8.21 (d, J = 8.4 Hz, 1H), 8.53 (dd, J_1 = 0.8 Hz, J_1 = 8.7 Hz 1H); ^{13}C{^{1}H} NMR (CDCl$_3$, 125 MHz) δ 117.7 (q, J_{HF}^1 = 276 Hz), 120.5, 130.2, 133.1, 135.5, 137.0, 146.6, 153.2 (q, J_{HF}^2 = 38 Hz); ^{19}F NMR (CDCl$_3$, 188 MHz) δ −69.4; HRMS (ESI-TOF) *m/z*: [M + H]$^+$ calcd for C$_8$H$_5$N$_3$OF$_3$ 216.0385, found 216.0389.

3,3-Bis(trifluoromethyl)-3,4-dihydro-benzo[*e*][1,2,4]-triazine-1-oxide (8). mp 132−134 °C (MeOH); ^{1}H NMR (CDCl$_3$, 500 MHz) δ 5.11 (s, 1H), 6.86 (dd, J_1 = 1.0 Hz, J_2 = 8.2 Hz, 1H), 6.96 (ddd, J_1 = 1.2 Hz, J_2 = 7.5 Hz, J_3 = 8.5 Hz, 1H), 7.46 (ddd, J_1 = 1.4 Hz, J_2 = 7.5 Hz, J_3 = 8.8 Hz, 1H), 8.02 (d, J = 8.4 Hz, 1H); ^{13}C{^{1}H} NMR (CDCl$_3$, 125 MHz) δ 77.5 (sept, J_{HF}^2 = 31 Hz), 114.8, 120.9, 121.3 (q, J_{HF}^1 = 291 Hz), 122.6, 127.7, 136.1, 136.9; ^{19}F NMR (CDCl$_3$, 188 MHz) δ −77.9; HRMS (ESI-TOF) *m/z*: [M + H]$^+$ calcd for C$_9$H$_6$N$_3$OF$_6$ 286.0415, found 286.0412.

Ethyl [(2-Nitrophenyl)hydrazono](chloro)acetate (3).[61] Following a similar literature procedure,[35] to a stirred mixture of *ortho*-nitroaniline (8.0 g, 58 mmol) in MeOH (126 mL) was added conc. HCl (34 mL). The mixture was cooled in an ice−water bath and a solution of NaNO$_2$ (4.4 g, 63.6 mmol) in H$_2$O (24 mL) was added dropwise with stirring over 15 min. The suspension was filtered, and to the clear solution was added ethyl 2-chloroacetoacetate (8.8 mL, 63.7 mmol) at rt. The resulting mixture was stirred at rt for 1.5 h. The suspension was filtered, and the filtered yellow solid was washed with H$_2$O and dried at 50 °C to give 11.36 g (73% yield) of chloro ester **3** as a yellow solid: mp (MeOH) 121−122 °C; ^{1}H NMR (CDCl$_3$, 600 MHz) δ 1.42 (t, J = 7.1 Hz, 3H), 4.41 (q, J = 7.1 Hz, 2H), 7.07 (t, J = 8.4 Hz, 1H), 7.63 (t, J = 8.0 Hz, 1H), 7.94 (d, J = 8.5 Hz, 1H), 8.21 (dd, J_1 = 11 Hz, J_2 = 8.5 Hz, 1H), 11.35 (s, 1H); ^{13}C{^{1}H} NMR (CDCl$_3$, 150 MHz) δ 14.3, 63.4, 117.3, 121.7, 122.0, 126.1, 133.7, 136.4, 139.0, 159.2. Anal. Calcd for C$_{10}$H$_{10}$ClN$_3$O$_4$: C, 44.21; H, 3.71; N, 15.47. Found: C, 44.16; H, 3.67; N, 15.45.

Ethyl[2-(2-nitrophenyl)hydrazine](imino)acetate (4).[61] Following a similar literature procedure,[35] a stirring solution of chloride **3** (10.0 g, 37.2 mmol) in dry THF (200 mL) was saturated with ammonia for 10 min. The mixture was stirred for 4 h and again saturated with ammonia for 20 min. The resulting solution was stirred overnight at rt under argon atmosphere. The reaction mixture was

poured into H_2O (200 mL) and extracted with CH_2Cl_2 (3×100 mL). The combined organic layers were dried ($MgSO_4$), and solvent was evaporated giving 9.24 g (100% yield) of **4** as red crystals: mp (MeOH) 119−121 °C; ^1H NMR ($CDCl_3$, 600 MHz) δ 1.41 (t, $J = 7.1$ Hz, 3H), 4.39 (q, $J = 7.1$ Hz, 2H), 4.99 (bs, 1H), 6.84 (t, $J = 8.2$ Hz, 1H), 7.53 (t, $J = 7.7$ Hz, 1H), 7.85 (d, $J = 8.5$ Hz, 1H), 8.13 (dd, $J_1 = 1.0$ Hz, $J_2 = 8.6$ Hz, 1H), 10.07 (s, 1H); $^{13}C\{^1H\}$ NMR ($CDCl_3$, 150 MHz) δ 14.3, 62.8, 116.9, 118.9, 125.9, 132.2, 136.4, 138.8, 142.4, 161.9. Anal. Calcd for $C_{10}H_{12}N_4O_4$: C, 47.62; H, 4.79; N, 22.21. Found: C, 47.70; H, 4.79; N, 22.20.

ASSOCIATED CONTENT

ⓢ Supporting Information

The Supporting Information is available free of charge on the ACS Publications website at DOI: 10.1021/acs.joc.9b00716.

Additional synthetic details, copies of NMR spectra, UV−vis data analysis, assignment of ^1H NMR chemical shifts and correlation analysis with Hammett constants, XRD data collection details, computation details, results and analysis for geometrical parameters, NMR chemical shifts, and electronic absorption spectra for selected derivatives **1**, archive for DFT calculation output files (PDF)

Crystallographic data (CIF)(CIF)(CIF)(CIF)(CIF)-(CIF)

AUTHOR INFORMATION

Corresponding Author

*E-mail: piotrk@cbmm.lodz.pl.

Author Contributions

The manuscript was written through contributions of all authors, and all authors have given approval to the final version of the manuscript.

Notes

The authors declare no competing financial interest.

ACKNOWLEDGMENTS

REFERENCES

(1) Charushin, V.; Rusinov, V.; Chupakhin, O. 1,2,4-Triazines and their Benzo Derivatives. *Comprehensive Heterocyclic Chemistry III*; Elsevier: 2008; Vol. 9, pp 95−196.

(2) Wolf, F. J.; Pfister, K., 3rd; Wilson, R. M., Jr.; Robinson, C. A. Benzotriazines. I. A New Series of Compounds Having Antimalarial Activity. *J. Am. Chem. Soc.* **1954**, *76*, 3551−3553.

(3) Noronha, G.; Barrett, K.; Cao, J.; Dneprovskaia, E.; Fine, R.; Gong, X.; Gritzen, C.; Hood, J.; Kang, X.; Klebansky, B.; Li, G.; Liao, W.; Lohse, D.; Mak, C. C.; McPherson, A.; Palanki, M. S. S.; Pathak, V. P.; Renick, J.; Soll, R.; Splittgerber, U.; Wrasidlo, W.; Zeng, B.; Zhao, N.; Zhou, Y. Discovery and preliminary structure−activity relationship studies of novel benzotriazine based compounds as Src inhibitors. *Bioorg. Med. Chem. Lett.* **2006**, *16*, 5546−5556.

(4) Noronha, G.; Barrett, K.; Boccia, A.; Brodhag, T.; Cao, J.; Chow, C. P.; Dneprovskaia, E.; Doukas, J.; Fine, R.; Gong, X.; Gritzen, C.; Gu, H.; Hanna, E.; Hood, J. D.; Hu, S.; Kang, X.; Key, J.; Klebansky, B.; Kousba, A.; Li, G.; Lohse, D.; Mak, C. C.; McPherson, A.; Palanki, M. S. S.; Pathak, V. P.; Renick, J.; Shi, F.; Soll, R.; Splittgerber, U.; Stoughton, S.; Tang, P.; Yee, S.; Zeng, B.; Ningning, Z.; Zhu, H. Discovery of [7-(2,6-dichlorophenyl)-5-methylbenzo[1,2,4]triazin-3-yl]-[4-(2-pyrrolidin-1-ylethoxy)phenyl]amine—a potent, orally active Src kinase inhibitor with anti-tumor activity in preclinical assays. *Bioorg. Med. Chem. Lett.* **2007**, *17*, 602−608.

(5) Cao, J.; Fine, R.; Gritzen, C.; Hood, J.; Kang, X.; Klebansky, B.; Lohse, D.; Mak, C. C.; McPherson, A.; Noronha, G.; Palanki, M. S. S.; Pathak, V. P.; Renick, J.; Soll, R.; Zeng, B.; Zhu, H. The design and preliminary structure−activity relationship studies of benzotriazines as potent inhibitors of Abl and Abl-T315I enzymes. *Bioorg. Med. Chem. Lett.* **2007**, *17*, 5812−5818.

(6) Boyle, R. G.; Travers, S. Pharmaceutical Compounds. WO2008015429, 2008.

(7) Lee, J.; Lee, S. H.; Seo, H. J.; Kim, M. J.; Kang, S. Y.; Kim, J.; Lee, S.-H.; Jung, M. E.; Son, E. J.; Song, K.-S.; Kim, M.-S. Novel C-Aryl Glucoside SGL T2 Inhibitors and Pharmaceutical Composition Comprising Same. WO2010147430, 2010.

(8) Zeller, M. N-Sulphonyl and N-Sulphinyl Amino Acid Amides as Microbiocides. WO9838161, 1998.

(9) Kotovskaya, S. K.; Zhumabaeva, G. A.; Perova, N. M.; Baskakova, Z. M.; Charushin, V. N.; Chupakhin, O. N.; Belanov, E. F.; Bormotov, N. I.; Balakhnin, S. M.; Serova, O. A. Synthesis and antiviral activity of fluorinated 3-phenyl-1,2,4-benzotriazines. *Pharm. Chem. J.* **2007**, *41*, 62−68.

(10) Boyd, M.; Hay, M. P.; Boyd, P. D. W. Complete ^1H, ^{13}C and ^{15}N NMR assignment of tirapazamine and related 1,2,4-benzotriazine N-oxides. *Magn. Reson. Chem.* **2006**, *44*, 948−954.

(11) Fuchs, T.; Chowdhury, G.; Barnes, C. L.; Gates, K. S. 3-Amino-1,2,4-benzotriazine 4-oxide: characterization of a new metabolite arising from bioreductive processing of the antitumor agent 3-amino-1,2,4-benzotriazine 1,4-dioxide (tirapazamine). *J. Org. Chem.* **2001**, *66*, 107−114.

(12) Xia, Q.; Zhang, L.; Zhang, J.; Sheng, R.; Yang, B.; He, Q.; Hu, Y. Synthesis, hypoxia-selective cytotoxicity of new 3-amino-1,2,4-benzotriazine-1,4-dioxide derivatives. *Eur. J. Med. Chem.* **2011**, *46*, 919−926.

(13) Kanitz, A.; Stark, D. Novel Compounds as ligands for transition metal complexes and materials made thereof, and use thereof, 2011,WO 2011/157546 A1. *Chem. Abstr.* **2011**, *165*, No. 99421.

(14) Constantinides, C. P.; Koutentis, P. A. Stable N- and N/S-rich heterocyclic radicals: synthesis and applications. *Adv. Heterocycl. Chem.* **2016**, *119*, 173−207.

(15) Nicoló, F.; Panzalorto, M.; Scopelliti, R.; Grassi, G.; Risitano, F. 5,7-Dimethyl-3-phenyl-1,2,4-benzotriazine. *Acta Crystallogr., Sect. C: Cryst. Struct. Commun.* **1998**, *54*, 405−407.

(16) Guo, H.; Liu, J.; Wang, X.; Huang, G. Copper-catalyzed domino reaction of 2-haloanilines with hydrazides: a new route for the synthesis of benzo[e][1,2,4]triazine derivatives. *Synlett* **2012**, *23*, 903−906.

(17) Tanaka, Y.; Oda, S.; Ito, S.; Kakehi, A. Base-induced Generation of Aryl(1,2,3-triazol-1-yl)carbenes from 1-[(N-Phenylsulfonyl)-benzohydrazonoyl]-1,2,3-triazoles and Their Ring Enlargement to 3-Aryl-1,2,4-triazines. *Heterocycles* **2005**, *65*, 279−286.

(18) Cortés, E.; Abonía, R.; Cobo, J.; Glidewell, C. Four related esters: two 4-(aroyl-hydrazinyl)-3-nitrobenzoates and two 3-aryl-1,2,4-benzotriazine-6-carboxylates. *Acta Crystallogr., Sect. C: Cryst. Struct. Commun.* **2013**, *69*, 754−760.

(19) Fauconnier, T.; Bain, A. D.; Hazendonk, P.; Bell, R. A.; Lock, C. J. L. Structure and dynamics of azapropazone derivatives studied by crystallography and nuclear magnetic resonance. *Can. J. Chem.* **1998**, *76*, 426−430.

(20) Abramovitch, R. A.; Schofield, K. Polyazabicyclic compounds. Part I. Preliminary experiments on the Bischler and the Bamberger synthesis of benzo-1,2,4-triazines. *J. Chem. Soc.* **1955**, 2326−2336.

(21) Cerri, R.; Boido, A.; Sparatore, F. Oxidation and acid-catalyzed cyclization of aldehyde 2-aminophenylhydrazones. Alternative syntheses for 1,2,4-benzotriazines and benzimidazoles. *J. Heterocycl. Chem.* **1979**, *16*, 1005−1008.

(22) Khodja, M.; Moulay, S.; Boutoumi, H.; Wilde, H. Two-step syntheses of 3-methyl and 3-phenyl-1,2,4-benzotriazines. *Heteroatom Chem.* **2006**, *17*, 166−172.

(23) Ito, S.; Tanaka, Y.; Kakehi, A. A novel synthesis of 3-aryl-1,2,4-benzotriazines via N-phenylsulfonyl-N″-arylbenzamidrazones. *Bull. Chem. Soc. Jpn.* **1982**, *55*, 859−864.

(24) Pozharskii, A. F.; Nanavyan, I. M.; Kuzmenko, V. V.; Chernyshev, A. I.; Orlov, Y. V.; Klyuev, N. A. Oxidation of 1-aminobenzimidazoles. Synthesis and properties of 1,1′-azobenzimidazoles. *Chem. Heterocycl. Compd.* **1989**, *25*, 1241−1253.

(25) Arndt, F. Ringschluss zwischen Nitro- und Aminogruppe unter Bildung von Triazinen. *Ber. Dtsch. Chem. Ges.* **1913**, *46*, 3522−3530.

(26) Jiu, J.; Mueller, G. P. Syntheses in the 1,2,4-benzotriazine series. *J. Org. Chem.* **1959**, *24*, 813−818.

(27) Carbon, J. A. Adjacent nitro and guanidino groups. II. The base-catalyzed rearrangement of benzotriazine *N*-oxides to benzotriazoles. *J. Org. Chem.* **1962**, *27*, 185−188.

(28) Messmer, A.; Hajós, G.; Tamás, J.; Neszmélyi, A. Structure elucidation of tetrazolo[5,1-*c*]benzo-*as*-triazine. An interesting ternary equilibrium of tetrazole-azide systems. *J. Org. Chem.* **1979**, *44*, 1823−1825.

(29) Zeiger, A. V.; Joullié, M. M. Oxidation of 1,2-diaminobenzimidazoles to 3-amino-1,2,4-benzotriazine. *J. Org. Chem.* **1977**, *42*, 542−545.

(30) Kumar, A.; Parshad, M.; Gupta, R. K.; Kumar, D. Hypervalent iodine mediated oxidation of 1,2-diaminobenzimidazole and its Schiff bases: efficient synthesis of 3-amino-1,2,4-benzotriazine and 2-aryl-1,2,4-triazolo[1,5-*a*]benzimidazoles. *Synthesis* **2009**, *2009*, 1663−1666.

(31) Ito, S.; Tanaka, Y.; Kakehi, A. Base-induced dehydrosulfinatocyclization of *N*-alkyl-*N*-phenylsulfonyl-*N″*-arylbenzamidrazones to 3,4-diaryl-4H-1,2,4-triazoles. *Bull. Chem. Soc. Jpn.* **1984**, *57*, 544−547.

(32) Uneyama, K.; Sugimoto, K. N-Substituted 2,2,2-trifluoroethanimidic acid l-methylethylidene hydrazides as synthetic blocks for trifluoromethylated nitrogen heterocycles: syntheses and oxidative cyclizations. *J. Org. Chem.* **1992**, *57*, 6014−6019.

(33) Wilde, H.; Hauptmann, S.; Kanitz, A.; Franzheld, M.; Mann, G. Synthese von 1,2,4-benzotriazin-3-ylessigsäureestern und amiden. *J. Prakt. Chem.* **1985**, *327*, 297−309.

(34) Reich, M. F.; Fabio, P. F.; Lee, V. J.; Kuck, N. A.; Testa, R. T. Pyrido[3,4-*e*]-1,2,4-triazines and related heterocycles as potential antifungal agents. *J. Med. Chem.* **1989**, *32*, 2474−2485.

(35) Bass, J. Y.; Caravella, J. A.; Chen, L.; Creech, K. L.; Deaton, D. N.; Madauss, K. P.; Marr, H. B.; McFadyen, R. B.; Miller, A. B.; Mills, W. Y.; Navas, F., III; Parks, D. J.; Smalley, T. L., Jr.; Spearing, P. K.; Todd, D.; Williams, S. P.; Wisely, G. B. Conformationally constrained farnesoid X receptor (FXR) agonists: Heteroaryl replacements of the naphthalene. *Bioorg. Med. Chem. Lett.* **2011**, *21*, 1206−1213.

(36) Zhou, Y.; Zhang, Z.; Jiang, Y.; Pan, X.; Ma, D. Synthesis of 1,2,4-benzotriazines via copper(I) iodide/1H-pyrrole-2-carboxylic Acid catalyzed coupling of o-haloacetanilides and *N*-Boc hydrazine. *Synlett* **2015**, *26*, 1586−1590.

(37) Zhong, Z.; Hong, R.; Wang, X. Construction of 3-aryl-1,2,4-benzotriazines via unprecedented rearrangement of bis(benzotriazol-1-yl)methylarenes. *Tetrahedron Lett.* **2010**, *51*, 6763−6766.

(38) Yin, R.; Zhou, L.; Liu, H.; Mao, H.; Lü, X.; Wang, X. Reactivity of AllylSmBr/HMPA: facile synthesis of 3-aryl-1,2,4-benzotriazines. *Chin. J. Chem.* **2013**, *31*, 143−148.

(39) Bamberger, E.; Wheelwright, E. Ueber die Einwirkung von Diazobenzol auf Acetessigäther. *Ber. Dtsch. Chem. Ges.* **1892**, *25*, 3201−3213.

(40) Robbins, R. F.; Schofield, K. Polyazabicyclic compounds. Part II. Further derivatives of benzo-l,2,4-triazine. *J. Chem. Soc.* **1957**, 3186−3194.

(41) Atallah, R. H.; Nazer, M. Z. Oxides of 3-methyl-1,2,4-benzotriazine. *Tetrahedron* **1982**, *38*, 1793−1796.

(42) Guirado, A.; Sanchéz, J. I. L.; Moreno, R.; Gálvez, J. First synthesis of 5,8-dichloro-3-(2-pyridyl)benzo[*e*][1,2,4]triazines by reaction of 3,3,6,6-tetrachloro-1,2-cyclohexanedione with 2-pyridylamidrazones. Characterization of unexpected bishemiaminal intermediates. *Tetrahedron Lett.* **2013**, *54*, 1542−1545.

(43) Alajarin, M.; Bonillo, B.; Marin-Luna, M.; Sanchez-Andrada, P.; Vidal, A. *N*-Phenyl-1,2,4-triazoline-3,5-dione (PTAD) as a dienophilic dinitrogen equivalent: a simple synthesis of 3-amino-1,2,4-benzotriazines from arylcarbodiimides. *Eur. J. Org. Chem.* **2010**, 694−704.

(44) Some of these methods are described in a recent microreview: Obijalska, E. A.; Kowalski, M. K. Recent progress in the synthesis of 1,2,4-benzotriazines. *Chem. Heterocycl. Compd.* **2017**, *53*, 846−848.

(45) Sasaki, T.; Murata, M. Chemie des 1.2.4-Triazins, X. Synthesen von kondensierten 1.2.4-Benzotriazinen. *Chem. Ber.* **1969**, *102*, 3818−3823.

(46) Rykowski, A.; van der Plas, H. C. Ring opening in the amination of 3-X-1,2,4-triazines [1,2]. A ^{15}N study. *J. Heterocycl. Chem.* **1984**, *21*, 433−444.

(47) Elkhoshnieh, Y. O.; Ibrahim, Y. A.; Abdou, W. M. On the search for the regioselective phosphorylation of 1,2,4-triazines by cyclic, acyclic phosphites and triphenylphosphine. *Phosphorus, Sulfur Silicon Relat. Elem.* **1995**, *101*, 67−73.

(48) Messmer, A.; Hajós, G.; Benko, P.; Pallos, L. Condensed *as*-triazines. VII. A simplified method for the synthesis of benzo-*as*-triazine derivatives. *Acta Chim. Acad. Sci. Hung.* **1980**, *103*, 123−133 data from SciFinder .

(49) Yamanaka, H.; Ohba, S. Reaction of methoxy-N-heteroarmatics with phenylacetonitrile under basic conditions. *Heterocycles* **1990**, *31*, 895−909.

(50) Sarkar, U.; Hillebrand, R.; Johnson, K. M.; Cummings, A. H.; Phung, N. L.; Rajapakse, A.; Zhou, H.; Willis, J. R.; Barnes, C. L.; Gates, K. S. Application of Suzuki−Miyaura and Buchwald−Hartwig cross-coupling reactions to the preparation of substituted 1,2,4-benzotriazine 1-oxides related to the antitumor agent tirapazamine. *J. Heterocycl. Chem.* **2017**, *54*, 155−160.

(51) Pchalek, K.; Hay, M. P. Stille coupling reactions in the synthesis of hypoxia-selective 3-alkyl-1,2,4-benzotriazine 1,4-dioxide anticancer agents. *J. Org. Chem.* **2006**, *71*, 6530−6535.

(52) Hay, M. P.; Denny, W. A. New and versatile syntheses of 3-alkyl- and 3-aryl-1,2,4-benzotriazine 1,4-dioxides: preparation of the bioreductive cytotoxins SR 4895 and SR 4941. *Tetrahedron Lett.* **2002**, *43*, 9569−9571.

(53) Hay, M. P.; Pchalek, K.; Pruijn, F. B.; Hicks, K. O.; Siim, B. G.; Anderson, R. F.; Shinde, S. S.; Phillips, V.; Denny, W. A.; Wilson, W. R. Hypoxia-selective 3-alkyl 1,2,4-benzotriazine 1,4-dioxides: the influence of hydrogen bond donors on extravascular transport and antitumor activity. *J. Med. Chem.* **2007**, *50*, 6654−6664.

(54) Jasiński, M.; Szymańska, K.; Gardias, A.; Pociecha, D.; Monobe, H.; Szczytko, J.; Kaszyński, P. Tuning the Magnetic Properties of Columnar Benzo[*e*][1,2,4]triazin-4-yls with the Molecular Shape. *ChemPhysChem* **2019**, *20*, 636−644.

(55) Jasiński, M.; Kapuściński, S.; Kaszyński, P. Stability of a columnar liquid crystalline phase in isomeric derivatives of the 1,4-dihydrobenzo[*e*][1,2,4]triazin-4-yl: conformational effects in the core. *J. Mol. Liq.* **2019**, *277*, 1054−1059.

(56) Kapuściński, S.; Gardias, A.; Pociecha, D.; Jasiński, M.; Szczytko, J.; Kaszyński, P. Magnetic behaviour of bent-core mesogens derived from the 1,4-dihydrobenzo[*e*][1,2,4]triazin-4-yl. *J. Mater. Chem. C* **2018**, *6*, 3079−3088.

(57) Jasiński, M.; Szczytko, J.; Pociecha, D.; Monobe, H.; Kaszyński, P. Substituent-Dependent Magnetic Behavior of Discotic Benzo[*e*]-[1,2,4]triazinyls. *J. Am. Chem. Soc.* **2016**, *138*, 9421−9424.

(58) Ligthart, G. B. W. L.; Guo, D.; Spek, A. L.; Kooijman, H.; Zuilhof, H.; Sijbesma, R. P. Ureidobenzotriazine multiple H-bonding arrays: the importance of geometrical details on the stability of H-bonds. *J. Org. Chem.* **2008**, *73*, 111−117.

(59) Doyle, M. P.; Siegfried, B.; Dellaria, J. F., Jr. Alkyl Nitrite-Metal Halide Deamination Reactions. 2. Substitutive Deamination of Arylamines by Alkyl Nitrites and Copper(I) Halides. A Direct and Remarkably Efficient Conversion of Arylamines to Aryl Halides. *J. Org. Chem.* **1977**, *42*, 2426−2431.

(60) Doyle, M. P.; Dellaria, J. F., Jr.; Siegfried, B.; Bishop, S. W. Reductive deamination of arylamines by alkyl nitrites in N,N-dimethylformamide. A direct conversion of arylamines to aromatic hydrocarbons. *J. Org. Chem.* **1977**, *42*, 3494−3498.

(61) Fusco, R.; Silvano, R. Asymmetrical triazines. VII. New synthesis of the benzo-1,2,4-triazine ring. *Gazz. Chim. Ital.* **1956**, *86*, 484−499 data from SciFinder .

(62) Menozzi-Smarrito, C.; Wong, C. C.; Meinl, W.; Glatt, H.; Fumeaux, R.; Munari, C.; Robert, F.; Williamson, G.; Barron, D. First Chemical Synthesis and in Vitro Characterization of the Potential Human Metabolites 5-O-Feruloylquinic Acid 4′-Sulfate and 4′-O-Glucuronide. *J. Agric. Food Chem.* **2011**, *59*, 5671−5676.

(63) Zhang, Z.; Sun, S.; Kodumuru, V.; Hou, D.; Liu, S.; Chakka, N.; Sviridov, S.; Chowdhury, S.; McLaren, D. G.; Ratkay, L. G.; Khakh, K.; Cheng, X.; Gschwend, H. W.; Kamboj, R.; Fu, J.; Winther, M. D. Discovery of piperazin-1-ylpyridazine-based potent and selective stearoyl-CoA desaturase-1 inhibitors for the treatment of obesity and metabolic syndrome. *J. Med. Chem.* **2013**, *56*, 568−583.

(64) Mantell, S. J.; Monaghan, S. M.; Stephenson, P. T. Purine Derivatives. WO2002000676A1, 2002.

(65) Rani, V. J.; Aminedi, R.; Polireddy, K.; Jagadeeswarareddy, K. Synthesis and spectral characterization of new bis(2-(pyrimidin-2-yl)ethoxy)alkanes and their pharmacological activity. *Arch. Pharm.* **2012**, *345*, 663.

(66) For details see the Supporting Information.

(67) Cacchi, S.; Fabrizi, G.; Goggiamani, A. Palladium-catalyzed hydroxycarbonylation of aryl and vinyl halides or triflates by acetic anhydride and formate anions. *Org. Lett.* **2003**, *5*, 4269−4272.

(68) Wu, F.-P.; Peng, J.-B.; Qi, X.; Wu, X.-F. Palladium-catalyzed carbonylative transformation of organic halides with formic acid as the coupling partner and CO source: synthesis of carboxylic acids. *J. Org. Chem.* **2017**, *82*, 9710−9714.

(69) Qi, X.; Li, C.-L.; Jiang, L.-B.; Zhang, W.-Q.; Wu, X.-F. Palladium-catalyzed alkoxycarbonylation of aryl halides with phenols employing formic acid as the CO source. *Catal. Sci. Technol.* **2016**, *6*, 3099−3107.

(70) Ueda, T.; Konishi, H.; Manabe, K. Trichlorophenyl formate: highly reactive and easily accessible crystalline CO surrogate for palladium-catalyzed carbonylation of aryl/alkenyl halides and triflates. *Org. Lett.* **2012**, *14*, 5370−5373.

(71) Tran-Vu, H.; Daugulis, O. Copper-catalyzed carboxylation of aryl iodides with carbon dioxide. *ACS Catal.* **2013**, *3*, 2417−2420.

(72) Güell, I.; Ribas, X. Ligand-free Ullmann-type C−heteroatom couplings under practical conditions. *Eur. J. Org. Chem.* **2014**, 3188−3195.

(73) Liu, X.; Xu, C.; Wang, M.; Liu, Q. Trifluoromethyltrimethylsilane: nucleophilic Ttrifluoromethylation and beyond. *Chem. Rev.* **2015**, *115*, 683−730.

(74) Oishi, M.; Kondo, H.; Amii, H. Aromatic trifluoromethylation catalytic in copper. *Chem. Commun.* **2009**, 1909−1911.

(75) Cottet, F.; Schlosser, M. Trifluoromethyl-Substituted Pyridines Through Displacement of Iodine by in situ Generated (Trifluoromethyl)copper. *Eur. J. Org. Chem.* **2002**, 327−330.

(76) Knauber, T.; Arikan, F.; Röschenthaler, G.-V.; Goossen, L. J. Copper-catalyzed trifluoromethylation of aryl iodides with potassium (trifluoromethyl)trimethoxyborate. *Chem. − Eur. J.* **2011**, *17*, 2689−2697.

(77) Hansch, C.; Leo, A.; Taft, R. W. A survey of Hammett substituent constants and resonance and field parameters. *Chem. Rev.* **1991**, *91*, 165−195.

(78) Rappoport, Z., Ed.; *The Cyano Group*; Wiley & Sons, 1970.

(79) Frisch, M. J.; Trucks, G. W.; Schlegel, H. B.; Scuseria, G. E.; Robb, M. A.; Cheeseman, J. R.; Scalmani, G.; Barone, V.; Mennucci, B.; Petersson, G. A.; Nakatsuji, H.; Caricato, M.; Li, X.; Hratchian, H. P.; Izmaylov, A. F.; Bloino, J.; Zheng, G.; Sonnenberg, J. L.; Hada, M.; Ehara, M.; Toyota, K.; Fukuda, R.; Hasegawa, J.; Ishida, M.; Nakajima, T.; Honda, Y.; Kitao, O.; Nakai, H.; Vreven, T.; Montgomery, J. A., Jr.; Peralta, J. E.; Ogliaro, F.; Bearpark, M.; Heyd, J. J.; Brothers, E.; Kudin, K. N.; Staroverov, V. N.; Kobayashi, R.; Normand, J.; Raghavachari, K.; Rendell, A.; Burant, J. C.; Iyengar, S. S.; Tomasi, J.; Cossi, M.; Rega, N.; Millam, J. M.; Klene, M.; Knox, J. E.; Cross, J. B.; Bakken, V.; Adamo, C.; Jaramillo, J.; Gomperts, R.; Stratmann, R. E.; Yazyev, O.; Austin, A. J.; Cammi, R.; Pomelli, C.; Ochterski, J. W.; Martin, R. L.; Morokuma, K.; Zakrzewski, V. G.; Voth, G. A.; Salvador, P.; Dannenberg, J. J.; Dapprich, S.; Daniels, A. D.; Farkas, O.; Foresman, J. B.; Ortiz, J. V.; Cioslowski, J.; Fox, D. J.. *Gaussian 09*, revision A.02; Gaussian, Inc.: Wallingford, CT, 2009.

(80) Scott, A. P.; Radom, L. Harmonic Vibrational Frequencies: An Evaluation of Hartree-Fock, Møller-Plesset, Quadratic Configuration Interaction, Density Functional Theory, and Semiempirical Scale Factors. *J. Phys. Chem.* **1996**, *100*, 16502−16513.

(81) Stratmann, R. E.; Scuseria, G. E.; Frisch, M. J. An efficient implementation of time-dependent density-functional theory for the calculation of excitation energies of large molecules. *J. Chem. Phys.* **1998**, *109*, 8218−8224.

(82) Cossi, M.; Scalmani, G.; Rega, N.; Barone, V. New developments in the polarizable continuum model for quantum mechanical and classical calculations on molecules in solution. *J. Chem. Phys.* **2002**, *117*, 43−54 and references therein .

(83) Fulmer, G. R.; Miller, A. J. M.; Sherden, N. H.; Gottlieb, H. E.; Nudelman, A.; Stoltz, B. M.; Bercaw, J. E.; Goldberg, K. I. NMR Chemical Shifts of Trace Impurities: Common Laboratory Solvents, Organics, and Gases in Deuterated Solvents Relevant to the Organometallic Chemist. *Organometallics* **2010**, *29*, 2176−2179.

(84) Preston, P. N.; Turnbull, K. Approaches to the synthesis of compounds containing fused mesoionic rings. *J. Chem. Soc., Perkin Trans. 1* **1977**, 1229−1233.

(85) Hübscher, J.; Seichter, W.; Gruber, T.; Kortus, J.; Weber, E. Synthesis and structural characterization of ethynylene-bridged bisazines featuring various α-substitution. *J. Heterocycl. Chem.* **2015**, *52*, 1062−1074.

Pomikło, D.; Bodzioch, A.; Pietrzak, A.; Kaszyński, P.

"C(3) Functional derivatives of the Blatter radical"

Org. Lett. **2019**, *21*, 6995–6999.

C(3) Functional Derivatives of the Blatter Radical

Dominika Pomikło,[†] Agnieszka Bodzioch,[†] Anna Pietrzak,[§,⊥] and Piotr Kaszyński*,[†,‡,§]

[†]Centre of Molecular and Macromolecular Studies, Polish Academy of Sciences, 90-363 Łódź, Poland
[§]Department of Chemistry, Middle Tennessee State University, Murfreesboro, Tennessee 37132, United States
[⊥]Faculty of Chemistry, Łódź University of Technology, 90-924 Łódź, Poland
[‡]Faculty of Chemistry, University of Łódź, 91-403 Łódź, Poland

Ⓢ *Supporting Information*

ABSTRACT: A series of 3-substituted 1-phenyl-1,4-dihydrobenzo[*e*][1,2,4]-triazin-4-yls **1** was prepared by addition of PhLi to 3-substituted benzo[*e*][1,2,4]-triazines **2** followed by aerial oxidation. The scope of the C(3) substituents in the reaction was investigated, and 10 structurally diverse radicals **1** were isolated, their stability was assessed and properties were investigated with spectroscopic and electrochemical methods. Two radicals were analyzed with single-crystal XRD methods. Experimental data are compared to DFT results and correlated with Hammett substituent parameters.

X = thienyl, CCPh, ferrocenyl, CF₃, alkyl, H, SBu-*t*, OEt, NH₂, morpholinyl
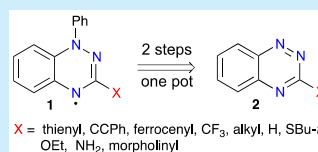
The exceptional stability, broad absorption in the visible range, and favorable electrochemical properties make the 1,4-dihydrobenzo[*e*][1,2,4]triazin-4-yl radical an attractive and increasingly important structural element of functional materials,[1,2] such as photoconductive liquid crystals[3−6] and those for molecular electronics,[7] energy storage,[8] controlled polymerization,[9] and biophysical[10] applications. Most of these applications require the presence of appropriate functional groups that enable the radical to be incorporated into more complex molecular architectures. Therefore, further progress in application of the 1,4-dihydrobenzo[*e*][1,2,4]triazin-4-yl hinges upon accessibility of its multifunctional derivatives.

There are three major methods leading to 1,4-dihydrobenzo-[*e*][1,2,4]triazin-4-yl radicals **1** (Figure 1): 6-π electrocycliza-
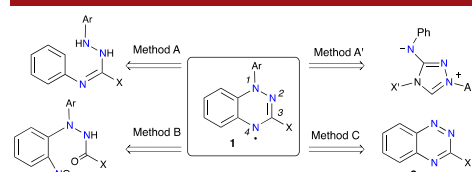
Figure 1. Selected methods for construction of the 1,4-dihydrobenzo-[*e*][1,2,4]triazin-4-yl skeleton.

tion of azoimines (methods A,[11−14] A′,[15] and the aza-Wittig modification[16]), reductive cyclocondensation of *N*-aryl hydrazides (method B),[17] and azaphilic addition of ArLi to benzo[*e*][1,2,4]triazines **2** followed by aerial oxidation of the resulting anion **3** (method C).[18] In methods A and B, substituent X in radical **1** is derived from the carboxylic acid, which, to large extent, defines its nature.

A review of the literature indicates that several functional groups have been introduced to the benzene ring of the benzo[*e*][1,2,4]triazinyl, and they include CN,[16,19] CHO,[19] NO₂,[16] halogens,[13,16] and OMe substituents.[13,16] Also transformations in the presence of the unpaired electron are numerous,[20,21] which have been extensively used in the preparation of some functional materials. Efficient methods have also been demonstrated for postcyclization ring substitution[13,14,20−22] and ring annulation.[23−25]

Functionalization of the C(3) atom is, however, much less developed. Arguably, this is a particularly important position since it is the only functionalizable position with a sizable negative spin density in the benzo[*e*][1,2,4]triazinyl system, and the substituent is expected[26] to have a significant impact on electronic properties of the radical. A literature search demonstrates that only a handful of substituents have been introduced into this position using mainly methods A and B, and they include aromatic (Ph,[11] substituted Ph,[3−6,16] 2-pyridinyl,[17] and 2-thienyl[16,17]), aliphatic (CH₃,[17] *t*-butyl,[27,28] and adamantyl[29]), CF₃,[17] and NHAr (in method A′ after basic hydrolysis of NH(CHO)Ar).[15] Surprisingly, there is no report on the C(3)-unsubstituted derivative (X = H).

Here, we present the preparation of C(3)-substituted 1-phenyl-1,4-dihydrobenzo[*e*][1,2,4]triazin-4-yl radicals **1** by addition of PhLi to the readily available benzo[*e*][1,2,4]-triazines[26] **2** followed by oxidation of the resulting anions **3** (method C, Figure 1). The scope of the substituents X is investigated, stability of radicals **1** is assessed, and the impact of the C(3) substituent X on spectroscopic and electrochemical properties in series **1** is analyzed.

Reactions of a series of 14 3-substituted benzo[*e*][1,2,4]-triazines[26] **2b−2o** with PhLi were conducted under conditions previously used to obtain the Blatter radical **1a** from **2a** in 70−78% yield,[18] and the results are shown in Table 1. Thus, 1,3

**Organic Letters**   Letter

Table 1. Preparation of 1-Phenyl-1,4-dihydrobenzo[e][1,2,4]triazin-4-yls 1 from Benzo[e][1,2,4]triazines 2[a]

X	yield (%) of 1[b]	X	yield (%) of 1[b]
a, Ph	70–78[c]	**i**, OEt	23
b, thien-2-yl	46	**j**, NH$_2$	13–15
c, ferrocenyl	29	**k**, morpholin-4-yl	67
d, C≡CPh	59	**l**, NHPh	0[d]
e, CF$_3$	81	**m**, COO$^-$[NMe$_4$]$^+$	0[d]
f, C$_5$H$_{11}$	31	**n**, CN	0, 59[e]
g, H	13–19	**o**, PO(OEt)$_2$	0, 58[e]
h, SBu-t	70		

[a]According to Scheme 1. Typical procedure: (1) 1.3 equiv of PhLi in Bu$_2$O (0.8 mL) was added to 0.5 mmol of **2** in THF (1.5 mL) at −78 °C; (2) H$_2$O (0.5 mL), air. [b]Yield of isolated compounds after chromatography. [c]Reference 18. [d]Complex mixture of products. [e]Yield of Blatter radical **1a**.

equiv of PhLi was added to 3-thienylbenzo[e][1,2,4]triazine (**2b**) in THF solution at −78 °C, the resulting **3b** was quenched with water and the formed *leuco* form was oxidized to **1b** by exposure to air (Scheme 1). The known[16,17] radical

Scheme 1. Preparation of Radicals 1 from Benzo[e][1,2,4]triazines 2
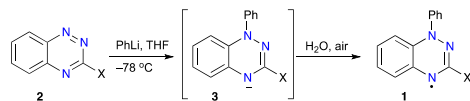
1b was isolated in 46% yield by column chromatography. A similar reaction of 3-ferrocenyl (**2c**), 3-C≡CPh (**2d**), 3-CF$_3$ (**2e**),[17] and 3-C$_5$H$_{11}$ (**2f**) derivatives gave the corresponding radicals in yields 31−81%. Radicals **1d** and **1f** exhibited limited stability in solutions and to chromatography. Instability of the latter radical is amplified by its liquid nature, while radical **1d** appears to be stable in the solid state.

Reactions of PhLi with 3-SBu-t and 3-(morpholin-4-yl) derivatives **2h** and **2k**, respectively, gave the corresponding radicals **1h** and **1k** in about 70% yield. In contrast, reactions of the 3-OEt (**2i**) and 3-NH$_2$ (**2j**) derivatives and the parent benzo[e][1,2,4]triazine (**2g**) gave complex mixtures of products, from which the desired radicals could be isolated in 13−23% yield. The 3-amino and 3-unsubstituted radicals, **1j** and **1g**, appear to be moderately stable after isolation, while the 3-OEt **1i** undergoes slow decomposition on standing, which precluded accurate combustion analysis. The formation of the Blatter radical **1a** by substitution of the OEt group was not observed.

No expected radicals were observed in reactions of PhLi with C(3)-NHPh (**2l**) and C(3)-COO$^-$[NMe$_4$]$^+$ (**2m**) derivatives. In the former case, a species with an apparently additional Ph group (addition of a total of two Ph groups) was isolated in 35% yield, but it was not investigated further.[30] This is presumably due to the dominant imino tautomeric form of **2l**[26] and the highest calculated electrophilicity, f^+, at the C(3) position of the corresponding anion.[30]

Finally, treatment of the 3-CN and 3-PO(OEt)$_2$ derivatives **2n** and **2o**, respectively, with PhLi led to the formation of the Blatter radical **1a** apparently by replacement of the C(3) substituent with the Ph group. When 0.25 equiv of PhLi was

used in the reaction with **2n**, the crude reaction mixture contained minor quantities of the expected radical **1n** along with the 3-phenylbenzo[e][1,2,4]triazine (**2a**), in addition to radical **1a**. This is consistent with the observed facile substitution of the CN group with OH, upon basic hydrolysis of **2n**,[26] and similar substitution of the 3-PO(OEt)$_2$ group in **2o**.[30]

Overall, C(3) substituents in benzo[e][1,2,4]triazines **2** fall into four categories: those that give high yields of radicals **1** upon reactions with PhLi (CF$_3$, aryl (Ph), CCPh, SBu-t, and morpholin-4-yl), those that give complex mixtures of products and the corresponding radicals **1** can be isolated in low yields (ferrocene, alkyl, OEt, NH$_2$, and H), those for which no desired products could be isolated (NHPh and COO$^-$), and those that undergo clean aromatic nucleophilic displacement with PhLi (CN and PO(OEt)$_2$). Most radicals are stable after isolation except for those containing H, C$_5$H$_{11}$, and OEt at the C(3) position, which slowly decompose upon standing.

Analysis of electrophilicity indices expressed as condensed electronic Fukui functions,[31,32] f^+,[30] indicates that the N(1) position is typically preferred for the Nu$^-$ addition, and the resulting anion is also most favored thermodynamically for addition of Ph$^-$ to **2a** and **2n**.[30] This regioselectivity is also predicted for anion **2j**$^-$, formed upon deprotonation of amine **2j**, but in anion **2l**$^-$, the C(3) position appears to be most electrophilic.

The structures of two radicals, **1h** and **1k**, were confirmed with single-crystal XRD analysis (Figure 2). Dimensions of the
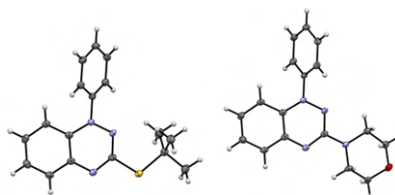
Figure 2. Molecular structures of **1h** (left) and **1k** (right). For selected geometrical parameters see the text and the SI. Displacement ellipsoids are drawn at the 50% probability level.

benzo[e][1,2,4]triazine heterocycle are typical with the ring being puckered (10.1°) along the N(1)···N(4) line in **1h** and essentially planar in **1k**. The C(3)−S distance in **1h** is 1.765(2) Å. In the two independent molecules of **1k** the C(3)−N distance is 1.372(2) Å and 1.386(2) Å with the nitrogen atoms away from the plane defined by the three connected C atoms by 0.171 and 0.302 Å, respectively.

Spectroscopic and electrochemical analyses of radicals in series **1** revealed the effects of the C(3) substituent. Thus, all radicals exhibit a broad, low intensity absorption in the visible range with poorly defined absorption maxima. The most pronounced effect on the absorption spectrum is exhibited by the 3-(morpholin-4-yl) derivative **1k** (Figure 3).

The observed trend in excitation energies is reproduced computationally. TD DFT analysis suggests that the two lowest energy excitations calculated at about 500 and 400 nm involve mainly the α-HOMO → α-LUMO and β-HOMO → β-LUMO transitions. Substitution of the C(3) position in the parent radical **1g** has stronger impact on the β-HOMO (Figure 4) energy (range in the series $\Delta E = 1.12$ eV) than on the α-

Organic Letters Letter
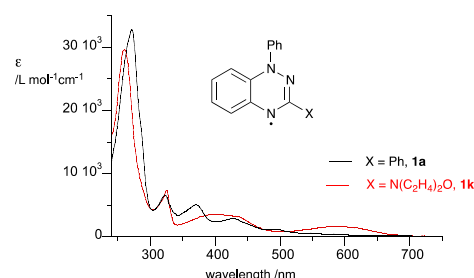
Figure 3. UV−vis spectra for radicals 3-Ph **1a** (black) and 3-(morpholin-4-yl) **1k** (red) in CH_2Cl_2.

$E = -7.58$ eV $E = -7.09$ eV
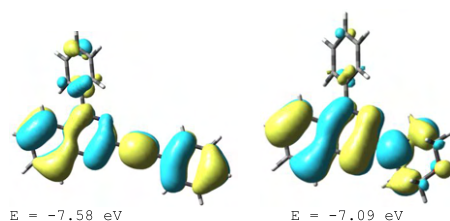
Figure 4. CAM-B3LYP/6-31++G(2d,p)//B3LYP/6-31G(2d,p)-derived β-HOMO contours and energies for radicals **1d** (left) and **1k** (right) in CH_2Cl_2 dielectric medium.

HOMO energy (range in the series $\Delta E = 0.44$ eV), and the observed trend approximately follows the Hammett σ_p parameter.[30] In general, π substituents, such as Ph, thienyl, and phenylethynyl, significantly stabilize the α-LUMO (by up to 0.93 eV in **1d**), while all substituents, with the exception of the CF_3, destabilize the β-HOMO orbital with the strongest effect observed in the 3-(morpholin-4-yl) derivative **1k** (by 0.89 eV). Consequently, the lowest energy excitation has the α-HOMO → α-LUMO character for 3-(het)aryl, 3-ethynyl and 3-CF_3 derivatives, while for those with substituents containing an electron pair (alkoxy and amines) it has the β-HOMO→ β-LUMO character.

Electrochemical analysis of series **1** gave more clear evidence of the C(3) substituent effect on the electronic structure of the benzo[e][1,2,4]triazinyl heterocycle.

A comparison of redox potentials in series **1** shows that replacement of the Ph substituent at the C(3) position in **1a** with CF_3, the most electron accepting substituent in the series, increases the $E_{1/2}^{0/+1}$ by 0.30 V in **1e**, while replacement with the most electron releasing morpholin-4-yl group lowers the oxidation potential by 0.20 V in **1k** (Figure 5, Table 2).[30] The reduction potentials $E_{1/2}^{-1/0}$ follow the same trend, which is consistent with other electrochemical studies[17] and correlates well with the Hammett σ_p parameters.[30,33] The observed nearly twice larger slope for the $E_{1/2}^{0/+1}$ potential vs σ_p plot[30] than for the $E_{1/2}^{-1/0}$ vs σ_p plot suggests a greater impact of the substituent on the HOMO than on the LUMO in series **1**. Interestingly, the ferrocenyl derivative **1c** exhibits two quasireversible oxidation processes due to the oxidation of the heterocycle (+0.38 V) and the ferrocenyl group (+0.72 V). Electrochemical analysis of **1g** and **1i** gave poor results due to instability of the sample.
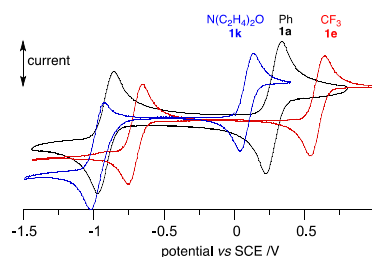
Figure 5. Cyclic voltammograms for 3-phenyl (**1a**, black), 3-CF_3 (**1e**, red), and 3-(morpholin-4-yl) (**1k**, blue) 1-phenyl-1,4-dihydrobenzo-[e][1,2,4]triazin-4-yls (∼0.5 mM) in CH_2Cl_2 [n-Bu$_4$N]$^+$ [PF$_6$]$^-$ (50 mM), ca. 20 °C, 50 mV s^{-1}, glassy carbon electrode.

Table 2. Electrochemical Data for 1-Phenyl-1,4-dihydrobenzo[e][1,2,4]triazin-4-yls 1[a]

X	$E_{1/2}^{-1/0}$ (V)	$E_{1/2}^{0/+1}$ (V)	E_{cell}[b] (V)	E_{LUMO}[c] (eV)	E_{HOMO}[c] (eV)
a, Ph[d]	−0.92	+0.28	1.20	−3.81	−4.81
b, thien-2-yl[e]	−0.88	+0.30	1.18	−3.92	−4.88
c, ferrocenyl	[f]	+0.38			−4.62
		+0.72[g]			
d, C≡CPh	−0.78	+0.40	1.18	−3.95	−4.94
e, CF_3[h]	−0.71	+0.58	1.29	−3.99	−5.15
f, C_5H_{11}[i]	−0.97	+0.24	1.21	−3.80	−4.78
h, SBu-t	−0.90	+0.30	1.20	−3.85	−4.87
j, NH_2	−0.96	+0.15	1.11	−3.83	−4.65
k, morpholin-4-yl	−0.98	+0.08	1.06	−3.80	−4.65

[a]Measured in CH_2Cl_2 [n-Bu$_4$N]$^+$ [PF$_6$]$^-$ (50 mM), *ca.* 20 °C, 50 mV s^{-1}, glassy carbon electrode. Potentials referenced to Fc/Fc$^+$ (0.46 V vs SCE; ref 34). [b]$E_{cell} = E_{1/2}^{0/+1} − E_{1/2}^{-1/0}$. [c]Calculated from the onset of oxidation or reduction: $E_{HOMO/LUMO} = -(E_{(onset\ ox/red\ vrs\ Fc+/Fc)} + 5.1)$ (eV); ref 35. [d]Reference 18. [e]Lit.[16] −0.82 and +0.32 V. [f]Ambiguous assignments. [g]The second oxidation potential is ascribed to the ferrocenyl group. [h]Lit.[17] −0.78 and +0.36 V vs SCE. [i]Lit.[17] for X = Me: −0.95 and +0.37 V vs SCE.

The C(3) substituent also impacts the *hfcc* and consequently the shape of EPR spectra of the radicals (e.g., Figure 6).[30] In all
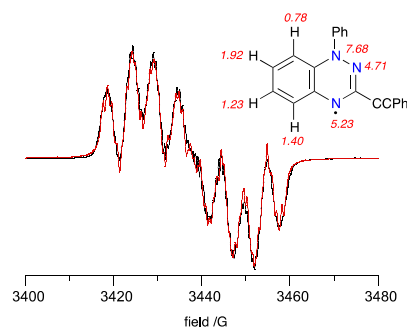
Figure 6. Experimental (black) and simulated (red) EPR spectra for radical **1d** recorded in CH_2Cl_2. Inset shows an assignment of the resulting *hfcc*.

radicals **1** the $a_{N(1)}$, $a_{N(2)}$, and $a_{N(4)}$ *hfcc* values fall into typical ranges of 7.4−8.1, 4.1−4.9, and 4.9−5.8 G, respectively. Correlation analysis of the data demonstrates that the a_{N1} *hfcc* are essentially independent of the C(3) substituent (slope = 0 within the error), the a_{N2} values show a weak increasing trend (when the CF$_3$ derivative is omitted), and a clear decreasing trend for a_{N4} *hfcc* is observed with increasing values of the substituent parameter σ_p.[30,33]

In summary, we have demonstrated access to benzo[*e*]-[1,2,4]triazin-4-yl with a significantly expanded range and diversity of substituents at the C(3) position. The newly available derivatives include the electroactive C(3)-ferrocenyl derivative **1c**, C(3)-acetylene derivative **1d**, and derivative **1j** containing a particularly important and versatile NH$_2$ functionality.[36] We have also established limitation of the azaphilic addition method and found its incompatibility with C(3) substituents such as COO$^−$, NHPh, CN, and PO(OR)$_2$. The expanded series of derivatives permitted analysis of C(3) substituent effects on electronic properties of the benzo[*e*]-[1,2,4]triazin-4-yl system, which, in turn, provides a tool for designing of radicals with greater functional flexibility and structural variety for modern materials applications.

■ ASSOCIATED CONTENT

Ⓢ Supporting Information

The Supporting Information is available free of charge on the ACS Publications website at DOI: 10.1021/acs.orglett.9b02563.

Synthetic and analytical details, UV−vis and EPR spectra, electrochemical data, details of XRD analysis, and computational results (PDF)

Accession Codes

CCDC 1915133 and 1915134 contain the supplementary crystallographic data for this paper. These data can be obtained free of charge via www.ccdc.cam.ac.uk/data_request/cif, or by emailing data_request@ccdc.cam.ac.uk, or by contacting The Cambridge Crystallographic Data Centre, 12 Union Road, Cambridge CB2 1EZ, UK; fax: +44 1223 336033.

■ AUTHOR INFORMATION

Corresponding Author

*E-mail: piotrk@cbmm.lodz.pl.
ORCID Ⓘ

Anna Pietrzak: 0000-0003-3415-8650
Piotr Kaszyński: 0000-0002-2325-8560

Notes

The authors declare no competing financial interest.

■ ACKNOWLEDGMENTS

■ REFERENCES

(1) *Functional Organic Materials: Syntheses, Strategies and Applications*; Müller, T. J. J., Bunz, U. H. F., Eds.; Wiley-VCH, 2007; Vol. *1*.
(2) Ratera, I.; Veciana, J. Playing with orgnic radicals as biulding blocks for functional molecular materials. *Chem. Soc. Rev.* **2012**, *41*, 303−349.
(3) Jasiński, M.; Kapuściński, S.; Kaszyński, P. Stability of a columnar liquid crystalline phase in isomeric derivatives of the 1,4-dihydrobenzo[*e*][1,2,4]triazin-4-yl: Conformational effects in the core. *J. Mol. Liq.* **2019**, *277*, 1054−1059.
(4) Jasiński, M.; Szczytko, J.; Pociecha, D.; Monobe, H.; Kaszyński, P. Substituent-Dependent Magnetic Behavior of Discotic Benzo[*e*]-[1,2,4]triazinyls. *J. Am. Chem. Soc.* **2016**, *138*, 9421−9424.
(5) Jasiński, M.; Szymańska, K.; Gardias, A.; Pociecha, D.; Monobe, H.; Szczytko, J.; Kaszyński, P. Tuning the Magnetic Properties of Columnar Benzo[*e*][1,2,4]triazin-4-yls with the Molecular Shape. *ChemPhysChem* **2019**, *20*, 636−644.
(6) Kapuściński, S.; Gardias, A.; Pociecha, D.; Jasiński, M.; Szczytko, J.; Kaszyński, P. Magnetic behaviour of bent-core mesogens derived from the 1,4-dihydrobenzo[e][1,2,4]triazin-4-yl. *J. Mater. Chem. C* **2018**, *6*, 3079−3088.
(7) Sanvito, S. Molecular Spintronics. *Chem. Soc. Rev.* **2011**, *40*, 3336−3355.
(8) Friebe, C.; Schubert, U. S. High-Power-Density Organic Radical Batteries. *Top. Curr. Chem.* **2017**, *375*, 19 DOI: 10.1007/s41061-017-0103-1.
(9) Demetriou, M.; Berezin, A. A.; Koutentis, P. A.; Krasia-Christoforou, T. Benzotriazinyl-mediated controlled radical polymerization of styrene. *Polym. Int.* **2014**, *63*, 674−679.
(10) Michaelis, V. K.; Smith, A. A.; Corzilius, B.; Haze, O.; Swager, T. M.; Griffin, R. G. High-Field 13C Dynamic Nuclear Polarization with a Radical Mixture. *J. Am. Chem. Soc.* **2013**, *135*, 2935−2938.
(11) Blatter, H. M.; Lukaszewski, H. A new stable free radical. *Tetrahedron Lett.* **1968**, *9*, 2701−2705.
(12) Koutentis, P. A.; Lo Re, D. Catalytic Oxidation of N-Phenylamidrazones to 1,3-Diphenyl-1,4-dihydro-1,2,4-benzotriazin-4-yls: An Improved Synthesis of Blatter's Radical. *Synthesis* **2010**, *2010*, 2075−2079.
(13) Constantinides, C. P.; Koutentis, P. A.; Loizou, G. Synthesis of 7-aryl/heteraryl-1,3-diphenyl-1,2,4-benzotriazinyls via palladium catalyzed Stille and Suzuki-Miyaura reactions. *Org. Biomol. Chem.* **2011**, *9*, 3122−3125.
(14) Constantinides, C. P.; Koutentis, P. A.; Rawson, J. M. Antiferromagnetic Interactions in 1D Heisenberg Linear Chains of 7-(4-Fluorophenyl) and 7-Phenyl-Substituted 1,3-Diphenyl-1,4-dihydro- 1,2,4-benzotriazin-4-yl Radicals. *Chem. - Eur. J.* **2012**, *18*, 15433−15438.
(15) Grant, J. A.; Lu, Z.; Tucker, D. E.; Hockin, B. M.; Yufit, D. S.; Fox, M. A.; Kataky, R.; Chechik, V.; O'Donoghue, A. C. New Blatter-type radicals from a bench-stable carbene. *Nature Commun.* **2017**, *8*, 15088.
(16) Savva, A. C.; Mirallai, S. I.; Zissimou, G. A.; Berezin, A. A.; Demetriades, M.; Kourtellaris, A.; Constantinides, C. P.; Nicolaides, C.; Trypiniotis, T.; Koutentis, P. A. Preparation of Blatter Radicals via Aza-Wittig Chemistry: The Reaction of N-Aryliminophosphoranes with 1-(Het)aroyl-2-aryldiazenes. *J. Org. Chem.* **2017**, *82*, 7564−7575.
(17) Berezin, A. A.; Zissimou, G.; Constantinides, C. P.; Beldjoudi, Y.; Rawson, J. M.; Koutentis, P. A. Route to Benzo- and Pyrido-Fused 1,2,4-Triazinyl Radicals *via* N'-(Het)aryl-N'-[2-nitro(het)aryl]-hydrazides. *J. Org. Chem.* **2014**, *79*, 314−327.
(18) Constantinides, C. P.; Obijalska, E.; Kaszyński, P. Access to 1,4-Dihydrobenzo[*e*][1,2,4]triazin-4-yl Derivtives. *Org. Lett.* **2016**, *18*, 916−919.
(19) Gallagher, N.; Zhang, H.; Junghoefer, T.; Giangrisostomi, E.; Ovsyannikov, R.; Pink, M.; Rajca, S.; Casu, M. B.; Rajca, A. Thermally and Magnetically Robust Triplet Ground State Diradical. *J. Am. Chem. Soc.* **2019**, *141*, 4764−4774.
(20) Bodzioch, A.; Zheng, M.; Kaszyński, P.; Utecht, G. Functional Group Transformations in Derivatives of 1,4-Dihydrobenzo[1,2,4]-triazinyl Radical. *J. Org. Chem.* **2014**, *79*, 7294−7310.
(21) Takahashi, Y.; Miura, Y.; Yoshioka, N. Introduction of Three Aryl Groups to Benzotriazinyl Radical by Suzuki-Miyaura Cross-coupling Reaction. *Chem. Lett.* **2014**, *43*, 1236−1238.
(22) Constantinides, C. P.; Carter, E.; Murphy, D. M.; Manoli, M.; Leitus, G. M.; Bendikov, M.; Rawson, J. M.; Koutentis, P. A. Spin-

triplet excitons in 1, 3-diphenyl-7-(fur-2-yl)-1,4-dihydro-1,2,4-benzo-triazin-4-yl. *Chem. Commun.* **2013**, *49*, 8662−8664.

(23) Berezin, A. A.; Constantinides, C. P.; Drouza, C.; Manoli, M.; Koutentis, P. A. From Blatter Radical to 7-Substituted 1,3-Diphenyl-1,4-dihydrothiazolo[5′,4′:4,5]benzo[1,2-e][1,2,4]triazin-4-yls: Toward Multifunctional Materials. *Org. Lett.* **2012**, *14*, 5586−5589.

(24) Berezin, A. A.; Constantinides, C. P.; Mirallai, S. I.; Manoli, M.; Cao, L. L.; Rawson, J. M.; Koutentis, P. A. Synthesis and properties of imidazolo-fused benzotriazinyl radicals. *Org. Biomol. Chem.* **2013**, *11*, 6780−6795.

(25) Constantinides, C. P.; Berezin, A. A.; Manoli, M.; Leitus, G. M.; Zissimou, G.; Bendikov, M.; Rawson, J. M.; Koutentis, P. A. Structural, Magnetic, and Computational Correlations of Some Imidazolo-Fused 1,2,4-Benzotriazinyl Radicals. *Chem. - Eur. J.* **2014**, *20*, 5388−5396.

(26) Bodzioch, A.; Pomikło, D.; Celeda, M.; Pietrzak, A.; Kaszyński, P. 3-Substituted Benzo[e][1,2,4]triazines: Synthesis and Electronic Effects of the C(3) Substituent. *J. Org. Chem.* **2019**, *84*, 6377−6394.

(27) Neugebauer, F. A.; Umminger, I. 1,4-Dihydro-1,2,4-benzo-triazin-Radikalkationen. *Chem. Ber.* **1981**, *114*, 2423−2430.

(28) Takahashi, Y.; Miura, Y.; Yoshioka, N. Synthesis and properties of the 3-tert-butyl-7-trifluoromethyl-1,4-dihydro-1-phenyl-1,2,4-ben-zotriazin-4-yl radical. *New J. Chem.* **2015**, *39*, 4783−4789.

(29) Constantinides, C. P.; Berezin, A. A.; Zissimou, G. A.; Manoli, M.; Leitus, G. M.; Koutentis, P. A. The Suppression of Columnar π-Stacking in 3-Adamantyl-1-phenyl-1,4-dihydrobenzo[e][1,2,4]triazin-4-yl. *Molecules* **2016**, *21*, 636−642.

(30) For details, see the Supporting Information.

(31) Parr, R. G.; Yang, W. Density functional approach to the frontier-electron theory of chemical reactivity. *J. Am. Chem. Soc.* **1984**, *106*, 4049−4050.

(32) Yang, W.; Mortier, W. J. The use of global and local molecular parameters for the analysis of the gas-phase basicity of amines. *J. Am. Chem. Soc.* **1986**, *108*, 5708−5711.

(33) Hansch, C.; Leo, A.; Taft, R. W. A survey of Hammett substituent constants and resonance and field parameters. *Chem. Rev.* **1991**, *91*, 165−195.

(34) Connelly, N. G.; Geiger, W. E. Chemical Redox Agents for Organometallic Chemistry. *Chem. Rev.* **1996**, *96*, 877−910.

(35) Cardona, C. M.; Li, W.; Kaifer, A. E.; Stockdale, D.; Bazan, G. C. Electrochemical Considerations for Determining Absolute Frontier Orbital Energy Levels of Conjugated Polymers for Solar Cell Applications. *Adv. Mater.* **2011**, *23*, 2367−2371.

(36) *The Amino Group*; Patai, S., Ed.; John Wiley & Sons, 1968.

Pomikło, D.; Bodzioch, A.; Kaszyński, P. "3-Substituted Blatter radicals: cyclization of *N*-arylguanidines and *N*-arylamidines to benzo[*e*][1,2,4]triazines and PhLi addition"

J. Org. Chem. **2023**, *88*, 2999–3011.

3-Substituted Blatter Radicals: Cyclization of *N*-Arylguanidines and *N*-Arylamidines to Benzo[*e*][1,2,4]triazines and PhLi Addition

Dominika Pomikło, Agnieszka Bodzioch,* and Piotr Kaszyński*

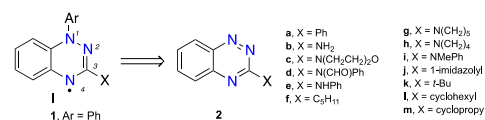ACCESS | Metrics & More | Article Recommendations | Supporting Information

ABSTRACT: A series of 3-amino- and 3-alkyl-substituted 1-phenyl-1,4-dihydrobenzo[*e*][1,2,4]triazin-4-yls was prepared in four steps involving N-arylation, cyclization of *N*-arylguanidines and *N*-arylamidines, reduction of the resulting *N*-oxides to benzo[*e*][1,2,4]triazines, and subsequent addition of PhLi followed by aerial oxidation. The resulting seven C(3)-substituted benzo[*e*][1,2,4]triazin-4-yls were analyzed by spectroscopic and electrochemical methods augmented with density functional theory (DFT) methods. Electrochemical data were compared to DFT results and correlated with substituent parameters.

X = morpholinyl, piperidinyl, pyrrolidinyl, NMePh, *t*-Bu, cyclohexyl, cyclopropyl
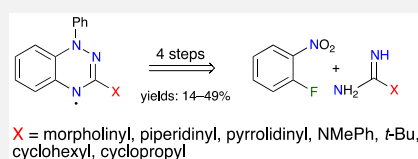
INTRODUCTION

Benzo[*e*][1,2,4]triazin-4-yls **I**,[1−3] derivatives of the prototypical Blatter radical[4] (**1a**, X = Ph, Figure 1), are increasingly important elements of advanced materials investigated in the context of controlled polymerization,[5] organic batteries,[6−8] photoconductive liquid crystals,[9−14] surface functionalization,[15] molecular electronics,[16] sensory,[17,18] and spintronic[19] applications. These investigations have stimulated advancement in chemistry of the benzo[*e*][1,2,4]triazinyls[20−22] and preparation of materials with tailored properties. One of the methods for the synthesis of Blatter radical derivatives of the general structure **I** involves azaphilic addition of ArLi to benzo[*e*][1,2,4]triazines **2** (Figure 1).[23] This method permitted the preparation of paramagnetic liquid crystals[9−13] and C(3) functional derivatives of Blatter radical, including the 3-amino **1b** and 3-(morpholin-4-yl) **1c**.[24] Another derivative, containing substituent X = N(CHO)Ph at the C(3) position (**1d**), was obtained by a rearrangement of a stable carbene and hydrolyzed to **1e** (X = NHPh).[25]

An analysis of literature data indicates that the 3-amino substituent in benzo[*e*][1,2,4]triazin-4-yl derivatives is particularly effective in the modification of electronic properties of the radicals: it effects a significant cathodic shift of the oxidation potential and a bathochromic shift in the electronic absorption, relative to the prototypical Blatter radical **1a**.[24]

a, X = Ph
b, X = NH₂
c, X = N(CH₂CH₂)₂O
d, X = N(CHO)Ph
e, X = NHPh
f, X = C₅H₁₁
g, X = N(CH₂)₅
h, X = N(CH₂)₄
i, X = NMePh
j, X = 1-imidazolyl
k, X = *t*-Bu
l, X = cyclohexyl
m, X = cyclopropyl

Figure 1. Preparation of Blatter radicals **I** by azaphilic addition of ArLi to benzo[*e*][1,2,4]triazines **2**.

Similar, although less pronounced effects, were observed for the 3-pentyl derivative **1f**.[24] For these reasons, 3-amino and 3-alkyl derivatives **1** are of interest for the fine-tuning of electronic properties of the benzo[*e*][1,2,4]triazinyl system and also in the context of our program in self-organizing paramagnetic materials[9−13] with controlled photophysical and redox behavior. In addition, 3-aminobenzo[*e*][1,2,4]-triazines, direct precursors to the radicals, have been demonstrated to possess antimalarial,[26] antitumor,[27,28] and *Abl* enzyme-inhibiting[29] activities, while their 1,4-dioxides are bioreductive antitumor agents with selective toxicity to oxygen-deprived (hypoxic) cells.[30−32]

The existing methods[24,25] for the preparation of 3-amino and 3-alkyl derivatives **I** rely mainly on benzo[*e*][1,2,4]-triazines **2**.[33,34] The requisite amines **2c** and **2e** were obtained from 3-chlorobenzo[*e*][1,2,4]triazine (**3**, Figure 2), while the 3-pentyl derivative **2f** was prepared in two steps from 3-iodobenzo[*e*][1,2,4]triazine-1-oxide (**4**).[33] Although the two halo derivatives **3** and **4** are general intermediates to a variety of such C(3)-substituted radicals,[24] their synthesis is a multistep process and involves poorly soluble intermediates, e.g., **5b**,[33,35] which is problematic for the preparation of polyradicals and more complex molecular systems. Therefore, in search for an alternative, more direct, and convenient method for the preparation of **2**, we focused on N-substituted guanidines **6** and amidines **7** as the starting materials. We have envisioned that their N-arylation with 1-fluoro-2-nitrobenzene
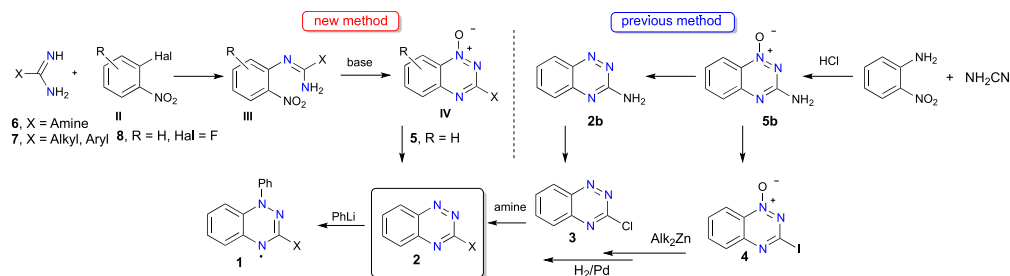
Figure 2. A comparison of two general strategies for the formation 3-substituted benzo[e][1,2,4]triazines **2**, precursors to radicals **1**.

(**8**) followed by cyclization could lead to the desired benzo[e][1,2,4]triazines **2** with the amino substituent of guanidine **6** and the alkyl residue of **7** incorporated at the C(3) position.

A literature search revealed that there are limited examples of N-arylation of the parent guanidine[35−39] **6** (X = NH$_2$) and amidines **7** (X = Me, Ph, RC$_6$H$_4$)[40] with 2-halonitroarenes **II**, via the S$_N$Ar mechanism, and formation of the substitution products **III** (Figure 2). In the absence of the activating NO$_2$ group, N-arylations of **6** and **7** are typically accomplished using Ullmann-type conditions (base and CuI).[41−45] Treatment of N-(2-nitroaryl)guanidine derivatives **III** (X = amine) with bases, such as NaOH, t-BuOK, or t-BuOLi, leads to 3-aminoareno[e][1,2,4]triazine-1-oxides **IV** (Figure 2).[30,35,38,46−49] The two processes, N-arylation and base-induced cyclization, are often combined into a one-pot reaction, and areno[1,2,4]triazine-1-oxides **IV** are isolated in good yields.[30] The analogous cyclization of N-(2-nitrophenyl)-amidines **III** (X = alkyl, aryl) in the presence of MeONa/MeOH was reported to lead also to benzo[e][1,2,4]triazine-1-oxides **IV**.[50] The substitution−cyclization tandem working for 2-halonitroarenes was different for reactions of nitronaphthalenes and nitroquinolines with guanidine and two amidines **7** (X = Ph, Me), for which a sequence of addition-oxidation-cyclization-deoxygenation was postulated as a one-pot process.[49]

Guanidines and amidines are often difficult to work with as reagents. Free guanidines are highly basic,[51] rapidly absorbing carbon dioxide and moisture and, like amidines, are thermally unstable undergoing decomposition with a release of ammonia.[30,49] On the other hand, the guanidine functionality has been found in many natural products and pharmaceuticals, playing key roles in various biological functions.[52−54] Guanidine derivatives serve also as nucleophilic catalysts,[53,55] auxiliaries in asymmetric synthesis,[56] precursors for the synthesis of heterocycles,[45,56] anion recognition, and as ligands for metal complexes and clusters.[54]

Herein, we explore the synthetic access to four C(3)-amino (X = morpholin-4-yl **c**, piperidin-1-yl **g**, pyrrolidin-1-yl **h**, NMePh **i**, and imidazol-1-yl **j**, Figure 1) and three C(3)-alkyl (X = t-Bu **k**, cyclohexyl **l**, and cylopropyl **m**) benzo[e][1,2,4]-triazines **2** by nucleophilic aromatic guanidinylation and amidinylation, respectively, of 1-fluoro-2-nitrobenzene (**8**). The cyclization of the corresponding N-arylguanidines and N-arylamidines gave a series of N-oxides **5**, which were deoxygenated. The resulting benzo[e][1,2,4]triazines **2** were converted by azaphilic addition of PhLi to radicals **1**, which were investigated by spectroscopic and electrochemical methods. The experimental data were compared with density functional theory (DFT) computational results and substituent parameters.

■ RESULTS AND DISCUSSION

Preparation of Guanidines 6. Classical syntheses of guanidines involve mainly cyanamides, carbodiimides, thiourea, and isocyanide-based precursors or guanylating reagents, such as S-methylisothioureas, pyrazole-1-carboximidamide and its derivatives, or triflyl guanidines.[57,58] In spite of a variety of known methods, most of them involve harmful precursors or harsh reaction conditions. For our purpose, substituted guanidines **6** were obtained as hydrochorides **6·HCl** using relatively safe reactions of amines with commercially available S-methylisothiourea guanylation agent **9** (Scheme 1, Method

Scheme 1. Preparation of Guanidine (6·HCl) and Amidine (7·HCl) Hydrochlorides[a]
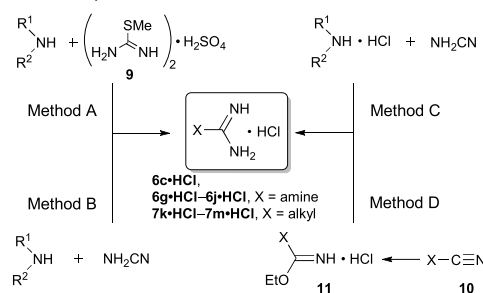
[a]*Reagents and conditions*: Method A: (1) H$_2$O, reflux, overnight; (2) BaCl$_2$, reflux, 1h. Method B: HCl, EtOH, reflux, overnight. Method C: pH 8−9, H$_2$O, reflux, overnight. Method D: (1) HCl, EtOH, 0 °C, overnight; (2) dry EtOH, NH$_3$ gas, rt, overnight.

A). Thus, following the literature procedure,[59] reaction of 2-methyl-2-thiopseudourea sulfate (**9**) with morpholine proceeded smoothly giving the desired morpholine-4-carboximidamide hydrochloride (**6c·HCl**) in 90% yield after 2 h. Contrary to the literature report,[59] the synthesis of piperidine-1-carboximidamide hydrochloride (**6g·HCl**) required significant elongation of the reaction time, and even after 48 h an inseparable mixture of the desired guanidine hydrochloride **6g·HCl** and piperidine hydrochloride was obtained. Therefore, an additional amount (1 equiv) of 2-methyl-2-thiopseudourea sulfate (**9**) was added, and the reaction was conducted for

another 24 h giving the complete transformation. A similar result was obtained in reaction of **9** with *N*-methylaniline. Therefore, a strategy involving reaction of the amine with cyanamide in the presence of HCl was explored (Scheme 1, Method B).[60] Thus, a reaction of cyanamide with morpholine and *N*-methylaniline gave the corresponding guanidine hydrochlorides **6c·HCl** and **6i·HCl** in 75% and 74% yields, respectively. On the other hand, attempts at a synthesis of piperidine-1-carboximidamide hydrochloride (**6g·HCl**) gave only piperidine hydrochloride under these conditions. Finally, condensing piperidine hydrochloride with cyanamide in a buffered solution (pH = 8−9) consisting of piperidine hydrochloride and piperidine provided **6g·HCl** in 91% yield (Scheme 1, Method C).[61] The same strategy was used for the preparation of guanidine hydrochlorides containing pyrrolidin-1-yl (**6h·HCl**) and imidazol-1-yl (**6j·HCl**) substituents in 86% and 48% yields, respectively.

Preparation of Amidines 7. Amidine hydrochlorides containing *t*-Bu (**7k·HCl**) and *c*-Hex (**7l·HCl**) substituents were obtained via the Pinner reaction.[57] Thus, an acid-induced reaction of the appropriate nitrile **10** with dry EtOH resulted in the formation of imino ester salts **11·HCl**, which were reacted with ammonia to form the desired amidine hydrochlorides **7k·HCl** and **7l·HCl** in 81% and 90% yields, respectively (Scheme 1, Method D). Cyclopropanecarboxamidine hydrochloride (**7m·HCl**) was commercially available.

N-Arylation and Cyclization to Benzo[e][1,2,4]-triazine-1-oxides 5. N-Substituted guanidine hydrochlorides **6·HCl** and amidine hydrochlorides **7·HCl** were used as key substrates for the synthesis of C(3)-amino and C(3)-alkyl derivatives of Blatter radicals **1** via a three-step procedure involving: (1) nucleophilic aromatic substitution of 1-fluoro-2-nitrobenzene (**8**) with free guanidine **6** or amidine **7** followed by base-induced cyclization,[30,38] (2) reduction of *N*-oxides **5**, and, finally (3) addition of PhLi to the obtained benzo[e]-[1,24]triazines **2** (Figure 2).

Initial experiments involved a reaction of **8** with morpholine-4-carboximidamide (**6c**), which was liberated from **6c·HCl** using equivalent amounts of EtONa in EtOH. The strong basicity of guanidine derivatives considerably limits the type of solvent, which can be used for this reaction. Following a literature report,[30] tetrahydrofuran (THF) was selected as the solvent for this reaction. However, due to low solubility of free guanidine **6c** in THF at both ambient and elevated temperatures, 25% v/v of dimethyl sulfoxide (DMSO) was added to the reaction mixture. After 12 h at 70 °C thin layer chromatography (TLC) showed a highly polar product suggesting the formation of substitution product **12c** (Scheme 2), which was accompanied by unreacted 1-fluoro-2-nitrobenzene (**8**). Addition of 1.5 equiv of *t*-BuOK initialized the cyclization reaction; however, after 3 h at 70 °C, TLC still showed the unreacted substitution product **12c**. Therefore, additional amounts of *t*-BuOK (1.5 equiv) were added, and the reaction time was extend for another 12 h giving the desired 3-(morpholin-4-yl)benzo[e][1,2,4]triazine-1-oxide (**5c**) in an overall yield of 65% (Scheme 2). A similar strategy was applied for substitution of 1-fluoro-2-nitrobenzene (**8**) with other guanidine derivatives containing piperidine and *N*-methylaniline moiety providing the corresponding *N*-oxides **5g** and **5i** in 25% and 42% yields, respectively.

In all cases TLC analysis showed the presence of unreacted 1-fluoro-2-nitrobenzene (**8**) after the substitution step. Therefore, to improve conversion of **8**, 6 equiv of guanidine **6** was

Scheme 2. Optimized Reaction Conditions for Synthesis of *N*-Oxide 5c[a]
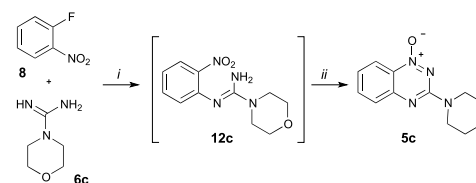
[a]*Reagents and conditions*: (*i*) **8**, MeCN, 78 °C, overnight; (*ii*) *t*-BuOK, MeCN, 78 °C, 3 h.

used. In addition, the solvent mixture (THF/DMSO) was replaced with MeCN to simplify the reaction workup procedure. Under these conditions, the nucleophilic aromatic guanidinylation of **8** with morpholine guanidine **6c** showed full conversion of **8** to **12c** (TLC analysis), which after *t*-BuOK-promoted cyclization, provided *N*-oxide **5c** in 72% yield (Table 1). Following this one-pot procedure, substitution of **8** with
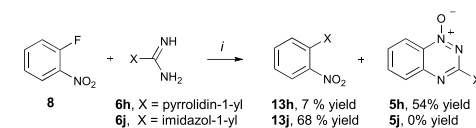
Table 1. Synthesis of Radicals 1

Guanidine **6**/ amidine **7**	*N*-Oxide **5** (yield %)[a]	Benzotriazine **2** (yield %)	Radical **1** (yield %)
c, X = morpholin-4-yl	72[b]	99	67
g, X = piperidin-1-yl	54[b]	99	86
h, X = pyrrolidin-1-yl	70[c]	95	72
i, X = NMePh	63[b]	99	73
k, X = *t*-Bu	25[d]	99	76
l, X = cyclohexyl	22[d]	99	79
m, X = cyclopropyl	17[d]	99	84

[a]Isolated yields obtained for optimized reaction conditions. [b]*t*-BuOK promoted cyclization. [c]Without *t*-BuOK. [d]Two-step procedure with MeONa-promoted cyclization.

piperidin-1-yl (**6g**) and *N*-methyl-*N*-phenyl (**6i**) guanidines gave the corresponding *N*-oxides **5** in 54% and 63% yields, respectively. Surprisingly, the reaction of **8** with pyrrolidine-1-carboxamidine (**6h**) proceeded smoothly providing the desired *N*-oxide **5h** in 70% yield during the substitution step (Table 1) without the need of *t*-BuOK. The formation of **5h** was accompanied by **13h** as a substitution product of the fluorine atom with pyrrolidine (Scheme 3). Under the reaction conditions, imidazole guanidine **6j** underwent a complete decomposition to imidazole, which reacted with 1-fluoro-2-nitrobenzene (**8**) giving **13j** as the substitution product isolated in 68% yield (Scheme 3). Subsequent catalytic (Pd/C) hydrogenation of *N*-oxides **5** in EtOH/AcOEt gave 3-

Scheme 3. Reaction of 8 with Guanidines 6h and 6j[a]

6h, X = pyrrolidin-1-yl   **13h**, 7 % yield   **5h**, 54% yield
6j, X = imidazol-1-yl   **13j**, 68 % yield   **5j**, 0% yield
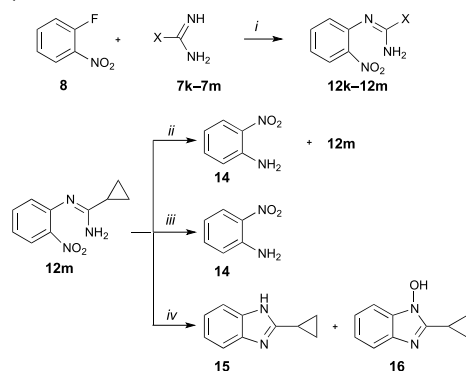
[a]*Reagents and conditions*: (*i*) **8**, MeCN, 78 °C, overnight.

aminobenzo[*e*][1,2,4]triazines **2** in nearly quantitative yields (Figure 2, Table 1).

The methodology developed for the synthesis of 3-amino derivatives **2** was extended to conversion of amidines **7** to 3-alkyl substituted benzo[*e*][1,2,4]triazines **2**. The formation of amidine-substituted products **12k−12m** was observed by TLC during the reaction of amidines **7** with **8**; however, cyclization under the previously applied conditions (*t*-BuOK) gave complex mixtures of products without formation of the desired *N*-oxides **5k−5m**. Therefore, the arylation products **12k−12m** were isolated (yields 88−94%) from the reaction of 1-fluoro-2-nitrobenzene (**8**) with amidines **7k−7m**, and several cyclization reactions were tested (Scheme 4). Thus, a reaction

Scheme 4. Nucleophilic Aromatic Substitution of 1-Fluoro-2-nitrobenzene (8) with Amidines 7k−7m and Attempts at Cyclization of 12m

[a]Reagents and conditions: (*i*) **8**, MeCN, 70 °C, overnight; (*ii*) 10% NaOH, EtOH, 78 °C, overnight; (*iii*) cat. HCl, EtOH, 78 °C, overnight; (*iv*) H₂, Pd/C, EtOH, rt, overnight.

of **12m** with 10% NaOH[46] or with catalytic amounts of HCl in EtOH gave only the unreacted substrate **12m** after overnight stirring at room temperature. Increasing the temperature to 60 °C resulted in the formation of trace amounts of 2-nitroaniline (**14**), which accompanied the unreacted **12m**. Finally, overnight reflux of an ethanolic solution of **12m** with 10% NaOH gave 16% of **14** (based on ¹H NMR), while the same with catalytic amounts of HCl gave **14** in 72% yield (based on ¹H NMR) (Scheme 4). Formation of small amounts of 2-nitroaniline (**14**) was also observed for **12m** in refluxing EtOH. The same results were obtained for reactions of **12l** and **12k** with NaOH and HCl in EtOH. On the other hand, an attempted transformation of **12m** to the corresponding *N*-oxide under reductive conditions (Pd/C, H₂) resulted in cyclization to benzimidazole derivatives **15** and **16** isolated in 16% and 82% yields, respectively (Scheme 4).

Due to the lack of success in the cyclization of **12m** to *N*-oxide **5m** using typical conditions, it was decided to use MeONa as the cyclization-promoting reagent previously reported for the synthesis of 3-phenylbenzo[*e*][1,2,4]triazine-1-oxide (**5a**).[50] In our hands a one-pot synthesis of *N*-oxide **5a**, involving N-arylation of **8** with amidine **7a** in MeOH and subsequent treatment with MeONa, provided the desired product **5a** in 61% yield. A similar strategy applied in the

synthesis of **5k−5m** resulted in the formation of 2-nitroanisole as the main product. To avoid this undesired process, it was decided to follow a two-step procedure with the isolation of substitution products **12k−12m**. Thus, cyclization of the isolated **12k−12m** using 1.5 equiv of MeONa in MeOH gave the corresponding *N*-oxides **5k−5m** in 17−25% yields (Table 1).

Preparation of C(3)-Substituted Radicals 1. 3-Amino- and 3-alkyl substituted benzo[*e*][1,2,4]triazines **2** were reacted with PhLi (Figure 2) giving the desired radicals **1** in good yields (Table 1). In comparison to morpholine derivative **1c**,[24] radicals **1g−1i** were unstable during purification by column chromatography (Et₃N passivated silica gel, neutral aluminum oxide, or neutral Florosil) and underwent fast decomposition to highly polar purple products, presumably iminoquinone type,[62,63] which could not be eluted from the column. Therefore, radicals **1g−1i** were purified by passing the crude mixture through a short diatomaceous earth pad (Cellite), washing the residue with *n*-pentane, and finally recrystallization from *n*-heptane. A similar purification process was used to obtain pure 3-alkyl-substituted radicals **1k−1m**. Following this procedure, radicals **1g−1i** and **1k−1m** were obtained in 67−86% yields from **2** (Table 1). All newly prepared radicals are solids except for cyclohexyl and cyclopropyl derivatives **1l** and **1m**, which are liquids and thus slowly decompose on standing.

Characterization of Radicals 1. Analysis of the radicals in series **1** revealed the effects of the C(3) substituent on the spectroscopic and electrochemical properties. Thus, all radicals exhibit broad, low-intensity absorption bands in the visible range up to 700 nm for C(3)-amino derivatives **1c** and **1g−1i** and up to 600 nm for C(3)-alkyl derivatives **1k−1m**, with poorly defined absorption maxima. The most pronounced bathochromic effect on the absorption spectrum is exhibited by the 3-pyrrolidinyl derivative **1h** (Figure 3). The observed trend
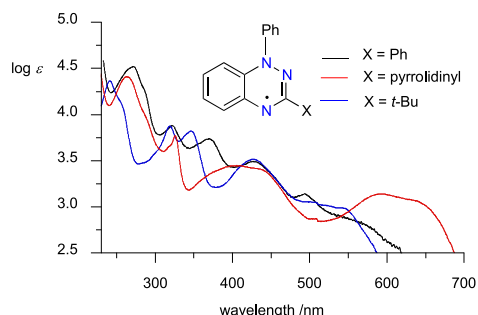
Figure 3. UV−Vis spectra for Blatter **1a** (black), 3-pyrrolidinyl **1h** (red), and 3-*t*-Bu **1k** (blue) radicals in CH₂Cl₂.

in excitation energies (Table 2) is well-reproduced computationally. A time-dependent density functional theory (TD DFT) analysis indicates that the lowest-energy excitation calculated at about 500 nm for C(3)-amino radicals **1c** and **1g−1i** is of the π−π* type involving the β-HOMO → β-LUMO transition (HOMO = highest occupied molecular orbital; LUMO = lowest unoccupied molecular orbital), while for C(3)-phenyl radical **1a** it involves mainly the α-HOMO → α-LUMO transition (Figure 4). On the other hand, a TD DFT analysis of C(3)-alkyl derivatives **1k−1m** suggests comparable

Table 2. Selected Experimental and Calculated Electronic Parameters for C(3)-Substituted Benzo[e][1,2,4]triazin-4-yls 1

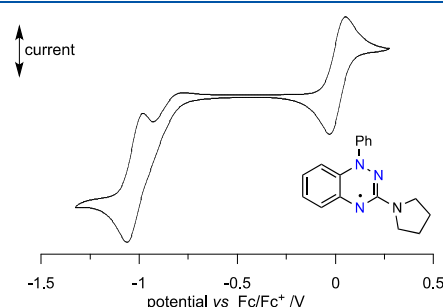| radical	λ_{max} exp[a] /nm	λ_{max} theor[b] /nm	$E_{\alpha\text{-HOMO}}$[b] /eV	$E_{\beta\text{-LUMO}}$[b] /eV	E1/2−1/0[c] /V	E1/2[0/ + 1c] /V	E_{cell}[d] /V	$a_{N(1)}$[e] /G	$a_{N(2)}$[e] /G	$a_{N(4)}$[e] /G
1a[f]	492	516	−6.240	−1.690	−0.92	0.28	1.20	7.65	4.87	4.90
1b[f]	565	478	−6.198	−1.607	−0.956	0.150	1.106	7.96	4.24	5.71
1c[f]	584	514	−6.127	−1.530	−0.981	0.083	1.064	7.99	4.13	5.75
1g	593	531	−6.060	−1.466	−1.001	0.021	1.022	7.79	4.09	5.88
1h	595	534	−6.047	−1.457	−1.021	0.012	1.033	7.83	4.07	5.93
1i	590	514	−6.128	−1.535	−0.921	0.088	1.009	7.78	4.21	5.72
1k	545	462	−6.171	−1.623	(−1.028)[g]	0.218	–	7.46	4.82	5.34
1l	545	462	−6.192	−1.639	(−0.994)[g]	0.218	–	7.54	5.02	5.02
1m	548	466	−6.196	−1.650	(−1.008)[g]	0.218	–	7.52	4.96	4.96

[a]The lowest-energy absorption band recorded in CH_2Cl_2. [b]Obtained at the TD UCAM-B3LYP/6-31++G(2d,p)//UB3LYP/6-31G(2d,p) level of theory in CH_2Cl_2 dielectric medium. [c]Potentials vs Fc/Fc$^+$ couple (0.46 V vs SCE).[64] Recorded in CH_2Cl_2 with $[n\text{-Bu}_4N]^+[PF_6]^-$ (50 mM), at ca. 20 °C, 50 mV s^{-1}, glassy carbon working electrode (2 mm disc). For details see the Supporting Information. [d]$E_{cell} = E_{1/2}^{0/+1} - E_{1/2}^{-1/0}$. [e]Recorded in benzene at ca. 20 °C. [f]Ref 24. [g]Cathodic potential for irreversible reduction process.
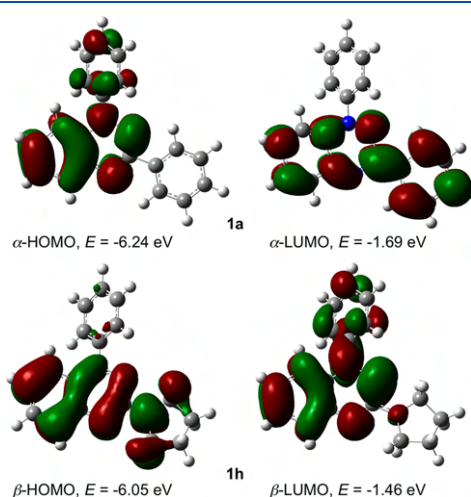
Figure 4. TD UCAM-B3LYP/6-31++G(2d,p)//UB3LYP/6-31G-(2d,p) derived contours (isovalue = 0.02) and energies of molecular orbitals in CH_2Cl_2 dielectric medium relevant to the lowest-energy excitations in **1a** and **1h**.

Figure 5. Cyclic voltammograms for **1h** (0.5 mM) in CH_2Cl_2 $[n\text{-Bu}_4N]^+[PF_6]^-$ (50 mM) vs Fc/Fc$^+$, ca. 20 °C, 50 mV s^{-1}, glassy carbon electrode (2 mm disc), scan starting at 0 V in the anodic direction. For details see the Supporting Information.

contributions of α-HOMO → α-LUMO and β-HOMO → β-LUMO transitions to the lowest-energy excitations calculated at about 460 nm. The difference in the origin of the lowest-energy excitation is due to destabilization of the β-HOMO by the amine lone pair and consequent narrowing of the β-HOMO-β-LUMO energy gap (Figure 4 and Supporting Information). Thus, the energy of the β-HOMO in amines is up to 0.7 eV higher than that in the prototypical **1a**.

Results of electrochemical analysis of radicals **1g**−**1i** are generally consistent with those previously obtained for morpholine derivative **1c**,[24] showing quasi-reversible oxidation and reduction processes. The only exception are two radicals with the most basic substituents, piperidinyl **1g** and pyrrolidinyl **1h**, for which reduction is a complex, presumably 2e$^-$ process involving a chemical step, such as protonation (Figure 5). Similar results were obtained for the C(3)−alkyl derivatives **1k**−**1m**, which exhibit an essentially irreversible, presumably 2e$^-$ reduction process (see the Supporting Information). For the purpose of comparative analyses, the
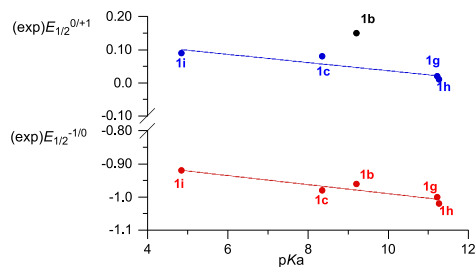
reduction potential $E_{1/2}^{-1/0}$ for two C(3)−amino radicals **1g** and **1h** was derived from the cathodic and anodic peak potentials ($\Delta E \approx 80$ mV).

A comparison of redox potentials in series **1** shows that replacement of the Ph substituent at the C(3) position in the parent Blatter radical **1a** with an amino group lowers the oxidation potential $E_{1/2}^{0/+1}$ by 0.19 V in **1i** and up to 0.27 V in **1h** (Table 2). Replacement of the Ph group in the Blatter radical **1a**, with an alkyl substituent in series **1k**−**1m**, also causes an anodic shift of the potentials, although to a lesser extent, when compared to the amines (Table 2).

For a quantitative analysis of the substituent effect on redox behavior of 3-amino-substituted derivatives **1**, the pK_a values of the corresponding amines[65] were used, since Hammett constants are not available for many of these substituents. Thus, both oxidation and reduction potentials correlate well with the pK_a values[65] of the corresponding amines (Figure 6); the increasing basicity of the amine corresponds to more cathodic redox potentials. The only exception from this trend is **1b** (X = NH$_2$), for which, $E_{1/2}^{0/+1}$ is too anodic by about 0.1 V, according to the correlation.

The oxidation process in series **1** shown in Figure 7 was modeled using the (U)B3LYP/6-31++G(2d,p)//(U)B3LYP/6-31G(2d,p) level of theory in CH_2Cl_2 dielectric medium. The obtained free energy of the process was expressed in volts and corrected for the absolute potential of the standard hydrogen electrode[66] (SHE) corrected for the Fc/Fc$^+$ potential versus

Figure 6. Plot of half-wave oxidation $(E_{1/2}^{0/+1})$ and reduction $(E_{1/2}^{-1/0})$ potentials in C(3)-amino series **1** vs pK_a for the corresponding amines.
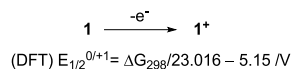
Figure 7. Oxidation of radicals **1** and conversion of the calculated ΔG_{298} in kcal mol^{-1} to the oxidation potential $E_{1/2}^{0/+1}$ in V vs Fc/Fc$^+$.

SHE (+0.71 V at 25 °C) giving the calculated oxidation potential (DFT)$E_{1/2}^{0/+1}$. Calculated potentials (DFT)$E_{1/2}^{0/+1}$ generally correlate well with the experimental $E_{1/2}^{0/+1}$ values, showing that the experimental potentials are systematically underestimated by 0.605(3) V by the DFT method (Figure 8).
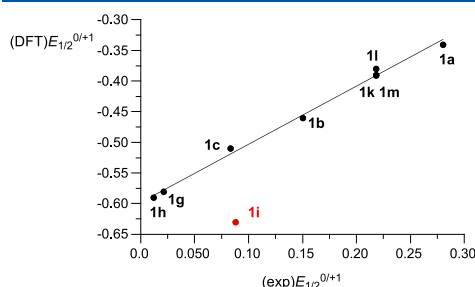
Figure 8. A comparison of experimental and DFT-calculated oxidation potentials $E_{1/2}$ in series **1**. Best-fit line excluding the data point for **1i**: (DFT)$E_{1/2}^{0/+1}$ = (exp)$E_{1/2}^{0/+1}$ − 0.605(3), r^2 = 0.992.

The only exception from this trend is **1i**, for which the calculated value of oxidation potential is underestimated by about 0.1 eV presumably due to conformational aspects of the NMePh substituent not correctly accounted for by calculations.

Radicals **1** exhibit typical EPR spectra consisting of seven principal lines resulting from splitting with three ^{14}N nuclei (e.g., **1m** in Figure 9). The experimental hyperfine coupling constants (*hfcc*) values depend on the C(3) substituent. Thus, in comparison to the prototypical Blatter radical **1a**, introduction of an amino substituent at C(3) increases the spin density at the N(1) and N(4) atoms resulting in higher $a_{N(1)}$ and $a_{N(4)}$ *hfcc* values. At the same time, concentration of the electron spin decreases on the N(2) atom and, consequently, diminishes the $a_{N(2)}$ *hfcc* values (Table 2). In the case of C(3)-alkyl derivatives **1k**−**1m** a slight decrease of
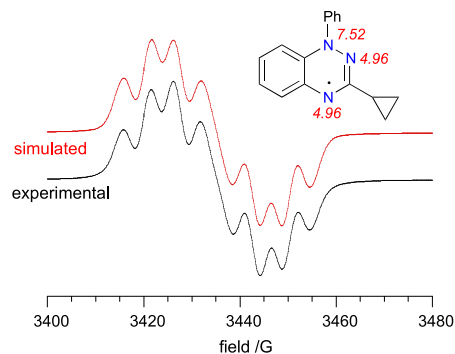
Figure 9. Experimental (black) and simulated (red) EPR spectra for radical **1m** recorded in benzene. (inset) An assignment of the resulting *hfcc*.

$a_{N(1)}$ *hfcc* values and slight increase of the $a_{N(4)}$ *hfcc* values are observed.

DFT calculations reproduced reasonably well the trend in the experimental *hfcc* values for series **1**. Correlations shown in Figure 10 demonstrate that the DFT method underestimates
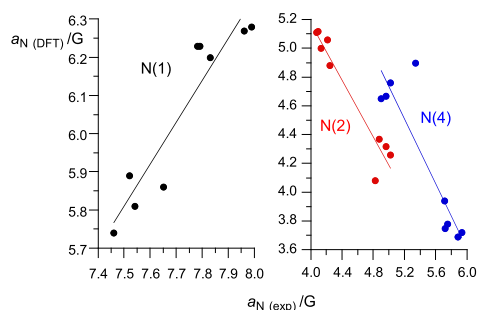
Figure 10. A comparison of experimental and DFT-calculated *hfcc* for the ring nitrogen atoms in series **1**. Calculated at the UCAM-B3LYP/EPR-III//UB3LYP/6-31G(2d,p) level of theory in benzene dielectric medium.

$a_{N(1)}$ values by 1.7 G and $a_{N(4)}$ up to 2.2 G for **1h** (X = pyrrolidyn-1-yl). The largest differences between the experimental and DFT-derived values are observed for **1l** (X = cyclohexyl), which may be related, in part, to the conformational mobility of the substituents not taken into account in calcuations.

■ CONCLUSIONS

In summary, we have demonstrated that benzo[*e*][1,2,4]-triazines **2** with a range of amino and alkyl substituents at the C(3) position are available by cyclization of the appropriate *N*-arylguanidines and *N*-arylamidines followed by reduction of the resulting *N*-oxides **5**. Thus, four C(3)-amino substituted *N*-oxides **5** have been prepared in good yields (up to 72%) using a one-pot process including *N*-arylation of 1-fluoro-2-nitro-benzene (**8**) with guanidines **6** followed by *t*-BuOK-promoted cyclization of the resulting *N*-arylguanidines. In contrast,

synthesis of three C(3)-alkyl *N*-oxides **5** required isolation of the intermediate *N*-arylamidines **12** and their subsequent MeONa-promoted cyclization to **5** isolated in lower yields (up to 25%). The deoxygenation of **5** proceeds smoothly in all cases giving the desired benzo[*e*][1,2,4]triazines **2**, which were finally converted in good yields (up to 86%) to the corresponding C(3)-substituted radicals **1** by addition of PhLi.

In contrast to most Blatter radicals, the radicals in series **1** exhibit limited stability to chromatographic solid support. They can, however, be easily purified by passing through a short diatomaceous earth pad, washing with *n*-pentane, and recrystallization from *n*-heptane. Most radicals **1** are stable after isolation except those containing cyclohexyl (**1l**) and cyclopropyl (**1m**) substituents at the C(3) position, which are liquids and thus slowly decompose on standing.

The experimental redox potentials of 3-amino derivatives **1** correlate well with pK_a values of the corresponding amines. A good correlation was also obtained for experimental and calculated (DFT) oxidation potentials ($E_{1/2}^{0/+1}$) of newly synthesized radicals **1**, which offers a tool for predicting oxidation potential values for other C(3)-amino derivatives.

A spectroscopic analysis augmented with TD DFT calculations revealed that the C(3) substituent impacts on the position and origin of the lowest π–π* excitation: The electron-donating group destabilizes the β-HOMO and narrows the HOMO–LUMO gap. Consequently, the lowest-energy excitation changes its character from a nearly pure α-HOMO → α-LUMO transition for the Blatter radical **1a**, through a comparable contribution of α-HOMO → α-LUMO and β-HOMO → β-LUMO transitions for C(3)-alkyl, to purely α-HOMO → α-LUMO for C(3)−amino derivatives **1**.

In comparison to the existing methods for the preparation of 3-amino and 3-alkyl derivatives of benzo[*e*][1,2,4]triazine **2**,[33] the presented methodology allows one to avoid multistep procedures with poorly soluble intermediates. It offers an alternative access to benzo[*e*][1,2,4]triazines **2**, which serve as convenient precursors to radicals **1** with greater control of their electrochemical and spectroscopic properties. This opens up new opportunities in structural manipulation with the C(3) substituent of benzo[*e*][1,2,4]triazin-4-yls providing a tool for the designing of radicals that show greater functional flexibility and structural variety for modern materials applications.

■ COMPUTATIONAL DETAILS

All calculations were carried out using the Gaussian 09 suite of programs.[67] Geometry optimizations were carried out at the UB3LYP/6-31G(2d,p) level of theory using tight convergence criteria and no symmetry constraints. Analytical second derivatives were computed using a vibrational analysis to confirm each stationary point to be a minimum by yielding zero imaginary frequencies.

Electronic excitation energies of radicals **1** in CH_2Cl_2 dielectric medium were obtained at the UCAM-B3LYP/6-31++G(2d,p) // UB3LYP/6-31G(2d,p) level of theory using the TD-DFT method.[68] The solvation model was implemented with the polarizable continuum model (PCM)[69] using the SCRF (solvent = CH_2Cl_2) keyword.

Isotropic Fermi contact coupling constants for radicals **1** were calculated using the UCAM-B3LYP/EPR-III // UB3LYP/6-31G(2d,p) method in benzene dielectric medium requested with the SCRF (solvent = benzene) keyword (PCM model).[69] Other computational details are provided in the Supporting Information.

■ EXPERIMENTAL SECTION

General. Commercially reagents and solvents were used as obtained. Reactions were carried out under inert atmosphere (N_2 or Ar gas), and subsequent reaction workups were conducted in air. Heat for the reactions requiring elevated temperatures was supplied using oil baths. Volatiles were removed under reduced pressure. Reaction mixtures and column eluents were monitored by TLC using aluminum-backed thin layer chromatography plates (Merck Kieselgel 60 F_{254}). The plates were observed under UV light at 254 and 365 nm. Melting points were determined on a Melt-Temp II Apparatus in capillaries, and they are uncorrected. ^{1}H and ^{13}C{^{1}H} NMR spectra were obtained at 400 and 100 MHz, respectively, on a Bruker Avance NMR spectrometer in CDCl$_3$ and referenced to the solvent (δ = 7.26 ppm for ^{1}H and δ = 77.16 ppm for ^{13}C{^{1}H})[70] or in DMSO-d_6 and referenced to the solvent (δ = 2.50 ppm for ^{1}H and δ = 39.52 ppm for ^{13}C{^{1}H}),[70] unless otherwise specified. UV−Vis spectra were recorded on a Jasco V770 spectrophotometer in spectroscopic-grade CH_2Cl_2 at concentrations in the range of $(1.5–10) \times 10^{-5}$ M. IR spectra were recorded using a Nexus FT-IR Thermo Nilolet IR spectrometer in KBr pellets. High-resolution mass spectrometry (HRMS) measurements were performed using SYNAPT G2-Si High-Definition Mass Spectrometry equipped with an electrospray ionization (ESI) mass analyzer.

Preparation of Radicals 1. General Procedure.[23,24] A 1.75 M solution of PhLi (1.3 mmol, 1.3 equiv) in *n*-dibutyl ether was added dropwise to a stirred solution of the 3-substituted benzo[*e*][1,2,4]-triazine **2** (1 mmol, 1 equiv) in dry THF (8 mL, 0.13 M) at −78 °C under Ar atmosphere, and the resulting mixture was stirred for 40 min at −78 °C and then for 1 h at rt. The reaction flask was opened, and the stirring was continued overnight in air at rt. After evaporation of the solvent, the residue was dissolved in CH_2Cl_2 and passed through a short diatomaceous earth pad, and the solvent was evaporated. The obtained solid was treated with *n*-pentane, the solution was filtered, and the solvent was evaporated giving crude radical **1**, which was recrystallized from *n*-heptane.

3-(Piperidin-1-yl)-1-phenyl-1,4-dihydrobenzo[e][1,2,4]triazin-4-yl (1g). Following the general procedure, radical **1g** (116.7 mg, 86% yield) was obtained as a dark green solid starting from 99.6 mg (0.465 mmol) of 3-(piperidin-1-yl)benzo[*e*][1,2,4]triazine (**2g**). mp 115−117 °C (*n*-heptane). IR ν 2932, 2850, 1512, 1481, 1445, 1333, 1281, 1245, 1207, 1117, 1027, 953, 778, 739, 699, 608 cm^{-1}. UV−Vis (CH_2Cl_2) λ_{max} (log ε) 265 (4.44), 326 (3.83), 413 (3.50), 593 (3.17) nm. ESI(+)-MS, *m/z* 291 (38, [M]$^+$), 293 (100, [M + 2H]$^+$). HRMS (ESI+-TOF) *m/z* [M]$^+$ calcd for $C_{18}H_{19}N_4$ 291.1610, found 291.1606. Anal. Calcd for $C_{18}H_{19}N_4$: C, 74.20; H, 6.57; N, 19.23. Found: C, 74.23; H, 6.59; N, 19.11%.

3-(Pyrrolidin-1-yl)-1-phenyl-1,4-dihydrobenzo[e][1,2,4]triazin-4-yl (1h). Following the general procedure, radical **1h** (46.0 mg, 72% yield) was obtained as a dark green solid starting from 46.2 mg (0.230 mmol) of benzo[*e*][1,2,4]triazine **2h**. mp 134−135 °C (*n*-heptane). IR ν 3052, 2963, 2923, 2860, 1517, 1477, 1448, 1329, 1261, 1022, 750, 698 cm^{-1}. UV−Vis (CH_2Cl_2) λ_{max} (log ε) 264 (4.41), 326 (3.75), 412 (3.44), 595 (3.13) nm. ESI(+)-MS, *m/z* 277 (70, [M]$^+$), 279 (100, [M + 2H]$^+$). HRMS (ESI+-TOF) *m/z* [M]$^+$ calcd for $C_{17}H_{17}N_4$ 277.1453, found 277.1442. Anal. Calcd for $C_{17}H_{17}N_4$: C, 73.63; H, 6.18; N, 20.20; for $C_{17}H_{17}N_4 \cdot 1/4H_2O$: C, 72.44; H, 6.26; N, 19.88. Found: C, 72.48; H, 6.39; N, 19.18%.

3-(N-Methyl-N-phenylamino)-1-phenyl-1,4-dihydrobenzo[e]-[1,2,4]triazin-4-yl (1i). Following the general procedure, radical **1i** (19.0 mg, 73% yield) was obtained as a dark green solid starting from 20.1 mg (0.085 mmol) of benzo[*e*][1,2,4]triazine **2i**. mp 142−144 °C (*n*-heptane). IR ν 2931, 2850, 1594, 1476, 1399, 1334, 1116, 1026, 754, 693 cm^{-1}. UV−Vis (CH_2Cl_2) λ_{max} (log ε) 284 (4.41), 326 (3.85), 412 (3.50), 590 (3.19) nm. ESI(+)-MS, *m/z* 313 (50, [M]$^+$), 315 (100, [M + 2H]$^+$). HRMS (ESI+-TOF) *m/z* [M]$^+$ calcd for $C_{20}H_{17}N_4$ 313.1453, found 313.1456. Anal. Calcd for $C_{20}H_{17}N_4$: C, 76.65; H, 5.47; N, 17.88. Found: C, 76.25; H, 5.56; N, 17.59%.

3-(tert-Butyl)-1-phenyl-1,4-dihydrobenzo[e][1,2,4]triazin-4-yl (1k). Following the general procedure, radical **1k** (71.6 mg, 76% yield) was obtained as a dark purple solid starting from 66.6 mg (0.356

mmol) of benzo[e][1,2,4]triazine **2k**. mp 106−108 °C (*n*-heptane). IR *ν* 2957, 2926, 2862, 1581, 1479, 1399, 1328, 1247, 1188, 1071, 999, 779, 748, 697, 591 cm⁻¹. UV−Vis (CH₂Cl₂) λ_{max} (log *ε*) 241 (4.36), 318 (3.87), 347 (3.82), 427 (3.51), 545 (2.98) nm. ESI(+)-MS, m/z 265 (100, [M + H]⁺). HRMS (ESI+-TOF) m/z [M + H]⁺ calcd for C₁₇H₁₉N₃ 265.1579, found 265.1572. Anal. Calcd for C₁₇H₁₈N₃: C, 77.24; H, 6.86; N, 15.90. Found: C, 77.23; H, 6.88; N, 15.91%.

3-(Cyclohexyl)-1-phenyl-1,4-dihydrobenzo[e][1,2,4]triazin-4-yl (1l). Following the general procedure, radical **1l** (61.8 mg, 79% yield) was obtained as a dark red oil starting from 57.5 mg (0.270 mmol) of benzo[e][1,2,4]triazine **2l**. IR *ν* 2923, 2850, 1584, 1481, 1402, 1328, 1199, 742, 692, 671, 516 cm⁻¹. UV−Vis (CH₂Cl₂) λ_{max} (log *ε*) 242 (4.30), 319 (3.81), 349 (3.77), 425 (3.38), 545 (2.80) nm. ESI(+)-MS, m/z 291 (100, [M + H]⁺). HRMS (ESI+-TOF) m/z [M + H]⁺ calcd for C₁₉H₂₁N₃ 291.1735, found 291.1736.

3-(Cyclopropyl)-1-phenyl-1,4-dihydrobenzo[e][1,2,4]triazin-4-yl (1m). Following the general procedure, radical **1m** (46.5 mg, 84% yield) was obtained as a dark red oil starting from 38.2 mg (0.223 mmol) of benzo[e][1,2,4]triazine **2m**. IR *ν* 2922, 2850, 1582, 1482, 1429, 1336, 1200, 1025, 926, 872, 822, 745, 697, 615, 504 cm⁻¹. UV−Vis (CH₂Cl₂) λ_{max} (log *ε*) 244 (4.27), 320 (3.76), 356 (3.66), 426 (3.30), 548 (2.81) nm. ESI(+)-MS, m/z 249 (100, [M + H]⁺). HRMS (ESI+-TOF) m/z [M]⁺ calcd for C₁₆H₁₄N₃ 248.1188, found 248.1189.

Preparation of Benzo[e][1,2,4]triazines 2. General Procedure. A mixture of the appropriate 3-substituted benzo[e][1,2,4]-triazine-1-oxide **5** (1 mmol, 1 equiv) and 10% Pd/C (10 mol %) in EtOH/AcOEt (1:1, 6 mL) was stirred at rt under H₂ atmosphere (balloon) until the TLC analysis showed the absence of the starting material. The mixture was filtered through a short diatomaceous earth (Cellite) pad, and the solvent was evaporated giving benzo[e][1,2,4]-triazine **2** as a yellow solid.

3-(Morpholin-4-yl)benzo[e][1,2,4]triazine (2c).[33] Following the general procedure, benzo[e][1,2,4]triazine **2c** (46.0 mg, 99% yield) was obtained as a yellow solid starting from 49.8 mg (0.210 mmol) of N-oxide **5c**. Analytical data was identical to that reported previously.[33]

3-(Piperidin-1-yl)benzo[e][1,2,4]triazine (2g). Following the general procedure, benzo[e][1,2,4]triazine **2g** (46.1 mg, 99% yield) was obtained from 50.0 mg (0.220 mmol) of N-oxide **5g** as a yellow oil. ¹H NMR (CDCl₃, 400 MHz) *δ* 8.18 (d, *J* = 8.2 Hz, 1H), 7.66 (ddd, J_1 = 8.3 Hz, J_2 = 7.0 Hz, J_3 = 1.3 Hz, 1H), 7.54 (d, *J* = 8.5 Hz, 1H), 7.34 (ddd, J_1 = 8.1 Hz, J_2 = 7.0 Hz, J_3 = 1.1 Hz, 1H), 4.05 (t, *J* = 3.3 Hz, 4H), 1.75−1.69 (m, 6H). ¹³C{¹H} NMR (CDCl₃, 100 MHz) *δ* 158.7, 142.6, 142.2, 135.4, 129.8, 126.5, 124.6, 45.0, 25.9, 24.9. ESI(+)-MS, m/z 215 (100, [M + H]⁺). HRMS (ESI+-TOF) m/z [M + H]⁺ calcd for C₁₂H₁₅N₄ 215.1297, found 215.1299.

3-(Pyrrolidin-1-yl)benzo[e][1,2,4]triazine (2h). Following the general procedure, benzo[e][1,2,4]triazine **2h** (106 mg, 95%) was obtained from 120 mg (0.556 mmol) of N-oxide **5h**. Recrystallization from *n*-heptane gave analytically pure product. mp 83−84 °C (*n*-heptane). ¹H NMR (CDCl₃, 400 MHz) *δ* 8.22 (dd, J_1 = 8.4 Hz, J_2 = 0.9 Hz, 1H), 7.68 (ddd, J_1 = 8.3 Hz, J_2 = 6.7 Hz, J_3 = 1.4 Hz, 1H), 7.60 (d, *J* = 8.1 Hz, 1H), 7.36 (ddd, J_1 = 8.2 Hz, J_2 = 6.7 Hz, J_3 = 1.4 Hz, 1H), 3.84 (bs, 4H), 2.10 (t, *J* = 8.1 Hz, 4H). ¹³C{¹H} NMR (CDCl₃, 100 MHz) *δ* 157.4, 142.9, 142.4, 135.4, 130.0, 126.5, 124.4, 47.0, 25.6. ESI(+)-MS, m/z 201 (100, [M + H]⁺). HRMS (ESI+-TOF) m/z [M + H]⁺ calcd for C₁₁H₁₃N₄ 201.1140, found 201.1136. Anal. Calcd for C₁₁H₁₂N₄: C, 65.98; H, 6.04; N, 27.98. Found: C, 65.71; H, 5.93; N, 27.84%.

3-(N-Methyl-N-phenylamino)benzo[e][1,2,4]triazine (2i). Following the general procedure, benzo[e][1,2,4]triazine **2i** (98.0 mg, 99% yield) was obtained from 106.0 mg (0.421 mmol) of N-oxide **5i** as a yellow solid. Recrystallization from *n*-heptane gave analytically pure product. mp 98−99 °C (*n*-heptane). ¹H NMR (CDCl₃, 400 MHz) *δ* 8.25 (dd, J_1 = 8.4 Hz, J_2 = 0.9 Hz, 1H), 7.73 (ddd, J_1 = 8.3 Hz, J_2 = 6.7 Hz, J_3 = 1.4 Hz, 1H), 7.64 (d, *J* = 8.1 Hz, 1H), 7.48−7.41 (m, 5H), 7.32−7.30 (m, 1H), 3.74 (s, 3H). ¹³C{¹H} NMR (CDCl₃, 100 MHz) *δ* 159.0, 144.8, 143.0, 142.1, 135.6, 129.9, 129.5, 127.0, 126.5, 126.4, 125.5, 39.1. ESI(+)-MS, m/z 237 (100, [M + H]⁺). HRMS (ESI

+-TOF) m/z [M + H]⁺ calcd for C₁₄H₁₃N₄ 237.1140, found 237.1134. Anal. Calcd for C₁₄H₁₂N₄: C, 71.17; H, 5.12; N, 23.71. Found: C, 70.84; H, 4.95; N, 23.40%.

3-(tert-Butyl)benzo[e][1,2,4]triazine (2k).[71] Following the general procedure, benzo[e][1,2,4]triazine **2k** (84.2 mg, 99% yield) was obtained from 92.3 mg (0.454 mmol) of N-oxide **5k** as a yellow solid. The analytical data was identical to that reported previously.[67]

3-(Cyclohexyl)benzo[e][1,2,4]triazine (2l). Following the general procedure, benzo[e][1,2,4]triazine **2l** (95.5 mg, 99% yield) was obtained from 103.07 mg (0.452 mmol) of N-oxide **5l** as a yellow solid. Recrystallization from *n*-heptane gave analytically pure product. mp 62−63 °C (*n*-heptane). ¹H NMR (CDCl₃, 400 MHz) *δ* 8.49 (dd, J_1 = 8.5 Hz, J_2 = 0.5 Hz, 1H), 8.00 (d, *J* = 8.3 Hz, 1H), 7.93 (ddd, J_1 = 8.8 Hz, J_2 = 7.1 Hz, J_3 = 1.3 Hz, 1H), 7.80 (ddd, J_1 = 8.2 Hz, J_2 = 7.0 Hz, J_3 = 1.2 Hz, 1H), 3.40 (tt, J_1 = 11.7 Hz, J_2 = 3.4 Hz, 1H), 2.17 (d, *J* = 14.1 Hz, 2H), 1.98−1.76 (m, 5H), 1.52 (qt, J_1 = 12.5 Hz, J_3 = 3.1 Hz, 2H), 1.40 (tt, J_1 = 12.0 Hz, J_2 = 3.3 Hz, 1H). ¹³C{¹H} NMR (CDCl₃, 100 MHz) *δ* 169.7, 146.5, 141.1, 135.3, 129.9, 129.7, 128.8, 46.2, 32.1, 26.4, 26.0. ESI(+)-MS, m/z 214 (100, [M + H]⁺). HRMS (ESI+-TOF) m/z [M + H]⁺ calcd for C₁₃H₁₆N₃ 214.1344, found 214.1350. Anal. Calcd for C₁₃H₁₅N₃: C, 73.21; H, 7.09; N, 19.70. Found: C, 73.22; H, 7.13; N, 19.71%.

3-(Cyclopropyl)benzo[e][1,2,4]triazine (2m). Following the general procedure, benzo[e][1,2,4]triazine **2m** (90.6 mg, 99% yield) was obtained from 100.0 mg (0.535 mmol) of N-oxide **5m** as a yellow solid. Recrystallization from *n*-heptane gave analytically pure product. mp 62−64 °C (*n*-heptane). ¹H NMR (CDCl₃, 400 MHz) *δ* 8.43 (d, *J* = 8.5 Hz, 1H), 7.89−7.88 (m, 2H), 7.75−7.71 (m, 1H), 2.70 (tt, J_1 = 8.2 Hz, J_2 = 4.8 Hz, 1H), 1.44−1.40 (m, 2H), 1.31−1.26 (m, 2H). ¹³C{¹H} NMR (CDCl₃, 100 MHz) *δ* 167.5, 146.5, 141.0, 135.4, 129.7, 129.3, 128.3, 17.3, 12.0. ESI(+)-MS, m/z 172 (100, [M + H]⁺). HRMS (ESI+-TOF) m/z [M + H]⁺ calcd for C₁₀H₁₀N₃ 172.0875, found 172.0876. Anal. Calcd for C₁₀H₉N₃: C, 70.16; H, 5.30; N, 24.54. Found: C, 70.14; H, 5.28; N, 24.52%.

3-Phenylbenzo[e][1,2,4]triazine-1-oxide (5a).[50] A mixture of substituted amidine hydrochloride **7a·HCl** (700.0 mg, 4.47 mmol, 1 equiv) and MeONa (4.47 mmol, 1 equiv) in dry MeOH was stirred under N₂ conditions for 30 min at rt. The resulting precipitated inorganic salt was filtered through a syringe filter under N₂ athomphere. After evaporation of the solvent, the free amidine was dried under vacuum and dissolved in dry MeOH (5 mL). 1-Fluoro-2-nitrobenzene (**8**, 105.1 mg, 0.078 mL, 0.745 mmol, 0.17 equiv) was added, and the resulting mixture was refluxed overnight. Additional amounts of MeONa (0.745 mmol, 0.17 equiv) were added, and the stirring was continued under reflux for 2 h. After cooling to rt, the reaction mixture was placed in a refrigerator for 2 h, and the resulting white crystalline product was collected giving 101.2 mg (61% yield) of 3-phenylbenzo[e][1,2,4]triazine-1-oxide (**5a**). Recrystallization from MeOH gave analytically pure product. mp 126−128 °C (MeOH; lit.[50] mp 118−119 °C). ¹H NMR (CDCl₃, 400 MHz) *δ* 8.54−6.46 (m, 3H), 8.10−8.06 (m, 1H), 7.97−7.91 (m, 1H), 7.72−7.67 (m, 1H), 7.58−7.50 (m, 3H). ¹³C{¹H} NMR (CDCl₃, 100 MHz) *δ* 160.8, 147.9, 135.8, 134.2, 133.6, 132.1, 130.2, 129.5, 128.9, 128.6, 120.4. ESI(+)-MS, m/z 224 (100, [M + H]⁺). HRMS (ESI+-TOF) m/z [M + H]⁺ calcd for C₁₃H₁₀N₃O 224.0824, found 224.0824. Anal. Calcd for C₁₃H₉N₃O: C, 69.95; H, 4.06; N, 18.82. Found: C, 70.01; H, 3.98; N, 18.77%.

Preparation of N-Oxides 5c, 5g−5i. General Procedure. A mixture of the appropriate guanidine hydrochloride **6c·HCl**, **6g·HCl**−**6i·HCl** (6 mmol, 6 equiv) and EtONa (6 mmol, 6 equiv) in dry EtOH (0.9 mL, 1.11 M) was stirred under N₂ conditions for 30 min at rt. The resulting precipitated inorganic salt was filtered through a syringe filter under N₂ atmosphere. After evaporation of the solvent, the free guanidine **6** was dried under vacuum and dissolved in dry MeCN (0.8 mL/1 mmol). 1-Fluoro-2-nitrobenzene (**8**, 1 mmol, 1 equiv) was added, and the resulting mixture was stirred overnight at 78 °C. *t*-BuOK (1.5 mmol, 1.5 equiv) was added, and the stirring was continued at 78 °C. After 1 h an additional portion of *t*-BuOK (1.5 mmol, 1.5 equiv) was added, and the reaction was continued for 3 h. The solvent was evaporated, and the residue was dissolved in AcOEt

(10 mL) and washed with water (2×10 mL); the solvents were evaporated, and the residue was purified by column chromatography (pet. ether/AcOEt, 4:1) giving pure 3-substituted benzo[*e*][1,2,4]-triazine-1-oxide **5**.

3-(Morpholin-4-yl)benzo[e][1,2,4]triazine-1-oxide (5c). Following the general procedure, *N*-oxide **5c** (49.8 mg, 72% yield) was obtained as a yellow solid starting from morpholine-4-carboxamidine hydrochloride (**6c·HCl**, 300 mg, 1.80 mmol) and 1-fluoro-2-nitrobenzene (**8**, 42.3 mg, 31.2 mL, 0.30 mmol). Recrystallization from ethanol gave analytically pure product. mp 172–174 °C (EtOH). ^{1}H NMR (DMSO-*d$_6$*, 400 MHz) δ 8.15 (d, *J* = 8.6 Hz, 1H), 7.82 (ddd, *J$_1$* = 8.4 Hz, *J$_2$* = 7.1 Hz, *J$_3$* = 1.4 Hz, 1H), 7.60 (d, *J* = 8.5 Hz, 1H), 7.39 (ddd, *J$_1$* = 8.4 Hz, *J$_2$* = 7.1 Hz, *J$_3$* = 1.1 Hz, 1H), 3.73–3.75 (m, 4H), 3.69–3.71 (m, 4H). ^{13}C{^{1}H} NMR (DMSO-*d$_6$*, 100 MHz) δ 157.9, 148.2, 136.1, 129.6, 126.3, 125.5, 119.9, 65.8, 44.1. IR ν 1549, 1430, 1346, 1233, 1114, 999, 864, 759 cm^{-1}. ESI(+)-MS, *m/z* 233 (100, [M + H]$^+$). HRMS (ESI+-TOF) *m/z* [M + H]$^+$ calcd for C$_{11}$H$_{13}$N$_4$O$_2$ 233.1039, found 233.1038. Anal. Calcd for C$_{11}$H$_{12}$N$_4$O$_2$: C, 56.89; H, 5.21; N, 24.12. Found: C, 56.87; H, 5.19; N, 24.08%.

3-(Piperidin-1-yl)benzo[e][1,2,4]triazine-1-oxide (5g). Following the general procedure, *N*-oxide **5g** (90.8 mg, 54% yield) was obtained as a yellow solid starting from piperidine-1-carboxamidine hydrochloride (**6g·HCl**, 717 mg, 4.38 mmol) and 1-fluoro-2-nitrobenzene (**8**, 103 mg, 76.9 mL, 0.73 mmol). Recrystallization from *n*-heptane gave analytically pure product. mp 104–106 °C (*n*-heptane). ^{1}H NMR (DMSO-*d$_6$*, 400 MHz) δ 8.13 (dd, *J$_1$* = 8.6 Hz, *J$_2$* = 0.7 Hz, 1H), 7.79 (ddd, *J$_1$* = 8.4 Hz, *J$_2$* = 6.9 Hz, *J$_3$* = 1.3 Hz, 1H), 7.57 (d, *J* = 8.5 Hz, 1H), 7.24 (ddd, *J$_1$* = 8.3 Hz, *J$_2$* = 6.9 Hz, *J$_3$* = 1.0 Hz, 1H), 3.77 (t, *J* = 5.1 Hz, 4H), 1.66–1.65 (m, 2H), 1.59–1.58 (m, 4H). ^{13}C{^{1}H} NMR (DMSO-*d$_6$*, 100 MHz) δ 157.7, 148.5, 136.0, 129.2, 126.2, 124.9, 120.0, 44.6, 25.2, 24.1. IR ν 1544, 1414, 1340, 1277, 1229, 1131, 992, 851, 768 cm^{-1}. ESI(+)-MS, *m/z* 231 (100, [M + H]$^+$). HRMS (ESI+-TOF) *m/z* [M + H]$^+$ calcd for C$_{12}$H$_{15}$N$_4$O 231.1246, found 231.1245. Anal. Calcd for C$_{12}$H$_{14}$N$_4$O: C, 62.59; H, 6.13; N, 24.33. Found: C, 62.65; H, 6.09; N, 24.28%.

3-(Pyrrolidin-1-yl)benzo[e][1,2,4]triazine-1-oxide (5h). Derivative **5h** was obtained following the general procedure without the use of *t*-BuOK. Thus, using pyrrolidine-1-carboxamidine hydrochloride (**6h·HCl**, 1.32 g, 8.82 mmol) and 1-fluoro-2-nitrobenzene (**8**, 133 mg, 0.99 mL, 0.942 mmol), 3-(pyrrolidin-1-yl)benzo[*e*][1,2,4]triazine-1-oxide (**5h**) was isolated in 70% yield (142 mg) by column chromatography (pet. ether/AcOEt, 3:1). Recrystallization from EtOH gave analytically pure product. mp 180–182 °C (EtOH). ^{1}H NMR (DMSO-*d$_6$*, 400 MHz) δ 8.15 (dd, *J$_1$* = 8.6 Hz, *J$_2$* = 1.4 Hz, 1H), 7.88 (ddd, *J$_1$* = 8.4 Hz, *J$_2$* = 6.9 Hz, *J$_3$* = 1.5 Hz, 1H), 7.60 (dd, *J$_1$* = 8.5 Hz, *J$_2$* = 0.7 Hz, 1H), 7.33 (ddd, *J$_1$* = 8.4 Hz, *J$_2$* = 6.9 Hz, *J$_3$* = 1.3 Hz, 1H), 3.55 (bs, 4H), 1.96–1.98 (m, 4H). ^{13}C{^{1}H} NMR (DMSO-*d$_6$*, 100 MHz) δ 156.7, 148.7, 135.8, 129.3, 126.1, 124.6, 120.0, 46.6, 24.8. ESI(+)-MS, *m/z* 217 (100, [M + H]$^+$). HRMS (ESI+-TOF) *m/z* [M + H]$^+$ calcd for C$_{11}$H$_{13}$N$_4$O 217.1089, found 217.1085. Anal. Calcd for C$_{11}$H$_{12}$N$_4$O: C, 61.10; H, 5.59; N, 25.91. Found: C, 61.12; H, 5.63; N, 26.03%.

3-(N-Methyl-N-phenylamino)benzo[e][1,2,4]triazine-1-oxide (5i). Following the general procedure *N*-oxide **5i** (110 mg, 63% yield) was obtained from *N*-methyl-*N*-phenyl-carboxamidine hydrochloride (**6i·HCl**, 1.01 g, 5.44 mmol) and 1-fluoro-2-nitrobenzene (**8**, 98.0 mg, 73.0 mL, 0.692 mmol). Product **5i** was isolated as the first fraction in column chromatography, which was followed by uncyclized intermediate **12i** (fraction 2). Recrystallization from ethanol gave analytically pure **5i** as a yellow solid. mp 120–122 °C (EtOH). ^{1}H NMR (DMSO-*d$_6$*, 400 MHz) δ 8.16 (dd, *J$_1$* = 8.6 Hz, *J$_2$* = 0.8 Hz, 1H), 7.84 (ddd, *J$_1$* = 8.4 Hz, *J$_2$* = 6.8 Hz, *J$_3$* = 1.3 Hz, 1H), 7.65 (d, *J* = 8.5 Hz, 1H), 7.48–7.40 (m, 5H), 7.32 (t, *J* = 7.0 Hz, 1H), 3.52 (s, 3H). ^{13}C{^{1}H} NMR (DMSO-*d$_6$*, 100 MHz) δ 158.2, 148.1, 144.1, 136.1, 130.0, 129.3, 126.7, 126.6, 126.4, 125.4, 125.8, 120.0, 38.8. IR ν 1534, 1421, 1361, 1173, 1104, 757, 694 cm^{-1}. ESI(+)-MS, *m/z* 253 (100, [M + H]$^+$). HRMS (ESI+-TOF) *m/z* [M + H]$^+$ calcd for C$_{14}$H$_{13}$N$_4$O 253.1089, found 253.1089. Anal. Calcd for C$_{14}$H$_{12}$N$_4$O: C, 66.65; H, 4.79; N, 22.21. Found: C, 66.38; H, 4.72; N, 22.19%.

Preparation of *N*-Oxides 5k–5m. General Procedure. To a solution of the appropriate *N*-(2-nitrophenyl)-alkylcarboxamidine **12** (1 mmol, 1 equiv) dissolved in MeOH (0.8 mL, 1.25 M) was added MeONa (1.5 mmol, 1.5 equiv), and the resulting reaction mixture was refluxed overnight. The solvent was evaporated, and the residue was purified by column chromatography (hexane/AcOEt, 4:1) giving pure 3-alkyl-substituted benzo[*e*][1,2,4]triazine-1-oxide **5**.

3-(tert-Butyl)benzo[e][1,2,4]triazine-1-oxide (5k). Following the general procedure, *N*-oxide **5k** (129.9 mg, 25% yield) was obtained as a pale yellow solid starting from *N*-(2-nitrophenyl)amidine **12k** (560.4 mg, 2.533 mmol). Recrystallization from *n*-heptane gave analytically pure product. mp 85–86 °C (*n*-heptane). ^{1}H NMR (CDCl$_3$, 400 MHz) δ 8.45 (d, *J* = 8.6 Hz, 1H), 8.00 (d, *J* = 8.4 Hz, 1H), 7.90 (td, *J$_1$* = 7.4 Hz, *J$_2$* = 1.0 Hz, 1H), 7.67 (td, *J$_1$* = 7.4 Hz, *J$_2$* = 1.0 Hz, 1H), 1.49 (s, 9H). ^{13}C{^{1}H} NMR (CDCl$_3$, 100 MHz) δ 173.2, 147.5, 135.3, 132.9, 130.0, 129.2, 120.2, 39.1, 29.3. ESI(+)-MS, *m/z* 204 (100, [M + H]$^+$). HRMS (ESI+-TOF) *m/z* [M + H]$^+$ calcd for C$_{11}$H$_{14}$N$_3$O 204.1137, found 204.1135. Anal. Calcd for C$_{11}$H$_{13}$N$_3$O: C, 65.01; H, 6.45; N, 20.68. Found: C, 65.03; H, 6.47; N, 20.71%.

3-(Cyclohexyl)benzo[e][1,2,4]triazine-1-oxide (5l). Following the general procedure, *N*-oxide **5l** (44.9 mg, 22% yield) was obtained as a pale yellow solid from *N*-(2-nitrophenyl)amidine **12l** (218.6 mg, 0.884 mmol). Recrystallization from *n*-heptane gave analytically pure product. mp 68–70 °C (*n*-heptane). ^{1}H NMR (CDCl$_3$, 400 MHz) δ 8.44 (d, *J* = 8.7 Hz, 1H), 7.97 (d, *J* = 8.4 Hz, 1H), 7.90 (td, *J$_1$* = 7.8 Hz, *J$_2$* = 1.2 Hz, 1H), 7.67 (td, *J$_1$* = 7.8 Hz, *J$_2$* = 1.2 Hz, 1H), 2.96 (tt, *J$_1$* = 8.4 Hz, *J$_2$* = 3.5 Hz, 1H), 2.08 (d, *J* = 11.8 Hz, 1H), 1.91–1.87 (m, 2H), 1.79–1.72 (m, 3H), 1.47–1.29 (m, 3H). ^{13}C{^{1}H} NMR (CDCl$_3$, 100 MHz) δ 170.6, 147.8, 135.5, 133.5, 129.9, 129.0, 120.2, 46.0, 31.5, 26.2, 25.9. ESI(+)-MS, *m/z* 230 (100, [M + H]$^+$). HRMS (ESI+-TOF) *m/z* [M + H]$^+$ calcd for C$_{13}$H$_{16}$N$_3$O 230.1293, found 230.1299. Anal. Calcd for C$_{13}$H$_{15}$N$_3$O: C, 68.10; H, 6.59; N, 18.33. Found: C, 68.11; H, 6.64; N, 18.32%.

3-(Cyclopropyl)benzo[e][1,2,4]triazine-1-oxide (5m).[72] Following the general procedure, *N*-oxide **5m** (12.1 mg, 17% yield) was obtained as a pale yellow solid starting from *N*-(2-nitrophenyl)-amidine **12m** (53.1 mg, 0.259 mmol). Recrystallization from *n*-heptane gave analytically pure product. mp 119–120 °C (*n*-heptane). ^{1}H NMR (CDCl$_3$, 400 MHz) δ 8.41 (d, *J* = 8.5 Hz, 1H), 7.91–7.85 (m, 2H), 7.62 (ddd, *J$_1$* = 8.5 Hz, *J$_2$* = 6.3 Hz, *J$_3$* = 2.2 Hz, 1H), 2.31 (tt, *J$_1$* = 8.2 Hz, *J$_2$* = 4.8 Hz, 1H), 1.34–1.30 (m, 2H), 1.22–1.17 (m, 2H). ^{13}C{^{1}H} NMR (CDCl$_3$, 100 MHz) δ 168.5, 147.8, 135.6, 133.5, 129.3, 128.5, 120.3, 16.9, 11.3. ESI(+)-MS, *m/z* 188 (100, [M + H]$^+$). HRMS (ESI+-TOF) *m/z* [M + H]$^+$ calcd for C$_{10}$H$_{10}$N$_3$O 188.0824, found 188.0823. Anal. Calcd for C$_{10}$H$_9$N$_3$O: C, 64.16; H, 4.85; N, 22.45. Found: C, 64.43; H, 4.96; N, 22.77%.

Attempted Preparation of 3-(Cyclopropyl)benzo[e][1,2,4]-triazine-1-oxide (5m) by a Two-Step Cyclization of 12m. *N*-(2-Nitrophenyl) amidine **12m** (100 mg, 0.49 mmol) was dissolved in EtOH (3 mL), and the mixture was stirred overnight with 10% Pd/C (5.2 mg, 0.049 mmol) under H$_2$ atmosphere (balloon). The mixture was filtered through a diatomaceous earth pad, which was washed with EtOH, and the filtrate was evaporated. The residue was purified by column chromatography (SiO$_2$, AcOEt/MeOH, gradient up to 100% MeOH) giving benzimidazoles **15** (12.1 mg, 16% yield) and **16** (69.5 mg, 82% yield).

Preparation of Guanidine Hydrochlorides 6·HCl. General Procedures. Method A. Following a modified literature procedure,[59] a solution of 2-methyl-2-thiopseudourea sulfate (**9**, 1 mmol, 1 equiv) and an appropriate amine (1 mmol, 1 equiv) in water (4 mL, 0.25 M) was heated overnight under reflux. A solution of BaCl$_2$ (1 mmol, 1 equiv) in water (2.5 mL, 0.4 M) was added dropwise over 30 min, and the resulting mixture was refluxed for 1 h. After cooling to rt, the resulting precipitate was filtered, and the filtrate was concentrated leaving a viscous syrup, which was dissolved in EtOH. The resulting solution was evaporated, and the residue was dried in vacuum. The obtained solid was recrystallized from a MeOH/acetone mixture (1:2) giving analytically pure salt **6·HCl**.

Method B. Following a modified literature procedure,[60] to a solution of appropriate amine (1 mmol, 1 equiv) in EtOH (1.5 mL, 0.67 M) was added conc. HCl (0.1 mL, 10 M) followed by a 50% aqueous solution of cyanamide (0.13 mL, 1.5 mmol, 1.5 equiv). The reaction mixture was refluxed overnight, then cooled to 0 °C followed by addition of diethyl ether. The mixture was refrigerated overnight, and the resulting solid was filtered giving the analytically pure product **6·HCl**.

Method C. Following a modified literature procedure,[61] to a mixture of the appropriate amine hydrochloride (1 mmol, 1 equiv) and cyanamide (1.5 mmol, 1.5 equiv) in water (1 mL, 1 M) some drops of the free amine were added until pH 8−9 was reached. The mixture was refluxed overnight. After cooling to rt the mixture was acidified with HCl to pH 4. Then water was removed in vacuum to give the guanidine salt **6·HCl**, which was recrystallized from a MeOH/acetone mixture (1:2) giving analytically pure product **6·HCl**.

Morpholine-4-carboxamidine Hydrochloride (6c·HCl).[59] Following Method A, 2.32 g (90% yield) of guanidinium salt **6c·HCl** was obtained as a white solid starting from morpholine (1.74 g, 19.6 mmol) and 2-methyl-2-thiopseudourea sulfate (**9**, 2.80 g, 20.1 mmol). mp 166−168 °C (MeOH/acetone; lit.[59] mp 138−139 °C). ^{1}H NMR (DMSO-d_6, 400 MHz) δ 7.74 (s, 4H), 3.62 (s, 4H), 3.44 (s, 4H). ^{13}C{^{1}H} NMR (DMSO-d_6, 100 MHz) δ 156.7, 65.3, 45.1. ESI(+)-MS, m/z 130 (100, [M − Cl]+; HRMS (ESI+-TOF) m/z [M + H]+ calcd for $C_5H_{12}N_3O$ 130.0980, found 130.0983.

Piperidine-1-carboximidamine Hydrochloride (6g·HCl).[59] Following Method C, 8.71 g (91% yield) of guanidinium salt **6g·HCl** was obtained as a white solid starting from 7.14 g of piperidine hydrochloride (7.14 g, 58.8 mmol) and cyanamide (3.70 g, 88.2 mmol). An analytical sample of the product could not be obtained by recrystallization, and crude product was used in the condensation reaction. ^{1}H NMR (DMSO-d_6, 400 MHz) δ major signals 7.52 (s, 4H), 3.38 (t, J = 5.5 Hz, 4H), 1.61−1.45 (m, 6H). ^{13}C{^{1}H} NMR (DMSO-d_6, 100 MHz) δ major signals 155.8, 46.1, 25.0, 23.3. ESI(+)-MS, m/z 128 (100, [M − Cl]+); HRMS (ESI+-TOF) m/z [M − Cl]+ calcd for $C_6H_{14}N_3$ 128.1188, found 128.1185.

Pyrrolidine-1-carboxamidine Hydrochloride (6h·HCl). Following Method C, 1.92 g (86% yield) of guanidinium salt **6h·HCl** was obtained as a white solid starting from of pyrrolidine hydrochloride (1.61 g, 14.9 mmol) and cyanamide (0.942 g, 22.4 mmol). mp 77−79 °C (MeOH/acetone). ^{1}H NMR (DMSO-d_6, 400 MHz) δ 7.37 (bs, 4H), 3.31 (t, J = 6.2 Hz, 4H), 1.92−1.87 (m, 4H). ^{13}C{^{1}H} NMR (DMSO-d_6, 100 MHz) δ 154.7, 47.1, 24.8. ESI(+)-MS, m/z 114 [100, [(M − HCl) + H]+]. HRMS (ESI-TOF) m/z [M + H]+ calcd for $C_5H_{12}N_3$ 114.1031, found 114.1035.

N-Methyl-N-phenylguanidine Hydrochloride (6i·HCl). Following Method B, 2.75 g (74% yield) of guanidinium salt **6i** was obtained as a white solid starting from N-methylaniline (2.15 g, 20.1 mmol) and cyanamide (1.26 g, 30.0 mmol). mp 180−183 °C (Et$_2$O). ^{1}H NMR (DMSO-d_6, 400 MHz) δ 7.52 (t, J = 7.7 Hz, 2H), 7.44 (t, J = 7.3 Hz, 1H), 7.38 (d, J = 7.3 Hz, 2H), 7.32 (bs, 2H) 3.27 (s, 3H). ^{13}C{^{1}H} NMR (DMSO-d_6, 100 MHz) δ 156.9, 141.0, 130.2, 128.6, 127.1 (Me under the solvent peak). ESI(+)-MS, m/z 150 [100, [(M − HCl) + H]+; HRMS (ESI+-TOF) m/z [M + H]+ calcd for $C_8H_{12}N_3$ 150.1031, found 150.1036.

Imidazole-1-carboxamidine Hydrochloride (6j·HCl). Following Method C, 2.09 g (48% yield) of guanidine salt **6j** was obtained as a white solid starting from imidazole hydrochloride (3.07 g, 29.2 mmol) and cyanamide (1.85 g, 43.8 mmol). ^{1}H NMR (DMSO-d_6, 400 MHz) δ 14.7 (bs, 1H), 9.13 (s, 1H), 7.68 (s, 2H), 6.71 (s, 2H). ^{13}C{^{1}H} NMR (DMSO-d_6, 100 MHz) δ 163.0, 134.1, 119.2, 118.5. ESI(+)-MS, m/z 111 [100, [(M − HCl) + H]+. HRMS (ESI+-TOF) m/z [(M − HCl) + H]+ calcd for $C_4H_7N_4$ 111.0671, found 111.0673.

Preparation of Amidine Hydrochlorides 7·HCl. Following a modified literature procedure,[57] an oven-dried three-necked round-bottom flask under Ar, equipped with a stirring bar, a gas inlet, and a reflux condenser, was charged with the appropriate nitrile **10** (1 mmol) and dry EtOH (2 mL, 0.5 M). The reaction was cooled in an ice-bath, before HCl gas was bubbled through the stirred reaction mixture for 4 h. The resulting mixture was stirred at rt overnight.

Subsequently, the solvent was evaporated under reduced pressure, and the resulting solid was suspended in Et$_2$O and filtered; the solid was rinsed with Et$_2$O and dried giving a white solid. The precipitate was then dissolved in dry EtOH under Ar, and NH$_3$ gas was bubbled through the solution for 3 h. The reaction mixture was left to stir overnight at rt. Then, the solvent was evaporated under reduced pressure, and the resulting sticky solid was dried. Recrystallization from a MeOH/acetone mixture gave the desired amidine hydrochloride **7·HCl** as white crystals.

tert-Butylcarboxamidine Hydrochloride (7k·HCl).[57] Following the general procedure, 6.66 g (48.7 mmol, 81% yield) of amidine salt **7k·HCl** was obtained from 5.00 g (6.65 mL, 60.2 mmol) of pivalonitrile (**10k**) as a white solid. ^{1}H NMR (DMSO-d_6, 400 MHz) δ 7.3 (bs, 4H), 1.23 (s, 9H). ^{13}C{^{1}H} NMR (DMSO-d_6, 100 MHz) δ 177.5, 36.3, 26.9. ESI(+)-MS, m/z 101 [100, [(M−Cl)+]. HRMS (ESI +-TOF) m/z [M − Cl]+ calcd for $C_5H_{13}N_2$ 101.1079, found 101.1075.

Cyclohexanecarboxamidine Hydrochloride (7l·HCl).[57] Following the general procedure, 6.71 g (41.2 mmol, 90% yield) of amidine salt **7l·HCl** was obtained from 5.00 g (5.44 mL, 45.8 mmol) of cyclohexanecarbonitrile (**10l**) as a white solid. mp 217−219 °C. ^{1}H NMR (DMSO-d_6, 400 MHz) δ 8.87 (bs, 4H), 2.44 (t, J = 12.1 Hz, 1H), 1.75 (bd, J = 8.1 Hz, 4H), 1.65 (d, J = 9.6 Hz, 1H), 1.55−1.45 (m, 2H), 1.26−1.13 (m, 3H). ^{13}C{^{1}H} NMR (DMSO-d_6, 100 MHz) δ 174.3, 41.4, 28.8, 25.1, 24.8. ESI(+)-MS, m/z 127 [100, (M − Cl)+]. HRMS (ESI+-TOF) m/z [M − Cl]+ calcd for $C_7H_{15}N_2$ 127.1235, found 127.1233.

N′-Methyl-N-(2-Nitrophenyl)-N′-phenylguanidine (12i). The guanidine **12i** (16 mg, 6% yield) was obtained as an unreacted intermediate in the one-pot preparation of N-oxide **5i** and isolated as the second fraction by column chromatography. ^{1}H NMR (DMSO-d_6, 400 MHz) δ 7.76 (d, J = 8.1 Hz, 1H), 7.44 (t, J = 7.8 Hz, 1H), 7.37 (t, J = 7.3 Hz, 2H), 7.29 (d, J = 7.9 Hz, 2H), 7.17 (t, J = 7.2 Hz, 1H), 6.99−6.94 (m, 2H), 5.49 (bs, 2H), 3.23 (s, 3H). ^{13}C{^{1}H} NMR (DMSO-d_6, 100 MHz) δ 152.5, 145.9, 145.3, 143.0, 133.5, 129.2, 126.2, 125.9, 125.1, 124.6, 120.2. ESI(+)-MS, m/z 271 (100, [M + H]+). HRMS (ESI+-TOF) m/z [M + H]+ calcd for $C_{14}H_{15}N_4O_2$ 271.1195, found 271.1191.

Preparation of N-Aryl Carboxamidines 12k−12m. General Procedure. A mixture of the appropriate amidine hydrochloride (7k−7m·HCl) (6 mmol, 6 equiv) and EtONa (6 mmol, 6 equiv) in dry EtOH (0.9 mL, 1.11 M) was stirred under N$_2$ atmosphere for 30 min at rt. The resulting precipitated inorganic salt was filtered through a syringe filter under N$_2$ atmosphere. After evaporation of the solvent, the free amidine was dried under vacuum and dissolved in dry MeCN (0.8 mL, 1.25 M). 1-Fluoro-2-nitrobenzene (**8**, 1 mmol, 1 equiv) was added, and the resulting mixture was stirred overnight at 78 °C. The solvent was evaporated, and the residue was dissolved in AcOEt (10 mL), washed with water (2 × 10 mL), and dried; the solvents were evaporated to dryness and purified by column chromatography (pet. ether/AcOEt, 2:1) giving N-substituted amidine **12**.

N-(2-Nitrophenyl)-tert-butylcarboxamidine (12k). Following the general procedure, **12k** (558.9 mg, 88% yield) was obtained as a yellow oil starting from tert-butylcarboxamidine hydrochloride (**7k·HCl**, 1.72 g, 17.2 mmol) and 1-fluoro-2-nitrobenzene (**8**, 405.0 mg, 2.87 mmol). ^{1}H NMR (CDCl$_3$, 400 MHz) δ 7.90 (d, J = 8.0 Hz, 1H), 7.46 (t, J = 7.8 Hz, 1H), 7.04 (t, J = 7.8 Hz, 2H), 4.50 (bs, 2H), 1.29 (s, 9H). ^{13}C{^{1}H} NMR (CDCl$_3$, 100 MHz) δ 165.4, 144.9, 141.8, 134.2, 125.4, 124.6, 122.4, 37.2, 28.3. ESI(+)-MS, m/z 222 (100, [M + H]+). HRMS (ESI+-TOF) m/z [M + H]+ calcd for $C_{11}H_{16}N_3O_2$ 222.1243, found 222.1236.

N-(2-Nitrophenyl)cyclohexanecarboxamidine (12l). Following the general procedure, **12l** (98.3 mg, 75% yield) was obtained from cyclohexanecarboxamidine hydrochloride (**7l·HCl**, 500 mg, 3.10 mmol) and 1-fluoro-2-nitrobenzene (**8**, 74.8 mg, 55.8 mL, 0.53 mmol) as a yellow oil. ^{1}H NMR (CDCl$_3$, 400 MHz) δ 7.83 (dd, J_1 = 8.3 Hz, J_1 = 1.2 Hz, 1H), 7.41 (ddd, J_1 = 8.4 Hz, J_2 = 7.0 Hz, J_3 = 1.5 Hz, 1H), 7.00 (ddd, J_1 = 8.3 Hz, J_2 = 7.1 Hz, J_3 = 1.2 Hz, 2H), 4.65 (bs, 2H), 2.15 (tt, J_1 = 11.9 Hz, J_2 = 3.4 Hz, 1H), 1.92 (dd, J_1 = 11.7 Hz, J_2 = 3.0 Hz, 2H), 1.78−1.75 (m, 2H), 1.66−1.63 (m, 1H), 1.39

(qd, J_1 = 9.8 Hz, J_2 = 2.6 Hz, 2H), 1.30−1.17 (m, 3H). ^{13}C{^{1}H} NMR (CDCl$_3$, 100 MHz) δ 163.3, 144.6, 141.8, 134.0, 125.2, 124.8, 122.4, 44.6, 30.6, 25.9, 25.8. ESI(+)-MS, m/z 248 (100, [M + H]$^+$). HRMS (ESI+-TOF) m/z [M + H]$^+$ calcd for C$_{13}$H$_{18}$N$_3$O$_2$ 248.1399, found 248.1397.

N-(2-Nitrophenyl)cyclopropanecarboxamidine (12m). Following the general procedure, **12m** (716.5 mg, 94% yield) was obtained from cyclopropanecarboxamidine hydrochloride (**7m·HCl**, 2.71 g, 22.5 mmol) and 1-fluoro-2-nitrobenzene (**8**, 522 mg, 0.39 mL, 3.7 mmol) as a yellow oil. ^{1}H NMR (CDCl$_3$, 400 MHz) δ 7.82 (d, J = 8.1 Hz, 1H), 7.42 (t, J = 8.0 Hz, 1H), 7.02 (ddd, J_1 = 8.3 Hz, J_2 = 7.2 Hz, J_3 = 1.1 Hz, 1H), 6.96 (bs, 1H), 4.7 (bs, 2H), 1.48−1.39 (m, 1H), 0.99 (d, J = 2.2 Hz, 2H), 0.82−0.79 (m, 2 H). ^{13}C{^{1}H} NMR (CDCl$_3$, 100 MHz) δ 160.6, 144.6, 142.2, 133.9, 125.2, 125.0, 122.4, 14.6, 7.4. ESI(+)-MS, m/z 206 (100, [M + H]$^+$). HRMS (ESI+-TOF) m/z [M + H]$^+$ calcd for C$_{10}$H$_{12}$N$_3$O$_2$ 206.0930, found 206.0928.

(1-Pyrrolidin-1-yl)-2-nitrobenzene (13h).[73] Compound **13h** (9 mg, 7% yield) was obtained as a byproduct in preparation of *N*-oxide **5h** and isolated as the first fraction by column chromatography as a pale, yellow oil. ^{1}H NMR (DMSO-d_6, 400 MHz) δ 7.71 (dd, J_1 = 8.2 Hz, J_2 = 1.6 Hz, 1H), 7.43 (ddd, J_1 = 8.6 Hz, J_2 = 7.0 Hz, J_3 = 1.7 Hz, 1H), 7.04 (dd, J_1 = 8.6 Hz, J_2 = 0.9 Hz, 1H), 6.75 (ddd, J_1 = 8.2 Hz, J_2 = 7.1 Hz, J_3 = 1.1 Hz, 1H), 3.13−3.10 (m, 4H), 1.92−1.89 (m, 4H). ^{13}C{^{1}H} NMR (DMSO-d_6, 100 MHz) δ 142.3, 136.4, 133.3, 126.2, 116.4, 115.4, 50.1, 25.3. Affinity purification (AP)(+)-MS, m/z 193 (61, [M + H]$^+$). HRMS (AP+-TOF) m/z [M + H]$^+$ calcd for C$_{10}$H$_{12}$N$_2$O$_2$ 193.0977, found 193.0978.

1-(Imidazol-1-yl)-2-nitrobenzene (13j).[74] **Attempted Preparation of 3-(imidazol-1-yl)benzo[e][1,2,4]triazine-1-oxide (5j).** Reaction of imidazole-1-carboxamidine hydrochloride (**6j·HCl**, 716 mg, 4.90 mmol) using the general procedure for preparation of *N*-oxides **5** gave 1-(imidazol-1-yl)-2-nitrobenzene (**13j**) isolated by column chromatography (pet. ether/AcOEt, 1:1) in 68% yield (102 mg) as a yellow solid. mp 98−99 °C (heptane/AcOEt; lit.[74] mp 97−98 °C). ^{1}H NMR (DMSO-d_6, 400 MHz) δ 8.17 (dd, J_1 = 8.1 Hz, J_2 = 1.2 Hz, 1H), 7.92 (s, 1H), 7.87 (ddd, J_1 = 7.8 Hz, J_2 = 6.4 Hz, J_3 = 1.4 Hz, 1H), 7.76−7.60 (m, 2H), 7.43 (s, 1H), 7.10 (s, 1H). ^{13}C{^{1}H} NMR (DMSO-d_6, 100 MHz) δ 144.6, 137.6, 134.5, 130.2, 129.9, 129.5, 128.9, 125.4, 120.7. ESI(+)-MS, m/z 190 (100, [M + H]$^+$). HRMS (ESI+-TOF) m/z [M + H]$^+$ calcd for C$_9$H$_8$N$_3$O$_2$ 190.0617, found 190.0616. Anal. Calcd for C$_9$H$_7$N$_3$O$_2$: C, 57.14; H, 3.73; N, 22.21. Found: C, 57.11; H, 3.89; N, 22.18%.

2-Nitroaniline (14). *N*-(2-Nitrophenyl) amidine **12m** (57.1 mg, 0.28 mmol) was dissolved in EtOH (3 mL), and the mixture was stirred overnight with a catalytic amount of HCl (0.1 mL, 1.18 mmol) at 78 °C. The mixture was evaporated to dryness, and the residue was purified by preparative TLC (SiO$_2$, hexane/AcOEt 2:1) giving aniline **14** (27.4 mg, 72% yield) as an orange solid. Analytical data was identical to that reported previously.[75]

2-Cyclopropyl-1H-benzimidazole (15).[76] This was obtained from the attempted preparation of **5m** from **12m**. Analytically pure benzimidazole **15** was obtained as colorless needles after recrystallization from CH$_2$Cl$_2$. mp 233−234 °C (CH$_2$Cl$_2$; lit.[76] mp 227−229 °C). ^{1}H NMR (DMSO-d_6, 400 MHz) δ 7.44−7.37 (m, 2H), 7.12−7.05 (m, 2H), 2.10 (tt, J_1 = 8.1 Hz, J_2 = 5.2 Hz, 1H), 1.12−0.96 (m, 4H). ^{13}C{^{1}H} NMR (DMSO-d_6, 100 MHz) δ 157.0, 138.5, 121.1 (2C), 114.0, 9.4, 8.77 (2C). ESI(+)-MS, m/z 159 (100, [M + H]$^+$). HRMS (ESI+-TOF) m/z [M + H]$^+$ calcd for C$_{10}$H$_{11}$N$_2$ 159.0922, found 159.0925. Anal. Calcd for C$_{10}$H$_{10}$N$_2$: C, 75.92; H, 6.37; N, 17.71. Found: C, 75.90; H, 6.35; N, 17.72%.

1-Hydroxy-2-cyclopropylbenzimidazole (16). This was obtained from the attempted preparation of **5m** from **12m**. Analytically pure benzimidazole **16** was obtained as white crystals after recrystallization from EtOH/AcOEt. mp 165−166 °C (EtOH/AcOEt). ^{1}H NMR (DMSO-d_6, 400 MHz) δ 11.77 (s, 1H), 7.44 (J = 7.9 Hz, 1H), 7.37 (J = 8.0 Hz, 1H), 7.16 (td, J_1 = 7.7 Hz, J_2 = 1.2 Hz, 1H), 7.10 (td, J_1 = 7.8 Hz, J_2 = 1.2 Hz, 1H), 2.28 (tt, J = 8.2 Hz, 4.9 Hz, 1H), 1.26−0.79 (m, 4H). ^{13}C{^{1}H} NMR (DMSO-d_6, 100 MHz) δ 153.0, 137.7, 132.6, 121.4, 121.3, 118.3, 108.1, 8.8, 6.3. ESI(+)-MS, m/z 175 (100, [M + H]$^+$). HRMS (ESI+-TOF) m/z [M + H]$^+$ calcd for C$_{10}$H$_{11}$N$_2$O

175.0871, found 175.0874. Anal. Calcd for C$_{10}$H$_{10}$N$_2$O: C, 68.95; H, 5.79; N, 16.08. Found: C, 68.95; H, 5.68; N, 16.05%.

■ ASSOCIATED CONTENT

Data Availability Statement

The data underlying this study are available in the published article and its online Supporting Information. These and also raw data are available upon request from the corresponding authors.

Ⓢ Supporting Information

The Supporting Information is available free of charge at https://pubs.acs.org/doi/10.1021/acs.joc.2c02703.

> NMR, IR, UV−vis, and EPR spectra, electrochemical data, and archive for DFT calculation (PDF)
> FAIR data, including the primary NMR FID files, for compounds **2**, **5**, **6·HCl**, **7·HCl**, **12**, **13**, **15**, and **16** (ZIP)

■ AUTHOR INFORMATION

Corresponding Authors

Piotr Kaszyński − *Centre of Molecular and Macromolecular Studies, Polish Academy of Sciences, 90-363 Łódź, Poland; Faculty of Chemistry, University of Łódź, 91-403 Łódź, Poland; Department of Chemistry, Middle Tennessee State University, 37132 Murfreesboro, Tennessee, United States;* orcid.org/0000-0002-2325-8560; Email: piotr.kaszynski@cbmm.lodz.pl

Agnieszka Bodzioch − *Centre of Molecular and Macromolecular Studies, Polish Academy of Sciences, 90-363 Łódź, Poland;* orcid.org/0000-0002-4501-4639; Email: agnieszka.bodzioch@cbmm.lodz.pl

Author

Dominika Pomikło − *Centre of Molecular and Macromolecular Studies, Polish Academy of Sciences, 90-363 Łódź, Poland;* orcid.org/0000-0003-1297-8922

Complete contact information is available at: https://pubs.acs.org/10.1021/acs.joc.2c02703

Author Contributions

The manuscript was written through contributions of all authors, and all authors have given approval to the final version of the manuscript.

Notes

The authors declare no competing financial interest.

■ REFERENCES

(1) Constantinides, C. P.; Koutentis, P. A. Stable N- and N/S-reach heterocyclic radicals: Synthesis and applications. *Adv. Heterocycl. Chem.* **2016**, *119*, 173−207.

(2) Ji, Y.; Long, L.; Zheng, Y. Recent advances of stable Blatter radicals: Synthesis, properties and applications. *Mater. Chem. Front.* **2020**, *4*, 3433−3443.

(3) Rogers, F. J. M.; Norcott, P. L.; Coote, M. L. Recent advances in the chemistry of benzo[e][1,2,4]triazinyl radicals. *Org. Biomol. Chem.* **2020**, *18*, 8255−8277.

(4) Blatter, H. M.; Łukaszewski, H. A new stable free radical. *Tetrahedron Lett.* **1968**, *9*, 2701−2705.

(5) Demetriou, M.; Berezin, A. A.; Koutentis, P. A.; Krasia-Christoforou, T. Benzotriazinyl-mediated controlled radical polymerization of styrene. *Polym. Int.* **2014**, *63*, 674−679.

(6) Steen, J. S.; Nuismer, J. L.; Eiva, V.; Wiglema, A. E. T.; Daub, N.; Hjelm, J.; Otten, E. Blatter radicals as bipolar materials for symmetrical redox-flow batteries. *J. Am. Chem. Soc.* **2022**, *144*, 5051−5058.

(7) Saal, A.; Friebe, C.; Schubert, U. S. Blatter radical as a polymeric active material in organic batteries. *J. Power Sources* **2022**, *524*, 231061.

(8) Friebe, C.; Schubert, U. S. High-power-density organic radical batteries. *Top. Curr. Chem.* **2017**, *375*, 19.

(9) Jasiński, M.; Kapuściński, S.; Kaszyński, P. Stability of a columnar liquid cristalline phase in isomeric derivatives of the 1,4-dihydrobenzo[*e*][1,2,4]triazin-4-yl: Conformational effect in the core. *J. Mol. Liq.* **2019**, *277*, 1054−1059.

(10) Jasiński, M.; Szczytko, J.; Pociecha, D.; Monobe, H.; Kaszyński, P. Substituent-dependent magnetic behavior of discotic benzo[*e*]-[1,2,4]triazinyls. *J. Am. Chem. Soc.* **2016**, *138*, 9421−9424.

(11) Jasiński, M.; Szymańska, K.; Gardias, A.; Pociecha, D.; Monobe, H.; Szczytko, J.; Kaszyński, P. Tuning the magnetic properties of columnar benzo[*e*][1,2,4]triazin-4-yls with the molecular shape. *ChemPhysChem* **2019**, *20*, 636−644.

(12) Kapuściński, S.; Gardias, A.; Pociecha, D.; Jasiński, M.; Szczytko, J.; Kaszyński, P. Magnetic behavior of bent-core mesogens derived from the 1,4-dihydrobenzo[*e*][1,2,4]triazin-4-yl. *J. Mater. Chem. C* **2018**, *6*, 3079−3088.

(13) Kapuściński, S.; Szczytko, J.; Pociecha, D.; Jasiński, M.; Kaszyński, P. Discs, dumbbels and superdiscs: Molecular and supermolecular architecture dependent magnetic behavior of mesogenic Blatter radical derivatives. *Mater. Chem. Front.* **2021**, *5*, 6512−6521.

(14) Shivakumar, K. I.; Pociecha, D.; Szczytko, J.; Kapuściński, S.; Monobe, H.; Kaszyński, P. Photocondutive bent-core liquid cristalline radicals with a paramagnetic polar switchable phase. *J. Mater. Chem. C* **2020**, *8*, 1083−1088.

(15) Low, J. Z.; Kladnik, G.; Patera, L. L.; Sokolov, S.; Lovat, G.; Kumarasamy, E.; Repp, J.; Campos, L. M.; Cvetko, D.; Morgante, A.; Venkataraman, L. The environment-dependent behavior of the Blatter radical at the metal-molecule interface. *Nano Lett.* **2019**, *19*, 2543−2548.

(16) Ciccullo, F.; Calzolari, A.; Bader, K.; Neugebauer, P.; Gallagher, N. M.; Rajca, A.; van Slageren, J.; Casu, M. B. Interfacing a potential purely organic molecular quantum bit with a real-life surface. *ACS Appl. Mater. Interfaces* **2019**, *11*, 1571−1578.

(17) Zheng, Y.; Miao, M.-s.; Dantelle, G.; Eisenmenger, N. D.; Wu, G.; Yavuz, I.; Chabinyc, M. L.; Houk, K. N.; Wudl, F. A solid-state effect responsible for an organic quintet state at room temperature and ambient pressure. *Adv. Mater.* **2015**, *27*, 1718−1723.

(18) Zheng, Y.; Miao, M.-s.; Kemei, M. C.; Seshadri, R.; Wudl, F. The pyreno-triazinyl radical − Magnetic and sensor properties. *Isr. J. Chem.* **2014**, *54*, 774−778.

(19) Casu, M. B. Nanoscale studies of organic radicals: Surface, interface, and spinterface. *Acc. Chem. Res.* **2018**, *51*, 753−760.

(20) Constantinides, C. P.; Koutentis, P. A.; Loizou, G. Synthesis of 7-aryl/heteraryl-1,3-diphenyl-1,2,4-benzotriazinyls *via* palladium catalyzed Stille and Suzuki-Miyaura reactions. *Org. Biomol. Chem.* **2011**, *9*, 3122−3125.

(21) Bodzioch, A.; Zheng, M.; Kaszyński, P.; Utecht, G. Functional group transformations in derivatives of 1,4-dihydrobenzo[*e*][1,2,4]-triazinyl radical. *J. Org. Chem.* **2014**, *79*, 7294−7310.

(22) Takahashi, Y.; Miura, Y.; Yoshioka, N. Introduction of three aryl groups to benzotriazynyl radical by Suzuki-Miyaura cross-coupling reaction. *Chem. Lett.* **2014**, *43*, 1236−1238.

(23) Constantinides, C. P.; Obijalska, E.; Kaszyński, P. Access to 1,4-dihydrobenzo[*e*][1,2,4]triazin-4-yl derivatives. *Org. Lett.* **2016**, *18*, 916−919.

(24) Pomikło, D.; Bodzioch, A.; Pietrzak, A.; Kaszyński, P. C(3) Functional derivatives of the Blatter radical. *Org. Lett.* **2019**, *21*, 6995−6999.

(25) Grant, J. A.; Lu, Z.; Tucker, D. E.; Hockin, B. M.; Yufit, D. S.; Fox, M. A.; Kataky, R.; Chechik, V.; o'Donoghue, A. C. New Blatter-type radicals from a bench-stable carbene. *Nature Commun.* **2017**, *8*, 15088.

(26) Wolf, F. J.; Pfister, R. K.; Wilson, J. R. M.; Robinson, C. A. Benzotriazines: A new series of compounds having antimalarial activity. *J. Am. Chem. Soc.* **1954**, *76*, 3551−3553.

(27) Noronha, G.; Barrett, K.; Boccia, A.; Brodhag, T.; Cao, J.; Chow, C. P.; Dneprovskaia, E.; Doukas, J.; Fine, R.; Gong, X.; Gritzen, C.; Gu, H.; Hanna, E.; Hood, J. D.; Hu, S.; Kang, X.; Key, J.; Klebansky, B.; Kousba, A.; Li, G.; Lohse, D.; Mak, C. C.; McPherson, A.; Palanki, M. S. S.; Pathak, V. P.; Renick, J.; Shi, F.; Soll, R.; Splittgerber, U.; Stoughton, S.; Tang, V. P.; Yee, S.; Zeng, B.; Zhao, N.; Zhu, H. Discovery of [7-(2,6-dichlorophenyl)-5-methylbenzo-[1,2,4]triazin-3-yl]-[4-(2-pyrrolidin-1-ylethoxy)phenyl]amine- a potent, orally active Src kinase inhibitor with anti-tumor activity in preclinical assays. *Bioorg. Med. Chem. Lett.* **2007**, *17*, 602−608.

(28) Noronha, G.; Barrett, K.; Cao, J.; Dneprovskaia, E.; Fine, R.; Gong, X.; Gritzen, C.; Hood, J.; Kang, X.; Klebansky, B.; Li, G.; Liao, W.; Lohse, D.; Mak, C. C.; McPherson, A.; Palanki, M. S. S.; Pathak, V. P.; Renick, J.; Soll, R.; Splittgerber, U.; Wrasidlo, W.; Zeng, B.; Zhao, N.; Zhou, Y. Discovery and preliminary structure-activity relationship studies of novel benzotriazine based compounds as Src inhibitors. *Bioorg. Med. Chem. Lett.* **2006**, *16*, 5546−5550.

(29) Cao, J.; Fine, R.; Gritzen, C.; Hood, J.; Kang, X.; Klebansky, B.; Lohse, D.; Mak, C. C.; McPherson, A.; Noronha, G.; Palanki, M. S. S.; Pathak, V. P.; Renick, J.; Soll, R.; Zeng, B.; Zhu, H. The design and preliminary structure-activity relationship studies of benzotriazines as potent inhibitors of Abl and Abl-T315I enzymes. *Bioorg. Med. Chem. Lett.* **2007**, *17*, 5812−5818.

(30) Suzuki, H.; Kawakami, T. A convenient synthesis of 3-amino-1,2,4-benzotriazine 1,4-dioxide (SR 4233) and related compounds *via* nucleophilic aromatic substitution between nitroarenes and guanidine base. *Synthesis* **1997**, *1997*, 855−857.

(31) Fuchs, T.; Chowdhury, G.; Barnes, C. L.; Gates, K. S. 3-Amino-1,2,4-benzotriazine-4-oxide: characterization of a new metabolite arising from bioreductive processing of the antitumor agent 3-amino-1,2,4-benzotriazine-1,4-dioxide (tirapazamine). *J. Org. Chem.* **2001**, *66*, 107−114.

(32) Xia, Q.; Zhang, L.; Zhang, J.; Sheng, R.; Yang, B.; He, Q.; Hu, Y. Synthesis, hypoxia-selective cytotoxicity of new 3-amino-1,2,4-benzotriazine-1,4-dioxide derivatives. *Eur. J. Med. Chem.* **2011**, *46*, 919−926.

(33) Bodzioch, A.; Pomikło, D.; Celeda, M.; Pietrzak, A.; Kaszyński, P. 3-substituted benzo[*e*][1,2,4]triazines: Synthesis and electronic effects of the C(3) substituent. *J. Org. Chem.* **2019**, *84*, 6377−6394.

(34) Epishina, M. A.; Kulikov, A. S.; Fershtat, L. L. Revisiting the synthesis of functionally substituted 1,3-dihydrobenzo[*e*][1,2,4]-triazines. *Molecules* **2022**, *27*, 2575−2588.

(35) Hay, M. P.; Gamage, S. A.; Kovacs, M. S.; Pruijn, F. B.; Anderson, R. F.; Patterson, A. V.; Wilson, W. R.; Brown, J. M.; Denny, W. A. Structure-activity relationship of 1,2,4-benzotriazine 1,4-dioxides as hypoxia-selective analogues of tirapazamine. *J. Med. Chem.* **2003**, *46*, 169−182.

(36) Yigiter, A. O.; Atakol, M. K.; Levent Aksu, M.; Atakol, O. Thermal characterization and theoretical and experimental comparison of picryl chloride derivatives of heterocyclic energetic compounds. *J. Therm. Anal. Calorim.* **2017**, *127*, 2199−2213.

(37) Grivas, J. C.; Navada, K. C. 2,6-Dinitro-*N*-(2-imidazolyl)-*p*-toluidine. *J. Org. Chem.* **1974**, *39*, 3165−3167.

(38) Ligthart, G. B. W. L.; Guo, D.; Spek, A. L.; Kooijman, H.; Zuilhof, H.; Sijbesma, R. P. Ureidobenzotriazine multiple H-bonding arrays: The importance of geometrical details on the stability of H-bonds. *J. Org. Chem.* **2008**, *73*, 111−117.

(39) Horner, J. K.; Henry, D. W. Analogs of 3-amino-7-chloro-1,2,4-benzotriazine 1-oxide as antimalarial agents. *J. Med. Chem.* **1968**, *11*, 946−949.

(40) Gupta, S.; Agarwal, P. K.; Kundu, B. Catalyst/ligand-free synthesis of benzimidazoles and quinazolinones from amidines *via* intramolecular transamination reaction. *Tetrahedron Lett.* **2010**, *51*, 1887−1890.

(41) Cortes-Salva, M.; Nguyen, B.-L.; Cuevas, J.; Pennypacker, K. R.; Antilla, J. C. Copper-catalyzed guanidinylation of aryl iodides: The formation of *N,N′*-disubstituted guanidines. *Org. Lett.* **2010**, *12*, 1316−1319.

(42) Xing, H.; Zhang, Y.; Lai, Y.; Jiang, Y.; Ma, D. Synthesis of symmetrical and unsymmetrical *N,N′*-diaryl guanidines *via* copper/*N*-methylglycine-catalyzed arylation of guanidine nitrate. *J. Org. Chem.* **2012**, *77*, 5449−5453.

(43) Lawson, C. P. A. T.; Slawin, A. M. Z.; Westwood, N. J. Application of the copper catalysed *N*-arylation of amidines in the synthesis of analogues of the chemical tool, blebbistatin. *Chemm. Commun.* **2011**, *47*, 1057−1059.

(44) Duan, F.; Liu, M.; Chen, J.; Ding, J.; Hu, Y.; Wu, H. Copper-catalyzed sequential arylation and intramolecular annulation of 2-(2-bromophenyl)-2,3-dihydroquinazolin-4(1*H*)-ones with amidines. *RSC Adv.* **2013**, *3*, 24001−24004.

(45) Deng, X.; McAllister, H.; Mani, M. S. CuI-catalyzed amination of arylhalides with guanidines or amidines: A facile synthesis of 1-*H*-2-substituted benzimidazoles. *J. Org. Chem.* **2009**, *74*, 5742−5745.

(46) Arndt, F. Ringschluss zwischen nitro- und aminogruppe unter bildung von triazinen. *Ber. Dtsch. Chem. Ges.* **1913**, *46*, 3522−3530.

(47) Arndt, F.; Rosenau, B. Uber cyclische azoxy-verbindungen. *Ber. Dtsch. Chem. Ges.* **1917**, *50*, 1248−1261.

(48) Berenyi, E.; Benkó, P.; Zólyomi, G.; Tamas, J. Ring transformation of condensed dihydro-*as*-triazines. *J. Heterocyc. Chem.* **1981**, *18*, 1537−1540.

(49) Suzuki, H.; Kawakami, T. Straightforward synthesis of some 2- or 3-substituted naphtho- and quinolino[1,2,4]triazines *via* the cyclocondensation of nitronaphthalenes and nitroquinolines with guanidine base. *J. Org. Chem.* **1999**, *64*, 3361−3363.

(50) Fusco, R.; Bianchetti, G. Sintesi di 1,2,4-benzotriazine-1-*N*-ossidi. XII Sulle triazine asimmetriche. *Rend., Sci. mat. fis. chim. geol., A (Ist. lomb. Accad. sci. lett.)* **1957**, *91*, 963−978.

(51) Quek, J. Y.; Davis, T. P.; Lowe, A. B. Amidine functionality as a stimulus-responsive building block. *Chem. Soc. Rev.* **2013**, *42*, 7326−7334.

(52) Castagnolo, D.; Schenone, S.; Botta, M. Guanylated diamines, triamines, and polyamines: Chemistry and biological properties. *Chem. Rev.* **2011**, *111*, 5247−5300.

(53) Taylor, J. E.; Bull, S. D.; Williams, J. M. J. Amidines, isothioureas, and guanidines as nucleophilic catalysts. *Chem. Soc. Rev.* **2012**, *41*, 2109−2121.

(54) Coles, M. P. Bicyclic-guanidines, -guanidinates and -guanidinium salts: Wide ranging applications from a simple family of molecules. *Chem. Commun.* **2009**, 3659−3676.

(55) Fu, X.; Tan, C.-H. Mechanistic considerations of guanidine-catalyzed reactions. *Chem. Commun.* **2011**, *47*, 8210−8222.

(56) Ishikawa, T. Guanidine Chemistry. *Chem. Pharm. Bull.* **2010**, *58*, 1555−1564.

(57) Baeten, M.; Maes, B. U. W. Guanidine synthesis: Use of amidines as guanylating agents. *Adv. Synth. Catal.* **2016**, *358*, 826−833.

(58) Demjén, A.; Angyal, A.; Wölfling, J.; Puskás, L. G.; Kanizsai, I. One-pot synthesis of diverse *N,N′*-disubstituted guanidines from *N*-chlorophthalimide, isocyanides and amines *via* N-phthaloyl-guanidines. *Org. Biomol. Chem.* **2018**, *16*, 2143−2149.

(59) Guo, D. X.; Liu, Y. J.; Li, T.; Wang, N.; Zhai, X.; Hu, C.; Gong, P. Synthesis and antitumor activities of a new series of 4,5-dihydro-1*H*-thiochromeno[4,3-*d*]pyrimidine derivatives. *Sci. China Chem.* **2012**, *55*, 347−351.

(60) Tavares, F. X.; Boucheron, J. A.; Dickerson, S. H.; Griffin, R. J.; Preugschat, F.; Thomson, S. A.; Wang, T. Y.; Zhou, H.-Q. *N*-Phenyl-4-pyrazolo[1,5-*b*]pyridazin-3-ylpyrimidin-2-amines as potent and selective inhibitors of glycogen synthase kinase 3 with good cellular efficacy. *J. Med. Chem.* **2004**, *47*, 4716−4730.

(61) Souza, M. C.; Macedo, W. P.; Silva, M. C. M.; Ramos, G. C. d. O.; Alt, H. G. One-pot synthesis of *N*-alkyl substituted phosphoryl guanidines. *Phosphorus, Sulfur, and Silicon* **2004**, *179*, 1047−1054.

(62) Neugebauer, F. A.; Umminger, I. Über 1,4-dihydro-1,2,4-benzotriazinyl-radikale. *Chem. Ber.* **1980**, *113*, 1205−1225.

(63) Constantinides, C. P.; Koutentis, P. A.; Krassos, H.; Rawson, J. M.; Tasiopoulos, A. J. Characterization and magnetic properties of a "super stable" radical 1,3-diphenyl-7-trifluoromethyl-1,4-dihydro-1,2,4-benzotriazin-4-yl. *J. Org. Chem.* **2011**, *76*, 2798−2806.

(64) Connelly, N. G.; Geiger, W. E. Chemical redox agents for organometallic chemistry. *Chem. Rev.* **1996**, *96*, 877−910.

(65) Hall, H. K., Jr Correlation of the base strengths of amines. *J. Am. Chem. Soc.* **1957**, *79*, 5441−5444.

(66) Trasatti, S. The absolute electrode potential: An explanatory note. *Pure Appl. Chem.* **1986**, *58*, 955−966.

(67) Frisch, M. J.; Trucks, G. W.; Schlegel, H. B.; Scuseria, G. E.; Robb, M. A.; Cheeseman, J. R.; Scalmani, G.; Barone, V.; Mennucci, B.; Petersson, G. A.; Nakatsuji, H.; Caricato, M.; Li, X.; Hratchian, H. P.; Izmaylov, A. F.; Bloino, J.; Zheng, G.; Sonnenberg, J. L.; Hada, M.; Ehara, M.; Toyota, K.; Fukuda, R.; Hasegawa, J.; Ishida, M.; Nakajima, T.; Honda, Y.; Kitao, O.; Nakai, H.; Vreven, T.; Montgomery, J. A., Jr.; Peralta, J. E.; Ogliaro, F.; Bearpark, M.; Heyd, J. J.; Brothers, E.; Kudin, K. N.; Staroverov, V. N.; Kobayashi, R.; Normand, J.; Raghavachari, K.; Rendell, A.; Burant, J. C.; Iyengar, S. S.; Tomasi, J.; Cossi, M.; Rega, N.; Millam, J. M.; Klene, M.; Knox, J. E.; Cross, J. B.; Bakken, V.; Adamo, C.; Jaramillo, J.; Gomperts, R.; Stratmann, R. E.; Yazyev, O.; Austin, A. J.; Cammi, R.; Pomelli, C.; Ochterski, J. W.; Martin, R. L.; Morokuma, K.; Zakrzewski, V. G.; Voth, G. A.; Salvador, P.; Dannenberg, J. J.; Dapprich, S.; Daniels, A. D.; Farkas, O.; Foresman, J. B.; Ortiz, J. V.; Cioslowski, J.; Fox, D. J. *Gaussian 09*, rev. A.02; Gaussian, Inc.: Wallingford, CT, 2009.

(68) Stratmann, R. E.; Scuseria, G. E.; Frisch, M. J. An efficient implementation of time-dependent density-functional theory for the calculation of excitation energies of large molecules. *J. Chem. Phys.* **1998**, *109*, 8218−8224.

(69) Cossi, M.; Scalmani, G.; Rega, N.; Barone, V. New developments in the polarazible continuum model for quantum mechanical and classical calculations on molecules in solution. *J. Chem. Phys.* **2002**, *117*, 43−54.

(70) Fulmer, G. R.; Miller, A. J. M.; Sherden, N. H.; Gottlieb, H. E.; Nudelman, A.; Stoltz, B. M.; Bercaw, J. E.; Goldberg, K. I. NMR chemical shifts of trace impurities: Common laboratory solvents, organics, and gases in deuterated solvents relevant to the organometallic chemist. *Organometallics* **2010**, *29*, 2176−2179.

(71) Bodzioch, A.; Pietrzak, A.; Kaszyński, P. Axially chiral stable radicals: Resolution and characterization of Blatter radical atropisomers. *Org. Lett.* **2021**, *23*, 7508−7512.

(72) Sarkar, U.; Hillebrand, R.; Johnson, K. M.; Cummings, A. H.; Phung, N. L.; Rajapakse, A.; Zhou, H.; Willis, J. R.; Barnes, C. L.; Gates, K. S. Application of Suzuki-Miyaura and Buchwald-Hartwig cross-coupling reactions to the preparation of substituted 1,2,4-benzotriazine 1-oxides related to the antitumor agent tirapazamine. *J. Heterocyclic Chem.* **2017**, *54*, 155−160.

(73) Irie, Y.; Koga, Y.; Matsumoto, T.; Matsubara, K. *o*-Amine-assisted cannizaro reaction of glyoxal with new 2,6-diaminoanilines. *Eur. J. Org. Chem.* **2009**, *2009*, 2243−2250.

(74) Yang, K.; Qiu, Y.; Li, Z.; Wang, Z.; Jiang, S. Ligands for copper-catalyzed C-N bond forming reactions with 1 mol% CuBr as catalyst. *J. Org. Chem.* **2011**, *76*, 3151−3159.

(75) Patil, V. V.; Shankarling, G. S. Steric-hindrance-induced regio- and chemoselective oxidation of aromatic amines. *J. Org. Chem.* **2015**, *80*, 7876−7883.

(76) Das, S.; Mallick, S.; De Sarkar, S. Cobalt-calatyzed sustainable synthesis of benzimidazoles by redox-economical coupling of *o*-nitroanilines and alcohols. *J. Org. Chem.* **2019**, *84*, 12111−12119.

10. Declarations of co-authors

prof. dr hab. inż. Piotr Kaszyński   Łódź, 28.08.2023
Wydział Chemii UŁ
ul. Tamka 12, 91-403 Łódź
e-mail: piotr.kaszynski@chemia.uni.lodz.pl

Oświadczenie

Niniejszym oświadczam, że w procesie powstawania publikacji:

D−1 Bodzioch, A.; Pomikło, D.; Celeda, M.; Pietrzak, A.; Kaszyński, P. 3-Substituted benzo[*e*][1,2,4]triazines: synthesis and electronic effects of the C(3) substituent. J. Org. Chem. 2019, 84, 6377–6394.

D−2 Pomikło, D.; Bodzioch, A.; Pietrzak, A.; Kaszyński, P. C(3) Functional derivatives of the Blatter radical. Org. Lett. 2019, 21, 6995–6999.

D−3 Pomikło, D.; Bodzioch, A.; Kaszyński, P. 3-Substituted Blatter radicals: cyclization of *N*-arylguanidines and *N*-arylamidines to benzo[*e*][1,2,4]triazines and PhLi addition. *J. Org. Chem.* **2023**, *88*, 2999–3011.

D−4 Pomikło, D.; Pietrzak, A.; Kishi, R.; Kaszyński, P. Bi-Blatter diradicals: convenient access to regioisomers with tunable electronic and magnetic properties. Mater. Chem. Front. 2023, doi.org/10.1039/D3QM00666B

D−5 Pomikło, D.; Kaszyński, P. Blatter diradicals with a spin coupler at the N(1) position. *Chem. Chem. Eur. J.* **2023**, Accepted Manuscript

Mój udział w każdej z powyższych publikacji polegał na sformułowaniu zakresu pracy, dyskusji wyników i przygotowaniu oraz złożeniu do publikacji ostatecznej wersji pracy jak również na opiece merytorycznej nad mgr inż. Dominiką Pomikło.

....
prof. dr hab. inż. Piotr Kaszyński

dr Agnieszka Bodzioch   Łódź, 28.08.2023
CBMM PAN
ul. Henryka Sienkiewicza 112, 90-363 Łódź
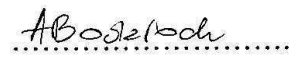e-mail: agnieszka.bodzioch@cbmm.lodz.pl

Oświadczenie

Niniejszym oświadczam, że w procesie powstawania publikacji:

D−1 Bodzioch, A.; Pomikło, D.; Celeda, M.; Pietrzak, A.; Kaszyński, P. 3-Substituted benzo[*e*][1,2,4]triazines: synthesis and electronic effects of the C(3) substituent. J. Org. Chem. 2019, 84, 6377–6394.

D−2 Pomikło, D.; Bodzioch, A.; Pietrzak, A.; Kaszyński, P. C(3) Functional derivatives of the Blatter radical. Org. Lett. 2019, 21, 6995–6999.

D−3 Pomikło, D.; Bodzioch, A.; Kaszyński, P. 3-Substituted Blatter radicals: cyclization of *N*-arylguanidines and *N*-arylamidines to benzo[*e*][1,2,4]triazines and PhLi addition. *J. Org. Chem.* **2023**, *88*, 2999–3011.

mój udział polegał na współpracy w obszarze syntezy i pomiarów elektrochemicznych oraz spektroskopowych badanych związków oraz udziale w opracowaniu oraz korekty manuskryptów.

ABodzioch
....
dr Agnieszka Bodzioch

dr inż. Anna Pietrzak   Łódź, 28.08.2023
Wydział Chemii PŁ
ul. Stefana Żeromskiego 114, 90-543 Łódź
e-mail: anna.pietrzak.1@p.lodz.pl

Oświadczenie

Niniejszym oświadczam, że w procesie powstawania publikacji:

D−1 Bodzioch, A.; Pomikło, D.; Celeda, M.; Pietrzak, A.; Kaszyński, P. 3-Substituted benzo[*e*][1,2,4]triazines: synthesis and electronic effects of the C(3) substituent. J. Org. Chem. 2019, 84, 6377–6394.

D−2 Pomikło, D.; Bodzioch, A.; Pietrzak, A.; Kaszyński, P. C(3) Functional derivatives of the Blatter radical. Org. Lett. 2019, 21, 6995–6999.

D−4 Pomikło, D.; Pietrzak, A.; Kishi, R.; Kaszyński, P. Bi-Blatter diradicals: convenient access to regioisomers with tunable electronic and magnetic properties. Mater. Chem. Front. 2023, doi.org/10.1039/D3QM00666B

mój udział polegał na wykonaniu oraz opracowaniu wyników pomiarów dyfrakcji rentgenowskiej w celu potwierdzenia struktury produktów końcowych.

Anna Pietrzak
dr inż. Anna Pietrzak

Dr. Ryohei Kishi   Osaka, 28.08.2023
Graduate School of Engineering Science,
Osaka University, Toyonaka, Osaka 560-8531, Japan
e-mail: kishi.ryohei.es@osaka-u.ac.jp

Declaration

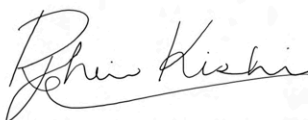I hereby declare that in the preparation of publication:

D−4 Pomikło, D.; Pietrzak, A.; Kishi, R.; Kaszyński, P. Bi-Blatter diradicals: convenient access to regioisomers with tunable electronic and magnetic properties. Mater. Chem. Front. 2023, doi.org/10.1039/D3QM00666B

My contribution was to perform the Density Functional Theory (DFT) calculations.

....
Dr. Ryohei Kishi

Małgorzata Celeda   Łódź, 28.08.2023
Wydział Chemii UŁ
ul. Tamka 12, 91-403 Łódź
e-mail: malgorzata.celeda@chemia.uni.lodz.pl

Oświadczenie

Niniejszym oświadczam, że w procesie powstawania publikacji:

D−1 Bodzioch, A.; Pomikło, D.; Celeda, M.; Pietrzak, A.; Kaszyński, P. 3-Substituted benzo[*e*][1,2,4]triazines: synthesis and electronic effects of the C(3) substituent. J. Org. Chem. 2019, 84, 6377–6394.

mój udział polegał na syntezie wybranych prekursorów.

Małgorzata Celeda